Universidad de Concepción
Dirección de Postgrado
Facultad de Ciencias Físicas y Matemáticas
Programa de Doctorado en Ciencias Aplicadas
con Mención en Ingeniería Matemática

MÉTODOS DE ELEMENTOS FINITOS MIXTOS Y AFINES PARA PROBLEMAS NO-LINEALES Y DE TRANSMISIÓN EN MECÁNICA DE MEDIOS CONTINUOS

(MIXED FINITE ELEMENT AND RELATED METHODS FOR NONLINEAR AND TRANSMISSION PROBLEMS IN CONTINUUM MECHANICS)

Tesis para optar al grado de Doctor en Ciencias
Aplicadas con mención en Ingeniería Matemática

FILÁNDER DE LOS ÁNGELES SEQUEIRA CHAVARRÍA
CONCEPCIÓN-CHILE

2015

Profesor Guía: Gabriel N. Gatica Pérez
CI^{2}MA y Departamento de Ingeniería Matemática
Universidad de Concepción, Chile

Cotutor: Johnny Guzmán
Division of Applied Mathematics
Brown University, USA

Mixed Finite Element and Related Methods for Nonlinear and Transmission Problems in Continuum Mechanics

Filánder A. Sequeira Chavarría

Directores de Tesis: Gabriel N. Gatica, Universidad de Concepción, Chile.
Johnny Guzmán, Brown University, USA.

Director de Programa: Raimund Bürger, Universidad de Concepción, Chile.

Comisión evaluadora

Prof.

Prof.

Prof.

Prof.

Comisión examinadora

Firma: ____________________
Prof. Gabriel N. Gatica, Universidad de Concepción, Chile.

Firma: ____________________
Prof. Luis F. Gatica, Universidad Católica de la Santísima Concepción, Chile.

Firma: ____________________
Prof. Norbert Heuer, Pontificia Universidad Católica de Chile, Chile.

Firma: ____________________
Prof. Ignacio Muga, Pontificia Universidad Católica de Valparaíso, Chile.

Firma: ____________________
Prof. Manuel E. Solano, Universidad de Concepción, Chile.

Calificación: ____________________

Concepción, 11 de Diciembre de 2015

Abstract

This dissertation deals with diverse mathematical and numerical aspects of new mixed finite element methods and hybridized discontinuous Galerkin schemes, based on the introduction of pseudostress auxiliary variables, for analyzing nonlinear and transmission problems governed by systems of partial differential equations arising in continuum mechanics.

Firstly, we present the *a priori* and *a posteriori* error analyses of a non-standard mixed finite element method for the linear elasticity problem with non-homogeneous Dirichlet boundary conditions, which does not require symmetric tensor spaces in the finite element discretization. Here, physical quantities such as the stress, the strain tensor of small deformations, and the rotation, are computed through a simple postprocessing in terms of the pseudostress variable. Furthermore, we also introduce a second element-by-element postprocessing formula for the stress, which yields an optimally convergent approximation of this unknown with respect to the broken $\mathbb{H}(\mathbf{div})$-norm. A reliable and efficient residual-based *a posteriori* error estimator for this problem, is also provided.

Next, we introduce and analyze an augmented mixed finite element method for the two-dimensional nonlinear Brinkman model of porous media flow with mixed boundary conditions. Here, we employ a dual-mixed formulation in which the main unknowns are given by the gradient of the velocity and the pseudostress. In this way, the original unknowns corresponding to the velocity and pressure are easily recovered through a simple postprocessing. We apply known results from nonlinear functional analysis to prove that the corresponding continuous and discrete schemes are both well-posed. In addition, we derive a reliable and efficient residual-based *a posteriori* error estimator for this nonlinear system.

On the other hand, we apply the hybridizable discontinuous Galerkin (HDG) method for numerically solving a class of nonlinear Stokes models arising in quasi-Newtonian fluids. We use the incompressibility condition to eliminate the pressure, and set the velocity gradient as an auxiliary unknown. Then, we enrich the HDG formulation with two suitable augmented equations, which allows us to apply a nonlinear version of Babuška-Brezzi theory and the classical Banach fixed-point theorem to show that the discrete scheme is well-posed, yielding in turn the derivation of the corresponding *a priori* error estimates. In addition, a second approach for this problem is also considered. For this new version, the main features of the aforementioned augmented formulation are maintained, but after introducing slight modifications of the finite element subspaces for the pseudostress and velocity, we are able to significantly improve our previous analyses and results. More precisely, on one hand we omit the utilization of any fixed-point argument and related parameters to establish the well-posedness of the discrete scheme, and on the other hand we now prove optimally convergent approximations for all the unknowns. Furthermore, we develop a reliable and efficient residual-based *a posteriori* error estimator, and propose the associated adaptive algorithm for our HDG approximation of the nonlinear model problem.

Additionally, we present an HDG method for the coupling of fluid flow with porous media flow. Flows are governed by the Stokes and Darcy equations, respectively, and the corresponding transmission conditions are given by mass conservation, balance of normal forces, and the Beavers-Joseph-Saffman law. We consider a fully-mixed formulation in which the main unknowns are given by the stress, the vorticity, the velocity, and the trace of the velocity, (all of them in the fluid), along with the velocity, the pressure, and the trace of the pressure in the porous medium. In addition, we enhance the finite dimensional subspace for the stress, in order to obtain optimally convergent approximations for all unknowns, as well as a superconvergent approximation of the trace variables. To do that, as in previous papers dealing with the development of *a priori* error estimates for HDG methods, we use the projection-based error analysis in order to simplify the corresponding study.

Finally, we close this thesis by providing H(div) conforming and discontinuous Galerkin (DG) methods for the incompressible Euler equation in two and three dimensions. More precisely, we consider velocity-pressure formulations in which the main goal is prove the L^2-stability of each scheme, along to the local conservative properties for the DG methods. Once we have developed H(div) conforming methods, it guides us in designing DG methods using the post-processing idea employed in previous papers. In addition, we obtain *a priori* error estimates for both the semi-discrete and fully-discrete methods using Backward Euler time stepping. In all the cases, we consider central and upwind fluxes.

For all the situations described above, several numerical experiments illustrating the correct performance of the methods, and confirming the theoretical results, are reported.

Resumen

Esta disertación aborda diversos aspectos matemáticos y numéricos acerca de nuevos métodos de elementos finitos mixtos y esquemas de Galerkin discontinuo hibridizado, basados en la introducción de variables auxiliares conocidas como pseudo-esfuerzos. Estas con el fin de analizar problemas no lineales y de transmisión, que se rigen por sistemas de ecuaciones diferenciales parciales, los cuales surgen en mecánica de medios continuos.

En primer lugar, se presenta el análisis de error *a priori* y *a posteriori* de un método de elementos finitos mixtos no estándar para el problema de elasticidad lineal con condiciones de contorno de Dirichlet no homogéneas, el cual no requiere espacios tensoriales simétricos en la discretización de elementos finitos. Además, cantidades de interés físico como el esfuerzo, el tensor de pequeñas deformaciones y la rotación, son calculadas a través de simples post-procesamientos en términos del pseudo-esfuerzo. Más aún, se introduce una segunda técnica de post-procesamiento para el esfuerzo, la cual proporciona una aproximación con convergencia óptima para esta incógnita, con respecto a la norma $\mathbb{H}(\mathbf{div})$ por tramos. Adicionalmente, se provee de un estimador de error *a posteriori* residual para este problema, el cual es confiable y eficiente.

A continuación, se introduce y se analiza un método de elementos mixtos aumentado para el modelo no lineal de Brinkman en dos dimensiones, referente a un flujo de medios porosos con condiciones de contorno mixtas. Se emplea una formulación dual-mixta en la cual las incógnitas principales corresponden al gradiente de la velocidad y al pseudo-esfuerzo. En este sentido, la velocidad y presión original son fácilmente recuperadas a través de simples post-procesamientos. Aquí se aplican resultados conocidos de análisis funcional no lineal para probar que los esquemas continuo y discreto correspondiente están bien puestos. Adicionalmente, se deriva un estimador de error *a posteriori* residual para este sistema no lineal, y se verifica que el mismo es confiable y eficiente.

Por otro lado, se aplica el método de Galerkin discontinuo hibridizado (HDG, por sus siglas en inglés) para resolver numéricamente una clase de modelos de Stokes no lineales que surgen en fluidos cuasi-Newtonianos. Se hace uso de la condición de incompresibilidad para eliminar la presión, y se introduce el gradiente de la velocidad como una incógnita auxiliar. Luego, se enriquece la formulación HDG con dos ecuaciones aumentadas adecuadas, las cuales permiten aplicar una versión no lineal de la teoría de Babuška-Brezzi y el teorema clásico del punto fijo de Banach, para probar que el esquema discreto esta bien puesto. Más aún, se derivan las estimaciones de error *a priori* correspondientes. Adicionalmente, se considera un segundo enfoque para este problema, en la cual se mantienen las características principales de la formulación aumentada previamente mencionada, pero introduciendo ahora ligeras modificaciones en los subespacios de elementos finitos para el pseudo-esfuerzo y la velocidad, con el fin de mejorar significativamente nuestros análisis y resultados anteriores. Más precisamente, por un lado omitimos la utilización de cualquier argumento de punto fijo (y los parámetros relacionados) para establecer que el esquema discreto esta bien puesto, y por el otro lado, ahora demostramos que las aproximaciones

convergen de manera óptima en todas las incógnitas. Además, se deriva un estimador de error *a posteriori* residual, confiable y eficiente, para este problema.

Posteriormente, se presenta un método HDG para la resolución numérica del acoplamiento de un fluido en un medio poroso. El modelo acoplado está determinado por las ecuaciones de Stokes y Darcy, respectivamente, y las condiciones de transmisión correspondientes están dadas por la conservación de masa, el balance de fuerzas normales y la ley de Beavers-Joseph-Saffman. Se considera una formulación completamente mixta, en la cual las incógnitas principales corresponden al esfuerzo, la vorticidad, la velocidad y la traza de la velocidad, todas ellas en el fluido; junto con la velocidad, la presión y la traza de la presión en el medio poroso. Además, se enriquece el subespacio de elementos finitos del esfuerzo, con el fin de obtener aproximaciones con convergencia óptima en todas las incógnitas, junto con superconvergencias para las variables de las trazas. Para hacer esto, de manera similar a artículos previos relacionados con el desarrollo de estimaciones de error *a priori* para métodos HDG, se utiliza un análisis de error basado en proyecciones, el cual simplifica el estudio correspondiente.

Finalmente, se cierra esta tesis con el desarrollo de métodos conformes en H(div) y de Galerkin discontinuos (DG, por sus siglas en inglés), para la ecuación incompresible de Euler en dos y tres dimensiones. Más precisamente, se consideran formulaciones de velocidad-presión que tienen como objetivo principal probar la estabilidad en L^2 de cada esquema, junto con las propiedades conservativas locales en el caso de los métodos DG. Una vez desarrollados los métodos conformes en H(div), esto nos guía en el diseño de aproximaciones DG usando un post-procesamiento introducido en artículos previos. Adicionalmente, se muestran estimaciones de error *a priori* para ambos métodos: parcialmente discreto y completamente discreto, usando el método de Euler regresivo. En todos los casos, se consideran flujos centrales y *upwind*.

Para todas las situaciones descritas previamente, se reportan varios experimentos numéricos, los cuales ilustran el correcto rendimiento de los métodos, y confirman además los resultados teóricos.

Agradecimientos

En este pequeño espacio, además de dar gracias a Dios, quiero agradecer a todas aquellas personas e instituciones que hicieron posible no sólo la realización de esta tesis, si no también mi agradable paso por Chile, así como mi crecimiento personal y profesional.

En primer lugar quiero agradecer a mi prometida Helen Guillén, quien no sólo me acompañó, me guió y me ayudó durante todo este proceso, sino que además si no fuera por ella yo no habría realizado mis estudios doctorales en Chile, ni sobrevivido a los mismos. A ella le dedico esta tesis.

A mi asesor Gabriel N. Gatica quien se tomó de su valioso tiempo para enseñarme a tener más confianza en mí mismo y a "no pasarme de revoluciones". Gracias por instruirme de la forma en que lo hizo, donde su orientación y apoyo no sólo me permitieron completar este trabajo, sino que además me abrió un nuevo mundo de posibilidades en el análisis matemático, el cual nunca consideré llegar a comprender. Siempre valoré todos sus consejos y opiniones, pero más que ellos quiero agradecerle de que no sólo fuera mi "Jefe", sino también un apreciado amigo.

A Johnny Guzmán y a su hermosa familia, les agradezco enormemente su hospitalidad durante mi visita en Providence. Gracias por el montón de tiempo que me dedicaste frente a la pizarra para entender los temas que eran nuevos para mí. Más aún, gracias por mostrarme esa preocupación sincera, pero más que eso, gracias por tu amistad y espero me sigas aconsejando en el futuro.

A mi asesor de maestría Paul Castillo quien me mostró el gusto por esta área y me dotó de herramientas fundamentales que me permitierón comprender lo nuevo con mayor facilidad. Además, a mi consejero Mario Marín en Costa Rica, quien me observó y guió en mi crecimiento y madurez. A ambos gracias por abrirme las puertas a mi desarrollo profesional y principalmente por brindarme su amistad.

A Mario Álvarez, a Eligio Antonio Colmenares y a Felipe Lepe, mis compañeros de numerosas y crueles batallas. Ha sido un honor caer y volverse a levantar con ustedes. Y a pesar de seguir al sabio que dijo que "el buen hijo regresa a casa y cuenta lo que le pasa", al menos yo, lo hago con ustedes. Dios me los bendiga siempre.

A mi familia por su apoyo constante y buenos deseos. Junto a ellos, gracias a mis amigos en Costa Rica y en otros países. En particular, gracias a Pablo Soto y a Carlos Garavito quienes siempre me tuvieron presente. Mil gracias a Manuel Solano por la amistad y el tiempo que dedicó a mis consultas triviales. A Manuel Sánchez y a su familia, gracias por su hospitalidad en Providence y por ser tan amables. Más aún, un sincero agradecimiento al profesor Luis Gatica, quien fue parte fundamental en el desarrollo de este trabajo, así como al profesor Chi-Wang Shu.

Al personal admistrativo y docente del Departamento de Ingeniería Matemática y del Centro de Investigación en Ingeniería Matemática (CI^{2}MA), de la Universidad de Concepción, por brindarme la oportunidad de realizar mis estudios doctorales. En particular, le agradezco profundamente al profesor Raimund Bürger, por su guía, consejos y preocupaciones como director.

Finalmente, pero no por eso menos importante, no tengo palabras para agradecer a la Comisión Nacional de Investigación Científica y Tecnológica (CONICYT) y a la Universidad Nacional de Costa Rica (UNA), por financiar mis estudios. Es gracias a ambos que siempre me pude concentrar en mi trabajo. Espero poder devolverles esto de la manera en que lo esperan.

Filánder A. Sequeira Ch.

Contents

List of Tables

List of Figures

Introduction

The devising of suitable numerical methods for solving linear and nonlinear problems in continuum mechanics has become a very active research area during the last two decades. In particular, mixed finite element methods, suitable augmented versions, and the introduction of pseudostress and post-processed variables, are important and useful techniques allowing to develop new schemes leading to the numerical solution of a wide range of problems arising in elasticity, plasticity, viscoelasticity and fluid mechanics.

In general, an interesting feature of mixed methods is given by the fact that, besides the original unknowns, they yield direct approximations of several other quantities of physical interest. For instance, an accurate direct calculation of the stresses is very desirable for flow problems involving interaction with solid structures. Regarding this, the pseudostress-based approaches provide an alternative strategy to approximate the stress variable without needing to impose neither strong nor weak symmetry of this unknown. In fact, this technique has become very popular, specially in fluid mechanics, and has gained considerable attention in recent years due to its applicability to diverse linear as well as nonlinear problems. Indeed, the velocity-pseudostress-pressure formulation of the Stokes equations was first presented in [62] (see also [63]), whereas the velocity-pseudostress formulation (now the definition of the pseudostress contains the pressure) was first studied in [25], and then reconsidered in [83], where further results, including the eventual incorporation of the pressure unknown and an associated a posteriori error analysis, were provided. In turn, augmented mixed finite element methods for pseudostress-based formulations of the stationary Stokes equations, which extend analogue results for linear elasticity problems (see [69, 70, 79]), were introduced and analyzed in [64]. Furthermore, the velocity-pressure-pseudostress formulation has also been applied to nonlinear Stokes problems. In particular, a new mixed finite element method for a class of models arising in quasi-Newtonian fluids was introduced in [76]. The results in [76] were extended in [58] to a setting in reflexive Banach spaces, thus allowing other nonlinear models such as the Carreau law for viscoplastic flows. Moreover, the dual-mixed approach from [76] and [58] was reformulated in [98] by restricting the space for the velocity gradient to that of trace-free tensors. For related contributions dealing with pseudostress-based formulations in incompressible flows, we refer to [59], [81], and the references therein. In turn, the corresponding extension to the Navier-Stokes equations has been developed in [26] and [27]. More recently, a new dual-mixed method for the aforementioned problem, in which the main unknowns are given by the velocity, its gradient, and a modified nonlinear pseudostress tensor linking the usual stress and the convective term, has been proposed in [99]. The idea from [99] has been modified in [30] through the introduction of a nonlinear pseudostress tensor linking now the pseudostress (instead of the stress) and the convective term, which, together with the velocity, constitute the only unknowns. Lately, the approach from [30] has been further extended in [53] and [29], where new augmented mixed-primal formulations for the stationary Boussinesq problem and the Navier-Stokes equations with variable viscosity, respectively, have been proposed and analyzed.

On the other hand, together with the mixed finite element methods, the utilization of discontinuous Galerkin (DG) methods for solving boundary value problems has been considered in different situations. The main reasons for the application of these methods, as compared to the continuous finite element schemes, are the high-order of approximation provided by them, their high degree of parallelism, and their suitability for h, p, and hp refinements. In particular, we are interested in the hybridizable discontinuous Galerkin (HDG) method, introduced in [42] for diffusion problems, as one of the several high-order discretization schemes that benefit from the hybridization technique originally applied in [50] to the local discontinuous Galerkin (LDG) method for time dependent convection-diffusion problems. The main advantages of HDG methods include a substantial reduction of the globally coupled degrees of freedom, which has been a criticism of the DG methods for elliptic problems during the last decade, and the fact that convergence is obtained even for a polynomial degree $k = 0$. Additionally, the approximate flux converges with order $k+1$ for $k \geq 0$, and an element-by-element computation of a new approximation of the scalar variable is possible, which converges with order $k+2$ for $k \geq 1$ (see e.g. [41, 45, 43]).

According to the above discussion, the purpose of this thesis is the introduction of new discretizations for several problems in continuum mechanics. In particular, our main interest is to deal with nonlinear and transmission systems by considering mixed schemes, augmented equations, HDG approximation, pseudostress-based approaches and postprocessing techniques, when required. More precisely, we focus on elasticity, Brinkman, Stokes, Stokes-Darcy and Euler problems. Furthermore, in all cases, we prove the well-posedness of each scheme and provide the corresponding *a priori* error estimates. Also, we derive reliable and efficient residual-based *a posteriori* error estimators for some of these problems. Additionally, several numerical experiments illustrating the correct performance of each method are reported, confirming the theoretical results.

The present work is organized as follows. In **Chapter 1**, and before considering nonlinear and transmission problems, we describe the 3D linear elasticity problem with non-homogeneous Dirichlet boundary conditions, in order to become familiar with the importance of the introduction of pseudostress-based formulations. Specifically, the approach introduced here is based on a simplified interpretation of the pseudostress-displacement formulation originally proposed in [6], which does not require symmetric tensor spaces in the finite element discretization. In addition we show that this formulation is well-posed, and we also analyze the associated mixed finite element method. In particular, we show that Raviart-Thomas spaces of order $k \geq 0$ for the pseudostress, and piecewise polynomials of degree $\leq k$ for the displacement can be employed, which, in the 3D case, yields a global number of unknowns behaving approximately as only 9 times the number of tetrahedra of the triangulation when $k = 0$. Next, a reliable and efficient residual-based *a posteriori* error estimator is developed for polyhedral domains in 3D. The contents of this chapter originally appeared in the following paper and preprint:

[74] Gabriel N. Gatica, Luis F. Gatica and Filánder A. Sequeira, *A* $\mathbb{RT}_k - \mathbf{P}_k$ *approximation for linear elasticity yielding a broken* $H(\mathbf{div})$ *convergent postprocessed stress.* **Applied Mathematics Letters**, vol. 49, pp. 133–140, (2015).

[75] Gabriel N. Gatica, Luis F. Gatica and Filánder A. Sequeira, *A priori and a posteriori error analyses of a pseudostress-based mixed formulation for linear elasticity.* Preprint 2015-14, Centro de Investigación en Ingeniería Matemática (CI^{2}MA), Universidad de Concepción, Chile, (2015).

In **Chapter 2** we introduce and analyze an augmented mixed finite element method for the two-dimensional nonlinear Brinkman model of porous media flow with mixed boundary conditions. Here, we extend a previous approach for the respective linear model (see [72]) to the present nonlinear case, and employ a dual-mixed formulation in which the main unknowns are given by the gradient of the velocity and the pseudostress. In this way, the original velocity and pressure unknowns are easily recovered through a simple postprocessing. Furthermore, since the Neumann boundary condition becomes essential, we impose it in a weak sense, which yields the introduction of the trace of the fluid velocity over the Neumann boundary as the associated Lagrange multiplier. We apply known results from nonlinear functional analysis to prove that the corresponding continuous and discrete schemes are well-posed. In addition, by applying basically the techniques from [66], [83], and [84], we derive a reliable and efficient residual-based *a posteriori* error estimator for our Galerkin scheme. The contents of this chapter originally appeared in the following paper:

> [73] Gabriel N. Gatica, Luis F. Gatica and Filánder A. Sequeira, *Analysis of an augmented pseudostress-based mixed formulation for a nonlinear Brinkman model of porous media flow.* **Computer Methods in Applied Mechanics and Engineering**, vol. 289, 1, pp. 104–130, (2015).

In **Chapter 3** we introduce and analyze a hybridizable discontinuous Galerkin method for numerically solving a class of nonlinear Stokes models arising in quasi-Newtonian fluids. Similarly as in previous papers dealing with the application of mixed finite element methods to these nonlinear models (see [23, 76, 54]), we first use the incompressibility condition to eliminate the pressure, and set the velocity gradient as an auxiliary unknown. We show the unique solvability of the augmented HDG scheme by considering an equivalent formulation, and then applying a nonlinear version of the Babuška-Brezzi theory and the classical Banach fixed-point theorem. The corresponding *a priori* error estimates are also derived using the equivalent formulation. Furthermore, in order to show that the implementation of the HDG scheme is quite simple, in this chapter we also discuss some general aspects concerning the computational implementation of the HDG method. The contents of this chapter originally appeared in the following paper:

> [89] Gabriel N. Gatica and Filánder A. Sequeira, *Analysis of an augmented HDG method for a class of quasi-Newtonian Stokes flows.* **Journal of Scientific Computing**, vol. 65, 3, pp. 1270–1308, (2015).

The corresponding analysis given in **Chapter 3**, which makes use of a fixed point strategy that depends on a suitably chosen parameter, yields optimal rates of convergence for only two of the six resulting unknowns, whereas the reported numerical results, showing higher orders than predicted, support the conjecture that the *a priori* error estimates are not sharp. In **Chapter 4**, the main features of the aforementioned augmented formulation are maintained, but after introducing slight modifications of the finite element subspaces for the pseudostress and velocity, we are able to significantly improve our previous analyses and results. More precisely, on one hand we omit the utilization of any fixed-point argument and related parameters to establish the well-posedness of the discrete scheme, and on the other hand we now prove optimally convergent approximations for all the unknowns. Furthermore, we develop a reliable and efficient residual-based *a posteriori* error estimator, and propose the associated adaptive algorithm for our HDG approximation of the nonlinear model problem. The contents of this chapter originally appeared in the following preprint:

> [91] Gabriel N. Gatica and Filánder A. Sequeira, *A priori and a posteriori error analyses of an augmented HDG method for a class of quasi-Newtonian Stokes flows.* Preprint 2015-32, Centro de Investigación en Ingeniería Matemática (CI^2MA), Universidad de Concepción, Chile, (2015).

In **Chapter 5** we consider a linear transmission problem. More precisely, we introduce and analyze an HDG method for numerically solving the coupling of fluid flow with porous media flow. Flows are governed by the Stokes and Darcy equations, respectively, and the corresponding transmission conditions are given by mass conservation, balance of normal forces, and the Beavers-Joseph-Saffman law. We consider a fully-mixed formulation in which the main unknowns in the fluid are given by the stress, the vorticity, the velocity, and the trace of the velocity, whereas the velocity, the pressure, and the trace of the pressure in the porous medium. In addition, we enrich the finite dimensional subspace for the stress, in order to obtain optimally convergent approximations for all unknowns, as well as a superconvergent approximation of the trace variables. To do that, similarly as in previous papers dealing with development of the *a priori* error estimates, we use the projection-based error analysis in order to simplify the corresponding study. The contents of this chapter originally appeared in the following preprint:

> [90] Gabriel N. Gatica and Filánder A. Sequeira, *Analysis of the HDG method for the Stokes-Darcy coupling.* Preprint 2015-23, Centro de Investigación en Ingeniería Matemática (CI^2MA), Universidad de Concepción, Chile, (2015).

Finally, in **Chapter 6** we aim to the extension of the results obtained in previous chapters regarding the unsteady state. Nevertheless, it is quite clear that in order to analyze transient problems, we need first to consider the steady state. After this, the extension is more natural and the main issue is to prove the stability in the numerical approximations. In **Chapters 1-5** we have already established the analysis of the steady state problems. Unfortunately, the proof of stability is not an easy task. In this sense, the incompressible Euler equation represents a usual way to begin understanding nonlinear time-evolution equations, whose natural formulation corresponds to the classical mixed form. Thus, the purpose of the chapter is to develop and study H(div) conforming and discontinuous Galerkin methods for the incompressible Euler's equation in two and three dimensions, using a velocity-pressure formulation. Here, we prove error estimates for both the semi-discrete and fully-discrete methods using Backward Euler time stepping. In addition, we also analyze central and upwind fluxes. The contents of this chapter originally appeared in the following preprint:

> [94] Johnny Guzmán, Filánder A. Sequeira and Chi-Wang Shu, *H(div) conforming and DG methods for incompressible Euler's equations.* Preprint 2015-19, Centro de Investigación en Ingeniería Matemática (CI^2MA), Universidad de Concepción, Chile, (2015).

In all the six chapters, we provide several numerical results illustrating the good performance of the proposed methods, and confirming the theoretical properties such as orders of convergence and reliability and efficiency of *a posteriori* error estimators. The set of numerical experiments includes examples in two and three dimensions, where we provided even examples not fully covered by the theory. In addition, all the computational implementations of the methods were obtained using C++ codes, and in the case of **Chapter 6**, MATLAB was also required.

Introducción

La elaboración de métodos numéricos adecuados para resolver problemas lineales y no lineales en mecánica de los medios continuos se ha convertido en un área de investigación bastante activa en las últimas dos décadas. En particular, los métodos mixtos de elementos finitos, versiones aumentadas y la introducción de pseudo-esfuerzos y variables post-procesadas, corresponden a técnicas importantes y útiles para desarrollar nuevos esquemas que conducen a la solución numérica de una amplia gama de problemas que surgen en elasticidad, plasticidad, visco-elasticidad y mecánica de fluidos.

En general, una característica interesante de los métodos mixtos corresponde al hecho de que, además de las incógnitas originales, con ellos se obtienen aproximaciones directas de varias otras cantidades de interés físico. Por ejemplo, un cálculo preciso y directo del esfuerzo es muy deseable para los problemas de flujo que implican la interacción con estructuras sólidas. En este sentido, los enfoques basados en pseudo-esfuerzos proporcionan una estrategia alternativa para aproximar la variable del esfuerzo sin la necesidad de imponer simetría fuerte o débil sobre esta incógnita. De hecho, esta técnica se ha vuelto muy popular, especialmente en mecánica de fluidos, y ha ganado considerable atención en los últimos años debido a su aplicabilidad a diversos problemas lineales, así como no lineales. En efecto, la formulación de velocidad−pseudo-esfuerzo−presión de las ecuaciones de Stokes se presentó por primera vez en [62] (ver además [63]), mientras que la formulación de velocidad−pseudo-esfuerzo (ahora la definición del pseudo-esfuerzo contiene la presión) se estudió por primera vez en [25], y luego se reconsideró en [83], donde se proporcionaron más resultados, incluyendo la eventual incorporación de la incógnita de la presión, así como el análisis de error *a posteriori* asociado. A su vez, en [64] se introdujeron y se analizaron métodos de elementos finitos mixtos aumentados para formulaciones basadas en pseudo-esfuerzos, para las ecuaciones estacionarias de Stokes. Dichos métodos extendieron resultados análogos para problemas de elasticidad lineal (ver [69, 70, 79]). Además, la formulación velocidad−presión−pseudo-esfuerzo también se ha aplicado a problemas de Stokes no lineales. En particular, un nuevo método de elementos finitos mixtos para una clase de modelos que surgen en fluidos cuasi-Newtonianos, se introdujo en [76]. Los resultados en [76] se extendieron en [58] para el caso de espacios de Banach reflexivos, permitiendo así otros modelos no lineales, como la ley de Carreau para flujos visco-plásticos. Por otra parte, el enfoque dual-mixto de [76] y [58] fue reformulado en [98] al restringir el espacio para el gradiente de velocidad a los tensores de traza nula. Con respecto a contribuciones relacionadas a formulaciones basadas en pseudo-esfuerzos en flujos incompresibles, nos referimos a [59], [81], y las referencias en ellos. A su vez, la extensión correspondiente a las ecuaciones de Navier-Stokes se ha desarrollado en [26] y [27]. Más recientemente, un nuevo método dual-mixto para el problema antes mencionado, en el cual las incógnitas principales corresponden a: la velocidad, su gradiente, y un tensor pseudo-esfuerzo no lineal modificado relacionado con el esfuerzo usual y el término convectivo, se ha propuesto en [99]. La idea de [99] ha sido modificada en [30] a través de la introducción de un tensor pseudo-esfuerzo no lineal relacionado con el ahora pseudo-esfuerzo (en vez del esfuerzo) y el término convectivo, el cual, junto con la velocidad, constituyen las únicas incógnitas.

Últimamente, el enfoque de [30] se ha ampliado aún más en [53] y [29], donde se proponen y se analizan nuevas formulaciones mixtas-primales aumentadas para el problema estacionario de Boussinesq y las ecuaciones de Navier-Stokes con viscosidad variable, respectivamente.

Por otro lado, junto con los métodos de elementos finitos mixtos, la utilización de métodos de Galerkin discontinuos (DG, por sus siglas en inglés) para la resolución numérica de problemas de valores de contorno, ha sido considerada en diferentes situaciones. Las razones principales de las aplicaciones de estos métodos, en comparación con los esquemas de elementos finitos continuos, corresponden al alto orden proporcionado por ellos en las aproximaciones, su alto grado de paralelismo, y su conveniencia para refinamientos h, p y hp. En particular, es de gran interés el método de Galerkin discontinuo hibridizado (HDG, por sus siglas en inglés), el cual fue introducido en [42] para problemas de difusión, como uno de los múltiples esquemas de discretización de orden superior que se benefician de la técnica de hibridización originalmente aplicada en [50] para el método de Galerkin discontinuo local (LDG, por sus siglas en inglés) a problemas de convección-difusión que dependen del tiempo. Las principales ventajas de los métodos HDG incluyen una reducción sustancial en el número global de grados de libertad, lo cual era una crítica de los métodos DG para problemas elípticos durante la última década. Además, se obtiene convergencia incluso para polinomios de grado $k = 0$. Adicionalmente, el flujo aproximado converge con orden $k+1$ para $k \geq 0$, y es posible calcular, elemento a elemento, una nueva aproximación de la variable escalar, la cual converge con orden $k + 2$ para $k \geq 1$ (ver por ejemplo, [41, 45, 43]).

De acuerdo con la discusión anterior, el propósito principal de esta tesis es la introducción de nuevas discretizaciones para varios problemas en mecánica de medios continuos. En particular, el interés se centra en los sistemas no lineales y de transmisión al considerar esquemas mixtos, ecuaciones aumentadas, aproximaciones HDG, enfoques basados en pseudo-esfuerzos y cuando se requiera, técnicas de post-procesado. Más precisamente, nos centramos en problemas de elasticidad, Brinkman, Stokes, Stokes-Darcy y Euler. Por otra parte, en todos los casos, se prueba que cada esquema esta bien puesto y se proporcionan las estimaciones de error *a priori* correspondientes. Además, para algunos de estos problemas, se deriva un estimador de error *a posteriori* residual, confiable y eficiente. Adicionalmente, se reportan varios experimentos numéricos que ilustran el correcto funcionamiento de cada método, lo que confirma los resultados teóricos predichos.

El presente trabajo está organizado como sigue. En el **Capítulo 1**, y previamente a la consideración de problemas no lineales y de transmisión, se describe el problema de elasticidad lineal 3D con condiciones de contorno de Dirichlet no homogéneas. Esto con el fin de familiarizarse con la importancia en la introducción de formulaciones basadas en pseudo-esfuerzos. Específicamente, el enfoque introducido aquí está basado en una interpretación simplificada de la formulación de pseudo-esfuerzo−desplazamiento, originalmente propuesta en [6], la cual no requiere espacios tensoriales simétricos en la discretización de elementos finitos. Además, se prueba que esta formulación está bien puesta y se analiza el método de elementos finitos mixtos asociado. En particular, se demuestra que es posible emplear los espacios de Raviart-Thomas de orden $k \geq 0$ para el pseudo-esfuerzo y polinomios a trozos de grado $\leq k$ para el desplazamiento. En el caso 3D, dichos espacios proporcionan en número global de incógnitas aproximado a 9 veces el número de tetraedros de la triangulación, cuando $k = 0$. Adicionalmente, se desarrolla un estimador de error *a posteriori* residual, el cual es confiable y eficiente para dominios poliédricos en 3D. Este capítulo está constituido por la siguiente publicación y pre-publicación:

[74] Gabriel N. Gatica, Luis F. Gatica and Filánder A. Sequeira, *A* $\mathbb{RT}_k - \mathbf{P}_k$ *approximation for linear elasticity yielding a broken* $H(\mathbf{div})$ *convergent postprocessed stress.* **Applied Mathematics Letters**, vol. 49, pp. 133–140, (2015).

[75] Gabriel N. Gatica, Luis F. Gatica and Filánder A. Sequeira, *A priori and a posteriori error analyses of a pseudostress-based mixed formulation for linear elasticity.* Preprint 2015-14, Centro de Investigación en Ingeniería Matemática ($\mathrm{CI^2MA}$), Universidad de Concepción, Chile, (2015).

En el **Capítulo 2** se introduce y se analiza un método de elementos finitos mixto aumentado para el modelo 2D no lineal de Brinkman de un medio poroso con condiciones de frontera mixtas. Aquí se extienden enfoques previos, aplicados al respectivo modelo lineal (ver [72]), al presente caso no lineal. Se emplea una formulación dual-mixta, en la cual las incógnitas principales corresponden al gradiente de la velocidad y al pseudo-esfuerzo. En este sentido, la velocidad y presión original son fácilmente recuperadas a través de simples post-procesamientos. Luego, dado que la condición de contorno de Neumann se vuelve esencial, esta se impone en el sentido débil, lo cual conlleva a la introducción de la traza de la velocidad del fluido sobre la frontera Neumann, como el multiplicador de Lagrange asociado. Se aplican resultados conocidos del análisis funcional no lineal para probar que los esquemas continuo y discreto correspondientes están bien puestos. Por otro lado, se utilizan las técnicas de [66], [83] y [84], para derivar un estimador de error *a posteriori* residual, el cual resulta ser confiable y eficiente para el esquema de Galerkin propuesto. Este capítulo está constituido por la siguiente publicación:

[73] Gabriel N. Gatica, Luis F. Gatica and Filánder A. Sequeira, *Analysis of an augmented pseudostress-based mixed formulation for a nonlinear Brinkman model of porous media flow.* **Computer Methods in Applied Mechanics and Engineering**, vol. 289, 1, pp. 104–130, (2015).

En el **Capítulo 3** se introduce y se analiza el método de Galerkin discontinuo hibridizado para la resolución numérica de una clase de modelos no lineales de Stokes, provenientes de fluidos cuasi-Newtonianos. Similar a artículos previos enfocados a la aplicación de métodos de elementos finitos mixtos para estos modelos no lineales (ver [23, 76, 54]), se utiliza primero la condición de incompresibilidad para eliminar la presión, y se establece el gradiente de la velocidad como una incógnita auxiliar. A continuación, se introduce una formulación equivalente del esquema HDG aumentado, la cual permite aplicar una versión no lineal de la teoría de Babuška-Brezzi, así como el teorema clásico del punto fijo de Banach, para garantizar la solubilidad única de nuestro esquema discreto. Las estimaciones de error *a priori* correspondientes son también derivadas a través de la formulación equivalente. Más aún, con el fin de mostrar que la implementación del esquema HDG no es complicada, en este capítulo también se discuten aspectos generales referentes a la implementación computacional del método HDG. Este capítulo está constituido por la siguiente publicación:

[89] Gabriel N. Gatica and Filánder A. Sequeira, *Analysis of an augmented HDG method for a class of quasi-Newtonian Stokes flows.* **Journal of Scientific Computing**, vol. 65, 3, pp. 1270–1308, (2015).

El análisis presentado en el **Capítulo 3** hace uso de una estrategia de punto fijo (la cual depende de la adecuada elección de un cierto parámetro), lo que provee de órdenes de convergencia óptimos sólo para dos de las seis incógnitas resultantes, mientras que los experimentos numéricos reportados, muestran órdenes superiores a lo previsto, apoyando así la conjetura de que las estimaciones de error *a priori* no son precisas. De acuerdo a esto, en el **Capítulo 4**, se mantienen las características principales de la formulación aumentada previamente mencionada, pero introduciendo ahora ligeras modificaciones en los subespacios de elementos finitos para el pseudo-esfuerzo y la velocidad, con el fin de mejorar significativamente nuestros análisis y resultados anteriores. En otras palabras, por un lado omitimos la utilización de cualquier argumento de punto fijo (y los parámetros relacionados) para establecer que el esquema discreto esta bien puesto, y por el otro lado, ahora demostramos que las aproximaciones convergen de manera óptima en todas las incógnitas. Más aún, se deriva un estimador de error *a posteriori* residual, confiable y eficiente para este problema; y se propone el algoritmo adaptativo asociado para la aproximación HDG no lineal. Este capítulo está constituido por la siguiente pre-publicación:

[91] Gabriel N. Gatica and Filánder A. Sequeira, *A priori and a posteriori error analyses of an augmented HDG method for a class of quasi-Newtonian Stokes flows.* Preprint 2015-32, Centro de Investigación en Ingeniería Matemática (CI^{2}MA), Universidad de Concepción, Chile, (2015).

En el **Capítulo 5** se considera un problema lineal de transmisión. Más precisamente, se introduce y se analiza un método HDG para la resolución numérica del acoplamiento de un fluido con un medio poroso. El modelo acoplado está determinado por las ecuaciones de Stokes y Darcy, respectivamente, y las condiciones de transmisión correspondientes están dadas por la conservación de masa, el balance de fuerzas normales y la ley de Beavers-Joseph-Saffman. Se considera una formulación completamente mixta, en la cual las principales incógnitas están dadas por el esfuerzo, la vorticidad, la velocidad y la traza de la velocidad, todas ellas en el fluido; junto con la velocidad, la presión y la traza de la presión en el medio poroso. Además, se enriquece el subespacio de dimensión finita del esfuerzo, con el fin de obtener aproximaciones con convergencia óptima para todas las incógnitas, así como aproximaciones superconvergentes para las variables de las trazas. Para hacer esto, se desarrollan las estimaciones de error *a priori* utilizando, como en árticulos previos, un análisis basado en proyecciones, el cual simplifica en gran medida dicho estudio. Este capítulo está constituido por la siguiente pre-publicación:

[90] Gabriel N. Gatica and Filánder A. Sequeira, *Analysis of the HDG method for the Stokes-Darcy coupling.* Preprint 2015-23, Centro de Investigación en Ingeniería Matemática (CI^{2}MA), Universidad de Concepción, Chile, (2015).

Finalmente, en el **Capítulo 6** se desea extender los resultados obtenidos en los capítulos previos al estado evolutivo. Sin embargo, para poder analizar estos problemas transitorios, se necesita primero considerar el caso estacionario. Luego de esto, la extensión es más natural y el problema principal consiste en probar la estabilidad en las aproximaciones numéricas. En las **Capítulos 1-5** se ha establecido el análisis de los problemas estacionarios. Lamentablemente, la demostración de la estabilidad no es una tarea fácil. En este sentido, la ecuación incompresible de Euler representa una ruta usual para iniciar a comprender ecuaciones no lineales que dependen del tiempo, cuya formulación natural viene dada en forma mixta. Así, el propósito de este capítulo es desarrollar y estudiar métodos conformes en

H(div) y de Galerkin discontinuo para la ecuación incompresible de Euler en dos y tres dimensiones, utilizando una formulación de velocidad-presión. Se prueban estimaciones de error para los métodos semi-discretos y para los completamente discretos, usando la aproximación temporal dada por Euler regresivo. También se analizan flujos centrales y *upwind*. Este capítulo está constituido por la siguiente pre-publicación:

[94] Johnny Guzmán, Filánder A. Sequeira and Chi-Wang Shu, *H(div) conforming and DG methods for incompressible Euler's equations.* Preprint 2015-19, Centro de Investigación en Ingeniería Matemática (CI^{2}MA), Universidad de Concepción, Chile, (2015).

En todos los seis capítulos, se proveen varios resultados numéricos que ilustran el buen comportamiento de los métodos propuestos. Además, que confirman las propiedades teóricas como órdenes de convergencia, así como la confiabilidad y la eficiencia de estimadores de error *a posteriori*. El conjunto de experimentos numéricos incluye ejemplos en dos y tres dimensiones, donde se proveen algunos de ellos no cubiertos completamente por la teoría. Adicionalmente, todos las implementaciones computacionales de los métodos fueron obtenidas usando códigos C^{++} y en el caso del **Capítulo 6**, también se requirió del programa MATLAB.

CHAPTER 1

A priori and a posteriori error analyses of a pseudostress-based mixed formulation for linear elasticity

1.1 Introduction

The introduction of further unknowns of physical interest, such as stresses, rotations, and tractions, and the need of locking-free numerical schemes when the corresponding Poisson ratio approaches $1/2$, have historically been the main reasons for the utilization of dual-mixed variational formulations and their associated mixed finite element methods to solve elasticity problems. The incompressible case can also be easily handled with this kind of formulations since the constants appearing in the stability and a priori error estimates do not depend on the unbounded Lamé parameter. Consequently, the derivation of appropriate finite element subspaces yielding corresponding well-posed Galerkin schemes has been extensively studied in the last three decades at least, and important early contributions with weakly imposed symmetry for the stress, which include the classical PEERS element and related approaches, were provided in [4], [121], and [122], to name a few. However, since the appearing of those first works, the main challenge in this direction has been the development of mixed finite element methods that incorporate the symmetry of the stress into the definition of the respective continuous and discrete spaces. In fact, the first stable mixed finite element methods for linear elasticity, with symmetric and weakly symmetric stresses, were derived, thanks to the finite element exterior calculus, about a decade ago (see, e.g. [8], [9], [7], [10]). In particular, the polynomial shape-functions provided in [10] yield the first stable elements for the symmetric stress-displacement approach in two dimensions. In this case, 24 degrees of freedom defining piecewise cubic polynomials for the stresses, and piecewise linear functions for the displacement, constitute the cheapest element. In turn, 162 degrees of freedom defining piecewise quartic stresses, and again piecewise linear displacements, form the lowest order element in 3D, which was introduced in [1]. Furthermore, stable elements with weak imposition of symmetric stresses have been derived in [8] and [7]. The corresponding element using the lowest polynomial degrees is determined by piecewise constants approximations for both the displacement and rotation, and piecewise linear functions for the stress. In addition, stable Stokes elements and interpolation operators keeping the reduced symmetry were employed in [16] to derive simpler proofs of the main results provided in [8] and [7].

On the other hand, an alternative way of dealing with dual-mixed variational formulations in continuum mechanics, without the need of imposing neither strong nor weak symmetry of the stresses, is given by the utilization of pseudostress-based approaches. In fact, this technique, which has become very popular, specially in fluid mechanics, has gained considerable attention in recent years due to its applicability to diverse linear as well as nonlinear problems. In particular, the velocity-pseudostress formulation of the Stokes equations was first studied in [25], and then reconsidered in [83], where further results, including the eventual incorporation of the pressure unknown and an associated *a posteriori* error analysis, were provided. In turn, augmented mixed finite element methods for pseudostress-based formulations of the stationary Stokes equations, which extend analogue results for linear elasticity problems (see [69], [70], [79]), were introduced and analyzed in [64]. Furthermore, the velocity-pressure-pseudostress formulation has also been applied to nonlinear Stokes problems. In particular, a new mixed finite element method for a class of models arising in quasi-Newtonian fluids, was introduced in [76]. The results in [76] were extended in [58] to a setting in reflexive Banach spaces, thus allowing other nonlinear models such as the Carreau law for viscoplastic flows. Moreover, the dual-mixed approach from [76] and [58] was reformulated in [98] by restricting the space for the velocity gradient to that of trace-free tensors. For related contributions dealing with pseudostress-based formulations in incompressible flows, we refer to [59], [81], and the references therein. In turn, the corresponding extension to the Navier-Stokes equations has been developed in [26] and [27]. More recently, a new dual-mixed method for the aforementioned problem, in which the main unknowns are given by the velocity, its gradient, and a modified nonlinear pseudostress tensor linking the usual stress and the convective term, has been proposed in [99]. The idea from [99] has been modified in [30] through the introduction of a nonlinear pseudostress tensor linking now the pseudostress (instead of the stress) and the convective term, which, together with the velocity, constitute the only unknowns. Lately, the approach from [30] has been further extended in [53] and [29], where new augmented mixed-primal formulations for the stationary Boussinesq problem and the Navier-Stokes equations with variable viscosity, respectively, have been proposed and analyzed.

In spite of the many aforedescribed works, it is quite surprising to realize that almost no contribution is available in the literature on the use of pseudostress-based formulations for the elasticity problem. Indeed, the search in MathScinet under the title words "*pseudostress*" and "*elasticity*" yields no results at all. Actually, up to the authors' knowledge, the only paper referring to this issue is [6], where a modified Hellinger-Reissner principle is employed to derive a new mixed variational formulation for the equations of linear elasticity. The resulting approach yields a pseudostress unknown defined in terms of the gradient of the displacement field, but depending also on a parameter to be chosen conveniently.

In the present paper we modify the approach from [6] by realizing that, under a suitable rewriting of the equilibrium equation, one can define a simpler pseudostress unknown in terms again of the gradient of the displacement field, but independent of any additional parameter. In addition, we introduce an element-by-element postprocessing formula for the symmetric stress, which yields an optimally convergent approximation of this unknown with respect to the broken $\mathbb{H}(\mathbf{div})$-norm. Moreover, a reliable and efficient residual-based *a posteriori* error estimator for the mixed finite element scheme is also derived. A very summarized version of the first part of this work is available in [74]. The rest of this paper is organized as follows. In Section 1.2 we describe the linear elasticity problem with non-homogeneous Dirichlet boundary conditions, derive its pseudostress-based dual-mixed formulation, and then show that it is well-posed. In Section 1.3 we introduce and analyze the associated mixed finite element method. In particular, we show that Raviart-Thomas spaces of order $k \geq 0$ for the pseudostress and piecewise polynomials of degree $\leq k$ for the displacement can be employed, which, in the 3D case, yields a global number of unknowns behaving approximately as only 9 times the number of tetrahedra of the triangulation when $k = 0$. Next, a reliable and efficient residual-based *a posteriori* error estimator is developed in Section 1.4. Finally, several numerical results showing the good performance of the mixed finite element method, confirming the reliability and efficiency of the estimator, and illustrating the expected behaviour of the associated adaptive algorithm, are reported in Section 1.5.

We end this section with some notations to be used below. Given $n \in \{2,3\}$, we denote $\mathrm{R}^{n\times n}$ the space of square matrices of order n with real entries, $\mathbb{I} := (\delta_{ij})$ is the identity matrix of $\mathrm{R}^{n\times n}$, and for any $\boldsymbol{\tau} := (\tau_{ij})$, $\boldsymbol{\zeta} := (\zeta_{ij}) \in \mathrm{R}^{n\times n}$, we write as usual

$$\boldsymbol{\tau}^{\mathtt{t}} := (\tau_{ji}), \qquad \mathrm{tr}(\boldsymbol{\tau}) := \sum_{i=1}^{n} \tau_{ii}, \qquad \boldsymbol{\tau}^{\mathtt{d}} := \boldsymbol{\tau} - \frac{1}{n}\,\mathrm{tr}(\boldsymbol{\tau})\,\mathbb{I}, \qquad \text{and} \qquad \boldsymbol{\tau} : \boldsymbol{\zeta} := \sum_{i,j=1}^{n} \tau_{ij}\zeta_{ij},$$

which corresponds, respectively, to the transpose, the trace, the deviator tensor of a tensor $\boldsymbol{\tau}$, and the tensorial product between $\boldsymbol{\tau}$ and $\boldsymbol{\zeta}$. In turn, in what follows we utilize standard simplified terminology for Sobolev spaces and norms. In particular, if $\mathcal{O} \subseteq \mathrm{R}^n$ is a domain, $\mathcal{S} \subseteq \mathrm{R}^n$ is an open or closed Lipschitz curve if $n = 2$ (resp. surface if $n = 3$), and $r \in \mathrm{R}$, we set

$$\mathbf{H}^r(\mathcal{O}) := [H^r(\mathcal{O})]^n\,, \quad \mathbb{H}^r(\mathcal{O}) := [H^r(\mathcal{O})]^{n\times n}\,, \quad \text{and} \quad \mathbf{H}^r(\mathcal{S}) := [H^r(\mathcal{S})]^n\,.$$

However, when $r = 0$ we usually write $\mathbf{L}^2(\mathcal{O})$, $\mathbb{L}^2(\mathcal{O})$, and $\mathbf{L}^2(\mathcal{S})$ instead of $\mathbf{H}^0(\mathcal{O})$, $\mathbb{H}^0(\mathcal{O})$, and $\mathbf{H}^0(\mathcal{S})$, respectively. The corresponding norms are denoted by $\|\cdot\|_{r,\mathcal{O}}$ (for $H^r(\mathcal{O})$, $\mathbf{H}^r(\mathcal{O})$, and $\mathbb{H}^r(\mathcal{O})$) and $\|\cdot\|_{r,\mathcal{S}}$ (for $H^r(\mathcal{S})$ and $\mathbf{H}^r(\mathcal{S})$). In general, given any Hilbert space H, we use $\mathbf{H}$ and $\mathbb{H}$ to denote H^n and $H^{n\times n}$, respectively. In addition, $\langle\cdot,\cdot\rangle_{\mathcal{S}}$ stands for the usual duality pairing between $H^{-1/2}(\mathcal{S})$ and $H^{1/2}(\mathcal{S})$, and $\mathbf{H}^{-1/2}(\mathcal{S})$ and $\mathbf{H}^{1/2}(\mathcal{S})$. Furthermore, with div denoting the usual divergence operator, the Hilbert space

$$\mathbf{H}(\mathrm{div};\mathcal{O}) := \left\{\mathbf{w} \in \mathbf{L}^2(\mathcal{O}) \ : \ \mathrm{div}(\mathbf{w}) \in L^2(\mathcal{O})\right\},$$

is standard in the realm of mixed problems (see [19], [92]). The space of matrix valued functions whose rows belong to $\mathbf{H}(\mathrm{div};\mathcal{O})$ will be denoted $\mathbb{H}(\mathbf{div};\mathcal{O})$, where $\mathbf{div}$ stands for the action of div along each row of a tensor. The Hilbert norms of $\mathbf{H}(\mathrm{div};\mathcal{O})$ and $\mathbb{H}(\mathbf{div};\mathcal{O})$ are denoted by $\|\cdot\|_{\mathrm{div},\mathcal{O}}$ and $\|\cdot\|_{\mathbf{div},\mathcal{O}}$, respectively. Note that if $\boldsymbol{\tau} \in \mathbb{H}(\mathbf{div};\mathcal{O})$, then $\mathbf{div}(\boldsymbol{\tau}) \in \mathbf{L}^2(\mathcal{O})$ and also $\boldsymbol{\tau}\mathbf{n} \in \mathbf{H}^{-1/2}(\partial\mathcal{O})$, where $\mathbf{n}$ denotes the outward unit vector normal to the boundary $\partial\mathcal{O}$. Finally, we employ $\mathbf{0}$ to denote a generic null vector (including the null functional and operator), and use C and c, with or without subscripts, bars, tildes or hats, to denote generic constants independent of the discretization parameters, which may take different values at different places.

1.2 The pseudostress-displacement formulation

1.2.1 The elasticity problem

Let Ω be a bounded and simply connected polyhedral domain in R^n, $n \in \{2,3\}$, and $\Gamma := \partial\Omega$ the boundary of Ω. Our goal is to determine the displacement $\mathbf{u}$ and stress tensor $\boldsymbol{\sigma}$ of a linear elastic material occupying the region Ω. In other words, given a volume force $\mathbf{f} \in \mathbf{L}^2(\Omega)$ and a Dirichlet datum $\mathbf{g} \in \mathbf{H}^{1/2}(\Gamma)$, we seek a symmetric tensor field $\boldsymbol{\sigma}$ and a vector field $\mathbf{u}$ such that

$$\begin{aligned} \boldsymbol{\sigma} &= 2\mu\,\mathbf{e}(\mathbf{u}) + \lambda\,\mathrm{tr}(\mathbf{e}(\mathbf{u}))\,\mathbb{I} \quad \text{in} \quad \Omega\,, \\ \mathbf{div}(\boldsymbol{\sigma}) &= -\mathbf{f} \quad \text{in} \quad \Omega\,, \quad \text{and} \quad \mathbf{u} = \mathbf{g} \quad \text{on} \quad \Gamma\,, \end{aligned} \tag{1.1}$$

where $\mathbf{e}(\mathbf{u}) := \frac{1}{2}(\nabla\,\mathbf{u} + (\nabla\,\mathbf{u})^{\mathtt{t}})$ is the strain tensor of small deformations, and λ, $\mu > 0$ denote the corresponding Lamé constants. Next, from

$$\mathbf{div}(\boldsymbol{\sigma}) \;=\; 2\mu\,\mathbf{div}(\mathbf{e}(\mathbf{u})) + \lambda\,\nabla\mathrm{div}(\mathbf{u})\,, \quad \text{and} \quad \mathbf{div}(\mathbf{e}(\mathbf{u})) \;=\; \frac{1}{2}\,\Delta\mathbf{u} + \frac{1}{2}\,\nabla\mathrm{div}(\mathbf{u})\,,$$

we deduce that

$$\mathbf{div}(\boldsymbol{\sigma}) \;=\; \mu\,\Delta\mathbf{u} + (\lambda+\mu)\,\nabla\mathrm{div}(\mathbf{u})\,.$$

Consequently, the formulation in displacement of (1.1) reduces to: Find $\mathbf{u}$ such that

$$\mu\,\Delta\mathbf{u} \;+\; (\lambda+\mu)\,\nabla\mathrm{div}(\mathbf{u}) \;=\; -\mathbf{f} \quad \text{in} \quad \Omega\,, \qquad \text{and} \qquad \mathbf{u} \;=\; \mathbf{g} \quad \text{on} \quad \Gamma\,.$$

Now, we define the non-symmetric pseudostress as the tensor

$$\boldsymbol{\rho} \;:=\; \mu\,\nabla\mathbf{u} \;+\; (\lambda+\mu)\,\mathrm{div}(\mathbf{u})\,\mathbb{I}$$

or (since $\mathrm{div}(\mathbf{u}) = \mathrm{tr}(\nabla\mathbf{u})$), equivalently

$$\boldsymbol{\rho} \;:=\; \mu\,\nabla\mathbf{u} \;+\; (\lambda+\mu)\,\mathrm{tr}(\nabla\mathbf{u})\,\mathbb{I}\,.$$

In this way, using that $\mathbf{div}(\boldsymbol{\rho}) = \mathbf{div}(\boldsymbol{\sigma})$, we can rewrite (1.1) as: Find the pseudostress $\boldsymbol{\rho}$ and the displacement $\mathbf{u}$ such that

$$\begin{aligned} \boldsymbol{\rho} \;&=\; \mu\,\nabla\mathbf{u} \;+\; (\lambda+\mu)\,\mathrm{tr}(\nabla\mathbf{u})\,\mathbb{I} \quad \text{in} \quad \Omega\,, \\ \mathbf{div}(\boldsymbol{\rho}) \;&=\; -\mathbf{f} \quad \text{in} \quad \Omega\,, \quad \text{and} \quad \mathbf{u} \;=\; \mathbf{g} \quad \text{on} \quad \Gamma\,. \end{aligned} \tag{1.2}$$

Furthermore, we find from the first equation of (1.2) that

$$\mathrm{tr}(\nabla\mathbf{u}) \;=\; \frac{1}{n\,\lambda + (n+1)\,\mu}\,\mathrm{tr}(\boldsymbol{\rho})\,, \tag{1.3}$$

which implies that the constitutive equation of (1.2) can also be established as

$$\frac{1}{\mu}\left\{\boldsymbol{\rho} - \frac{\lambda+\mu}{n\,\lambda + (n+1)\,\mu}\,\mathrm{tr}(\boldsymbol{\rho})\,\mathbb{I}\right\} \;=\; \nabla\,\mathbf{u}\,.$$

Hence, the new formulation of the problem (1.1) is given by: Find $(\boldsymbol{\rho}, \mathbf{u})$ such that

$$\begin{aligned} \frac{1}{\mu}\left\{\boldsymbol{\rho} - \frac{\lambda+\mu}{n\,\lambda + (n+1)\,\mu}\,\mathrm{tr}(\boldsymbol{\rho})\,\mathbb{I}\right\} \;&=\; \nabla\,\mathbf{u} \quad \text{in} \quad \Omega\,, \\ \mathbf{div}(\boldsymbol{\rho}) \;&=\; -\mathbf{f} \quad \text{in} \quad \Omega\,, \quad \text{and} \quad \mathbf{u} \;=\; \mathbf{g} \quad \text{on} \quad \Gamma\,. \end{aligned} \tag{1.4}$$

1.2.2 The dual-mixed variational formulation

Multiplying the first equation in (1.4) by $\boldsymbol{\tau} \in \mathbb{H}(\mathbf{div};\Omega)$, integrating by parts in Ω, and using the Dirichlet boundary condition, we obtain

$$\frac{1}{\mu}\int_\Omega \boldsymbol{\rho} : \boldsymbol{\tau} - \frac{\lambda+\mu}{\mu(n\,\lambda + (n+1)\,\mu)}\int_\Omega \mathrm{tr}(\boldsymbol{\rho})\,\mathrm{tr}(\boldsymbol{\tau}) \;+\; \int_\Omega \mathbf{u}\cdot\mathbf{div}(\boldsymbol{\tau}) \;=\; \langle \boldsymbol{\tau}\mathbf{n}\,, \mathbf{g}\rangle_\Gamma\,,$$

which together with the equilibrium equation (second equation in (1.4)) tested against $\mathbf{v} \in \mathbf{L}^2(\Omega)$, yields the variational formulation of (1.4) given by: Find $(\boldsymbol{\rho}, \mathbf{u}) \in \mathbb{H} \times \mathbf{Q}$ such that

$$\begin{aligned} a(\boldsymbol{\rho}, \boldsymbol{\tau}) \;+\; b(\boldsymbol{\tau}, \mathbf{u}) \;&=\; F(\boldsymbol{\tau}) \qquad \forall\, \boldsymbol{\tau} \in \mathbb{H}\,, \\ b(\boldsymbol{\rho}, \mathbf{v}) \;&=\; G(\mathbf{v}) \qquad \forall\, \mathbf{v} \in \mathbf{Q}\,, \end{aligned} \tag{1.5}$$

where $\mathbb{H} := \mathbb{H}(\mathbf{div}; \Omega)$, $\mathbf{Q} := \mathbf{L}^2(\Omega)$, the bilinear forms $a : \mathbb{H} \times \mathbb{H} \to \mathrm{R}$ and $b : \mathbb{H} \times \mathbf{Q} \to \mathrm{R}$ are defined by

$$a(\boldsymbol{\xi}, \boldsymbol{\tau}) \;:=\; \frac{1}{\mu} \int_\Omega \boldsymbol{\xi} : \boldsymbol{\tau} - \frac{\lambda + \mu}{\mu(n\,\lambda + (n+1)\,\mu)} \int_\Omega \mathrm{tr}(\boldsymbol{\xi})\,\mathrm{tr}(\boldsymbol{\tau}) \quad \forall\, \boldsymbol{\xi}, \boldsymbol{\tau} \,\in\, \mathbb{H}\,, \tag{1.6}$$

$$b(\boldsymbol{\tau}, \mathbf{v}) \;:=\; \int_\Omega \mathbf{v} \cdot \mathbf{div}(\boldsymbol{\tau}) \quad \forall\, \boldsymbol{\tau} \,\in\, \mathbb{H}\,, \quad \forall\, \mathbf{v} \,\in\, \mathbf{Q}\,, \tag{1.7}$$

and the functionals $F \in \mathbb{H}'$ and $G \in \mathbf{Q}'$ are given by

$$F(\boldsymbol{\tau}) := \langle \boldsymbol{\tau}\mathbf{n} \,, \mathbf{g} \rangle_\Gamma \quad \text{ and } \quad G(\mathbf{v}) := -\int_\Omega \mathbf{f} \cdot \mathbf{v}.$$

We noted from (1.6) that

$$a(\mathbb{I}, \boldsymbol{\tau}) \;=\; \frac{1}{(n\lambda + (n+1)\mu)} \int_\Omega \mathrm{tr}(\boldsymbol{\tau}) \qquad \forall\, \boldsymbol{\tau} \in \mathbb{H}\,, \tag{1.8}$$

and from (1.7) that

$$b(\mathbb{I}, \mathbf{v}) \;=\; 0 \qquad \forall\, \mathbf{v} \in \mathbf{Q}\,. \tag{1.9}$$

Moreover, replacing $\boldsymbol{\xi} = \boldsymbol{\xi}^{\mathrm{d}} + \dfrac{1}{n}\,\mathrm{tr}(\boldsymbol{\xi})\,\mathbb{I}$ in (1.6), and using that $\boldsymbol{\xi}^{\mathrm{d}} : \boldsymbol{\tau} = \boldsymbol{\xi}^{\mathrm{d}} : \boldsymbol{\tau}^{\mathrm{d}}$, and that $\mathrm{tr}(\boldsymbol{\xi}^{\mathrm{d}}) = 0$, for all $\boldsymbol{\xi} \in \mathbb{L}^2(\Omega)$, we arrive at the following equivalent expression for the bilinear form a

$$a(\boldsymbol{\xi}, \boldsymbol{\tau}) \;=\; \frac{1}{\mu} \int_\Omega \boldsymbol{\xi}^{\mathrm{d}} : \boldsymbol{\tau}^{\mathrm{d}} + \frac{1}{n(n\,\lambda + (n+1)\,\mu)} \int_\Omega \mathrm{tr}(\boldsymbol{\xi})\,\mathrm{tr}(\boldsymbol{\tau}) \qquad \forall\, \boldsymbol{\xi}, \boldsymbol{\tau} \in \mathbb{H}\,. \tag{1.10}$$

The convenience of writing a in the form (1.10) will become clear later on when we analyze the solvability of (1.5).

We now define $\mathbb{H}_0 := \left\{ \boldsymbol{\tau} \in \mathbb{H}(\mathbf{div}; \Omega) \;:\; \int_\Omega \mathrm{tr}(\boldsymbol{\tau}) = 0 \right\}$ and note that $\mathbb{H} = \mathbb{H}_0 \oplus \mathrm{R}\mathbb{I}$, that is for any $\boldsymbol{\tau} \in \mathbb{H}$ there exist unique $\boldsymbol{\tau}_0 \in \mathbb{H}_0$ and $d := \dfrac{1}{n|\Omega|} \displaystyle\int_\Omega \mathrm{tr}(\boldsymbol{\tau}) \in \mathrm{R}$, where $|\Omega|$ denotes the measure of Ω, such that $\boldsymbol{\tau} = \boldsymbol{\tau}_0 + d\,\mathbb{I}$. In particular, taking $\boldsymbol{\tau} = \mathbb{I}$ in the first equation of (1.5), we deduce that

$$\int_\Omega \mathrm{tr}(\boldsymbol{\rho}) \;=\; (n\,\lambda + (n+1)\,\mu) \int_\Gamma \mathbf{g} \cdot \mathbf{n}\,,$$

which yields $\boldsymbol{\rho} = \boldsymbol{\rho}_0 + c\,\mathbb{I}$, with $\boldsymbol{\rho}_0 \in \mathbb{H}_0$ and the constant c given explicitly by

$$c \;:=\; \frac{(n\lambda + (n+1)\mu)}{n\,|\Omega|} \int_\Gamma \mathbf{g} \cdot \mathbf{n}\,. \tag{1.11}$$

In this way, replacing $\boldsymbol{\rho}$ by the expression $\boldsymbol{\rho}_0 + c\,\mathbb{I}$ in (1.5), with the bilinear form a given by (1.10), applying the identities (1.8) and (1.9), using that $\boldsymbol{\rho}^{\mathrm{d}} = \boldsymbol{\rho}_0^{\mathrm{d}}$ and $\mathbf{div}(\boldsymbol{\rho}) = \mathbf{div}(\boldsymbol{\rho}_0)$, and denoting from now on the remaining unknown $\boldsymbol{\rho}_0 \in \mathbb{H}_0$ simply by $\boldsymbol{\rho}$, we find that the dual-mixed variational formulation (1.5) is equivalent to the following saddle point problem: Find $(\boldsymbol{\rho}, \mathbf{u}) \in \mathbb{H}_0 \times \mathbf{Q}$ such that

$$\begin{aligned} a(\boldsymbol{\rho}, \boldsymbol{\tau}) \;+\; b(\boldsymbol{\tau}, \mathbf{u}) \;&=\; F(\boldsymbol{\tau}) \qquad \forall\, \boldsymbol{\tau} \in \mathbb{H}_0\,, \\ b(\boldsymbol{\rho}, \mathbf{v}) \;&=\; G(\mathbf{v}) \qquad \forall\, \mathbf{v} \in \mathbf{Q}\,. \end{aligned} \tag{1.12}$$

Lemma 1.1. *Problems* (1.5) *and* (1.12) *are equivalent in the following sense:*

i) If $(\boldsymbol{\rho}, \mathbf{u}) \in \mathbb{H} \times \mathbf{Q}$ *is a solution of* (1.5)*, and* $\boldsymbol{\rho} = \boldsymbol{\rho}_0 + c\,\mathbb{I}$*, with* $\boldsymbol{\rho}_0 \in \mathbb{H}_0$ *and* $c \in R$*, then* $(\boldsymbol{\rho}_0, \mathbf{u}) \in \mathbb{H}_0 \times \mathbf{Q}$ *is a solution of* (1.12)*.*

ii) If $(\boldsymbol{\rho}_0, \mathbf{u}) \in \mathbb{H}_0 \times \mathbf{Q}$ *is a solution of* (1.12)*, and* $\boldsymbol{\rho} := \boldsymbol{\rho}_0 + c\,\mathbb{I}$*, with* c *given by* (1.11)*, then* $(\boldsymbol{\rho}, \mathbf{u}) \in \mathbb{H} \times \mathbf{Q}$ *is a solution of* (1.5)*.*

Proof. Let $(\boldsymbol{\rho}, \mathbf{u}) \in \mathbb{H} \times \mathbf{Q}$ a solution of (1.5), such that $\boldsymbol{\rho} = \boldsymbol{\rho}_0 + c\,\mathbb{I}$, with $\boldsymbol{\rho}_0 \in \mathbb{H}_0$ and $c \in \mathrm{R}$. Then from the first equation of (1.5) we have

$$a(\boldsymbol{\rho}_0, \boldsymbol{\tau}) \;+\; b(\boldsymbol{\tau}, \mathbf{u}) \;=\; F(\boldsymbol{\tau}) \;-\; c\,a(\mathbb{I}, \boldsymbol{\tau}) \qquad \forall\, \boldsymbol{\tau} \in \mathbb{H}\,,$$

which using (1.8), yields

$$a(\boldsymbol{\rho}_0, \boldsymbol{\tau}) \;+\; b(\boldsymbol{\tau}, \mathbf{u}) \;=\; F(\boldsymbol{\tau}) \qquad \forall\, \boldsymbol{\tau} \in \mathbb{H}_0\,.$$

In turn, from the second equation of (1.5) we can write

$$b(\boldsymbol{\rho}_0, \mathbf{v}) \;+\; c\,b(\mathbb{I}, \mathbf{v}) \;=\; G(\mathbf{v}) \qquad \forall\, \mathbf{v} \,\in\, \mathbf{Q}\,,$$

which according to (1.9), gives

$$b(\boldsymbol{\rho}_0, \mathbf{v}) \;=\; G(\mathbf{v}) \qquad \forall\, \mathbf{v} \,\in\, \mathbf{Q}\,,$$

and hence $(\boldsymbol{\rho}_0, \mathbf{u}) \in \mathbb{H}_0 \times \mathbf{Q}$ is a solution of (1.12). Conversely, let $(\boldsymbol{\rho}_0, \mathbf{u}) \in \mathbb{H}_0 \times \mathbf{Q}$ be a solution of (1.12), and set $\boldsymbol{\rho} := \boldsymbol{\rho}_0 + c\,\mathbb{I}$, with c given by (1.11). Then, given $\boldsymbol{\tau} = \boldsymbol{\tau}_0 + d\,\mathbb{I} \in \mathbb{H}$, with $\boldsymbol{\tau}_0 \in \mathbb{H}_0$ and $d \in \mathrm{R}$, we deduce

$$\begin{aligned} a(\boldsymbol{\rho}, \boldsymbol{\tau}) \;+\; b(\boldsymbol{\tau}, \mathbf{u}) \;&=\; a(\boldsymbol{\rho}_0, \boldsymbol{\tau}_0) \,+\, b(\boldsymbol{\tau}_0, \mathbf{u}) \,+\, d\,a(\mathbb{I}, c\,\mathbb{I}) \;=\; F(\boldsymbol{\tau}_0) \,+\, d \int_\Gamma \mathbf{g}\cdot\mathbf{n} \\ &=\; F(\boldsymbol{\tau}_0) \,+\, d\,F(\mathbb{I}) \;=\; F(\boldsymbol{\tau})\,. \end{aligned}$$

On the other hand, using (1.9) we deduce

$$b(\boldsymbol{\rho}, \mathbf{v}) \;=\; b(\boldsymbol{\rho}_0, \mathbf{v}) \;+\; c\,b(\mathbb{I}, \mathbf{v}) \;=\; G(\mathbf{v}) \qquad \forall\, \mathbf{v} \,\in\, \mathbf{Q}\,,$$

which shows that $(\boldsymbol{\rho}, \mathbf{u}) \in \mathbb{H} \times \mathbf{Q}$ is a solution of (1.5). □

Furthermore, according to the new meaning of $\boldsymbol{\rho}$, we deduce from (1.4) and (1.11) that the constitutive equation in (1.4) now becomes

$$\frac{1}{\mu}\left\{\boldsymbol{\rho} - \frac{\lambda+\mu}{n\,\lambda + (n+1)\,\mu}\,\mathrm{tr}(\boldsymbol{\rho})\,\mathbb{I}\right\} \;+\; \left\{\frac{1}{n\,|\Omega|}\int_\Gamma \mathbf{g}\cdot\mathbf{n}\right\}\mathbb{I} \;=\; \nabla\,\mathbf{u} \quad \text{in} \quad \Omega\,,$$

whereas the equilibrium equation remains the same, that is

$$\mathbf{div}(\boldsymbol{\rho}) \;=\; -\mathbf{f} \quad \text{in} \quad \Omega\,. \tag{1.13}$$

At this point we remark that the stress $\boldsymbol{\sigma}$ can be expressed in terms of the pseudostress $\boldsymbol{\rho}$ and displacement $\mathbf{u}$ as

$$\boldsymbol{\sigma} \;=\; \boldsymbol{\rho} \;+\; \boldsymbol{\rho}^{\mathrm{t}} \;-\; (\lambda + 2\mu)\,\mathrm{tr}(\nabla\mathbf{u})\,\mathbb{I}\,,$$

whence using the identity (1.3) we can calculate the symmetric stress tensor field in terms of the pseudostress $\boldsymbol{\rho}$ by

$$\boldsymbol{\sigma} \,=\, \boldsymbol{\rho} \,+\, \boldsymbol{\rho}^{\mathrm{t}} \,-\, \left\{ \frac{\lambda + 2\mu}{n\lambda + (n+1)\mu} \right\} \mathrm{tr}(\boldsymbol{\rho})\, \mathbb{I}\,. \tag{1.14}$$

In addition, other physical quantities of interest such as the strain tensor of small deformations $\mathbf{e}(\mathbf{u})$ and the rotation $\boldsymbol{\gamma} := \frac{1}{2}(\nabla\, \mathbf{u} - (\nabla\, \mathbf{u})^{\mathrm{t}})$, can be computed in terms of the pseudostress $\boldsymbol{\rho}$ by

$$\mathbf{e}(\mathbf{u}) \,=\, \frac{1}{2\,\mu} \left\{ \boldsymbol{\rho} \,+\, \boldsymbol{\rho}^{\mathrm{t}} \,-\, \frac{2(\lambda + \mu)}{n\lambda + (n+1)\mu} \mathrm{tr}(\boldsymbol{\rho})\, \mathbb{I} \right\}\,, \quad \text{and} \quad \boldsymbol{\gamma} \,=\, \frac{1}{2\mu}(\boldsymbol{\rho} \,-\, \boldsymbol{\rho}^{\mathrm{t}})\,,$$

respectively. On the other hand, in terms of the $\mathbb{H}_0$-component of pseudostress, the stress is given by

$$\boldsymbol{\sigma} \,=\, \boldsymbol{\rho} \,+\, \boldsymbol{\rho}^{\mathrm{t}} \,-\, \left(\frac{\lambda + 2\mu}{n\lambda + (n+1)\mu} \mathrm{tr}(\boldsymbol{\rho}) - \frac{n\lambda + 2\mu}{n|\Omega|} \int_\Gamma \mathbf{g} \cdot \mathbf{n} \right) \mathbb{I}\,. \tag{1.15}$$

1.2.3 Analysis of the dual-mixed formulation

In this section we show the well-posedness of (1.12) by using the classical Babuška-Brezzi theory (see, e.g., [19, 71]). The following lemma will be required.

Lemma 1.2. *There exists $c_1 > 0$, depending only on Ω, such that*

$$c_1 \|\boldsymbol{\tau}\|_{0,\Omega}^2 \,\leq\, \|\boldsymbol{\tau}^{\mathrm{d}}\|_{0,\Omega}^2 \,+\, \|\mathbf{div}(\boldsymbol{\tau})\|_{0,\Omega}^2 \quad \forall\, \boldsymbol{\tau} \,\in\, \mathbb{H}_0. \tag{1.16}$$

Proof. It is analogous to the corresponding proof for the two-dimensional case (see [5, Lemma 3.1] or [19, Proposition 3.1 of Chapter IV]). □

We note that, the inequality (1.16), being valid only in $\mathbb{H}_0$, explains the need of replacing (1.5) by the variational formulation (1.12). Thus, the following theorem provides the well-posedness of (1.12).

Theorem 1.1. *Assume that $\mathbf{f} \in \mathbf{L}^2(\Omega)$ and $\mathbf{g} \in \mathbf{H}^{1/2}(\Gamma)$. Then, there exists a unique solution $(\boldsymbol{\rho}, \mathbf{u}) \in \mathbb{H}_0 \times \mathbf{Q}$ to (1.12). In addition, there exists $c_2 > 0$, independent of λ, such that*

$$\|\boldsymbol{\rho}\|_{\mathbf{div},\Omega} \,+\, \|\mathbf{u}\|_{0,\Omega} \,\leq\, c_2 \left\{ \|\mathbf{f}\|_{0,\Omega} \,+\, \|\mathbf{g}\|_{1/2,\Gamma} \right\}.$$

Proof. It suffices to check that the bilinear forms a and b satisfy the hypotheses of the Babuška-Brezzi theory. The proof is similar to that of [83, Theorem 2.1]. For sake of completeness we now provide the details. We first observe from (1.6) and (1.7) that a and b are bounded with $\|a\| = \frac{2}{\mu}$ and $\|b\| = 1$, respectively. In fact, applying the Cauchy-Schwarz inequality and using that $\dfrac{\lambda + \mu}{n\lambda + (n+1)\mu} < \dfrac{1}{n}$, we find from definition of bilinear form a (cf. (1.6)) that

$$\begin{aligned} |a(\boldsymbol{\xi}, \boldsymbol{\tau})| \;&=\; \left| \frac{1}{\mu} \int_\Omega \boldsymbol{\xi} : \boldsymbol{\tau} - \frac{\lambda + \mu}{\mu\,(n\,\lambda + (n+1)\,\mu)} \int_\Omega \mathrm{tr}(\boldsymbol{\xi})\, \mathrm{tr}(\boldsymbol{\tau}) \right| \\ &\leq\; \frac{1}{\mu} \|\boldsymbol{\xi}\|_{0,\Omega} \|\boldsymbol{\tau}\|_{0,\Omega} + \frac{1}{n\mu} \|\mathrm{tr}(\boldsymbol{\xi})\|_{0,\Omega} \|\mathrm{tr}(\boldsymbol{\tau})\|_{0,\Omega} \\ &\leq\; \frac{2}{\mu} \|\boldsymbol{\xi}\|_{0,\Omega} \|\boldsymbol{\tau}\|_{0,\Omega} \;\leq\; \frac{2}{\mu} \|\boldsymbol{\xi}\|_{\mathbf{div},\Omega} \|\boldsymbol{\tau}\|_{\mathbf{div},\Omega} \quad \forall\, \boldsymbol{\xi}, \boldsymbol{\tau} \in \mathbb{H}_0. \end{aligned}$$

Analogously, applying the Cauchy-Schwarz inequality, we obtain from definition of bilinear form b (cf. (1.7)) that

$$|b(\boldsymbol{\tau}, \mathbf{v})| \;=\; \left| \int_{\Omega} \mathbf{v} \cdot \mathbf{div}(\boldsymbol{\tau}) \right| \;\leq\; \|\mathbf{div}(\boldsymbol{\tau})\|_{0,\Omega} \, \|\mathbf{v}\|_{0,\Omega} \;\leq\; \|\boldsymbol{\tau}\|_{\mathbf{div},\Omega} \, \|\mathbf{v}\|_{0,\Omega} \quad \forall\, \boldsymbol{\tau} \in \mathbb{H}_0, \quad \forall\, \mathbf{v} \in \mathbf{Q}\,.$$

On the other hand, we deduce that $\mathbb{V} := \{\boldsymbol{\tau} \in \mathbb{H}_0 : \mathbf{div}(\boldsymbol{\tau}) = \mathbf{0}\}$ is the null space of b, whence (1.10) and Lemma 1.2 imply

$$a(\boldsymbol{\tau}, \boldsymbol{\tau}) \;\geq\; \frac{1}{\mu} \, \|\boldsymbol{\tau}^{\mathtt{d}}\|_{0,\Omega}^2 \;\geq\; \frac{c_1}{\mu} \, \|\boldsymbol{\tau}\|_{0,\Omega}^2 \;=\; \frac{c_1}{\mu} \, \|\boldsymbol{\tau}\|_{\mathbf{div},\Omega}^2 \qquad \forall\, \boldsymbol{\tau} \in \mathbb{V}\,. \tag{1.17}$$

This shows that a is $\mathbb{V}$-elliptic, with constant $\alpha := \frac{c_1}{\mu}$ independent of the Lamé constant λ. Finally, given $\mathbf{v} \in \mathbf{Q}$, $\mathbf{v} \neq \mathbf{0}$, we let $\mathbf{z} \in \mathbf{H}_0^1(\Omega)$ be the unique weak solution of the auxiliary problem

$$\Delta\, \mathbf{z} \;=\; \mathbf{v} \quad \text{in} \quad \Omega\,, \qquad \mathbf{z} \;=\; \mathbf{0} \quad \text{on} \quad \Gamma\,.$$

Then, we let $\hat{\boldsymbol{\tau}}$ be the $\mathbb{H}_0$-component of $\nabla \mathbf{z}$, which implies $\mathbf{div}(\hat{\boldsymbol{\tau}}) = \mathbf{div}(\nabla \mathbf{z}) = \mathbf{v}$ in Ω. This shows that the bounded linear operator $\mathbf{div} : \mathbb{H}_0 \to \mathbf{Q}$ is surjective, which completes the proof. $\square$

1.3 The mixed finite element method

In this section, we define explicit finite element subspaces $\mathbb{H}_{0,h}$ of $\mathbb{H}_0(\mathbf{div};\Omega)$, and $\mathbf{Q}_h$ of $\mathbf{L}^2(\Omega)$ such that the corresponding mixed finite element scheme associated with the continuous formulation (1.12) is well-posed and stable.

1.3.1 Preliminaries

Let $\{\mathcal{T}_h\}_{h>0}$ be a regular family of triangulations of the region $\bar{\Omega} \subset \mathrm{R}^n$ by tetrahedrons T of diameter h_T such that $\bar{\Omega} = \cup\{T : T \in \mathcal{T}_h\}$, and define $h := \max\{h_T : T \in \mathcal{T}_h\}$. The faces of the tetrahedrons of $\mathcal{T}_h$ are denoted by e and their corresponding diameters by h_e. Certainly, we are assuming here that $n = 3$. In the case $n = 2$ we just need to replace tetrahedrons by triangles and faces by edges in what follows. Now, given an integer $\ell \geq 0$ and a subset U of R^n, we denote by $\mathrm{P}_\ell(U)$ the space of polynomials defined in U of total degree at most ℓ. According to the notational convention given in the introduction, we denote $\mathbf{P}_\ell(U) := [\mathrm{P}_\ell(U)]^n$ and $\mathbb{P}_\ell(U) := [\mathrm{P}_\ell(U)]^{n\times n}$. Then, for each integer $k \geq 0$ and for each $T \in \mathcal{T}_h$, we define the local Raviart-Thomas space of order k (see, e.g. [19])

$$\mathbf{RT}_k(T) \;:=\; \mathbf{P}_k(T) \;\oplus\; \mathrm{P}_k(T)\,\mathbf{x}$$

where $\mathbf{x} = \begin{pmatrix} x_1 \\ \vdots \\ x_n \end{pmatrix}$ is a generic vector of R^n, and let $\mathbb{RT}_k(\mathcal{T}_h)$ be the corresponding global space, that is,

$$\mathbb{RT}_k(\mathcal{T}_h) \;:=\; \Big\{ \boldsymbol{\tau} \in \mathbb{H}(\mathbf{div};\Omega) \;:\; (\tau_{i1}, \dots, \tau_{in})^{\mathtt{t}}|_T \;\in\; \mathbf{RT}_k(T) \quad \forall\, i \in \{1,\dots,n\}, \quad \forall\, T \in \mathcal{T}_h \Big\}\,.$$

We also let $\mathrm{P}_k(\mathcal{T}_h)$ be the global space of piecewise polynomials of degree $\leq k$, that is

$$\mathrm{P}_k(\mathcal{T}_h) \;:=\; \Big\{ v \in L^2(\Omega) \;:\; v|_T \in \mathrm{P}_k(T) \quad \forall\, T \in \mathcal{T}_h \Big\}\,. \tag{1.18}$$

We now introduce the following finite element subspaces of $\mathbb{H}_0$, and $\mathbf{Q}$, respectively,

$$\begin{aligned}\mathbb{H}_{0,h} &:= \mathbb{RT}_k(\mathcal{T}_h)\cap\mathbb{H}_0(\mathbf{div};\Omega) = \left\{\boldsymbol{\tau}_h \in \mathbb{RT}_k(\mathcal{T}_h) : \int_\Omega \operatorname{tr}(\boldsymbol{\tau}_h) = 0\right\},\\ \mathbf{Q}_h &:= \mathbf{P}_k(\mathcal{T}_h).\end{aligned} \tag{1.19}$$

Then, the mixed finite element scheme associated with (1.12) reads : Find $(\boldsymbol{\rho}_h, \mathbf{u}_h) \in \mathbb{H}_{0,h}\times\mathbf{Q}_h$, such that

$$\begin{aligned} a(\boldsymbol{\rho}_h,\boldsymbol{\tau}_h) + b(\boldsymbol{\tau}_h,\mathbf{u}_h) &= \langle\boldsymbol{\tau}_h\mathbf{n}\,,\mathbf{g}\rangle_\Gamma \qquad \forall\,\boldsymbol{\tau}_h\in\mathbb{H}_{0,h},\\ b(\boldsymbol{\rho}_h,\mathbf{v}_h) &= -\int_\Omega \mathbf{f}\cdot\mathbf{v}_h \qquad \forall\,\mathbf{v}_h\in\mathbf{Q}_h.\end{aligned} \tag{1.20}$$

We remark at this point that when $k = 0$ and $n = 3$ the number of unknowns N involved in (1.20) behaves approximately as 9 times the number of tetrahedra of the triangulation. In fact, having in mind that: each row of $\boldsymbol{\tau}_h \in \mathbb{RT}_0(\mathcal{T}_h)$ is locally defined by 4 degrees of freedom, most of the sides of the triangulation belong to 2 tetrahedra each, and each $\mathbf{v}_h \in \mathbf{P}_0(\mathcal{T}_h)$ is locally determined by 3 degrees of freedom, we find that N is asymptotically given by

$$\left(\frac{4\times 3}{2} + 3\right)\times\text{number of tetrahedra} = 9\times\text{number of tetrahedra}. \tag{1.21}$$

In turn, it is easy to show (see, e.g. formulae given in [71, Section 3.3]) that the factor 9 changes to 39 and 102 when $k = 1$ and $k = 2$, respectively. On the other hand, it is important to notice that the identity (1.15) certainly suggests to approximate the symmetric stress tensor field $\boldsymbol{\sigma}$ by the postprocessing formula

$$\boldsymbol{\sigma}_h = \boldsymbol{\rho}_h + \boldsymbol{\rho}_h^{\mathtt{t}} - \left(\frac{\lambda+2\mu}{n\lambda+(n+1)\mu}\operatorname{tr}(\boldsymbol{\rho}_h) - \frac{n\lambda+2\mu}{n|\Omega|}\int_\Gamma \mathbf{g}\cdot\mathbf{n}\right)\mathbb{I}. \tag{1.22}$$

Moreover, in Section 1.3.3 below we propose a second-step postprocessed approximation of $\boldsymbol{\sigma}_h$ and provide the corresponding error estimate.

1.3.2 Solvability analysis

In order to provide the unique solvability of the Galerkin scheme (1.20), we need to introduce the Raviart-Thomas interpolation operator (see [19]), $\mathscr{E}_h^k : \mathbb{H}^1(\Omega) \to \mathbb{RT}_k(\mathcal{T}_h)$, which, given $\boldsymbol{\tau} \in \mathbb{H}^1(\Omega)$, and denoting by $\mathbf{n}$ the outward unit normal on each face/edge of the triangulation, is characterized by the following identities:

$$\int_e \mathscr{E}_h^k(\boldsymbol{\tau})\mathbf{n}\cdot\mathbf{p} = \int_e \boldsymbol{\tau}\mathbf{n}\cdot\mathbf{p} \qquad \forall\text{ face/edge } e\in\mathcal{T}_h,\quad \forall\,\mathbf{p}\in\mathbf{P}_k(e),\quad \text{when } k\geq 0, \tag{1.23}$$

and

$$\int_T \mathscr{E}_h^k(\boldsymbol{\tau}) : \boldsymbol{\xi} = \int_T \boldsymbol{\tau} : \boldsymbol{\xi} \qquad \forall\,T\in\mathcal{T}_h,\quad \forall\,\boldsymbol{\xi}\in\mathbb{P}_{k-1}(T),\quad \text{when}\quad k\geq 1. \tag{1.24}$$

Then, using (1.23) and (1.24), it is easy to show that

$$\mathbf{div}(\mathscr{E}_h^k(\boldsymbol{\tau})) = \mathscr{P}_h^k(\,\mathbf{div}(\boldsymbol{\tau})\,), \tag{1.25}$$

where $\mathscr{P}_h^k : \mathbf{L}^2(\Omega) \to \mathbf{Q}_h$ is the $\mathbf{L}^2(\Omega)$ - orthogonal projector. The interpolation operator $\mathscr{E}_h^k$ can also be defined as a bounded linear operator from the larger space $\mathbb{H}^s(\Omega)\cap\mathbb{H}(\mathbf{div};\Omega)$ into $\mathbb{RT}_k(\mathcal{T}_h)$ for all

$s \in (0,1]$ (see, e.g. Theorem 3.16 in [96]), and in this case there holds the following interpolation error estimate

$$\|\boldsymbol{\tau} - \mathscr{E}_h^k(\boldsymbol{\tau})\|_{0,T} \;\leq\; C\, h_T^s \left\{ \|\boldsymbol{\tau}\|_{s,T} \;+\; \|\mathbf{div}(\boldsymbol{\tau})\|_{0,T} \right\} \qquad \forall\, T \,\in\, \mathcal{T}_h\,. \tag{1.26}$$

Furthermore, we need the following approximation properties of the operators $\mathscr{P}_h^k$ and $\mathscr{E}_h^k$. It is well known (see, e.g. [37]) that for each $\mathbf{v} \in \mathbf{H}^m(\Omega)$, with $0 \leq m \leq k+1$, there holds

$$\|\mathbf{v} - \mathscr{P}_h^k(\mathbf{v})\|_{0,T} \;\leq\; C\, h_T^m\, |\mathbf{v}|_{m,T} \quad \forall\, T \,\in\, \mathcal{T}_h\,. \tag{1.27}$$

In addition, the operator $\mathscr{E}_h^k$ satisfies the following approximation properties (see, e.g. [19]): For each $\boldsymbol{\tau} \in \mathbb{H}^m(\Omega)$, with $1 \leq m \leq k+1$,

$$\|\boldsymbol{\tau} - \mathscr{E}_h^k(\boldsymbol{\tau})\|_{0,T} \;\leq\; C\, h_T^m\, |\boldsymbol{\tau}|_{m,T} \quad \forall\, T \in \mathcal{T}_h\,. \tag{1.28}$$

For each $\boldsymbol{\tau} \in \mathbb{H}^1(\Omega)$ such that $\mathbf{div}(\boldsymbol{\tau}) \in \mathbf{H}^m(\Omega)$, with $0 \leq m \leq k+1$,

$$\|\mathbf{div}(\boldsymbol{\tau} - \mathscr{E}_h^k(\boldsymbol{\tau}))\|_{0,T} \;\leq\; C\, h_T^m\, |\mathbf{div}(\boldsymbol{\tau})|_{m,T} \quad \forall\, T \in \mathcal{T}_h\,. \tag{1.29}$$

For each $\boldsymbol{\tau} \in \mathbb{H}^1(\Omega)$, where T_e is any tetrahedron/triangle of $\mathcal{T}_h$ having e as a face/edge,

$$\|\boldsymbol{\tau}\mathbf{n} - \mathscr{E}_h^k(\boldsymbol{\tau})\mathbf{n}\|_{0,e} \;\leq\; C\, h_e^{1/2}\, \|\boldsymbol{\tau}\|_{1,T_e} \quad \forall \text{ face/edge } e \,\in\, \mathcal{T}_h\,. \tag{1.30}$$

In particular, note that (1.29) follows easily from the property (1.25) and (1.27).

Then, as a consequence of (1.26), (1.27), (1.28), (1.29), (1.30), and the usual interpolation estimates, we find that $\mathbb{H}_{0,h}$ and $\mathbf{Q}_h$ satisfy the following approximation properties:

($\mathrm{AP}_h^{\boldsymbol{\rho}}$) For each $s \in (0, k+1]$ and for each $\boldsymbol{\tau} \in \mathbb{H}^s(\Omega) \cap \mathbb{H}_0(\mathbf{div};\Omega)$ with $\mathbf{div}(\boldsymbol{\tau}) \in \mathbf{H}^s(\Omega)$ there exists $\boldsymbol{\tau}_h \in \mathbb{H}_{0,h}$ such that

$$\|\boldsymbol{\tau} - \boldsymbol{\tau}_h\|_{\mathbf{div},\Omega} \;\leq\; C\, h^s \left\{ \|\boldsymbol{\tau}\|_{s,\Omega} + \|\mathbf{div}(\boldsymbol{\tau})\|_{s,\Omega} \right\}.$$

($\mathrm{AP}_h^{\mathbf{u}}$) For each $s \in [0, k+1]$ and for each $\mathbf{v} \in \mathbf{H}^s(\Omega)$, there exists $\mathbf{v}_h \in \mathbf{Q}_h$ such that

$$\|\mathbf{v} - \mathbf{v}_h\|_{0,\Omega} \;\leq\; C\, h^s\, \|\mathbf{v}\|_{s,\Omega}\,.$$

Next, we establish the unique solvability, stability, and convergence of the Galerkin scheme (1.20) with the finite element subspaces given by (1.19). We begin with the proof of the discrete inf-sup condition for the bilinear form b.

Lemma 1.3. *Let $\mathbb{H}_{0,h}$ and $\mathbf{Q}_h$ be given by* (1.19)*. Then, there exists $\beta > 0$, independent of h and λ, such that*

$$\sup_{\substack{\boldsymbol{\tau}_h \in \mathbb{H}_{0,h} \\ \boldsymbol{\tau}_h \neq \mathbf{0}}} \frac{b(\boldsymbol{\tau}_h, \mathbf{v}_h)}{\|\boldsymbol{\tau}_h\|_{\mathbf{div},\Omega}} \;\geq\; \beta\, \|\mathbf{v}_h\|_{0,\Omega} \qquad \forall\;\, \mathbf{v}_h \in \mathbf{Q}_h\,.$$

Proof. See [83, Lemma 3.2]. $\square$

The following theorem establishes the well-posedness of (1.20) and the associated Céa estimate.

Theorem 1.2. *The Galerkin scheme* (1.20) *has a unique solution* $(\boldsymbol{\rho}_h, \mathbf{u}_h) \in \mathbb{H}_{0,h} \times \mathbf{Q}_h$*, which satisfies the corresponding stability and Céa estimates, i.e. there exist positive constants* C, $\widetilde{C}$*, independent of* h *and* λ*, such that*

$$\|(\boldsymbol{\rho}_h\,,\,\mathbf{u}_h)\|_{\mathbb{H}_0\times\mathbf{Q}} \;\leq\; C\,\Big\{\|\mathbf{f}\|_{0,\Omega} \;+\; \|\mathbf{g}\|_{1/2,\Gamma}\Big\}\,,$$

and

$$\|(\boldsymbol{\rho}\,,\,\mathbf{u}) - (\boldsymbol{\rho}_h\,,\,\mathbf{u}_h)\|_{\mathbb{H}_0\times\mathbf{Q}} \;\leq\; \widetilde{C} \inf_{(\boldsymbol{\tau}_h\,,\,\mathbf{v}_h)\,\in\,\mathbb{H}_{0,h}\,\times\,\mathbf{Q}_h} \|(\boldsymbol{\rho}\,,\,\mathbf{u}) - (\boldsymbol{\tau}_h\,,\,\mathbf{v}_h)\|_{\mathbb{H}_0\times\mathbf{Q}}\,. \tag{1.31}$$

Proof. Since $\mathbf{div}(\mathbb{H}_{0,h}) \subseteq \mathbf{Q}_h$, we find that the discrete kernel of b is given by

$$\mathbb{V}_h \;:=\; \Big\{\boldsymbol{\tau}_h \in \mathbb{H}_{0,h}\;:\; b(\boldsymbol{\tau}_h, \mathbf{v}_h) = 0 \quad \forall\; \mathbf{v}_h \in \mathbf{Q}_h\Big\} \;=\; \Big\{\boldsymbol{\tau}_h \in \mathbb{H}_{0,h}\;:\; \mathbf{div}(\boldsymbol{\tau}_h) = \mathbf{0} \;\text{ in } \Omega\Big\} \;\subseteq\; \mathbb{V}\,,$$

which, thanks to (1.17), shows that a is strongly coercive in $\mathbb{V}_h$. This fact, Lemma 3.1, and a direct application of the discrete Babuška-Brezzi theory (see, e.g. [92, Theorem 1.1, Chapter II] or [19, Theorem II.1.1]) complete the proof. $\square$

The following theorem provides the theoretical rate of convergence of the Galerkin scheme (1.20), under suitable regularity assumptions on the exact solution.

Theorem 1.3. *Let* $(\boldsymbol{\rho}, \mathbf{u}) \in \mathbb{H}_0 \times \mathbf{Q}$ *and* $(\boldsymbol{\rho}_h, \mathbf{u}_h) \in \mathbb{H}_{0,h} \times \mathbf{Q}_h$ *be the unique solutions of the continuous and discrete formulations* (1.12) *and* (1.20)*, respectively. Assume that* $\boldsymbol{\rho} \in \mathbb{H}^s(\Omega)$, $\mathbf{div}(\boldsymbol{\rho}) \in \mathbf{H}^s(\Omega)$ *and* $\mathbf{u} \in \mathbf{H}^s(\Omega)$*, for some* $s \in (0, k+1]$*. Then, there exists* $C > 0$*, independent of* h*, such that*

$$\|(\boldsymbol{\rho}, \mathbf{u}) - (\boldsymbol{\rho}_h, \mathbf{u}_h)\|_{\mathbb{H}_0\times\mathbf{Q}} \;\leq\; C\,h^s\,\Big\{\|\boldsymbol{\rho}\|_{s,\Omega} \;+\; \|\mathbf{div}(\boldsymbol{\rho})\|_{s,\Omega} \;+\; \|\mathbf{u}\|_{s,\Omega}\Big\}\,.$$

Proof. It is a straightforward consequence of the Céa estimate (1.31) and the approximation properties $(\mathrm{AP}_h^{\boldsymbol{\rho}})$ and $(\mathrm{AP}_h^{\mathbf{u}})$. $\square$

1.3.3 A fully postprocessed stress

We end this section by proposing a second-step postprocessed stress and deriving the corresponding a priori error estimate. To do that, we first observe from (1.15) and (1.22) that there holds

$$\|\boldsymbol{\sigma} - \boldsymbol{\sigma}_h\|_{0,\Omega} \quad\leq\quad (2+n)\,\|\boldsymbol{\rho} - \boldsymbol{\rho}_h\|_{0,\Omega}, \tag{1.32}$$

which shows that the rate of convergence of $\|\boldsymbol{\sigma} - \boldsymbol{\sigma}_h\|_{0,\Omega}$ is the same of $\|\boldsymbol{\rho} - \boldsymbol{\rho}_h\|_{0,\Omega}$. Unfortunately, numerical experiments (cf. Section 5) confirm that the rate of convergence of $\sum\limits_{T\in\mathcal{T}_h} \|\boldsymbol{\sigma} - \boldsymbol{\sigma}_h\|^2_{\mathbf{div},T}$ is of lower order than $\sum\limits_{T\in\mathcal{T}_h} \|\boldsymbol{\rho}-\boldsymbol{\rho}_h\|^2_{\mathbf{div},T}$. This fact has motivated the construction of a second approximation for the stress variable $\boldsymbol{\sigma}$, which has a better rate of convergence in the broken $\mathbb{H}(\mathbf{div})$-norm. Indeed, we first note that $\boldsymbol{\sigma}_h$ gives us a good approximation for $\boldsymbol{\sigma}$ in the $\mathbb{L}^2$-norm (cf. (1.32)). Hence, the problem lies on the approximation that $\mathbf{div}(\boldsymbol{\sigma}_h)$ implies for $\mathbf{div}(\boldsymbol{\sigma})$. Furthermore, we know from (1.1) that $\mathbf{div}(\boldsymbol{\sigma}) = -\mathbf{f}$, and then we try to approximate $\mathbf{div}(\boldsymbol{\sigma}_h)$ by $-\mathbf{f}$ in each $T \in \mathcal{T}_h$. The above discussion suggests to define the following postprocessed approximation for $\boldsymbol{\sigma}$: Given $T \in \mathcal{T}_h$, we find $\boldsymbol{\sigma}_h^\star|_T := \boldsymbol{\sigma}_{h,T}^\star \in \mathbb{RT}_k(T)$ such that

$$\big\langle \boldsymbol{\sigma}_{h,T}^\star, \boldsymbol{\tau}_h \big\rangle_{\mathbf{div},T} \;:=\; \int_T \boldsymbol{\sigma}_{h,T}^\star : \boldsymbol{\tau}_h \;+\; \int_T \mathbf{div}(\boldsymbol{\sigma}_{h,T}^\star)\cdot\mathbf{div}(\boldsymbol{\tau}_h) \;=\; \int_T \boldsymbol{\sigma}_h : \boldsymbol{\tau}_h \;-\; \int_T \mathbf{f}\cdot\mathbf{div}(\boldsymbol{\tau}_h), \tag{1.33}$$

for all $\boldsymbol{\tau}_h \in \mathbb{RT}_k(T) := \big\{\boldsymbol{\tau} \in \mathbb{L}^2(T) \,:\, (\tau_{i1},\dots,\tau_{in})^{\mathtt{t}}|_T \,\in\, \mathbf{RT}_k(T) \quad \forall\, i \in \{1,\dots,n\}\big\}$. It is important to note that $\boldsymbol{\sigma}^\star_{h,T}$ can be explicitly (and efficiently) calculated for each $T \in \mathcal{T}_h$ independently. Moreover, the following result establishes an estimate for the local error $\|\boldsymbol{\sigma} - \boldsymbol{\sigma}^\star_{h,T}\|_{\mathbf{div},T}$.

Lemma 1.4. *Assume that $\boldsymbol{\sigma}|_T \in \mathbb{H}^1(T)$ for each $T \in \mathcal{T}_h$. Then there holds*

$$\|\boldsymbol{\sigma} - \boldsymbol{\sigma}^\star_{h,T}\|_{\mathbf{div},T} \;\leq\; \|\boldsymbol{\sigma} - \boldsymbol{\sigma}_h\|_{0,T} \,+\, 2\,\|\boldsymbol{\sigma} - \mathscr{E}^k_{h,T}(\boldsymbol{\sigma})\|_{\mathbf{div},T}, \tag{1.34}$$

where $\mathscr{E}^k_{h,T}$ is the local Raviart-Thomas interpolation operator on T.

Proof. We first notice, using that $\mathbf{div}(\boldsymbol{\sigma}) = -\mathbf{f}$ in Ω, that there holds

$$\langle \boldsymbol{\sigma}, \boldsymbol{\tau}_h\rangle_{\mathbf{div},T} \;=\; \int_T \boldsymbol{\sigma} : \boldsymbol{\tau}_h \;-\; \int_T \mathbf{f}\cdot\mathbf{div}(\boldsymbol{\tau}_h) \quad \forall\, \boldsymbol{\tau}_h \in \mathbb{RT}_k(T),$$

which, using (1.33), implies the error equation:

$$\big\langle \boldsymbol{\sigma} - \boldsymbol{\sigma}^\star_{h,T}, \boldsymbol{\tau}_h\big\rangle_{\mathbf{div},T} \;=\; \int_T (\boldsymbol{\sigma} - \boldsymbol{\sigma}_h) : \boldsymbol{\tau}_h \quad \forall\, \boldsymbol{\tau}_h \in \mathbb{RT}_k(T),$$

and then, adding $\mathscr{E}^k_{h,T}(\boldsymbol{\sigma})$ to both sides and rearranging, we find that

$$\Big\langle \mathscr{E}^k_{h,T}(\boldsymbol{\sigma}) - \boldsymbol{\sigma}^\star_{h,T}, \boldsymbol{\tau}_h\Big\rangle_{\mathbf{div},T} \;=\; \int_T (\boldsymbol{\sigma} - \boldsymbol{\sigma}_h) : \boldsymbol{\tau}_h \,+\, \Big\langle \mathscr{E}^k_{h,T}(\boldsymbol{\sigma}) - \boldsymbol{\sigma}, \boldsymbol{\tau}_h\Big\rangle_{\mathbf{div},T} \quad \forall\, \boldsymbol{\tau}_h \in \mathbb{RT}_k(T).$$

Next, taking $\boldsymbol{\tau}_h := \mathscr{E}^k_{h,T}(\boldsymbol{\sigma}) - \boldsymbol{\sigma}^\star_{h,T} \in \mathbb{RT}_k(T)$ in the above identity, and applying the Cauchy-Schwarz inequality, we deduce that

$$\|\mathscr{E}^k_{h,T}(\boldsymbol{\sigma}) - \boldsymbol{\sigma}^\star_{h,T}\|_{\mathbf{div},T} \;\leq\; \|\boldsymbol{\sigma} - \boldsymbol{\sigma}_h\|_{0,T} \,+\, \|\boldsymbol{\sigma} - \mathscr{E}^k_{h,T}(\boldsymbol{\sigma})\|_{\mathbf{div},T}. \tag{1.35}$$

Finally, from the triangle inequality we note that

$$\|\boldsymbol{\sigma} - \boldsymbol{\sigma}^\star_{h,T}\|_{\mathbf{div},T} \;\leq\; \|\boldsymbol{\sigma} - \mathscr{E}^k_{h,T}(\boldsymbol{\sigma})\|_{\mathbf{div},T} \,+\, \|\mathscr{E}^k_{h,T}(\boldsymbol{\sigma}) - \boldsymbol{\sigma}^\star_{h,T}\|_{\mathbf{div},T},$$

which, together with (1.35), yields (1.34) and complete the proof. □

A straightforward consequence of the previous lemma is given by the following global rate of convergence for $\boldsymbol{\sigma}^\star_h$.

Theorem 1.4. *Let $(\boldsymbol{\rho}, \mathbf{u}) \in \mathbb{H}_0 \times \mathbf{Q}$ and $(\boldsymbol{\rho}_h, \mathbf{u}_h) \in \mathbb{H}_{0,h} \times \mathbf{Q}_h$ be the unique solutions of the continuous and discrete formulations* (1.12) *and* (1.20)*, respectively. In addition, let $\boldsymbol{\sigma}$ be the stress tensor given by* (1.15)*, and let $\boldsymbol{\sigma}_h$ and $\boldsymbol{\sigma}^\star_h$ be its discrete approximations introduced in* (1.22) *and* (1.33)*, respectively. Assume that $\boldsymbol{\rho} \in \mathbb{H}^s(\Omega)$, $\mathbf{div}(\boldsymbol{\rho}) \in \mathbf{H}^s(\Omega)$, and $\mathbf{u} \in \mathbf{H}^s(\Omega)$, for some $s \in (0, k+1]$. Then, there exists $C > 0$, independent of h, such that*

$$\left\{\sum_{T\in\mathcal{T}_h} \|\boldsymbol{\sigma} - \boldsymbol{\sigma}^\star_h\|^2_{\mathbf{div},T}\right\}^{1/2} \quad\leq\quad C\,h^s \Big\{\|\boldsymbol{\rho}\|_{s,\Omega} \,+\, \|\mathbf{div}(\boldsymbol{\rho})\|_{s,\Omega} \,+\, \|\mathbf{u}\|_{s,\Omega}\Big\}.$$

Proof. We first observe from (1.15) that the regularity of $\boldsymbol{\sigma}$ depends on the regularity of $\boldsymbol{\rho}$. Indeed, given $\boldsymbol{\rho} \in \mathbb{H}^s(\Omega)$, this establish that $\boldsymbol{\rho}^{\mathtt{t}} \in \mathbb{H}^s(\Omega)$ and $\mathrm{tr}(\boldsymbol{\rho}) \in H^s(\Omega)$, which imply that $\boldsymbol{\sigma} \in \mathbb{H}^s(\Omega)$. In addition, from the fact that $\mathbf{div}(\boldsymbol{\sigma}) = \mathbf{div}(\boldsymbol{\rho})$, we deduce that $\mathbf{div}(\boldsymbol{\sigma}) \in \mathbf{H}^s(\Omega)$. Then, the proof follows straightforwardly from the estimate (1.34), after summing up over $T \in \mathcal{T}_h$, using (1.28), (1.29) and (1.32) together with Theorem 1.3. □

We end this section by emphasizing, as it has become clear from the foregoing analysis, that the present pseudostress-based formulation for linear elasticity is very suitable to handle corresponding Dirichlet boundary conditions. In other words, as long as no tractions are imposed on Γ or part of it, there is no need of introducing the symmetric stress tensor $\boldsymbol{\sigma}$ as the main unknown of the associated mixed formulation. In spite of it, and if approximations of $\boldsymbol{\sigma}$ are anyway required, we also showed that this can be easily obtained through a simple postprocessing procedure yielding optimal rates of convergence in the broken $\mathbb{H}(\mathbf{div};\Omega)$-norm. Nevertheless, it is still not clear whether the pseudostress-based approach can also be applied/adapted to Neumann or mixed boundary conditions, so that additional work in this direction needs certainly to be done. Perhaps, as a first attempt, one could try to explore a further use of formula (1.14) expressing $\boldsymbol{\sigma}$ in terms of the pseudostress $\boldsymbol{\rho}$. More precisely, assuming for instance that one has the Neumann boundary condition: $\boldsymbol{\sigma}\,\mathbf{n} \,=\, \mathbf{g}_{_N} \in \mathbf{H}^{-1/2}(\Gamma)$ on Γ, we find from (1.14) that

$$\boldsymbol{\rho}\,\mathbf{n} \,=\, \mathbf{g}_{_N} \,-\, \left(\boldsymbol{\rho}^{\mathtt{t}} \,-\, \left\{\frac{\lambda+2\mu}{n\lambda+(n+1)\mu}\right\} \operatorname{tr}(\boldsymbol{\rho})\,\mathbb{I}\right)\mathbf{n} \quad \text{on} \quad \Gamma\,,$$

and hence, the resulting Neumann boundary value problem arising now from (1.4) becomes: Find $(\boldsymbol{\rho},\mathbf{u})$ such that

$$\begin{aligned} \frac{1}{\mu}\left\{\boldsymbol{\rho} - \frac{\lambda+\mu}{n\,\lambda+(n+1)\,\mu}\operatorname{tr}(\boldsymbol{\rho})\,\mathbb{I}\right\} \,&=\, \nabla\mathbf{u} \quad \text{in} \quad \Omega\,, \quad \mathbf{div}(\boldsymbol{\rho}) \,=\, -\mathbf{f} \quad \text{in} \quad \Omega\,, \\ \boldsymbol{\rho}\,\mathbf{n} \,&=\, \mathbf{g}_{_N} \,-\, \left(\boldsymbol{\rho}^{\mathtt{t}} \,-\, \left\{\frac{\lambda+2\mu}{n\lambda+(n+1)\mu}\right\} \operatorname{tr}(\boldsymbol{\rho})\,\mathbb{I}\right)\mathbf{n} \quad \text{on} \quad \Gamma\,. \end{aligned} \tag{1.36}$$

In this way, a fixed-point strategy based on the unknown $\boldsymbol{\rho}$ could be suggested to analyze the well-posedness of (1.36) and its Galerkin approximation. We plan to address this and other eventual approaches arising from (1.14) and (1.36), at least numerically, in a future work.

1.4 A residual-based a posteriori error estimator

In this section we develop a residual-based *a posteriori* error analysis for the mixed finite element scheme (1.20) with the subspaces $\mathbb{H}_{0,h}$ and $\mathbf{Q}_h$ defined by (1.19) for $n = 3$. To this end, we require additional notations. We first recall that the curl of a 3D vector $\mathbf{v} := (v_1, v_2, v_3)$ is the 3D vector

$$\operatorname{curl}(\mathbf{v}) \;=\; \nabla\times\mathbf{v} \;:=\; \left(\frac{\partial v_3}{\partial x_2} - \frac{\partial v_2}{\partial x_3}\,,\, \frac{\partial v_1}{\partial x_3} - \frac{\partial v_3}{\partial x_1}\,,\, \frac{\partial v_2}{\partial x_1} - \frac{\partial v_1}{\partial x_2}\right).$$

Then, given a tensor function $\boldsymbol{\tau} := (\tau_{ij})_{3\times 3}$, the operator $\underline{\mathbf{curl}}$ denotes curl acting along each row of $\boldsymbol{\tau}$, that is, $\underline{\mathbf{curl}}(\boldsymbol{\tau})$ is the 3×3 tensor whose rows are given by

$$\underline{\mathbf{curl}}(\boldsymbol{\tau}) \;:=\; \begin{pmatrix} \operatorname{curl}(\tau_{11},\tau_{12},\tau_{13}) \\ \operatorname{curl}(\tau_{21},\tau_{22},\tau_{23}) \\ \operatorname{curl}(\tau_{31},\tau_{32},\tau_{33}) \end{pmatrix}.$$

Also, we denote by $\boldsymbol{\tau}\times\mathbf{n}$, the 3×3 tensor whose rows are given by the tangential components of each row of $\boldsymbol{\tau}$, that is,

$$\boldsymbol{\tau}\times\mathbf{n} \;:=\; \begin{pmatrix} (\tau_{11},\tau_{12},\tau_{13})\times\mathbf{n} \\ (\tau_{21},\tau_{22},\tau_{23})\times\mathbf{n} \\ (\tau_{31},\tau_{32},\tau_{33})\times\mathbf{n} \end{pmatrix}.$$

In addition, we define the Sobolev space

$$\mathbb{H}(\underline{\mathbf{curl}};\Omega) := \left\{ \mathbf{w} \in \mathbb{L}^2(\Omega) \,:\, \underline{\mathbf{curl}}(\mathbf{w}) \in \mathbb{L}^2(\Omega) \right\}.$$

On the other hand, given $T \in \mathcal{T}_h$, we let $\mathcal{E}(T)$ be the set of its faces, and let $\mathcal{E}_h$ be the set of all faces of the triangulation $\mathcal{T}_h$. Then, we write $\mathcal{E}_h = \mathcal{E}_h(\Omega) \cup \mathcal{E}_h(\Gamma)$, where $\mathcal{E}_h(\Omega) := \{e \in \mathcal{E}_h : e \subseteq \Omega\}$ and $\mathcal{E}_h(\Gamma) := \{e \in \mathcal{E}_h : e \subseteq \Gamma\}$. Also, for each face $e \in \mathcal{E}_h$ we fix a unit normal $\mathbf{n}_e$ to e. In addition, given $\boldsymbol{\tau} \in \mathbb{H}(\underline{\mathbf{curl}};\Omega)$ and $e \in \mathcal{E}_h(\Omega)$, we let $[\![\boldsymbol{\tau} \times \mathbf{n}_e]\!]$ be the corresponding jump of the tangential traces (which exist in a variational sense) across e, that is, $[\![\boldsymbol{\tau} \times \mathbf{n}_e]\!] := (\boldsymbol{\tau}|_T - \boldsymbol{\tau}|_{T'})|_e \times \mathbf{n}_e$, where T and T' are the elements of $\mathcal{T}_h$ having e as a common face. From now on, when no confusion arises, we simple write $\mathbf{n}$ instead of $\mathbf{n}_e$.

1.4.1 The a posteriori error estimator

Given $(\boldsymbol{\rho}, \mathbf{u}) \in \mathbb{H}_0 \times \mathbf{Q}$ and $(\boldsymbol{\rho}_h, \mathbf{u}_h) \in \mathbb{H}_{0,h} \times \mathbf{Q}_h$ be the unique solutions of the continuous and discrete formulations (1.12) and (1.20), respectively, we define for each $T \in \mathcal{T}_h$ a local error indicator θ_T as follows:

$$\begin{aligned}
\theta_T^2 \;:=\;& \|\mathbf{f} + \mathbf{div}(\boldsymbol{\rho}_h)\|_{0,T}^2 \;+\; h_T^2 \left\| \nabla \mathbf{u}_h - \frac{1}{\mu}\left\{ \boldsymbol{\rho}_h - \frac{\lambda+\mu}{3\lambda+4\mu}\,\mathrm{tr}(\boldsymbol{\rho}_h)\,\mathbb{I} \right\} - c_{\mathbf{g}}\,\mathbb{I} \right\|_{0,T}^2 \\
&+ h_T^2 \left\| \underline{\mathbf{curl}}\left(\frac{1}{\mu}\left\{ \boldsymbol{\rho}_h - \frac{\lambda+\mu}{3\lambda+4\mu}\,\mathrm{tr}(\boldsymbol{\rho}_h)\,\mathbb{I} \right\}\right) \right\|_{0,T}^2 \\
&+ \sum_{e \in \mathcal{E}(T)\cap\mathcal{E}_h(\Omega)} h_e \left\| \left[\!\!\left[\left(\frac{1}{\mu}\left\{ \boldsymbol{\rho}_h - \frac{\lambda+\mu}{3\lambda+4\mu}\,\mathrm{tr}(\boldsymbol{\rho}_h)\,\mathbb{I} \right\} + c_{\mathbf{g}}\,\mathbb{I} \right) \times \mathbf{n} \right]\!\!\right] \right\|_{0,e}^2 \\
+& \sum_{e \in \mathcal{E}(T)\cap\mathcal{E}_h(\Gamma)} h_e \left\{ \left\| \nabla \mathbf{g} \times \mathbf{n} - \left(\frac{1}{\mu}\left\{ \boldsymbol{\rho}_h - \frac{\lambda+\mu}{3\lambda+4\mu}\,\mathrm{tr}(\boldsymbol{\rho}_h)\,\mathbb{I} \right\} + c_{\mathbf{g}}\,\mathbb{I} \right) \times \mathbf{n} \right\|_{0,e}^2 \;+\; \|\mathbf{g} - \mathbf{u}_h\|_{0,e}^2 \right\},
\end{aligned} \tag{1.37}$$

where

$$c_{\mathbf{g}} \;:=\; \frac{1}{3|\Omega|} \int_\Gamma \mathbf{g}\cdot\mathbf{n}\,. \tag{1.38}$$

The residual character of each term on the right hand side of (1.37) is quite clear from the continuous identities provided in Section 1.2. As usual the expression

$$\boldsymbol{\theta} \;:=\; \left\{ \sum_{T\in\mathcal{T}_h} \theta_T^2 \right\}^{1/2} \tag{1.39}$$

is employed as the global residual error estimator.

The following theorem constitutes the main result of this section.

Theorem 1.5. *Assume that Ω is a polyhedral domain and that $\mathbf{g} \in \mathbf{H}^1(\Gamma)$. In addition, let $(\boldsymbol{\rho}, \mathbf{u}) \in \mathbb{H}_0 \times \mathbf{Q}$ and $(\boldsymbol{\rho}_h, \mathbf{u}_h) \in \mathbb{H}_{0,h} \times \mathbf{Q}_h$ be the unique solutions of* (1.12) *and* (1.20)*, respectively. Then, there exist positive constants $C_{\mathtt{eff}}$ and $C_{\mathtt{rel}}$, independent of h and λ, such that*

$$C_{\mathtt{eff}}\,\boldsymbol{\theta} \;+\; h.o.t. \;\le\; \|(\boldsymbol{\rho}, \mathbf{u}) - (\boldsymbol{\rho}_h, \mathbf{u}_h)\|_{\mathbb{H}_0\times\mathbf{Q}} \;\le\; C_{\mathtt{rel}}\,\boldsymbol{\theta}\,, \tag{1.40}$$

where h.o.t. stands for one or several terms of higher order.

The proof of Theorem 1.5 is separated into the parts given by the next subsections. Firstly, we prove the reliability (upper bound in (1.40)) of the global error estimator, and then in Subsection 4.3 we show the efficiency of the global error estimator (lower bound in (1.40)).

1.4.2 Reliability

We begin with the following preliminary estimate.

Lemma 1.5. *Let* $(\boldsymbol{\rho}, \mathbf{u}) \in \mathbb{H}_0 \times \mathbf{Q}$ *and* $(\boldsymbol{\rho}_h, \mathbf{u}_h) \in \mathbb{H}_{0,h} \times \mathbf{Q}_h$ *be the unique solutions of* (1.12) *and* (1.20)*, respectively. Then there exists* $C > 0$*, independent of* h*, such that*

$$C \, \|(\boldsymbol{\rho} - \boldsymbol{\rho}_h, \mathbf{u} - \mathbf{u}_h)\|_{\mathbb{H}_0 \times \mathbf{Q}} \;\le\; \sup_{\substack{\boldsymbol{\tau} \in \mathbb{H}_0 \\ \boldsymbol{\tau} \neq \mathbf{0}}} \frac{|E(\boldsymbol{\tau})|}{\|\boldsymbol{\tau}\|_{\mathbb{H}_0}} \;+\; \|\mathbf{f} + \mathbf{div}(\boldsymbol{\rho}_h)\|_{0,\Omega} \,, \tag{1.41}$$

where

$$E(\boldsymbol{\tau}) \;:=\; a(\boldsymbol{\rho} - \boldsymbol{\rho}_h, \boldsymbol{\tau}) \;+\; b(\boldsymbol{\tau}, \mathbf{u} - \mathbf{u}_h) \qquad \forall\, \boldsymbol{\tau} \in \mathbb{H}_0 \,. \tag{1.42}$$

Proof. We first observe from Theorem 1.1 that the bounded linear operator $\mathcal{A} : \mathbb{H}_0 \times \mathbf{Q} \to (\mathbb{H}_0 \times \mathbf{Q})' \equiv \mathbb{H}_0' \times \mathbf{Q}'$, which is induced by the left-hand side of the equations in (1.12), is an isomorphism. Then there exists $C > 0$ such that

$$\|\mathcal{A}(\boldsymbol{\xi}, \mathbf{w})\|_{\mathbb{H}_0' \times \mathbf{Q}'} \;\ge\; C \|(\boldsymbol{\xi}, \mathbf{w})\|_{\mathbb{H}_0 \times \mathbf{Q}} \qquad \forall\, (\boldsymbol{\xi}, \mathbf{w}) \,\in\, \mathbb{H}_0 \times \mathbf{Q} \,.$$

Equivalently

$$C \, \|(\boldsymbol{\xi}, \mathbf{w})\|_{\mathbb{H}_0 \times \mathbf{Q}} \;\le\; \sup_{\substack{(\boldsymbol{\tau}, \mathbf{v}) \in \mathbb{H}_0 \times \mathbf{Q} \\ (\boldsymbol{\tau}, \mathbf{v}) \neq \mathbf{0}}} \frac{a(\boldsymbol{\xi}, \boldsymbol{\tau}) + b(\boldsymbol{\tau}, \mathbf{w}) + b(\boldsymbol{\xi}, \mathbf{v})}{\|(\boldsymbol{\tau}, \mathbf{v})\|_{\mathbb{H}_0 \times \mathbf{Q}}} \qquad \forall\, (\boldsymbol{\xi}, \mathbf{w}) \,\in\, \mathbb{H}_0 \times \mathbf{Q} \,.$$

In particular, for the error $(\boldsymbol{\xi}, \mathbf{w}) := (\boldsymbol{\rho} - \boldsymbol{\rho}_h, \mathbf{u} - \mathbf{u}_h)$, and using the notation introduced by (1.42) we have

$$\begin{aligned}
C \, \|(\boldsymbol{\rho} - \boldsymbol{\rho}_h, \mathbf{u} - \mathbf{u}_h)\|_{\mathbb{H}_0 \times \mathbf{Q}} \;&\le\; \sup_{\substack{(\boldsymbol{\tau}, \mathbf{v}) \in \mathbb{H}_0 \times \mathbf{Q} \\ (\boldsymbol{\tau}, \mathbf{v}) \neq \mathbf{0}}} \frac{a(\boldsymbol{\rho} - \boldsymbol{\rho}_h, \boldsymbol{\tau}) + b(\boldsymbol{\tau}, \mathbf{u} - \mathbf{u}_h) + b(\boldsymbol{\rho} - \boldsymbol{\rho}_h, \mathbf{v})}{\|(\boldsymbol{\tau}, \mathbf{v})\|_{\mathbb{H}_0 \times \mathbf{Q}}} \\
&\le\; \sup_{\substack{(\boldsymbol{\tau}, \mathbf{v}) \in \mathbb{H}_0 \times \mathbf{Q} \\ (\boldsymbol{\tau}, \mathbf{v}) \neq \mathbf{0}}} \left\{ \frac{E(\boldsymbol{\tau})}{\|\boldsymbol{\tau}\|_{\mathbb{H}_0}} \;+\; \frac{b(\boldsymbol{\rho} - \boldsymbol{\rho}_h, \mathbf{v})}{\|\mathbf{v}\|_{\mathbf{Q}}} \right\} \;\le\; \sup_{\substack{\boldsymbol{\tau} \in \mathbb{H}_0 \\ \boldsymbol{\tau} \neq \mathbf{0}}} \frac{E(\boldsymbol{\tau})}{\|\boldsymbol{\tau}\|_{\mathbb{H}_0}} \;+\; \sup_{\substack{\mathbf{v} \in \mathbf{Q} \\ \mathbf{v} \neq \mathbf{0}}} \frac{b(\boldsymbol{\rho} - \boldsymbol{\rho}_h, \mathbf{v})}{\|\mathbf{v}\|_{\mathbf{Q}}} \,.
\end{aligned}$$

In turn, according to the definition of the bilinear operator b (cf. (1.7)), and using Cauchy-Schwarz inequality, and the second equation of (1.5), we get

$$\sup_{\substack{\mathbf{v} \in \mathbf{Q} \\ \mathbf{v} \neq \mathbf{0}}} \frac{b(\boldsymbol{\rho} - \boldsymbol{\rho}_h, \mathbf{v})}{\|\mathbf{v}\|_{\mathbf{Q}}} \;=\; \sup_{\substack{\mathbf{v} \in \mathbf{Q} \\ \mathbf{v} \neq \mathbf{0}}} \frac{-\displaystyle\int_\Omega \mathbf{v} \cdot \Big\{ \mathbf{f} + \mathbf{div}(\boldsymbol{\rho}_h) \Big\}}{\|\mathbf{v}\|_{\mathbf{Q}}} \;\le\; \|\mathbf{f} + \mathbf{div}(\boldsymbol{\rho}_h)\|_{0,\Omega} \,,$$

which, completes the proof of (1.41). $\square$

Our next goal is to estimate the supremum in (1.41). For this purpose, we now deduce from the first equations of (1.12) and (1.20) that

$$E(\boldsymbol{\tau}) \;=\; F(\boldsymbol{\tau}) - a(\boldsymbol{\rho}_h, \boldsymbol{\tau}) - b(\boldsymbol{\tau}, \mathbf{u}_h) \quad \forall\, \boldsymbol{\tau} \,\in\, \mathbb{H}_0 \,, \quad \text{and} \quad E(\boldsymbol{\tau}_h) \;=\; 0 \quad \forall\, \boldsymbol{\tau}_h \,\in\, \mathbb{H}_{0,h} \,,$$

whence, given a particular $\boldsymbol{\tau}_h \in \mathbb{H}_{0,h}$, and denoting $\widehat{\boldsymbol{\tau}} := \boldsymbol{\tau} - \boldsymbol{\tau}_h$, we can write

$$E(\boldsymbol{\tau}) \;=\; E(\widehat{\boldsymbol{\tau}}) \;=\; \langle \widehat{\boldsymbol{\tau}}\mathbf{n}\,, \mathbf{g}\rangle_\Gamma - \frac{1}{\mu}\int_\Omega \boldsymbol{\rho}_h^{\mathtt{d}} : \widehat{\boldsymbol{\tau}}^{\mathtt{d}} - \frac{1}{3(3\lambda+4\mu)}\int_\Omega \operatorname{tr}(\boldsymbol{\rho}_h)\operatorname{tr}(\widehat{\boldsymbol{\tau}}) - \int_\Omega \mathbf{u}_h \cdot \mathbf{div}(\widehat{\boldsymbol{\tau}})\,. \tag{1.43}$$

In this way, estimating the supremum in (1.41) reduces now to bound $|E(\widehat{\boldsymbol{\tau}})|$ for a suitable choice of $\boldsymbol{\tau}_h \in \mathbb{H}_{0,h}$ (cf. (1.19)). To this end, we will need the Clément interpolation operator $I_h : H^1(\Omega) \to X_h$ (cf. [40]), where

$$X_h \;:=\; \Big\{ v \in C(\bar{\Omega}) \,:\, v|_T \in \mathrm{P}_1(T) \quad \forall\, T \in \mathcal{T}_h \Big\}\,.$$

A vectorial version of I_h, say $\mathbf{I}_h : \mathbf{H}^1(\Omega) \to \mathbf{X}_h := [X_h]^3$, which is defined componentwise by I_h, is also required. The following lemma establishes the local approximation properties of I_h.

Lemma 1.6. *There exist constants $c_1, c_2 > 0$, independent of h, such that for all $v \in H^1(\Omega)$ there holds*

$$\|v - I_h(v)\|_{0,T} \;\le\; c_1\, h_T\, \|v\|_{1,\triangle(T)} \quad \forall\, T \in \mathcal{T}_h\,,$$

and

$$\|v - I_h(v)\|_{0,e} \;\le\; c_2\, h_e^{1/2}\, \|v\|_{1,\triangle(e)} \quad \forall\, e \in \mathcal{E}_h\,,$$

where $\triangle(T) := \cup\{T' \in \mathcal{T}_h \;:\; T' \cap T \neq \varnothing\}$ and $\triangle(e) := \cup\{T' \in \mathcal{T}_h \;:\; T' \cap e \neq \varnothing\}$.

Proof. See [40]. $\square$

In turn, we now establish a suitable Helmholtz decomposition for $\mathbb{H}(\mathbf{div};\Omega)$.

Lemma 1.7. *For each $\boldsymbol{\tau} \in \mathbb{H}(\mathbf{div};\Omega)$ there exist $\mathbf{z} \in \mathbf{H}^2(\Omega)$ and $\boldsymbol{\chi} \in \mathbb{H}^1(\Omega)$ such that*

$$\boldsymbol{\tau} \;=\; \nabla\mathbf{z} + \underline{\mathbf{curl}}(\boldsymbol{\chi}) \quad \textit{in} \quad \Omega \quad \textit{and} \quad \|\mathbf{z}\|_{2,\Omega} + \|\boldsymbol{\chi}\|_{1,\Omega} \;\le\; c\,\|\boldsymbol{\tau}\|_{\mathbf{div},\Omega}\,, \tag{1.44}$$

where c is a positive constant independent of all the foregoing variables.

Proof. We begin by introducing a sufficiently large convex domain $\widetilde{\Omega}$ such that $\overline{\Omega} \subset \widetilde{\Omega}$. Then, we proceed as in the second part of the proof of [87, Lemma 3.3] and perform a suitable extension of $\boldsymbol{\tau}$ to the whole domain $\widetilde{\Omega}$. More precisely, given $\boldsymbol{\tau} \in \mathbb{H}(\mathbf{div};\Omega)$, we consider the boundary value problem:

$$\Delta\mathbf{w} \;=\; \mathbf{0} \quad \text{in} \quad \widetilde{\Omega}\setminus\overline{\Omega}\,, \quad \frac{\partial\mathbf{w}}{\partial\mathbf{n}} \;=\; \boldsymbol{\tau}\,\mathbf{n} \quad \text{on} \quad \Gamma\,, \quad \mathbf{w} = \mathbf{0} \quad \text{on} \quad \partial\widetilde{\Omega}\,, \tag{1.45}$$

where $\mathbf{n}$ stands here for the inward unit normal on Γ. It follows, thanks to the Lax-Milgram Theorem, that (1.45) has a unique solution $\mathbf{w} \in \mathbf{H}^1(\widetilde{\Omega}\setminus\overline{\Omega})$, which satisfies

$$\|\mathbf{w}\|_{1,\widetilde{\Omega}\setminus\overline{\Omega}} \le \widetilde{c}\,\|\boldsymbol{\tau}\,\mathbf{n}\|_{-1/2,\Gamma} \;\le\; \widetilde{c}\,\|\boldsymbol{\tau}\|_{\mathbf{div},\Omega}\,, \tag{1.46}$$

with a constant $\widetilde{c} > 0$, independent of $\boldsymbol{\tau}$. Then, we define $\widetilde{\boldsymbol{\tau}} := \begin{cases} \boldsymbol{\tau} & \text{in} \quad \Omega \\ \nabla\mathbf{w} & \text{in} \quad \widetilde{\Omega}\setminus\overline{\Omega} \end{cases}$, and observe, according to (1.45) and (1.46), that $\widetilde{\boldsymbol{\tau}} \in \mathbb{H}(\mathbf{div};\widetilde{\Omega})$ and

$$\|\widetilde{\boldsymbol{\tau}}\|_{\mathbf{div},\widetilde{\Omega}} \le \Big\{1 + \widetilde{c}^2\Big\}^{1/2}\,\|\boldsymbol{\tau}\|_{\mathbf{div},\Omega}\,. \tag{1.47}$$

In this way, applying the Helmholtz decomposition provided by [127, Proposition 4.52] (see also [2, Theorems 2.17 and 3.12] for the original reference) to the convex region $\widetilde{\Omega}$ and $\widetilde{\boldsymbol{\tau}} \in \mathbb{H}(\mathbf{div};\widetilde{\Omega})$, we deduce that there exist $\widetilde{\mathbf{z}} \in \mathbf{H}^2(\widetilde{\Omega})$ and $\widetilde{\boldsymbol{\chi}} := \begin{pmatrix} \widetilde{\boldsymbol{\chi}}_1 \\ \widetilde{\boldsymbol{\chi}}_2 \\ \widetilde{\boldsymbol{\chi}}_3 \end{pmatrix} \in \mathbb{H}^1(\widetilde{\Omega})$, with $\widetilde{\boldsymbol{\chi}}_i := (\widetilde{\chi}_{i1}, \widetilde{\chi}_{i2}, \widetilde{\chi}_{i3})^{\mathtt{t}} \in \mathbf{H}^1(\widetilde{\Omega})$, $i \in \{1,2,3\}$, such that

$$\widetilde{\boldsymbol{\tau}} = \nabla \widetilde{\mathbf{z}} + \underline{\mathbf{curl}}(\widetilde{\boldsymbol{\chi}}) \quad \text{in} \quad \widetilde{\Omega} \quad \text{and} \quad \|\widetilde{\mathbf{z}}\|_{2,\widetilde{\Omega}} + \|\widetilde{\boldsymbol{\chi}}\|_{1,\widetilde{\Omega}} \leq C\,\|\widetilde{\boldsymbol{\tau}}\|_{\mathbf{div},\widetilde{\Omega}} \leq \widetilde{C}\,\|\boldsymbol{\tau}\|_{\mathbf{div},\Omega}\,, \tag{1.48}$$

where the last inequality makes use of (1.47), thus yielding $\widetilde{C} = C\left\{1 + \widetilde{c}^2\right\}^{1/2}$. Finally, defining $\mathbf{z} := \widetilde{\mathbf{z}}|_{\Omega} \in \mathbf{H}^2(\Omega)$ and $\boldsymbol{\chi} := \widetilde{\boldsymbol{\chi}}|_{\Omega} \in \mathbb{H}^1(\Omega)$, noting that certainly $\widetilde{\boldsymbol{\tau}}|_{\Omega} = \boldsymbol{\tau}$, and employing (1.48), we arrive at (1.44) and conclude the proof. □

Now we are in conditions to estimate $E(\widehat{\boldsymbol{\tau}})$ (cf. (1.43)). To do that, we let $\boldsymbol{\tau} \in \mathbb{H}_0$ and bound $|E(\widehat{\boldsymbol{\tau}})|$ for a specific choice of $\boldsymbol{\tau}_h \in \mathbb{H}_{0,h}$. More precisely, the Helmholtz decomposition of $\boldsymbol{\tau}$ given by Lemma 1.7 suggests to define $\boldsymbol{\tau}_h$ through what we call a discrete Helmholtz decomposition. In other words, with the notations employed in the above proof we now let $\boldsymbol{\chi}_h := \begin{pmatrix} \boldsymbol{\chi}_{1h} \\ \boldsymbol{\chi}_{2h} \\ \boldsymbol{\chi}_{3h} \end{pmatrix}$, where $\boldsymbol{\chi}_{ih} := \mathbf{I}_h(\boldsymbol{\chi}_i)$, $i \in \{1,2,3\}$, and define

$$\boldsymbol{\tau}_h \;:=\; \mathscr{E}_h^k(\nabla \mathbf{z}) \;+\; \underline{\mathbf{curl}}(\boldsymbol{\chi}_h) \;-\; d_h\,\mathbb{I}\,, \tag{1.49}$$

where $\mathscr{E}_h^k$ is the Raviart-Thomas interpolation operator introduced before (cf. (1.23) and (1.24)), and the constant d_h is chosen so that $\boldsymbol{\tau}_h$, which is already in $\mathbb{RT}_k(\mathcal{T}_h)$, belongs to $\mathbb{H}_{0,h}$. Equivalently, $\boldsymbol{\tau}_h$ is the $\mathbb{H}_0$-component of $\mathscr{E}_h^k(\nabla \mathbf{z}) + \underline{\mathbf{curl}}(\boldsymbol{\chi}_h) \in \mathbb{RT}_k(\mathcal{T}_h)$, which yields

$$d_h \;=\; \frac{1}{3\,|\Omega|}\int_{\Omega} \operatorname{tr}\big(\mathscr{E}_h^k(\nabla \mathbf{z}) \;+\; \underline{\mathbf{curl}}(\boldsymbol{\chi}_h)\big) \;=\; -\,\frac{1}{3\,|\Omega|}\int_{\Omega} \operatorname{tr}\big(\nabla \mathbf{z} - \mathscr{E}_h^k(\nabla \mathbf{z}) \;+\; \underline{\mathbf{curl}}(\boldsymbol{\chi} - \boldsymbol{\chi}_h)\big)\,, \tag{1.50}$$

where the second equality makes use of the fact that $\boldsymbol{\tau} = \nabla \mathbf{z} + \underline{\mathbf{curl}}(\boldsymbol{\chi})$ is taken in $\mathbb{H}_0$. According to the aforementioned Helmholtz decomposition of $\boldsymbol{\tau}$, we refer to (1.49) as the announced discrete Helmholtz decomposition of $\boldsymbol{\tau}_h$. Therefore, we can write

$$\widehat{\boldsymbol{\tau}} \;:=\; \nabla \mathbf{z} \;-\; \mathscr{E}_h^k(\nabla \mathbf{z}) \;+\; \underline{\mathbf{curl}}(\boldsymbol{\chi} - \boldsymbol{\chi}_h) \;+\; d_h\,\mathbb{I}\,, \tag{1.51}$$

which, using the property (1.25), yields

$$\mathbf{div}(\widehat{\boldsymbol{\tau}}) \;=\; \mathbf{div}(\nabla \mathbf{z} - \mathscr{E}_h^k(\nabla \mathbf{z})) \;=\; (\mathbf{I} - \mathscr{P}_h^k)(\mathbf{div}(\nabla \mathbf{z})) \;=\; (\mathbf{I} - \mathscr{P}_h^k)(\mathbf{div}(\boldsymbol{\tau}))\,.$$

In this way, since $\mathscr{P}_h^k : \mathbf{L}^2(\Omega) \to \mathbf{Q}_h$ is the orthogonal projector and $\mathbf{u}_h \in \mathbf{Q}_h$, we readily see from the foregoing equation that

$$\int_{\Omega} \mathbf{u}_h \cdot \mathbf{div}(\widehat{\boldsymbol{\tau}}) \;=\; \int_{\Omega} \mathbf{u}_h \cdot (\mathbf{I} - \mathscr{P}_h^k)(\mathbf{div}(\boldsymbol{\tau})) \;=\; 0\,. \tag{1.52}$$

In turn, taking into account that $\boldsymbol{\rho}_h \in \mathbb{H}_{0,h}$, and recalling the expressions for $c_{\mathbf{g}}$ and d_h given by (1.38) and (1.50), respectively, we easily deduce from the definition of E (cf. (1.43)) that

$$E(d_h\,\mathbb{I}) \;=\; d_h \int_{\Gamma} \mathbf{g} \cdot \mathbf{n} \;=\; -\,c_{\mathbf{g}} \int_{\Omega} \operatorname{tr}\big(\nabla \mathbf{z} - \mathscr{E}_h^k(\nabla \mathbf{z}) \;+\; \underline{\mathbf{curl}}(\boldsymbol{\chi} - \boldsymbol{\chi}_h)\big)\,. \tag{1.53}$$

Hence, replacing (1.51) into (1.43), and employing (1.52) and (1.53), we find that $E(\widehat{\boldsymbol{\tau}})$ can be decomposed as

$$E(\widehat{\boldsymbol{\tau}}) \;=\; E_1(\mathbf{z}) \;+\; E_2(\boldsymbol{\chi})\,, \tag{1.54}$$

where

$$E_1(\mathbf{z}) := \langle(\nabla\mathbf{z} - \mathscr{E}_h^k(\nabla\mathbf{z}))\mathbf{n}, \mathbf{g}\rangle_\Gamma - c_{\mathbf{g}}\int_\Omega \mathrm{tr}(\nabla\mathbf{z} - \mathscr{E}_h^k(\nabla\mathbf{z}))$$
$$- \frac{1}{\mu}\int_\Omega \boldsymbol{\rho}_h^{\mathtt{d}} : (\nabla\mathbf{z} - \mathscr{E}_h^k(\nabla\mathbf{z})) - \frac{1}{3(3\lambda+4\mu)}\int_\Omega \mathrm{tr}(\boldsymbol{\rho}_h)\,\mathrm{tr}(\nabla\mathbf{z} - \mathscr{E}_h^k(\nabla\mathbf{z}))\,,$$

and

$$E_2(\boldsymbol{\chi}) := \langle\underline{\mathbf{curl}}(\boldsymbol{\chi} - \boldsymbol{\chi}_h)\mathbf{n}, \mathbf{g}\rangle_\Gamma - c_{\mathbf{g}}\int_\Omega \mathrm{tr}(\underline{\mathbf{curl}}(\boldsymbol{\chi} - \boldsymbol{\chi}_h))$$
$$- \frac{1}{\mu}\int_\Omega \boldsymbol{\rho}_h^{\mathtt{d}} : \underline{\mathbf{curl}}(\boldsymbol{\chi} - \boldsymbol{\chi}_h) - \frac{1}{3(3\lambda+4\mu)}\int_\Omega \mathrm{tr}(\boldsymbol{\rho}_h)\,\mathrm{tr}(\underline{\mathbf{curl}}(\boldsymbol{\chi} - \boldsymbol{\chi}_h))\,.$$

Furthermore, we note from the definition of $\boldsymbol{\rho}_h^{\mathtt{d}}$ and the equality $\mathrm{tr}(\boldsymbol{\xi}) = \boldsymbol{\xi} : \mathbb{I}$, that

$$E_1(\mathbf{z}) = \langle(\nabla\mathbf{z} - \mathscr{E}_h^k(\nabla\mathbf{z}))\mathbf{n}, \mathbf{g}\rangle_\Gamma - \int_\Omega \left(\frac{1}{\mu}\left\{\boldsymbol{\rho}_h - \frac{\lambda+\mu}{3\lambda+4\mu}\mathrm{tr}(\boldsymbol{\rho}_h)\,\mathbb{I}\right\} + c_{\mathbf{g}}\,\mathbb{I}\right) : (\nabla\mathbf{z} - \mathscr{E}_h^k(\nabla\mathbf{z}))\,, \tag{1.55}$$

and

$$E_2(\boldsymbol{\chi}) = \langle\underline{\mathbf{curl}}(\boldsymbol{\chi} - \boldsymbol{\chi}_h)\mathbf{n}, \mathbf{g}\rangle_\Gamma - \int_\Omega \left(\frac{1}{\mu}\left\{\boldsymbol{\rho}_h - \frac{\lambda+\mu}{3\lambda+4\mu}\mathrm{tr}(\boldsymbol{\rho}_h)\,\mathbb{I}\right\} + c_{\mathbf{g}}\,\mathbb{I}\right) : \underline{\mathbf{curl}}(\boldsymbol{\chi} - \boldsymbol{\chi}_h)\,. \tag{1.56}$$

The following two lemmas provide upper bounds for $|E_1(\mathbf{z})|$ and $|E_2(\boldsymbol{\chi})|$.

Lemma 1.8. *There exists $C > 0$, independent of λ and h, such that*

$$|E_1(\mathbf{z})| \le C\left\{\sum_{T\in\mathcal{T}_h}\theta_{1,T}^2\right\}^{1/2}\|\boldsymbol{\tau}\|_{\mathbf{div};\Omega}\,, \tag{1.57}$$

where

$$\theta_{1,T}^2 := h_T^2\left\|\nabla\mathbf{u}_h - \left(\frac{1}{\mu}\left\{\boldsymbol{\rho}_h - \frac{\lambda+\mu}{3\lambda+4\mu}\mathrm{tr}(\boldsymbol{\rho}_h)\,\mathbb{I}\right\} + c_{\mathbf{g}}\,\mathbb{I}\right)\right\|_{0,T}^2 + \sum_{e\in\mathcal{E}(T)\cap\mathcal{E}_h(\Gamma)} h_e\,\|\mathbf{g} - \mathbf{u}_h\|_{0,e}^2\,.$$

Proof. Since $\nabla\mathbf{z} \in \mathbb{H}^1(\Omega)$, it follows that $(\nabla\mathbf{z} - \mathscr{E}_h^k(\nabla\mathbf{z}))\mathbf{n}|_\Gamma$ belongs to $\mathbf{L}^2(\Gamma)$, whence $E_1(\mathbf{z})$ (cf. (1.55)) can be redefined as:

$$\begin{aligned} E_1(\mathbf{z}) &= \sum_{e\in\mathcal{E}_h(\Gamma)}\int_e (\nabla\mathbf{z} - \mathscr{E}_h^k(\nabla\mathbf{z}))\mathbf{n}\cdot\mathbf{g} \\ &\quad - \int_\Omega \left(\frac{1}{\mu}\left\{\boldsymbol{\rho}_h - \frac{\lambda+\mu}{3\lambda+4\mu}\mathrm{tr}(\boldsymbol{\rho}_h)\,\mathbb{I}\right\} + c_{\mathbf{g}}\,\mathbb{I}\right) : (\nabla\mathbf{z} - \mathscr{E}_h^k(\nabla\mathbf{z}))\,. \end{aligned} \tag{1.58}$$

On the other hand, since $\mathbf{u}_h|_e \in \mathbf{P}_k(e)$ for each face $e \in \mathcal{E}_h$ (in particular for each face $e \in \mathcal{E}_h(\Gamma)$), and $\nabla\mathbf{u}_h|_T \in \mathbb{P}_{k-1}(T)$ for each $T \in \mathcal{T}_h$, the identities (1.23) and (1.24) characterizing $\mathscr{E}_h^k$, yield, respectively,

$$\int_e (\nabla\mathbf{z} - \mathscr{E}_h^k(\nabla\mathbf{z}))\,\mathbf{n}\cdot\mathbf{u}_h = 0 \qquad \forall\, e \in \mathcal{E}_h(\Gamma)\,,$$

and

$$\int_T (\nabla\mathbf{z} - \mathscr{E}_h^k(\nabla\mathbf{z})) : \nabla\mathbf{u}_h = 0 \qquad \forall\, T \in \mathcal{T}_h\,.$$

Hence, introducing the above expressions into (1.58), we can write $E_1(\mathbf{z})$ as

$$
\begin{aligned}
E_1(\mathbf{z}) = & \sum_{e\in\mathcal{E}_h(\Gamma)} \int_e (\nabla\,\mathbf{z} - \mathscr{E}_h^k(\nabla\,\mathbf{z}))\mathbf{n}\cdot(\mathbf{g}-\mathbf{u}_h) \\
& + \sum_{T\in\mathcal{T}_h} \int_T \left[\nabla \mathbf{u}_h - \left(\frac{1}{\mu}\left\{\boldsymbol{\rho}_h - \frac{\lambda+\mu}{3\lambda+4\mu}\,\mathrm{tr}(\boldsymbol{\rho}_h)\,\mathbb{I}\right\} + c_{\mathbf{g}}\,\mathbb{I}\right)\right] : (\nabla\,\mathbf{z} - \mathscr{E}_h^k(\nabla\,\mathbf{z}))\,.
\end{aligned}
$$

Finally, applying the Cauchy-Schwarz inequality, the approximation properties (1.28) (with $m=1$) and (1.30), and then the fact that $\|\nabla\mathbf{z}\|_{1,\Omega} \le \|\mathbf{z}\|_{2,\Omega} \le C\|\boldsymbol{\tau}\|_{\mathbf{div},\Omega}$ by (1.44), we obtain the upper bound (1.57). □

Lemma 1.9. *Assume that $\mathbf{g}\in\mathbf{H}^1(\Gamma)$. Then, there exists $C>0$, independent of λ and h, such that*

$$
|E_2(\boldsymbol{\chi})| \;\le\; C\left\{\sum_{T\in\mathcal{T}_h}\theta_{2,T}^2\right\}^{1/2} \|\boldsymbol{\tau}\|_{\mathbf{div},\Omega}\,, \tag{1.59}
$$

where

$$
\begin{aligned}
\theta_{2,T}^2 \;:=\; & h_T^2\left\|\underline{\mathbf{curl}}\left(\frac{1}{\mu}\left\{\boldsymbol{\rho}_h - \frac{\lambda+\mu}{3\lambda+4\mu}\,\mathrm{tr}(\boldsymbol{\rho}_h)\,\mathbb{I}\right\}\right)\right\|_{0,T}^2 \\
& + \sum_{e\in\mathcal{E}(T)\cap\mathcal{E}_h(\Omega)} h_e\left\|\left[\!\left[\left(\frac{1}{\mu}\left\{\boldsymbol{\rho}_h - \frac{\lambda+\mu}{3\lambda+4\mu}\,\mathrm{tr}(\boldsymbol{\rho}_h)\,\mathbb{I}\right\} + c_{\mathbf{g}}\,\mathbb{I}\right)\times\mathbf{n}\right]\!\right]\right\|_{0,e}^2 \\
& + \sum_{e\in\mathcal{E}(T)\cap\mathcal{E}_h(\Gamma)} h_e\left\|\nabla\mathbf{g}\times\mathbf{n} - \left(\frac{1}{\mu}\left\{\boldsymbol{\rho}_h - \frac{\lambda+\mu}{3\lambda+4\mu}\,\mathrm{tr}(\boldsymbol{\rho}_h)\,\mathbb{I}\right\} + c_{\mathbf{g}}\,\mathbb{I}\right)\times\mathbf{n}\right\|_{0,e}^2 .
\end{aligned}
$$

Proof. Using the fact that $\underline{\mathbf{curl}}(\boldsymbol{\chi}-\boldsymbol{\chi}_h)\,\mathbf{n} = \mathbf{div}\,((\boldsymbol{\chi}-\boldsymbol{\chi}_h)\times\mathbf{n})$, and then integrating by parts on Γ, we find that

$$
\langle\underline{\mathbf{curl}}(\boldsymbol{\chi}-\boldsymbol{\chi}_h)\,\mathbf{n},\mathbf{g}\rangle_\Gamma \;=\; \langle\boldsymbol{\chi}-\boldsymbol{\chi}_h,\nabla\mathbf{g}\times\mathbf{n}\rangle_\Gamma \;=\; \sum_{e\in\mathcal{E}_h(\Gamma)}\int_e(\boldsymbol{\chi}-\boldsymbol{\chi}_h):(\nabla\mathbf{g}\times\mathbf{n})\,.
$$

Next, integrating by parts on each $T\in\mathcal{T}_h$, we obtain that

$$
\begin{aligned}
& \int_\Omega\left(\frac{1}{\mu}\left\{\boldsymbol{\rho}_h - \frac{\lambda+\mu}{3\lambda+4\mu}\,\mathrm{tr}(\boldsymbol{\rho}_h)\,\mathbb{I}\right\} + c_{\mathbf{g}}\,\mathbb{I}\right) : \underline{\mathbf{curl}}(\boldsymbol{\chi}-\boldsymbol{\chi}_h) \\
& = \sum_{T\in\mathcal{T}_h}\left[\int_T \underline{\mathbf{curl}}\left(\frac{1}{\mu}\left\{\boldsymbol{\rho}_h - \frac{\lambda+\mu}{3\lambda+4\mu}\,\mathrm{tr}(\boldsymbol{\rho}_h)\,\mathbb{I}\right\}\right) : (\boldsymbol{\chi}-\boldsymbol{\chi}_h)\right. \\
& \qquad \left. + \int_{\partial T}\left(\frac{1}{\mu}\left\{\boldsymbol{\rho}_h - \frac{\lambda+\mu}{3\lambda+4\mu}\,\mathrm{tr}(\boldsymbol{\rho}_h)\,\mathbb{I}\right\} + c_{\mathbf{g}}\,\mathbb{I}\right)\times\mathbf{n} : (\boldsymbol{\chi}-\boldsymbol{\chi}_h)\right] \\
& = \sum_{T\in\mathcal{T}_h}\int_T \underline{\mathbf{curl}}\left(\frac{1}{\mu}\left\{\boldsymbol{\rho}_h - \frac{\lambda+\mu}{3\lambda+4\mu}\,\mathrm{tr}(\boldsymbol{\rho}_h)\,\mathbb{I}\right\}\right) : (\boldsymbol{\chi}-\boldsymbol{\chi}_h) \\
& \qquad + \sum_{e\in\mathcal{E}_h(\Omega)}\int_e \left[\!\left[\left(\frac{1}{\mu}\left\{\boldsymbol{\rho}_h - \frac{\lambda+\mu}{3\lambda+4\mu}\,\mathrm{tr}(\boldsymbol{\rho}_h)\,\mathbb{I}\right\} + c_{\mathbf{g}}\,\mathbb{I}\right)\times\mathbf{n}\right]\!\right] : (\boldsymbol{\chi}-\boldsymbol{\chi}_h) \\
& \qquad + \sum_{e\in\mathcal{E}_h(\Gamma)}\int_e \left(\frac{1}{\mu}\left\{\boldsymbol{\rho}_h - \frac{\lambda+\mu}{3\lambda+4\mu}\,\mathrm{tr}(\boldsymbol{\rho}_h)\,\mathbb{I}\right\} + c_{\mathbf{g}}\,\mathbb{I}\right)\times\mathbf{n} : (\boldsymbol{\chi}-\boldsymbol{\chi}_h)\,.
\end{aligned}
$$

Hence, replacing the above expressions into (1.56), we can write

$$
\begin{aligned}
E_2(\boldsymbol{\chi}) \;=\; & -\sum_{T\in\mathcal{T}_h}\int_T \underline{\mathbf{curl}}\left(\frac{1}{\mu}\left\{\boldsymbol{\rho}_h - \frac{\lambda+\mu}{3\lambda+4\mu}\,\mathrm{tr}(\boldsymbol{\rho}_h)\,\mathbb{I}\right\}\right) : (\boldsymbol{\chi}-\boldsymbol{\chi}_h) \\
& - \sum_{e\in\mathcal{E}_h(\Omega)}\int_e \left[\!\!\left[\left(\frac{1}{\mu}\left\{\boldsymbol{\rho}_h - \frac{\lambda+\mu}{3\lambda+4\mu}\,\mathrm{tr}(\boldsymbol{\rho}_h)\,\mathbb{I}\right\} + c_{\mathbf{g}}\,\mathbb{I}\right)\times\mathbf{n}\right]\!\!\right] : (\boldsymbol{\chi}-\boldsymbol{\chi}_h) \\
& + \sum_{e\in\mathcal{E}_h(\Gamma)}\int_e \left[\nabla\mathbf{g}\times\mathbf{n} - \left(\frac{1}{\mu}\left\{\boldsymbol{\rho}_h - \frac{\lambda+\mu}{3\lambda+4\mu}\,\mathrm{tr}(\boldsymbol{\rho}_h)\,\mathbb{I}\right\} + c_{\mathbf{g}}\,\mathbb{I}\right)\times\mathbf{n}\right] : (\boldsymbol{\chi}-\boldsymbol{\chi}_h)\,.
\end{aligned}
$$

In addition, since $\boldsymbol{\chi}_h := \mathbf{I}_h(\boldsymbol{\chi})$, the approximation properties of $\mathbf{I}_h$ (cf. Lemma 1.6) yields

$$
\|\boldsymbol{\chi}-\boldsymbol{\chi}_h\|_{0,T} \;\leq\; c_1\, h_T\, \|\boldsymbol{\chi}\|_{1,\triangle(T)} \qquad \forall\, T\in\mathcal{T}_h\,, \tag{1.60}
$$

and

$$
\|\boldsymbol{\chi}-\boldsymbol{\chi}_h\|_{0,e} \;\leq\; c_2\, h_e^{1/2}\, \|\boldsymbol{\chi}\|_{1,\triangle(e)} \qquad \forall\, e\in\mathcal{E}_h\,. \tag{1.61}
$$

Thus, applying the Cauchy-Schwarz inequality to each term in the above expression for $E_2(\boldsymbol{\chi})$, and making use of the estimates (1.60), (1.61) and (1.44), together with the fact that $\triangle(T)$ and $\triangle(e)$ are bounded (since $\{\mathcal{T}_h\}_{h>0}$ is shape-regular), we derive the upper bound (1.59). □

Finally, it follows from the decomposition (1.54) of E and Lemmas 4.3 and 4.4 that

$$
|E(\widehat{\boldsymbol{\tau}})| \;\leq\; C\left\{\sum_{T\in\mathcal{T}_h}(\theta_{1,T}^2+\theta_{2,T}^2)\right\}^{1/2} \|\boldsymbol{\tau}\|_{\mathbf{div},\Omega} \quad \forall\,\boldsymbol{\tau}\in\mathbb{H}_0\,,
$$

which, gives an upper bound for the supremum on the right hand side of (1.41) (cf. Lemma 4.1).

In this way, and noting that

$$
\|\mathbf{f}+\mathbf{div}(\boldsymbol{\rho}_h)\|_{0,\Omega}^2 \;=\; \sum_{T\in\mathcal{T}_h}\|\mathbf{f}+\mathbf{div}(\boldsymbol{\rho}_h)\|_{0,T}^2\,,
$$

we conclude from Lemma 4.1 the reliability of $\boldsymbol{\theta}$ (upper bound in (1.40)).

1.4.3 Efficiency

In this section we prove the efficiency of our *a posteriori* error estimator $\boldsymbol{\theta}$ (lower bound in (1.40)). In other words, we derive suitable upper bounds for the six terms defining the local error indicator θ_T^2 (cf. (1.37)). We first notice, using that $\mathbf{f} = -\mathbf{div}(\boldsymbol{\rho})$ in Ω, that there holds

$$
\|\mathbf{f}+\mathbf{div}(\boldsymbol{\rho}_h)\|_{0,T}^2 \;=\; \|\mathbf{div}(\boldsymbol{\rho}-\boldsymbol{\rho}_h)\|_{0,T}^2 \;\leq\; \|\boldsymbol{\rho}-\boldsymbol{\rho}_h\|_{\mathbf{div},T}^2\,. \tag{1.62}
$$

Next, in order to bound the terms involving the mesh parameters h_T and h_e, we proceed similarly as in [32] and [33] (see also [68]), and apply results ultimately based on inverse inequalities (see [37]) and the localization technique introduced in [126], which is based on tetrahedron-bubble and face-bubble functions. To this end, we now introduce further notations and preliminary results. Given $T\in\mathcal{T}_h$ and $e\in\mathcal{E}(T)$, we let ψ_T and ψ_e be the usual tetrahedron-bubble and face-bubble functions, respectively (see (1.5) and (1.6) in [126]), which satisfy:

i) $\psi_T \in \mathrm{P}_4(T)$, $\mathrm{supp}(\psi_T) \subseteq T$, $\psi_T = 0$ on ∂T, and $0 \le \psi_T \le 1$ in T.

ii) $\psi_e|_T \in \mathrm{P}_3(T)$, $\mathrm{supp}(\psi_e) \subseteq \omega_e := \cup\{T' \in \mathcal{T}_h \,:\, e \in \mathcal{E}(T')\}$, $\psi_e = 0$ on $\partial T \setminus e$, and $0 \le \psi_e \le 1$ in ω_e.

We also recall from [125] that, given $k \in \mathbb{N} \cup \{0\}$, there exists a linear operator $L : C(e) \to C(T)$ that satisfies $L(p) \in \mathrm{P}_k(T)$ and $L(p)|_e = p \quad \forall\, p \in \mathrm{P}_k(e)$. A corresponding vectorial version of L, that is the componentwise application of L, is denoted by $\mathbf{L}$. Additional properties of ψ_T, ψ_e and L are collected in the following lemma.

Lemma 1.10. *Given $k \in \mathbb{N} \cup \{0\}$, there exist positive constants c_1, c_2, and c_3, depending only on k and the shape regularity of the triangulations (minimum angle condition), such that for each $T \in \mathcal{T}_h$ and $e \in \mathcal{E}(T)$, there hold*

$$\|q\|_{0,T}^2 \;\le\; c_1\, \|\psi_T^{1/2}\, q\|_{0,T}^2 \qquad \forall\, q \in P_k(T)\,, \tag{1.63}$$

$$\|p\|_{0,e}^2 \;\le\; c_2\, \|\psi_e^{1/2}\, p\|_{0,e}^2 \qquad \forall\, p \in P_k(e)\,, \tag{1.64}$$

and

$$\|\psi_e^{1/2}\, L(p)\|_{0,T}^2 \;\le\; c_3\, h_e\, \|p\|_{0,e}^2 \quad \forall\, p \in P_k(e)\,. \tag{1.65}$$

Proof. See [125, Lemma 4.1]. □

The following inverse estimate will also be used.

Lemma 1.11. *Let $\ell, m \in \mathbb{N} \cup \{0\}$ such that $\ell \le m$. Then, there exists $c_4 > 0$, depending only on k, ℓ, m and the shape regularity of the triangulations, such that for each $T \in \mathcal{T}_h$ there holds*

$$|q|_{m,T} \;\le\; c_4\, h_T^{\ell - m}\, |q|_{\ell,T} \quad \forall\, q \in P_k(T)\,. \tag{1.66}$$

Proof. See [37, Theorem 3.2.6]. □

In order to bound the boundary term of the local error estimator θ_T given by $h_e\, \|\mathbf{g} - \mathbf{u}_h\|_{0,e}^2$, $e \in \mathcal{E}_h(\Gamma)$, we will need the following discrete trace inequality.

Lemma 1.12. *There exists $c_5 > 0$, depending only on the shape regularity of the triangulations, such that for each $T \in \mathcal{T}_h$ and $e \in \mathcal{E}(T)$, there holds*

$$\|v\|_{0,e}^2 \;\le\; c_5\, \left\{ h_e^{-1}\, \|v\|_{0,T}^2 \;+\; h_e\, |v|_{1,T}^2 \right\} \quad \forall\, v \in H^1(T)\,. \tag{1.67}$$

Proof. See [3, equation (2.4)]. □

Lemma 1.13. *Let $\boldsymbol{\zeta}_h \in \mathbb{L}^2(\Omega)$ be a piecewise polynomial of degree $k \ge 0$ on each $T \in \mathcal{T}_h$. In addition, let $\boldsymbol{\zeta} \in \mathbb{L}^2(\Omega)$ be such that $\underline{\mathbf{curl}}(\boldsymbol{\zeta}) = \mathbf{0}$ on each $T \in \mathcal{T}_h$. Then, there exists $c_6 > 0$, independent of h, such that*

$$\|\underline{\mathbf{curl}}(\boldsymbol{\zeta}_h)\|_{0,T} \;\le\; c_6\, h_T^{-1}\, \|\boldsymbol{\zeta} - \boldsymbol{\zeta}_h\|_{0,T} \quad \forall\, T \in \mathcal{T}_h\,. \tag{1.68}$$

Proof. We adapt the proof of [13, Lemma 4.3]. Indeed, applying (1.63), integrating by parts, recalling that $\psi_T = 0$ on ∂T, and using the Cauchy-Schwarz inequality, we obtain

$$\begin{aligned}
\|\underline{\mathbf{curl}}(\boldsymbol{\zeta}_h)\|_{0,T}^2 &\leq c_1 \|\psi_T^{1/2}\underline{\mathbf{curl}}(\boldsymbol{\zeta}_h)\|_{0,T}^2 \;=\; c_1 \int_T \underline{\mathbf{curl}}(\boldsymbol{\zeta}_h - \boldsymbol{\zeta}) : \psi_T\, \underline{\mathbf{curl}}(\boldsymbol{\zeta}_h) \\
&= c_1 \int_T (\boldsymbol{\zeta}_h - \boldsymbol{\zeta}) : \underline{\mathbf{curl}}(\psi_T\, \underline{\mathbf{curl}}(\boldsymbol{\zeta}_h)) \;\leq\; c_1 \|\boldsymbol{\zeta} - \boldsymbol{\zeta}_h\|_{0,T} \|\underline{\mathbf{curl}}(\psi_T\, \underline{\mathbf{curl}}(\boldsymbol{\zeta}_h))\|_{0,T}\,.
\end{aligned}$$

From the inverse estimate (1.66) and the fact that $0 \leq \psi_T \leq 1$, it follows

$$\|\underline{\mathbf{curl}}(\psi_T\, \underline{\mathbf{curl}}(\boldsymbol{\zeta}_h))\|_{0,T} \;\leq\; \widetilde{c}_4\, h_T^{-1} \|\psi_T\, \underline{\mathbf{curl}}(\boldsymbol{\zeta}_h)\|_{0,T} \;\leq\; \widetilde{c}_4\, h_T^{-1}\, \|\underline{\mathbf{curl}}(\boldsymbol{\zeta}_h)\|_{0,T}\,,$$

where $\widetilde{c}_4$ depends only on c_4 (see (1.66)). This proves the lemma with $c_6 := c_1\widetilde{c}_4$. □

Lemma 1.14. *Let $\boldsymbol{\zeta}_h \in \mathbb{L}^2(\Omega)$ be a piecewise polynomial of degree $k \geq 0$ on each $T \in \mathcal{T}_h$, and let $\boldsymbol{\zeta} \in \mathbb{L}^2(\Omega)$ be such that $\underline{\mathbf{curl}}(\boldsymbol{\zeta}) = \mathbf{0}$ in Ω. Then, there exists $c_7 > 0$, independent of h, such that*

$$\|[\![\boldsymbol{\zeta}_h \times \mathbf{n}]\!]\|_{0,e} \;\leq\; c_7\, h_e^{-1/2}\, \|\boldsymbol{\zeta} - \boldsymbol{\zeta}_h\|_{0,\omega_e} \quad \forall\; e \in \mathcal{E}_h\,. \tag{1.69}$$

Proof. We adapt the proof of [13, Lemma 4.4]. Given a face $e \in \mathcal{E}_h$, we denote $\mathbf{r}_h := [\![\boldsymbol{\zeta}_h \times \mathbf{n}]\!]$ the corresponding tangential jump of $\boldsymbol{\zeta}_h$. Then, employing (1.64) and integrating by parts on each tetrahedron of ω_e, we obtain

$$\begin{aligned}
c_2^{-1}\|\mathbf{r}_h\|_{0,e}^2 &\leq \|\psi_e^{1/2}\mathbf{r}_h\|_{0,e}^2 \;=\; \|\psi_e^{1/2}\mathbf{L}(\mathbf{r}_h)\|_{0,e}^2 \;=\; \int_e \psi_e \mathbf{L}(\mathbf{r}_h) : [\![\boldsymbol{\zeta}_h \times \mathbf{n}]\!] \\
&= -\int_{\omega_e} \psi_e \mathbf{L}(\mathbf{r}_h) : \underline{\mathbf{curl}}(\boldsymbol{\zeta}_h) \;+\; \int_{\omega_e} \underline{\mathbf{curl}}(\psi_e \mathbf{L}(\mathbf{r}_h)) : \boldsymbol{\zeta}_h\,.
\end{aligned}$$

Next, since $[\![\boldsymbol{\zeta} \times \mathbf{n}]\!] = \mathbf{0}$, we deduce that

$$0 \;=\; -\int_{\omega_e} \psi_e \mathbf{L}(\mathbf{r}_h) : \underline{\mathbf{curl}}(\boldsymbol{\zeta}) \;+\; \int_{\omega_e} \underline{\mathbf{curl}}(\psi_e \mathbf{L}(\mathbf{r}_h)) : \boldsymbol{\zeta}\,,$$

and therefore

$$\begin{aligned}
c_2^{-1}\|\mathbf{r}_h\|_{0,e}^2 &\leq \int_{\omega_e} \psi_e \mathbf{L}(\mathbf{r}_h) : \underline{\mathbf{curl}}(\boldsymbol{\zeta} - \boldsymbol{\zeta}_h) - \int_{\omega_e} \underline{\mathbf{curl}}(\psi_e \mathbf{L}(\mathbf{r}_h)) : (\boldsymbol{\zeta} - \boldsymbol{\zeta}_h) \\
&= -\int_{\omega_e} \psi_e \mathbf{L}(\mathbf{r}_h) : \underline{\mathbf{curl}}(\boldsymbol{\zeta}_h) - \int_{\omega_e} \underline{\mathbf{curl}}(\psi_e \mathbf{L}(\mathbf{r}_h)) : (\boldsymbol{\zeta} - \boldsymbol{\zeta}_h)\,,
\end{aligned}$$

which, using the Cauchy-Schwarz inequality, yields

$$c_2^{-1}\|\mathbf{r}_h\|_{0,e}^2 \;\leq\; \|\psi_e \mathbf{L}(\mathbf{r}_h)\|_{0,\omega_e} \|\underline{\mathbf{curl}}(\boldsymbol{\zeta}_h)\|_{0,\omega_e} + \|\underline{\mathbf{curl}}(\psi_e \mathbf{L}(\mathbf{r}_h))\|_{0,\omega_e} \|\boldsymbol{\zeta} - \boldsymbol{\zeta}_h\|_{0,\omega_e}\,.$$

Now, applying Lemma 1.13 to each element of ω_e, and using the fact that $h_{T_e}^{-1} \leq h_e^{-1}$, it follows the existence of a constant $\widetilde{c}_6 > 0$ that depends only on c_6 (see (1.68)) such that

$$\|\underline{\mathbf{curl}}(\boldsymbol{\zeta}_h)\|_{0,\omega_e} \;\leq\; \widetilde{c}_6\, h_e^{-1}\, \|\boldsymbol{\zeta} - \boldsymbol{\zeta}_h\|_{0,\omega_e}\,. \tag{1.70}$$

On the other hand, from inverse estimate (1.66) applied to each element of ω_e, there exists a constant $\widetilde{c}_4 > 0$ that depends only on c_4 (see (1.66)) such that

$$\|\underline{\mathbf{curl}}(\psi_e \mathbf{L}(\mathbf{r}_h))\|_{0,\omega_e} \;\leq\; \widetilde{c}_4\, h_e^{-1} \|\psi_e \mathbf{L}(\mathbf{r}_h)\|_{0,\omega_e}\,, \tag{1.71}$$

whereas employing (1.65) and the fact that $0 \leq \psi_e \leq 1$, we deduce that

$$\|\psi_e \mathbf{L}(\mathbf{r}_h)\|_{0,\omega_e} \;\leq\; c_3^{1/2}\, h_e^{1/2} \|\mathbf{r}_h\|_{0,e}\,. \tag{1.72}$$

Finally (1.69) follows easily from (1.70), (1.71) and (1.72), with $c_7 := c_2 c_3^{1/2} \max\{\widetilde{c}_4, \widetilde{c}_6\}$. □

We now apply Lemmas 1.13 and 1.14 to bound the other two terms defining θ_T^2. For this purpose, we define for each $T \in \mathcal{T}_h$ the tensors

$$\boldsymbol{\zeta}_h \;:=\; \frac{1}{\mu}\left\{\boldsymbol{\rho}_h - \frac{\lambda+\mu}{3\lambda+4\mu}\,\mathrm{tr}(\boldsymbol{\rho}_h)\,\mathbb{I}\right\} \,+\, c_{\mathbf{g}}\,\mathbb{I} \quad \text{in} \quad T \tag{1.73}$$

and

$$\boldsymbol{\zeta} \;:=\; \frac{1}{\mu}\left\{\boldsymbol{\rho} - \frac{\lambda+\mu}{3\lambda+4\mu}\,\mathrm{tr}(\boldsymbol{\rho})\,\mathbb{I}\right\} \,+\, c_{\mathbf{g}}\,\mathbb{I} \quad \text{in} \quad T\,, \tag{1.74}$$

then, using the triangle inequality, the fact that $\dfrac{\lambda+\mu}{3\lambda+4\mu} < 1$, and the continuity of $\boldsymbol{\tau} \mapsto \mathrm{tr}(\boldsymbol{\tau})$, we readily deduce that

$$\|\boldsymbol{\zeta} - \boldsymbol{\zeta}_h\|_{0,T} \;\le\; \frac{4}{\mu}\|\boldsymbol{\rho} - \boldsymbol{\rho}_h\|_{0,T} \qquad \forall\, T \in \mathcal{T}_h\,. \tag{1.75}$$

Lemma 1.15. *There exist $C_1, C_2 > 0$, independent of h and λ, such that*

$$h_T^2 \left\| \underline{\mathbf{curl}}\left(\frac{1}{\mu}\left\{\boldsymbol{\rho}_h - \frac{\lambda+\mu}{3\lambda+4\mu}\,\mathrm{tr}(\boldsymbol{\rho}_h)\,\mathbb{I}\right\}\right)\right\|_{0,T}^2 \;\le\; C_1\,\|\boldsymbol{\rho} - \boldsymbol{\rho}_h\|_{0,T}^2 \quad \forall\, T \in \mathcal{T}_h \tag{1.76}$$

and

$$h_e \left\| \left[\!\left[\left(\frac{1}{\mu}\left\{\boldsymbol{\rho}_h - \frac{\lambda+\mu}{3\lambda+4\mu}\,\mathrm{tr}(\boldsymbol{\rho}_h)\,\mathbb{I}\right\} + c_{\mathbf{g}}\,\mathbb{I}\right) \times \mathbf{n} \right]\!\right] \right\|_{0,e}^2 \;\le\; C_2\,\|\boldsymbol{\rho} - \boldsymbol{\rho}_h\|_{0,\omega_e}^2 \quad \forall\, e \in \mathcal{E}_h(\Omega). \tag{1.77}$$

Proof. We begin by applying Lemma 1.13 to the tensors (1.73) and (1.74), and then using (1.75), we obtain (1.76) with $C_1 := \frac{16}{\mu^2} c_6$. Analogously, applying Lemma 1.14 to the tensors (1.73) and (1.74), and then using (1.75), we obtain (1.77) with $C_2 := \frac{16}{\mu^2} c_7$. $\square$

The remaining three terms are bounded next. For this purpose, we will apply Lemmas 1.10, 1.11 and 1.12.

Lemma 1.16. *There exists $C_3 > 0$, independent of h and λ, such that for each $T \in \mathcal{T}_h$*

$$h_T^2 \left\| \nabla \mathbf{u}_h - \left(\frac{1}{\mu}\left\{\boldsymbol{\rho}_h - \frac{\lambda+\mu}{3\lambda+4\mu}\,\mathrm{tr}(\boldsymbol{\rho}_h)\,\mathbb{I}\right\} + c_{\mathbf{g}}\,\mathbb{I}\right)\right\|_{0,T}^2 \;\le\; C_3\,\left\{\|\mathbf{u} - \mathbf{u}_h\|_{0,T}^2 + h_T^2\,\|\boldsymbol{\rho} - \boldsymbol{\rho}_h\|_{0,T}^2\right\}. \tag{1.78}$$

Proof. We adapt the proof of [72, Lemma 4.13]. In fact, given $T \in \mathcal{T}_h$, we denote $\boldsymbol{\chi}_T := \nabla \mathbf{u}_h - \boldsymbol{\zeta}_h$ in T, where $\boldsymbol{\zeta}_h$ is given by (1.73). Then, applying (1.63), using that $\nabla \mathbf{u} = \boldsymbol{\zeta}$ in Ω, where $\boldsymbol{\zeta}$ is given by (1.74), and integrating by parts, we find that

$$\begin{aligned}
\|\boldsymbol{\chi}_T\|_{0,T}^2 \;&\le\; c_1\,\|\psi_T^{1/2}\,\boldsymbol{\chi}_T\|_{0,T}^2 \;=\; c_1 \int_T \psi_T\,\boldsymbol{\chi}_T : (\nabla \mathbf{u}_h - \boldsymbol{\zeta}_h) \\
&=\; c_1 \int_T \psi_T\,\boldsymbol{\chi}_T : \left\{\nabla(\mathbf{u}_h - \mathbf{u}) + (\boldsymbol{\zeta} - \boldsymbol{\zeta}_h)\right\} \\
&=\; c_1 \left\{\int_T \mathbf{div}(\psi_T\,\boldsymbol{\chi}_T)\cdot(\mathbf{u} - \mathbf{u}_h) + \int_T \psi_T\,\boldsymbol{\chi}_T : (\boldsymbol{\zeta} - \boldsymbol{\zeta}_h)\right\}.
\end{aligned}$$

Then, applying the Cauchy-Schwarz inequality, the inverse estimate (1.66), the fact that $0 \le \psi_T \le 1$, and the estimate (1.75), we get

$$\|\boldsymbol{\chi}_T\|_{0,T}^2 \;\le\; c_1\,\left\{(3\bar{c}_4)^{1/2}\,h_T^{-1}\,\|\mathbf{u} - \mathbf{u}_h\|_{0,T} + \frac{4}{\mu}\|\boldsymbol{\rho} - \boldsymbol{\rho}_h\|_{0,T}\right\}\,\|\boldsymbol{\chi}_T\|_{0,T}\,,$$

where $\bar{c}_4$ is a constant that depends only on c_4 (see (1.66)). Hence,

$$h_T^2 \|\boldsymbol{\chi}_T\|_{0,T} \;\leq\; C_3 \left\{ \|\mathbf{u} - \mathbf{u}_h\|_{0,T}^2 + h_T^2 \|\boldsymbol{\rho} - \boldsymbol{\rho}_h\|_{0,T}^2 \right\},$$

where $C_3 := c_1^2 \left(\frac{4\sqrt{3\bar{c}_4}}{\mu} + \max\left\{ 3\bar{c}_4, \frac{16}{\mu^2} \right\} \right)$ is independent of h and λ, which completes the proof. □

Lemma 1.17. *Assume that* $\mathbf{g}$ *is piecewise polynomial. Then, there exists* $C_4 > 0$*, independent of* h *and* λ*, such that for each* $e \in \mathcal{E}_h(\Gamma)$ *there holds*

$$h_e \left\| \left(\nabla \mathbf{g} - \frac{1}{\mu} \left\{ \boldsymbol{\rho}_h - \frac{\lambda + \mu}{3\lambda + 4\mu} \operatorname{tr}(\boldsymbol{\rho}_h) \mathbb{I} \right\} - c_{\mathbf{g}} \mathbb{I} \right) \times \mathbf{n} \right\|_{0,e}^2 \;\leq\; C_4 \|\boldsymbol{\rho} - \boldsymbol{\rho}_h\|_{0,T_e}^2, \tag{1.79}$$

where T_e *is the tetrahedron of* $\mathcal{T}_h$ *having* e *as a face.*

Proof. Given $e \in \mathcal{E}_h(\Gamma)$ we denote $\boldsymbol{\chi}_e := (\nabla \mathbf{g} - \boldsymbol{\zeta}_h) \times \mathbf{n}$ on e. Then, applying (1.64) and the extension operator $\mathbf{L} : \mathbf{C}(e) \to \mathbf{C}(T)$, we obtain that

$$\begin{aligned} \|\boldsymbol{\chi}_e\|_{0,e}^2 \;&\leq\; c_2 \|\psi_e^{1/2} \boldsymbol{\chi}_e\|_{0,e}^2 \;=\; c_2 \int_e \psi_e \, \boldsymbol{\chi}_e : \left\{ (\nabla \mathbf{g} - \boldsymbol{\zeta}_h) \times \mathbf{n} \right\} \\ &=\; c_2 \int_{\partial T_e} \psi_e \, \mathbf{L}(\boldsymbol{\chi}_e) : \left\{ (\nabla \mathbf{u} - \boldsymbol{\zeta}_h) \times \mathbf{n} \right\}. \end{aligned}$$

Now, integrating by parts, and using that $\nabla \mathbf{u} = \boldsymbol{\zeta}$ in T_e, we find that

$$\int_{\partial T_e} \psi_e \, \mathbf{L}(\boldsymbol{\chi}_e) : \left\{ (\nabla \mathbf{u} - \boldsymbol{\zeta}_h) \times \mathbf{n} \right\} \;=\; \int_{T_e} (\boldsymbol{\zeta} - \boldsymbol{\zeta}_h) : \underline{\mathbf{curl}}(\psi_e \, \mathbf{L}(\boldsymbol{\chi}_e)) + \int_{T_e} \underline{\mathbf{curl}}(\boldsymbol{\zeta}_h) : \psi_e \, \mathbf{L}(\boldsymbol{\chi}_e).$$

Then, applying the Cauchy-Schwarz inequality, the inverse estimate (1.66) and Lemma 1.13, we deduce that

$$\|\boldsymbol{\chi}_e\|_{0,e}^2 \;\leq\; c_2 (c_4 + c_6) \, h_{T_e}^{-1} \, \|\boldsymbol{\zeta} - \boldsymbol{\zeta}_h\|_{0,T_e} \|\psi_e \mathbf{L}(\boldsymbol{\chi}_e)\|_{0,T_e}.$$

In turn, recalling that $0 \leq \psi_e \leq 1$ and using (1.65), we can write

$$\|\psi_e \mathbf{L}(\boldsymbol{\chi}_e)\|_{0,T_e} \;\leq\; \|\psi_e^{1/2} \mathbf{L}(\boldsymbol{\chi}_e)\|_{0,T_e} \;\leq\; c_3^{1/2} \, h_e^{1/2} \|\boldsymbol{\chi}_e\|_{0,T_e},$$

which, combined with the foregoing inequality, the fact that $h_e \leq h_{T_e}$, and the estimate (1.75), yield

$$h_e \, \|\boldsymbol{\chi}_e\|_{0,e}^2 \;\leq\; \frac{16}{\mu^2} c_2^2 c_3 (c_4 + c_6)^2 \, \|\boldsymbol{\rho} - \boldsymbol{\rho}_h)\|_{0,T_e}^2.$$

This completes the proof of (1.79) with $C_4 := \frac{16}{\mu^2} c_2^2 c_3 (c_4 + c_6)^2$. □

We remark here that if $\mathbf{g}$ were not piecewise polynomial but sufficiently smooth, then higher order terms given by the errors arising from suitable polynomial approximations would appear in (1.40). This explains the eventual expression *h.o.t.* in (1.40).

Lemma 1.18. *There exists* $C_5 > 0$*, independent of* h *and* λ*, such that for each* $e \in \mathcal{E}_h(\Gamma)$ *there holds*

$$h_e \, \|\mathbf{g} - \mathbf{u}_h\|_{0,e}^2 \;\leq\; C_5 \left\{ \|\mathbf{u} - \mathbf{u}_h\|_{0,T_e}^2 + h_{T_e}^2 \, \|\boldsymbol{\rho} - \boldsymbol{\rho}_h\|_{0,T_e}^2 \right\}, \tag{1.80}$$

where T_e *is the tetrahedron of* $\mathcal{T}_h$ *having* e *as a face.*

Proof. We adapt the proof of [83, Lemma 4.14]. Indeed, applying the discrete trace inequality given by (1.67) of Lemma 1.12, together with the fact that $\mathbf{u} = \mathbf{g}$ on Γ and $\nabla \mathbf{u} = \boldsymbol{\zeta}$ in Ω, we easily obtain that for each $e \in \mathcal{E}_h(\Gamma)$ there holds

$$\begin{aligned}
\|\mathbf{g} - \mathbf{u}_h\|_{0,e}^2 &= \|\mathbf{u} - \mathbf{u}_h\|_{0,e}^2 \;\leq\; c_5 \left\{ h_e^{-1} \|\mathbf{u} - \mathbf{u}_h\|_{0,T_e}^2 + h_e |\mathbf{u} - \mathbf{u}_h|_{1,T_e}^2 \right\} \\
&= c_5 \left\{ h_e^{-1} \|\mathbf{u} - \mathbf{u}_h\|_{0,T_e}^2 + h_e \|\nabla \mathbf{u} - \nabla \mathbf{u}_h\|_{0,T_e}^2 \right\} \\
&\leq c_5 \left\{ h_e^{-1} \|\mathbf{u} - \mathbf{u}_h\|_{0,T_e}^2 + h_e \|\boldsymbol{\zeta} - \boldsymbol{\zeta}_h + \boldsymbol{\zeta}_h - \nabla \mathbf{u}_h\|_{0,T_e}^2 \right\} \\
&= c_5 \left\{ h_e^{-1} \|\mathbf{u} - \mathbf{u}_h\|_{0,T_e}^2 + 2 h_e \left\{ \|\boldsymbol{\zeta} - \boldsymbol{\zeta}_h\|_{0,T_e}^2 + \|\nabla \mathbf{u}_h - \boldsymbol{\zeta}_h\|_{0,T_e}^2 \right\} \right\} ,
\end{aligned}$$

which, using that $h_e \leq h_{T_e}$, gives

$$h_e \, \|\mathbf{g} - \mathbf{u}_h\|_{0,e}^2 \;\leq\; c_5 \left\{ \|\mathbf{u} - \mathbf{u}_h\|_{0,T_e}^2 + 2 h_{T_e}^2 \left\{ \|\boldsymbol{\zeta} - \boldsymbol{\zeta}_h\|_{0,T_e}^2 + \|\nabla \mathbf{u}_h - \boldsymbol{\zeta}_h\|_{0,T_e}^2 \right\} \right\} .$$

This estimate, the upper bound given by (1.75), and Lemma 1.16 yield (1.80) with the constant $C_5 := c_5 \left(2 C_3 + \max\{1, \frac{32}{\mu}\}\right)$. □

Finally, the efficiency of $\boldsymbol{\theta}$ follows straightforwardly from the estimate (1.62), together with Lemmas 1.15 throughout 1.18, after summing up over $T \in \mathcal{T}_h$ and using that the number of tetrahedra on each domain ω_e is bounded by two.

1.5 Numerical results

In this section, we present some numerical results in R^3 illustrating the performance of the mixed finite element scheme (1.20), confirming the reliability and efficiency of the *a posteriori* error estimator $\boldsymbol{\theta}$ (cf. (1.39)) analyzed in Section 4, and showing the behaviour of the associated adaptive algorithm. In all the computations we consider the specific finite element subspaces $\mathbb{H}_{0,h}$ and $\mathbf{Q}_h$ given by (1.19) with $k \in \{0, 1, 2\}$. In addition, similarly as in [64] and [69], the zero integral mean condition for tensors in the space $\mathbb{H}_{0,h}$ is imposed via a real Lagrange multiplier, which actually means that, instead of (1.20), we solve the modified discrete scheme given by: Find $(\boldsymbol{\rho}_h, (\mathbf{u}_h, \xi_h)) \in \mathbb{H}_h \times (\mathbf{Q}_h \times \mathrm{R})$ such that

$$\begin{aligned}
a(\boldsymbol{\rho}_h, \boldsymbol{\tau}_h) \,+\, b(\boldsymbol{\tau}_h, \mathbf{u}_h) \,+\, \xi_h \int_\Omega \operatorname{tr}(\boldsymbol{\tau}_h) &= \langle \boldsymbol{\tau}_h \mathbf{n} \,, \mathbf{g} \rangle_\Gamma \qquad \forall\, \boldsymbol{\tau}_h \in \mathbb{H}_h \,, \\
b(\boldsymbol{\rho}_h, \mathbf{v}_h) \,+\, \eta_h \int_\Omega \operatorname{tr}(\boldsymbol{\rho}_h) &= -\int_\Omega \mathbf{f} \cdot \mathbf{v}_h \qquad \forall\, (\mathbf{v}_h, \eta_h) \in \mathbf{Q}_h \times \mathrm{R} \,.
\end{aligned} \tag{1.81}$$

Notice that ξ_h, known in advance to be equal to $c_{\mathbf{g}}$ (cf. (1.38)), which arises after taking $\boldsymbol{\tau}_h = \mathbb{I}$ and $(\mathbf{v}_h, \eta_h) = (\mathbf{0}, 1)$ in (1.81), is an artificial unknown introduced here just to keep the symmetry of (1.81).

We begin by introducing additional notations. In what follows N stands for the total number of degrees of freedom (unknowns) of (1.20), which, as proved by (1.21) for $k = 0$ (see also [79, Section 4]), behaves asymptotically as 9 times the number of tetrahedra of each triangulation. This factor increases to 12.5 when we use the three-dimensional PEERS (see, e.g. [107, Definition 3.1]). In order to confirm the above factor and those indicated for $k = 1$ and $k = 2$ right after (1.21), in all the numerical tables to be displayed below we include a column with the ratio N/m, where m is the number of tetrahedra of each triangulation. In turn, the individual and total errors of the unknowns pseudostress $\boldsymbol{\rho}$ and displacement $\mathbf{u}$ are given by

$$\mathtt{e}(\boldsymbol{\rho}) \;:=\; \|\boldsymbol{\rho}-\boldsymbol{\rho}_h\|_{\mathbf{div},\Omega}\,, \quad \mathtt{e}(\mathbf{u}) \;:=\; \|\mathbf{u}-\mathbf{u}_h\|_{0,\Omega}\,, \quad \text{and} \quad \mathtt{e}(\boldsymbol{\rho},\mathbf{u}) \;:=\; \Big\{[\mathtt{e}(\boldsymbol{\rho})]^2+[\mathtt{e}(\mathbf{u})]^2\Big\}^{1/2},$$

whereas the effectivity index with respect to $\boldsymbol{\theta}$ is defined by

$$\mathtt{eff}(\boldsymbol{\theta}) \;:=\; \mathtt{e}(\boldsymbol{\rho},\mathbf{u})\;/\;\boldsymbol{\theta}\,.$$

Then, we define the experimental rates of convergence

$$\mathtt{r}(\boldsymbol{\rho}) \;:=\; \frac{\log(\mathtt{e}(\boldsymbol{\rho})/\mathtt{e}'(\boldsymbol{\rho}))}{\log(h/h')}\,, \quad \mathtt{r}(\mathbf{u}) \;:=\; \frac{\log(\mathtt{e}(\mathbf{u})/\mathtt{e}'(\mathbf{u}))}{\log(h/h')}\,, \quad \text{and} \quad \mathtt{r}(\boldsymbol{\rho},\mathbf{u}) \;:=\; \frac{\log(\mathtt{e}(\boldsymbol{\rho},\mathbf{u})/\mathtt{e}'(\boldsymbol{\rho},\mathbf{u}))}{\log(h/h')}\,,$$

where $\mathtt{e}$ and $\mathtt{e}'$ denote the corresponding errors at two consecutive triangulations with mesh sizes h and h', respectively. However, when the adaptive algorithm is applied (see details below), the expression $\log(h/h')$ appearing in the computation of the above rates is replaced by $-\frac{1}{2}\log(N/N')$, where N and N', denote the corresponding degrees of freedom of each triangulation. In addition, we also define

$$\mathtt{e}_0(\boldsymbol{\sigma}) \;:=\; \|\boldsymbol{\sigma}-\boldsymbol{\sigma}_h\|_{0,\Omega}\,, \quad \mathtt{e}_{\mathbf{div}}(\boldsymbol{\sigma}) \;:=\; \left\{\sum_{T\in\mathcal{T}_h}\|\boldsymbol{\sigma}-\boldsymbol{\sigma}_h\|^2_{\mathbf{div},T}\right\}^{1/2},$$

$$\mathtt{e}_0^\star(\boldsymbol{\sigma}) \;:=\; \|\boldsymbol{\sigma}-\boldsymbol{\sigma}_h^\star\|_{0,\Omega}\,, \quad \text{and} \quad \mathtt{e}^\star_{\mathbf{div}}(\boldsymbol{\sigma}) \;:=\; \left\{\sum_{T\in\mathcal{T}_h}\|\boldsymbol{\sigma}-\boldsymbol{\sigma}_h^\star\|^2_{\mathbf{div},T}\right\}^{1/2},$$

the corresponding errors of stress $\boldsymbol{\sigma}$. Hence, similarly as before, we also denote by $\mathtt{r}_0(\boldsymbol{\sigma})$, $\mathtt{r}_{\mathbf{div}}(\boldsymbol{\sigma})$, $\mathtt{r}_0^\star(\boldsymbol{\sigma})$ and $\mathtt{r}^\star_{\mathbf{div}}(\boldsymbol{\sigma})$, the experimental rates of convergence. Here, $\boldsymbol{\sigma}_h$ is the approximation given by the postprocesing formula (1.22), whereas $\boldsymbol{\sigma}_h^\star$ is introduced in (1.33).

Next, we recall that given the Young modulus E and the Poisson ratio ν of an isotropic linear elastic solid, the corresponding Lamé parameters are defined as

$$\mu \;:=\; \frac{E}{2(1+\nu)} \quad \text{and} \quad \lambda \;:=\; \frac{E\nu}{(1+\nu)(1-2\nu)}\,.$$

In the examples we fix $E = 1$ and take $\nu \in \{0.3000, 0.4900, 0.4999\}$, which gives the following values of μ and λ:

ν	μ	λ
0.3000	0.3846	0.5769
0.4900	0.3356	16.4430
0.4999	0.3333	1666.4444

The cases $\nu = 0.4900$ and $\nu = 0.4999$ correspond to materials showing nearly incompressible behaviour.

The numerical results presented below were obtained using a C^{++} code. In turn, the linear systems were solved using the Conjugate Gradient method as main solver, and the individual errors are computed on each tetrahedron using a Gaussian quadrature rule. For the adaptive mesh generation, we use the software TetGen developed in [120]. The three examples to be considered in this section are described next. Example 1 is employed to illustrate the performance of the mixed finite element scheme and to confirm the reliability and efficiency of the *a posteriori* error estimator. Then, Example 2 and 3 are utilized to show the behaviour of the adaptive algorithm associated with $\boldsymbol{\theta}$, which apply the following procedure from [126]:

(1) Start with a coarse mesh $\mathcal{T}_h$.

(2) Solve the discrete problem (1.20) for the actual mesh $\mathcal{T}_h$.

(3) Compute θ_T for each tetrahedron $T \in \mathcal{T}_h$.

(4) Evaluate stopping criterion ($\boldsymbol{\theta} \leq$ given tolerance) and decide to finish or go to next step.

(5) Use *blue-green* procedure to refine each $T' \in \mathcal{T}_h$ whose indicator $\theta_{T'}$ satisfies

$$\theta_{T'} \;\geq\; \frac{1}{2} \max \left\{ \theta_T \;:\; T \in \mathcal{T}_h \right\}.$$

(6) Define resulting mesh as actual mesh $\mathcal{T}_h$ and go to step 2.

We take the domain Ω either as the unit cube $]0,1[^3$, the L-shaped domain

$$]-1/2,1/2[\, \times \,]0,1[\, \times \,]-1/2,1/2[\, \setminus \, \Big( ]0,1/2[\, \times \,]0,1[\, \times \,]0,1/2[\Big) \,,$$

or the T-shaped domain

$$]-1,1[\, \times \,]-1,1[\, \times \,]0,1[\, \setminus \, \Big( ]-1,-1/3[\, \times \,]-1,1/2[\, \times \,]0,1[\, \cup \,]1/3,1[\, \times \,]-1,1/2[\, \times \,]0,1[\Big) \,,$$

and choose $\mathbf{f}$ and $\mathbf{g}$ so that the Poisson ratio ν and the exact solution $\mathbf{u}$ are given as follows:

Example	Ω	ν	$\mathbf{u}(x_1, x_2, x_3)$
1	Unit cube	0.4900	$(x_1^2+1)(x_2^2+1)(x_3^2+1)e^{x_1+x_2+x_3} \begin{pmatrix} 1 \\ 1 \\ 1 \end{pmatrix}$
2	L-shaped	0.3000	$\begin{pmatrix} e^{x_2}\,(x_3-0.1)\,(x_1+1)^2\,/\,r \\ e^{x_2}\,(x_1+1)^2\,r \\ -e^{x_2}\,(x_1+1)\,(150x_1^2+25x_1+100x_3^2-20x_3-3)\,/\,(50r) \end{pmatrix}$
3	T-shaped	0.4999	$\begin{pmatrix} (x_1+0.38)/r_1 \;+\; (x_1-0.38)/r_2 \\ (x_2-0.45)(1/r_1+1/r_2) \\ (x_3-1.05)(1/r_1+1/r_2) \end{pmatrix}$

where $r := \sqrt{(x_1-0.1)^2+(x_3-0.1)^2}$ in Example 2, whereas

$$r_1 \;:=\; \sqrt{(x_1+0.38)^2+(x_2-0.45)^2+(x_3-1.05)^2}$$

and

$$r_2 \ := \ \sqrt{(x_1 - 0.38)^2 + (x_2 - 0.45)^2 + (x_3 - 1.05)^2}$$

in Example 3. Note that the solution of Example 2 is singular at $(0.1, x_2, 0.1)$, and then we should expect regions of high gradients around that line, which is the line in the middle corner of the L along x_2-axis. Similarly, the solution of Example 3 is singular at $(-0.38, 0.45, 1.05)$ and $(0.38, 0.45, 1.05)$, which are the middle corners of the T with respect the plane $x_3 = 1$.

In Tables 1.1 and 1.2, we summarize the convergence history of the mixed finite element scheme (1.20) as applied to Example 1, for a sequence of quasi-uniform triangulations (generated as in [79]) of the domain. We notice there that the rate of convergence $O(h^{k+1})$ predicted by Theorems 1.3 and 1.4 (when $s = k + 1$) is attained by all the unknowns. In particular, these results confirm that our new postprocessed stress $\boldsymbol{\sigma}_h^*$ clearly improves in one power the non-satisfactory order provided by the first approximation $\boldsymbol{\sigma}_h$ with respect to the broken $\mathbb{H}(\mathbf{div})$-norm. In addition, as observed in the eighth column of Table 1.1, the convergence of $\mathtt{e}(\mathbf{u})$ is a bit faster than expected, which is a special behaviour of this particular solution $\mathbf{u}$, as it is also mentioned in [79]. We also remark the good behaviour of the *a posteriori* error estimator $\boldsymbol{\theta}$ in this case. More precisely, in Table 1.1, we see that the effectivity indices $\mathtt{eff}(\boldsymbol{\theta})$ remain always bounded above and below, which illustrates the reliability and efficiency result provided by Theorem 1.5.

Next, in Tables 1.3 - 1.10, we provide the convergence history of the quasi-uniform and adaptive schemes as applied to Examples 2 and 3. The stopping criterion in the adaptive refinements is $\boldsymbol{\theta} \leq 1.8$ $(k = 0)$, $\boldsymbol{\theta} \leq 0.6$ $(k = 1)$, and $\boldsymbol{\theta} \leq 0.4$ $(k = 2)$ for Example 2, whereas $\boldsymbol{\theta} \leq 4000$ $(k = 0)$, $\boldsymbol{\theta} \leq 1200$ $(k = 1)$, and $\boldsymbol{\theta} \leq 900$ $(k = 2)$ for Example 3. We observe here that the errors of the adaptive methods decrease faster than those obtained by the quasi-uniform ones. This fact is better illustrated in Figures 1.1 and 1.4 where we display the errors $\mathtt{e}(\boldsymbol{\rho}, \mathbf{u})$ and $\mathtt{e}^\star_{\mathbf{div}}(\boldsymbol{\sigma})$ vs. the degrees of freedom N for both refinements. In addition, the effectivity indices remain also bounded from above and below, which confirms the reliability and efficiency of $\boldsymbol{\theta}$ for the associated adaptive algorithm as well. Some intermediate meshes obtained with this procedure are displayed in Figures 1.2 and 1.5. Notice here that the adapted meshes concentrate the refinements around the line $(0, x_2, 0)$ in Example 2, and around the points $(-1/3, 1/2, 1)$ and $(1/3, 1/2, 1)$ in Example 3, which means that the method is able to recognize the regions with high gradients of the solutions. Finally, in Figures 1.3 and 1.6, we display iso-surfaces for some components of the pseudostress $\boldsymbol{\rho}_h$, the displacement $\mathbf{u}_h$, and the stress tensor $\boldsymbol{\sigma}_h$ (or $\boldsymbol{\sigma}_h^\star$), for both examples.

k	h	N	N/m	$\mathtt{e}(\boldsymbol{\rho})$	$\mathtt{r}(\boldsymbol{\rho})$	$\mathtt{e}(\mathbf{u})$	$\mathtt{r}(\mathbf{u})$	$\mathtt{e}(\boldsymbol{\rho},\mathbf{u})$	$\mathtt{r}(\boldsymbol{\rho},\mathbf{u})$	$\mathtt{eff}(\boldsymbol{\theta})$
0	0.4330	3745	9.753	8.89e+2	−−	3.76e+1	−−	8.90e+2	−−	0.2035
	0.3464	7201	9.601	7.09e+2	1.01	2.61e+1	1.63	7.10e+2	1.01	0.1944
	0.2887	12313	9.501	5.89e+2	1.02	1.92e+1	1.69	5.89e+2	1.02	0.1878
	0.2474	19405	9.429	5.02e+2	1.03	1.47e+1	1.74	5.03e+2	1.03	0.1828
	0.2165	28801	9.375	4.38e+2	1.03	1.16e+1	1.77	4.38e+2	1.03	0.1790
	0.1925	40825	9.334	3.88e+2	1.03	9.39e-0	1.79	3.88e+2	1.03	0.1759
	0.1732	55801	9.300	3.48e+2	1.03	7.76e-0	1.81	3.48e+2	1.03	0.1735
	0.1575	74053	9.273	3.15e+2	1.03	6.52e-0	1.82	3.15e+2	1.03	0.1714
	0.1443	95905	9.250	2.88e+2	1.03	5.56e-0	1.83	2.88e+2	1.03	0.1697
	0.1332	121681	9.231	2.65e+2	1.03	4.80e-0	1.84	2.65e+2	1.03	0.1683
1	0.4330	15841	41.253	4.83e+1	−−	1.12e-0	−−	4.84e+1	−−	0.0536
	0.3464	30601	40.801	3.09e+1	2.00	6.00e-1	2.80	3.09e+1	2.00	0.0523
	0.2887	52489	40.501	2.15e+1	2.00	3.59e-1	2.81	2.15e+1	2.00	0.0516
	0.2165	123265	40.125	1.21e+1	2.00	1.60e-1	2.81	1.21e+1	2.00	0.0506
	0.1925	174961	40.000	9.56e-0	2.00	1.15e-1	2.80	9.56e-0	2.00	0.0503
	0.1732	239401	39.900	7.74e-0	2.00	8.59e-2	2.78	7.74e-0	2.00	0.0501
	0.1575	317989	39.818	6.40e-0	2.00	6.60e-2	2.76	6.40e-0	2.00	0.0499
	0.1443	412129	39.750	5.38e-0	2.00	5.20e-2	2.74	5.38e-0	2.00	0.0497
	0.1332	523225	39.692	4.58e-0	2.00	4.19e-2	2.72	4.59e-0	2.00	0.0496
2	0.4330	40897	106.503	1.89e-0	−−	3.17e-2	−−	1.89e-0	−−	0.0310
	0.3464	79201	105.601	9.68e-1	3.00	1.35e-2	3.81	9.68e-1	3.00	0.0304
	0.2887	136081	105.001	5.60e-1	3.00	6.77e-3	3.79	5.60e-1	3.00	0.0300
	0.2165	320257	104.250	2.36e-1	2.99	2.31e-3	3.72	2.37e-1	2.99	0.0296
	0.1925	454897	104.000	1.67e-1	2.98	1.49e-3	3.69	1.67e-1	2.98	0.0296
	0.1732	622801	103.800	1.22e-1	2.95	1.02e-3	3.64	1.22e-1	2.95	0.0296
	0.1575	827641	103.636	9.19e-2	2.98	7.20e-4	3.64	9.19e-2	2.98	0.0296
	0.1443	1073089	103.500	7.09e-2	2.98	5.25e-4	3.63	7.09e-2	2.98	0.0293
	0.1332	1362817	103.385	5.57e-2	3.01	3.93e-4	3.61	5.57e-2	3.01	0.0293

Table 1.1: Example 1, quasi-uniform scheme.

k	h	N	$\mathtt{e}_0(\boldsymbol{\sigma})$	$\mathtt{r}_0(\boldsymbol{\sigma})$	$\mathtt{e}_{\mathtt{div}}(\boldsymbol{\sigma})$	$\mathtt{r}_{\mathtt{div}}(\boldsymbol{\sigma})$	$\mathtt{e}_0^\star(\boldsymbol{\sigma})$	$\mathtt{r}_0^\star(\boldsymbol{\sigma})$	$\mathtt{e}_{\mathtt{div}}^\star(\boldsymbol{\sigma})$	$\mathtt{r}_{\mathtt{div}}^\star(\boldsymbol{\sigma})$
	0.4330	3745	6.44e+2	−−	1.80e+3	−−	6.08e+2	−−	9.34e+2	−−
	0.3464	7201	5.22e+2	0.94	1.71e+3	0.23	4.93e+2	0.94	7.52e+2	0.97
	0.2887	12313	4.37e+2	0.97	1.66e+3	0.17	4.13e+2	0.97	6.28e+2	0.99
0	0.2165	28801	3.29e+2	1.00	1.60e+3	0.10	3.11e+2	1.00	4.72e+2	1.00
	0.1732	55801	2.62e+2	1.01	1.58e+3	0.06	2.48e+2	1.01	3.77e+2	1.00
	0.1575	74053	2.38e+2	1.01	1.57e+3	0.05	2.25e+2	1.02	3.43e+2	1.01
	0.1443	95905	2.18e+2	1.02	1.56e+3	0.05	2.06e+2	1.02	3.14e+2	1.01
	0.1332	121681	2.01e+2	1.02	1.56e+3	0.04	1.90e+2	1.02	2.90e+2	1.01
	0.4330	15841	3.47e+1	−−	6.91e+2	−−	3.04e+1	−−	5.09e+1	−−
	0.3464	30601	2.26e+1	1.92	5.63e+2	0.92	1.98e+1	1.93	3.27e+1	1.97
	0.2887	52489	1.59e+1	1.94	4.75e+2	0.93	1.39e+1	1.94	2.28e+1	1.98
1	0.2165	123265	9.05e-0	1.95	3.62e+2	0.95	7.94e-0	1.95	1.29e+1	1.98
	0.1925	174961	7.19e-0	1.96	3.23e+2	0.95	6.31e-0	1.96	1.02e+1	1.98
	0.1575	317989	4.85e-0	1.96	2.67e+2	0.96	4.26e-0	1.96	6.86e-0	1.99
	0.1443	412129	4.09e-0	1.97	2.45e+2	0.97	3.59e-0	1.96	5.77e-0	1.99
	0.1332	523225	3.49e-0	1.97	2.27e+2	0.97	3.06e-0	1.97	4.93e-0	1.99
	0.4330	40897	1.41e-0	−−	4.87e+1	−−	1.21e-0	−−	1.99e-0	−−
	0.3464	79201	7.31e-1	2.94	3.16e+1	1.93	6.28e-1	2.94	1.02e-0	2.98
	0.2887	136081	4.27e-1	2.95	2.22e+1	1.94	3.66e-1	2.95	5.93e-1	2.98
	0.2474	215209	2.71e-1	2.96	1.64e+1	1.95	2.32e-1	2.96	3.74e-1	2.99
2	0.2165	320257	1.82e-1	2.96	1.27e+1	1.96	1.56e-1	2.96	2.51e-1	2.99
	0.1732	622801	9.40e-2	2.97	8.16e-0	1.97	8.06e-2	2.97	1.29e-1	2.99
	0.1575	827641	7.07e-2	2.98	6.76e-0	1.97	6.07e-2	2.98	9.69e-2	2.99
	0.1443	1073089	5.46e-2	2.98	5.69e-0	1.97	4.68e-2	2.99	7.47e-2	3.00
	0.1332	1362817	4.29e-2	2.99	4.85e-0	2.00	3.68e-2	2.99	5.88e-2	3.00

Table 1.2: Example 1, quasi-uniform scheme for the postprocessed unknowns: $\boldsymbol{\sigma}_h$ and $\boldsymbol{\sigma}_h^\star$.

k	h	N	N/m	$\mathtt{e}(\boldsymbol{\rho})$	$\mathtt{r}(\boldsymbol{\rho})$	$\mathtt{e}(\mathbf{u})$	$\mathtt{r}(\mathbf{u})$	$\mathtt{e}(\boldsymbol{\rho},\mathbf{u})$	$\mathtt{r}(\boldsymbol{\rho},\mathbf{u})$	$\mathtt{eff}(\boldsymbol{\theta})$
0	0.7500	757	10.514	6.58e-0	−−	6.65e-1	−−	6.62e-0	−−	0.3313
	0.3750	5617	9.752	4.32e-0	0.61	3.34e-1	1.00	4.34e-0	0.61	0.3322
	0.2500	18469	9.501	3.20e-0	0.74	2.21e-1	1.01	3.21e-0	0.74	0.3304
	0.1875	43201	9.375	2.59e-0	0.75	1.66e-1	1.00	2.59e-0	0.75	0.3342
	0.1500	83701	9.300	2.17e-0	0.78	1.33e-1	1.00	2.17e-0	0.78	0.3386
	0.1250	143857	9.250	1.83e-0	0.94	1.11e-1	0.99	1.83e-0	0.94	0.3335
	0.1071	227557	9.214	1.59e-0	0.91	9.49e-2	1.00	1.59e-0	0.91	0.3326
	0.0938	338689	9.188	1.40e-0	0.92	8.30e-2	1.00	1.41e-0	0.92	0.3321
	0.0833	481141	9.167	1.26e-0	0.93	7.38e-2	1.00	1.26e-0	0.93	0.3316
	0.0750	658801	9.150	1.14e-0	0.90	6.64e-2	1.01	1.15e-0	0.90	0.3342
	0.0682	875557	9.136	1.04e-0	0.96	6.03e-2	1.00	1.05e-0	0.96	0.3337
	0.0625	1135297	9.125	9.57e-1	1.01	5.54e-2	0.99	9.58e-1	1.01	0.3304
	0.0577	1441909	9.115	8.89e-1	0.92	5.11e-2	1.01	8.91e-1	0.92	0.3326
	0.0536	1799281	9.107	8.24e-1	1.02	4.74e-2	0.99	8.26e-1	1.02	0.3298
	0.0500	2211301	9.100	7.73e-1	0.93	4.43e-2	1.01	7.75e-1	0.93	0.3318
	0.0469	2681857	9.094	7.24e-1	1.02	4.15e-2	0.99	7.25e-1	1.02	0.3293
	0.0441	3214837	9.088	6.82e-1	0.98	3.91e-2	1.00	6.83e-1	0.98	0.3291
	0.0417	3814129	9.083	6.45e-1	0.98	3.69e-2	1.00	6.46e-1	0.98	0.3289
	0.0395	4483621	9.079	6.11e-1	1.00	3.50e-2	1.00	6.12e-1	1.00	0.3280
	0.0375	5227201	9.075	5.81e-1	0.99	3.32e-2	1.00	5.82e-1	0.99	0.3272
1	0.7500	3133	43.514	3.46e-0	−−	1.08e-1	−−	3.46e-0	−−	0.2256
	0.3750	23761	41.252	1.74e-0	0.99	3.59e-2	1.59	1.74e-0	0.99	0.2444
	0.2500	78733	40.501	1.00e-0	1.36	1.77e-2	1.75	1.00e-0	1.36	0.2365
	0.1875	184897	40.125	6.24e-1	1.65	1.03e-2	1.87	6.24e-1	1.65	0.2383
	0.1500	359101	39.900	4.34e-1	1.63	6.51e-3	2.06	4.34e-1	1.63	0.2507
	0.1250	618193	39.750	3.11e-1	1.82	4.67e-3	1.82	3.11e-1	1.82	0.2388
	0.1071	979021	39.643	2.39e-1	1.71	3.46e-3	1.96	2.39e-1	1.71	0.2353
	0.0938	1458433	39.563	1.88e-1	1.78	2.66e-3	1.96	1.88e-1	1.78	0.2359
	0.0833	2073277	39.500	1.52e-1	1.83	2.11e-3	1.97	1.52e-1	1.83	0.2374
	0.0750	2840401	39.450	1.26e-1	1.77	1.69e-3	2.09	1.26e-1	1.77	0.2418
2	0.7500	7993	111.014	2.01e-0	−−	3.81e-2	−−	2.01e-0	−−	0.1693
	0.3750	61345	106.502	7.66e-1	1.40	9.87e-3	1.95	7.66e-1	1.40	0.1788
	0.2500	204121	105.001	3.07e-1	2.25	3.37e-3	2.65	3.07e-1	2.25	0.1643
	0.1875	480385	104.250	1.50e-1	2.48	1.44e-3	2.96	1.51e-1	2.48	0.1605
	0.1500	934201	103.800	9.02e-2	2.29	7.39e-4	2.98	9.02e-2	2.29	0.1783
	0.1250	1609633	103.500	5.65e-2	2.56	4.28e-4	2.99	5.65e-2	2.56	0.1734

Table 1.3: Example 2, quasi-uniform scheme.

k	h	N	$\mathtt{e}_0(\boldsymbol{\sigma})$	$\mathtt{r}_0(\boldsymbol{\sigma})$	$\mathtt{e}_{\mathtt{div}}(\boldsymbol{\sigma})$	$\mathtt{r}_{\mathtt{div}}(\boldsymbol{\sigma})$	$\mathtt{e}_0^\star(\boldsymbol{\sigma})$	$\mathtt{r}_0^\star(\boldsymbol{\sigma})$	$\mathtt{e}_{\mathtt{div}}^\star(\boldsymbol{\sigma})$	$\mathtt{r}_{\mathtt{div}}^\star(\boldsymbol{\sigma})$
	0.7500	757	2.17e-0	−−	7.16e-0	−−	2.12e-0	−−	6.78e-0	−−
	0.3750	5617	1.33e-0	0.71	5.06e-0	0.50	1.33e-0	0.67	4.44e-0	0.61
	0.2500	18469	9.39e-1	0.86	4.12e-0	0.51	9.39e-1	0.86	3.28e-0	0.75
	0.1875	43201	7.23e-1	0.91	3.65e-0	0.42	7.22e-1	0.91	2.64e-0	0.75
	0.1500	83701	5.88e-1	0.93	3.36e-0	0.36	5.85e-1	0.94	2.21e-0	0.79
	0.1250	143857	4.99e-1	0.90	3.15e-0	0.36	4.98e-1	0.89	1.86e-0	0.94
	0.1071	227557	4.30e-1	0.96	3.02e-0	0.28	4.30e-1	0.96	1.62e-0	0.91
	0.0938	338689	3.78e-1	0.97	2.93e-0	0.23	3.78e-1	0.97	1.43e-0	0.92
	0.0833	481141	3.37e-1	0.97	2.86e-0	0.20	3.37e-1	0.97	1.28e-0	0.93
0	0.0750	658801	3.03e-1	1.00	2.81e-0	0.16	3.03e-1	1.01	1.17e-0	0.90
	0.0682	875557	2.76e-1	0.98	2.77e-0	0.15	2.76e-1	0.98	1.06e-0	0.96
	0.0625	1135297	2.54e-1	0.96	2.74e-0	0.13	2.54e-1	0.95	9.75e-1	1.01
	0.0577	1441909	2.35e-1	1.01	2.72e-0	0.11	2.34e-1	1.02	9.06e-1	0.92
	0.0536	1799281	2.18e-1	0.97	2.70e-0	0.10	2.18e-1	0.95	8.40e-1	1.02
	0.0500	2211301	2.04e-1	1.01	2.68e-0	0.08	2.03e-1	1.02	7.88e-1	0.93
	0.0469	2681857	1.91e-1	0.97	2.67e-0	0.08	1.91e-1	0.96	7.38e-1	1.02
	0.0441	3214837	1.80e-1	0.99	2.66e-0	0.07	1.80e-1	0.99	6.95e-1	0.98
	0.0417	3814129	1.70e-1	0.99	2.65e-0	0.06	1.70e-1	0.99	6.57e-1	0.98
	0.0395	4483621	1.61e-1	1.00	2.64e-0	0.05	1.61e-1	1.00	6.23e-1	0.99
	0.0375	5227201	1.53e-1	1.00	2.64e-0	0.04	1.53e-1	1.00	5.92e-1	0.99
	0.7500	3133	1.02e-0	−−	6.04e-0	−−	1.04e-0	−−	3.56e-0	−−
	0.3750	23761	4.42e-1	1.21	4.99e-0	0.28	4.57e-1	1.18	1.78e-0	1.00
	0.2500	78733	2.36e-1	1.54	4.41e-0	0.30	2.45e-1	1.54	1.02e-0	1.37
	0.1875	184897	1.42e-1	1.77	3.67e-0	0.64	1.47e-1	1.76	6.35e-1	1.65
1	0.1500	359101	9.53e-2	1.79	3.07e-0	0.80	9.84e-2	1.81	4.41e-1	1.63
	0.1250	618193	6.90e-2	1.77	2.78e-0	0.55	7.16e-2	1.75	3.16e-1	1.82
	0.1071	979021	5.18e-2	1.86	2.53e-0	0.60	5.38e-2	1.86	2.43e-1	1.71
	0.0938	1458433	4.03e-2	1.89	2.28e-0	0.80	4.18e-2	1.89	1.91e-1	1.78
	0.0833	2073277	3.22e-2	1.90	2.05e-0	0.89	3.34e-2	1.90	1.54e-1	1.84
	0.0750	2840401	2.63e-2	1.92	1.86e-0	0.91	2.72e-2	1.94	1.28e-1	1.77
	0.7500	7993	5.49e-1	−−	5.00e-0	−−	5.70e-1	−−	2.07e-0	−−
	0.3750	61345	1.90e-1	1.53	3.58e-0	0.48	2.00e-1	1.51	7.84e-1	1.40
2	0.2500	204121	7.44e-2	2.32	2.40e-0	0.99	7.96e-2	2.27	3.14e-1	2.26
	0.1875	480385	3.42e-2	2.70	1.60e-0	1.41	3.68e-2	2.68	1.53e-1	2.49
	0.1500	934201	1.90e-2	2.64	1.05e-0	1.90	2.03e-2	2.67	9.17e-2	2.31
	0.1250	1609633	1.17e-2	2.67	7.38e-1	1.91	1.27e-2	2.56	5.74e-2	2.56

Table 1.4: Example 2, quasi-uniform scheme for the postprocessed unknowns: $\boldsymbol{\sigma}_h$ and $\boldsymbol{\sigma}_h^\star$.

k	h	N	N/m	$\mathtt{e}(\boldsymbol{\rho})$	$\mathtt{r}(\boldsymbol{\rho})$	$\mathtt{e}(\mathbf{u})$	$\mathtt{r}(\mathbf{u})$	$\mathtt{e}(\boldsymbol{\rho},\mathbf{u})$	$\mathtt{r}(\boldsymbol{\rho},\mathbf{u})$	$\mathtt{eff}(\boldsymbol{\theta})$
0	0.7500	757	10.514	6.58e-0	$--$	6.65e-1	$--$	6.62e-0	$--$	0.3313
	0.7500	2473	9.892	4.72e-0	0.56	4.42e-1	0.69	4.74e-0	0.56	0.3334
	0.5000	8380	9.534	3.13e-0	0.67	3.10e-1	0.58	3.15e-0	0.67	0.3193
	0.5000	10348	9.529	2.94e-0	0.58	2.81e-1	0.96	2.96e-0	0.59	0.3231
	0.4146	36898	9.337	1.89e-0	0.70	1.69e-1	0.80	1.89e-0	0.70	0.3139
	0.2864	93637	9.254	1.40e-0	0.63	1.36e-1	0.46	1.41e-0	0.63	0.3100
	0.2795	202747	9.213	1.07e-0	0.70	9.41e-2	0.96	1.07e-0	0.71	0.3092
	0.1768	485527	9.147	8.05e-1	0.65	7.69e-2	0.46	8.09e-1	0.65	0.3094
	0.1768	1033678	9.123	6.23e-1	0.68	5.50e-2	0.89	6.25e-1	0.68	0.3080
	0.1250	2251543	9.094	4.81e-1	0.66	4.48e-2	0.53	4.83e-1	0.66	0.3082
1	0.7500	3133	43.514	3.46e-0	$--$	1.08e-1	$--$	3.46e-0	$--$	0.2256
	0.7071	9586	41.498	1.97e-0	1.01	7.00e-2	0.78	1.97e-0	1.01	0.2243
	0.5590	27331	40.732	9.21e-1	1.45	3.51e-2	1.32	9.22e-1	1.45	0.2008
	0.5590	41794	40.656	6.34e-1	1.76	2.62e-2	1.38	6.34e-1	1.76	0.1891
	0.5000	101143	40.232	3.65e-1	1.25	1.58e-2	1.14	3.66e-1	1.25	0.1846
	0.3692	156802	40.072	2.61e-1	1.53	1.21e-2	1.24	2.61e-1	1.53	0.1806
	0.3668	300970	39.858	1.81e-1	1.13	7.31e-3	1.54	1.81e-1	1.13	0.1848
	0.2613	583252	39.704	1.07e-1	1.58	4.16e-3	1.70	1.07e-1	1.58	0.1843
2	0.7500	7993	111.014	2.01e-0	$--$	3.81e-2	$--$	2.01e-0	$--$	0.1693
	0.7071	25447	106.920	8.44e-1	1.50	1.44e-2	1.68	8.44e-1	1.50	0.1716
	0.7071	53473	105.887	3.19e-1	2.62	7.52e-3	1.74	3.19e-1	2.62	0.1234
	0.7071	78949	105.688	1.97e-1	2.48	6.06e-3	1.12	1.97e-1	2.48	0.1070
	0.4566	141883	104.943	1.21e-1	1.66	2.37e-3	3.20	1.21e-1	1.66	0.1253
	0.4566	256903	104.475	6.72e-2	1.98	1.75e-3	1.02	6.72e-2	1.98	0.1172
	0.3604	383023	104.224	4.53e-2	1.98	1.10e-3	2.34	4.53e-2	1.98	0.1151

Table 1.5: Example 2, adaptive scheme.

k	h	N	$\mathtt{e}_0(\boldsymbol{\sigma})$	$\mathtt{r}_0(\boldsymbol{\sigma})$	$\mathtt{e}_{\mathtt{div}}(\boldsymbol{\sigma})$	$\mathtt{r}_{\mathtt{div}}(\boldsymbol{\sigma})$	$\mathtt{e}_0^\star(\boldsymbol{\sigma})$	$\mathtt{r}_0^\star(\boldsymbol{\sigma})$	$\mathtt{e}_{\mathtt{div}}^\star(\boldsymbol{\sigma})$	$\mathtt{r}_{\mathtt{div}}^\star(\boldsymbol{\sigma})$
	0.7500	757	2.17e-0	−−	7.16e-0	−−	2.12e-0	−−	6.78e-0	−−
	0.7500	2473	1.61e-0	0.50	5.44e-0	0.46	1.63e-0	0.44	4.89e-0	0.55
	0.5000	8380	1.05e-0	0.70	4.08e-0	0.47	1.07e-0	0.70	3.23e-0	0.68
	0.5000	10348	9.63e-1	0.83	3.93e-0	0.35	9.74e-1	0.86	3.04e-0	0.60
0	0.4146	36898	6.30e-1	0.67	3.20e-0	0.32	6.35e-1	0.67	1.95e-0	0.70
	0.2864	93637	4.61e-1	0.67	2.93e-0	0.19	4.66e-1	0.66	1.45e-0	0.64
	0.2795	202747	3.59e-1	0.65	2.79e-0	0.13	3.62e-1	0.66	1.10e-0	0.70
	0.1768	485527	2.63e-1	0.71	2.69e-0	0.08	2.66e-1	0.71	8.30e-1	0.66
	0.1768	1033678	2.07e-1	0.64	2.64e-0	0.05	2.09e-1	0.64	6.42e-1	0.68
	0.1250	2251543	1.58e-1	0.70	2.61e-0	0.03	1.59e-1	0.70	4.96e-1	0.67
	0.7500	3133	1.02e-0	−−	6.04e-0	−−	1.04e-0	−−	3.56e-0	−−
	0.7071	9586	5.53e-1	1.09	5.47e-0	0.18	5.76e-1	1.05	2.03e-0	1.01
	0.5590	27331	2.88e-1	1.25	4.13e-0	0.54	2.99e-1	1.25	9.52e-1	1.44
1	0.5590	41794	1.90e-1	1.96	3.81e-0	0.38	1.99e-1	1.92	6.53e-1	1.78
	0.5000	101143	1.12e-1	1.20	2.92e-0	0.60	1.17e-1	1.20	3.77e-1	1.24
	0.3692	156802	7.86e-2	1.62	2.53e-0	0.66	8.19e-2	1.62	2.69e-1	1.54
	0.3668	300970	5.30e-2	1.21	2.10e-0	0.57	5.52e-2	1.21	1.86e-1	1.13
	0.2613	583252	2.97e-2	1.75	1.66e-0	0.72	3.11e-2	1.74	1.05e-1	1.73
	0.7500	7993	5.49e-1	−−	5.00e-0	−−	5.70e-1	−−	2.07e-0	−−
	0.7071	25447	2.26e-1	1.53	3.71e-0	0.52	2.41e-1	1.48	8.67e-1	1.50
	0.7071	53473	1.07e-1	2.01	2.39e-0	1.18	1.15e-1	2.00	3.32e-1	2.58
2	0.7071	78949	6.15e-2	2.86	1.90e-0	1.18	6.61e-2	2.83	2.04e-1	2.51
	0.4566	141883	3.30e-2	2.13	1.40e-0	1.05	3.54e-2	2.13	1.24e-1	1.69
	0.4566	256903	1.98e-2	1.72	9.62e-1	1.26	1.83e-2	2.22	6.94e-2	1.96
	0.3604	383023	1.39e-2	1.78	6.92e-1	1.65	1.04e-2	2.84	3.99e-2	2.77

Table 1.6: Example 2, adaptive scheme for the postprocessed unknowns: $\boldsymbol{\sigma}_h$ and $\boldsymbol{\sigma}_h^\star$.

k	h	N	N/m	$\mathtt{e}(\boldsymbol{\rho})$	$\mathtt{r}(\boldsymbol{\rho})$	$\mathtt{e}(\mathbf{u})$	$\mathtt{r}(\mathbf{u})$	$\mathtt{e}(\boldsymbol{\rho},\mathbf{u})$	$\mathtt{r}(\boldsymbol{\rho},\mathbf{u})$	$\mathtt{eff}(\boldsymbol{\theta})$
	0.6509	2905	10.087	1.50e+4	−−	4.48e+2	−−	1.50e+4	−−	0.5604
	0.3254	21985	9.542	1.03e+4	0.55	1.68e+2	1.42	1.03e+4	0.55	0.5755
	0.2170	72793	9.361	7.77e+3	0.69	8.74e+1	1.61	7.77e+3	0.69	0.5801
	0.1627	170881	9.271	6.22e+3	0.77	5.36e+1	1.70	6.22e+3	0.77	0.5803
	0.1302	331801	9.217	5.16e+3	0.84	3.63e+1	1.75	5.16e+3	0.84	0.5774
0	0.1085	571105	9.181	4.40e+3	0.88	2.62e+1	1.77	4.40e+3	0.88	0.5739
	0.0930	904345	9.155	3.82e+3	0.91	1.99e+1	1.81	3.82e+3	0.91	0.5697
	0.0814	1347073	9.135	3.38e+3	0.93	1.56e+1	1.82	3.38e+3	0.93	0.5662
	0.0723	1914841	9.120	3.02e+3	0.94	1.25e+1	1.84	3.02e+3	0.94	0.5632
	0.0651	2623201	9.108	2.73e+3	0.96	1.03e+1	1.86	2.73e+3	0.96	0.5601
	0.0592	3487705	9.098	2.49e+3	0.99	8.61e-0	1.88	2.49e+3	0.99	0.5569
	0.0542	4523905	9.090	2.29e+3	0.94	7.33e-0	1.86	2.29e+3	0.94	0.5550
	0.6509	12169	42.253	8.74e+3	−−	6.18e+1	−−	8.75e+3	−−	0.4299
	0.3254	93601	40.625	4.40e+3	0.99	1.37e+1	2.18	4.40e+3	0.99	0.5118
	0.2170	311689	40.083	2.66e+3	1.24	5.27e-0	2.35	2.66e+3	1.24	0.5460
1	0.1627	733825	39.813	1.78e+3	1.40	2.56e-0	2.51	1.78e+3	1.40	0.5622
	0.1302	1427401	39.650	1.26e+3	1.54	1.44e-0	2.58	1.26e+3	1.54	0.5678
	0.1085	2459809	39.542	9.36e+2	1.64	8.81e-1	2.69	9.36e+2	1.64	0.5697
	0.0930	3898441	39.464	7.27e+2	1.63	5.99e-1	2.50	7.27e+2	1.63	0.5637
	0.6509	31249	108.503	5.04e+3	−−	1.87e+1	−−	5.04e+3	−−	0.3386
	0.3254	242497	105.250	1.90e+3	1.40	2.94e-0	2.67	1.90e+3	1.40	0.4172
2	0.2170	810001	104.167	9.31e+2	1.76	9.18e-1	2.87	9.31e+2	1.76	0.4647
	0.1627	1910017	103.625	5.76e+2	1.67	4.00e-1	2.89	5.76e+2	1.67	0.4643
	0.1302	3718801	103.300	3.97e+2	1.67	2.10e-1	2.88	3.97e+2	1.67	0.4651

Table 1.7: Example 3, quasi-uniform scheme.

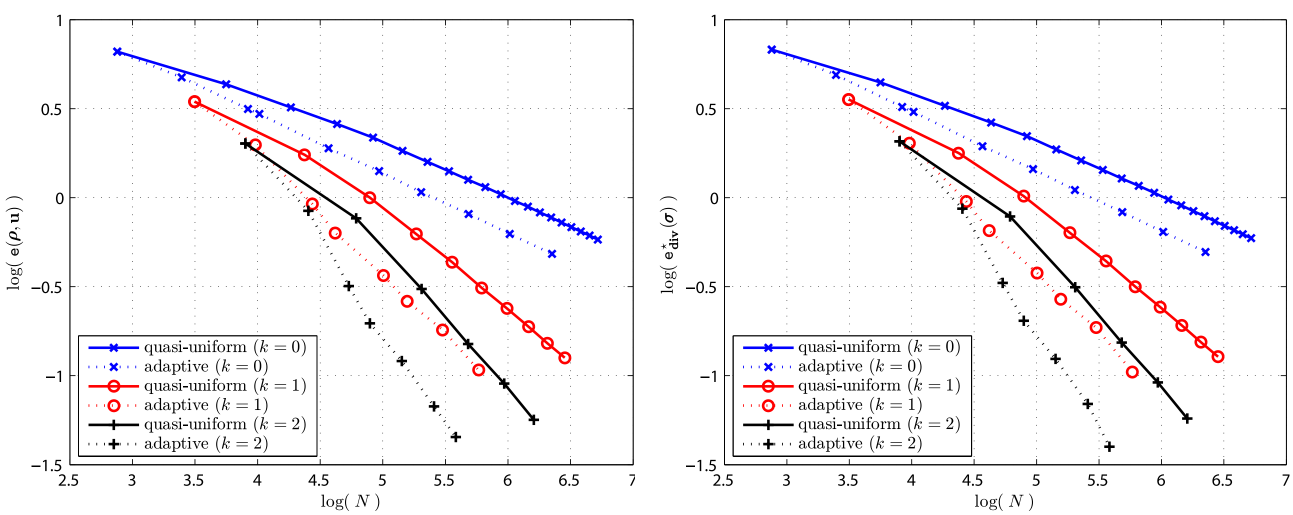

Figure 1.1: Example 2, $\mathtt{e}(\boldsymbol{\rho},\mathbf{u})$ vs. N (left) and $\mathtt{e}^{\star}_{\mathbf{div}}(\boldsymbol{\sigma})$ vs. N (right).

k	h	N	$\mathtt{e}_0(\boldsymbol{\sigma})$	$\mathtt{r}_0(\boldsymbol{\sigma})$	$\mathtt{e}_{\mathtt{div}}(\boldsymbol{\sigma})$	$\mathtt{r}_{\mathtt{div}}(\boldsymbol{\sigma})$	$\mathtt{e}_0^\star(\boldsymbol{\sigma})$	$\mathtt{r}_0^\star(\boldsymbol{\sigma})$	$\mathtt{e}_{\mathtt{div}}^\star(\boldsymbol{\sigma})$	$\mathtt{r}_{\mathtt{div}}^\star(\boldsymbol{\sigma})$
	0.6509	2905	4.48e+3	−−	1.58e+4	−−	4.37e+3	−−	1.51e+4	−−
	0.3254	21985	2.63e+3	0.77	1.15e+4	0.46	2.56e+3	0.77	1.03e+4	0.55
	0.2170	72793	1.84e+3	0.87	9.40e+3	0.50	1.80e+3	0.87	7.83e+3	0.69
	0.1627	170881	1.42e+3	0.91	8.20e+3	0.47	1.38e+3	0.91	6.27e+3	0.77
	0.1302	331801	1.15e+3	0.93	7.45e+3	0.43	1.12e+3	0.93	5.20e+3	0.84
0	0.1085	571105	9.69e+2	0.95	6.96e+3	0.37	9.47e+2	0.94	4.44e+3	0.88
	0.0930	904345	8.36e+2	0.96	6.62e+3	0.32	8.17e+2	0.96	3.86e+3	0.91
	0.0814	1347073	7.35e+2	0.97	6.38e+3	0.28	7.18e+2	0.97	3.41e+3	0.93
	0.0723	1914841	6.55e+2	0.97	6.21e+3	0.24	6.40e+2	0.97	3.05e+3	0.94
	0.0651	2623201	5.91e+2	0.98	6.08e+3	0.20	5.77e+2	0.98	2.76e+3	0.96
	0.0592	3487705	5.37e+2	1.00	5.97e+3	0.18	5.24e+2	1.00	2.51e+3	0.99
	0.0542	4523905	4.93e+2	0.97	5.90e+3	0.15	4.82e+2	0.97	2.31e+3	0.94
	0.6509	12169	1.29e+3	−−	1.03e+4	−−	1.22e+3	−−	8.76e+3	−−
	0.3254	93601	5.41e+2	1.26	6.24e+3	0.72	5.13e+2	1.25	4.41e+3	0.99
	0.2170	311689	2.99e+2	1.46	4.52e+3	0.80	2.84e+2	1.45	2.67e+3	1.24
1	0.1627	733825	1.89e+2	1.60	3.53e+3	0.86	1.80e+2	1.60	1.78e+3	1.40
	0.1302	1427401	1.30e+2	1.68	2.93e+3	0.83	1.23e+2	1.68	1.26e+3	1.54
	0.1085	2459809	9.40e+1	1.77	2.49e+3	0.89	8.95e+1	1.77	9.37e+2	1.64
	0.0930	3898441	7.24e+1	1.69	2.16e+3	0.95	6.91e+1	1.68	7.33e+2	1.59
	0.6509	31249	5.54e+2	−−	6.79e+3	−−	5.12e+2	−−	5.04e+3	−−
	0.3254	242497	1.66e+2	1.74	3.39e+3	1.00	1.55e+2	1.73	1.91e+3	1.40
2	0.2170	810001	7.36e+1	2.01	2.07e+3	1.21	6.85e+1	2.01	9.32e+2	1.76
	0.1627	1910017	4.44e+1	1.75	1.35e+3	1.48	4.12e+1	1.76	5.67e+2	1.72
	0.1302	3718801	3.06e+1	1.68	9.56e+2	1.56	2.82e+1	1.70	3.89e+2	1.69

Table 1.8: Example 3, quasi-uniform scheme for the postprocessed unknown: $\boldsymbol{\sigma}_h$ and $\boldsymbol{\sigma}_h^\star$.

k	h	N	N/m	$\mathtt{e}(\boldsymbol{\rho})$	$\mathtt{r}(\boldsymbol{\rho})$	$\mathtt{e}(\mathbf{u})$	$\mathtt{r}(\mathbf{u})$	$\mathtt{e}(\boldsymbol{\rho},\mathbf{u})$	$\mathtt{r}(\boldsymbol{\rho},\mathbf{u})$	$\mathtt{eff}(\boldsymbol{\theta})$
	0.6509	2905	10.087	1.50e+4	−−	4.48e+2	−−	1.50e+4	−−	0.5604
	0.6509	4657	9.825	1.04e+4	1.56	3.37e+2	1.21	1.04e+4	1.56	0.4900
	0.6509	6868	9.756	7.38e+3	1.76	2.85e+2	0.86	7.39e+3	1.76	0.4144
	0.6509	13672	9.601	5.90e+3	0.65	1.82e+2	1.30	5.90e+3	0.65	0.4091
0	0.6009	42169	9.396	4.05e+3	0.67	9.05e+1	1.24	4.05e+3	0.67	0.3960
	0.4167	81979	9.307	3.19e+3	0.71	5.77e+1	1.35	3.19e+3	0.71	0.3827
	0.3560	204958	9.221	2.28e+3	0.73	3.47e+1	1.11	2.28e+3	0.73	0.3644
	0.3125	412942	9.183	1.83e+3	0.62	2.10e+1	1.44	1.83e+3	0.62	0.3659
	0.2763	861778	9.137	1.41e+3	0.72	1.33e+1	1.23	1.41e+3	0.72	0.3555
	0.6509	12169	42.253	8.74e+3	−−	6.18e+1	−−	8.75e+3	−−	0.4299
	0.6509	17875	41.667	4.14e+3	3.89	2.65e+1	4.41	4.14e+3	3.89	0.4143
	0.6509	25642	41.492	2.12e+3	3.71	1.85e+1	1.98	2.12e+3	3.71	0.3112
	0.6509	46606	40.954	1.38e+3	1.44	1.30e+1	1.18	1.38e+3	1.44	0.3000
1	0.6509	103993	40.417	8.08e+2	1.33	5.13e-0	2.32	8.08e+2	1.33	0.3054
	0.6009	158200	40.203	5.68e+2	1.68	3.13e-0	2.35	5.68e+2	1.68	0.3094
	0.4566	253738	40.047	4.04e+2	1.45	1.78e-0	2.39	4.04e+2	1.45	0.3141
	0.4566	455698	39.837	2.53e+2	1.59	1.05e-0	1.80	2.53e+2	1.59	0.2925
	0.6509	31249	108.503	5.04e+3	−−	1.87e+1	−−	5.04e+3	−−	0.3386
	0.6509	46759	107.245	1.75e+3	5.26	4.26e-0	7.34	1.75e+3	5.26	0.3854
2	0.6509	66439	106.987	5.62e+2	6.46	2.75e-0	2.50	5.62e+2	6.46	0.2274
	0.6509	100765	105.957	3.87e+2	1.80	1.47e-0	3.01	3.87e+2	1.80	0.2547
	0.6509	160993	105.224	2.24e+2	2.33	9.24e-1	1.98	2.24e+2	2.33	0.2456
	0.6509	270037	104.909	1.35e+2	1.95	3.91e-1	3.32	1.35e+2	1.95	0.2523

Table 1.9: Example 3, adaptive scheme.

k	h	N	$\mathtt{e}_0(\boldsymbol{\sigma})$	$\mathtt{r}_0(\boldsymbol{\sigma})$	$\mathtt{e}_{\mathbf{div}}(\boldsymbol{\sigma})$	$\mathtt{r}_{\mathbf{div}}(\boldsymbol{\sigma})$	$\mathtt{e}_0^\star(\boldsymbol{\sigma})$	$\mathtt{r}_0^\star(\boldsymbol{\sigma})$	$\mathtt{e}_{\mathbf{div}}^\star(\boldsymbol{\sigma})$	$\mathtt{r}_{\mathbf{div}}^\star(\boldsymbol{\sigma})$
	0.6509	2905	4.48e+3	−−	1.58e+4	−−	4.37e+3	−−	1.51e+4	−−
	0.6509	4657	3.70e+3	0.82	1.17e+4	1.29	3.62e+3	0.80	1.05e+4	1.54
	0.6509	6868	3.24e+3	0.68	9.20e+3	1.23	3.17e+3	0.67	7.53e+3	1.72
	0.6509	13672	2.55e+3	0.69	8.05e+3	0.39	2.50e+3	0.69	6.03e+3	0.65
0	0.6009	42169	1.66e+3	0.76	6.80e+3	0.30	1.62e+3	0.77	4.15e+3	0.66
	0.4167	81979	1.29e+3	0.76	6.33e+3	0.22	1.26e+3	0.77	3.28e+3	0.71
	0.3560	204958	9.35e+2	0.70	5.92e+3	0.15	9.14e+2	0.70	2.35e+3	0.73
	0.3125	412942	7.21e+2	0.74	5.75e+3	0.08	7.04e+2	0.74	1.89e+3	0.62
	0.2763	861778	5.56e+2	0.71	5.63e+3	0.06	5.42e+2	0.71	1.45e+3	0.72
	0.6509	12169	1.29e+3	−−	1.03e+4	−−	1.22e+3	−−	8.76e+3	−−
	0.6509	17875	6.62e+2	3.48	6.31e+3	2.54	6.32e+2	3.41	4.16e+3	3.88
	0.6509	25642	4.53e+2	2.10	4.68e+3	1.65	4.32e+2	2.11	2.14e+3	3.69
1	0.6509	46606	3.06e+2	1.31	3.58e+3	0.89	2.91e+2	1.32	1.39e+3	1.44
	0.6509	103993	1.78e+2	1.35	2.76e+3	0.65	1.69e+2	1.35	8.15e+2	1.33
	0.6009	158200	1.26e+2	1.67	2.29e+3	0.90	1.19e+2	1.68	5.73e+2	1.68
	0.4566	253738	8.67e+1	1.58	1.92e+3	0.73	8.20e+1	1.58	4.07e+2	1.45
	0.4566	455698	5.86e+1	1.33	1.53e+3	0.78	5.55e+1	1.33	2.56e+2	1.59
	0.6509	31249	5.54e+2	−−	6.79e+3	−−	5.12e+2	−−	5.05e+3	−−
	0.6509	46759	1.69e+2	5.91	3.38e+3	3.46	1.57e+2	5.87	1.75e+3	5.26
2	0.6509	66439	9.03e+1	3.55	1.81e+3	3.55	8.40e+1	3.55	5.65e+2	6.44
	0.6509	100765	5.78e+1	2.15	1.37e+3	1.35	5.34e+1	2.18	3.88e+2	1.80
	0.6509	160993	3.32e+1	2.36	1.00e+3	1.32	3.07e+1	2.36	2.25e+2	2.33
	0.6509	270037	2.02e+1	1.92	7.33e+2	1.22	1.86e+1	1.94	1.36e+2	1.95

Table 1.10: Example 3, adaptive scheme for the postprocessed unknown: $\boldsymbol{\sigma}_h$ and $\boldsymbol{\sigma}_h^\star$.

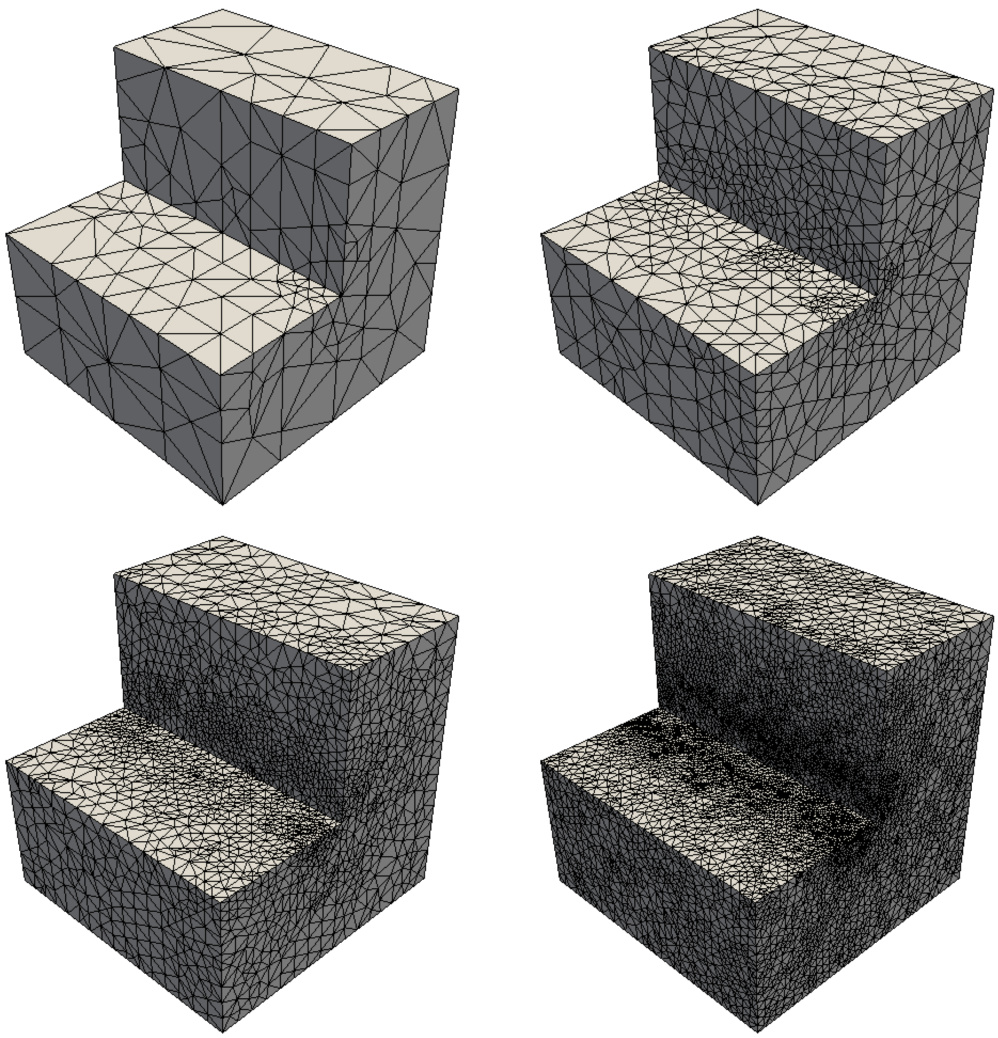

Figure 1.2: Example 2, adapted meshes for $k = 0$ with 10348, 93637, 485527, and 2251543 degrees of freedom.

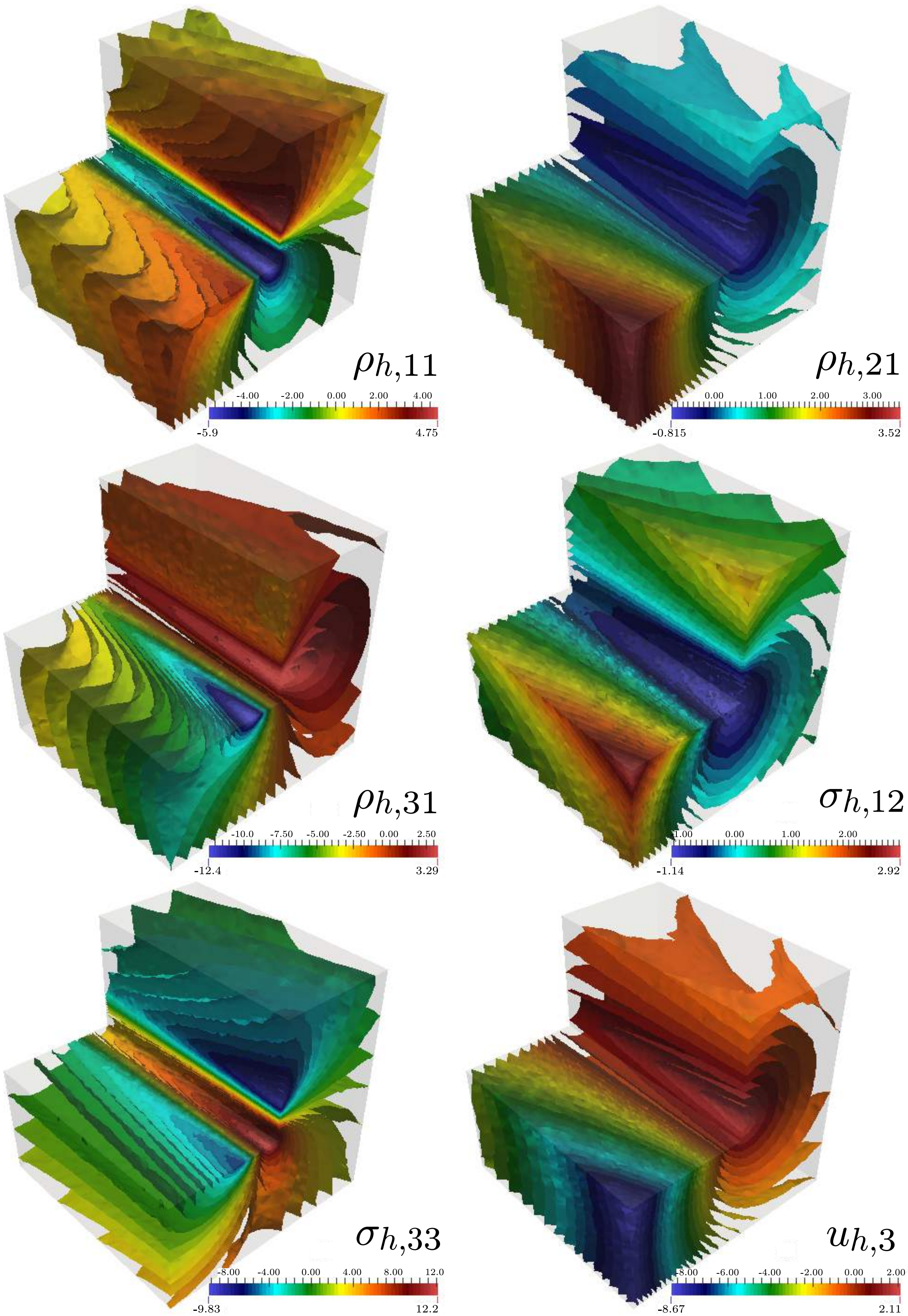

Figure 1.3: Example 2, iso-surfaces of some components of the approximate solutions ($k = 0$ and $N = 2251543$) for adaptive scheme.

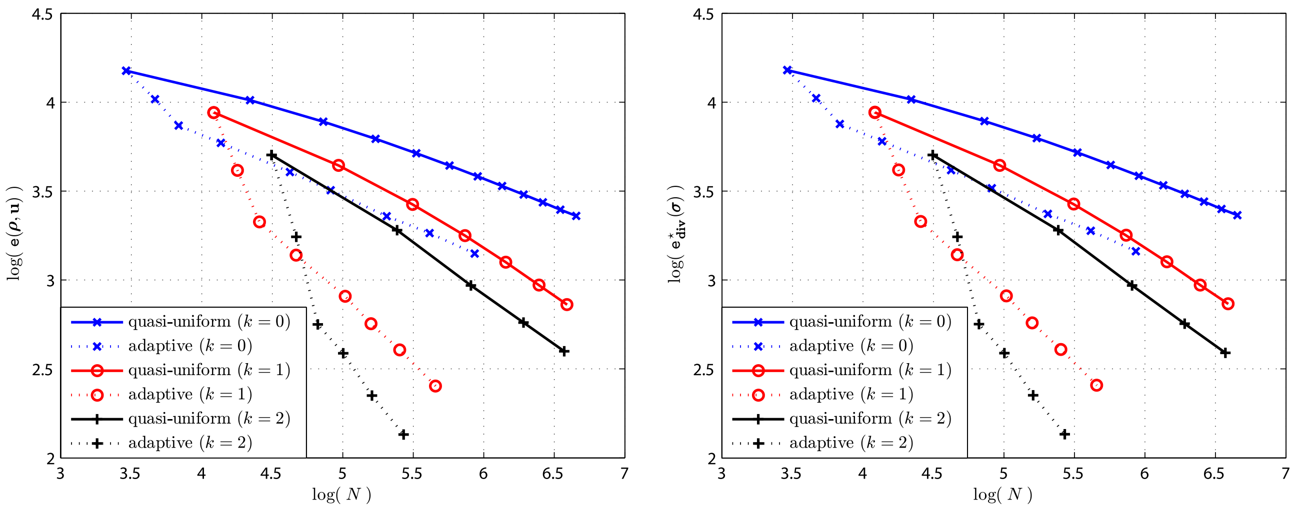

Figure 1.4: Example 3, $\mathsf{e}(\boldsymbol{\rho}, \mathbf{u})$ vs. N (left) and $\mathsf{e}^{\star}_{\mathbf{div}}(\boldsymbol{\sigma})$ vs. N (right).

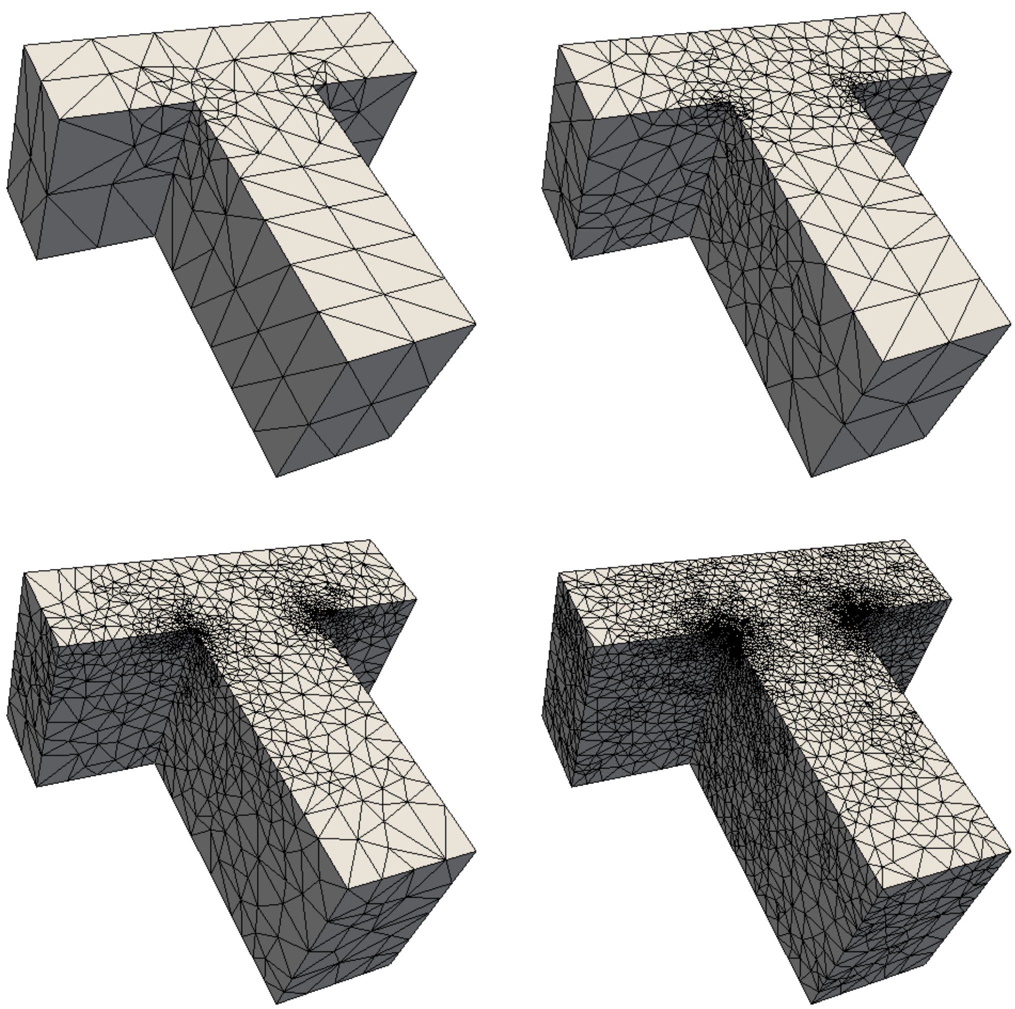

Figure 1.5: Example 3, adapted meshes for $k = 0$ with 6868, 42169, 204958, and 861778 degrees of freedom.

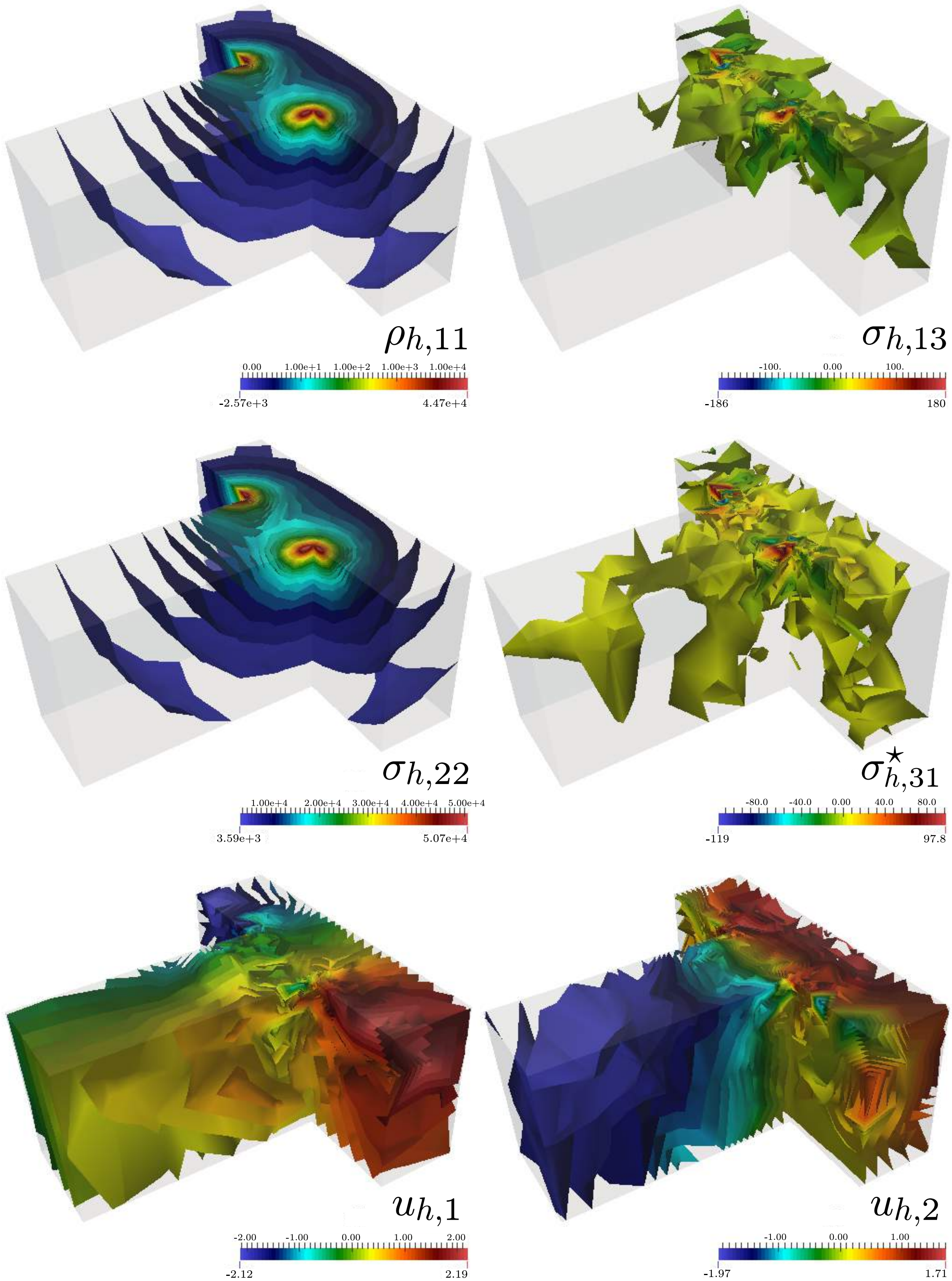

Figure 1.6: Example 3, iso-surfaces of some components of the approximate solutions ($k = 2$ and $N = 270037$) for adaptive scheme.

CHAPTER 2

Analysis of an augmented pseudostress-based mixed formulation for a nonlinear Brinkman model of porous media flow

2.1 Introduction

The Brinkman model of porous media flow, which can be seen as a mixture of Darcy's and Stokes' equations, is usually hard to solve, firstly because of the wide range of possible permeability ratios, and secondly due to the nature of the mixed boundary conditions involved. One way of solving the first issue is by means of stabilized methods (see, e.g. [21], [100]), whereas the weak imposition of the Dirichlet boundary conditions, using Nitsche's method, has been applied recently to deal with the second difficulty (see, e.g. [95] and the references therein). However, most of the variational formulations found in the literature are based on the typical Stokes-type (also called primal-mixed) approach in which the velocity and the pressure are kept as the main unknowns. Actually, up to the authors' knowledge, no stress-based or pseudostress-based approaches seemed to be available until the recent contribution [72], where an alternative way of dealing with the mixed boundary conditions and the *a priori* and *a posteriori* error analyses of a dual-mixed approach for the two-dimensional Brinkman problem were provided. Indeed, the pseudostress $\boldsymbol{\sigma}$ is the main unknown of the resulting saddle point problem in [72], and the velocity and pressure are easily recovered in terms of $\boldsymbol{\sigma}$ through simple postprocessing formulae. In addition, as it is usual for dual-mixed methods, the Dirichlet boundary condition for the velocity becomes natural in this case, and the Neumann boundary condition, being essential, is imposed weakly through the introduction of the trace of the velocity on that boundary as the associated Lagrange multiplier. In this way, the Babuška-Brezzi theory is applied first in [72] to establish sufficient conditions for the well-posedness of the resulting continuous and discrete formulations. In particular, a feasible choice of finite element subspaces is given by Raviart-Thomas elements of order $k \geq 0$ for the pseudostress, and continuous piecewise polynomials of degree $k+1$ for the Lagrange multiplier. Next, a reliable and efficient residual-based *a posteriori* error estimator is derived there. Suitable auxiliary problems, the continuous inf-sup conditions satisfied by the bilinear forms involved, a discrete Helmholtz decomposition, and the local approximation properties of the Raviart-Thomas and Clément interpolation operators are the main tools for proving the reliability. In turn, Helmholtz's decomposition, inverse inequalities, and the localization technique based on triangle-bubble and edge-bubble functions are employed to show the efficiency.

The purpose of the present chapter is to extend the analysis and results from [72] to a class of Brinkman models whose viscosity depends nonlinearly on the gradient of the velocity, which is a characteristic feature of quasi-Newtonian Stokes flows (see, e.g. [76, 84, 98]). To this end, we introduce the gradient of the velocity as a new unknown and follow the approach from [84] to deal with the aforedescribed nonlinearity. Moreover, in order to be able to apply the abstract theory from [118] dealing with nonlinear saddle point problems (see also [67], [77]), we need to modify the resulting variational formulation by augmenting it with a redundant equation arising from the constitutive law relating the pseudostress and the velocity gradient. The rest of this work is organized as follows. In Section 2.2 we define our nonlinear Brinkman model. Then, in Section 2.3 we introduce the augmented continuous formulation and analize its solvability. The associated mixed finite element method is introduced and analyzed in Section 2.4. Next, in Section 2.5 we basically apply the techniques from [66], [83], and [84], to derive a reliable and efficient residual-based *a posteriori* error estimator for our Galerkin scheme. Finally, some numerical results showing the good performance and robustness of the mixed finite element method, confirming the reliability and efficiency of the estimator, and illustrating the behavior of the associated adaptive algorithm are reported in Section 2.6.

We end this section with some notations to be used below. Given $\boldsymbol{\tau} := (\tau_{ij})$, $\boldsymbol{\zeta} := (\zeta_{ij}) \in \mathrm{R}^{2\times 2}$, we write as usual

$$\boldsymbol{\tau}^{\mathrm{t}} := (\tau_{ji}), \quad \mathrm{tr}\,(\boldsymbol{\tau}) := \sum_{i=1}^{2} \tau_{ii}, \quad \boldsymbol{\tau}^{\mathrm{d}} := \boldsymbol{\tau} - \frac{1}{2}\mathrm{tr}\,(\boldsymbol{\tau})\,\mathbb{I}, \quad \text{and} \quad \boldsymbol{\tau} : \boldsymbol{\zeta} := \sum_{i,j=1}^{2} \tau_{ij}\zeta_{ij},$$

where $\mathbb{I}$ is the identity matrix of $\mathrm{R}^{2\times 2}$. In addition, in what follows we utilize standard simplified terminology for Sobolev spaces and norms. In particular, if $\mathcal{O} \subset \mathrm{R}^2$ is a domain, $\mathcal{S} \subset \mathrm{R}^2$ is a Lipschitz curve, and $r \in \mathrm{R}$, we define

$$\mathbf{H}^r(\mathcal{O}) := [H^r(\mathcal{O})]^2, \quad \mathbb{H}^r(\mathcal{O}) := [H^r(\mathcal{O})]^{2\times 2}, \quad \text{and} \quad \mathbf{H}^r(\mathcal{S}) := [H^r(\mathcal{S})]^2.$$

However, when $r = 0$ we usually write $\mathbf{L}^2(\mathcal{O})$, $\mathbb{L}^2(\mathcal{O})$, and $\mathbf{L}^2(\mathcal{S})$ instead of $\mathbf{H}^0(\mathcal{O})$, $\mathbb{H}^0(\mathcal{O})$, and $\mathbf{H}^0(\mathcal{S})$, respectively. The corresponding norms are denoted by $\|\cdot\|_{r,\mathcal{O}}$ (for $H^r(\mathcal{O})$, $\mathbf{H}^r(\mathcal{O})$, and $\mathbb{H}^r(\mathcal{O})$) and $\|\cdot\|_{r,\mathcal{S}}$ (for $H^r(\mathcal{S})$ and $\mathbf{H}^r(\mathcal{S})$). In general, given any Hilbert space H, we use $\mathbf{H}$ and $\mathbb{H}$ to denote H^2 and $H^{2\times 2}$, respectively. In turn, the Hilbert space

$$\mathbf{H}(\mathrm{div};\mathcal{O}) := \left\{ \mathbf{w} \in \mathbf{L}^2(\mathcal{O}) \;:\; \mathrm{div}(\mathbf{w}) \in L^2(\mathcal{O}) \right\},$$

is standard in the realm of mixed problems (see [19]). The space of matrix valued functions whose rows belong to $\mathbf{H}(\mathrm{div};\mathcal{O})$ will be denoted $\mathbb{H}(\mathbf{div};\mathcal{O})$. Hereafter, $\mathbf{div}$ denotes the usual divergence operator div acting along each row of the corresponding tensor. The Hilbert norms of $\mathbf{H}(\mathrm{div};\mathcal{O})$ and $\mathbb{H}(\mathbf{div};\mathcal{O})$ are denoted by $\|\cdot\|_{\mathrm{div},\mathcal{O}}$ and $\|\cdot\|_{\mathbf{div},\mathcal{O}}$, respectively. Note that if $\boldsymbol{\tau} \in \mathbb{H}(\mathbf{div};\mathcal{O})$, then $\mathbf{div}(\boldsymbol{\tau}) \in \mathbf{L}^2(\mathcal{O})$. Finally, we employ $\mathbf{0}$ to denote a generic null vector (including the null functional and operator), and use C and c, with or without subscripts, bars, tildes or hats, to denote generic constants independent of the discretization parameters, which may take different values at different places.

2.2 The nonlinear Brinkman model

Let Ω be a bounded and simply connected open domain in R^2 with polygonal boundary Γ, and such that all its interior angles lie in $(0, 2\pi)$. Also, let Γ_D and Γ_N be disjoint open subsets of Γ, with $|\Gamma_D|$, $|\Gamma_N| \neq 0$, such that $\Gamma = \bar{\Gamma}_D \cup \bar{\Gamma}_N$. Then, given $\mathbf{f} \in \mathbf{L}^2(\Omega)$ and $\mathbf{g} \in \mathbf{H}^{-1/2}(\Gamma_N)$, our boundary value problem reads as follows: Find a tensor field $\boldsymbol{\sigma}$ (pseudostress), a vector field $\mathbf{u}$ (velocity), and a scalar field p (pressure) in appropriate spaces such that

$$\begin{aligned} \boldsymbol{\sigma} &= \mu(|\nabla\mathbf{u}|)\nabla\mathbf{u} - p\,\mathbb{I} \quad \text{in } \Omega, \quad \alpha\,\mathbf{u} - \mathbf{div}(\boldsymbol{\sigma}) = \mathbf{f} \quad \text{in } \Omega, \\ \operatorname{div}(\mathbf{u}) &= 0 \quad \text{in } \Omega, \quad \mathbf{u} = \mathbf{0} \quad \text{on } \Gamma_D, \quad \boldsymbol{\sigma\nu} = \mathbf{g} \quad \text{on } \Gamma_N, \end{aligned} \tag{2.1}$$

where $\mu : \mathrm{R}^+ \to \mathrm{R}^+$ is the nonlinear dynamic viscosity function, $\alpha > 0$ is a constant approximation of the viscosity divided by the permeability, $|\cdot|$ is the euclidean norm of $\mathrm{R}^{2\times 2}$, and $\boldsymbol{\nu}$ is the unit outward normal to Γ. Alternatively, one could also assume that α is a known positive function approximating the viscosity divided by the permeability, which is lowerly and upperly bounded, in which case the corresponding analysis would be a slight variation of the one to be developed in what follows. Furthermore, we recall here that the Sobolev space $\mathbf{H}^{-1/2}(\Gamma_N)$ is defined as the dual of $\mathbf{H}^{1/2}_{00}(\Gamma_N)$, where

$$\mathbf{H}^{1/2}_{00}(\Gamma_N) := \left\{ \mathbf{v}|_{\Gamma_N} \; : \; \mathbf{v} \in \mathbf{H}^1(\Omega), \quad \mathbf{v} = \mathbf{0} \;\text{ on }\; \Gamma_D \right\}.$$

The corresponding duality pairing with respect to the $\mathbf{L}^2(\Gamma_N)$ - inner product is denoted by $\langle\cdot,\cdot\rangle_{\Gamma_N}$. In addition, throughout the chapter $\|\cdot\|_{0;1/2,\Gamma_N}$ stands for the usual norm of both $H^{1/2}_{00}(\Gamma_N)$ and $\mathbf{H}^{1/2}_{00}(\Gamma_N)$ (see [72]) .

On the other hand, in what follows we let $\psi_{ij} : \mathrm{R}^{2\times 2} \to \mathrm{R}$ be the mapping given by $\psi_{ij}(\mathbf{r}) := \mu(|\mathbf{r}|)r_{ij}$ for all $\mathbf{r} := (r_{ij}) \in \mathrm{R}^{2\times 2}$, for all $i, j \in \{1, 2\}$. Then, throughout this chapter we assume that μ is of class C^1 and that there exist $\gamma_0, \alpha_0 > 0$ such that for all $\mathbf{r} := (r_{ij})$, $\mathbf{s} := (s_{ij}) \in \mathrm{R}^{2\times 2}$, there holds

$$|\psi_{ij}(\mathbf{r})| \;\leq\; \gamma_0\|\mathbf{r}\|_{\mathrm{R}^{2\times 2}}, \qquad \left|\frac{\partial}{\partial r_{kl}}\psi_{ij}(\mathbf{r})\right| \;\leq\; \gamma_0, \quad \forall\, i,j,k,l \in \{1,2\}, \tag{2.2}$$

and

$$\sum_{i,j,k,l=1}^{2} \frac{\partial}{\partial r_{kl}}\psi_{ij}(\mathbf{r})s_{ij}s_{kl} \;\;\geq\;\; \alpha_0\|\mathbf{s}\|^2_{\mathrm{R}^{2\times 2}}. \tag{2.3}$$

For example, the Carreau law for viscoplastic flows (see, e.g. [108, 117]), given by

$$\mu(t) := \mu_0 + \mu_1(1 + t^2)^{(\beta-2)/2} \quad \forall\, t \in \mathrm{R}^+\,,$$

satisfies (2.2) and (2.3) for all $\mu_0, \mu_1 > 0$, and for all $\beta \in [1, 2]$. In particular, note that with $\beta = 2$ we recover the usual linear Brinkman model.

Now, we observe that the pair of equations given by

$$\boldsymbol{\sigma} = \mu(|\nabla\mathbf{u}|)\nabla\mathbf{u} - p\,\mathbb{I} \quad \text{in } \Omega, \quad \text{and} \quad \operatorname{div}(\mathbf{u}) = 0 \quad \text{in } \Omega,$$

is equivalent to

$$\boldsymbol{\sigma} = \mu(|\nabla\mathbf{u}|)\nabla\mathbf{u} - p\,\mathbb{I} \quad \text{in } \Omega, \quad \text{and} \quad p = -\frac{1}{2}\operatorname{tr}(\boldsymbol{\sigma}) \quad \text{in } \Omega, \tag{2.4}$$

whence introducing the gradient $\mathbf{t} := \nabla\mathbf{u}$ in Ω, as an auxiliary unknown, we can rewrite (2.1) as follows

$$\begin{aligned} \mathbf{t} &= \nabla\mathbf{u} \quad \text{in } \Omega, \quad \boldsymbol{\sigma}^{\mathrm{d}} = \boldsymbol{\psi}(\mathbf{t}) \quad \text{in } \Omega, \quad \alpha\,\mathbf{u} - \mathbf{div}(\boldsymbol{\sigma}) = \mathbf{f} \quad \text{in } \Omega, \\ \operatorname{tr}(\mathbf{t}) &= 0 \quad \text{in } \Omega, \quad \mathbf{u} = \mathbf{0} \quad \text{on } \Gamma_D, \quad \boldsymbol{\sigma\nu} = \mathbf{g} \quad \text{on } \Gamma_N, \end{aligned} \tag{2.5}$$

where $\boldsymbol{\psi} : \mathrm{R}^{2\times 2} \to \mathrm{R}^{2\times 2}$ is given by $\boldsymbol{\psi}(\mathbf{r}) := (\psi_{ij}(\mathbf{r})) = (\mu(|\mathbf{r}|)r_{ij})$ for all $\mathbf{r} := (r_{ij}) \in \mathrm{R}^{2\times 2}$.

2.3 The continuous formulation

2.3.1 The augmented approach

Initially we test the first and second equations of (2.5) with $\boldsymbol{\tau} \in \mathbb{H}(\mathbf{div};\Omega)$ and $\mathbf{s} \in \mathbb{L}^2_{\mathrm{tr}}(\Omega)$, respectively, where

$$\mathbb{L}^2_{\mathrm{tr}}(\Omega) \ := \ \left\{ \mathbf{s} \in \mathbb{L}^2(\Omega) \ : \ \mathrm{tr}\,(\mathbf{s}) \ = \ 0 \right\} .$$

Then, integrating by parts the expression $\int_\Omega \nabla \mathbf{u} : \boldsymbol{\tau}$, using the Dirichlet boundary condition, recalling that $\mathrm{tr}\,(\mathbf{t}) \ = \ 0$, and introducing the auxiliary unknown $\boldsymbol{\xi} := -\mathbf{u}|_{\Gamma_N} \in \mathbf{H}^{1/2}_{00}(\Gamma_N)$, we arrive at

$$\begin{aligned} \int_\Omega \boldsymbol{\psi}(\mathbf{t}) : \mathbf{s} - \int_\Omega \mathbf{s} : \boldsymbol{\sigma}^{\mathrm{d}} \ &= \ 0 \quad \forall\, \mathbf{s} \in \mathbb{L}^2_{\mathrm{tr}}(\Omega), \\ \int_\Omega \mathbf{t} : \boldsymbol{\tau}^{\mathrm{d}} + \int_\Omega \mathbf{u} \cdot \mathbf{div}(\boldsymbol{\tau}) + \langle \boldsymbol{\tau\nu}, \boldsymbol{\xi} \rangle_{\Gamma_N} \ &= \ 0 \quad \forall\, \boldsymbol{\tau} \in \mathbb{H}(\mathbf{div};\Omega). \end{aligned} \tag{2.6}$$

In turn, the Neumann boundary condition is imposed weakly as

$$\langle \boldsymbol{\sigma\nu}, \boldsymbol{\lambda} \rangle_{\Gamma_N} \ = \ \langle \mathbf{g}, \boldsymbol{\lambda} \rangle_{\Gamma_N} \quad \forall\, \boldsymbol{\lambda} \in \mathbf{H}^{1/2}_{00}(\Gamma_N)\,,$$

and replacing $\mathbf{u}$ in (2.6) by

$$\mathbf{u} \ = \ \frac{1}{\alpha} \Big\{ \mathbf{f} \ + \ \mathbf{div}(\boldsymbol{\sigma}) \Big\} \quad \text{in } \Omega, \tag{2.7}$$

we obtain that

$$\int_\Omega \mathbf{t} : \boldsymbol{\tau}^{\mathrm{d}} + \frac{1}{\alpha} \int_\Omega \mathbf{div}(\boldsymbol{\sigma}) \cdot \mathbf{div}(\boldsymbol{\tau}) + \langle \boldsymbol{\tau\nu}, \boldsymbol{\xi} \rangle_{\Gamma_N} \ = \ -\frac{1}{\alpha} \int_\Omega \mathbf{f} \cdot \mathbf{div}(\boldsymbol{\tau}) \quad \forall\, \boldsymbol{\tau} \in \mathbb{H}(\mathbf{div};\Omega).$$

Finally, for sake of feasibility of the forthcoming analysis, namely to be able to apply the abstract theory from [118], we enrich the foregoing equations with the introduction of the constitutive law relating $\boldsymbol{\sigma}$ and $\mathbf{t}$ (written as in the second equation of (2.5)) multiplied by a stabilization parameter. More precisely, given $\kappa > 0$, to be chosen later, we add

$$\kappa \int_\Omega \big(\boldsymbol{\sigma}^{\mathrm{d}} - \boldsymbol{\psi}(\mathbf{t}) \big) : \boldsymbol{\tau}^{\mathrm{d}} \ = \ 0 \quad \forall\, \boldsymbol{\tau} \in \mathbb{H}(\mathbf{div};\Omega),$$

and then, we obtain the variational formulation: Find $((\mathbf{t},\boldsymbol{\sigma}),\boldsymbol{\xi}) \in H \times Q$ such that

$$\begin{aligned} [\mathcal{A}(\mathbf{t},\boldsymbol{\sigma}),(\mathbf{s},\boldsymbol{\tau})] \ + \ [\mathcal{B}(\mathbf{s},\boldsymbol{\tau}),\boldsymbol{\xi}] \ &= \ [\mathcal{F},(\mathbf{s},\boldsymbol{\tau})] \quad \forall\, (\mathbf{s},\boldsymbol{\tau}) \in H, \\ [\mathcal{B}(\mathbf{t},\boldsymbol{\sigma}),\boldsymbol{\lambda}] \ &= \ [\mathcal{G},\boldsymbol{\lambda}] \quad \forall\, \boldsymbol{\lambda} \in Q, \end{aligned} \tag{2.8}$$

where $H := \mathbb{L}^2_{\mathrm{tr}}(\Omega) \times \mathbb{H}(\mathbf{div};\Omega)$, $Q := \mathbf{H}^{1/2}_{00}(\Gamma_N)$, and the nonlinear operator $\mathcal{A} : H \to H'$, the linear operator $\mathcal{B} : H \to Q'$, and the functionals $\mathcal{F} \in H'$ and $\mathcal{G} \in Q'$, are defined by

$$\begin{aligned} [\mathcal{A}(\mathbf{t},\boldsymbol{\sigma}),(\mathbf{s},\boldsymbol{\tau})] \ := \ &\int_\Omega \boldsymbol{\psi}(\mathbf{t}) : \mathbf{s} \ - \ \int_\Omega \mathbf{s} : \boldsymbol{\sigma}^{\mathrm{d}} + \int_\Omega \mathbf{t} : \boldsymbol{\tau}^{\mathrm{d}} \\ + \kappa &\int_\Omega \Big(\boldsymbol{\sigma}^{\mathrm{d}} \ - \ \boldsymbol{\psi}(\mathbf{t}) \Big) : \boldsymbol{\tau}^{\mathrm{d}} + \frac{1}{\alpha} \int_\Omega \mathbf{div}(\boldsymbol{\sigma}) \cdot \mathbf{div}(\boldsymbol{\tau})\,, \end{aligned} \tag{2.9}$$

$$[\mathcal{B}(\mathbf{s},\boldsymbol{\tau}),\boldsymbol{\lambda}] \ := \ \langle \boldsymbol{\tau\nu}, \boldsymbol{\lambda} \rangle_{\Gamma_N}\ , \tag{2.10}$$

$$[\mathcal{F},(\mathbf{s},\boldsymbol{\tau})] \ := \ -\frac{1}{\alpha} \int_\Omega \mathbf{f} \cdot \mathbf{div}(\boldsymbol{\tau})\,,$$

$$[\mathcal{G},\boldsymbol{\lambda}] \ := \ \langle \mathbf{g}, \boldsymbol{\lambda} \rangle_{\Gamma_N}\ , \tag{2.11}$$

where $[\cdot,\cdot]$ stands in each case for the duality pairing induced by the corresponding operators and functionals.

2.3.2 Analysis of the augmented formulation

The purpose of this section is to establish the well-posedness of (2.8). We begin the analysis by recalling from [118] the following abstract theorem.

Theorem 2.1. *Let X and M be Hilbert spaces, and let $\mathcal{A} : X \to X'$ and $\mathcal{B} : X \to M'$ be nonlinear and linear operators, respectively. Let $V := Ker(\mathcal{B}) = \{x \in X : [\mathcal{B}(x), q] = 0\ \forall q \in M\}$. Assume that $\mathcal{A}$ is Lipschitz-continuous on X and that for all $\widetilde{z} \in X$, $\mathcal{A}(\widetilde{z} + \cdot\ )$ is uniformly strongly monotone on V, that is, there exist constants c_1, $c_2 > 0$ such that*

$$\|\mathcal{A}(x) - \mathcal{A}(y)\|_{X'} \ \le\ c_1 \|x - y\|_X \quad \forall\, x, y \in X,$$

and

$$[\mathcal{A}(\widetilde{z} + x) - \mathcal{A}(\widetilde{z} + y)] \ \ge\ c_2 \|x - y\|_X^2,$$

for all $\widetilde{z} \in X$ and for all $x, y \in V$. In addition, assume that there exists $\beta > 0$ such that for all $q \in M$

$$\sup_{\substack{x \in X\\ x \neq \mathbf{0}}} \frac{[\mathcal{B}(x), q]}{\|x\|_X} \ \ge\ \beta \|q\|_M .$$

Then, given $(\mathcal{F}, \mathcal{G}) \in X' \times M'$, there exists a unique $(x, p) \in X \times M$ such that

$$\begin{aligned} [\mathcal{A}(x), y] \ +\ [\mathcal{B}(y), p] &= [\mathcal{F}, y] \quad \forall\, y \in X, \\ [\mathcal{B}(x), q] \qquad\qquad &= [\mathcal{G}, q] \quad \forall\, q \in M. \end{aligned}$$

Further, the following estimates hold

$$\|x\|_X \ \le\ \frac{1}{c_2} \|\mathcal{F}\| + \frac{1}{\beta}\left(1 + \frac{c_1}{c_2}\right) \|\mathcal{G}\|, \tag{2.12}$$

$$\|p\|_M \ \le\ \frac{1}{\beta}\left(1 + \frac{c_1}{c_2}\right)\left(\|\mathcal{F}\| + \frac{c_1}{\beta}\|\mathcal{G}\|\right). \tag{2.13}$$

Proof. See [118, Proposition 2.3] or [84, Theorem 3.1]. □

In what follows we apply Theorem 2.1 to the augmented formulation (2.8). The inf-sup condition for the linear operator $\mathcal{B}$ is proved first.

Lemma 2.1. *There exists a positive constant β, depending only on Ω, such that*

$$\sup_{\substack{(\mathbf{s}, \boldsymbol{\tau}) \in H\\ (\mathbf{s}, \boldsymbol{\tau}) \neq \mathbf{0}}} \frac{[\mathcal{B}(\mathbf{s}, \boldsymbol{\tau}), \boldsymbol{\lambda}]}{\|(\mathbf{s}, \boldsymbol{\tau})\|_H} \ \ge\ \beta \|\boldsymbol{\lambda}\|_{0;1/2,\Gamma_N} \quad \forall\, \boldsymbol{\lambda} \in Q.$$

Proof. Note that $\mathcal{B} : H \to Q'$ is given by $\mathcal{B}(\mathbf{s}, \boldsymbol{\tau}) := \boldsymbol{\tau}\boldsymbol{\nu}|_{\Gamma_N} \in \mathbf{H}^{-1/2}(\Gamma_N) = Q' \quad \forall\, (\mathbf{s}, \boldsymbol{\tau}) \in H$, and hence the fact that the normal trace operator $\gamma_{\boldsymbol{\nu}} : \mathbb{H}(\mathbf{div}; \Omega) \to \mathbf{H}^{-1/2}(\Gamma_N)$ is surjective implies the same property for $\mathcal{B}$. □

Next, in order to verify the assumptions required by Theorem 2.1 for our nonlinear operator $\mathcal{A}$, we define the auxiliary nonlinear operator $\mathbb{A} : \mathbb{L}^2_{\mathrm{tr}}(\Omega) \to [\mathbb{L}^2_{\mathrm{tr}}(\Omega)]'$ given by

$$[\mathbb{A}(\mathbf{r}), \mathbf{s}] \ :=\ \int_\Omega \boldsymbol{\psi}(\mathbf{r}) : \mathbf{s} \quad \forall\, \mathbf{r}, \mathbf{s} \in \mathbb{L}^2_{\mathrm{tr}}(\Omega). \tag{2.14}$$

It is easy to show from (2.2) and (2.3) (see e.g. [84, Lemma 2.1]) that $\mathbb{A}$ is Lipschitz-continuous and strongly monotone.

Lemma 2.2. *Let γ_0 and α_0 be the constants of* (2.2) *and* (2.3)*, respectively. Then, for each $\mathbf{r}, \mathbf{s} \in \mathbb{L}^2_{\mathrm{tr}}(\Omega)$ there hold*

$$\|\mathbb{A}(\mathbf{r}) - \mathbb{A}(\mathbf{s})\|_{[\mathbb{L}^2(\Omega)]'} \;\leq\; \gamma_0 \|\mathbf{r} - \mathbf{s}\|_{0,\Omega}, \tag{2.15}$$

and

$$[\mathbb{A}(\mathbf{r}) - \mathbb{A}(\mathbf{s}), \mathbf{r} - \mathbf{s}] \;\geq\; \alpha_0 \|\mathbf{r} - \mathbf{s}\|^2_{0,\Omega}. \tag{2.16}$$

Proof. It suffices to observe that for each $\widetilde{\mathbf{r}} \in \mathbb{L}^2_{\mathrm{tr}}(\Omega)$ the Gâteuax derivative $\mathcal{D}\mathbb{A}(\widetilde{\mathbf{r}})$ is a bilinear form on $\mathbb{L}^2_{\mathrm{tr}}(\Omega) \times \mathbb{L}^2_{\mathrm{tr}}(\Omega)$, which is uniformly bounded and uniformly $\mathbb{L}^2_{\mathrm{tr}}(\Omega)$-elliptic (see [84, Lemma 2.1] for details). $\square$

We are now ready to establish that the nonlinear operator $\mathcal{A}$ (cf. (2.9)) is also Lipschitz-continuous on H.

Lemma 2.3. *Let $\mathcal{A}$ be the nonlinear operator defined in* (2.9)*. Then, there exists a constant $C_{\mathrm{LC}} > 0$ such that*

$$\|\mathcal{A}(\mathbf{t}, \boldsymbol{\sigma}) - \mathcal{A}(\mathbf{s}, \boldsymbol{\tau})\|_{H'} \;\leq\; C_{\mathrm{LC}} \|(\mathbf{t}, \boldsymbol{\sigma}) - (\mathbf{s}, \boldsymbol{\tau})\|_H \quad \forall\, (\mathbf{t}, \boldsymbol{\sigma}), (\mathbf{s}, \boldsymbol{\tau}) \in H.$$

Proof. Given $(\mathbf{t}, \boldsymbol{\sigma}), (\mathbf{s}, \boldsymbol{\tau})$ and $(\mathbf{r}, \boldsymbol{\rho}) \in H$, we obtain, according to the definition of $\mathcal{A}$ and $\mathbb{A}$, that

$$\begin{aligned}
[\mathcal{A}(\mathbf{t}, \boldsymbol{\sigma}) - \mathcal{A}(\mathbf{s}, \boldsymbol{\tau}), (\mathbf{r}, \boldsymbol{\rho})] \;=\; & [\mathbb{A}(\mathbf{t}) - \mathbb{A}(\mathbf{s}), \mathbf{r}] \;-\; \kappa[\mathbb{A}(\mathbf{t}) - \mathbb{A}(\mathbf{s}), \boldsymbol{\rho}^{\mathrm{d}}] \;-\; \int_\Omega \mathbf{r} : (\boldsymbol{\sigma} - \boldsymbol{\tau})^{\mathrm{d}} \\
+ \;\; & \int_\Omega (\mathbf{t} - \mathbf{s}) : \boldsymbol{\rho}^{\mathrm{d}} \;+\; \kappa \int_\Omega (\boldsymbol{\sigma} - \boldsymbol{\tau})^{\mathrm{d}} : \boldsymbol{\rho}^{\mathrm{d}} + \frac{1}{\alpha} \int_\Omega \mathbf{div}(\boldsymbol{\sigma} - \boldsymbol{\tau}) \cdot \mathbf{div}(\boldsymbol{\rho})\,.
\end{aligned} \tag{2.17}$$

Hence, it follows easily from (2.17), (2.15), and the Cauchy-Schwarz inequality, that $\mathcal{A}$ is Lipschitz-continuous on H with the constant $C_{\mathrm{LC}} := 3\max\{1, \gamma_0, \kappa, \kappa\gamma_0, \alpha^{-1}\}$. $\square$

Our next goal is to show that for all $(\mathbf{r}, \boldsymbol{\rho}) \in H$, $\mathcal{A}((\mathbf{r}, \boldsymbol{\rho}) + \cdot\,)$ is uniformly strongly monotone on the kernel of $\mathcal{B}$, given by $V := \{(\mathbf{s}, \boldsymbol{\tau}) \in H \;:\; \boldsymbol{\tau}\boldsymbol{\nu} \;=\; \mathbf{0} \;\text{ on } \Gamma_N\}$. To this end, we first consider the decomposition

$$\mathbb{H}(\mathbf{div}; \Omega) \;=\; \mathbb{H}_0(\mathbf{div}; \Omega) \oplus \mathrm{R}\mathbb{I},$$

where $\mathbb{H}_0(\mathbf{div}; \Omega) := \{\boldsymbol{\tau} \in \mathbb{H}(\mathbf{div}; \Omega) \;:\; \int_\Omega \mathrm{tr}\,(\boldsymbol{\tau}) \;=\; 0\}$. This means that for any $\boldsymbol{\tau} \in \mathbb{H}(\mathbf{div}; \Omega)$ there exist unique $\boldsymbol{\tau}_0 \in \mathbb{H}_0(\mathbf{div}; \Omega)$ and $d := \frac{1}{2|\Omega|} \int_\Omega \mathrm{tr}\,(\boldsymbol{\tau}) \in \mathrm{R}$ such that $\boldsymbol{\tau} \;=\; \boldsymbol{\tau}_0 + d\mathbb{I}$, whence $\|\boldsymbol{\tau}\|^2_{\mathbf{div},\Omega} = \|\boldsymbol{\tau}_0\|^2_{\mathbf{div},\Omega} + 2d^2|\Omega|$. In addition, we have the following lemmas.

Lemma 2.4. *There exists $C_1 > 0$, depending only on Ω, such that*

$$C_1 \|\boldsymbol{\tau}_0\|^2_{0,\Omega} \;\leq\; \|\boldsymbol{\tau}^{\mathrm{d}}\|^2_{0,\Omega} \;+\; \|\mathbf{div}(\boldsymbol{\tau})\|^2_{0,\Omega} \quad \forall\, \boldsymbol{\tau} \in \mathbb{H}(\mathbf{div}; \Omega).$$

Proof. See [5, Lemma 3.1] or [19, Proposition 3.1, Chapter IV]. $\square$

Lemma 2.5. *There exists $C_2 > 0$, depending only on Γ_N and Ω, such that*

$$C_2 \|\boldsymbol{\tau}\|^2_{\mathbf{div},\Omega} \;\leq\; \|\boldsymbol{\tau}_0\|^2_{\mathbf{div},\Omega} \quad \forall\, \boldsymbol{\tau} \in \mathbb{H}(\mathbf{div}; \Omega) \quad \textit{such that} \quad \boldsymbol{\tau}\boldsymbol{\nu} \;=\; \mathbf{0} \quad \textit{on} \;\; \Gamma_N.$$

Proof. See [69, Lemma 2.2]. $\square$

The uniform strong monotonicity of $\mathcal{A}((\mathbf{r},\boldsymbol{\rho})+\cdot\,)$ on V, for all $(\mathbf{r},\boldsymbol{\rho})\in H$, is proved as follows.

Lemma 2.6. *Let $\mathcal{A}$ and $\mathcal{B}$ be the operators defined in* (2.9) *and* (2.10)*, respectively, and let V be the kernel of $\mathcal{B}$. Assume that the parameter κ lies in $\left(0,\frac{2\alpha_0\delta}{\gamma_0}\right)$ for each $\delta\in\left(0,\frac{2}{\gamma_0}\right)$, where α_0 and γ_0 are the positive constants from* (2.2) *and* (2.3)*. Then, there exists a constant $C_{\mathrm{SM}}>0$ such that for all $(\mathbf{r},\boldsymbol{\rho})\in H$, and for all $(\mathbf{t},\boldsymbol{\sigma}),(\mathbf{s},\boldsymbol{\tau})\in V$ there holds*

$$[\mathcal{A}((\mathbf{r},\boldsymbol{\rho})+(\mathbf{t},\boldsymbol{\sigma}))-\mathcal{A}((\mathbf{r},\boldsymbol{\rho})+(\mathbf{s},\boldsymbol{\tau})),(\mathbf{t},\boldsymbol{\sigma})-(\mathbf{s},\boldsymbol{\tau})]\;\geq\;C_{\mathrm{SM}}\|(\mathbf{t},\boldsymbol{\sigma})-(\mathbf{s},\boldsymbol{\tau})\|_H^2\,.$$

Proof. Given $(\mathbf{r},\boldsymbol{\rho})\in H$ and $(\mathbf{t},\boldsymbol{\sigma}),(\mathbf{s},\boldsymbol{\tau})\in V$, we obtain from (2.17) that

$$\begin{aligned}&[\mathcal{A}((\mathbf{r},\boldsymbol{\rho})+(\mathbf{t},\boldsymbol{\sigma}))-\mathcal{A}((\mathbf{r},\boldsymbol{\rho})+(\mathbf{s},\boldsymbol{\tau})),(\mathbf{t},\boldsymbol{\sigma})-(\mathbf{s},\boldsymbol{\tau})]\\&\quad=\;[\mathbb{A}(\mathbf{r}+\mathbf{t})-\mathbb{A}(\mathbf{r}+\mathbf{s}),\mathbf{t}-\mathbf{s}]-\kappa[\mathbb{A}(\mathbf{r}+\mathbf{t})-\mathbb{A}(\mathbf{r}+\mathbf{s}),(\boldsymbol{\sigma}-\boldsymbol{\tau})^{\mathrm{d}}]\\&\qquad+\;\kappa\|(\boldsymbol{\sigma}-\boldsymbol{\tau})^{\mathrm{d}}\|_{0,\Omega}^2+\frac{1}{\alpha}\|\mathbf{div}(\boldsymbol{\sigma}-\boldsymbol{\tau})\|_{0,\Omega}^2.\end{aligned}$$

Then, using that $[\mathbb{A}(\mathbf{r}+\mathbf{t})-\mathbb{A}(\mathbf{r}+\mathbf{s}),\mathbf{t}-\mathbf{s}]=[\mathbb{A}(\mathbf{r}+\mathbf{t})-\mathbb{A}(\mathbf{r}+\mathbf{s}),(\mathbf{r}+\mathbf{t})-(\mathbf{r}+\mathbf{s})]$, and applying the strong monotonicity and Lipschitz-continuity of $\mathbb{A}$ (cf. Lemma 2.2), we deduce from the foregoing equation that

$$\begin{aligned}&[\mathcal{A}((\mathbf{r},\boldsymbol{\rho})+(\mathbf{t},\boldsymbol{\sigma}))-\mathcal{A}((\mathbf{r},\boldsymbol{\rho})+(\mathbf{s},\boldsymbol{\tau})),(\mathbf{t},\boldsymbol{\sigma})-(\mathbf{s},\boldsymbol{\tau})]\\&\quad\geq\;\alpha_0\|\mathbf{t}-\mathbf{s}\|_{0,\Omega}^2-\kappa\gamma_0\|\mathbf{t}-\mathbf{s}\|_{0,\Omega}\|(\boldsymbol{\sigma}-\boldsymbol{\tau})^{\mathrm{d}}\|_{0,\Omega}+\kappa\|(\boldsymbol{\sigma}-\boldsymbol{\tau})^{\mathrm{d}}\|_{0,\Omega}^2+\frac{1}{\alpha}\|\mathbf{div}(\boldsymbol{\sigma}-\boldsymbol{\tau})\|_{0,\Omega}^2\\&\quad\geq\;\alpha_0\|\mathbf{t}-\mathbf{s}\|_{0,\Omega}^2-\kappa\gamma_0\left\{\frac{\|\mathbf{t}-\mathbf{s}\|_{0,\Omega}^2}{2\delta}+\frac{\delta\|(\boldsymbol{\sigma}-\boldsymbol{\tau})^{\mathrm{d}}\|_{0,\Omega}^2}{2}\right\}+\kappa\|(\boldsymbol{\sigma}-\boldsymbol{\tau})^{\mathrm{d}}\|_{0,\Omega}^2\;+\;\frac{1}{\alpha}\|\mathbf{div}(\boldsymbol{\sigma}-\boldsymbol{\tau})\|_{0,\Omega}^2\\&\quad=\;\left(\alpha_0-\frac{\kappa\gamma_0}{2\delta}\right)\|\mathbf{t}-\mathbf{s}\|_{0,\Omega}^2+\kappa\left(1-\frac{\gamma_0\delta}{2}\right)\|(\boldsymbol{\sigma}-\boldsymbol{\tau})^{\mathrm{d}}\|_{0,\Omega}^2+\frac{1}{\alpha}\|\mathbf{div}(\boldsymbol{\sigma}-\boldsymbol{\tau})\|_{0,\Omega}^2\,,\end{aligned}$$

for all $\delta>0$. It follows that the constants multiplying the norms above become positive if $\delta\in\left(0,\frac{2}{\gamma_0}\right)$ and $\kappa\in\left(0,\frac{2\alpha_0\delta}{\gamma_0}\right)$. Then, applying Lemmas 2.4 and 2.5, we deduce that

$$\begin{aligned}&[\mathcal{A}((\mathbf{r},\boldsymbol{\rho})+(\mathbf{t},\boldsymbol{\sigma}))-\mathcal{A}((\mathbf{r},\boldsymbol{\rho})+(\mathbf{s},\boldsymbol{\tau})),(\mathbf{t},\boldsymbol{\sigma})-(\mathbf{s},\boldsymbol{\tau})]\\&\quad\geq\;\left(\alpha_0-\frac{\kappa\gamma_0}{2\delta}\right)\|\mathbf{t}-\mathbf{s}\|_{0,\Omega}^2+\beta_1\|(\boldsymbol{\sigma}-\boldsymbol{\tau})_0\|_{0,\Omega}^2+\frac{1}{2\alpha}\|\mathbf{div}((\boldsymbol{\sigma}-\boldsymbol{\tau})_0)\|_{0,\Omega}^2\\&\quad\geq\;\left(\alpha_0-\frac{\kappa\gamma_0}{2\delta}\right)\|\mathbf{t}-\mathbf{s}\|_{0,\Omega}^2+\beta_2\|(\boldsymbol{\sigma}-\boldsymbol{\tau})_0\|_{\mathbf{div},\Omega}^2\\&\quad\geq\;\left(\alpha_0-\frac{\kappa\gamma_0}{2\delta}\right)\|\mathbf{t}-\mathbf{s}\|_{0,\Omega}^2+C_2\beta_2\|(\boldsymbol{\sigma}-\boldsymbol{\tau})\|_{\mathbf{div},\Omega}^2,\end{aligned}$$

where $\beta_1:=C_1\min\left\{1-\frac{\gamma_0\delta}{2},\frac{1}{2\alpha}\right\}>0$ and $\beta_2:=\min\left\{\beta_1,\frac{1}{2\alpha}\right\}>0$. Finally, the proof is completed by choosing $C_{\mathrm{SM}}:=\min\left\{\alpha_0-\frac{\kappa\gamma_0}{2\delta},C_2\beta_2\right\}$. $\square$

We remark here that the optimal choice of the stabilization parameter κ, that is the one yielding the largest value of the strong monotonicity constant C_{SM}, arises by taking $\delta=\frac{1}{\gamma_0}$ and $\kappa=\frac{\alpha_0}{\gamma_0^2}$.

The well-posedness of our variational formulation (2.8) is provided by the following theorem.

Theorem 2.2. *Assume that $\mathbf{f}\in\mathbf{L}^2(\Omega)$, $\mathbf{g}\in\mathbf{H}^{-1/2}(\Gamma_N)$, and that the parameter κ lies in $\left(0,\frac{2\alpha_0\delta}{\gamma_0}\right)$ for each $\delta\in\left(0,\frac{2}{\gamma_0}\right)$, where α_0 and γ_0 are the positive constants from* (2.2) *and* (2.3)*. Then, there exists a* *unique* $((\mathbf{t},\boldsymbol{\sigma}),\boldsymbol{\xi}) \in H \times Q$ *solution of* (2.8). *In addition, there exists a positive constant* C, *depending on* Γ_N, Ω, β, α_0, γ_0, κ, *and* α, *such that*

$$\|\mathbf{t}\|_{0,\Omega} \;+\; \|\boldsymbol{\sigma}\|_{\mathbf{div},\Omega} \;+\; \|\boldsymbol{\xi}\|_{0;1/2,\Gamma_N} \;\leq\; C\left\{\|\mathbf{f}\|_{0,\Omega} \;+\; \|\mathbf{g}\|_{-1/2,\Gamma_N}\right\}.$$

Proof. Thanks to Lemmas 2.1, 2.3, and 2.6, the proof is a direct application of Theorem 2.1. □

2.4 The mixed finite element method

In this section we adapt the approach from [72] and define explicit finite element subspaces H_h of $\mathbb{L}^2_{\mathrm{tr}}(\Omega) \times \mathbb{H}(\mathbf{div};\Omega)$ and Q_h of $\mathbf{H}^{1/2}_{00}(\Gamma_N)$ such that the mixed finite element scheme associated with the continuous formulation (2.8) is well-posed. For this purpose, let $\{\mathcal{T}_h\}_{h>0}$ be a shape-regular family of triangulations of the polygonal region $\bar{\Omega}$ by triangles T of diameter h_T, with mesh size $h := \max\{h_T : T \in \mathcal{T}_h\}$, and such that all the points in $\bar{\Gamma}_D \cap \bar{\Gamma}_N$ become vertices of $\mathcal{T}_h$ for all $h > 0$. Also, given an integer $k \geq 0$ and a subset S of R^2, we denote by $\mathrm{P}_k(S)$ the space of polynomials defined in S of total degree at most k. Then, for each integer $k \geq 0$ and for each $T \in \mathcal{T}_h$, we define the local Raviart-Thomas space of order k (see, e.g. [19], [116])

$$\mathbf{RT}_k(T) \;:=\; \mathbf{P}_k(T) \;\oplus\; \mathrm{P}_k(T)\mathbf{x},$$

where $\mathbf{x} = \binom{x_1}{x_2}$ is a generic vector of R^2, and $\mathbf{P}_k(T) := [\mathrm{P}_k(T)]^2$. Now, let $\mathbb{RT}_k(\mathcal{T}_h)$ be the corresponding global Raviart-Thomas tensor space of order k, that is,

$$\mathbb{RT}_k(\mathcal{T}_h) \;:=\; \left\{\boldsymbol{\tau} \in \mathbb{H}(\mathbf{div};\Omega) \;:\; (\tau_{i1},\tau_{i2})^{\mathrm{t}}|_T \in \mathbf{RT}_k(T) \;\; \forall\, i \in \{1,2\}, \quad \forall\, T \in \mathcal{T}_h\right\}.$$

We also let $\mathbb{X}_h$ be the global tensor space of piecewise polynomials of degree $\leq k$ with zero trace, that is

$$\mathbb{X}_h \;:=\; \left\{\mathbf{s} \in \mathbb{L}^2_{\mathrm{tr}}(\Omega) \;:\; \mathbf{s}|_T \in \mathbb{P}_k(T) \quad \forall\, T \in \mathcal{T}_h\right\},$$

so that the corresponding finite element subspace H_h for $(\mathbf{t},\boldsymbol{\sigma}) \in \mathbb{L}^2_{\mathrm{tr}}(\Omega) \times \mathbb{H}(\mathbf{div};\Omega)$ is given by

$$H_h \;:=\; \mathbb{X}_h \times \mathbb{RT}_k(\mathcal{T}_h). \tag{2.18}$$

In turn, an eventual finite element subspace for the fluid velocity $\mathbf{u}$ would be given by the global vector space of piecewise polynomials of degree $\leq k$, that is

$$\mathcal{Q}^{\mathbf{u}}_h \;:=\; \left\{\mathbf{v} \in \mathbf{L}^2(\Omega) \;:\; \mathbf{v}|_T \in \mathbf{P}_k(T) \quad \forall\, T \in \mathcal{T}_h\right\}. \tag{2.19}$$

Next, let Σ_h be the partition on Γ_N induced by the triangulation $\mathcal{T}_h$, and define the mesh size $h_\Sigma := \max\{|e| : e \in \Sigma_h\}$. Then, proceeding exactly as in [72], we consider in what follows two possible choices for Q_h, the finite element subspace approximating the unknown $\boldsymbol{\xi} \in \mathbf{H}^{1/2}_{00}(\Gamma_N)$.

A first choice for Q_h: Let $\Sigma_{\tilde{h}}$ be another partition of Γ_N, completely independent from Σ_h, with $\tilde{h} := \max\{|e| : e \in \Sigma_{\tilde{h}}\}$. Then, given an integer $k \geq 0$, we define

$$Q_h \;:=\; \left\{\boldsymbol{\lambda}_{\tilde{h}} \in \mathbf{H}^{1/2}_{00}(\Gamma_N) \;:\; \boldsymbol{\lambda}_{\tilde{h}}|_e \in \mathbf{P}_{k+1}(e) \quad \forall\, e \in \Sigma_{\tilde{h}}\right\}. \tag{2.20}$$

A second choice for Q_h: Let us assume that the number of edges of Σ_h is an even number. Then, we let Σ_{2h} be the partition of Γ_N arising by joining pairs of adjacent elements, and define for $k = 0$

$$Q_h \;:=\; \left\{\boldsymbol{\lambda}_h \in \mathbf{H}^{1/2}_{00}(\Gamma_N) \;:\; \boldsymbol{\lambda}_h|_e \in \mathbf{P}_1(e) \quad \forall\, e \in \Sigma_{2h}\right\}. \tag{2.21}$$

As already stated in [72], the advantages and disadvantages of one choice or the other will become clear below from Lemma 2.7. More precisely, under quasi-uniformity assumptions on Σ_h and $\Sigma_{\tilde{h}}$, (2.20) allows any polynomial degree $k \geq 0$, whereas (2.21) is restricted to $k = 0$, but without requiring any further condition on these meshes.

Then, the mixed finite element scheme associated with (2.8) reads: Find $((\mathbf{t}_h, \boldsymbol{\sigma}_h), \boldsymbol{\xi}_h) \in H_h \times Q_h$ such that

$$\begin{aligned} [\mathcal{A}(\mathbf{t}_h, \boldsymbol{\sigma}_h), (\mathbf{s}_h, \boldsymbol{\tau}_h)] \; + \; [\mathcal{B}(\mathbf{s}_h, \boldsymbol{\tau}_h), \boldsymbol{\xi}_h] \quad &= \quad [\mathcal{F}, (\mathbf{s}_h, \boldsymbol{\tau}_h)] \qquad \forall\, (\mathbf{s}_h, \boldsymbol{\tau}_h) \in H_h, \\ [\mathcal{B}(\mathbf{t}_h, \boldsymbol{\sigma}_h), \boldsymbol{\lambda}_h] \quad &= \quad [\mathcal{G}, \boldsymbol{\lambda}_h] \qquad \forall\, \boldsymbol{\lambda}_h \in Q_h. \end{aligned} \tag{2.22}$$

We remark that the second identity in (2.4) suggests that the pressure p can be approximated later on by the postprocessing formula

$$p_h \;:=\; -\frac{1}{2}\,\mathrm{tr}\,(\boldsymbol{\sigma}_h)\,. \tag{2.23}$$

In what follows we apply again Theorem 2.1 to show that (2.22) is well-posed. We begin by recalling from [72] the discrete inf-sup condition for $\mathcal{B}$, which establishes the existence of $\beta > 0$, independent of h, such that

$$\sup_{\substack{(\mathbf{s}_h, \boldsymbol{\tau}_h) \in H_h \\ (\mathbf{s}_h, \boldsymbol{\tau}_h) \neq \mathbf{0}}} \frac{[\mathcal{B}(\mathbf{s}_h, \boldsymbol{\tau}_h), \boldsymbol{\lambda}_h]}{\|(\mathbf{s}_h, \boldsymbol{\tau}_h)\|_H} \;\geq\; \beta \|\boldsymbol{\lambda}_h\|_{0;1/2,\Gamma_N} \quad \forall\, \boldsymbol{\lambda}_h \in Q_h. \tag{2.24}$$

More precisely, we have the following result (cf. [72]).

Lemma 2.7. *Let H_h and Q_h be given by* (2.18) *and* (2.20) *(with $k \geq 1$), respectively, and assume that both Σ_h and $\Sigma_{\tilde{h}}$ are quasi-uniform. Then there exist constants $C_0 \in (0, 1]$ and $\beta > 0$, independent of h and $\tilde{h}$, such that whenever $h_\Sigma \leq C_0 \tilde{h}$, there holds* (2.24). *Furthermore, let H_h and Q_h be given by* (2.18) *(with $k = 0$) and* (2.21), *respectively. Then there exists $\beta > 0$, independent of h, such that* (2.24) *holds.*

Proof. We first recall that the quasi-uniformity of Σ_h and, analogously, of $\Sigma_{\tilde{h}}$, means that there exists $c > 0$, independent of h, such that $\max\limits_{e \in \Sigma_h} |e| \leq c \min\limits_{e \in \Sigma_h} |e|$. Note that these assumptions, which are required for the first part of this lemma only, are utilized to prove the existence of suitable discrete liftings. Indeed, the proof of the first statement proceeds similarly as in [11, Lemmas 3.2 and 3.3], whereas the second one follows by applying [86, Lemma 4.2], the analysis from [86, Section 5.1], and the recent result provided by [109, Theorem A.1]. $\square$

On the other hand, the Lipschitz-continuity of $\mathcal{A}$ on $H_h \subseteq H$, follows similarly to the proof of Lemma 2.3. Hence, it remains to prove that for each $(\mathbf{r}_h, \boldsymbol{\rho}_h) \in H_h$, $\mathcal{A}((\mathbf{r}_h, \boldsymbol{\rho}_h) + \cdot\,)$ is uniformly strongly monotone on V_h, where V_h is the discrete kernel of the operator $\mathcal{B}$, that is

$$V_h \;:=\; \mathbb{X}_h \times \widetilde{V}_h,$$

with

$$\widetilde{V}_h \;:=\; \Big\{ \boldsymbol{\tau}_h \in \mathbb{RT}_k(\mathcal{T}_h) \;:\; \langle \boldsymbol{\tau}_h \boldsymbol{\nu}, \boldsymbol{\lambda}_h \rangle_{\Gamma_N} \;=\; 0 \quad \forall\, \boldsymbol{\lambda}_h \in Q_h \Big\}\,.$$

The following lemma provides the discrete analogue of Lemma 2.5.

Lemma 2.8. *There exists $C > 0$, independent of h, such that*

$$C\|\boldsymbol{\tau}_h\|^2_{\mathbf{div},\Omega} \;\leq\; \|\boldsymbol{\tau}_{0h}\|^2_{\mathbf{div},\Omega}, \quad \forall\, \boldsymbol{\tau}_h \;:=\; \boldsymbol{\tau}_{0h} + d_h\mathbb{I} \in \widetilde{V}_h,$$

where $\boldsymbol{\tau}_{0h} \in \mathbb{RT}_k(\mathcal{T}_h) \cap \mathbb{H}_0(\mathbf{div};\Omega)$ and $d_h \in R$.

Proof. See [72, Lemma 7]. $\square$

Now, we are in a position to show the required discrete property of $\mathcal{A}$ on V_h, for all $(\mathbf{r}_h, \boldsymbol{\rho}_h) \in H_h$.

Lemma 2.9. *Assume that the parameter κ lies in $\left(0, \frac{2\alpha_0\delta}{\gamma_0}\right)$ for each $\delta \in \left(0, \frac{2}{\gamma_0}\right)$, where α_0 and γ_0 are the positive constants from* (2.2) *and* (2.3)*. Then, there exists a constant $C > 0$, independent of h, such that*

$$[\mathcal{A}((\mathbf{r}_h, \boldsymbol{\rho}_h) + (\mathbf{t}_h, \boldsymbol{\sigma}_h)) - \mathcal{A}((\mathbf{r}_h, \boldsymbol{\rho}_h) + (\mathbf{s}_h, \boldsymbol{\tau}_h)), (\mathbf{t}_h, \boldsymbol{\sigma}_h) - (\mathbf{s}_h, \boldsymbol{\tau}_h)] \;\geq\; C\|(\mathbf{t}_h, \boldsymbol{\sigma}_h) - (\mathbf{s}_h, \boldsymbol{\tau}_h)\|^2_H\,,$$

for all $(\mathbf{r}_h, \boldsymbol{\rho}_h) \in H_h$, and for all $(\mathbf{t}_h, \boldsymbol{\sigma}_h), (\mathbf{s}_h, \boldsymbol{\tau}_h) \in V_h$.

Proof. It follows straightforwardly from the proof of Lemma 2.6, using now Lemma 2.8 instead of Lemma 2.5. $\square$

The following theorem establishes the well posedness of (2.22) and the associated Céa estimate.

Theorem 2.3. *Let Q_h be any of the two choices described above with the conditions assumed in* Lemma 2.7*. Also, suppose that the parameter κ lies in $\left(0, \frac{2\alpha_0\delta}{\gamma_0}\right)$ for each $\delta \in \left(0, \frac{2}{\gamma_0}\right)$, where α_0 and γ_0 are the positive constants from* (2.2) *and* (2.3)*. Then the Galerkin scheme* (2.22) *has a unique solution $((\mathbf{t}_h, \boldsymbol{\sigma}_h), \boldsymbol{\xi}_h) \in H_h \times Q_h$ and there exist positive constants $C_1, C_2 > 0$, independent of h, such that*

$$\|((\mathbf{t}_h, \boldsymbol{\sigma}_h), \boldsymbol{\xi}_h)\|_{H\times Q} \;\leq\; C_1\Big\{\|\mathbf{f}\|_{0,\Omega} \;+\; \|\mathbf{g}\|_{-1/2,\Gamma_N}\Big\}\,,$$

and

$$\begin{aligned} &\|((\mathbf{t}, \boldsymbol{\sigma}), \boldsymbol{\xi}) - ((\mathbf{t}_h, \boldsymbol{\sigma}_h), \boldsymbol{\xi}_h)\|_{H\times Q} \\ &\quad\leq\; C_2\left\{\inf_{(\mathbf{s}_h, \boldsymbol{\tau}_h)\in H_h} \|(\mathbf{t}, \boldsymbol{\sigma}) - (\mathbf{s}_h, \boldsymbol{\tau}_h)\|_H \;+\; \inf_{\boldsymbol{\lambda}_h\in Q_h} \|\boldsymbol{\xi} - \boldsymbol{\lambda}_h\|_{0;1/2,\Gamma_N}\right\}. \end{aligned} \tag{2.25}$$

Proof. Thanks to the previous results given by Lemmas 2.7, 2.3 and 2.9, the proof is again a direct application of Theorem 2.1. In turn, the Céa estimate (2.25) follows from a particular application of the general result given by [118, Theorem 2.1]. $\square$

Next, in order to provide the rate of convergence of the Galerkin scheme (2.22), we need the approximation properties of the finite element subspaces involved. For this purpose, we now introduce the Raviart-Thomas interpolation operator (see [19, 116]) $\Pi_h^k : \mathbb{H}^1(\Omega) \to \mathbb{RT}_k(\mathcal{T}_h)$, which, given $\boldsymbol{\tau} \in \mathbb{H}^1(\Omega)$, is characterized by the following identities:

$$\int_e \Pi_h^k(\boldsymbol{\tau})\boldsymbol{\nu}\cdot\mathbf{p} \;=\; \int_e \boldsymbol{\tau}\boldsymbol{\nu}\cdot\mathbf{p}, \quad \forall\, \mathbf{p} \in \mathbf{P}_k(e), \quad \forall \text{ edge } e \in \mathcal{T}_h, \quad \text{when } k \geq 0, \tag{2.26}$$

and

$$\int_T \Pi_h^k(\boldsymbol{\tau}) : \boldsymbol{\rho} \;=\; \int_T \boldsymbol{\tau} : \boldsymbol{\rho}, \quad \forall\, \boldsymbol{\rho} \in \mathbb{P}_{k-1}(T), \quad \forall\, T \in \mathcal{T}_h, \quad \text{when } k \geq 1. \tag{2.27}$$

Recall, according to the notations introduced at the beginning of the present section (see also the last paragraph of Section 2.1), that $\mathbf{P}_k(e) := [\mathrm{P}_k(e)]^2$ and $\mathbb{P}_{k-1}(T) := [\mathrm{P}_{k-1}(T)]^{2\times 2}$. Then, it is easy to show, using (2.26) and (2.27), that (cf. [113, Section 3.4.2, eq. (3.4.23)])

$$\mathbf{div}(\Pi_h^k(\boldsymbol{\tau})) \;=\; \mathcal{P}_h^k(\mathbf{div}(\boldsymbol{\tau})), \tag{2.28}$$

where $\mathcal{P}_h^k : \mathbf{L}^2(\Omega) \to \mathcal{Q}_h^{\mathbf{u}}$ is the $\mathbf{L}^2(\Omega)$-orthogonal projector. Since $\mathcal{Q}_h^{\mathbf{u}}$ is the subspace of $\mathbf{L}^2(\Omega)$ formed by piecewise polynomial vectors of degree $\le k$ [cf. (2.19)], it is easy to see that $\mathcal{P}_h^k(\mathbf{v})|_T = \mathcal{P}_{h,T}^k(\mathbf{v}|_T)$ for each $T \in \mathcal{T}_h$, for each $\mathbf{v} \in \mathbf{L}^2(\Omega)$, where $\mathcal{P}_{h,T}^k : \mathbf{L}^2(T) \to \mathbf{P}_k(T)$ is the local orthogonal projector. Hence, for each $\mathbf{v} \in \mathbf{H}^m(\Omega)$, with $0 \le m \le k+1$, there holds (see, e.g. [37])

$$\|\mathbf{v} - \mathcal{P}_h^k(\mathbf{v})\|_{0,T} \;=\; \|\mathbf{v} - \mathcal{P}_{h,T}^k(\mathbf{v})\|_{0,T} \;\le\; C h_T^m |\mathbf{v}|_{m,T} \quad \forall\, T \in \mathcal{T}_h. \tag{2.29}$$

In addition, the operator Π_h^k satisfies the following approximation properties (see, e.g. [19, 116]): for each $\boldsymbol{\tau} \in \mathbb{H}^m(\Omega)$, with $1 \le m \le k+1$, there holds

$$\|\boldsymbol{\tau} - \Pi_h^k(\boldsymbol{\tau})\|_{0,T} \;\le\; C h_T^m |\boldsymbol{\tau}|_{m,T} \quad \forall\, T \in \mathcal{T}_h, \tag{2.30}$$

for each $\boldsymbol{\tau} \in \mathbb{H}^1(\Omega)$ such that $\mathbf{div}(\boldsymbol{\tau}) \in \mathbf{H}^m(\Omega)$, with $0 \le m \le k+1$, there holds

$$\|\mathbf{div}(\boldsymbol{\tau} - \Pi_h^k(\boldsymbol{\tau}))\|_{0,T} \;\le\; C h_T^m |\mathbf{div}(\boldsymbol{\tau})|_{m,T} \quad \forall\, T \in \mathcal{T}_h, \tag{2.31}$$

and for each $\boldsymbol{\tau} \in \mathbb{H}^1(\Omega)$, there holds

$$\|\boldsymbol{\tau}\boldsymbol{\nu}_e - \Pi_h^k(\boldsymbol{\tau})\boldsymbol{\nu}_e\|_{0,e} \;\le\; C h_e^{1/2} \|\boldsymbol{\tau}\|_{1,T_e} \quad \forall \text{ edge } e \in \mathcal{T}_h, \tag{2.32}$$

where $T_e \in \mathcal{T}_h$ contains e on its boundary. In particular, note that (2.31) follows easily from (2.28) and (2.29). Moreover, the interpolation operator Π_h^k can also be defined as a bounded linear operator from the larger space $\mathbb{H}^s(\Omega) \cap \mathbb{H}(\mathbf{div};\Omega)$ into $\mathbb{RT}_k(\mathcal{T}_h)$ for all $s \in (0,1]$ (see, e.g. [96, Theorem 3.16]), and in this case there holds the following interpolation error estimate

$$\|\boldsymbol{\tau} - \Pi_h^k(\boldsymbol{\tau})\|_{0,T} \;\le\; C h_T^s \Big\{ \|\boldsymbol{\tau}\|_{s,T} \;+\; \|\mathbf{div}(\boldsymbol{\tau})\|_{0,T} \Big\} \quad \forall\, T \in \mathcal{T}_h. \tag{2.33}$$

Then, as a consequence of (2.29)–(2.33) and the usual estimates for the interpolation in Sobolev spaces (cf. [110, Appendix B]), we find that $\mathbb{X}_h$, $\mathbb{RT}_k(\mathcal{T}_h)$ and Q_h satisfy the following approximation properties:

$(\mathbf{AP}_h^{\mathbf{t}})$ For each $s \in [0, k+1]$ and for each $\mathbf{s} \in \mathbb{H}^s(\Omega)$ there exists $\mathbf{s}_h \in \mathbb{X}_h$ such that

$$\|\mathbf{s} - \mathbf{s}_h\|_{0,\Omega} \;\le\; C h^s \|\mathbf{s}\|_{s,\Omega}.$$

$(\mathbf{AP}_h^{\boldsymbol{\sigma}})$ For each $s \in (0, k+1]$ and for each $\boldsymbol{\tau} \in \mathbb{H}^s(\Omega)$ with $\mathbf{div}(\boldsymbol{\tau}) \in \mathbf{H}^s(\Omega)$ there exists $\boldsymbol{\tau}_h \in \mathbb{RT}_k(\mathcal{T}_h)$ such that

$$\|\boldsymbol{\tau} - \boldsymbol{\tau}_h\|_{\mathbf{div},\Omega} \;\le\; C h^s \Big\{ \|\boldsymbol{\tau}\|_{s,\Omega} \;+\; \|\mathbf{div}(\boldsymbol{\tau})\|_{s,\Omega} \Big\}.$$

$(\mathbf{AP}_h^{\boldsymbol{\xi}})$ For each $s \in [0, k+1]$ and for each $\boldsymbol{\lambda} \in \mathbf{H}_{00}^{s+1/2}(\Gamma_N)$, there exists $\boldsymbol{\lambda}_h \in Q_h$ such that

$$\|\boldsymbol{\lambda} - \boldsymbol{\lambda}_h\|_{0;1/2,\Gamma_N} \;\le\; C h^s \|\boldsymbol{\lambda}\|_{s+1/2,\Gamma_N}.$$

The following theorem provides the theoretical rate of convergence of the Galerkin scheme (2.22), under suitable regularity assumptions on the exact solution.

Theorem 2.4. *Let* $((\mathbf{t},\boldsymbol{\sigma}),\boldsymbol{\xi}) \in H \times Q$ *and* $((\mathbf{t}_h,\boldsymbol{\sigma}_h),\boldsymbol{\xi}_h) \in H_h \times Q_h$ *be the unique solutions of the continuous and discrete formulations* (2.8) *and* (2.22), *respectively. Assume that* $\mathbf{t} \in \mathbb{H}^s(\Omega)$, $\boldsymbol{\sigma} \in \mathbb{H}^s(\Omega)$, $\mathbf{div}(\boldsymbol{\sigma}) \in \mathbf{H}^s(\Omega)$ *and* $\boldsymbol{\xi} \in \mathbf{H}_{00}^{s+1/2}(\Gamma_N)$, *for some* $s \in (0, k+1]$. *Then, there exists* $C > 0$, *independent of* h, *such that*

$$\|((\mathbf{t},\boldsymbol{\sigma}),\boldsymbol{\xi}) - ((\mathbf{t}_h,\boldsymbol{\sigma}_h),\boldsymbol{\xi}_h)\|_{H\times Q} \;\leq\; C h^s \left\{ \|\mathbf{t}\|_{s,\Omega} + \|\boldsymbol{\sigma}\|_{s,\Omega} + \|\mathbf{div}(\boldsymbol{\sigma})\|_{s,\Omega} + \|\boldsymbol{\xi}\|_{s+1/2,\Gamma_N} \right\}.$$

Proof. It follows from the Céa estimate (2.25) (cf. Theorem 2.3) and the approximation properties $(\mathbf{AP}_h^{\mathbf{t}})$, $(\mathbf{AP}_h^{\boldsymbol{\sigma}})$ and $(\mathbf{AP}_h^{\boldsymbol{\xi}})$. □

2.5 A residual-based a posteriori error estimator

In this section we develop a residual-based *a posteriori* error analysis for the mixed finite element scheme (2.22).

2.5.1 Preliminaries

First we introduce several notations. Given $T \in \mathcal{T}_h$, we let $\mathcal{E}(T)$ be the set of its edges, and let $\mathcal{E}_h$ be the set of all edges of the triangulation $\mathcal{T}_h$. Then we write $\mathcal{E}_h = \mathcal{E}_h(\Omega) \cup \mathcal{E}_h(\Gamma_D) \cup \mathcal{E}_h(\Gamma_N)$, where $\mathcal{E}_h(\Omega) := \{e \in \mathcal{E}_h : e \subseteq \Omega\}$, $\mathcal{E}_h(\Gamma_D) := \{e \in \mathcal{E}_h : e \subseteq \Gamma_D\}$ and $\mathcal{E}_h(\Gamma_N) := \{e \in \mathcal{E}_h : e \subseteq \Gamma_N\}$. Also, for each edge $e \in \mathcal{E}_h$ we fix a unit normal vector $\boldsymbol{\nu}_e := (\nu_1,\nu_2)^{\mathrm{t}}$, and let $\boldsymbol{s}_e := (-\nu_2,\nu_1)^{\mathrm{t}}$ be the corresponding fixed unit tangential vector along e. Then, given $e \in \mathcal{E}_h(\Omega)$ and $\boldsymbol{\tau} \in \mathbb{L}^2(\Omega)$ such that $\boldsymbol{\tau}|_T \in \mathbb{C}(T) := [C(T)]^{2\times 2}$ on each $T \in \mathcal{T}_h$, we let $[\![\boldsymbol{\tau}\boldsymbol{s}_e]\!]$ be the corresponding tangential jump across e, that is, $[\![\boldsymbol{\tau}\boldsymbol{s}_e]\!] := (\boldsymbol{\tau}|_T - \boldsymbol{\tau}|_{T'})|_e \boldsymbol{s}_e$, where T and T' are the triangles of $\mathcal{T}_h$ having e as a common edge. Abusing notation, when $e \in \mathcal{E}_h(\Gamma)$, we also write $[\![\boldsymbol{\tau}\boldsymbol{s}_e]\!] := \boldsymbol{\tau}|_e \boldsymbol{s}_e$. From now on, when no confusion arises, we simple write $\boldsymbol{s}$ and $\boldsymbol{\nu}$ instead of $\boldsymbol{s}_e$ and $\boldsymbol{\nu}_e$, respectively. Finally, given scalar, vector and tensor valued fields v, $\boldsymbol{\varphi} := (\varphi_1,\varphi_2)$ and $\boldsymbol{\tau} := (\tau_{ij})$, respectively, we let

$$\mathbf{curl}(v) := \begin{pmatrix} \frac{\partial v}{\partial x_2} \\ -\frac{\partial v}{\partial x_1} \end{pmatrix}, \quad \underline{\mathbf{curl}}(\boldsymbol{\varphi}) := \begin{pmatrix} \mathbf{curl}(\varphi_1)^{\mathrm{t}} \\ \mathbf{curl}(\varphi_2)^{\mathrm{t}} \end{pmatrix}, \quad \text{and} \quad \mathrm{curl}(\boldsymbol{\tau}) := \begin{pmatrix} \frac{\partial \tau_{12}}{\partial x_1} - \frac{\partial \tau_{11}}{\partial x_2} \\ \frac{\partial \tau_{22}}{\partial x_1} - \frac{\partial \tau_{21}}{\partial x_2} \end{pmatrix}.$$

Then, letting $((\mathbf{t},\boldsymbol{\sigma}),\boldsymbol{\xi}) \in H \times Q$ and $((\mathbf{t}_h,\boldsymbol{\sigma}_h),\boldsymbol{\xi}_h) \in H_h \times Q_h$ be the unique solutions of the continuous and discrete formulations (2.8) and (2.22), respectively, we define for each $T \in \mathcal{T}_h$ a local error indicator θ_T as follows:

$$\begin{aligned}
\theta_T^2 \;:=\;& \frac{1}{\alpha^2}\|\mathbf{f} - \mathcal{P}_h^k(\mathbf{f})\|_{0,T}^2 + h_T^2\,\|\mathbf{t}_h - \nabla \mathbf{u}_h\|_{0,T}^2 + h_T^2\|\mathrm{curl}(\mathbf{t}_h)\|_{0,T}^2 \\
&+ \sum_{e\in\mathcal{E}(T)\cap\mathcal{E}_h(\Omega)} h_e\|[\![\mathbf{t}_h\boldsymbol{s}]\!]\|_{0,e}^2 + \sum_{e\in\mathcal{E}(T)\cap\mathcal{E}_h(\Gamma_D)} h_e\|[\![\mathbf{t}_h\boldsymbol{s}]\!]\|_{0,e}^2 \\
&+ \sum_{e\in\mathcal{E}(T)\cap\mathcal{E}_h(\Gamma_N)} h_e \left\{ \left\| \mathbf{t}_h\boldsymbol{s} + \frac{d\boldsymbol{\xi}_h}{d\boldsymbol{s}} \right\|_{0,e}^2 + \|\boldsymbol{\xi}_h + \mathbf{u}_h\|_{0,e}^2 + \|\mathbf{g} - \boldsymbol{\sigma}_h\boldsymbol{\nu}\|_{0,e}^2 \right\} \\
&+ \|\boldsymbol{\sigma}_h^{\mathrm{d}} - \boldsymbol{\psi}(\mathbf{t}_h)\|_{0,T}^2 + h_T^2\|\mathrm{curl}\left(\boldsymbol{\sigma}_h^{\mathrm{d}} - \boldsymbol{\psi}(\mathbf{t}_h)\right)\|_{0,T}^2 \\
&+ \sum_{e\in\mathcal{E}(T)} h_e\|[\![(\boldsymbol{\sigma}_h^{\mathrm{d}} - \boldsymbol{\psi}(\mathbf{t}_h))\boldsymbol{s}]\!]\|_{0,e}^2,
\end{aligned} \tag{2.34}$$

where, resembling (2.7), we set

$$\mathbf{u}_h \;:=\; \frac{1}{\alpha}\Big\{\mathcal{P}_h^k(\mathbf{f}) \;+\; \mathbf{div}(\boldsymbol{\sigma}_h)\Big\} \quad \text{in } \Omega. \tag{2.35}$$

Note that the term $\|\mathbf{g}-\boldsymbol{\sigma}_h\boldsymbol{\nu}\|_{0,e}^2$, defining θ_T^2, requires that $\mathbf{g}|_e \in \mathbf{L}^2(e)\ \forall\, e \in \mathcal{E}_h(\Gamma_N)$. The residual character of each term on the right hand side of (2.34) is quite clear. As usual the expression

$$\boldsymbol{\theta} \;:=\; \left\{\sum_{T\in\mathcal{T}_h} \theta_T^2\right\}^{1/2} \tag{2.36}$$

is employed as the global residual error estimator.

The following theorem constitutes the main result of this section.

Theorem 2.5. *Let $((\mathbf{t},\boldsymbol{\sigma}),\boldsymbol{\xi}) \in H\times Q$ and $((\mathbf{t}_h,\boldsymbol{\sigma}_h),\boldsymbol{\xi}_h) \in H_h\times Q_h$ be the unique solutions of* (2.8) *and* (2.22)*, respectively. In addition, let $\mathbf{u}\in\mathbf{L}^2(\Omega)$ be defined according to* (2.7)*, that is $\mathbf{u} := \frac{1}{\alpha}\{\mathbf{f}+\mathbf{div}(\boldsymbol{\sigma})\}$, and assume that the Neumann datum $\mathbf{g}$ belongs to $\mathbf{L}^2(\Gamma_N)$. Then, there exists positive constants $C_{\mathtt{eff}}$ and $C_{\mathtt{rel}}$, independent of h, such that*

$$C_{\mathtt{eff}}\boldsymbol{\theta} + h.o.t. \;\le\; \|\mathbf{u}-\mathbf{u}_h\|_{0,\Omega} \;+\; \|((\mathbf{t}-\mathbf{t}_h,\boldsymbol{\sigma}-\boldsymbol{\sigma}_h),\boldsymbol{\xi}-\boldsymbol{\xi}_h)\|_{H\times Q} \;\le\; C_{\mathtt{rel}}\boldsymbol{\theta}, \tag{2.37}$$

where h.o.t. stands for one or several terms of higher order.

The proof of Theorem 2.5, which follows closely the approaches in [66] and [72], is separated into the two parts given by the next subsections. The efficiency of the global error estimator (lower bound in (2.37)) is proved below in Section 2.5.3, whereas the corresponding reliability (upper bound in (2.37)) is derived next. The meaning of *h.o.t.* is explained below right after Theorem 2.6.

2.5.2 Reliability

We begin by recalling from the proof of Lemma 2.2 that $\mathcal{D}\mathbb{A}(\widetilde{\mathbf{r}})$ is a uniformly bounded and uniformly elliptic bilinear form on $\mathbb{L}^2_{\mathrm{tr}}(\Omega)\times\mathbb{L}^2_{\mathrm{tr}}(\Omega)$ for all $\widetilde{\mathbf{r}}\in\mathbb{L}^2_{\mathrm{tr}}(\Omega)$. Moreover, we observe from (2.9) and (2.14), that the nonlinear operator $\mathcal{A}$ can be rewritten as:

$$[\mathcal{A}(\mathbf{t},\boldsymbol{\sigma}),(\mathbf{s},\boldsymbol{\tau})] \;:=\; [\mathbb{A}(\mathbf{t}),\mathbf{s}-\kappa\boldsymbol{\tau}^{\mathrm{d}}] - \int_\Omega \mathbf{s}:\boldsymbol{\sigma}^{\mathrm{d}} + \int_\Omega \mathbf{t}:\boldsymbol{\tau}^{\mathrm{d}} + \kappa\int_\Omega \boldsymbol{\sigma}^{\mathrm{d}}:\boldsymbol{\tau}^{\mathrm{d}} + \frac{1}{\alpha}\int_\Omega \mathbf{div}(\boldsymbol{\sigma})\cdot\mathbf{div}(\boldsymbol{\tau})\,. \tag{2.38}$$

Hence, as a consequence of the continuous dependence result provided by the linear version of Theorem 2.1 (cf. (2.12) and (2.13) with $\mathcal{A}$ linear), which is actually the usual estimate provided by the Babuška-Brezzi theory (see, e.g. [19, Theorem 1.1 in Chapter II]), we can conclude that the linear operator $\mathcal{M}$ obtained by adding the two equations of the left hand side of (2.8), after replacing $\mathbb{A}$ within $\mathcal{A}$ (see (2.38)) by the Gâteaux derivative $\mathcal{D}\mathbb{A}(\widetilde{\mathbf{r}})$ at any $\widetilde{\mathbf{r}}\in\mathbb{L}^2_{\mathrm{tr}}(\Omega)$, satisfies a global inf-sup condition. More precisely, there exists a constant $C>0$ such that

$$C\|((\mathbf{r},\boldsymbol{\rho}),\boldsymbol{\zeta})\|_{H\times Q} \;\le\; \sup_{\substack{((\mathbf{s},\boldsymbol{\tau}),\boldsymbol{\lambda})\in H\times Q\\ ((\mathbf{s},\boldsymbol{\tau}),\boldsymbol{\lambda})\neq\mathbf{0}}} \frac{[\mathcal{M}((\mathbf{s},\boldsymbol{\tau}),\boldsymbol{\lambda}),((\mathbf{r},\boldsymbol{\rho}),\boldsymbol{\zeta})]}{\|((\mathbf{s},\boldsymbol{\tau}),\boldsymbol{\lambda})\|_{H\times Q}}, \tag{2.39}$$

for all $\widetilde{\mathbf{r}}\in\mathbb{L}^2_{\mathrm{tr}}(\Omega)$ and for all $((\mathbf{r},\boldsymbol{\rho}),\boldsymbol{\zeta})\in H\times Q$, where

$$\begin{aligned}[\mathcal{M}((\mathbf{s},\boldsymbol{\tau}),\boldsymbol{\lambda}),((\mathbf{r},\boldsymbol{\rho}),\boldsymbol{\zeta})] \;:=\;& \mathcal{D}\mathbb{A}(\widetilde{\mathbf{r}})(\mathbf{r},\mathbf{s}-\kappa\boldsymbol{\tau}^{\mathrm{d}}) - \int_\Omega \mathbf{s}:\boldsymbol{\rho}^{\mathrm{d}} + \int_\Omega \mathbf{r}:\boldsymbol{\tau}^{\mathrm{d}}\\ +\;\; \kappa\int_\Omega \boldsymbol{\rho}^{\mathrm{d}}:\boldsymbol{\tau}^{\mathrm{d}} + \frac{1}{\alpha}\int_\Omega \mathbf{div}(\boldsymbol{\rho})\cdot\mathbf{div}(\boldsymbol{\tau}) \;+\; &[\mathcal{B}(\mathbf{s},\boldsymbol{\tau}),\boldsymbol{\zeta}] \;+\; [\mathcal{B}(\mathbf{r},\boldsymbol{\rho}),\boldsymbol{\lambda}]\,.\end{aligned}$$

We now have the following preliminary estimate.

Lemma 2.10. *Let* $((\mathbf{t},\boldsymbol{\sigma}),\boldsymbol{\xi}) \in H \times Q$ *and* $((\mathbf{t}_h,\boldsymbol{\sigma}_h),\boldsymbol{\xi}_h) \in H_h \times Q_h$ *be the unique solutions of* (2.8) *and* (2.22)*, respectively. Then there exists* $C > 0$*, independent of* h*, such that*

$$\begin{aligned} & C\,\|((\mathbf{t}-\mathbf{t}_h,\boldsymbol{\sigma}-\boldsymbol{\sigma}_h),\boldsymbol{\xi}-\boldsymbol{\xi}_h)\|_{H\times Q} \\ & \quad \le\ \|\boldsymbol{\sigma}_h^{\mathrm{d}} - \boldsymbol{\psi}(\mathbf{t}_h)\|_{0,\Omega} \ +\ \|\mathbf{g}-\boldsymbol{\sigma}_h\boldsymbol{\nu}\|_{-1/2,\Gamma_N} \ +\ \sup_{\substack{\boldsymbol{\tau}\in\mathbb{H}(\mathbf{div};\Omega)\\ \boldsymbol{\tau}\neq\mathbf{0}}} \frac{\big(E_1+E_2\big)(\boldsymbol{\tau})}{\|\boldsymbol{\tau}\|_{\mathbf{div},\Omega}}\,, \end{aligned} \tag{2.40}$$

where the functionals E_1 *and* E_2*, defined as*

$$E_1(\boldsymbol{\tau}) \ :=\ \langle \boldsymbol{\tau}\boldsymbol{\nu},\boldsymbol{\xi}_h\rangle_{\Gamma_N} + \int_\Omega \mathbf{t}_h : \boldsymbol{\tau} + \frac{1}{\alpha}\int_\Omega (\mathbf{f}+\mathbf{div}(\boldsymbol{\sigma}_h))\cdot\mathbf{div}(\boldsymbol{\tau})\,, \tag{2.41}$$

and

$$E_2(\boldsymbol{\tau}) \ :=\ \kappa\int_\Omega (\boldsymbol{\sigma}_h^{\mathrm{d}} - \boldsymbol{\psi}(\mathbf{t}_h)) : \boldsymbol{\tau}\,, \tag{2.42}$$

satisfy

$$\big(E_1+E_2\big)(\boldsymbol{\tau}_h) \ =\ 0 \qquad \forall\,\boldsymbol{\tau}_h \in \mathbb{RT}_k(\mathcal{T}_h)\,. \tag{2.43}$$

Proof. Since $\mathbf{t}$ and $\mathbf{t}_h$ belong to $\mathbb{L}^2_{\mathrm{tr}}(\Omega)$, a straightforward application of the mean value theorem yields the existence of a convex combination of $\mathbf{t}$ and $\mathbf{t}_h$, say $\widetilde{\mathbf{r}}_h \in \mathbb{L}^2_{\mathrm{tr}}(\Omega)$, such that

$$\mathcal{D}\mathbb{A}(\widetilde{\mathbf{r}}_h)(\mathbf{t}-\mathbf{t}_h,\mathbf{s}) \ =\ [\mathbb{A}(\mathbf{t})-\mathbb{A}(\mathbf{t}_h),\mathbf{s}] \quad \forall\,\mathbf{s}\in\mathbb{L}^2_{\mathrm{tr}}(\Omega).$$

Then, applying (2.39) to the Galerkin error $((\mathbf{r},\boldsymbol{\rho}),\boldsymbol{\zeta}) := ((\mathbf{t}-\mathbf{t}_h,\boldsymbol{\sigma}-\boldsymbol{\sigma}_h),\boldsymbol{\xi}-\boldsymbol{\xi}_h)$, we obtain that

$$\begin{aligned} & C\|((\mathbf{t}-\mathbf{t}_h,\boldsymbol{\sigma}-\boldsymbol{\sigma}_h),\boldsymbol{\xi}-\boldsymbol{\xi}_h)\|_{H\times Q} \\ & \quad \le \sup_{\substack{((\mathbf{s},\boldsymbol{\tau}),\boldsymbol{\lambda})\in H\times Q\\ ((\mathbf{s},\boldsymbol{\tau}),\boldsymbol{\lambda})\neq\mathbf{0}}} \frac{[\mathcal{A}(\mathbf{t},\boldsymbol{\sigma})-\mathcal{A}(\mathbf{t}_h,\boldsymbol{\sigma}_h),(\mathbf{s},\boldsymbol{\tau})] + [\mathcal{B}(\mathbf{s},\boldsymbol{\tau}),\boldsymbol{\xi}-\boldsymbol{\xi}_h] + [\mathcal{B}(\mathbf{t}-\mathbf{t}_h,\boldsymbol{\sigma}-\boldsymbol{\sigma}_h),\boldsymbol{\lambda}]}{\|((\mathbf{s},\boldsymbol{\tau}),\boldsymbol{\lambda})\|_{H\times Q}} \\ & \quad \le \sup_{\substack{(\mathbf{s},\boldsymbol{\tau})\in H\\ (\mathbf{s},\boldsymbol{\tau})\neq\mathbf{0}}} \frac{\mathcal{R}(\mathbf{s},\boldsymbol{\tau})}{\|(\mathbf{s},\boldsymbol{\tau})\|_H} + \sup_{\substack{\boldsymbol{\lambda}\in Q\\ \boldsymbol{\lambda}\neq\mathbf{0}}} \frac{[\mathcal{B}(\mathbf{t}-\mathbf{t}_h,\boldsymbol{\sigma}-\boldsymbol{\sigma}_h),\boldsymbol{\lambda}]}{\|\boldsymbol{\lambda}\|_{0;1/2,\Gamma_N}}, \end{aligned} \tag{2.44}$$

where $\mathcal{R}(\mathbf{s},\boldsymbol{\tau}) := [\mathcal{A}(\mathbf{t},\boldsymbol{\sigma})-\mathcal{A}(\mathbf{t}_h,\boldsymbol{\sigma}_h),(\mathbf{s},\boldsymbol{\tau})] + [\mathcal{B}(\mathbf{s},\boldsymbol{\tau}),\boldsymbol{\xi}-\boldsymbol{\xi}_h]$. But, from the second equation of (2.8) and the definitions of $\mathcal{B}$ (cf. (2.10)) and $\mathcal{G}$ (cf. (2.11)), we see that $[\mathcal{B}(\mathbf{t}-\mathbf{t}_h,\boldsymbol{\sigma}-\boldsymbol{\sigma}_h),\boldsymbol{\lambda}] = \langle \mathbf{g}-\boldsymbol{\sigma}_h\boldsymbol{\nu},\boldsymbol{\lambda}\rangle_{\Gamma_N}$, which yields

$$\sup_{\substack{\boldsymbol{\lambda}\in Q\\ \boldsymbol{\lambda}\neq\mathbf{0}}} \frac{[\mathcal{B}(\mathbf{t}-\mathbf{t}_h,\boldsymbol{\sigma}-\boldsymbol{\sigma}_h),\boldsymbol{\lambda}]}{\|\boldsymbol{\lambda}\|_{0;1/2,\Gamma_N}} \ =\ \sup_{\substack{\boldsymbol{\lambda}\in Q\\ \boldsymbol{\lambda}\neq\mathbf{0}}} \frac{\langle \mathbf{g}-\boldsymbol{\sigma}_h\boldsymbol{\nu},\boldsymbol{\lambda}\rangle_{\Gamma_N}}{\|\boldsymbol{\lambda}\|_{0;1/2,\Gamma_N}} \ =\ \|\mathbf{g}-\boldsymbol{\sigma}_h\boldsymbol{\nu}\|_{-1/2,\Gamma_N}\,. \tag{2.45}$$

Next, according to the first equation of (2.8) we observe that

$$\mathcal{R}(\mathbf{s},\boldsymbol{\tau}) \ =\ [\mathcal{F},(\mathbf{s},\boldsymbol{\tau})] - [\mathcal{A}(\mathbf{t}_h,\boldsymbol{\sigma}_h),(\mathbf{s},\boldsymbol{\tau})] - [\mathcal{B}(\mathbf{s},\boldsymbol{\tau}),\boldsymbol{\xi}_h] \quad \forall\,(\mathbf{s},\boldsymbol{\tau})\in H\,,$$

which gives

$$\mathcal{R}(\mathbf{s},\boldsymbol{\tau}) \ =\ -E_1(\boldsymbol{\tau}) - E_2(\boldsymbol{\tau}) + \int_\Omega (\boldsymbol{\sigma}_h^{\mathrm{d}} - \boldsymbol{\psi}(\mathbf{t}_h)) : \mathbf{s} \quad \forall\,(\mathbf{s},\boldsymbol{\tau})\in H\,. \tag{2.46}$$

Then, applying the Cauchy-Schwarz inequality to the last term on the right hand side of (2.46), and replacing the resulting expression together with (2.45) back into (2.44), we obtain (2.40). Finally, it is easy to see from (2.46) and the first equation of (2.22) that (2.43) holds. $\square$

We now aim to bound the supremum on the right hand side of (2.40), for which we write

$$\big(E_1 + E_2\big)(\boldsymbol{\tau}) \;=\; E_1(\boldsymbol{\tau} - \boldsymbol{\tau}_h) \;+\; E_2(\boldsymbol{\tau} - \boldsymbol{\tau}_h) \tag{2.47}$$

with a suitable choice of $\boldsymbol{\tau}_h \in \mathbb{RT}_k(\mathcal{T}_h)$. To this end, and proceeding exactly as in [72, Section 4.2], we need the Clément interpolation operator $\mathcal{I}_h : H^1(\Omega) \to X_h$ (cf. [40]), where

$$X_h \;:=\; \big\{ v \in C(\bar{\Omega}) \;:\; v|_T \in \mathrm{P}_1(T) \quad \forall\, T \in \mathcal{T}_h \big\}\,.$$

A vectorial version of $\mathcal{I}_h$, say $\boldsymbol{\mathcal{I}}_h : \mathbf{H}^1(\Omega) \to \mathbf{X}_h$, which is defined componentwise by $\mathcal{I}_h$, is also required. The following lemma establishes the local approximation properties of $\mathcal{I}_h$.

Lemma 2.11. *There exist constants $c_1, c_2 > 0$, independent of h, such that for all $v \in H^1(\Omega)$ there holds*

$$\|v - \mathcal{I}_h(v)\|_{0,T} \;\leq\; c_1 h_T \|v\|_{1,\Delta(T)} \quad \forall\, T \in \mathcal{T}_h,$$

and

$$\|v - \mathcal{I}_h(v)\|_{0,e} \;\leq\; c_2 h_e^{1/2} \|v\|_{1,\Delta(e)} \quad \forall\, e \in \mathcal{E}_h,$$

where $\Delta(T)$ and $\Delta(e)$ are the union of all elements intersecting with T and e, respectively.

Proof. See [40]. □

Next, for each $\boldsymbol{\tau} \in \mathbb{H}(\mathbf{div};\Omega)$ we consider its Helmholtz decomposition (see, e.g. [72, Section 4.2] for details)

$$\boldsymbol{\tau} \;=\; \nabla \mathbf{z} + \underline{\mathbf{curl}}(\boldsymbol{\chi})\,,$$

where $\mathbf{z} \in \mathbf{H}^2(\Omega)$ and $\boldsymbol{\chi} \in \mathbf{H}^1(\Omega)$ satisfy $\boldsymbol{\Delta} \mathbf{z} = \mathbf{div}(\boldsymbol{\tau})$ in Ω, $\int_\Omega \boldsymbol{\chi} = \mathbf{0}$, and

$$\|\mathbf{z}\|_{2,\Omega} \;+\; \|\boldsymbol{\chi}\|_{1,\Omega} \;\leq\; C \|\boldsymbol{\tau}\|_{\mathbf{div},\Omega}\,. \tag{2.48}$$

Then, we let $\boldsymbol{\zeta} := \nabla \mathbf{z} \in \mathbb{H}^1(\Omega)$, $\boldsymbol{\chi}_h := \boldsymbol{\mathcal{I}}_h(\boldsymbol{\chi})$, and define

$$\boldsymbol{\tau}_h \;:=\; \Pi_h^k(\boldsymbol{\zeta}) \;+\; \underline{\mathbf{curl}}(\boldsymbol{\chi}_{\boldsymbol{h}}) \in \mathbb{RT}_k(\mathcal{T}_h), \tag{2.49}$$

where Π_h^k is the Raviart-Thomas interpolation operator introduced before (cf. (2.26) and (2.27)). We refer to (2.49) as a discrete Helmholtz decomposition of $\boldsymbol{\tau}_h$. Therefore, we can write

$$\boldsymbol{\tau} - \boldsymbol{\tau}_h \;=\; \boldsymbol{\tau} - \Pi_h^k(\boldsymbol{\zeta}) - \underline{\mathbf{curl}}(\boldsymbol{\chi}_{\boldsymbol{h}}) \;=\; \boldsymbol{\zeta} - \Pi_h^k(\boldsymbol{\zeta}) + \underline{\mathbf{curl}}(\boldsymbol{\chi} - \boldsymbol{\chi}_{\boldsymbol{h}})\,,$$

which, using (2.28) and the fact that $\mathbf{div}(\boldsymbol{\zeta}) = \boldsymbol{\Delta}\mathbf{z} = \mathbf{div}(\boldsymbol{\tau})$ in Ω, and denoting by $\mathbf{I}$ a generic identity operator, yields

$$\mathbf{div}(\boldsymbol{\tau} - \boldsymbol{\tau}_h) \;=\; \mathbf{div}\left(\boldsymbol{\zeta} - \Pi_h^k(\boldsymbol{\zeta})\right) \;=\; (\mathbf{I} - \mathcal{P}_h^k)(\mathbf{div}(\boldsymbol{\zeta})) \;=\; (\mathbf{I} - \mathcal{P}_h^k)(\mathbf{div}(\boldsymbol{\tau})).$$

Hence, according to (2.41), (2.42), and (2.43), and using the foregoing identities, we find that

$$\begin{aligned} E_1(\boldsymbol{\tau} - \boldsymbol{\tau}_h) \;&=\; \frac{1}{\alpha}\int_\Omega (\mathbf{f} + \mathbf{div}(\boldsymbol{\sigma}_h)) \cdot (\mathbf{I} - \mathcal{P}_h^k)(\mathbf{div}(\boldsymbol{\tau})) \\ &\quad + \int_\Omega \mathbf{t}_h : (\boldsymbol{\zeta} - \Pi_h^k(\boldsymbol{\zeta})) \;+\; \Big\langle (\boldsymbol{\zeta} - \Pi_h^k(\boldsymbol{\zeta})\boldsymbol{\nu}, \boldsymbol{\xi}_h \Big\rangle_{\Gamma_N} \\ &\quad + \int_\Omega \mathbf{t}_h : \underline{\mathbf{curl}}(\boldsymbol{\chi} - \boldsymbol{\chi}_h) \;+\; \langle \underline{\mathbf{curl}}(\boldsymbol{\chi} - \boldsymbol{\chi}_h)\boldsymbol{\nu}, \boldsymbol{\xi}_h \rangle_{\Gamma_N}\,, \end{aligned}$$

and

$$E_2(\boldsymbol{\tau} - \boldsymbol{\tau}_h) \;=\; \kappa \int_\Omega (\boldsymbol{\sigma}_h^{\mathrm{d}} - \boldsymbol{\psi}(\mathbf{t}_h)) : \underline{\mathbf{curl}}(\boldsymbol{\chi} - \boldsymbol{\chi}_h) \,+\, \kappa \int_\Omega (\boldsymbol{\sigma}_h^{\mathrm{d}} - \boldsymbol{\psi}(\mathbf{t}_h)) : (\boldsymbol{\zeta} - \Pi_h^k(\boldsymbol{\zeta}))\,.$$

The following two lemmas provide the upper bounds for $|E_1(\boldsymbol{\tau} - \boldsymbol{\tau}_h)|$ and $|E_2(\boldsymbol{\tau} - \boldsymbol{\tau}_h)|$.

Lemma 2.12. *There exists $C > 0$, independent of h and α, such that*

$$\begin{aligned} |E_1(\boldsymbol{\tau} - \boldsymbol{\tau}_h)| \;\leq\; C \Bigg\{ & \sum_{T\in\mathcal{T}_h} \left\{ \frac{1}{\alpha^2} \|\mathbf{f} - \mathcal{P}_h^k(\mathbf{f})\|_{0,T}^2 + h_T^2 \, \|\mathbf{t}_h - \nabla \mathbf{u}_h\|_{0,T}^2 + h_T^2 \|\mathrm{curl}(\mathbf{t}_h)\|_{0,T}^2 \right\} \\ & + \sum_{e\in\mathcal{E}_h(\Omega)} h_e \|[\![\mathbf{t}_h \boldsymbol{s}]\!]\|_{0,e}^2 + \sum_{e\in\mathcal{E}_h(\Gamma_D)} h_e \|[\![\mathbf{t}_h \boldsymbol{s}]\!]\|_{0,e}^2 \\ & + \sum_{e\in\mathcal{E}_h(\Gamma_N)} h_e \left\{ \left\| \mathbf{t}_h \boldsymbol{s} + \frac{d\boldsymbol{\xi}_h}{d\boldsymbol{s}} \right\|_{0,e}^2 + \|\boldsymbol{\xi}_h + \mathbf{u}_h\|_{0,e}^2 \right\} \Bigg\}^{1/2} \|\boldsymbol{\tau}\|_{\mathbf{div},\Omega}. \end{aligned}$$

Proof. It follows exactly as in [72, Lemma 14], with $\mathbf{t}_h$ instead of $\frac{1}{\mu}\boldsymbol{\sigma}_h^{\mathrm{d}}$. The main tools employed are integration by parts, the Cauchy-Schwarz inequality, the approximation properties provided by Lemma 2.11, the identities (2.26) and (2.27) characterizing Π_h^k, the fact that the number of triangles in $\Delta(T)$ and $\Delta(e)$ are bounded, the approximation properties (2.30) and (2.32) (with $m = 1$), and the estimate (2.48). We omit further details here. □

Lemma 2.13. *There exists $C > 0$, independent of h, such that*

$$\begin{aligned} |E_2(\boldsymbol{\tau} - \boldsymbol{\tau}_h)| \;\leq\; C \Bigg\{ \sum_{T\in\mathcal{T}_h} \Bigg\{ & h_T^2 \|\boldsymbol{\sigma}_h^{\mathrm{d}} - \boldsymbol{\psi}(\mathbf{t}_h)\|_{0,T}^2 + h_T^2 \|\mathrm{curl}(\boldsymbol{\sigma}_h^{\mathrm{d}} - \boldsymbol{\psi}(\mathbf{t}_h))\|_{0,T}^2 \\ & + \sum_{e\in\mathcal{E}(T)} h_e \|[\![(\boldsymbol{\sigma}_h^{\mathrm{d}} - \boldsymbol{\psi}(\mathbf{t}_h))\boldsymbol{s}]\!]\|_{0,e}^2 \Bigg\} \Bigg\}^{1/2} \|\boldsymbol{\tau}\|_{\mathbf{div},\Omega}. \end{aligned}$$

Proof. It follows analogously to the proof of [84, Lemma 4.6], whose main ideas are taken from [83, Lemmas 4.3 and 4.4]. □

Having established the above bounds for $|E_1(\boldsymbol{\tau} - \boldsymbol{\tau}_h)|$ and $|E_2(\boldsymbol{\tau} - \boldsymbol{\tau}_h)|$, we conclude from Lemma 2.10 and (2.47) that there exists $C > 0$, independent of h, such that

$$\|((\mathbf{t} - \mathbf{t}_h, \boldsymbol{\sigma} - \boldsymbol{\sigma}_h), \boldsymbol{\xi} - \boldsymbol{\xi}_h)\|_{H\times Q} \;\leq\; C \left\{ \sum_{T\in\mathcal{T}_h} \widehat{\theta}_T^2 + \|\mathbf{g} - \boldsymbol{\sigma}_h \boldsymbol{\nu}\|_{-1/2,\Gamma_N}^2 \right\}^{1/2}, \tag{2.50}$$

where

$$
\begin{aligned}
\widehat{\theta}_T^2 \quad := \quad & \frac{1}{\alpha^2}\|\mathbf{f}-\mathcal{P}_h^k(\mathbf{f})\|_{0,T}^2 + h_T^2\,\|\mathbf{t}_h - \nabla\mathbf{u}_h\|_{0,T}^2 + h_T^2\|\mathrm{curl}(\mathbf{t}_h)\|_{0,T}^2 \\
& + \sum_{e\in\mathcal{E}(T)\cap\mathcal{E}_h(\Omega)} h_e\|[\![\mathbf{t}_h\boldsymbol{s}]\!]\|_{0,e}^2 + \sum_{e\in\mathcal{E}(T)\cap\mathcal{E}_h(\Gamma_D)} h_e\|[\![\mathbf{t}_h\boldsymbol{s}]\!]\|_{0,e}^2 \\
& + \sum_{e\in\mathcal{E}(T)\cap\mathcal{E}_h(\Gamma_N)} h_e\left\{\left\|\mathbf{t}_h\boldsymbol{s} + \frac{d\boldsymbol{\xi}_h}{d\boldsymbol{s}}\right\|_{0,e}^2 + \|\boldsymbol{\xi}_h + \mathbf{u}_h\|_{0,e}^2\right\} \\
& + \|\boldsymbol{\sigma}_h^{\mathrm{d}} - \boldsymbol{\psi}(\mathbf{t}_h)\|_{0,T}^2 + h_T^2\|\mathrm{curl}(\boldsymbol{\sigma}_h^{\mathrm{d}} - \boldsymbol{\psi}(\mathbf{t}_h))\|_{0,T}^2 \\
& + \sum_{e\in\mathcal{E}(T)} h_e\|[\![(\boldsymbol{\sigma}_h^{\mathrm{d}} - \boldsymbol{\psi}(\mathbf{t}_h))\boldsymbol{s}]\!]\|_{0,e}^2.
\end{aligned}
$$

Now, in order to complete the upper bound for $\|((\mathbf{t}-\mathbf{t}_h,\boldsymbol{\sigma}-\boldsymbol{\sigma}_h),\boldsymbol{\xi}-\boldsymbol{\xi}_h)\|_{H\times Q}$ in terms of local error indicators, we need to estimate the Neumann residual $\|\mathbf{g}-\boldsymbol{\sigma}_h\boldsymbol{\nu}\|_{-1/2,\Gamma_N}$. Actually, this result was already proved in [72]. It is stated as follows.

Lemma 2.14. *Assume that the Neumann datum $\mathbf{g}\in\mathbf{L}^2(\Gamma_N)$. Then there exists $C>0$, independent of h, such that*

$$\|\mathbf{g}-\boldsymbol{\sigma}_h\boldsymbol{\nu}\|_{-1/2,\Gamma_N}^2 \;\le\; C\sum_{e\in\mathcal{E}_h(\Gamma_N)} h_e\|\mathbf{g}-\boldsymbol{\sigma}_h\boldsymbol{\nu}\|_{0,e}^2.$$

Proof. See [72, Lemma 15]. □

It is important to recall here, as remarked in [72, Remark after Lemma 15], that the shape-regularity of the mesh $\mathcal{T}_h$ insures that the constant C in Lemma 2.14 is independent of h, whence the estimate provided there in terms of the computable local quantities $\|\mathbf{g}-\boldsymbol{\sigma}_h\boldsymbol{\nu}\|_{0,e}$ becomes suitable for the associated adaptive algorithm. Without this assumption, it would not make sense to apply this theorem, and we would have just to keep the expression $\|\mathbf{g}-\boldsymbol{\sigma}_h\boldsymbol{\nu}\|_{-1/2,\Gamma_N}$ in the *a posteriori* error estimator, thus rendering a non-local and hence useless quantity for adaptivity.

Then, as a consequence of Lemmas 2.10 and 2.14, together with the estimate (2.50), we conclude that there exists $C>0$, independent of h, such that

$$\|((\mathbf{t}-\mathbf{t}_h,\boldsymbol{\sigma}-\boldsymbol{\sigma}_h),\boldsymbol{\xi}-\boldsymbol{\xi}_h)\|_{H\times Q} \quad\le\quad C\,\boldsymbol{\theta}, \tag{2.51}$$

where $\boldsymbol{\theta}$ is the global *a posteriori* error estimator defined by (2.36) and (2.34).

On the other hand, the upper bound for $\|\mathbf{u}-\mathbf{u}_h\|_{0,\Omega}$ is quite straightforward from the definition of $\mathbf{u}$ and $\mathbf{u}_h$. Indeed, recalling that

$$\mathbf{u} \;=\; \frac{1}{\alpha}\{\mathbf{f}+\mathbf{div}(\boldsymbol{\sigma})\} \qquad\text{and}\qquad \mathbf{u}_h \;=\; \frac{1}{\alpha}\left\{\mathcal{P}_h^k(\mathbf{f})+\mathbf{div}(\boldsymbol{\sigma}_h)\right\},$$

we easily obtain

$$\|\mathbf{u}-\mathbf{u}_h\|_{0,\Omega} \quad\le\quad \frac{1}{\alpha}\left\{\|\mathbf{f}-\mathcal{P}_h^k(\mathbf{f})\|_{0,\Omega} + \|\boldsymbol{\sigma}-\boldsymbol{\sigma}_h\|_{\mathbf{div},\Omega}\right\}. \tag{2.52}$$

Finally, from (2.52) and (2.51) we have that there exists $C_{\mathtt{rel}}>0$, independent of h, such that

$$\|\mathbf{u}-\mathbf{u}_h\|_{0,\Omega} \;+\; \|((\mathbf{t}-\mathbf{t}_h,\boldsymbol{\sigma}-\boldsymbol{\sigma}_h),\boldsymbol{\xi}-\boldsymbol{\xi}_h)\|_{H\times Q} \;\le\; C_{\mathtt{rel}}\boldsymbol{\theta},$$

which proves the reliability of the estimator $\boldsymbol{\theta}$.

2.5.3 Efficiency

In this section we prove the efficiency of our *a posteriori* error estimator $\boldsymbol{\theta}$ (lower bound in (2.37)). In other words, we derive suitable upper bounds for the eleven terms defining the local error indicator θ_T^2 (cf. (2.34)). We first notice, using the definitions of $\mathbf{u}$ (cf. (2.7)) and $\mathbf{u}_h$ (cf. (2.35)), that

$$\|\mathbf{f} - \mathcal{P}_h^k(\mathbf{f})\|_{0,T}^2 \;\leq\; 2\alpha^2\|\mathbf{u}-\mathbf{u}_h\|_{0,T}^2 \;+\; 2\|\mathbf{div}\big(\boldsymbol{\sigma}-\boldsymbol{\sigma}_h\big)\|_{0,T}^2\,. \tag{2.53}$$

On the other hand, we notice that the converse of the derivation of (2.8) from (2.5) holds true. Indeed, it is easy to show, applying integration by parts backwardly and using appropriate test functions, that the unique solution $((\mathbf{t},\boldsymbol{\sigma}),\boldsymbol{\xi}) \in H \times Q$ of (2.8) solves the original problem (2.5). Then, using that $\boldsymbol{\sigma}^{\mathrm{d}} = \boldsymbol{\psi}(\mathbf{t})$ in Ω and applying the Lipschitz-continuity of $\mathbb{A}$ (cf. Lemma 2.2), but restricted to the triangle $T \in \mathcal{T}_h$ instead of Ω, we deduce that

$$\begin{aligned}\|\boldsymbol{\sigma}_h^{\mathrm{d}} - \boldsymbol{\psi}(\mathbf{t}_h)\|_{0,T} \;&\leq\; \|(\boldsymbol{\sigma}-\boldsymbol{\sigma}_h)^{\mathrm{d}}\|_{0,T} + \|\mu(|\mathbf{t}|)\mathbf{t} - \mu(|\mathbf{t}_h|)\mathbf{t}_h\|_{0,T},\\ &\leq\; \|\boldsymbol{\sigma}-\boldsymbol{\sigma}_h\|_{0,T} + \gamma_0\|\mathbf{t}-\mathbf{t}_h\|_{0,T}.\end{aligned} \tag{2.54}$$

Next, in order to bound the terms involving the mesh parameters h_T and h_e, we make use of the results and estimates available for the corresponding linear case (cf. [72, Section 4.3]). The techniques applied there are based on triangle-bubble and edge-bubble functions, extension operators, and discrete trace and inverse inequalities. For further details on these tools we refer particularly to [72, Lemmas 16 and 17, and eq. (67)].

Hence, the estimates of the remaining nine terms defining θ_T^2 (cf. (2.34)) are established next. In what follows, given $e \in \mathcal{E}_h(\Gamma_D) \cup \mathcal{E}_h(\Gamma_N)$, T_e stands for the triangle of $\mathcal{T}_h$ having e as an edge. Also, for each $e \in \mathcal{E}_h(\Omega)$ we set $\omega_e := \cup\{\, T \in \mathcal{T}_h \;:\; e \in \mathcal{E}(T)\}$.

Theorem 2.6. *Assume that* $\mathbf{g}$ *is piecewise polynomial. Then, there exist* $C_i > 0$*,* $i \in \{1,2,...,8\}$*, independent of* h*, such that*

$$h_T^2\|\mathrm{curl}(\mathbf{t}_h)\|_{0,T}^2 \;\leq\; C_1\|\mathbf{t}-\mathbf{t}_h\|_{0,T}^2 \quad \forall\, T \in \mathcal{T}_h\,,$$

$$h_e\|[\![\mathbf{t}_h\boldsymbol{s}_e]\!]\|_{0,e}^2 \;\leq\; C_2\|\mathbf{t}-\mathbf{t}_h\|_{0,\omega_e}^2 \quad \forall\, e \in \mathcal{E}_h(\Omega)\,,$$

$$h_T^2\,\|\mathbf{t}_h - \nabla\mathbf{u}_h\|_{0,T}^2 \;\leq\; C_3\left\{\|\mathbf{u}-\mathbf{u}_h\|_{0,T}^2 + h_T^2\|\mathbf{t}-\mathbf{t}_h\|_{0,T}^2\right\} \quad \forall\, T \in \mathcal{T}_h\,,$$

$$h_e\,\|[\mathbf{t}_h\boldsymbol{s}]\|_{0,e}^2 \;\leq\; C_4\|\mathbf{t}-\mathbf{t}_h\|_{0,T_e}^2 \quad \forall\, e \in \mathcal{E}_h(\Gamma_D)\,,$$

$$h_e\|\boldsymbol{\xi}_h + \mathbf{u}_h\|_{0,e}^2 \;\leq\; C_5\Big\{h_e\|\boldsymbol{\xi}-\boldsymbol{\xi}_h\|_{0,e}^2 + \|\mathbf{u}-\mathbf{u}_h\|_{0,T_e}^2 + h_{T_e}^2\|\mathbf{t}-\mathbf{t}_h\|_{0,T_e}^2\Big\} \quad \forall\, e \in \mathcal{E}_h(\Gamma_N)\,,$$

$$h_e\|\mathbf{g} - \boldsymbol{\sigma}_h\boldsymbol{\nu}\|_{0,e}^2 \;\leq\; C_6\Big\{\|\boldsymbol{\sigma}-\boldsymbol{\sigma}_h\|_{0,T_e}^2 + h_{T_e}^2\|\mathbf{div}(\boldsymbol{\sigma}-\boldsymbol{\sigma}_h)\|_{0,T_e}^2\Big\} \quad \forall\, e \in \mathcal{E}_h(\Gamma_N)\,,$$

$$h_T^2\|\mathrm{curl}(\boldsymbol{\sigma}_h^{\mathrm{d}} - \boldsymbol{\psi}(\mathbf{t}_h))\|_{0,T}^2 \;\leq\; C_7\left\{\|\mathbf{t}-\mathbf{t}_h\|_{0,T}^2 + \|\boldsymbol{\sigma}-\boldsymbol{\sigma}_h\|_{0,T}^2\right\} \quad \forall\, T \in \mathcal{T}_h\,,$$

and

$$h_e\|[\![(\boldsymbol{\sigma}_h^{\mathrm{d}} - \boldsymbol{\psi}(\mathbf{t}_h))\boldsymbol{s}]\!]\|_{0,e}^2 \;\leq\; C_8\left\{\|\mathbf{t}-\mathbf{t}_h\|_{0,\omega_e}^2 + \|\boldsymbol{\sigma}-\boldsymbol{\sigma}_h\|_{0,\omega_e}^2\right\} \quad \forall\, e \in \mathcal{E}_h\,.$$

Proof. The first six estimates follow as in the proofs of the corresponding results in [72] by replacing $\frac{1}{\mu}\boldsymbol{\sigma}_h$ by $\mathbf{t}_h$, and by using that $\mathbf{t} = \nabla\mathbf{u}$ in Ω, $\mathbf{u} = \mathbf{0}$ in Γ_D, $\boldsymbol{\xi} = -\mathbf{u}$ on Γ_N, and $\mathbf{g} = \boldsymbol{\sigma}\boldsymbol{\nu}$ on Γ_N. In turn, the last two follow analogously to the proof of [84, Lemma 4.11], which applies [72, Lemma 18] to $\boldsymbol{\rho}_h = \boldsymbol{\sigma}_h^{\mathrm{d}} - \boldsymbol{\psi}(\mathbf{t}_h)$ and $\boldsymbol{\rho} = \boldsymbol{\sigma}^{\mathrm{d}} - \boldsymbol{\psi}(\mathbf{t})$ in Ω, and then uses the Lipschitz-continuity of $\mathbb{A}$ (cf. Lemma 2.2) restricted to T and ω_e. $\square$

Note here that if $\mathbf{g}$ were not piecewise polynomial but sufficiently smooth, then higher order terms given by the errors arising from suitable polynomial approximations would appear in the foregoing sixth inequality. This explains the eventual expression *h.o.t.* in (2.37).

We continue with the following result.

Lemma 2.15. *Assume that Σ_h is quasi-uniform. Then there exists $C_9 > 0$, independent of h, such that*

$$\sum_{e\in\mathcal{E}_h(\Gamma_N)} h_e \left\| \mathbf{t}_h \boldsymbol{s} + \frac{d\boldsymbol{\xi}_h}{d\boldsymbol{s}} \right\|_{0,e}^2 \;\leq\; C_9 \left\{ \sum_{e\in\mathcal{E}_h(\Gamma_N)} \|\mathbf{t} - \mathbf{t}_h\|_{0,T_e}^2 + \|\boldsymbol{\xi} - \boldsymbol{\xi}_h\|_{0;1/2,\Gamma_N}^2 \right\}.$$

Proof. It follows as in the proof of [72, Lemma 22], by replacing there $\frac{1}{\mu}\boldsymbol{\sigma}_h^{\mathrm{d}}$ by $\mathbf{t}_h$, and then using that $\mathbf{t} = \nabla \mathbf{u}$ in Ω. $\square$

Note, as in [72], that the estimate provided by Lemma 2.15 is the only nonlocal bound of the present efficiency analysis. In addition, this lemma is the only one needing to assume that Σ_h is quasi-uniform, which is required to apply the inverse inequality of piecewise polynomials on Σ_h. Certainly, in order to preserve that assumption, the eventual adaptive refinements must hold away of Γ_N. However, under an additional local regularity assumption on $\boldsymbol{\xi}$, but without assuming any quasi-uniformity condition, we are able to prove the following local bound.

Lemma 2.16. *Assume that $\boldsymbol{\xi}|_e \in \mathbf{H}^1(e)$ for each $e \in \mathcal{E}_h(\Gamma_N)$. Then there exists $\widetilde{C}_9 > 0$, independent of h, such that for each $e \in \mathcal{E}_h(\Gamma_N)$ there holds*

$$h_e \left\| \mathbf{t}_h \boldsymbol{s} + \frac{d\boldsymbol{\xi}_h}{d\boldsymbol{s}} \right\|_{0,e}^2 \;\leq\; \widetilde{C}_9 \left\{ \|\mathbf{t} - \mathbf{t}_h\|_{0,T_e}^2 + h_e \left\| \frac{d}{d\boldsymbol{s}}(\boldsymbol{\xi} - \boldsymbol{\xi}_h) \right\|_{0,e}^2 \right\}.$$

Proof. It suffices to replace again $\frac{1}{\mu}\boldsymbol{\sigma}_h^{\mathrm{d}}$ by $\mathbf{t}_h$ in [72, Lemma 23]. $\square$

Consequently, the efficiency of $\boldsymbol{\theta}$ follows straightforwardly from estimates (2.53) and (2.54), together with Theorem 2.6 and Lemma 2.15, after summing up over $T \in \mathcal{T}_h$.

2.6 Numerical results

In this section, we present four numerical examples demonstrating a good performance of the augmented mixed finite element scheme (2.22), confirming the reliability and efficiency of the *a posteriori* error estimator $\boldsymbol{\theta}$ derived in Section 2.5, and showing the behaviour of the associated adaptive algorithm. In all the computations we consider the specific finite element subspaces H_h and Q_h given respectively by (2.18) and (2.20), with $k \in \{0, 1, 2\}$ and $\Sigma_{\tilde{h}} := \Sigma_{2h}$. We begin by introducing additional notations. In what follows N stands for the total number of degrees of freedom (unknowns) of (2.22), that is,

$$\begin{aligned} N \;&:=\; 2(k+1) \times (\#\text{ of edges in } \mathcal{T}_h) \;+\; \{3d_k + 2k(k+2)\} \times (\#\text{ of elements in } \mathcal{T}_h) \\ &\quad + 2\left\{(k+1) \times (\#\text{ of edges in } \Sigma_{\tilde{h}}) + 1\right\}, \end{aligned}$$

with $d_k := \frac{1}{2}(k+1)(k+2)$. Also, the individual and total errors are defined by

$$\begin{array}{rclrcl} \mathtt{e}(\mathbf{t}) & := & \|\mathbf{t}-\mathbf{t}_h\|_{0,\Omega}, & \mathtt{e}(\boldsymbol{\sigma}) & := & \|\boldsymbol{\sigma}-\boldsymbol{\sigma}_h\|_{\mathbf{div},\Omega}, \\ \mathtt{e}(\boldsymbol{\xi}) & := & \|\boldsymbol{\xi}-\boldsymbol{\xi}_h\|_{0;1/2,\Gamma_N}, & \mathtt{e}(\mathbf{u}) & := & \|\mathbf{u}-\mathbf{u}_h\|_{0,\Omega}, \\ \mathtt{e}(\mathbf{t},\boldsymbol{\sigma},\boldsymbol{\xi}) & := & \Big\{[\mathtt{e}(\mathbf{t})]^2+[\mathtt{e}(\boldsymbol{\sigma})]^2+[\mathtt{e}(\boldsymbol{\xi})]^2\Big\}^{1/2}, & \mathtt{e}(p) & := & \|p-p_h\|_{0,\Omega}, \end{array}$$

$$\mathtt{e}(\mathbf{t},\boldsymbol{\sigma},\boldsymbol{\xi},\mathbf{u}) := \Big\{[\mathtt{e}(\mathbf{t})]^2+[\mathtt{e}(\boldsymbol{\sigma})]^2+[\mathtt{e}(\boldsymbol{\xi})]^2+[\mathtt{e}(\mathbf{u})]^2\Big\}^{1/2},$$

where p_h and $\mathbf{u}_h$ are computed by the postprocessing formulae (2.23) and (2.35), whereas the effectivity index with respect to $\boldsymbol{\theta}$ is given by

$$\mathtt{eff}(\boldsymbol{\theta}) := \mathtt{e}(\mathbf{t},\boldsymbol{\sigma},\boldsymbol{\xi},\mathbf{u}) \,/\, \boldsymbol{\theta}.$$

Then, we define the experimental rates of convergence

$$\begin{array}{rclrcl} \mathtt{r}(\mathbf{t}) & := & \dfrac{\log(\mathtt{e}(\mathbf{t})/\mathtt{e}'(\mathbf{t}))}{\log(h/h')} & \mathtt{r}(\boldsymbol{\sigma}) & := & \dfrac{\log(\mathtt{e}(\boldsymbol{\sigma})/\mathtt{e}'(\boldsymbol{\sigma}))}{\log(h/h')}, \\ \mathtt{r}(\boldsymbol{\xi}) & := & \dfrac{\log(\mathtt{e}(\boldsymbol{\xi})/\mathtt{e}'(\boldsymbol{\xi}))}{\log(h/h')}, & \mathtt{r}(\mathbf{t},\boldsymbol{\sigma},\boldsymbol{\xi}) & := & \dfrac{\log(\mathtt{e}(\mathbf{t},\boldsymbol{\sigma},\boldsymbol{\xi})/\mathtt{e}'(\mathbf{t},\boldsymbol{\sigma},\boldsymbol{\xi}))}{\log(h/h')}, \end{array}$$

and similarly for $\mathtt{r}(p)$ and $\mathtt{r}(\mathbf{u})$, where $\mathtt{e}$ and $\mathtt{e}'$ denote the corresponding errors for two consecutive triangulations with mesh sizes h and h', respectively. Nevertheless, when the adaptive algorithm is applied (see details below), the expression $\log(h/h')$ appearing in the computation of the above rates is replaced by $-\frac{1}{2}\log(N/N')$, where N and N' denote the corresponding degrees of freedom of each triangulation.

The numerical results presented below were obtained using a C^{++} code. The corresponding nonlinear algebraic systems arising from (2.8) are solved by the Newton-Raphson method with a tolerance of 10^{-6} and taking the solution of the associated linear Brinkman problem ($\mu = 1$) as initial iteration for the quasi-uniform scheme. In all the examples no more than four iterations were required to achieve the given tolerance. In turn, the linear systems were solved using the Conjugate Gradient method as main solver, and applying a stopping criterion determined by a relative tolerance of 10^{-10}.

The examples to be considered in this section, some of them taken from [72], are described next. Example 1 is employed to illustrate the performance of the augmented mixed finite element scheme (2.22) and to confirm the reliability and efficiency of the *a posteriori* error estimator $\boldsymbol{\theta}$. Examples 2 and 3 are utilized to show the behaviour of the associated adaptive algorithm, which applies the following procedure:

(1) Start with a coarse mesh $\mathcal{T}_h$.

(2) Solve the linear version of the discrete problem (2.22), in order to obtain an initial guess $\mathbf{x}_0$, for the Newton iterations.

(3) Solve the discrete problem (2.22) for the actual mesh $\mathcal{T}_h$, with the actual initial guess $\mathbf{x}_0$.

(4) Compute θ_T (cf. (2.34)) for each triangle $T \in \mathcal{T}_h$,

(5) Evaluate stopping criterion ($\boldsymbol{\theta} \leq$ given tolerance) and decide to finish or go to next step.

(6) Use *red-green-blue* procedure (cf. [126]) to refine each $T' \in \mathcal{T}_h$ whose indicator $\theta_{T'}$ satisfies

$$\theta_{T'} \;\geq\; \frac{1}{2}\max\{\theta_T \;:\; T \in \mathcal{T}_h\}\,.$$

(7) Use the solution given by step 3 and the new mesh to interpolate a new initial guess $\widetilde{\mathbf{x}}_0$ and then replace $\mathbf{x}_0$ by $\widetilde{\mathbf{x}}_0$.

(8) Define the new mesh as actual mesh $\mathcal{T}_h$ and go to step 3.

For the three examples we consider the nonlinear function $\mu : \mathrm{R}^+ \to \mathrm{R}^+$ given by the Carreau law

$$\mu(t) \;:=\; \mu_0 \;+\; \mu_1(1+t^2)^{(\beta-2)/2} \quad \forall\, t \in \mathrm{R}^+,$$

with $\mu_0 = \mu_1 = 0.5$ and $\beta = 1.5$. It is easy to check that the assumptions (2.2) and (2.3) are satisfied with

$$\gamma_0 \;=\; \mu_0 \;+\; \mu_1\left\{\frac{|\beta-2|}{2}+1\right\} \qquad \text{and} \qquad \alpha_0 \;=\; \mu_0.$$

Hence, for the implementation of the augmented scheme (2.22) we use the stabilization parameter $\kappa = \frac{\alpha_0}{\gamma_0^2}$, which certainly satisfies the required hypothesis $\kappa \in \left(0, \frac{2\alpha_0}{\gamma_0^2}\right)$. Nevertheless, similarly as observed in [82, Figures 9 and 11], one can check that for a wide range of values of κ within the above interval, the Galerkin schemes are still stable in the sense that all the errors remain bounded, which confirms the robustness of the method with respect to this stabilization parameter.

In Example 1 we consider $\Omega = (0,1)^2$, $\Gamma_D = \big\{(w,0),(0,w) \in \mathrm{R}^2 \;:\; 0 \leq w \leq 1\big\}$, $\Gamma_N = \Gamma \setminus \bar{\Gamma}_D$, $\alpha = \frac{1}{2\pi}$, and choose the data $\mathbf{f}$ and $\mathbf{g}$ so that the exact solution is given for each $\mathbf{x} := (x_1,x_2)^{\mathrm{t}} \in \Omega$ by

$$\mathbf{u}(\mathbf{x}) \;=\; \begin{pmatrix} (1+x_1-\exp(x_1))\,(1-\cos(x_2)) \\ (\exp(x_1)-1)\,(x_2-\sin(x_2)) \end{pmatrix}$$

and

$$p(\mathbf{x}) \;=\; \frac{1}{2}\,\exp(2\pi x_1).$$

Note that $\mathbf{u}$ is divergence free and $(\mathbf{u},p)$ is regular in the whole domain Ω.

In Example 2 we consider $\Omega =]-1,1[^2 \setminus [0,1]^2$, $\Gamma_D = \{(-1,x_2) \in \mathrm{R}^2 : -1 \leq x_2 \leq 1\}$, $\Gamma_N = \Gamma \setminus \bar{\Gamma}_D$, $\alpha = 1$, and choose $\mathbf{f}$ and $\mathbf{g}$ so that the exact solution is given for each $\mathbf{x} := (x_1,x_2)^{\mathrm{t}} \in \Omega$ by

$$\mathbf{u}(\mathbf{x}) \;=\; \mathbf{curl}\left((x_1+1)^2\sqrt{(x_1-0.1)^2 \;+\; (x_2-0.1)^2}\right)$$

and

$$p(\mathbf{x}) \;=\; \frac{1}{x_2 \;+\; 1.1}.$$

Note that Ω is an L-shaped domain and that $\mathbf{u}$ and p are singular at $(0.1,0.1)$ and along the line $x_2 = -1.1$, respectively. Hence, we should expect regions of high gradients around the origin, which is the middle corner of the L, and along the line $x_2 = -1$.

Finally, in Example 3 we consider $\Omega =]-1,1[^2 \setminus ([-1,-0.25] \times [-1,0.5] \cup [0.25,1] \times [-1,0.5])$, $\Gamma_D = \{(x_1,1) \in \mathrm{R}^2 : -1 \leq x_1 \leq 1\}$, $\Gamma_N = \Gamma \setminus \bar{\Gamma}_D$, $\alpha = 10$, and choose the data $\mathbf{f}$ and $\mathbf{g}$ so that the exact solution is given for each $\mathbf{x} := (x_1,x_2)^{\mathrm{t}} \in \Omega$ by

$$\mathbf{u}(\mathbf{x}) \;=\; \mathbf{curl}\Big((x_2-1)^2\Big\{\sqrt{(x_1+0.3)^2 \;+\; (x_2-0.45)^2} \;+\; \sqrt{(x_1-0.3)^2 \;+\; (x_2-0.45)^2}\Big\}\Big)$$

and

$$p(\mathbf{x}) \;=\; \frac{1}{x_2 \;+\; 1.1}.$$

Note that Ω is a T-shaped domain and that $\mathbf{u}$ and p are singular at $(-0.3, 0.45)$ and $(0.3, 0.45)$, and along the line $x_2 = -1.1$, respectively. Hence, similarly to Example 2, we should expect regions of high gradients around $(-0.25, 0.5)$ and $(0.25, 0.5)$, which are the middle corners of the T, and along the line $x_2 = -1$.

In Tables 2.1 and 2.2 we summarize the convergence history of the augmented mixed finite element scheme (2.8) as applied to Example 1 for a sequence of quasi-uniform triangulations of each domain. We notice there that the rate of convergence $O(h^{k+1})$ predicted by Theorem 2.4 (when $s = k + 1$) is attained by all the unknowns, including the postprocessed $\mathbf{u}_h$ and p_h (cf. Table 2.2). In particular, as observed in the ninth column of Table 2.1, the convergence of $\boldsymbol{\xi}_h$ is a bit faster than expected, which could correspond to either a superconvergence phenomenon or a special feature of this example. A similar phenomenon holds for the variable $\mathbf{u}$ in Table 2.2 for $k \geq 1$. We also remark the good behaviour of the *a posteriori* error estimator $\boldsymbol{\theta}$ in this case. In particular, in Table 2.1, we see that the effectivity index $\mathtt{eff}(\boldsymbol{\theta})$ remains always in a neighborhood of 0.167 for $k = 0$, which illustrates the reliability and efficiency result provided by Theorem 2.5.

Next, in Tables 2.3, 2.4, 2.5, and 2.6, we provide the convergence history of the quasi-uniform and adaptive schemes as applied to Examples 3 and 4. The stopping criterion in both adaptive refinements is $\boldsymbol{\theta} \leq 0.2$. We observe here, as expected, that the errors of the adaptive methods decrease faster than those obtained by the quasi-uniform ones. This fact is better illustrated in Figures. 2.1 and 2.3 where we display the errors $\mathtt{e}(\mathbf{t}, \boldsymbol{\sigma}, \boldsymbol{\xi})$ vs. the degrees of freedom N for both refinements. In addition, the effectivity indices remain again bounded from above and below, which confirms the reliability and efficiency of $\boldsymbol{\theta}$ for the associated adaptive algorithm as well. Some intermediate meshes obtained with this procedure are displayed in Figures 2.2 and 2.4. Notice here that the adapted meshes concentrate the refinements around the origin and the line $x_2 = -1$ in Example 3, and around the points $(-0.25, 0.5)$ and $(0.25, 0.5)$ and the line $x_2 = -1$ in Example 4, which means that the method is in fact able to recognize the regions with high gradients of the solutions. Finally, in order to illustrate the accurateness of the adaptive scheme, in Figures 2.5, 2.6, 2.7, and 2.8, we display some components of the solutions for both examples. For the field unknowns, the approximate ones are placed at the left side whereas the exact ones are placed at the right side. In turn, the components of the boundary unknown $\boldsymbol{\xi}$ are depicted along straight lines beginning at the points $(-1, -1)$ and $(-1, 1)$ for the L-shaped and T-shaped domains, respectively, and then continuing counterclockwise. This gives the 1D graphs in which the two approximate components of $\boldsymbol{\xi}$ are identified by red bullets whereas the exact ones are identified by continuous blue lines.

k	h	N	e($\mathbf{t}$)	r($\mathbf{t}$)	e($\boldsymbol{\sigma}$)	r($\boldsymbol{\sigma}$)	e($\boldsymbol{\xi}$)	r($\boldsymbol{\xi}$)	e($\mathbf{t},\boldsymbol{\sigma},\boldsymbol{\xi}$)	r($\mathbf{t},\boldsymbol{\sigma},\boldsymbol{\xi}$)	eff($\boldsymbol{\theta}$)
	1/16	7266	8.58e-0	−−	3.20e+01	−−	1.44e-0	−−	3.31e+01	−−	0.1686
	1/20	11322	6.72e-0	1.09	2.56e+01	0.99	7.33e-1	3.03	2.65e+01	1.00	0.1683
	1/24	16274	5.49e-0	1.11	2.14e+01	0.99	4.28e-1	2.95	2.21e+01	1.00	0.1681
	1/28	22122	4.63e-0	1.12	1.83e+01	1.00	2.77e-1	2.82	1.89e+01	1.00	0.1679
0	1/32	28866	3.98e-0	1.13	1.60e+01	1.00	1.94e-1	2.67	1.65e+01	1.00	0.1678
	1/36	36506	3.48e-0	1.13	1.43e+01	1.00	1.44e-1	2.52	1.47e+01	1.01	0.1677
	1/48	64802	2.50e-0	1.14	1.07e+01	1.00	7.57e-2	2.25	1.10e+01	1.01	0.1674
	1/64	115074	1.80e-0	1.16	8.03e-0	1.00	4.43e-2	1.86	8.23e-0	1.01	0.1671
	1/96	258626	1.12e-0	1.17	5.36e-0	1.00	2.42e-2	1.49	5.47e-0	1.01	0.1668
	1/128	459522	8.01e-1	1.16	4.02e-0	1.00	1.64e-2	1.35	4.10e-0	1.01	0.1666
	1/16	22722	2.08e-1	−−	1.21e-0	−−	2.04e-3	−−	1.22e-0	−−	0.1623
	1/20	35442	1.32e-1	2.04	7.75e-1	1.99	9.23e-4	3.55	7.86e-1	1.99	0.1624
	1/24	50978	9.13e-2	2.02	5.39e-1	1.99	4.80e-4	3.59	5.47e-1	1.99	0.1624
	1/28	69330	6.71e-2	2.00	3.97e-1	1.99	2.76e-4	3.57	4.02e-1	1.99	0.1624
1	1/32	90498	5.14e-2	1.99	3.04e-1	1.99	1.72e-4	3.53	3.08e-1	1.99	0.1625
	1/36	114482	4.06e-2	1.99	2.40e-1	2.00	1.14e-4	3.49	2.44e-1	2.00	0.1625
	1/48	203330	2.29e-2	1.99	1.35e-1	2.00	4.30e-5	3.40	1.37e-1	2.00	0.1625
	1/64	361218	1.29e-2	1.99	7.61e-2	2.00	1.68e-5	3.27	7.72e-2	2.00	0.1626
	1/96	812162	5.77e-3	1.99	3.39e-2	2.00	4.51e-6	3.24	3.44e-2	2.00	0.1625
	1/128	1443330	3.25e-3	1.99	1.91e-2	2.00	1.78e-6	3.24	1.93e-2	2.00	0.1626
	1/16	46370	4.69e-3	−−	3.33e-2	−−	1.38e-5	−−	3.36e-2	−−	0.1581
	1/20	72362	2.41e-3	2.98	1.71e-2	2.98	5.77e-6	3.89	1.73e-2	2.98	0.1580
	1/24	104114	1.40e-3	2.98	9.91e-3	2.99	2.83e-6	3.91	1.00e-2	2.99	0.1580
	1/28	141626	8.84e-4	2.99	6.25e-3	2.99	1.55e-6	3.92	6.31e-3	2.99	0.1580
2	1/32	184898	5.93e-4	2.99	4.19e-3	2.99	9.14e-7	3.93	4.23e-3	2.99	0.1580
	1/36	233930	4.17e-4	2.99	2.94e-3	3.00	5.75e-7	3.94	2.97e-3	3.00	0.1580
	1/48	415586	1.77e-4	2.99	1.24e-3	2.99	1.85e-7	3.94	1.26e-3	2.99	0.1580
	1/64	738434	7.47e-5	2.99	5.25e-4	3.00	5.94e-8	3.94	5.31e-4	3.00	0.1580
	1/96	1660610	2.22e-5	2.99	1.56e-4	3.00	1.20e-8	3.94	1.58e-4	3.00	0.1580
	1/128	2951426	9.39e-6	2.99	6.59e-5	3.00	3.86e-9	3.94	6.65e-5	3.00	0.1581

Table 2.1: Example 1, quasi-uniform scheme.

k	h	N	$\mathtt{e}(\mathbf{u})$	$\mathtt{r}(\mathbf{u})$	$\mathtt{e}(\mathtt{p})$	$\mathtt{r}(\mathtt{p})$
	1/16	7266	1.24e-1	−−	3.90e-0	−−
	1/20	11322	8.19e-2	1.84	3.12e-0	1.01
	1/24	16274	5.93e-2	1.77	2.60e-0	1.01
	1/28	22122	4.58e-2	1.68	2.22e-0	1.01
0	1/32	28866	3.71e-2	1.58	1.94e-0	1.00
	1/36	36506	3.11e-2	1.49	1.73e-0	1.00
	1/48	64802	2.12e-2	1.34	1.29e-0	1.00
	1/64	115074	1.51e-2	1.18	9.70e-1	1.00
	1/96	258626	9.54e-3	1.13	6.46e-1	1.00
	1/128	459522	6.77e-3	1.19	4.85e-1	1.00
	1/16	22722	1.56e-3	−−	1.38e-1	−−
	1/20	35442	7.70e-4	3.17	8.87e-2	1.99
	1/24	50978	4.35e-4	3.14	6.17e-2	1.99
	1/28	69330	2.69e-4	3.10	4.54e-2	1.99
1	1/32	90498	1.79e-4	3.08	3.48e-2	2.00
	1/36	114482	1.25e-4	3.06	2.75e-2	2.00
	1/48	203330	5.21e-5	3.03	1.55e-2	2.00
	1/64	361218	2.20e-5	3.00	8.71e-3	2.00
	1/96	812162	6.52e-6	3.00	3.87e-3	2.00
	1/128	1443330	2.75e-6	3.00	2.18e-3	2.00
	1/16	46370	1.96e-5	−−	3.60e-3	−−
	1/20	72362	8.04e-6	4.00	1.84e-3	3.01
	1/24	104114	3.88e-6	4.00	1.06e-3	3.01
	1/28	141626	2.09e-6	4.00	6.67e-4	3.01
2	1/32	184898	1.23e-6	3.96	4.46e-4	3.01
	1/36	233930	7.65e-7	4.05	3.13e-4	3.01
	1/48	415586	2.42e-7	4.01	1.32e-4	3.01
	1/64	738434	7.64e-8	4.00	5.54e-5	3.01
	1/96	1660610	1.51e-8	4.00	1.63e-5	3.01
	1/128	2951426	4.78e-9	4.00	6.86e-6	3.01

Table 2.2: Example 1, quasi-uniform scheme for the postprocessed unknowns.

k	h	N	$\texttt{e}(\mathbf{t})$	$\texttt{r}(\mathbf{t})$	$\texttt{e}(\boldsymbol{\sigma})$	$\texttt{r}(\boldsymbol{\sigma})$	$\texttt{e}(\boldsymbol{\xi})$	$\texttt{r}(\boldsymbol{\xi})$	$\texttt{e}(\mathbf{t},\boldsymbol{\sigma},\boldsymbol{\xi})$	$\texttt{r}(\mathbf{t},\boldsymbol{\sigma},\boldsymbol{\xi})$	$\texttt{eff}(\boldsymbol{\theta})$
	1/2	366	3.39e-0	−−	1.59e+01	−−	1.55e+01	−−	2.25e+01	−−	1.1530
	1/4	1402	2.15e-0	0.66	1.11e+01	0.52	6.37e-0	1.29	1.30e+01	0.79	1.0015
	1/6	3110	1.50e-0	0.90	8.70e-0	0.61	3.65e-0	1.37	9.55e-0	0.76	0.9548
	1/8	5490	1.12e-0	1.02	7.16e-0	0.68	2.25e-0	1.68	7.58e-0	0.80	0.9281
	1/10	8542	9.00e-1	0.96	6.05e-0	0.76	1.53e-0	1.74	6.30e-0	0.83	0.9170
	1/12	12266	7.70e-1	0.86	5.22e-0	0.80	1.15e-0	1.56	5.40e-0	0.84	0.9148
	1/14	16662	6.77e-1	0.83	4.59e-0	0.83	9.21e-1	1.45	4.73e-0	0.86	0.9151
	1/16	21730	6.01e-1	0.89	4.09e-0	0.86	7.50e-1	1.54	4.21e-0	0.88	0.9149
0	1/18	27470	5.35e-1	0.98	3.69e-0	0.88	6.11e-1	1.74	3.78e-0	0.91	0.9137
	1/20	33882	4.78e-1	1.06	3.36e-0	0.90	4.97e-1	1.96	3.43e-0	0.93	0.9119
	1/40	134962	2.25e-1	1.09	1.75e-0	0.94	1.01e-1	2.29	1.76e-0	0.96	0.9056
	1/80	538722	1.11e-1	1.02	8.84e-1	0.98	2.28e-2	2.15	8.91e-1	0.99	0.9066
	1/160	2152642	5.53e-2	1.00	4.43e-1	1.00	5.51e-3	2.05	4.47e-1	1.00	0.9065
	1/200	3362802	4.42e-2	1.00	3.55e-1	1.00	3.51e-3	2.02	3.58e-1	1.00	0.9064
	1/220	4068682	4.02e-2	1.00	3.23e-1	1.00	2.90e-3	2.02	3.25e-1	1.00	0.9063
	1/240	4841762	3.68e-2	1.00	2.96e-1	1.00	2.43e-3	2.01	2.98e-1	1.00	0.9067
	1/300	7564202	2.95e-2	1.00	2.37e-1	1.00	1.55e-3	2.01	2.38e-1	1.00	0.9067
	1/400	13445602	2.21e-2	1.00	1.77e-1	1.00	8.70e-4	2.01	1.79e-1	1.00	0.9065
	1/2	1114	1.51e-0	−−	7.34e-0	−−	5.12e-0	−−	9.08e-0	−−	0.8729
	1/4	4338	6.63e-1	1.18	3.84e-0	0.94	1.95e-0	1.39	4.35e-0	1.06	0.8278
	1/6	9674	4.50e-1	0.96	2.36e-0	1.20	1.16e-0	1.28	2.66e-0	1.21	0.8336
	1/8	17122	3.58e-1	0.79	1.60e-0	1.34	7.85e-1	1.35	1.82e-0	1.33	0.8606
	1/10	26682	2.57e-1	1.49	1.16e-0	1.45	5.02e-1	2.01	1.29e-0	1.54	0.8561
1	1/12	38354	1.71e-1	2.24	8.75e-1	1.54	3.00e-1	2.81	9.40e-1	1.73	0.8281
	1/14	52138	1.12e-1	2.76	6.81e-1	1.62	1.76e-1	3.48	7.12e-1	1.80	0.8031
	1/16	68034	7.59e-2	2.89	5.44e-1	1.68	1.06e-1	3.75	5.59e-1	1.81	0.7919
	1/18	86042	5.59e-2	2.60	4.44e-1	1.72	7.17e-2	3.36	4.53e-1	1.79	0.7920
	1/20	106162	4.50e-2	2.06	3.69e-1	1.75	5.45e-2	2.61	3.76e-1	1.78	0.7979
	1/40	423522	1.19e-2	1.92	1.02e-1	1.85	9.66e-3	2.50	1.03e-1	1.86	0.8356
	1/2	2246	7.37e-1	−−	3.52e-0	−−	2.42e-0	−−	4.33e-0	−−	0.6759
	1/4	8810	4.43e-1	0.73	1.34e-0	1.39	1.15e-0	1.07	1.82e-0	1.25	0.7723
	1/6	19694	2.98e-1	0.98	6.60e-1	1.75	6.33e-1	1.48	9.61e-1	1.58	0.8532
2	1/8	34898	1.61e-1	2.15	3.73e-1	1.98	3.02e-1	2.57	5.06e-1	2.23	0.6371
	1/10	54422	8.71e-2	2.74	2.29e-1	2.19	1.44e-1	3.32	2.84e-1	2.59	0.5190
	1/12	78266	5.31e-2	2.72	1.50e-1	2.34	7.77e-2	3.38	1.77e-1	2.61	0.5272
	1/14	106430	3.45e-2	2.79	1.03e-1	2.43	4.66e-2	3.32	1.18e-1	2.62	0.5931

Table 2.3: Example 2, quasi-uniform scheme.

k	h	N	$\mathtt{e}(\mathbf{t})$	$\mathtt{r}(\mathbf{t})$	$\mathtt{e}(\boldsymbol{\sigma})$	$\mathtt{r}(\boldsymbol{\sigma})$	$\mathtt{e}(\boldsymbol{\xi})$	$\mathtt{r}(\boldsymbol{\xi})$	$\mathtt{e}(\mathbf{t},\boldsymbol{\sigma},\boldsymbol{\xi})$	$\mathtt{r}(\mathbf{t},\boldsymbol{\sigma},\boldsymbol{\xi})$	$\mathtt{eff}(\boldsymbol{\theta})$
	0.5000	366	3.39e-0	−−	1.59e+01	−−	1.55e+01	−−	2.25e+01	−−	1.1530
	0.5000	484	3.00e-0	0.88	1.52e+01	0.36	8.34e-0	4.45	1.76e+01	1.78	0.9389
	0.5000	674	2.48e-0	1.15	1.14e+01	1.74	7.01e-0	1.05	1.36e+01	1.55	0.9263
	0.5000	1032	1.90e-0	1.26	1.01e+01	0.57	3.88e-0	2.78	1.09e+01	1.01	0.8639
	0.5000	1396	1.59e-0	1.16	7.51e-0	1.93	3.61e-0	0.48	8.49e-0	1.68	0.8574
	0.5000	2138	1.24e-0	1.16	6.15e-0	0.94	1.77e-0	3.36	6.52e-0	1.24	0.8077
	0.5000	3506	9.55e-1	1.07	4.61e-0	1.16	1.38e-0	1.00	4.91e-0	1.15	0.8192
	0.2500	6558	6.93e-1	1.02	3.39e-0	0.98	9.43e-1	1.21	3.59e-0	1.00	0.8037
	0.2500	10426	5.35e-1	1.12	2.66e-0	1.05	3.67e-1	4.07	2.74e-0	1.17	0.7843
0	0.1768	17278	4.15e-1	1.00	2.02e-0	1.10	2.26e-1	1.92	2.07e-0	1.10	0.7757
	0.1250	33354	2.98e-1	1.00	1.42e-0	1.07	1.05e-1	2.32	1.45e-0	1.08	0.7645
	0.0884	59296	2.23e-1	1.01	1.04e-0	1.08	5.83e-2	2.06	1.06e-0	1.08	0.7579
	0.0625	103338	1.70e-1	0.99	7.91e-1	0.97	3.36e-2	1.98	8.10e-1	0.98	0.7555
	0.0625	177166	1.28e-1	1.04	5.91e-1	1.08	1.86e-2	2.19	6.05e-1	1.08	0.7519
	0.0442	324068	9.58e-2	0.97	4.44e-1	0.95	1.08e-2	1.81	4.54e-1	0.95	0.7552
	0.0313	559566	7.24e-2	1.02	3.35e-1	1.03	6.35e-3	1.94	3.43e-1	1.03	0.7560
	0.0221	859962	5.86e-2	0.98	2.71e-1	0.99	3.58e-3	2.66	2.77e-1	0.99	0.7550
	0.0156	1582206	4.37e-2	0.97	2.01e-1	0.98	2.38e-3	1.35	2.06e-1	0.98	0.7524
	0.0156	2413766	3.50e-2	1.05	1.58e-1	1.13	1.29e-3	2.88	1.62e-1	1.13	0.7481
	0.0110	4324014	2.65e-2	0.95	1.22e-1	0.89	7.59e-4	1.83	1.25e-1	0.90	0.7568
	0.5000	1114	1.51e-0	−−	7.34e-0	−−	5.12e-0	−−	9.08e-0	−−	0.8729
	0.5000	1322	9.65e-1	5.21	7.01e-0	0.54	2.19e-0	9.94	7.40e-0	2.38	0.7937
	0.5000	2058	7.06e-1	1.41	3.90e-0	2.64	2.10e-0	0.19	4.49e-0	2.26	0.7891
	0.5000	2546	5.16e-1	2.95	3.61e-0	0.72	1.11e-0	6.02	3.81e-0	1.53	0.7893
	0.5000	4162	4.18e-1	0.86	1.67e-0	3.14	1.08e-0	0.09	2.03e-0	2.56	0.7705
1	0.5000	4626	1.91e-1	14.85	1.59e-0	0.94	1.68e-1	35.21	1.61e-0	4.41	0.7206
	0.5000	7098	1.35e-1	1.61	1.00e-0	2.16	1.66e-1	0.07	1.03e-0	2.11	0.7158
	0.5000	11198	8.37e-2	2.10	6.14e-1	2.15	1.15e-1	1.62	6.30e-1	2.14	0.7141
	0.3536	17566	5.41e-2	1.94	3.72e-1	2.22	6.04e-2	2.84	3.81e-1	2.24	0.6854
	0.2500	27334	3.47e-2	2.01	2.25e-1	2.27	2.55e-2	3.90	2.29e-1	2.29	0.6636
	0.2500	41090	2.17e-2	2.30	1.47e-1	2.10	1.59e-2	2.32	1.49e-1	2.11	0.6543
	0.1768	59146	1.42e-2	2.35	1.11e-1	1.56	7.09e-3	4.45	1.12e-1	1.59	0.7023
	0.5000	2246	7.37e-1	−−	3.52e-0	−−	2.42e-0	−−	4.33e-0	−−	0.6759
	0.5000	2552	4.95e-1	6.22	3.06e-0	2.18	1.15e-0	11.65	3.31e-0	4.23	0.6437
	0.5000	4106	4.51e-1	0.40	2.04e-0	1.70	1.16e-0	-0.03	2.39e-0	1.36	0.7652
	0.5000	4718	1.73e-1	13.76	1.15e-0	8.25	3.06e-1	19.15	1.20e-0	9.87	0.6242
2	0.5000	5936	1.73e-1	0.03	1.11e-0	0.32	3.13e-1	-0.20	1.17e-0	0.28	0.7404
	0.5000	8810	4.63e-2	6.66	3.49e-1	5.86	8.74e-2	6.46	3.63e-1	5.91	0.6054
	0.5000	9992	3.33e-2	5.23	3.36e-1	0.59	3.27e-2	15.63	3.40e-1	1.05	0.7023
	0.5000	15290	2.17e-2	2.02	1.55e-1	3.65	2.49e-2	1.29	1.58e-1	3.59	0.6374
	0.5000	20648	1.02e-2	5.03	8.33e-2	4.12	1.16e-2	5.05	8.48e-2	4.15	0.5758

Table 2.4: Example 2, adaptive scheme.

k	h	N	$\mathtt{e}(\mathbf{t})$	$\mathtt{r}(\mathbf{t})$	$\mathtt{e}(\boldsymbol{\sigma})$	$\mathtt{r}(\boldsymbol{\sigma})$	$\mathtt{e}(\boldsymbol{\xi})$	$\mathtt{r}(\boldsymbol{\xi})$	$\mathtt{e}(\mathbf{t},\boldsymbol{\sigma},\boldsymbol{\xi})$	$\mathtt{r}(\mathbf{t},\boldsymbol{\sigma},\boldsymbol{\xi})$	$\mathtt{eff}(\boldsymbol{\theta})$
0	0.3750	724	1.40e-0	−−	7.46e-0	−−	6.08e-0	−−	9.73e-0	−−	1.7390
	0.1875	2790	8.60e-1	0.70	4.68e-0	0.67	2.57e-0	1.24	5.41e-0	0.85	1.7570
	0.1250	6200	6.18e-1	0.82	3.43e-0	0.77	1.69e-0	1.04	3.87e-0	0.82	1.7718
	0.0938	10954	4.64e-1	1.00	2.73e-0	0.79	1.14e-0	1.34	3.00e-0	0.89	1.7505
	0.0750	17052	3.65e-1	1.07	2.27e-0	0.83	8.01e-1	1.60	2.44e-0	0.93	1.7282
	0.0625	24494	3.02e-1	1.05	1.94e-0	0.88	5.82e-1	1.75	2.04e-0	0.96	1.7154
	0.0536	33280	2.59e-1	1.00	1.68e-0	0.92	4.45e-1	1.75	1.76e-0	0.98	1.7116
	0.0469	43410	2.28e-1	0.96	1.48e-0	0.95	3.57e-1	1.64	1.54e-0	0.99	1.7126
	0.0417	54884	2.04e-1	0.94	1.32e-0	0.96	2.98e-1	1.53	1.37e-0	0.99	1.7146
	0.0375	67702	1.85e-1	0.94	1.19e-0	0.97	2.55e-1	1.48	1.23e-0	0.99	1.7150
	0.0188	269802	8.70e-2	1.09	6.05e-1	0.98	6.44e-2	1.99	6.14e-1	1.01	1.6799
	0.0094	1077202	4.12e-2	1.08	3.03e-1	1.00	1.34e-2	2.26	3.06e-1	1.00	1.7048
1	0.3750	2214	5.81e-1	−−	3.15e-0	−−	2.18e-0	−−	3.87e-0	−−	1.6991
	0.1875	8650	2.96e-1	0.97	1.56e-0	1.02	9.92e-1	1.14	1.87e-0	1.05	1.5416
	0.1250	19310	1.87e-1	1.12	9.19e-1	1.30	5.55e-1	1.43	1.09e-0	1.33	1.3667
	0.0938	34194	1.44e-1	0.91	5.84e-1	1.58	3.76e-1	1.35	7.09e-1	1.49	1.3268
	0.0750	53302	1.16e-1	0.97	3.93e-1	1.77	2.76e-1	1.39	4.95e-1	1.62	1.3085
	0.0625	76634	9.21e-2	1.27	2.82e-1	1.82	2.02e-1	1.72	3.59e-1	1.76	1.2165
	0.0536	104190	7.09e-2	1.70	2.13e-1	1.85	1.43e-1	2.22	2.66e-1	1.95	1.0810
	0.0469	135970	5.31e-2	2.16	1.66e-1	1.86	9.95e-2	2.73	2.00e-1	2.11	0.9717
	0.0417	171974	3.94e-2	2.54	1.33e-1	1.88	6.90e-2	3.11	1.55e-1	2.19	0.9067
2	0.3750	4472	3.23e-1	−−	1.69e-0	−−	1.17e-0	−−	2.08e-0	−−	1.1581
	0.1875	17582	1.74e-1	0.89	7.14e-1	1.25	5.10e-1	1.19	8.95e-1	1.22	1.0612
	0.1250	39332	1.31e-1	0.69	3.17e-1	2.01	3.24e-1	1.12	4.71e-1	1.58	1.1396
	0.0938	69722	9.33e-2	1.19	1.65e-1	2.27	2.05e-1	1.60	2.79e-1	1.83	0.9407
	0.0750	108752	6.23e-2	1.81	1.00e-1	2.22	1.22e-1	2.31	1.70e-1	2.22	0.7126
	0.0625	156422	4.04e-2	2.38	6.30e-2	2.55	7.23e-2	2.88	1.04e-1	2.69	0.5927

Table 2.5: Example 3, quasi-uniform scheme.

k	h	N	$\mathtt{e}(\mathbf{t})$	$\mathtt{r}(\mathbf{t})$	$\mathtt{e}(\boldsymbol{\sigma})$	$\mathtt{r}(\boldsymbol{\sigma})$	$\mathtt{e}(\boldsymbol{\xi})$	$\mathtt{r}(\boldsymbol{\xi})$	$\mathtt{e}(\mathbf{t},\boldsymbol{\sigma},\boldsymbol{\xi})$	$\mathtt{r}(\mathbf{t},\boldsymbol{\sigma},\boldsymbol{\xi})$	$\mathtt{eff}(\boldsymbol{\theta})$
	0.3750	724	1.40e-0	−−	7.46e-0	−−	6.08e-0	−−	9.73e-0	−−	1.7390
	0.3750	942	1.17e-0	1.37	6.65e-0	0.88	3.21e-0	4.86	7.47e-0	2.00	1.5176
	0.3750	1334	1.02e-0	0.81	4.91e-0	1.74	2.93e-0	0.51	5.81e-0	1.45	1.4362
	0.2500	2414	7.23e-1	1.15	4.09e-0	0.61	1.56e-0	2.13	4.44e-0	0.91	1.4099
	0.2500	3324	6.09e-1	1.08	3.01e-0	1.92	1.42e-0	0.59	3.38e-0	1.70	1.3028
	0.1875	4516	4.87e-1	1.46	2.49e-0	1.24	7.03e-1	4.58	2.63e-0	1.64	1.1800
	0.1875	6676	3.94e-1	1.09	2.02e-0	1.07	5.18e-1	1.56	2.12e-0	1.10	1.1806
	0.1250	11264	2.93e-1	1.12	1.58e-0	0.95	2.67e-1	2.53	1.62e-0	1.02	1.1825
0	0.1250	16740	2.47e-1	0.86	1.25e-0	1.17	1.73e-1	2.21	1.29e-0	1.18	1.1262
	0.1250	27176	1.86e-1	1.17	9.96e-1	0.93	9.37e-2	2.52	1.02e-0	0.96	1.1629
	0.0884	41338	1.51e-1	1.02	7.97e-1	1.06	6.74e-2	1.57	8.14e-1	1.07	1.1508
	0.0625	69714	1.18e-1	0.92	6.13e-1	1.01	3.47e-2	2.54	6.25e-1	1.01	1.1347
	0.0625	110000	9.18e-2	1.11	4.84e-1	1.04	2.19e-2	2.02	4.93e-1	1.04	1.1440
	0.0442	168592	7.39e-2	1.02	3.95e-1	0.95	1.60e-2	1.47	4.02e-1	0.96	1.1607
	0.0442	232804	6.39e-2	0.91	3.39e-1	0.95	9.24e-3	3.41	3.45e-1	0.95	1.1568
	0.0313	372780	5.00e-2	1.04	2.67e-1	1.02	6.48e-3	1.51	2.71e-1	1.02	1.1598
	0.0313	542152	4.14e-2	1.02	2.20e-1	1.02	4.46e-3	1.99	2.24e-1	1.02	1.1673
	0.3750	2214	5.81e-1	−−	3.15e-0	−−	2.18e-0	−−	3.87e-0	−−	1.6991
	0.3750	2518	3.58e-1	7.51	2.61e-0	2.89	1.02e-0	11.81	2.83e-0	4.89	1.4725
	0.3750	3150	3.09e-1	1.33	1.63e-0	4.21	1.03e-0	-0.10	1.95e-0	3.30	1.3267
	0.3750	3798	1.93e-1	5.02	1.23e-0	2.99	4.82e-1	8.13	1.34e-0	4.05	1.1749
1	0.3750	5090	1.69e-1	0.90	8.04e-1	2.91	4.84e-1	-0.03	9.54e-1	2.30	1.2067
	0.3750	5490	8.81e-2	17.27	6.98e-1	3.75	1.13e-1	38.54	7.12e-1	7.72	1.1211
	0.3750	7706	7.38e-2	1.05	3.88e-1	3.46	1.11e-1	0.10	4.10e-1	3.26	0.8694
	0.2500	10582	4.30e-2	3.41	3.31e-1	1.00	4.99e-2	5.03	3.37e-1	1.23	1.0209
	0.2500	18142	2.62e-2	1.83	1.56e-1	2.79	4.16e-2	0.67	1.64e-1	2.68	0.8562
	0.3750	4472	3.23e-1	−−	1.69e-0	−−	1.17e-0	−−	2.08e-0	−−	1.1581
	0.3750	4880	1.86e-1	12.70	1.19e-0	8.03	4.98e-1	19.48	1.31e-0	10.67	0.9807
	0.3750	6062	1.77e-1	0.45	8.94e-1	2.66	5.10e-1	-0.23	1.04e-0	2.06	1.0595
2	0.3750	6830	9.99e-2	9.56	6.44e-1	5.50	2.02e-1	15.57	6.82e-1	7.14	0.9906
	0.3750	9104	9.37e-2	0.44	2.37e-1	6.97	2.05e-1	-0.10	3.27e-1	5.13	0.8652
	0.3750	9512	2.38e-2	62.55	1.88e-1	10.41	3.21e-2	84.45	1.93e-1	24.09	0.7652
	0.3750	11786	2.21e-2	0.68	1.78e-1	0.54	3.27e-2	-0.17	1.82e-1	0.52	0.9934

Table 2.6: Example 3, adaptive scheme.

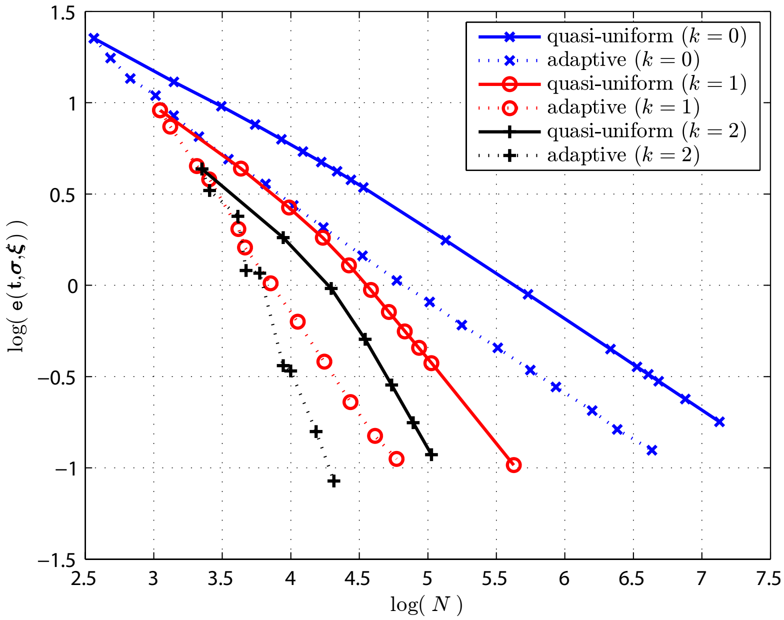

Figure 2.1: Example 3, $\mathsf{e}(\mathbf{t}, \boldsymbol{\sigma}, \boldsymbol{\xi})$ vs. N.

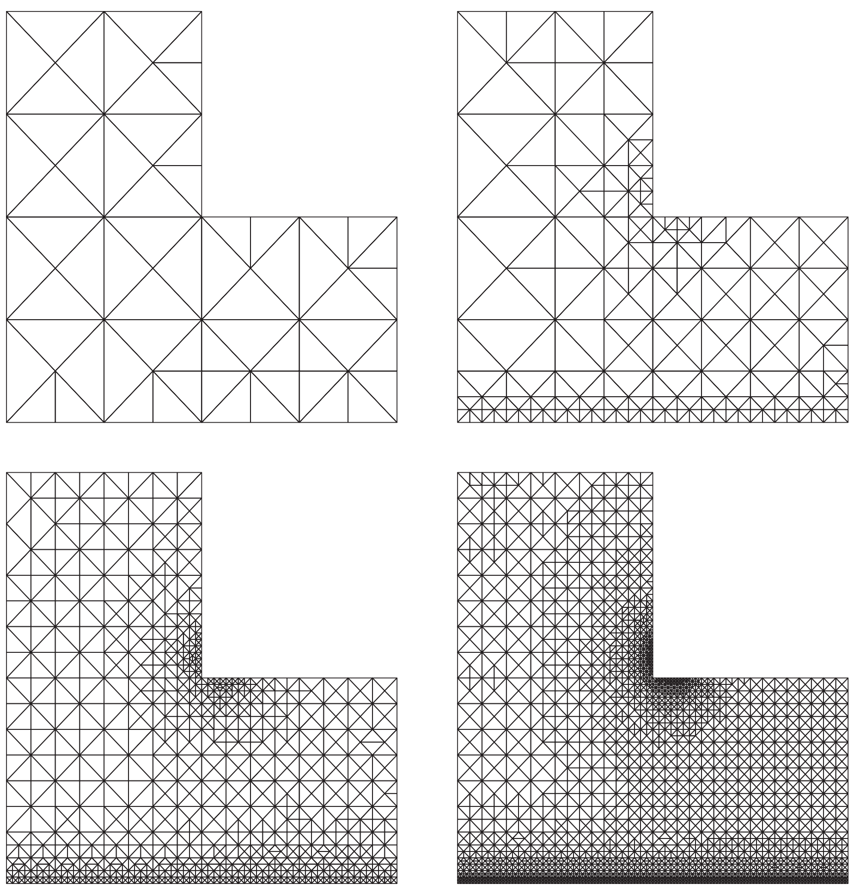

Figure 2.2: Example 3, adapted meshes for $k = 0$ with 484, 2138, 10426, and 33354 degrees of freedom.

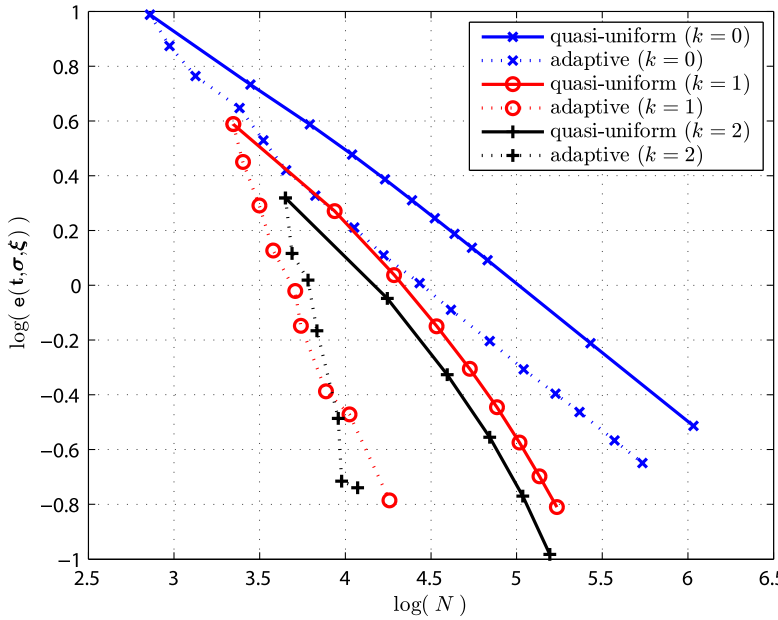

Figure 2.3: Example 4, $\mathsf{e}(\mathbf{t}, \boldsymbol{\sigma}, \boldsymbol{\xi})$ vs. N.

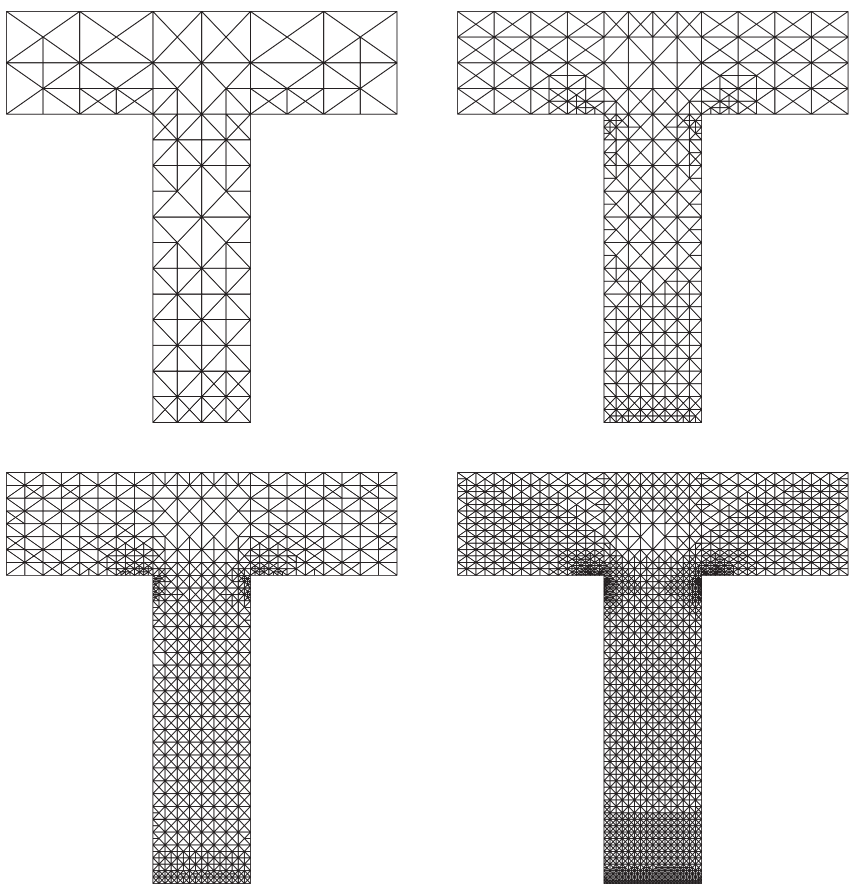

Figure 2.4: Example 4, adapted meshes for $k = 0$ with 1334, 4516, 11264, and 27176 degrees of freedom.

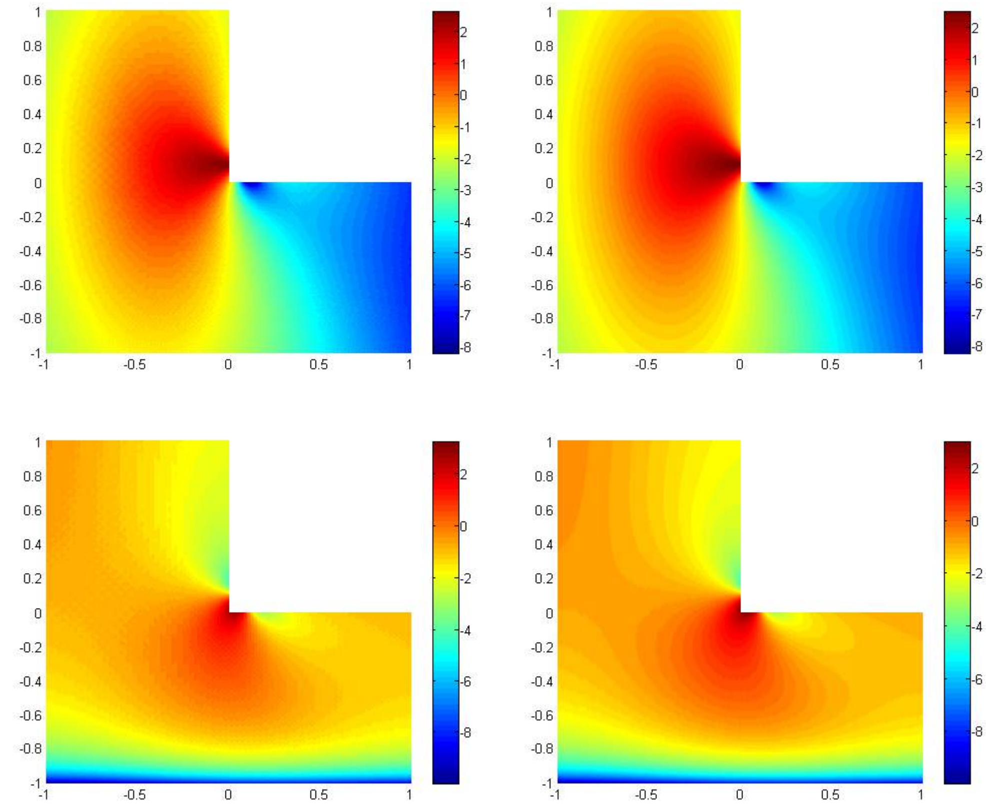

Figure 2.5: Example 3, approximate and exact σ_{21} and σ_{22} ($k = 0$ and $N = 177166$) for adaptive scheme.

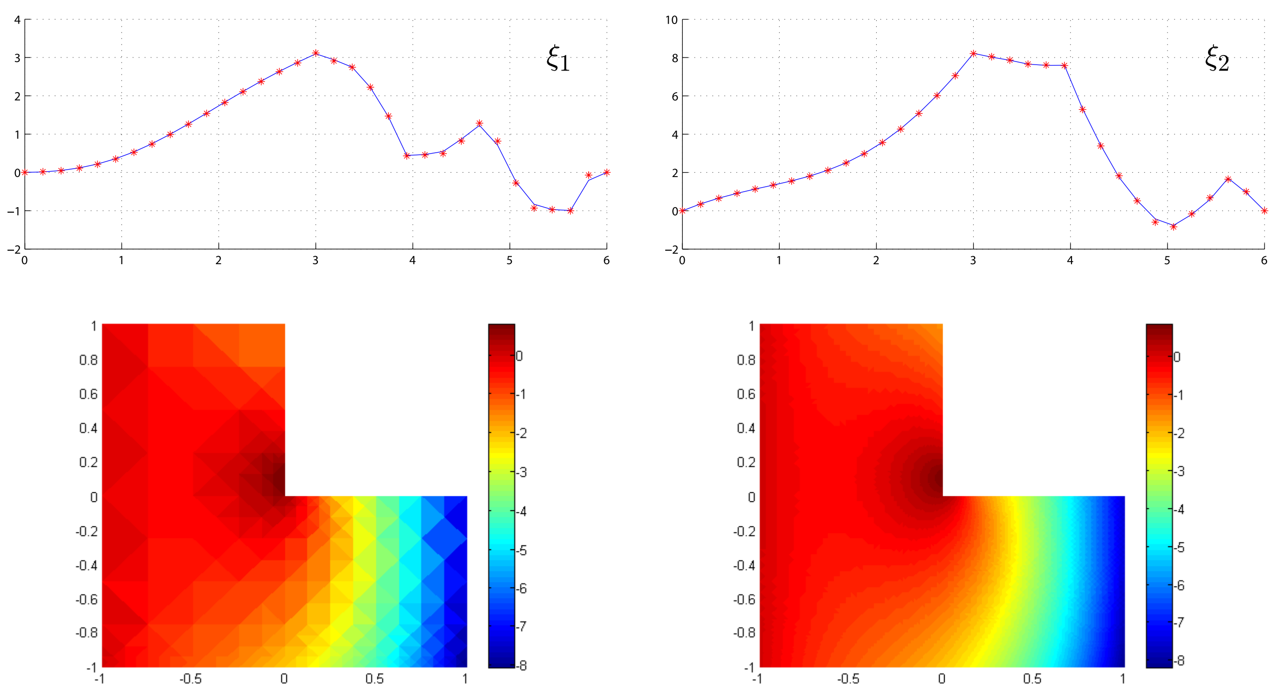

Figure 2.6: Example 3, approximate and exact $\boldsymbol{\xi}$ and u_2 ($k = 0$ and $N = 3506, 177166$) for adaptive scheme.

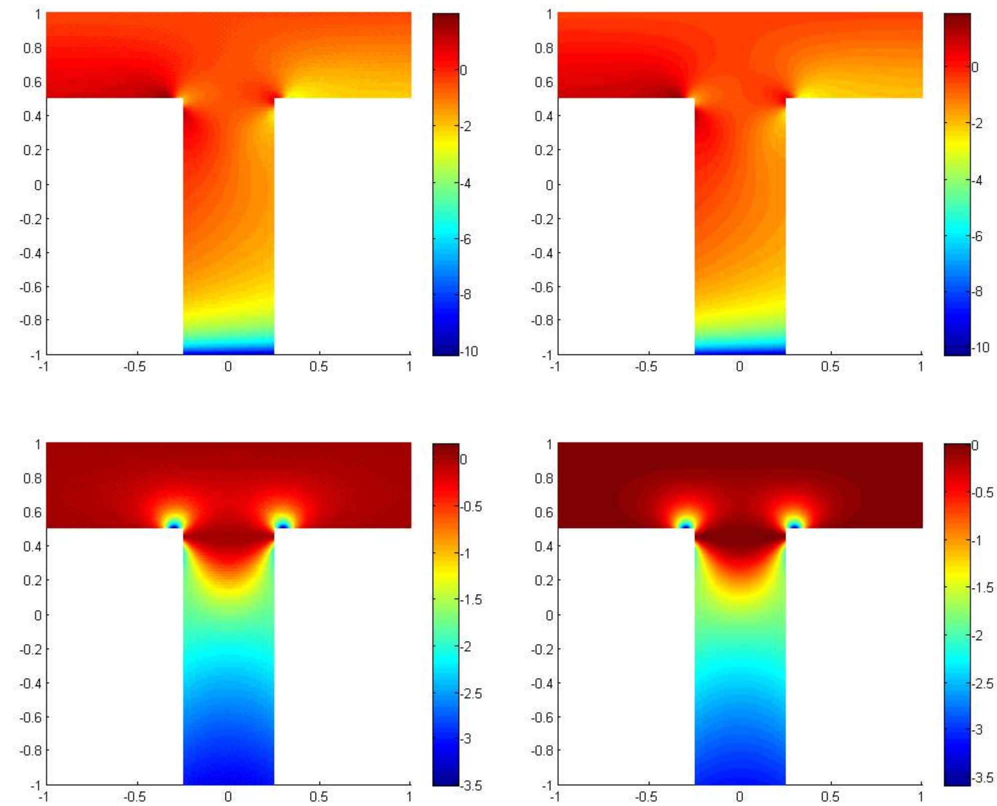

Figure 2.7: Example 4, approximate and exact σ_{11} and σ_{21} ($k = 0$ and $N = 168592$) for adaptive scheme.

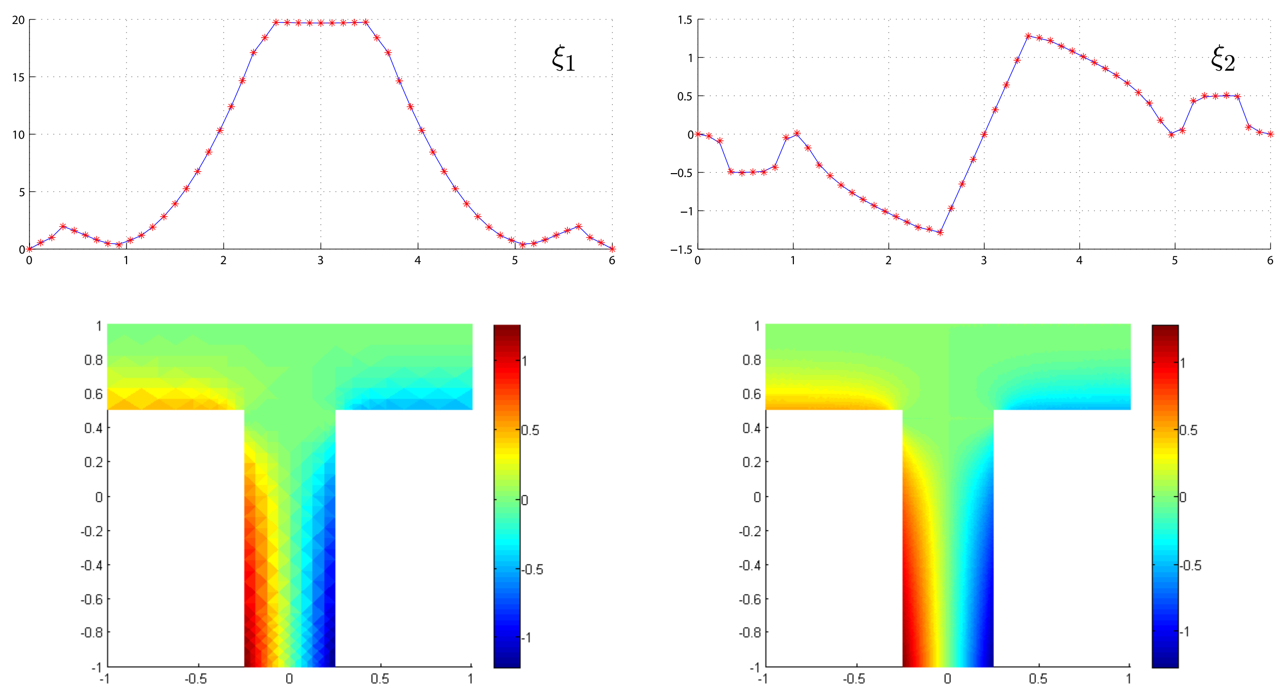

Figure 2.8: Example 4, approximate and exact $\boldsymbol{\xi}$ and u_2 ($k = 0$ and $N = 6676, 168592$) for adaptive scheme.

CHAPTER 3

Analysis of an augmented HDG method for a class of quasi-Newtonian Stokes flows

3.1 Introduction

The devising of suitable numerical methods for solving the linear and nonlinear Stokes and related problems has become a very active research area during the last decade. In particular, a mixed finite element method and a suitable augmented version of the latter for a nonlinear Stokes flow problem involving a non-Newtonian fluid, are introduced and analized in [84]. In addition, the velocity-pressure-stress formulation for incompressible flows has gained considerable attention in recent years due to its natural applicability to non-Newtonian flows, where the corresponding constitutive equations are nonlinear. In general, an interesting feature of the mixed methods is given by the fact that, besides the original unknowns, they yield direct approximations of several other quantities of physical interest. For instance, an accurate direct calculation of the stresses is very desirable for flow problems involving interaction with solid structures.

On the other hand, the hybridizable discontinuous Galerkin (HDG) method, introduced in [42] for diffusion problems, is one of the several high-order discretization schemes that benefit from the hybridization technique originally applied in [50] to the local discontinuous Galerkin (LDG) method for time dependent convection-diffusion problems. The main advantages of HDG methods include a substantial reduction of the globally coupled degrees of freedom, which was a criticism for the discontinuous Galerkin (DG) methods for elliptic problems during the last decade, and the fact that convergence is obtained even for a polynomial degree $k = 0$. Additionally, the approximate flux converges with order $k+1$ for $k \geq 0$, and an element-by-element computation of a new approximation of the scalar variable is possible, which converges with order $k+2$ for $k \geq 1$ (see e.g. [41, 45, 43]). In the context of the linear Stokes equation, the hybridization for DG methods was initially introduced in [31] and then analyzed in [112, 43]. Lately, an overview of the recent work by Cockburn and co-workers on the devising of hybridizable discontinuous Galerkin (HDG) methods for the Stokes equations of incompressible flow was provided in [49].

Now, the utilization of DG methods to numerically solve nonlinear boundary value problems has been first considered in [22] and [97]. Indeed, the application of the local discontinuous Galerkin (LDG) method to a class of nonlinear diffusion problems was developed in [22], whereas the extension of the interior penalty *hp* DG method to quasilinear elliptic equations was studied in [97]. The results from [22] were generalized in [23], where the *a priori* and *a posteriori* error analyses of the LDG method as applied to certain type of nonlinear Stokes models (whose kinematic viscosities are nonlinear monotone functions of the gradient of the velocity) were derived. The approach in [23] is based on the introduction of the flux and the tensor gradient of the velocity as further unknowns. A suitable Lagrange multiplier is also needed to ensure that the corresponding discrete variational formulation is well-posed. A two-fold saddle point operator equation is obtained as the resulting LDG mixed formulation, which is then reduced to a dual mixed formulation. A nonlinear version of the well known Babuška-Brezzi theory is applied to prove that the discrete formulation is well-posed and derive the corresponding *a priori* error analysis. In turn, the analysis from [97] was extended in [54], where the *a priori* and *a posteriori* error analysis, with respect to a mesh-dependent energy norm, of a class of interior penalty *hp* DGFEM for the numerical approximation of basically the same quasi-Newtonian fluid flow problems studied in [23], were provided. Furthermore, an HDG approach was employed in [111] for the numerical solution of steady and time-dependent nonlinear convection-diffusion equations. In fact, the approximate scalar variable and corresponding flux are first expressed in [111] in terms of an approximate trace of the scalar variable, and then the jump condition of the numerical fluxes are explicitly enforced across the element boundaries. As a consequence, a global equation system solely in terms of the approximate trace of the scalar variable is obtained at every Newton iteration. At the end, and similarly as in previous papers on HDG, an element-by-element postprocessing scheme is applied to obtain new approximations of the flux and the scalar variable, which converge with order $k+1$ and $k+2$, respectively, in the L^2-norm. Nevertheless, and up to our knowledge, there is still no contribution in the literature concerning HDG for nonlinear Stokes systems.

According to the above discussion, we are interested in this chapter in applying the HDG approach to the class of quasi-Newtonian Stokes flows studied in [23, 76, 54] (see also [84, 98]). To this end, we plan to employ the same velocity-pseudostress formulation from [84]. In what follows, given any Hilbert space U, $\mathbf{U} := U^n$ and $\mathbb{U} := U^{n\times n}$ denote, respectively, the space of vector and square matrices of order n, $n \in \{2,3\}$, with entries in U. In order to define the boundary value problem of interest, we now let Ω be a bounded and simply connected polygonal domain in R^n with boundary Γ. As in [84], our goal is to determine the velocity $\mathbf{u}$, the pseudostress tensor $\boldsymbol{\sigma}$, and the pressure p of a steady flow occupying the region Ω, under the action of external forces. More precisely, given a volume force $\mathbf{f} \in \mathbf{L}^2(\Omega)$ and $\mathbf{g} \in \mathbf{H}^{1/2}(\Gamma)$, we seek a tensor field $\boldsymbol{\sigma}$, a vector field $\mathbf{u}$, and a scalar field p such that

$$\begin{aligned} \boldsymbol{\sigma} \,=\, \mu(|\nabla\mathbf{u}|)\,\nabla\mathbf{u} - p\,\mathbb{I} \quad \text{in} \quad \Omega, \qquad & \mathbf{div}(\boldsymbol{\sigma}) \,=\, -\mathbf{f} \quad \text{in} \quad \Omega\,, \\ \operatorname{div}(\mathbf{u}) \,=\, 0 \quad \text{in} \quad \Omega\,, \qquad \mathbf{u} \,=\, \mathbf{g} \quad \text{on} \quad \Gamma\,, \qquad & \int_\Omega p \,=\, 0\,, \end{aligned} \tag{3.1}$$

where $\mu : \mathrm{R}^+ \to \mathrm{R}^+$ is the nonlinear kinematic velocity function of the fluids, $\mathbf{div}$ stands for the usual divergence operator div acting along each row of tensor, $\nabla\mathbf{u}$ is the tensor gradient of $\mathbf{u}$, $|\cdot|$ is the euclidean norm of $\mathrm{R}^{n\times n}$, and $\mathbb{I}$ is the identity matrix of $\mathrm{R}^{n\times n}$. As required by the incompressibility condition, we assume from now on that the datum $\mathbf{g}$ satisfies the compatibility condition $\int_\Gamma \mathbf{g}\cdot\boldsymbol{\nu} = 0$, where $\boldsymbol{\nu}$ stands for the unit outward normal at Γ. The kind of nonlinear Stokes problem given by (3.1) appears in the modeling of a large class of non-Newtonian fluids (see, e.g. [12, 104, 108, 117]). In particular, the Ladyzhenskaya law, is given by $\mu(t) := \mu_0 + \mu_1 t^{\beta-2}\ \forall\ t \in \mathrm{R}^+$, with $\mu_0 \geq 0$, $\mu_1 > 0$, and $\beta > 1$, and the Carreau law for viscoplastic flows (see, e.g. [108, 117]) reads $\mu(t) := \mu_0 + \mu_1(1+t^2)^{(\beta-2)/2}\ \forall\ t \in \mathrm{R}^+$, with $\mu_0 \geq 0$, $\mu_1 > 0$, and $\beta \geq 1$.

The rest of the work is organized as follows. In Section 3.2 we introduce the augmented hybridizable discontinuous Galerkin formulation involving the velocity, the pseudostress, the velocity gradient and the trace of the velocity, as unknowns. In Section 3.3 we show the unique solvability of the augmented

HDG scheme by considering an equivalent formulation and then applying a nonlinear version of the Babuška-Brezzi theory and the classical Banach fixed-point Theorem. The corresponding *a priori* error estimates are derived in Section 3.4. Next, in Section 3.5 we discuss some general aspects concerning the computational implementation of the HDG method. Finally, several numerical experiments validating the good performance of the method and confirming the rates of convergence derived are reported in Section 3.6. We end the present section with further notations to be used below. Given $\boldsymbol{\tau} := (\tau_{ij})$, $\boldsymbol{\zeta} := (\zeta_{ij}) \in \mathrm{R}^{n\times n}$, we write as usual

$$\mathrm{tr}\,(\boldsymbol{\tau}) \;:=\; \sum_{i=1}^{n} \tau_{ii}, \quad \boldsymbol{\tau}^{\mathrm{d}} \;:=\; \boldsymbol{\tau} - \frac{1}{n}\mathrm{tr}\,(\boldsymbol{\tau})\,\mathbb{I}, \quad \text{and} \quad \boldsymbol{\tau} : \boldsymbol{\zeta} \;:=\; \sum_{i,j=1}^{n} \tau_{ij}\zeta_{ij}.$$

Also, in what follows we utilize the standard terminology for Sobolev spaces and norms, employ $\mathbf{0}$ to denote a generic null vector, null tensor or null operator, and use C, with or without subscripts, bars, tildes or hats, to denote generic constants independent of the discretization parameters, which may take different values at different places.

3.2 The augmented HDG method

3.2.1 The hybridizable discontinuous Galerkin method

We begin by eliminating the pressure. Indeed, we know from [84, Section 2.1] that the pair given by the first and third equations in (3.1) is equivalent to

$$\boldsymbol{\sigma} \;=\; \mu(|\nabla \mathbf{u}|)\nabla \mathbf{u} - p\,\mathbb{I} \;\text{ in } \Omega \quad \text{and} \quad p \;=\; -\frac{1}{n}\,\mathrm{tr}\,(\boldsymbol{\sigma}) \;\text{ in } \Omega. \tag{3.2}$$

In what follows we let $\psi_{ij} : \mathrm{R}^{n\times n} \to \mathrm{R}$ be the mapping given by $\psi_{ij}(\mathbf{r}) := \mu(|\mathbf{r}|)r_{ij}$ for all $\mathbf{r} := (r_{ij}) \in \mathrm{R}^{n\times n}$, for all $i, j \in \{1, \ldots, n\}$. Then, throughout this chapter we assume that μ is of class C^1 and that there exist $\gamma_0, \alpha_0 > 0$ such that for all $\mathbf{r} := (r_{ij})$, $\mathbf{s} := (s_{ij}) \in \mathrm{R}^{n\times n}$, there holds

$$|\psi_{ij}(\mathbf{r})| \;\leq\; \gamma_0 \|\mathbf{r}\|_{\mathrm{R}^{n\times n}}, \qquad \left|\frac{\partial}{\partial r_{kl}}\psi_{ij}(\mathbf{r})\right| \;\leq\; \gamma_0, \quad \forall\, i, j, k, l \in \{1, \ldots, n\}, \tag{3.3}$$

and

$$\sum_{i,j,k,l=1}^{n} \frac{\partial}{\partial r_{kl}}\psi_{ij}(\mathbf{r}) s_{ij} s_{kl} \;\;\geq\;\; \alpha_0 \|\mathbf{s}\|^2_{\mathrm{R}^{n\times n}}. \tag{3.4}$$

It is easy to check that the Carreau law satisfies (3.3) and (3.4) for all $\mu_0 > 0$, and for all $\beta \in [1, 2]$. In particular, with $\beta = 2$ we recover the usual linear Stokes model. We observe in advance that the above assumptions are required to prove later on the strong monotonicity and Lipschitz-continuity properties of the continuous and discrete nonlinear operators involving the viscosity function μ (see Lemmas 3.4, 3.5 and 3.6 below).

Observe that we can rewrite (3.2) as

$$\boldsymbol{\sigma} \;=\; \boldsymbol{\psi}(\nabla \mathbf{u}) - p\,\mathbb{I} \;\text{ in } \Omega \quad \text{and} \quad p \;=\; -\frac{1}{n}\mathrm{tr}\,(\boldsymbol{\sigma}) \;\text{ in } \Omega,$$

where $\boldsymbol{\psi} : \mathrm{R}^{n\times n} \to \mathrm{R}^{n\times n}$ is given by $\boldsymbol{\psi}(\mathbf{r}) := (\psi_{ij}(\mathbf{r}))$ for all $\mathbf{r} := (r_{ij}) \in \mathrm{R}^{n\times n}$. Hence, replacing p by $-\frac{1}{n}\mathrm{tr}\,(\boldsymbol{\sigma})$ in the first equation of (3.1), and introducing the gradient $\mathbf{t} := \nabla\mathbf{u}$ in Ω as an auxiliary unknown, we arrive at the system

$$\begin{array}{rclcrcl} \boldsymbol{\psi}(\mathbf{t}) - \boldsymbol{\sigma}^{\mathrm{d}} = \mathbf{0} & \text{in} & \Omega\,, & \quad & \mathbf{t} - \nabla\mathbf{u} = \mathbf{0} & \text{in} & \Omega\,, \\ -\mathbf{div}(\boldsymbol{\sigma}) = \mathbf{f} & \text{in} & \Omega\,, & & \mathrm{tr}\,(\mathbf{t}) = 0 & \text{in} & \Omega\,, \\ \mathbf{u} = \mathbf{g} & \text{on} & \Gamma\,, & & \displaystyle\int_\Omega \mathrm{tr}\,(\boldsymbol{\sigma}) = 0\,. & & \end{array} \tag{3.5}$$

We recall here that a well-posed continuous formulation of (3.5) has been proposed in [84, Section 2], which reads: Find $(\mathbf{t},\boldsymbol{\sigma},\mathbf{u}) \in X_1 \times M_1 \times \mathbf{L}^2(\Omega)$ such that

$$\begin{aligned} \int_\Omega \boldsymbol{\psi}(\mathbf{t}) : \mathbf{s} - \int_\Omega \boldsymbol{\sigma}^{\mathrm{d}} : \mathbf{s} \quad &= \quad 0 \quad \forall\, \mathbf{s} \in X_1, \\ -\int_\Omega \mathbf{t} : \boldsymbol{\tau}^{\mathrm{d}} - \int_\Omega \mathbf{u}\cdot\mathbf{div}(\boldsymbol{\tau}) \quad &= \quad -\langle \boldsymbol{\tau\nu}, \mathbf{g}\rangle_\Gamma \quad \forall\, \boldsymbol{\tau} \in M_1, \\ -\int_\Omega \mathbf{v}\cdot\mathbf{div}(\boldsymbol{\sigma}) \quad &= \quad \int_\Omega \mathbf{f}\cdot\mathbf{v} \quad \forall\, \mathbf{v} \in \mathbf{L}^2(\Omega), \end{aligned} \tag{3.6}$$

where $X_1 := \{\mathbf{s} \in \mathbb{L}^2(\Omega) \;:\; \mathrm{tr}\,(\mathbf{s}) = 0\}$ and $M_1 = \left\{\boldsymbol{\tau} \in \mathbb{H}(\mathbf{div};\Omega) \;:\; \int_\Omega \mathrm{tr}\,(\boldsymbol{\tau}) = 0\right\}$. The purpose of reminding here (3.6) will become clear in the *a priori* error analysis given below in Section 3.4.

Next, in order to introduce the HDG method for the system (3.5), we first need some preliminary notations. Let $\mathcal{T}_h$ be a shape-regular triangulation of $\bar\Omega$ without the presence of hanging nodes, and let $\mathcal{E}_h$ be the set of faces F of $\mathcal{T}_h$. Then, we set

$$\partial\mathcal{T}_h \;:=\; \cup\{\partial T \;:\; T \in \mathcal{T}_h\}\,,$$

and introduce the inner products:

$$\begin{aligned} (\mathbf{u},\mathbf{v})_{\mathcal{T}_h} \quad &:= \quad \sum_{T\in\mathcal{T}_h} \int_T \mathbf{u}\cdot\mathbf{v} \quad \forall\, \mathbf{u},\mathbf{v} \in \mathbf{L}^2(\mathcal{T}_h), \\ (\boldsymbol{\sigma},\boldsymbol{\tau})_{\mathcal{T}_h} \quad &:= \quad \sum_{T\in\mathcal{T}_h} \int_T \boldsymbol{\sigma} : \boldsymbol{\tau} \quad \forall\, \boldsymbol{\sigma},\boldsymbol{\tau} \in \mathbb{L}^2(\mathcal{T}_h), \\ \langle \mathbf{u},\mathbf{v}\rangle_{\partial\mathcal{T}_h} \quad &:= \quad \sum_{T\in\mathcal{T}_h} \int_{\partial T} \mathbf{u}\cdot\mathbf{v} \quad \forall\, \mathbf{u},\mathbf{v} \in \mathbf{L}^2(\partial\mathcal{T}_h), \\ \langle \mathbf{u},\mathbf{v}\rangle_{\partial\mathcal{T}_h\backslash\Gamma} \quad &:= \quad \sum_{T\in\mathcal{T}_h} \sum_{F\in\partial T\backslash\Gamma} \int_F \mathbf{u}\cdot\mathbf{v} \quad \forall\, \mathbf{u},\mathbf{v} \in \mathbf{L}^2(\partial\mathcal{T}_h), \end{aligned}$$

with the induced norm

$$\|\mathbf{v}\|_{\mathcal{T}_h} \;:=\; (\mathbf{v},\mathbf{v})_{\mathcal{T}_h}^{1/2} \quad \forall\, \mathbf{v} \in \mathbf{L}^2(\mathcal{T}_h).$$

In addition, we let $\mathrm{P}_k(U)$ be the space of polynomials of total degree at most k defined on the domain U, and denote by $\mathcal{E}_h^i$ and $\mathcal{E}_h^\partial$ the set of interior and boundary faces, respectively, of $\mathcal{E}_h$.

On the other hand, let $\boldsymbol{\nu}^+$ and $\boldsymbol{\nu}^-$ be the outward unit normal vectors on the boundaries of two neighboring elements T^+ and T^-, respectively. We use $(\boldsymbol{\tau}^\pm,\mathbf{v}^\pm)$ to denote the traces of $(\boldsymbol{\tau},\mathbf{v})$ on $F := \partial T^+ \cap \partial T^-$ from the interior of $T^\pm$, where $\boldsymbol{\tau}$ and $\mathbf{v}$ are second-order tensorial and vectorial functions, respectively. Then, we define the means $\{\!\{\cdot\}\!\}$ and jumps $[\![\cdot]\!]$ for $F \in \mathcal{E}_h^i$, as follows

$$\begin{aligned} \{\!\{\boldsymbol{\tau}\}\!\} &:= \frac{1}{2}\left(\boldsymbol{\tau}^+ + \boldsymbol{\tau}^-\right), & \{\!\{\mathbf{v}\}\!\} &:= \frac{1}{2}\left(\mathbf{v}^+ + \mathbf{v}^-\right), \\ [\![\boldsymbol{\tau}]\!] &:= \boldsymbol{\tau}^+\boldsymbol{\nu}^+ + \boldsymbol{\tau}^-\boldsymbol{\nu}^-, & [\![\mathbf{v}]\!] &:= \mathbf{v}^+ \otimes \boldsymbol{\nu}^+ + \mathbf{v}^- \otimes \boldsymbol{\nu}^-, \end{aligned}$$

where $\otimes$ denotes the usual dyadic or tensor product. Next, given $k \geq 1$, the finite dimensional discontinuous subspaces are given by

$$\begin{aligned} S_h &:= \left\{\mathbf{s} \in \mathbb{L}^2(\Omega) \;:\; \mathbf{s}|_T \in \mathbb{P}_k(T) \quad \forall\, T \in \mathcal{T}_h\right\}, \\ \Sigma_h &:= \left\{\boldsymbol{\tau} \in \mathbb{L}^2(\Omega) \;:\; \boldsymbol{\tau}|_T \in \mathbb{P}_k(T) \quad \forall\, T \in \mathcal{T}_h, \quad \text{and} \quad \int_\Omega \operatorname{tr}(\boldsymbol{\tau}) = 0\right\}, \\ V_h &:= \left\{\mathbf{v} \in \mathbf{L}^2(\Omega) \;:\; \mathbf{v}|_T \in \mathbf{P}_{k-1}(T) \quad \forall\, T \in \mathcal{T}_h\right\}, \\ M_h &:= \left\{\boldsymbol{\mu} \in \mathbf{L}^2(\mathcal{E}_h^i) \;:\; \boldsymbol{\mu}|_F \in \mathbf{P}_k(F) \quad \forall\, F \in \mathcal{E}_h^i\right\}. \end{aligned}$$

At this point we remark in advance that the choice of the polynomial degree $k-1$ in the definition of V_h is justified by the need of satisfying later on a joint discrete inf-sup condition with the space Σ_h (see Lemma 3.7 below).

We now proceed similarly as in [43] to derive the HDG formulation of (3.5). In fact, testing the equations in (3.5) with elements in the foregoing subspaces, integrating by parts, and introducing the numerical fluxes $\widehat{\mathbf{u}}_h$ and $\widehat{\boldsymbol{\sigma}_h\boldsymbol{\nu}}$, we arrive at: Find $(\mathbf{t}_h, \boldsymbol{\sigma}_h, \mathbf{u}_h, \boldsymbol{\lambda}_h) \in S_h \times \Sigma_h \times V_h \times M_h$, such that

$$(\boldsymbol{\psi}(\mathbf{t}_h), \mathbf{s}_h)_{\mathcal{T}_h} - (\mathbf{s}_h, \boldsymbol{\sigma}_h^{\mathrm{d}})_{\mathcal{T}_h} = 0 \quad \forall\, \mathbf{s}_h \in S_h, \tag{3.7a}$$

$$(\mathbf{t}_h, \boldsymbol{\tau}_h^{\mathrm{d}})_{\mathcal{T}_h} + (\mathbf{u}_h, \mathbf{div}_h(\boldsymbol{\tau}_h))_{\mathcal{T}_h} - \langle \boldsymbol{\tau}_h\boldsymbol{\nu}, \widehat{\mathbf{u}}_h\rangle_{\partial\mathcal{T}_h} = 0 \quad \forall\, \boldsymbol{\tau}_h \in \Sigma_h, \tag{3.7b}$$

$$(\boldsymbol{\sigma}_h, \nabla_h \mathbf{v}_h)_{\mathcal{T}_h} - \langle \widehat{\boldsymbol{\sigma}_h\boldsymbol{\nu}}, \mathbf{v}_h\rangle_{\partial\mathcal{T}_h} = (\mathbf{f}, \mathbf{v}_h)_{\mathcal{T}_h} \quad \forall\, \mathbf{v}_h \in V_h, \tag{3.7c}$$

$$\langle \widehat{\boldsymbol{\sigma}_h\boldsymbol{\nu}}, \boldsymbol{\mu}_h\rangle_{\partial\mathcal{T}_h\setminus\Gamma} = 0 \quad \forall\, \boldsymbol{\mu}_h \in M_h, \tag{3.7d}$$

where, letting Π_Γ be the $\mathbf{L}^2(\Gamma)$ projection onto the space of piecewise polynomials of degree less than or equals to k on $\mathcal{E}_h^\partial$, we set

$$\widehat{\mathbf{u}}_h := \begin{cases} \Pi_\Gamma(\mathbf{g}) & \text{on } \mathcal{E}_h^\partial, \\ \boldsymbol{\lambda}_h & \text{on } \mathcal{E}_h^i, \end{cases} \qquad \text{and} \qquad \widehat{\boldsymbol{\sigma}_h\boldsymbol{\nu}} := \boldsymbol{\sigma}_h\boldsymbol{\nu} - \mathbf{S}(\mathbf{u}_h - \widehat{\mathbf{u}}_h) \;\text{ on } \partial\mathcal{T}_h, \tag{3.7e}$$

where $\mathbf{S}$ is a stabilization operator to be defined below. Note that the condition $\widehat{\mathbf{u}}_h = \Pi_\Gamma(\mathbf{g})$ on $\mathcal{E}_h^\partial$ is usually imposed in the equivalent way $\langle \widehat{\mathbf{u}}_h, \boldsymbol{\mu}_h\rangle_\Gamma = \langle \mathbf{g}, \boldsymbol{\mu}_h\rangle_\Gamma \;\forall\, \boldsymbol{\mu}_h \in \mathbf{P}_k(\mathcal{E}_h)$, which is employed to perform the solvability analysis of (3.7). In this sense, note first that problem (3.7) can be reformulated as

$$\begin{aligned} (\boldsymbol{\psi}(\mathbf{t}_h), \mathbf{s}_h)_{\mathcal{T}_h} - (\mathbf{s}_h, \boldsymbol{\sigma}_h^{\mathrm{d}})_{\mathcal{T}_h} &= 0, \\ (\mathbf{t}_h, \boldsymbol{\tau}_h^{\mathrm{d}})_{\mathcal{T}_h} + (\mathbf{u}_h, \mathbf{div}_h(\boldsymbol{\tau}_h))_{\mathcal{T}_h} - \langle \boldsymbol{\tau}_h\boldsymbol{\nu}, \boldsymbol{\lambda}_h\rangle_{\partial\mathcal{T}_h\setminus\Gamma} &= \langle \boldsymbol{\tau}_h\boldsymbol{\nu}, \mathbf{g}\rangle_\Gamma, \\ -(\mathbf{v}_h, \mathbf{div}_h(\boldsymbol{\sigma}_h))_{\mathcal{T}_h} + \langle \mathbf{S}(\mathbf{u}_h - \boldsymbol{\lambda}_h), \mathbf{v}_h\rangle_{\partial\mathcal{T}_h\setminus\Gamma} + \langle \mathbf{S}\mathbf{u}_h, \mathbf{v}_h\rangle_\Gamma &= (\mathbf{f}, \mathbf{v}_h)_{\mathcal{T}_h} + \langle \mathbf{S}\mathbf{g}, \mathbf{v}_h\rangle_\Gamma, \\ \langle \boldsymbol{\sigma}_h\boldsymbol{\nu}, \boldsymbol{\mu}_h\rangle_{\partial\mathcal{T}_h\setminus\Gamma} - \langle \mathbf{S}(\mathbf{u}_h - \boldsymbol{\lambda}_h), \boldsymbol{\mu}_h\rangle_{\partial\mathcal{T}_h\setminus\Gamma} &= 0, \end{aligned}$$

for all $(\mathbf{s}_h, \boldsymbol{\tau}_h, \mathbf{v}_h, \boldsymbol{\mu}_h) \in S_h \times \Sigma_h \times V_h \times M_h$, where (3.7c) has been rewritten using that

$$\begin{aligned}(\boldsymbol{\sigma}_h, \nabla_h \mathbf{v}_h)_{\mathcal{T}_h} &= \sum_{T\in\mathcal{T}_h} \int_T \boldsymbol{\sigma}_h : \nabla \mathbf{v}_h = \sum_{T\in\mathcal{T}_h} \left\{ -\int_T \mathbf{div}(\boldsymbol{\sigma}_h)\cdot \mathbf{v}_h + \int_{\partial T} \boldsymbol{\sigma}_h \boldsymbol{\nu}\cdot \mathbf{v}_h \right\},\\ &= -(\mathbf{v}_h, \mathbf{div}_h(\boldsymbol{\sigma}_h))_{\mathcal{T}_h} + \langle \boldsymbol{\sigma}_h \boldsymbol{\nu}, \mathbf{v}_h\rangle_{\partial\mathcal{T}_h}.\end{aligned}$$

We complete the definition of the HDG method by describing the stabilization tensor $\mathbf{S}$. In [43], general conditions for $\mathbf{S}$ were proposed, where in particular $\mathbf{S}^+$ does not necessarily match $\mathbf{S}^-$ for each $F \in \mathcal{E}_h^i$. Here, we consider the special case in which $\mathbf{S}^+ = \mathbf{S}^-$ in each $F \in \mathcal{E}_h^i$, that is, $\mathbf{S}$ has only one value on each $F \in \mathcal{E}_h$. More precisely, given $F \in \mathcal{E}_h$, the tensor $\mathbf{S}$ satisfies the following conditions:

$$\mathbf{S}|_F \text{ is constant, and } \mathbf{S}|_F \text{ is symmetric and positive definite.}$$

Observe that $\mathbf{S}^{-1}$ is well defined and symmetric and positive definite as well on each $F \in \mathcal{E}_h$. In (3.18) below, we select a particular choice for tensor $\mathbf{S}$ in order to establish the well-posedness of (3.8).

3.2.2 The augmented HDG formulation

In order to establish the unique solvability of the nonlinear problem (3.8), we now enrich the HDG formulation with two augmented equations arising from the constitutive and equilibrium equations, that is

$$\kappa_1(\boldsymbol{\sigma}_h^{\mathrm{d}} - \boldsymbol{\psi}(\mathbf{t}_h), \boldsymbol{\tau}_h^{\mathrm{d}})_{\mathcal{T}_h} = 0 \quad \forall\, \boldsymbol{\tau}_h \in \Sigma_h,$$

and

$$\kappa_2(\mathbf{div}_h(\boldsymbol{\sigma}_h), \mathbf{div}_h(\boldsymbol{\tau}_h))_{\mathcal{T}_h} = -\kappa_2(\mathbf{f}, \mathbf{div}_h(\boldsymbol{\tau}_h))_{\mathcal{T}_h} \quad \forall\, \boldsymbol{\tau}_h \in \Sigma_h,$$

where $\kappa_1, \kappa_2 > 0$ are parameters to be determined later on. In this way, our problem becomes: Find $(\mathbf{t}_h, \boldsymbol{\sigma}_h, \mathbf{u}_h, \boldsymbol{\lambda}_h) \in S_h \times \Sigma_h \times V_h \times M_h$ such that

$$(\boldsymbol{\psi}(\mathbf{t}_h), \mathbf{s}_h)_{\mathcal{T}_h} - (\mathbf{s}_h, \boldsymbol{\sigma}_h^{\mathrm{d}})_{\mathcal{T}_h} = 0, \tag{3.8a}$$

$$(\mathbf{t}_h, \boldsymbol{\tau}_h^{\mathrm{d}})_{\mathcal{T}_h} + (\mathbf{u}_h, \mathbf{div}_h(\boldsymbol{\tau}_h))_{\mathcal{T}_h} - \langle \boldsymbol{\tau}_h\boldsymbol{\nu}, \boldsymbol{\lambda}_h\rangle_{\partial\mathcal{T}_h\setminus\Gamma} = \langle \boldsymbol{\tau}_h\boldsymbol{\nu}, \mathbf{g}\rangle_{\Gamma}, \tag{3.8b}$$

$$-(\mathbf{v}_h, \mathbf{div}_h(\boldsymbol{\sigma}_h))_{\mathcal{T}_h} + \langle \mathbf{S}(\mathbf{u}_h - \boldsymbol{\lambda}_h), \mathbf{v}_h\rangle_{\partial\mathcal{T}_h\setminus\Gamma} + \langle \mathbf{S}\mathbf{u}_h, \mathbf{v}_h\rangle_{\Gamma} = (\mathbf{f}, \mathbf{v}_h)_{\mathcal{T}_h} + \langle \mathbf{S}\mathbf{g}, \mathbf{v}_h\rangle_{\Gamma}, \tag{3.8c}$$

$$\langle \boldsymbol{\sigma}_h\boldsymbol{\nu}, \boldsymbol{\mu}_h\rangle_{\partial\mathcal{T}_h\setminus\Gamma} - \langle \mathbf{S}(\mathbf{u}_h - \boldsymbol{\lambda}_h), \boldsymbol{\mu}_h\rangle_{\partial\mathcal{T}_h\setminus\Gamma} = 0, \tag{3.8d}$$

$$\kappa_1(\boldsymbol{\sigma}_h^{\mathrm{d}} - \boldsymbol{\psi}(\mathbf{t}_h), \boldsymbol{\tau}_h^{\mathrm{d}})_{\mathcal{T}_h} = 0, \tag{3.8e}$$

$$\kappa_2(\mathbf{div}_h(\boldsymbol{\sigma}_h), \mathbf{div}_h(\boldsymbol{\tau}_h))_{\mathcal{T}_h} = -\kappa_2(\mathbf{f}, \mathbf{div}_h(\boldsymbol{\tau}_h))_{\mathcal{T}_h}, \tag{3.8f}$$

for all $(\mathbf{s}_h, \boldsymbol{\tau}_h, \mathbf{v}_h, \boldsymbol{\mu}_h) \in S_h \times \Sigma_h \times V_h \times M_h$. Hence, in what follows we proceed as in [22, 23] and derive an equivalent formulation to (3.8) (see (3.10) below), for which we prove its unique solvability. In addition, the *a priori* error estimates for (3.8) will also be based on the analysis of (3.10). We emphasize, however, that the introduction of this equivalent formulation is just for theoretical purposes and by no means for the explicit computation of the solution of (3.8), which is solved directly as we explain below in Section 3.5.

First, we consider equation (3.8d) and note that

$$\begin{aligned}
0 &= \langle \boldsymbol{\sigma}_h \boldsymbol{\nu}, \boldsymbol{\mu}_h \rangle_{\partial\mathcal{T}_h\setminus\Gamma} - \langle \mathbf{S}\mathbf{u}_h, \boldsymbol{\mu}_h \rangle_{\partial\mathcal{T}_h\setminus\Gamma} + \langle \mathbf{S}\boldsymbol{\lambda}_h, \boldsymbol{\mu}_h \rangle_{\partial\mathcal{T}_h\setminus\Gamma} \\
&= \sum_{T\in\mathcal{T}_h} \sum_{F\in\partial T\setminus\Gamma} \int_F \boldsymbol{\sigma}_h \boldsymbol{\nu} \cdot \boldsymbol{\mu}_h - \sum_{T\in\mathcal{T}_h} \sum_{F\in\partial T\setminus\Gamma} \int_F \mathbf{S}\mathbf{u}_h \cdot \boldsymbol{\mu}_h + \sum_{T\in\mathcal{T}_h} \sum_{F\in\partial T\setminus\Gamma} \int_F \mathbf{S}\boldsymbol{\lambda}_h \cdot \boldsymbol{\mu}_h \\
&= \sum_{F\in\mathcal{E}_h^i} \int_F [\![\boldsymbol{\sigma}_h]\!] \cdot \boldsymbol{\mu}_h - 2 \sum_{F\in\mathcal{E}_h^i} \int_F \Big(\mathbf{S}\{\!\{\mathbf{u}_h\}\!\} \cdot \boldsymbol{\mu}_h - \mathbf{S}\boldsymbol{\lambda}_h \cdot \boldsymbol{\mu}_h \Big) \\
&= \int_{\mathcal{E}_h^i} \Big([\![\boldsymbol{\sigma}_h]\!] - 2\mathbf{S}\{\!\{\mathbf{u}_h\}\!\} + 2\mathbf{S}\boldsymbol{\lambda}_h \Big) \cdot \boldsymbol{\mu}_h \quad \forall\, \boldsymbol{\mu}_h \in M_h.
\end{aligned}$$

Hence, using that $[\![\boldsymbol{\sigma}_h]\!] - 2\mathbf{S}\{\!\{\mathbf{u}_h\}\!\} + 2\mathbf{S}\boldsymbol{\lambda}_h \in M_h$, we find that

$$[\![\boldsymbol{\sigma}_h]\!] - 2\,\mathbf{S}\{\!\{\mathbf{u}_h\}\!\} + 2\,\mathbf{S}\boldsymbol{\lambda}_h \;=\; \mathbf{0} \quad \text{on } \mathcal{E}_h^i,$$

which yields

$$\boldsymbol{\lambda}_h \;=\; \{\!\{\mathbf{u}_h\}\!\} - \frac{1}{2}\mathbf{S}^{-1}[\![\boldsymbol{\sigma}_h]\!] \quad \text{on } \mathcal{E}_h^i. \tag{3.9}$$

Observe that (3.9) coincides with the expression for $\widehat{\mathbf{u}}_h$ given in [43]. We now replace $\boldsymbol{\lambda}_h$ from (3.9) in (3.8b) and (3.8c). For this purpose, we first observe that

$$\begin{aligned}
-\langle \boldsymbol{\tau}_h \boldsymbol{\nu}, \boldsymbol{\lambda}_h \rangle_{\partial\mathcal{T}_h\setminus\Gamma} &= -\sum_{T\in\mathcal{T}_h} \sum_{F\in\partial T\setminus\Gamma} \boldsymbol{\tau}_h \boldsymbol{\nu} \cdot \boldsymbol{\lambda}_h \;=\; -\int_{\mathcal{E}_h^i} [\![\boldsymbol{\tau}_h]\!] \cdot \boldsymbol{\lambda}_h, \\
&= \frac{1}{2} \int_{\mathcal{E}_h^i} \mathbf{S}^{-1}[\![\boldsymbol{\sigma}_h]\!] \cdot [\![\boldsymbol{\tau}_h]\!] \;-\; \int_{\mathcal{E}_h^i} \{\!\{\mathbf{u}_h\}\!\} \cdot [\![\boldsymbol{\tau}_h]\!],
\end{aligned}$$

and

$$\begin{aligned}
-\langle \mathbf{S}\boldsymbol{\lambda}_h, \mathbf{v}_h \rangle_{\partial\mathcal{T}_h\setminus\Gamma} &= -\langle \mathbf{S}\mathbf{v}_h, \boldsymbol{\lambda}_h \rangle_{\partial\mathcal{T}_h\setminus\Gamma} \;=\; -\sum_{T\in\mathcal{T}_h} \sum_{F\in\partial T\setminus\Gamma} \mathbf{S}\mathbf{v}_h \cdot \boldsymbol{\lambda}_h, \\
&= -2 \int_{\mathcal{E}_h^i} \mathbf{S}\{\!\{\mathbf{v}_h\}\!\} \cdot \boldsymbol{\lambda}_h \;=\; \int_{\mathcal{E}_h^i} \{\!\{\mathbf{v}_h\}\!\} \cdot [\![\boldsymbol{\sigma}_h]\!] \;-\; 2 \int_{\mathcal{E}_h^i} \mathbf{S}\{\!\{\mathbf{u}_h\}\!\} \cdot \{\!\{\mathbf{v}_h\}\!\}.
\end{aligned}$$

In this way, the foregoing equations together with (3.8a), (3.8b), (3.8c), (3.8e) and (3.8f) lead to the problem: Find $((\mathbf{t}_h, \boldsymbol{\sigma}_h), \mathbf{u}_h) \in H_h \times V_h$ such that

$$\begin{aligned}
[\mathcal{A}_h(\mathbf{t}_h, \boldsymbol{\sigma}_h), (\mathbf{s}_h, \boldsymbol{\tau}_h)] \;+\; [\mathcal{B}_h(\mathbf{s}_h, \boldsymbol{\tau}_h), \mathbf{u}_h] &= [\mathcal{F}_h, (\mathbf{s}_h, \boldsymbol{\tau}_h)] \quad \forall\, (\mathbf{s}_h, \boldsymbol{\tau}_h) \in H_h, \\
[\mathcal{B}_h(\mathbf{t}_h, \boldsymbol{\sigma}_h), \mathbf{v}_h] \;-\; [\mathcal{S}_h(\mathbf{u}_h), \mathbf{v}_h] &= [\mathcal{G}_h, \mathbf{v}_h] \;+\; [\mathcal{C}_h(\mathbf{u}_h), \mathbf{v}_h] \quad \forall\, \mathbf{v}_h \in V_h,
\end{aligned} \tag{3.10}$$

where $H_h := S_h \times \Sigma_h$, and the operators $\mathcal{A}_h : H_h \to H_h'$, $\mathcal{B}_h : H_h \to V_h'$, $\mathcal{S}_h : V_h \to V_h'$ and $\mathcal{C}_h : V_h \to V_h'$, and the functionals $\mathcal{F}_h : H_h \to \mathrm{R}$ and $\mathcal{G}_h : V_h \to \mathrm{R}$, are defined by

$$\begin{aligned}
[\mathcal{A}_h(\mathbf{t}_h, \boldsymbol{\sigma}_h), (\mathbf{s}_h, \boldsymbol{\tau}_h)] \;:=\; & (\boldsymbol{\psi}(\mathbf{t}_h), \mathbf{s}_h)_{\mathcal{T}_h} - (\mathbf{s}_h, \boldsymbol{\sigma}_h^{\mathrm{d}})_{\mathcal{T}_h} \;+\; (\mathbf{t}_h, \boldsymbol{\tau}_h^{\mathrm{d}})_{\mathcal{T}_h} \;+\; \frac{1}{2} \int_{\mathcal{E}_h^i} \mathbf{S}^{-1}[\![\boldsymbol{\sigma}_h]\!] \cdot [\![\boldsymbol{\tau}_h]\!] \\
+ \quad & \kappa_1(\boldsymbol{\sigma}_h^{\mathrm{d}} - \boldsymbol{\psi}(\mathbf{t}_h), \boldsymbol{\tau}_h^{\mathrm{d}})_{\mathcal{T}_h} + \kappa_2(\mathbf{div}_h(\boldsymbol{\sigma}_h), \mathbf{div}_h(\boldsymbol{\tau}_h))_{\mathcal{T}_h}\,,
\end{aligned} \tag{3.11}$$

$$[\mathcal{B}_h(\mathbf{s}_h, \boldsymbol{\tau}_h), \mathbf{v}_h] \;:=\; (\mathbf{v}_h, \mathbf{div}_h(\boldsymbol{\tau}_h))_{\mathcal{T}_h} - \int_{\mathcal{E}_h^i} \{\!\{\mathbf{v}_h\}\!\} \cdot [\![\boldsymbol{\tau}_h]\!]\,, \tag{3.12}$$

$$[\mathcal{S}_h(\mathbf{u}_h), \mathbf{v}_h] \;:=\; \langle \mathbf{S}\mathbf{u}_h, \mathbf{v}_h \rangle_{\partial\mathcal{T}_h}\,, \tag{3.13}$$

$$[\mathcal{C}_h(\mathbf{u}_h), \mathbf{v}_h] := -2\int_{\mathcal{E}_h^i} \mathbf{S}\{\!\{\mathbf{u}_h\}\!\} \cdot \{\!\{\mathbf{v}_h\}\!\},$$

$$[\mathcal{F}_h, (\mathbf{s}_h, \boldsymbol{\tau}_h)] := \langle \boldsymbol{\tau}_h \boldsymbol{\nu}, \mathbf{g}\rangle_\Gamma - \kappa_2(\mathbf{f}, \mathbf{div}_h(\boldsymbol{\tau}_h))_{\mathcal{T}_h},$$

$$[\mathcal{G}_h, \mathbf{v}_h] := -(\mathbf{f}, \mathbf{v}_h)_{\mathcal{T}_h} - \langle \mathbf{S}\mathbf{g}, \mathbf{v}_h\rangle_\Gamma,$$

where $[\cdot,\cdot]$ stands in each case for the duality pairing induced by the corresponding operators and functionals. Note, for purposes that will become clear below, that the expression $[\mathcal{C}_h(\mathbf{u}_h), \mathbf{v}_h]$ has been placed on the right-hand side of the second equation in (3.10). In addition, while the above operators and functionals are defined on discrete spaces, it is not difficult to see that they can act on continuous spaces as well. For example, $\mathcal{A}_h$ can actually be defined on $(S_h + \mathbb{L}^2(\Omega)) \times (\Sigma_h + \mathbb{H}(\mathbf{div};\Omega))$ and similarly for the other ones. In particular, this fact will be employed at the beginning of Section 3.4.

3.3 Solvability analysis

In this section, we establish the unique solvability of the nonlinear problem (3.10). To this end, and following [22, 23], we let $\mathtt{h} \in L^\infty(\mathcal{E}_h)$ be the function related to the local meshsizes, that is

$$\mathtt{h}(x) := \begin{cases} \min\{h_{T_1}, h_{T_2}\} & \text{if } x \in \operatorname{int}(\partial T_1 \cap \partial T_2), \\ h_T & \text{if } x \in \operatorname{int}(\partial T \cap \Gamma), \end{cases}$$

and assume that the meshsize is bounded, that is, that there exists a constant $h_0 > 0$ such that

$$h := \max_{T\in\mathcal{T}_h}\{h_T\} \le h_0. \tag{3.14}$$

The main idea of our analysis consist of redefining (3.10) as a fixed point problem.

3.3.1 Preliminaries

The analysis below requires the following preliminary results.

Lemma 3.1 (Discrete trace's inequality)**.** *There exists $C_{\mathrm{tr}} > 0$, depending only on the shape regularity of the mesh, such that for each $T \in \mathcal{T}_h$ and $F \in \partial T$ there holds*

$$\|\mathbf{z}\|_{0,F}^2 \le C_{\mathrm{tr}}\left\{h_T^{-1}\|\mathbf{z}\|_{0,T}^2 + h_T|\mathbf{z}|_{1,T}^2\right\} \quad \forall\, \mathbf{z} \in \mathbf{H}^1(T). \tag{3.15}$$

Proof. The proof uses a trace theorem and a scaling argument (see [39] for details). □

Lemma 3.2. *There exists $c_0 > 0$, independent of h, such that for all $\mathbf{z} \in \mathbf{H}^1(\Omega)$ there holds*

$$\|\mathtt{h}^{1/2}\mathbf{z}\|_{0,\mathcal{E}_h^i} \le c_0\|\mathbf{z}\|_{1,\Omega}. \tag{3.16}$$

Proof. Given $\mathbf{z} \in \mathbf{H}^1(\Omega)$, we have

$$\|\mathtt{h}^{1/2}\mathbf{z}\|_{0,\mathcal{E}_h^i}^2 = \int_{\mathcal{E}_h^i} \mathtt{h}|\mathbf{z}|^2 = \frac{1}{2}\int_{\mathcal{E}_h^i} \mathtt{h}\left(|\mathbf{z}^+|^2 + |\mathbf{z}^-|^2\right) \le \frac{1}{2}\sum_{T\in\mathcal{T}_h}\int_{\partial T} \mathtt{h}|\mathbf{z}|^2 \le C\sum_{T\in\mathcal{T}_h} h_T\|\mathbf{z}\|_{0,\partial T}^2,$$

where C depends on the regularity of $\mathcal{T}_h$. Next, using (3.15) and (3.14), we deduce from the foregoing inequalities that

$$\|\mathrm{h}^{1/2}\mathbf{z}\|^2_{0,\mathcal{E}_h^i} \;\leq\; CC_{\mathrm{tr}}\sum_{T\in\mathcal{T}_h} h_T\left\{h_T^{-1}\|\mathbf{z}\|^2_{0,T}+h_T|\mathbf{z}|^2_{1,T}\right\} \;\leq\; CC_{\mathrm{tr}}(1+h^2)\sum_{T\in\mathcal{T}_h}\|\mathbf{z}\|^2_{1,T} \;\leq\; c_0^2\|\mathbf{z}\|^2_{1,\Omega},$$

with $c_0 := (CC_{\mathrm{tr}}(1+h_0^2))^{1/2}$, which completes the proof. □

Lemma 3.3. *There exists a constant $c_1 > 0$, independent of h, such that*

$$\|\boldsymbol{\tau}_h\|^2_{0,\Omega} \;\leq\; c_1\left\{\|\boldsymbol{\tau}_h^{\mathrm{d}}\|^2_{0,\Omega} \;+\; \|\mathbf{div}_h(\boldsymbol{\tau}_h)\|^2_{\mathcal{T}_h} \;+\; \|\mathrm{h}^{-1/2}[\![\boldsymbol{\tau}_h]\!]\|^2_{0,\mathcal{E}_h^i}\right\} \quad \forall\ \boldsymbol{\tau}_h\in\Sigma_h.$$

Proof. We follow similarly as in the proof of [19, Proposition 3.1, Chapter IV]. Indeed, given $\boldsymbol{\tau}_h\in\Sigma_h$, we know from [92, Corollary 2.4 in Chapter I] that there is a unique $\mathbf{z}\in\mathbf{H}_0^1(\Omega)$ such that $\mathrm{div}(\mathbf{z}) = \mathrm{tr}\,(\boldsymbol{\tau}_h)$ and

$$\|\mathbf{z}\|_{1,\Omega} \;\;\leq\;\; C\|\mathrm{tr}\,(\boldsymbol{\tau}_h)\,\|_{0,\Omega}. \tag{3.17}$$

Now, utilizing that $\mathbf{z}\in\mathbf{H}_0^1(\Omega)$, we have that

$$\begin{aligned}
\|\mathrm{tr}\,(\boldsymbol{\tau}_h)\,\|^2_{0,\Omega} \;&=\; \int_\Omega \mathrm{tr}\,(\boldsymbol{\tau}_h)\,\mathrm{div}(\mathbf{z}) \;=\; \int_\Omega \boldsymbol{\tau}_h : \{\mathrm{tr}\,(\nabla\mathbf{z})\,\mathbb{I}\}\,,\\
&=\; n\int_\Omega \boldsymbol{\tau}_h : (\nabla\mathbf{z}-(\nabla\mathbf{z})^{\mathrm{d}}) \;=\; n\int_\Omega \boldsymbol{\tau}_h:\nabla\mathbf{z} - n\int_\Omega \boldsymbol{\tau}_h^{\mathrm{d}}:\nabla\mathbf{z},\\
&=\; n\sum_{T\in\mathcal{T}_h}\left\{-\int_T \mathbf{z}\cdot\mathbf{div}(\boldsymbol{\tau}_h)+\int_{\partial T}\boldsymbol{\tau}_h\boldsymbol{\nu}\cdot\mathbf{z}\right\} - n\int_\Omega \boldsymbol{\tau}_h^{\mathrm{d}}:\nabla\mathbf{z},\\
&=\; -n(\mathbf{z},\mathbf{div}_h(\boldsymbol{\tau}_h))_{\mathcal{T}_h} + n\int_{\mathcal{E}_h^i}[\![\boldsymbol{\tau}_h]\!]\cdot\mathbf{z} - n\int_\Omega \boldsymbol{\tau}_h^{\mathrm{d}}:\nabla\mathbf{z}.
\end{aligned}$$

Next, applying Cauchy-Schwarz inequality, and then (3.16) and (3.17), we find that

$$\begin{aligned}
\|\mathrm{tr}\,(\boldsymbol{\tau}_h)\,\|^2_{0,\Omega} \;&\leq\; n\|\mathbf{z}\|_{0,\Omega}\|\mathbf{div}_h(\boldsymbol{\tau}_h)\|_{\mathcal{T}_h} + n\|\mathrm{h}^{-1/2}[\![\boldsymbol{\tau}_h]\!]\|_{0,\mathcal{E}_h^i}\|\mathrm{h}^{1/2}\mathbf{z}\|_{0,\mathcal{E}_h^i} + n\|\boldsymbol{\tau}_h^{\mathrm{d}}\|_{0,\Omega}|\mathbf{z}|_{1,\Omega}\\
&\leq\; n\|\mathbf{z}\|_{0,\Omega}\|\mathbf{div}_h(\boldsymbol{\tau}_h)\|_{\mathcal{T}_h} + nc_0\|\mathrm{h}^{-1/2}[\![\boldsymbol{\tau}_h]\!]\|_{0,\mathcal{E}_h^i}\|\mathbf{z}\|_{1,\Omega} + n\|\boldsymbol{\tau}_h^{\mathrm{d}}\|_{0,\Omega}|\mathbf{z}|_{1,\Omega}\\
&\leq\; C\|\mathbf{z}\|_{1,\Omega}\left\{\|\boldsymbol{\tau}_h^{\mathrm{d}}\|^2_{0,\Omega}+\|\mathbf{div}_h(\boldsymbol{\tau}_h)\|^2_{\mathcal{T}_h}+\|\mathrm{h}^{-1/2}[\![\boldsymbol{\tau}_h]\!]\|^2_{0,\mathcal{E}_h^i}\right\}^{1/2}\\
&\leq\; C\|\mathrm{tr}\,(\boldsymbol{\tau}_h)\,\|_{0,\Omega}\left\{\|\boldsymbol{\tau}_h^{\mathrm{d}}\|^2_{0,\Omega}+\|\mathbf{div}_h(\boldsymbol{\tau}_h)\|^2_{\mathcal{T}_h}+\|\mathrm{h}^{-1/2}[\![\boldsymbol{\tau}_h]\!]\|^2_{0,\mathcal{E}_h^i}\right\}^{1/2},
\end{aligned}$$

which gives

$$\|\mathrm{tr}\,(\boldsymbol{\tau}_h)\,\|^2_{0,\Omega} \;\;\leq\;\; C\left\{\|\boldsymbol{\tau}_h^{\mathrm{d}}\|^2_{0,\Omega}+\|\mathbf{div}_h(\boldsymbol{\tau}_h)\|^2_{\mathcal{T}_h}+\|\mathrm{h}^{-1/2}[\![\boldsymbol{\tau}_h]\!]\|^2_{0,\mathcal{E}_h^i}\right\}.$$

This inequality and the fact that $\|\boldsymbol{\tau}_h\|^2_{0,\Omega} = \|\boldsymbol{\tau}_h^{\mathrm{d}}\|^2_{0,\Omega}+\frac{1}{n}\|\mathrm{tr}\,(\boldsymbol{\tau}_h)\,\|^2_{0,\Omega}$, complete the proof. □

We now realize, thanks to the previous lemma, that for convenience of further analysis, we need to establish a particular choice of the stabilization tensor $\mathbf{S}$. For this purpose, we let $\tau > 0$ be a constant and set the tensor $\mathbf{S}$ as follows

$$\mathbf{S}|_F \;\;:=\;\; \tau\,\mathrm{h}\,\mathbb{I} \quad \forall\ F\in\mathcal{E}_h, \tag{3.18}$$

which certainly yields

$$\mathbf{S}^{-1}|_F \;:=\; (\tau\mathtt{h})^{-1}\mathbb{I} \quad \forall\, F \in \mathcal{E}_h. \tag{3.19}$$

The parameter τ introduced here will play a key role later on for proving that the fixed point operator derived from our solvability analysis is in fact a contraction (see Lemma 3.12 below). In addition, we consider the following definition of a norm onto Σ_h

$$\|\boldsymbol{\tau}_h\|^2_{\Sigma_h} \;:=\; \|\boldsymbol{\tau}_h^{\mathrm{d}}\|^2_{0,\Omega} \;+\; \|\mathbf{div}_h(\boldsymbol{\tau}_h)\|^2_{\mathcal{T}_h} \;+\; \|(\tau\mathtt{h})^{-1/2}[\![\boldsymbol{\tau}_h]\!]\|^2_{0,\mathcal{E}_h^i} \quad \forall\, \boldsymbol{\tau}_h \in \Sigma_h$$

which, according to Lemma 3.3, satisfies

$$\|\boldsymbol{\tau}_h\|_{0,\Omega} \;\leq\; c_2\|\boldsymbol{\tau}_h\|_{\Sigma_h} \quad \forall\, \boldsymbol{\tau}_h \in \Sigma_h, \tag{3.20}$$

where $c_2^2 := c_1 \max\{1,\tau\} > 0$ is independent of h. Note that the above suggests the following norm on $H_h := S_h \times \Sigma_h$

$$\|(\mathbf{s}_h,\boldsymbol{\tau}_h)\|_{H_h} \;:=\; \left\{\|\mathbf{s}_h\|^2_{0,\Omega} \;+\; \|\boldsymbol{\tau}_h\|^2_{\Sigma_h}\right\}^{1/2} \quad \forall\, (\mathbf{s}_h,\boldsymbol{\tau}_h) \in H_h.$$

On the other hand, we define the nonlinear operator $\mathbb{A} : S_h \to S_h'$ by

$$[\mathbb{A}(\mathbf{t}_h),\mathbf{s}_h] \;:=\; (\boldsymbol{\psi}(\mathbf{t}_h),\mathbf{s}_h)_{\mathcal{T}_h} \quad \forall\, \mathbf{t}_h,\mathbf{s}_h \in S_h.$$

Then, we have the following result.

Lemma 3.4. *Let γ_0 and α_0 be the constants from* (3.3) *and* (3.4)*, respectively. Then, for all $\mathbf{t}_h,\mathbf{s}_h \in S_h$ there hold*

$$\|\mathbb{A}(\mathbf{t}_h) - \mathbb{A}(\mathbf{s}_h)\|_{S_h'} \;\leq\; \gamma_0\|\mathbf{t}_h - \mathbf{s}_h\|_{0,\Omega} \tag{3.21}$$

and

$$[\mathbb{A}(\mathbf{t}_h) - \mathbb{A}(\mathbf{s}_h),\mathbf{t}_h - \mathbf{s}_h] \;\geq\; \alpha_0\|\mathbf{t}_h - \mathbf{s}_h\|^2_{0,\Omega}. \tag{3.22}$$

Proof. See [84, Lemma 2.1] or [23, Section 3]. □

We are now ready to establish that the nonlinear operator $\mathcal{A}_h$ defining the problem (3.10) is also Lipschitz-continuous and strongly monotone. In particular, the second property will depend on a suitable choice of the parameter κ_1.

Lemma 3.5. *Let $\mathcal{A}_h$ be the nonlinear operator defined by* (3.11)*. Then, there exists a constant $C_{\mathrm{LC}} > 0$, independent of h and τ, such that*

$$\|\mathcal{A}_h(\mathbf{t}_h,\boldsymbol{\sigma}_h) - \mathcal{A}_h(\mathbf{s}_h,\boldsymbol{\tau}_h)\|_{H_h'} \;\leq\; C_{\mathrm{LC}}\,\|(\mathbf{t}_h,\boldsymbol{\sigma}_h) - (\mathbf{s}_h,\boldsymbol{\tau}_h)\|_{H_h} \quad \forall\, (\mathbf{t}_h,\boldsymbol{\sigma}_h),(\mathbf{s}_h,\boldsymbol{\tau}_h) \in H_h.$$

Proof. Given $(\mathbf{t}_h,\boldsymbol{\sigma}_h),(\mathbf{s}_h,\boldsymbol{\tau}_h)$ and $(\mathbf{r}_h,\boldsymbol{\rho}_h) \in H_h$, we obtain from the definition of $\mathbb{A}$ and (3.19) that

$$\begin{aligned}
[\mathcal{A}_h(\mathbf{t}_h,\boldsymbol{\sigma}_h) - \mathcal{A}_h(\mathbf{s}_h,\boldsymbol{\tau}_h),(\mathbf{r}_h,\boldsymbol{\rho}_h)] \;&=\; [\mathbb{A}(\mathbf{t}_h) - \mathbb{A}(\mathbf{s}_h),\mathbf{r}_h] - \kappa_1[\mathbb{A}(\mathbf{t}_h) - \mathbb{A}(\mathbf{s}_h),\boldsymbol{\rho}_h^{\mathrm{d}}] \\
&- (\mathbf{r}_h,(\boldsymbol{\sigma}_h - \boldsymbol{\tau}_h)^{\mathrm{d}})_{\mathcal{T}_h} + (\mathbf{t}_h - \mathbf{s}_h,\boldsymbol{\rho}_h^{\mathrm{d}})_{\mathcal{T}_h} + \frac{1}{2}\sum_{F\in\mathcal{E}_h^i}\int_F (\tau\mathtt{h})^{-1/2}[\![(\boldsymbol{\sigma}_h - \boldsymbol{\tau}_h)]\!]\cdot(\tau\mathtt{h})^{-1/2}[\![\boldsymbol{\rho}_h]\!] \\
&+ \kappa_1((\boldsymbol{\sigma}_h - \boldsymbol{\tau}_h)^{\mathrm{d}},\boldsymbol{\rho}_h^{\mathrm{d}})_{\mathcal{T}_h} + \kappa_2(\mathbf{div}_h(\boldsymbol{\sigma}_h - \boldsymbol{\tau}_h),\mathbf{div}_h(\boldsymbol{\rho}_h))_{\mathcal{T}_h},
\end{aligned} \tag{3.23}$$

from which, applying Cauchy-Schwarz inequality and (3.21), it follows that

$$
\begin{aligned}
[\mathcal{A}(\mathbf{t}_h,\boldsymbol{\sigma}_h) - \mathcal{A}(\mathbf{s}_h,\boldsymbol{\tau}_h),(\mathbf{r}_h,\boldsymbol{\rho}_h)] \;&\le\; \|\mathbb{A}(\mathbf{t}_h) - \mathbb{A}(\mathbf{s}_h)\|_{S'_h}\|\mathbf{r}_h\|_{0,\Omega} + \kappa_1\|\mathbb{A}(\mathbf{t}_h) - \mathbb{A}(\mathbf{s}_h)\|_{S'_h}\,\|\boldsymbol{\rho}_h^{\mathrm{d}}\|_{0,\Omega}\\
&+ \|\mathbf{r}_h\|_{0,\Omega}\,\|(\boldsymbol{\sigma}_h-\boldsymbol{\tau}_h)^{\mathrm{d}}\|_{0,\Omega} + \|\mathbf{t}_h-\mathbf{s}_h\|_{0,\Omega}\,\|\boldsymbol{\rho}_h^{\mathrm{d}}\|_{0,\Omega}\\
&+ \frac{1}{2}\|(\tau\mathtt{h})^{-1/2}[\![(\boldsymbol{\sigma}_h-\boldsymbol{\tau}_h)]\!]\|_{0,\mathcal{E}_h^i}\,\|(\tau\mathtt{h})^{-1/2}[\![\boldsymbol{\rho}_h]\!]\|_{0,\mathcal{E}_h^i} + \kappa_1\|(\boldsymbol{\sigma}_h-\boldsymbol{\tau}_h)^{\mathrm{d}}\|_{0,\Omega}\,\|\boldsymbol{\rho}_h^{\mathrm{d}}\|_{0,\Omega}\\
&+ \kappa_2\|\mathbf{div}_h(\boldsymbol{\sigma}_h-\boldsymbol{\tau}_h)\|_{\mathcal{T}_h}\,\|\mathbf{div}_h(\boldsymbol{\rho}_h)\|_{\mathcal{T}_h},\\
&\le\; \gamma_0\|\mathbf{t}_h-\mathbf{s}_h\|_{0,\Omega}\,\|\mathbf{r}_h\|_{0,\Omega} + \gamma_0\kappa_1\|\mathbf{t}_h-\mathbf{s}_h\|_{0,\Omega}\,\|\boldsymbol{\rho}_h^{\mathrm{d}}\|_{0,\Omega}\\
&+ \|\mathbf{r}_h\|_{0,\Omega}\,\|(\boldsymbol{\sigma}_h-\boldsymbol{\tau}_h)^{\mathrm{d}}\|_{0,\Omega} + \|\mathbf{t}_h-\mathbf{s}_h\|_{0,\Omega}\,\|\boldsymbol{\rho}_h^{\mathrm{d}}\|_{0,\Omega}\\
&+ \frac{1}{2}\|(\tau\mathtt{h})^{-1/2}[\![(\boldsymbol{\sigma}_h-\boldsymbol{\tau}_h)]\!]\|_{0,\mathcal{E}_h^i}\,\|(\tau\mathtt{h})^{-1/2}[\![\boldsymbol{\rho}_h]\!]\|_{0,\mathcal{E}_h^i} + \kappa_1\|(\boldsymbol{\sigma}_h-\boldsymbol{\tau}_h)^{\mathrm{d}}\|_{0,\Omega}\,\|\boldsymbol{\rho}_h^{\mathrm{d}}\|_{0,\Omega}\\
&+ \kappa_2\|\mathbf{div}_h(\boldsymbol{\sigma}_h-\boldsymbol{\tau}_h)\|_{\mathcal{T}_h}\,\|\mathbf{div}_h(\boldsymbol{\rho}_h)\|_{\mathcal{T}_h}.
\end{aligned}
$$

In this way, setting

$$C_{\mathrm{LC}} \;:=\; 3\,\max\{1,\gamma_0,\kappa_1,\gamma_0\kappa_1,\kappa_2\}\,,$$

we conclude that

$$[\mathcal{A}(\mathbf{t}_h,\boldsymbol{\sigma}_h) - \mathcal{A}(\mathbf{s}_h,\boldsymbol{\tau}_h),(\mathbf{r}_h,\boldsymbol{\rho}_h)] \;\le\; C_{\mathrm{LC}}\,\|(\mathbf{t}_h,\boldsymbol{\sigma}_h)-(\mathbf{s}_h,\boldsymbol{\tau}_h)\|_{H_h}\,\|(\mathbf{r}_h,\boldsymbol{\rho}_h)\|_{H_h},$$

which ends the proof. □

Lemma 3.6. *Let $\mathcal{A}_h$ be the nonlinear operator defined by* (3.11)*, and assume that the parameter κ_1 lies in $\left(0,\frac{2\alpha_0}{\gamma_0^2}\right)$, where α_0 and γ_0 are the positive constants from* (3.3) *and* (3.4)*. Then, there exists a constant $C_{\mathrm{SM}}>0$, independent of h and τ, such that*

$$[\mathcal{A}_h(\mathbf{t}_h,\boldsymbol{\sigma}_h) - \mathcal{A}_h(\mathbf{s}_h,\boldsymbol{\tau}_h),(\mathbf{t}_h,\boldsymbol{\sigma}_h)-(\mathbf{s}_h,\boldsymbol{\tau}_h)] \;\ge\; C_{\mathrm{SM}}\,\|(\mathbf{t}_h,\boldsymbol{\sigma}_h)-(\mathbf{s}_h,\boldsymbol{\tau}_h)\|_{H_h}^2,$$

for all $(\mathbf{t}_h,\boldsymbol{\sigma}_h),(\mathbf{s}_h,\boldsymbol{\tau}_h)\in H_h$.

Proof. Given $(\mathbf{t}_h,\boldsymbol{\sigma}_h)$ and $(\mathbf{s}_h,\boldsymbol{\tau}_h)\in H_h$, we take $(\mathbf{r}_h,\boldsymbol{\rho}_h)=(\mathbf{t}_h,\boldsymbol{\sigma}_h)-(\mathbf{s}_h,\boldsymbol{\tau}_h)$ in (3.23), to obtain

$$
\begin{aligned}
[\mathcal{A}_h(\mathbf{t}_h,\boldsymbol{\sigma}_h) - \mathcal{A}_h(\mathbf{s}_h,\boldsymbol{\tau}_h),(\mathbf{t}_h,\boldsymbol{\sigma}_h)-(\mathbf{s}_h,\boldsymbol{\tau}_h)] \;&=\; [\mathbb{A}(\mathbf{t}_h)-\mathbb{A}(\mathbf{s}_h),\mathbf{t}_h-\mathbf{s}_h]\\
&-\;\kappa_1[\mathbb{A}(\mathbf{t}_h)-\mathbb{A}(\mathbf{s}_h),(\boldsymbol{\sigma}_h-\boldsymbol{\tau}_h)^{\mathrm{d}}] + \frac{1}{2}\|(\tau\mathtt{h})^{-1/2}[\![\boldsymbol{\sigma}_h-\boldsymbol{\tau}_h]\!]\|_{0,\mathcal{E}_h^i}^2\\
&+\;\kappa_1\|(\boldsymbol{\sigma}_h-\boldsymbol{\tau}_h)^{\mathrm{d}}\|_{0,\Omega}^2 + \kappa_2\|\mathbf{div}_h(\boldsymbol{\sigma}_h-\boldsymbol{\tau}_h)\|_{\mathcal{T}_h}^2,
\end{aligned}
$$

which, according to (3.21) and (3.22), implies that

$$
\begin{aligned}
&[\mathcal{A}_h(\mathbf{t}_h,\boldsymbol{\sigma}_h) - \mathcal{A}_h(\mathbf{s}_h,\boldsymbol{\tau}_h),(\mathbf{t}_h,\boldsymbol{\sigma}_h)-(\mathbf{s}_h,\boldsymbol{\tau}_h)]\\
&\quad\ge\; \alpha_0\,\|\mathbf{t}_h-\mathbf{s}_h\|_{0,\Omega}^2 - \gamma_0\kappa_1\,\|\mathbf{t}_h-\mathbf{s}_h\|_{0,\Omega}\,\|(\boldsymbol{\sigma}_h-\boldsymbol{\tau}_h)^{\mathrm{d}}\|_{0,\Omega} + \frac{1}{2}\|(\tau\mathtt{h})^{-1/2}[\![\boldsymbol{\sigma}_h-\boldsymbol{\tau}_h]\!]\|_{0,\mathcal{E}_h^i}^2\\
&\qquad+\;\kappa_1\,\|(\boldsymbol{\sigma}_h-\boldsymbol{\tau}_h)^{\mathrm{d}}\|_{0,\Omega}^2 + \kappa_2\,\|\mathbf{div}_h(\boldsymbol{\sigma}_h-\boldsymbol{\tau}_h)\|_{\mathcal{T}_h}^2,\\
&\quad\ge\; \alpha_0\,\|\mathbf{t}_h-\mathbf{s}_h\|_{0,\Omega}^2 - \gamma_0\kappa_1\left\{\frac{\|\mathbf{t}_h-\mathbf{s}_h\|_{0,\Omega}^2}{2\delta} \;+\; \frac{\delta\,\|(\boldsymbol{\sigma}_h-\boldsymbol{\tau}_h)^{\mathrm{d}}\|_{0,\Omega}^2}{2}\right\}\\
&\qquad+\;\frac{1}{2}\|(\tau\mathtt{h})^{-1/2}[\![\boldsymbol{\sigma}_h-\boldsymbol{\tau}_h]\!]\|_{0,\mathcal{E}_h^i}^2 \;+\; \kappa_1\,\|(\boldsymbol{\sigma}_h-\boldsymbol{\tau}_h)^{\mathrm{d}}\|_{0,\Omega}^2 + \kappa_2\,\|\mathbf{div}_h(\boldsymbol{\sigma}_h-\boldsymbol{\tau}_h)\|_{\mathcal{T}_h}^2,\\
&\quad=\; \left(\alpha_0-\frac{\gamma_0\kappa_1}{2\delta}\right)\|\mathbf{t}_h-\mathbf{s}_h\|_{0,\Omega}^2 + \kappa_1\left(1-\frac{\gamma_0\delta}{2}\right)\|(\boldsymbol{\sigma}_h-\boldsymbol{\tau}_h)^{\mathrm{d}}\|_{0,\Omega}^2\\
&\qquad+\;\kappa_2\,\|\mathbf{div}_h(\boldsymbol{\sigma}_h-\boldsymbol{\tau}_h)\|_{\mathcal{T}_h}^2 + \frac{1}{2}\|(\tau\mathtt{h})^{-1/2}[\![\boldsymbol{\sigma}_h-\boldsymbol{\tau}_h]\!]\|_{0,\mathcal{E}_h^i}^2 \quad \forall\,\delta>0.
\end{aligned}
$$

It follows that the constants multiplying the norms above become positive if $\delta \in \left(0, \frac{2}{\gamma_0}\right)$ and $\kappa_1 \in \left(0, \frac{2\alpha_0\delta}{\gamma_0}\right)$. In particular, for $\delta = \frac{1}{\gamma_0}$ we require $\kappa_1 \in \left(0, \frac{2\alpha_0}{\gamma_0^2}\right)$, whence we find that

$$\begin{aligned}
&[\mathcal{A}_h(\mathbf{t}_h, \boldsymbol{\sigma}_h) - \mathcal{A}_h(\mathbf{s}_h, \boldsymbol{\tau}_h), (\mathbf{t}_h, \boldsymbol{\sigma}_h) - (\mathbf{s}_h, \boldsymbol{\tau}_h)] \\
&\quad \geq \left(\alpha_0 - \frac{\gamma_0^2\kappa_1}{2}\right) \|\mathbf{t}_h - \mathbf{s}_h\|_{0,\Omega}^2 + \frac{\kappa_1}{2}\|(\boldsymbol{\sigma}_h - \boldsymbol{\tau}_h)^{\mathrm{d}}\|_{0,\Omega}^2 \\
&\qquad + \kappa_2 \, \|\mathbf{div}_h(\boldsymbol{\sigma}_h - \boldsymbol{\tau}_h)\|_{\mathcal{T}_h}^2 + \frac{1}{2}\|(\tau \mathtt{h})^{-1/2}[\![\boldsymbol{\sigma}_h - \boldsymbol{\tau}_h]\!]\|_{0,\mathcal{E}_h^i}^2 \\
&\quad \geq C_{\mathrm{SM}}\|(\mathbf{t}_h, \boldsymbol{\sigma}_h) - (\mathbf{s}_h, \boldsymbol{\tau}_h)\|_{H_h}^2,
\end{aligned}$$

with $C_{\mathrm{SM}} := \min\left\{\alpha_0 - \frac{\gamma_0^2\kappa_1}{2}, \frac{\kappa_1}{2}, \kappa_2, \frac{1}{2}\right\}$, thus completing the proof of the lemma. □

Our next goal is to show the discrete inf-sup condition for the linear operator $\mathcal{B}_h$. More precisely, we have the following result.

Lemma 3.7. *There exists a constant $C_{\mathrm{inf}} > 0$, independent of h and τ, such that*

$$\sup_{\substack{(\mathbf{s}_h, \boldsymbol{\tau}_h) \in H_h \\ (\mathbf{s}_h, \boldsymbol{\tau}_h) \neq \mathbf{0}}} \frac{[\mathcal{B}_h(\mathbf{s}_h, \boldsymbol{\tau}_h), \mathbf{v}_h]}{\|(\mathbf{s}_h, \boldsymbol{\tau}_h)\|_{H_h}} \;\geq\; C_{\mathrm{inf}} \, \|\mathbf{v}_h\|_{0,\Omega} \quad \forall\, \mathbf{v}_h \in V_h.$$

Proof. We begin by recalling from (3.12) that $\mathcal{B}_h$ does not depend on $\mathbf{s}_h$, and hence it suffices to show the existence of $C_{\mathrm{inf}} > 0$ such that

$$\sup_{\substack{\boldsymbol{\tau}_h \in \Sigma_h \\ \boldsymbol{\tau}_h \neq \mathbf{0}}} \frac{\displaystyle\int_\Omega \mathbf{v}_h \cdot \mathbf{div}_h(\boldsymbol{\tau}_h) - \int_{\mathcal{E}_h^i} \{\!\{\mathbf{v}_h\}\!\} \cdot [\![\boldsymbol{\tau}_h]\!]}{\|\boldsymbol{\tau}_h\|_{\Sigma_h}} \;\geq\; C_{\mathrm{inf}} \, \|\mathbf{v}_h\|_{0,\Omega} \quad \forall\, \mathbf{v}_h \in V_h.$$

To this end we let $\mathrm{RT}_{k-1}(\Omega)$ be the global Raviart-Thomas space of degree $k-1$, which is clearly contained in S_h, and note that

$$\sup_{\substack{\boldsymbol{\tau}_h \in \Sigma_h \\ \boldsymbol{\tau}_h \neq \mathbf{0}}} \frac{\displaystyle\int_\Omega \mathbf{v}_h \cdot \mathbf{div}_h(\boldsymbol{\tau}_h) - \int_{\mathcal{E}_h^i} \{\!\{\mathbf{v}_h\}\!\} \cdot [\![\boldsymbol{\tau}_h]\!]}{\|\boldsymbol{\tau}_h\|_{\Sigma_h}} \;\geq\; \sup_{\substack{\boldsymbol{\tau}_h \in \mathrm{RT}_{k-1}(\Omega)\backslash\{\mathbf{0}\} \\ \int_\Omega \mathrm{tr}(\boldsymbol{\tau}_h) = 0}} \frac{\displaystyle\int_\Omega \mathbf{v}_h \cdot \mathbf{div}(\boldsymbol{\tau}_h)}{\|\boldsymbol{\tau}_h\|_{\Sigma_h}}.$$

In this way, and observing that $\|\boldsymbol{\tau}_h\|_{\Sigma_h}$ is equivalent to $\|\boldsymbol{\tau}_h\|_{\mathbf{div},\Omega}$ $\forall\ \boldsymbol{\tau}_h \in \mathrm{RT}_{k-1}(\Omega)$ such that $\int_\Omega \mathrm{tr}\,(\boldsymbol{\tau}_h) = 0$, with constants independent of h and τ, the rest of the proof follows from classical results from mixed finite element methods (see, e.g. [71, Section 4.2 and Lemma 2.6]). □

The following three lemmas establish the positive semidefiniteness of $\mathcal{S}_h$ and some discrete trace, inverse, and boundedness inequalities to be employed later on.

Lemma 3.8. *The operator $\mathcal{S}_h : V_h \to V_h'$, defined by* (3.13) *is positive semidefinite, that is,*

$$[\mathcal{S}_h(\mathbf{v}_h), \mathbf{v}_h] \;\geq\; 0 \quad \forall\, \mathbf{v}_h \in V_h.$$

Proof. It is clear from (3.13) that

$$[\mathcal{S}_h(\mathbf{v}_h), \mathbf{v}_h] \;=\; \sum_{T \in \mathcal{T}_h} \sum_{F \in \partial T} \int_F \mathbf{S}\mathbf{v}_h \cdot \mathbf{v}_h \quad \forall\, \mathbf{v}_h \in\; V_h,$$

which, thanks to the fact that $\mathbf{S}$ is a positive definite tensor on $\mathcal{E}_h$, completes the proof. □

Lemma 3.9 (Discrete trace's inequality + inverse's inequality). *There exists $C_{\rm inv} > 0$, depending only on k and the shape regularity of the mesh, such that*

$$\|\mathbf{v}\|^2_{0,\partial T} \;\leq\; C_{\rm inv}\, h_T^{-1}\|\mathbf{v}\|^2_{0,T} \quad \forall\, \mathbf{v} \in \mathbf{P}_k(T), \quad \forall\, T \in \mathcal{T}_h, \tag{3.24}$$

and

$$\|\boldsymbol{\tau}\|^2_{0,\partial T} \;\leq\; C_{\rm inv}\, h_T^{-1}\|\boldsymbol{\tau}\|^2_{0,T} \quad \forall\, \boldsymbol{\tau} \in \mathbb{P}_k(T), \quad \forall\, T \in \mathcal{T}_h. \tag{3.25}$$

Proof. The proof uses the discrete trace inequality from Lemma 3.1 and an inverse inequality. See also [22, Lemma 3.2]. □

Lemma 3.10. *There exist constants $\widehat{C}_1, \widehat{C}_2, \widehat{C}_3 > 0$, independent of h and τ, such that*

i) $\|\mathtt{h}^{1/2}\{\!\{\mathbf{v}_h\}\!\}\|_{0,\mathcal{E}_h^i} \;\leq\; \widehat{C}_1\|\mathbf{v}_h\|_{0,\Omega} \quad \forall\, \mathbf{v}_h \in V_h.$

ii) $\|\mathtt{h}^{1/2}\mathbf{v}_h\|_{0,\mathcal{E}_h^\partial} \;\leq\; \widehat{C}_2\|\mathbf{v}_h\|_{0,\Omega} \qquad \forall\, \mathbf{v}_h \in V_h.$

iii) $\|\mathtt{h}^{1/2}\boldsymbol{\tau}_h\boldsymbol{\nu}\|_{0,\mathcal{E}_h^\partial} \;\leq\; \widehat{C}_3\|\boldsymbol{\tau}_h\|_{0,\Omega} \quad \forall\, \boldsymbol{\tau}_h \in \Sigma_h.$

Proof. Given $\mathbf{v}_h \in V_h$, we use (3.24) to deduce that

$$\begin{aligned}
\|\mathtt{h}^{1/2}\{\!\{\mathbf{v}_h\}\!\}\|^2_{0,\mathcal{E}_h^i} \;&=\; \frac{1}{4}\int_{\mathcal{E}_h^i} \mathtt{h}|\mathbf{v}_h^+ + \mathbf{v}_h^-|^2 \;\leq\; \frac{1}{2}\int_{\mathcal{E}_h^i} \mathtt{h}\left(|\mathbf{v}_h^+|^2 + |\mathbf{v}_h^-|^2\right) \;\leq\; \frac{1}{2}\sum_{T\in\mathcal{T}_h}\int_{\partial T} \mathtt{h}|\mathbf{v}_h|^2 \\
&\leq\; C_1\sum_{T\in\mathcal{T}_h} h_T\|\mathbf{v}_h\|^2_{0,\partial T} \;\leq\; C_1 C_{\rm inv}\sum_{T\in\mathcal{T}_h}\|\mathbf{v}_h\|^2_{0,T} \;=\; C_1 C_{\rm inv}\|\mathbf{v}_h\|^2_{0,\Omega},
\end{aligned}$$

which shows *i)* with $\widehat{C}_1 := (C_1 C_{\rm inv})^{1/2} > 0$. Next, using that $\mathtt{h} = h_T$ on $\mathcal{E}_h^\partial$, and applying again (3.24), we find that

$$\|\mathtt{h}^{1/2}\mathbf{v}_h\|^2_{0,\mathcal{E}_h^\partial} \;=\; \int_{\mathcal{E}_h^\partial}\mathtt{h}|\mathbf{v}_h|^2 \;\leq\; \sum_{T\in\mathcal{T}_h} h_T\|\mathbf{v}_h\|^2_{0,\partial T} \;\leq\; C_{\rm inv}\|\mathbf{v}_h\|^2_{0,\Omega},$$

which proves *ii)* with $\widehat{C}_2 := (C_{\rm inv})^{1/2}$. Finally, the proof of *iii)* follows from (3.25). □

Using Lemma 3.10, the definition of tensor $\mathbf{S}$ given in (3.18), and the Cauchy-Schwarz inequality, it is easy to check that the operators $\mathcal{B}_h$, $\mathcal{S}_h$ and $\mathcal{C}_h$, and the functionals $\mathcal{F}_h$ and $\mathcal{G}_h$, are all bounded with respect to the corresponding norms. More precisely, the corresponding bounds are established in the following lemma.

Lemma 3.11. *Let $\mathbf{s}_h \in S_h$, $\boldsymbol{\tau}_h \in \Sigma_h$ and $\mathbf{u}_h, \mathbf{v}_h \in V_h$. Then there hold*

$$\begin{aligned}
|[\mathcal{B}_h(\mathbf{s}_h,\boldsymbol{\tau}_h),\mathbf{v}_h]| \;&\leq\; (1+\tau\widehat{C}_1)\,\|(\mathbf{s}_h,\boldsymbol{\tau}_h)\|_{H_h}\,\|\mathbf{v}_h\|_{0,\Omega} \\
|[\mathcal{S}_h(\mathbf{u}_h),\mathbf{v}_h]| \;&\leq\; \tau\widehat{C}_1\,\|\mathbf{u}_h\|_{0,\Omega}\,\|\mathbf{v}_h\|_{0,\Omega} \\
|[\mathcal{C}_h(\mathbf{u}_h),\mathbf{v}_h]| \;&\leq\; 2\tau\widehat{C}_1^2\,\|\mathbf{u}_h\|_{0,\Omega}\,\|\mathbf{v}_h\|_{0,\Omega} \\
|[\mathcal{F}_h,(\mathbf{s}_h,\boldsymbol{\tau}_h)]| \;&\leq\; \left(\kappa_2 + c_2\widehat{C}_3\right)\mathbb{B}(\mathbf{f},\mathbf{g})\,\|(\mathbf{s}_h,\boldsymbol{\tau}_h)\|_{H_h} \\
|[\mathcal{G}_h,\mathbf{v}_h]| \;&\leq\; \left(1+\tau h_0\widehat{C}_2\right)\mathbb{B}(\mathbf{f},\mathbf{g})\,\|\mathbf{v}_h\|_{0,\Omega}
\end{aligned} \tag{3.26}$$

where

$$\mathbb{B}(\mathbf{f},\mathbf{g}) \;:=\; \|\mathbf{f}\|_{0,\Omega} \;+\; \|\mathtt{h}^{-1/2}\mathbf{g}\|_{0,\mathcal{E}_h^\partial}.$$

Proof. The proof uses Lemma 3.10 and the definitions of each operator and functional. We omit further details and refer to [22, Lemma 4.4]. $\square$

We end this section, by recalling from [77] the following abstract theorem.

Theorem 3.1. *Let X, M be Hilbert spaces and assume that*

i) the operator $\mathcal{A} : X \to X'$ is Lipschitz continuous and strongly monotonic, that is, there exist γ, $\alpha > 0$ such that

$$\|\mathcal{A}(\mathbf{s}_1) - \mathcal{A}(\mathbf{s}_2)\|_{X'} \;\leq\; \gamma\, \|\mathbf{s}_1 - \mathbf{s}_2\|_X \quad \forall\, \mathbf{s}_1, \mathbf{s}_2 \in X$$

and

$$[\mathcal{A}(\mathbf{s}_1) - \mathcal{A}(\mathbf{s}_2), \mathbf{s}_1 - \mathbf{s}_2] \;\geq\; \alpha\, \|\mathbf{s}_1 - \mathbf{s}_2\|_X^2 \quad \forall\, \mathbf{s}_1, \mathbf{s}_2 \in X;$$

ii) the linear operator $\mathcal{S}$ is positive semidefinite on M, that is

$$[\mathcal{S}(\boldsymbol{\tau}), \boldsymbol{\tau}] \;\geq\; 0 \quad \forall\, \boldsymbol{\tau} \in M;$$

iii) the linear operator $\mathcal{B}$ satisfies an inf-sup condition on $X \times M$, that is, there exists $\beta > 0$ such that

$$\sup_{\substack{\mathbf{s}\in X\\ \mathbf{s}\neq \mathbf{0}}} \frac{[\mathcal{B}(\mathbf{s}), \boldsymbol{\tau}]}{\|\mathbf{s}\|_X} \;\geq\; \beta\, \|\boldsymbol{\tau}\|_M \quad \forall\, \boldsymbol{\tau} \in M.$$

Then, given $\mathcal{F} \in X'$ and $\mathcal{G} \in M'$, there exists a unique solution $(\mathbf{t}, \boldsymbol{\sigma}) \in X \times M$ of

$$\begin{aligned} [\mathcal{A}(\mathbf{t}), \mathbf{s}] + [\mathcal{B}^*(\boldsymbol{\sigma}), \mathbf{s}] &= [\mathcal{F}, \mathbf{s}] \quad \forall\, \mathbf{s} \in X, \\ [\mathcal{B}(\mathbf{t}), \boldsymbol{\tau}] - [\mathcal{S}(\boldsymbol{\sigma}), \boldsymbol{\tau}] &= [\mathcal{G}, \boldsymbol{\tau}] \quad \forall\, \boldsymbol{\tau} \in M. \end{aligned}$$

In addition, the following estimates hold

$$\begin{aligned} \|\mathbf{t}\|_X &\leq C_1 \Big\{ \|\mathcal{F}\|_{X'} + \|\mathcal{G}\|_{M'} + \|\mathcal{A}(\mathbf{0})\|_{X'} \Big\}, \\ \|\boldsymbol{\sigma}\|_M &\leq C_2 \Big\{ \|\mathcal{F}\|_{X'} + \|\mathcal{G}\|_{M'} + \|\mathcal{A}(\mathbf{0})\|_{X'} \Big\}, \end{aligned}$$

where

$$C_1 \;:=\; \frac{1}{\alpha} + \frac{\|\mathcal{B}\|}{\alpha} C_2 \quad \text{and} \quad C_2 \;:=\; \frac{\gamma^2}{\alpha\beta^2}\left(1 + \frac{\|\mathcal{B}\|}{\alpha}\right).$$

Proof. See [77, Lemma 2.1], where it is easy to show the last estimates from expressions (2.8) and (2.9) in [77]. $\square$

3.3.2 Main result

In order to prove existence and uniqueness of solution of (3.10), we now introduce the nonlinear mapping $\mathbb{T}_h : H_h \times V_h \to H_h \times V_h$ that, given $((\mathbf{r}_h, \boldsymbol{\rho}_h), \mathbf{w}_h) \in H_h \times V_h$, defines $\mathbb{T}_h((\mathbf{r}_h, \boldsymbol{\rho}_h), \mathbf{w}_h) := ((\mathbf{t}_h, \boldsymbol{\sigma}_h), \mathbf{u}_h) \in H_h \times V_h$ as the unique solution of the problem

$$\begin{aligned} [\mathcal{A}_h(\mathbf{t}_h, \boldsymbol{\sigma}_h), (\mathbf{s}_h, \boldsymbol{\tau}_h)] + [\mathcal{B}_h(\mathbf{s}_h, \boldsymbol{\tau}_h), \mathbf{u}_h] &= [\mathcal{F}_h, (\mathbf{s}_h, \boldsymbol{\tau}_h)] \quad \forall\, (\mathbf{s}_h, \boldsymbol{\tau}_h) \in H_h, \\ [\mathcal{B}_h(\mathbf{t}_h, \boldsymbol{\sigma}_h), \mathbf{v}_h] - [\mathcal{S}_h(\mathbf{u}_h), \mathbf{v}_h] &= [\mathcal{G}_h, \mathbf{v}_h] + [\mathcal{C}_h(\mathbf{w}_h), \mathbf{v}_h] \quad \forall\, \mathbf{v}_h \in V_h. \end{aligned}$$

Note that actually $\mathbb{T}_h((\mathbf{r}_h,\boldsymbol{\rho}_h),\mathbf{w}_h)$ depends only on the third component $\mathbf{w}_h \in V_h$. In addition, bearing in mind Lemmas 3.5, 3.6, 3.7 and 3.8, it follows from Theorem 3.1 that $\mathbb{T}_h$ is well-defined and there holds

$$\|(\mathbf{t}_h,\boldsymbol{\sigma}_h)\|_{H_h} \;\le\; \widehat{C}_a\widetilde{C}\,\mathbb{B}(\mathbf{f},\mathbf{g}) \;+\; 2\widehat{C}_1^2\widehat{C}_a\tau\,\|\mathbf{w}_h\|_{0,\Omega}, \tag{3.27}$$

and

$$\|\mathbf{u}_h\|_{0,\Omega} \;\le\; \widehat{C}_b\widetilde{C}\,\mathbb{B}(\mathbf{f},\mathbf{g}) \;+\; 2\widehat{C}_1^2\widehat{C}_b\tau\,\|\mathbf{w}_h\|_{0,\Omega}, \tag{3.28}$$

where

$$\begin{aligned}
\widetilde{C} &:= 1+\kappa_2+\tau h_0\widehat{C}_2 + c_1^{1/2}\widehat{C}_3(1+\tau)^{1/2},\\
\widehat{C}_a &:= \frac{1}{C_{\mathrm{SM}}}\left(1+(1+\tau\widehat{C}_1)\widehat{C}_b\right),\\
\widehat{C}_b &:= \frac{C_{\mathrm{LC}}^2}{C_{\mathrm{SM}}C_{\inf}^2}\left(1+\frac{1+\tau\widehat{C}_1}{C_{\mathrm{SM}}}\right),
\end{aligned}$$

and the constants $\widehat{C}_1$, $\widehat{C}_2$, and $\widehat{C}_3$ are those from Lemma 3.10. Observe here that the identity $\mathcal{A}_h(\mathbf{0},\mathbf{0}) = (\mathbf{0},\mathbf{0})$ and Lemma 3.11 have been employed to establish the estimates (3.27) and (3.28). Also, we remark that the relevance of the introduction of $\mathbb{T}_h$ has to do with the fact that any eventual solution of (3.10) becomes a fixed point of $\mathbb{T}_h$ and conversely. Moreover, the following lemma establishes that $\mathbb{T}_h$ is indeed a contraction mapping and hence, thanks to the Banach Fixed-Point Theorem, it has a unique fixed point in $H_h \times V_h$.

Lemma 3.12. *Assume that the parameter τ lies in $\left(0,\frac{1}{\theta}\right)$, where*

$$\theta \;:=\; \left(\frac{2\widehat{C}_1^2}{C_{\mathrm{SM}}}\right)\left(\frac{C_{\mathrm{LC}}}{C_{\inf}}\right)\left(1+\frac{C_{\mathrm{LC}}}{C_{\inf}}\right) \;>\; 0.$$

Then, $\mathbb{T}_h$ is a contraction.

Proof. Given $((\mathbf{t}_h,\boldsymbol{\sigma}_h),\mathbf{u}_h)$, $((\widetilde{\mathbf{t}}_h,\widetilde{\boldsymbol{\sigma}}_h),\widetilde{\mathbf{u}}_h)$, $((\mathbf{r}_h,\boldsymbol{\rho}_h),\mathbf{w}_h)$, and $((\widetilde{\mathbf{r}}_h,\widetilde{\boldsymbol{\rho}}_h),\widetilde{\mathbf{w}}_h)$ in $H_h \times V_h$ such that

$$\mathbb{T}_h((\mathbf{r}_h,\boldsymbol{\rho}_h),\mathbf{w}_h) \;=\; ((\mathbf{t}_h,\boldsymbol{\sigma}_h),\mathbf{u}_h) \quad\text{and}\quad \mathbb{T}_h((\widetilde{\mathbf{r}}_h,\widetilde{\boldsymbol{\rho}}_h),\widetilde{\mathbf{w}}_h) \;=\; ((\widetilde{\mathbf{t}}_h,\widetilde{\boldsymbol{\sigma}}_h),\widetilde{\mathbf{u}}_h),$$

we know from the definition of $\mathbb{T}_h$ that

$$[\mathcal{A}_h(\mathbf{t}_h,\boldsymbol{\sigma}_h)-\mathcal{A}_h(\widetilde{\mathbf{t}}_h,\widetilde{\boldsymbol{\sigma}}_h),(\mathbf{s}_h,\boldsymbol{\tau}_h)] \;+\; [\mathcal{B}_h(\mathbf{s}_h,\boldsymbol{\tau}_h),\mathbf{u}_h-\widetilde{\mathbf{u}}_h] \;=\; 0, \tag{3.29a}$$

$$[\mathcal{B}_h(\mathbf{t}_h-\widetilde{\mathbf{t}}_h,\boldsymbol{\sigma}_h-\widetilde{\boldsymbol{\sigma}}_h),\mathbf{v}_h] \;-\; [\mathcal{S}_h(\mathbf{u}_h-\widetilde{\mathbf{u}}_h),\mathbf{v}_h] \;=\; [\mathcal{C}_h(\mathbf{w}_h-\widetilde{\mathbf{w}}_h),\mathbf{v}_h], \tag{3.29b}$$

for all $((\mathbf{s}_h,\boldsymbol{\tau}_h),\mathbf{v}_h) \in H_h \times V_h$. Next, taking $(\mathbf{s}_h,\boldsymbol{\tau}_h) = (\mathbf{t}_h-\widetilde{\mathbf{t}}_h,\boldsymbol{\sigma}_h-\widetilde{\boldsymbol{\sigma}}_h)$ and $\mathbf{v}_h = \mathbf{u}_h-\widetilde{\mathbf{u}}_h$, we obtain from (3.29) that

$$\begin{aligned}
&[\mathcal{A}_h(\mathbf{t}_h,\boldsymbol{\sigma}_h)-\mathcal{A}_h(\widetilde{\mathbf{t}}_h,\widetilde{\boldsymbol{\sigma}}_h),(\mathbf{t}_h,\boldsymbol{\sigma}_h)-(\widetilde{\mathbf{t}}_h,\widetilde{\boldsymbol{\sigma}}_h)]\\
&\qquad\qquad + [\mathcal{S}_h(\mathbf{u}_h-\widetilde{\mathbf{u}}_h),\mathbf{u}_h-\widetilde{\mathbf{u}}_h] \;=\; -[\mathcal{C}_h(\mathbf{w}_h-\widetilde{\mathbf{w}}_h),\mathbf{u}_h-\widetilde{\mathbf{u}}_h].
\end{aligned} \tag{3.30}$$

Then, using the strong monotonicity of $\mathcal{A}_h$, the fact that $\mathcal{S}_h$ is positive semidefinite, and the boundedness of $\mathcal{C}_h$ (cf. (3.26)), we deduce from (3.30) that

$$\|(\mathbf{t}_h,\boldsymbol{\sigma}_h)-(\widetilde{\mathbf{t}}_h,\widetilde{\boldsymbol{\sigma}}_h)\|_{H_h}^2 \;\le\; \frac{2\tau\widehat{C}_1^2}{C_{\mathrm{SM}}}\,\|\mathbf{w}_h-\widetilde{\mathbf{w}}_h\|_{0,\Omega}\,\|\mathbf{u}_h-\widetilde{\mathbf{u}}_h\|_{0,\Omega}. \tag{3.31}$$

On the other hand, employing the inf-sup condition for $\mathcal{B}_h$ (cf. Lemma 3.7), (3.29a), and the Lipschitz-continuity of $\mathcal{A}_h$ (cf. Lemma 3.6), we find that

$$\begin{aligned}
\|\mathbf{u}_h - \widetilde{\mathbf{u}}_h\|_{0,\Omega} &\leq \frac{1}{C_{\inf}} \sup_{\substack{(\mathbf{s}_h,\boldsymbol{\tau}_h)\in H_h \\ (\mathbf{s}_h,\boldsymbol{\tau}_h)\neq \mathbf{0}}} \frac{|[\mathcal{B}_h(\mathbf{s}_h,\boldsymbol{\tau}_h),\mathbf{u}_h - \widetilde{\mathbf{u}}_h]|}{\|(\mathbf{s}_h,\boldsymbol{\tau}_h)\|_{H_h}}, \\
&= \frac{1}{C_{\inf}} \sup_{\substack{(\mathbf{s}_h,\boldsymbol{\tau}_h)\in H_h \\ (\mathbf{s}_h,\boldsymbol{\tau}_h)\neq \mathbf{0}}} \frac{|-[\mathcal{A}_h(\mathbf{t}_h,\boldsymbol{\sigma}_h) - \mathcal{A}_h(\widetilde{\mathbf{t}}_h,\widetilde{\boldsymbol{\sigma}}_h),(\mathbf{s}_h,\boldsymbol{\tau}_h)]|}{\|(\mathbf{s}_h,\boldsymbol{\tau}_h)\|_{H_h}}, \\
&\leq \frac{C_{\mathrm{LC}}}{C_{\inf}} \|(\mathbf{t}_h,\boldsymbol{\sigma}_h) - (\widetilde{\mathbf{t}}_h,\widetilde{\boldsymbol{\sigma}}_h)\|_{H_h},
\end{aligned}$$

which, together with (3.31), implies that

$$\|(\mathbf{t}_h,\boldsymbol{\sigma}_h) - (\widetilde{\mathbf{t}}_h,\widetilde{\boldsymbol{\sigma}}_h)\|_{H_h} \leq \left(\frac{2\tau\widehat{C}_1^2}{C_{\mathrm{SM}}}\right)\left(\frac{C_{\mathrm{LC}}}{C_{\inf}}\right)\|\mathbf{w}_h - \widetilde{\mathbf{w}}_h\|_{0,\Omega}$$

and

$$\|\mathbf{u}_h - \widetilde{\mathbf{u}}_h\|_{0,\Omega} \leq \left(\frac{2\tau\widehat{C}_1^2}{C_{\mathrm{SM}}}\right)\left(\frac{C_{\mathrm{LC}}}{C_{\inf}}\right)^2\|\mathbf{w}_h - \widetilde{\mathbf{w}}_h\|_{0,\Omega}.$$

In this way, we conclude that

$$\|\mathbb{T}_h((\mathbf{r}_h,\boldsymbol{\rho}_h),\mathbf{w}_h) - \mathbb{T}_h((\widetilde{\mathbf{r}}_h,\widetilde{\boldsymbol{\rho}}_h),\widetilde{\mathbf{w}}_h)\|_{H_h\times V_h} \leq L\,\|((\mathbf{r}_h,\boldsymbol{\rho}_h),\mathbf{w}_h) - ((\widetilde{\mathbf{r}}_h,\widetilde{\boldsymbol{\rho}}_h),\widetilde{\mathbf{w}}_h)\|_{H_h\times V_h},$$

with $L := \tau\theta$. Finally, since $C_{\inf}$, C_{LC}, and C_{SM}, are independent of $\tau > 0$, we can choose $\tau \in \big(0,\frac{1}{\theta}\big)$, which insures that $\mathbb{T}_h$ is a contraction and completes the proof. □

Now we are ready to establish the main result of this section.

Theorem 3.2. *Assume that*

$$0 < \tau < \min\left\{\frac{1}{\theta},\ \frac{1}{2}\left(\frac{C_{\mathrm{SM}}}{(1+C_{\mathrm{SM}})\theta + \widehat{C}_1}\right)\right\}.$$

Then, there exists a unique $((\mathbf{t}_h,\boldsymbol{\sigma}_h),\mathbf{u}_h)\in H_h\times V_h$ *solution of* (3.10). *Moreover, there holds*

$$\|(\mathbf{t}_h,\boldsymbol{\sigma}_h)\|_{H_h} \leq C_{\mathrm{a}}\,\mathbb{B}(\mathbf{f},\mathbf{g}) \quad \textit{and} \quad \|\mathbf{u}_h\|_{0,\Omega} \leq C_{\mathrm{b}}\,\mathbb{B}(\mathbf{f},\mathbf{g}),$$

where

$$C_{\mathrm{a}} := \widehat{C}_a\,(\widetilde{C} + 2\widehat{C}_1^2 C_b\tau) \quad \textit{and} \quad C_{\mathrm{b}} := 2\widehat{C}_b\widetilde{C}.$$

Proof. The unique solvability of (3.10) follows straightforwardly from its equivalence with the fixed-point equation for $\mathbb{T}_h$, the corresponding Banach Theorem, and the fact that $\mathbb{T}_h$ becomes a contraction when $\tau < \frac{1}{\theta}$ (cf. Lemma 3.12). Then, denoting by $((\mathbf{t}_h,\boldsymbol{\sigma}_h),\mathbf{u}_h)\in H_h\times V_h$ the unique solution of (3.10), we have from (3.27) and (3.28) that

$$\|(\mathbf{t}_h,\boldsymbol{\sigma}_h)\|_{H_h} \leq \widehat{C}_a\widetilde{C}\,\mathbb{B}(\mathbf{f},\mathbf{g}) + 2\widehat{C}_1^2\widehat{C}_a\tau\,\|\mathbf{u}_h\|_{0,\Omega} \tag{3.32}$$

and

$$\|\mathbf{u}_h\|_{0,\Omega} \leq \widehat{C}_b\widetilde{C}\,\mathbb{B}(\mathbf{f},\mathbf{g}) + 2\widehat{C}_1^2\widehat{C}_b\tau\,\|\mathbf{u}_h\|_{0,\Omega}. \tag{3.33}$$

It remain to handle the second term on the right-hand side of (3.33). For this purpose, we now note that

$$\begin{aligned} 2\widehat{C}_1^2\widehat{C}_b\tau &= 2\widehat{C}_1^2\frac{C_{\mathrm{LC}}^2}{C_{\mathrm{SM}}C_{\mathrm{inf}}^2}\left(1+\frac{1+\tau\widehat{C}_1}{C_{\mathrm{SM}}}\right)\tau \\ &= \left(\frac{2\widehat{C}_1^2}{C_{\mathrm{SM}}}\right)\left(\frac{C_{\mathrm{LC}}}{C_{\mathrm{inf}}}\right)\left(\frac{C_{\mathrm{LC}}}{C_{\mathrm{inf}}}\right)\left(1+\frac{1+\tau\widehat{C}_1}{C_{\mathrm{SM}}}\right)\tau \\ &\leq \theta\left(1+\frac{1+\tau\widehat{C}_1}{C_{\mathrm{SM}}}\right)\tau = \left(\theta+\frac{\theta+(\theta\tau)\widehat{C}_1}{C_{\mathrm{SM}}}\right)\tau \end{aligned}$$

which, using the assumption on τ, gives

$$2\widehat{C}_1^2\widehat{C}_b\tau < \left(\theta+\frac{\theta+\widehat{C}_1}{C_{\mathrm{SM}}}\right)\tau = \left(\frac{(1+C_{\mathrm{SM}})\theta+\widehat{C}_1}{C_{\mathrm{SM}}}\right)\tau < \frac{1}{2}.$$

In this way, replacing the foregoing inequality back into (3.33), we deduce that

$$\|\mathbf{u}_h\|_{0,\Omega} \leq 2\widehat{C}_b\widetilde{C}\,\mathbb{B}(\mathbf{f},\mathbf{g}) = C_{\mathrm{b}}\,\mathbb{B}(\mathbf{f},\mathbf{g}),$$

which, together with (3.32), yields

$$\|(\mathbf{t}_h,\boldsymbol{\sigma}_h)\|_{H_h} \leq \left(\widehat{C}_a\widetilde{C}+2\widehat{C}_1^2\widehat{C}_aC_{\mathrm{b}}\tau\right)\mathbb{B}(\mathbf{f},\mathbf{g}) = C_{\mathrm{a}}\,\mathbb{B}(\mathbf{f},\mathbf{g}),$$

thus completing the proof of the theorem. □

3.4 A priori error analysis

We now aim to derive the *a priori* error estimates for the augmented HDG scheme (3.10). We begin by remarking that the eventual extension to the present nonlinear case of the projection-based error analysis developed in [43] (see also [49]) does not seem straightforward, precisely because of the nonlinearity, and hence in what follows we adopt a more classical approach. Next, since $\mathbf{u}\in\mathbf{L}^2(\Omega)$ and $\nabla\mathbf{u}=\mathbf{t}\in\mathbb{L}^2(\Omega)$ (cf. (3.5)), we observe that actually $\mathbf{u}\in\mathbf{H}^1(\Omega)$, which guarantees that the jump $[\![\mathbf{u}]\!]$ vanish on any interior face of $\mathcal{T}_h$ and there holds $\{\!\{\mathbf{u}\}\!\}=\mathbf{u}$. In addition, since $\boldsymbol{\sigma}=\boldsymbol{\psi}(\nabla\mathbf{u})-p\mathbb{I}\in\mathbb{L}^2(\Omega)$ and $\mathbf{div}(\boldsymbol{\sigma})=-\mathbf{f}$ in Ω, with $\mathbf{f}\in\mathbf{L}^2(\Omega)$, we conclude that $\boldsymbol{\sigma}\in\mathbb{H}(\mathbf{div};\Omega)$, whence $[\![\boldsymbol{\sigma}]\!]=\mathbf{0}$ on each $F\in\mathcal{E}_h^i$. Then, it is easy to check that $(\mathbf{t},\boldsymbol{\sigma},\mathbf{u})$ satisfies the equations of (3.10), and then we obtain the error equations

$$[\mathcal{A}_h(\mathbf{t},\boldsymbol{\sigma})-\mathcal{A}_h(\mathbf{t}_h,\boldsymbol{\sigma}_h),(\mathbf{s}_h,\boldsymbol{\tau}_h)]+[\mathcal{B}_h(\mathbf{s}_h,\boldsymbol{\tau}_h),\mathbf{u}-\mathbf{u}_h] = 0 \quad \forall\,(\mathbf{s}_h,\boldsymbol{\tau}_h)\in H_h, \tag{3.34a}$$

$$[\mathcal{B}_h((\mathbf{t},\boldsymbol{\sigma})-(\mathbf{t}_h,\boldsymbol{\sigma}_h)),\mathbf{v}_h]-[\mathcal{S}_h(\mathbf{u}-\mathbf{u}_h),\mathbf{v}_h]-[\mathcal{C}_h(\mathbf{u}-\mathbf{u}_h),\mathbf{v}_h] = 0 \quad \forall\,\mathbf{v}_h\in V_h. \tag{3.34b}$$

The following result establishes the Céa estimate for (3.6) and (3.10).

Lemma 3.13. *Assume that*

$$0 < \tau < \min\left\{\frac{1}{\theta},\ \frac{1}{2}\left(\frac{C_{\mathrm{SM}}}{(1+C_{\mathrm{SM}})\theta+\widehat{C}_1}\right),\ \frac{1}{\vartheta}\right\},$$

with $\theta > 0$ *defined in Lemma* 3.12 *and*

$$\vartheta \;:=\; 2\left(1+\frac{C_{\rm LC}}{C_{\rm SM}}\right)\left(\frac{C_{\rm LC}}{C_{\rm inf}}\right)\left(\frac{\widehat{C}_1+2\widehat{C}_2^2}{C_{\rm inf}}\right) \;>\; 0.$$

Let $(\mathbf{t},\boldsymbol{\sigma},\mathbf{u}) \in \mathbb{L}^2(\Omega)\times\mathbb{H}(\mathbf{div};\Omega)\times\mathbf{L}^2(\Omega)$ *and* $((\mathbf{t}_h,\boldsymbol{\sigma}_h),\mathbf{u}_h) \in H_h\times V_h$ *be the unique solutions of* (3.6) *and* (3.10)*, respectively. Then, there hold the Céa error estimates*

$$\begin{aligned}\|(\mathbf{t},\boldsymbol{\sigma})-(\mathbf{t}_h,\boldsymbol{\sigma}_h)\|_{H_h} \;&\le\; 2\left(1+\frac{C_{\rm LC}}{C_{\rm SM}}\right)\left(1+\frac{\|\mathcal{B}_h\|}{C_{\rm inf}}\right)\inf_{(\mathbf{s}_h,\boldsymbol{\tau}_h)\in H_h}\|(\mathbf{t},\boldsymbol{\sigma})-(\mathbf{s}_h,\boldsymbol{\tau}_h)\|_{H_h}\\ &+\;\left\{\frac{\|\mathcal{B}_h\|}{C_{\rm SM}}+\left\{1+\left(1+\frac{C_{\rm LC}}{C_{\rm SM}}\right)\frac{\|\mathcal{B}_h\|}{C_{\rm inf}}\right\}\left(\frac{C_{\rm inf}}{C_{\rm LC}}\right)\right\}\inf_{\mathbf{v}_h\in V_h}\|\mathbf{u}-\mathbf{v}_h\|_{0,\Omega},\end{aligned} \tag{3.35}$$

and

$$\begin{aligned}\|\mathbf{u}-\mathbf{u}_h\|_{0,\Omega} \;&\le\; 2\left(1+\frac{C_{\rm LC}}{C_{\rm SM}}\right)\left(\frac{C_{\rm LC}}{C_{\rm inf}}\right)\left(1+\frac{\|\mathcal{B}_h\|}{C_{\rm inf}}\right)\inf_{(\mathbf{s}_h,\boldsymbol{\tau}_h)\in H_h}\|(\mathbf{t},\boldsymbol{\sigma})-(\mathbf{s}_h,\boldsymbol{\tau}_h)\|_{H_h}\\ &+\;2\left\{1+\left(1+\frac{C_{\rm LC}}{C_{\rm SM}}\right)\frac{\|\mathcal{B}_h\|}{C_{\rm inf}}\right\}\inf_{\mathbf{v}_h\in V_h}\|\mathbf{u}-\mathbf{v}_h\|_{0,\Omega}.\end{aligned} \tag{3.36}$$

Proof. We proceed as in [119, Proposition 4.1]. In fact, we first set $H_h = \widetilde{H}_h \oplus \widetilde{H}_h^{\perp}$, with $\widetilde{H}_h$ being the kernel of $\mathcal{B}_h$. Hence, given $(\mathbf{s}_h,\boldsymbol{\tau}_h) \in H_h$, we let $(\mathbf{r}_h,\boldsymbol{\rho}_h)\in\widetilde{H}_h^{\perp}$ be the unique solution of

$$[\mathcal{B}_h(\mathbf{r}_h,\boldsymbol{\rho}_h),\mathbf{v}_h] \;=\; [\mathcal{B}_h((\mathbf{t},\boldsymbol{\sigma})-(\mathbf{s}_h,\boldsymbol{\tau}_h))-\mathcal{S}_h(\mathbf{u}-\mathbf{u}_h)-\mathcal{C}_h(\mathbf{u}-\mathbf{u}_h),\mathbf{v}_h] \quad \forall\,\mathbf{v}_h\in V_h,$$

which there exists thanks to the discrete inf-sup condition and the continuity of $\mathcal{B}_h$. Then, there holds

$$\begin{aligned}C_{\rm inf}\,\|(\mathbf{r}_h,\boldsymbol{\rho}_h)\|_{H_h} \;&\le\; \sup_{\substack{\mathbf{v}_h\in V_h\\ \mathbf{v}_h\neq\mathbf{0}}}\frac{[\mathcal{B}_h(\mathbf{r}_h,\boldsymbol{\rho}_h),\mathbf{v}_h]}{\|\mathbf{v}_h\|_{0,\Omega}}\\ &=\; \sup_{\substack{\mathbf{v}_h\in V_h\\ \mathbf{v}_h\neq\mathbf{0}}}\frac{[\mathcal{B}_h((\mathbf{t},\boldsymbol{\sigma})-(\mathbf{s}_h,\boldsymbol{\tau}_h))-\mathcal{S}_h(\mathbf{u}-\mathbf{u}_h)-\mathcal{C}_h(\mathbf{u}-\mathbf{u}_h),\mathbf{v}_h]}{\|\mathbf{v}_h\|_{0,\Omega}}\\ &\le\; \|\mathcal{B}_h\|\,\|(\mathbf{t},\boldsymbol{\sigma})-(\mathbf{s}_h,\boldsymbol{\tau}_h)\|_{H_h}+\{\,\|\mathcal{S}_h\|+\|\mathcal{C}_h\|\,\}\,\|\mathbf{u}-\mathbf{u}_h\|_{0,\Omega}\end{aligned}$$

that is

$$\|(\mathbf{r}_h,\boldsymbol{\rho}_h)\|_{H_h} \;\le\; \frac{\|\mathcal{B}_h\|}{C_{\rm inf}}\|(\mathbf{t},\boldsymbol{\sigma})-(\mathbf{s}_h,\boldsymbol{\tau}_h)\|_{H_h}+\left\{\frac{\|\mathcal{S}_h\|+\|\mathcal{C}_h\|}{C_{\rm inf}}\right\}\|\mathbf{u}-\mathbf{u}_h\|_{0,\Omega}. \tag{3.37}$$

Also, note by construction of $(\mathbf{r}_h,\boldsymbol{\rho}_h)\in\widetilde{H}_h^{\perp}$ and (3.34b) that there holds

$$[\mathcal{B}_h((\mathbf{s}_h,\boldsymbol{\tau}_h)+(\mathbf{r}_h,\boldsymbol{\rho}_h)-(\mathbf{t}_h,\boldsymbol{\sigma}_h)),\mathbf{v}_h] \;=\; 0 \quad \forall\,\mathbf{v}_h\in V_h. \tag{3.38}$$

Next, applying the strong monotonicity of $\mathcal{A}_h$ and (3.34a), we get

$$\begin{aligned}&C_{\rm SM}\,\|(\mathbf{s}_h,\boldsymbol{\tau}_h)+(\mathbf{r}_h,\boldsymbol{\rho}_h)-(\mathbf{t}_h,\boldsymbol{\sigma}_h)\|_{H_h}^2\\ &\le\; [\mathcal{A}_h((\mathbf{s}_h,\boldsymbol{\tau}_h)+(\mathbf{r}_h,\boldsymbol{\rho}_h))-\mathcal{A}_h(\mathbf{t}_h,\boldsymbol{\sigma}_h),(\mathbf{s}_h,\boldsymbol{\tau}_h)+(\mathbf{r}_h,\boldsymbol{\rho}_h)-(\mathbf{t}_h,\boldsymbol{\sigma}_h)]\\ &=\; [\mathcal{A}_h((\mathbf{s}_h,\boldsymbol{\tau}_h)+(\mathbf{r}_h,\boldsymbol{\rho}_h))-\mathcal{A}_h(\mathbf{t},\boldsymbol{\sigma}),(\mathbf{s}_h,\boldsymbol{\tau}_h)+(\mathbf{r}_h,\boldsymbol{\rho}_h)-(\mathbf{t}_h,\boldsymbol{\sigma}_h)]\\ &\quad+\;[\mathcal{A}_h(\mathbf{t},\boldsymbol{\sigma})-\mathcal{A}_h(\mathbf{t}_h,\boldsymbol{\sigma}_h),(\mathbf{s}_h,\boldsymbol{\tau}_h)+(\mathbf{r}_h,\boldsymbol{\rho}_h)-(\mathbf{t}_h,\boldsymbol{\sigma}_h)]\\ &=\; [\mathcal{A}_h((\mathbf{s}_h,\boldsymbol{\tau}_h)+(\mathbf{r}_h,\boldsymbol{\rho}_h))-\mathcal{A}_h(\mathbf{t},\boldsymbol{\sigma}),(\mathbf{s}_h,\boldsymbol{\tau}_h)+(\mathbf{r}_h,\boldsymbol{\rho}_h)-(\mathbf{t}_h,\boldsymbol{\sigma}_h)]\\ &\quad-\;[\mathcal{B}_h((\mathbf{s}_h,\boldsymbol{\tau}_h)+(\mathbf{r}_h,\boldsymbol{\rho}_h)-(\mathbf{t}_h,\boldsymbol{\sigma}_h)),\mathbf{u}-\mathbf{u}_h].\end{aligned}$$

In turn, it follows from (3.38) that we can replace $\mathbf{u}_h$ by $\mathbf{v}_h \in V_h$ in the foregoing expression involving $\mathcal{B}_h$, and hence we obtain

$$\begin{aligned}
& C_{\mathrm{SM}} \, \|(\mathbf{s}_h, \boldsymbol{\tau}_h) + (\mathbf{r}_h, \boldsymbol{\rho}_h) - (\mathbf{t}_h, \boldsymbol{\sigma}_h)\|_{H_h}^2 \\
& \quad \leq \; [\mathcal{A}_h((\mathbf{s}_h, \boldsymbol{\tau}_h) + (\mathbf{r}_h, \boldsymbol{\rho}_h)) - \mathcal{A}_h(\mathbf{t}, \boldsymbol{\sigma}), (\mathbf{s}_h, \boldsymbol{\tau}_h) + (\mathbf{r}_h, \boldsymbol{\rho}_h) - (\mathbf{t}_h, \boldsymbol{\sigma}_h)] \\
& \qquad - \; [\mathcal{B}_h((\mathbf{s}_h, \boldsymbol{\tau}_h) + (\mathbf{r}_h, \boldsymbol{\rho}_h) - (\mathbf{t}_h, \boldsymbol{\sigma}_h)), \mathbf{u} - \mathbf{v}_h] \\
& \quad \leq \; C_{\mathrm{LC}} \, \|(\mathbf{s}_h, \boldsymbol{\tau}_h) + (\mathbf{r}_h, \boldsymbol{\rho}_h) - (\mathbf{t}, \boldsymbol{\sigma})\|_{H_h} \, \|(\mathbf{s}_h + \mathbf{r}_h, \boldsymbol{\tau}_h + \boldsymbol{\rho}_h) - (\mathbf{t}_h, \boldsymbol{\sigma}_h)\|_{H_h} \\
& \qquad + \; \|\mathcal{B}_h\| \, \|(\mathbf{s}_h, \boldsymbol{\tau}_h) + (\mathbf{r}_h, \boldsymbol{\rho}_h) - (\mathbf{t}_h, \boldsymbol{\sigma}_h)\|_{H_h} \, \|\mathbf{u} - \mathbf{v}_h\|_{0,\Omega},
\end{aligned}$$

which yields

$$\|(\mathbf{s}_h, \boldsymbol{\tau}_h) + (\mathbf{r}_h, \boldsymbol{\rho}_h) - (\mathbf{t}_h, \boldsymbol{\sigma}_h)\|_{H_h} \;\; \leq \;\; \frac{C_{\mathrm{LC}}}{C_{\mathrm{SM}}} \|(\mathbf{t}, \boldsymbol{\sigma}) - (\mathbf{s}_h, \boldsymbol{\tau}_h) - (\mathbf{r}_h, \boldsymbol{\rho}_h)\|_{H_h} + \frac{\|\mathcal{B}_h\|}{C_{\mathrm{SM}}} \|\mathbf{u} - \mathbf{v}_h\|_{0,\Omega}.$$

Thus, by triangle inequality we deduce that

$$\begin{aligned}
\|(\mathbf{t}, \boldsymbol{\sigma}) - (\mathbf{t}_h, \boldsymbol{\sigma}_h)\|_{H_h} \; & \leq \; \|(\mathbf{t}, \boldsymbol{\sigma}) - (\mathbf{s}_h, \boldsymbol{\tau}_h) - (\mathbf{r}_h, \boldsymbol{\rho}_h)\|_{H_h} + \|(\mathbf{s}_h, \boldsymbol{\tau}_h) + (\mathbf{r}_h, \boldsymbol{\rho}_h) - (\mathbf{t}_h, \boldsymbol{\sigma}_h)\|_{H_h} \\
& \leq \; \left(1 + \frac{C_{\mathrm{LC}}}{C_{\mathrm{SM}}}\right) \|(\mathbf{t}, \boldsymbol{\sigma}) - (\mathbf{s}_h, \boldsymbol{\tau}_h) - (\mathbf{r}_h, \boldsymbol{\rho}_h)\|_{H_h} \; + \; \frac{\|\mathcal{B}_h\|}{C_{\mathrm{SM}}} \, \|\mathbf{u} - \mathbf{v}_h\|_{0,\Omega} \\
& \leq \; \left(1 + \frac{C_{\mathrm{LC}}}{C_{\mathrm{SM}}}\right) \|(\mathbf{t}, \boldsymbol{\sigma}) - (\mathbf{s}_h, \boldsymbol{\tau}_h)\|_{H_h} \; + \; \left(1 + \frac{C_{\mathrm{LC}}}{C_{\mathrm{SM}}}\right) \|(\mathbf{r}_h, \boldsymbol{\rho}_h)\|_{H_h} \; + \; \frac{\|\mathcal{B}_h\|}{C_{\mathrm{SM}}} \|\mathbf{u} - \mathbf{v}_h\|_{0,\Omega},
\end{aligned}$$

which, together with (3.37) and the fact that $(\mathbf{s}_h, \boldsymbol{\tau}_h) \in H_h$ and $\mathbf{v}_h \in V_h$ are arbitrary, imply

$$\begin{aligned}
\|(\mathbf{t}, \boldsymbol{\sigma}) - (\mathbf{t}_h, \boldsymbol{\sigma}_h)\|_{H_h} \; & \leq \; \left(1 + \frac{C_{\mathrm{LC}}}{C_{\mathrm{SM}}}\right) \left(1 + \frac{\|\mathcal{B}_h\|}{C_{\inf}}\right) \inf_{(\mathbf{s}_h, \boldsymbol{\tau}_h) \in H_h} \|(\mathbf{t}, \boldsymbol{\sigma}) - (\mathbf{s}_h, \boldsymbol{\tau}_h)\|_{H_h} \\
& + \frac{\|\mathcal{B}_h\|}{C_{\mathrm{SM}}} \inf_{\mathbf{v}_h \in V_h} \|\mathbf{u} - \mathbf{v}_h\|_{0,\Omega} + \left(1 + \frac{C_{\mathrm{LC}}}{C_{\mathrm{SM}}}\right) \left(\frac{\|\mathcal{S}_h\| + \|\mathcal{C}_h\|}{C_{\inf}}\right) \|\mathbf{u} - \mathbf{u}_h\|_{0,\Omega}.
\end{aligned} \tag{3.39}$$

On the other hand, using the inf-sup condition for $\mathcal{B}_h$, (3.34a), and the Lipschitz-continuity of $\mathcal{A}_h$, we find that for each $\mathbf{v}_h \in V_h$ there holds

$$\begin{aligned}
C_{\inf} \, \|\mathbf{v}_h - \mathbf{u}_h\|_{0,\Omega} \;\; & \leq \;\; \sup_{\substack{(\mathbf{s}_h, \boldsymbol{\tau}_h) \in H_h \\ (\mathbf{s}_h, \boldsymbol{\tau}_h) \neq \mathbf{0}}} \frac{[\mathcal{B}_h(\mathbf{s}_h, \boldsymbol{\tau}_h), \mathbf{v}_h - \mathbf{u}_h]}{\|(\mathbf{s}_h, \boldsymbol{\tau}_h)\|_{H_h}} \\
& = \;\; \sup_{\substack{(\mathbf{s}_h, \boldsymbol{\tau}_h) \in H_h \\ (\mathbf{s}_h, \boldsymbol{\tau}_h) \neq \mathbf{0}}} \frac{[\mathcal{B}_h(\mathbf{s}_h, \boldsymbol{\tau}_h), \mathbf{v}_h - \mathbf{u}] \; + \; [\mathcal{B}_h(\mathbf{s}_h, \boldsymbol{\tau}_h), \mathbf{u} - \mathbf{u}_h]}{\|(\mathbf{s}_h, \boldsymbol{\tau}_h)\|_{H_h}} \\
& = \;\; \sup_{\substack{(\mathbf{s}_h, \boldsymbol{\tau}_h) \in H_h \\ (\mathbf{s}_h, \boldsymbol{\tau}_h) \neq \mathbf{0}}} \frac{[\mathcal{B}_h(\mathbf{s}_h, \boldsymbol{\tau}_h), \mathbf{v}_h - \mathbf{u}] \; - \; [\mathcal{A}_h(\mathbf{t}, \boldsymbol{\sigma}) - \mathcal{A}_h(\mathbf{t}_h, \boldsymbol{\sigma}_h), (\mathbf{s}_h, \boldsymbol{\tau}_h)]}{\|(\mathbf{s}_h, \boldsymbol{\tau}_h)\|_{H_h}} \\
& \leq \;\; \|\mathcal{B}_h\| \, \|\mathbf{u} - \mathbf{v}_h\|_{0,\Omega} \; + \; C_{\mathrm{LC}} \, \|(\mathbf{t}, \boldsymbol{\sigma}) - (\mathbf{t}_h, \boldsymbol{\sigma}_h)\|_{H_h},
\end{aligned}$$

which, together with an application of the triangle inequality, gives

$$\|\mathbf{u} - \mathbf{u}_h\|_{0,\Omega} \;\; \leq \;\; \left(1 + \frac{\|\mathcal{B}_h\|}{C_{\inf}}\right) \inf_{\mathbf{v}_h \in V_h} \|\mathbf{u} - \mathbf{v}_h\|_{0,\Omega} \; + \; \frac{C_{\mathrm{LC}}}{C_{\inf}} \, \|(\mathbf{t}, \boldsymbol{\sigma}) - (\mathbf{t}_h, \boldsymbol{\sigma}_h)\|_{H_h}. \tag{3.40}$$

Next, by substituting (3.39) into (3.40), we arrive at

$$\begin{aligned}
\|\mathbf{u} - \mathbf{u}_h\|_{0,\Omega} \;\; \leq \;\; & \left(1 + \frac{C_{\mathrm{LC}}}{C_{\mathrm{SM}}}\right) \left(\frac{C_{\mathrm{LC}}}{C_{\inf}}\right) \left(1 + \frac{\|\mathcal{B}_h\|}{C_{\inf}}\right) \inf_{(\mathbf{s}_h, \boldsymbol{\tau}_h) \in H_h} \|(\mathbf{t}, \boldsymbol{\sigma}) - (\mathbf{s}_h, \boldsymbol{\tau}_h)\|_{H_h} \\
& + \; \left\{1 + \left(1 + \frac{C_{\mathrm{LC}}}{C_{\mathrm{SM}}}\right) \frac{\|\mathcal{B}_h\|}{C_{\inf}}\right\} \inf_{\mathbf{v}_h \in V_h} \|\mathbf{u} - \mathbf{v}_h\|_{0,\Omega} \\
& + \; \left(1 + \frac{C_{\mathrm{LC}}}{C_{\mathrm{SM}}}\right) \left(\frac{C_{\mathrm{LC}}}{C_{\inf}}\right) \left(\frac{\|\mathcal{S}_h\| + \|\mathcal{C}_h\|}{C_{\inf}}\right) \|\mathbf{u} - \mathbf{u}_h\|_{0,\Omega}.
\end{aligned}$$

In turn, we know from Lemma 3.11 that $\|\mathcal{S}_h\| \le \tau \widehat{C}_1$ and $\|\mathcal{C}_h\| \le 2\tau \widehat{C}_1^2$, and hence, recalling that $\tau < \frac{1}{\vartheta}$, we deduce that

$$\left(1 + \frac{C_{\rm LC}}{C_{\rm SM}}\right)\left(\frac{C_{\rm LC}}{C_{\rm inf}}\right)\left(\frac{\|\mathcal{S}_h\| + \|\mathcal{C}_h\|}{C_{\rm inf}}\right) \;\le\; \left(1 + \frac{C_{\rm LC}}{C_{\rm SM}}\right)\left(\frac{C_{\rm LC}}{C_{\rm inf}}\right)\left(\frac{\widehat{C}_1 + 2\widehat{C}_1^2}{C_{\rm inf}}\right)\tau \;<\; \frac{1}{2},$$

which allows to conclude from the previous inequality that

$$\begin{aligned} \|\mathbf{u} - \mathbf{u}_h\|_{0,\Omega} \;\le\; & 2\left(1 + \frac{C_{\rm LC}}{C_{\rm SM}}\right)\left(\frac{C_{\rm LC}}{C_{\rm inf}}\right)\left(1 + \frac{\|\mathcal{B}_h\|}{C_{\rm inf}}\right) \inf_{(\mathbf{s}_h,\boldsymbol{\tau}_h)\in H_h} \|(\mathbf{t},\boldsymbol{\sigma}) - (\mathbf{s}_h,\boldsymbol{\tau}_h)\|_{H_h} \\ & + 2\left\{1 + \left(1 + \frac{C_{\rm LC}}{C_{\rm SM}}\right)\frac{\|\mathcal{B}_h\|}{C_{\rm inf}}\right\} \inf_{\mathbf{v}_h\in V_h} \|\mathbf{u} - \mathbf{v}_h\|_{0,\Omega}. \end{aligned} \tag{3.41}$$

Finally, it is easy to see that (3.39) and (3.41) provide (3.35) and (3.36), thus finishing the proof. □

Next, in order to provide the rate of convergence of the discontinuous Galerkin scheme (3.10), we need the approximation properties of the finite element subspaces involved. For this purpose, given $T \in \mathcal{T}_h$, we let $\boldsymbol{\mathcal{P}}_T^k : \mathbb{L}^2(T) \to \mathbb{P}_k(T)$ and $\mathcal{P}_T^{k-1} : \mathbf{L}^2(T) \to \mathbf{P}_{k-1}(T)$ be the $\mathbb{L}^2(T)$ and $\mathbf{L}^2(T)$ – orthogonal projectors, respectively. It is well known (see, e.g. [37, 71]) that for each $\mathbf{s} \in \mathbb{H}^\ell(T)$ and $\mathbf{v} \in \mathbf{H}^{\ell+1}(T)$ there holds

$$\|\mathbf{s} - \boldsymbol{\mathcal{P}}_T^k(\mathbf{s})\|_{0,T} \;\le\; C h_T^{\min\{\ell,k+1\}} |\mathbf{s}|_{\ell,T} \quad \forall\, T \in \mathcal{T}_h, \tag{3.42}$$

and

$$\|\mathbf{v} - \mathcal{P}_T^{k-1}(\mathbf{v})\|_{0,T} \;\le\; C h_T^{\min\{\ell+1,k\}} |\mathbf{v}|_{\ell+1,T} \quad \forall\, T \in \mathcal{T}_h. \tag{3.43}$$

On the other hand, let $\Pi_T^{k-1} : \mathbb{H}^1(T) \to \mathbb{P}_k(T)$ be the Raviart-Thomas interpolation operator (see [19, 71, 116]), which satisfies the approximation property

$$\|\boldsymbol{\tau} - \Pi_T^{k-1}(\boldsymbol{\tau})\|_{\mathbf{div},T} \;\le\; C h_T^{\min\{\ell,k\}} \Big\{ |\boldsymbol{\tau}|_{\ell,T} \;+\; |\mathbf{div}(\boldsymbol{\tau})|_{\ell,T} \Big\} \quad \forall\, T \in \mathcal{T}_h, \tag{3.44}$$

and for each $\boldsymbol{\tau} \in \mathbb{H}^\ell(T)$ such that $\mathbf{div}(\boldsymbol{\tau}) \in \mathbf{H}^\ell(T)$, with $\ell \ge 1$. Moreover, the interpolation operator Π_T^{k-1} can also be defined as a bounded linear operator from the larger space $\mathbb{H}^\ell(T) \cap \mathbb{H}(\mathbf{div};T)$ into $\mathbb{P}_k(T)$ for all $\ell \in (0,1]$ (see, e.g. [96, Theorem 3.16]). In this case there holds the following interpolation error estimate (see [71, Lemma 3.19])

$$\|\boldsymbol{\tau} - \Pi_T^{k-1}(\boldsymbol{\tau})\|_{0,T} \;\le\; C h_T^{\ell} \Big\{ |\boldsymbol{\tau}|_{\ell,T} \;+\; \|\mathbf{div}(\boldsymbol{\tau})\|_{0,T} \Big\} \quad \forall\, T \in \mathcal{T}_h,$$

which, together with (3.44), implies for $\ell > 0$ that

$$\|\boldsymbol{\tau} - \Pi_T^{k-1}(\boldsymbol{\tau})\|_{\mathbf{div},T} \;\le\; C h_T^{\min\{\ell,k\}} \Big\{ |\boldsymbol{\tau}|_{\ell,T} \;+\; \|\mathbf{div}(\boldsymbol{\tau})\|_{\ell,T} \Big\} \quad \forall\, T \in \mathcal{T}_h.$$

On the other hand, observe that, given $Z := \{\boldsymbol{\tau} \in \mathbb{L}^2(\Omega) \,:\, \boldsymbol{\tau}|_T \in \mathbb{H}^\ell(T) \quad \forall\, T \in \mathcal{T}_h\}$, we can define $\Pi_{\Sigma_h} : \mathbb{H}(\mathbf{div};\Omega) \cap Z \to \Sigma_h$ by

$$\Pi_{\Sigma_h}(\boldsymbol{\tau})|_T \;:=\; \Pi_T^{k-1}(\boldsymbol{\tau}|_T) \;+\; d\,\mathbb{I} \quad \forall\, T \in \mathcal{T}_h,$$

with $d := -\frac{1}{n|\Omega|} \sum\limits_{T\in\mathcal{T}_h} \int_T \operatorname{tr}\Big(\Pi_T^{k-1}(\boldsymbol{\tau}|_T)\Big) \in \mathrm{R}$. Then, it is easy to prove that

$$\|\boldsymbol{\tau} - \Pi_{\Sigma_h}(\boldsymbol{\tau})\|_{\Sigma_h}^2 \;\le\; \sum_{T\in\mathcal{T}_h} \|\boldsymbol{\tau} - \Pi_T^{k-1}(\boldsymbol{\tau})\|_{\mathbf{div},T}^2 \quad \forall\, \boldsymbol{\tau} \in \mathbb{H}(\mathbf{div};\Omega) \cap Z,$$

and hence

$$\|\boldsymbol{\tau} - \Pi_{\Sigma_h}(\boldsymbol{\tau})\|_{\Sigma_h} \;\leq\; C \sum_{T\in\mathcal{T}_h} h_T^{\min\{\ell,k\}} \Big\{ |\boldsymbol{\tau}|_{\ell,T} \;+\; \|\mathbf{div}(\boldsymbol{\tau})\|_{\ell,T} \Big\}. \tag{3.45}$$

In this way, as a consequence of (3.42), (3.43), (3.45), and the usual interpolation estimates, we find that S_h, Σ_h and V_h satisfy the following approximation properties:

($\mathbf{AP}_h^{\mathbf{t}}$) For each $\ell \geq 0$ and for each $\mathbf{s} \in \mathbb{H}^\ell(\Omega)$ there exists $\mathbf{s}_h \in S_h$ such that

$$\|\mathbf{s} - \mathbf{s}_h\|_{0,\Omega} \;\leq\; C \sum_{T\in\mathcal{T}_h} h_T^{\min\{\ell,k+1\}} |\mathbf{s}|_{\ell,T}.$$

($\mathbf{AP}_h^{\boldsymbol{\sigma}}$) For each $\ell > 0$ and for each $\boldsymbol{\tau} \in \mathbb{H}^\ell(\Omega)$ with $\mathbf{div}(\boldsymbol{\tau}) \in \mathbf{H}^\ell(\Omega)$ there exists $\boldsymbol{\tau}_h \in \Sigma_h$ such that

$$\|\boldsymbol{\tau} - \boldsymbol{\tau}_h\|_{\Sigma_h} \;\leq\; C \sum_{T\in\mathcal{T}_h} h_T^{\min\{\ell,k\}} \Big\{ |\boldsymbol{\tau}|_{\ell,T} \;+\; \|\mathbf{div}(\boldsymbol{\tau})\|_{\ell,T} \Big\}.$$

($\mathbf{AP}_h^{\mathbf{u}}$) For each $\ell \geq 0$ and for each $\mathbf{v} \in \mathbf{H}^\ell(\Omega)$ there exists $\mathbf{v}_h \in V_h$ such that

$$\|\mathbf{v} - \mathbf{v}_h\|_{0,\Omega} \;\leq\; C \sum_{T\in\mathcal{T}_h} h_T^{\min\{\ell+1,k\}} |\mathbf{v}|_{\ell+1,T}.$$

The following theorem establishes the theoretical rates of convergence of the discrete scheme (3.10), under suitable regularity assumptions on the exact solution.

Theorem 3.3. *Assume the same hypotheses of Lemma* 3.13. *In addition, suppose that there exists an integer $\ell > 0$ such that $\mathbf{t}|_T \in \mathbb{H}^\ell(T)$, $\boldsymbol{\sigma}|_T \in \mathbb{H}^\ell(T)$, $\mathbf{div}(\boldsymbol{\sigma}|_T) \in \mathbf{H}^\ell(T)$ and $\mathbf{u}|_T \in \mathbf{H}^{\ell+1}(T)$, for all $T \in \mathcal{T}_h$. Then, there exists $C > 0$, independent of h and the polynomial approximation degree k, such that*

$$\begin{aligned} &\|\mathbf{t} - \mathbf{t}_h\|_{0,\Omega} \;+\; \|\boldsymbol{\sigma} - \boldsymbol{\sigma}_h\|_{\Sigma_h} \;+\; \|\mathbf{u} - \mathbf{u}_h\|_{0,\Omega} \\ &\quad\leq\; C \sum_{T\in\mathcal{T}_h} h_T^{\min\{\ell,k\}} \Big\{ |\mathbf{t}|_{\ell,T} \;+\; |\boldsymbol{\sigma}|_{\ell,T} \;+\; \|\mathbf{div}(\boldsymbol{\sigma})\|_{\ell,T} \;+\; |\mathbf{u}|_{\ell+1,T} \Big\}. \end{aligned}$$

Proof. It follows from the Céa estimate (cf. Lemma 3.13) and the approximation properties ($\mathbf{AP}_h^{\mathbf{t}}$), ($\mathbf{AP}_h^{\boldsymbol{\sigma}}$) and ($\mathbf{AP}_h^{\mathbf{u}}$). □

Note from the previous theorem and (3.20) that we can also conclude that

$$\|\boldsymbol{\sigma} - \boldsymbol{\sigma}_h\|_{0,\Omega} \;\;\leq\;\; C \sum_{T\in\mathcal{T}_h} h_T^{\min\{\ell,k\}} \Big\{ |\mathbf{t}|_{\ell,T} + |\boldsymbol{\sigma}|_{\ell,T} + \|\mathbf{div}(\boldsymbol{\sigma})\|_{\ell,T} + |\mathbf{u}|_{\ell+1,T} \Big\}. \tag{3.46}$$

Furthermore, we know from (3.2) that $p = -\frac{1}{n}\mathrm{tr}\,(\boldsymbol{\sigma})$, which suggests to define the following postprocessed approximation of the pressure:

$$p_h \;:=\; -\frac{1}{n}\,\mathrm{tr}\,(\boldsymbol{\sigma}_h) \quad \text{in} \quad \Omega\,,$$

and therefore

$$\|p - p_h\|_{0,\Omega} \;\;=\;\; \frac{1}{n}\|\mathrm{tr}\,(\boldsymbol{\sigma} - \boldsymbol{\sigma}_h)\,\|_{0,\Omega} \;\leq\; \frac{1}{\sqrt{n}}\,\|\boldsymbol{\sigma} - \boldsymbol{\sigma}_h\|_{0,\Omega}, \tag{3.47}$$

which, thanks to (3.46), gives the *a priori* error estimate for the pressure.

Now, as in [43], we measure the errors of quantities defined on $\partial\mathcal{T}_h$ with the seminorm:

$$\|\boldsymbol{\mu}\|_h \;:=\; \left\{\sum_{T\in\mathcal{T}_h} h_T\|\boldsymbol{\mu}\|_{0,\partial T}^2\right\}^{1/2},$$

and we let $\Pi_{\mathcal{E}_h}:\mathbf{L}^2(\mathcal{E}_h)\to\mathbf{P}_k(\mathcal{E}_h)$ be the orthogonal projection onto the space of piecewise polynomials of degree less than or equals to k on $\mathcal{E}_h$. Next, we end this section with the *a priori* error estimate for the trace of the velocity unknown, which is established next.

Theorem 3.4. *Assume the same hypotheses of Theorem* 3.3*. Then, there exists* $C>0$*, independent of* h *and the polynomial approximation degree* k*, such that*

$$\|\Pi_{\mathcal{E}_h}(\mathbf{u})-\widehat{\mathbf{u}}_h\|_h \;\leq\; C\sum_{T\in\mathcal{T}_h} h_T^{\min\{\ell,k\}}\left\{|\mathbf{t}|_{\ell,T}+|\boldsymbol{\sigma}|_{\ell,T}+\|\mathbf{div}(\boldsymbol{\sigma})\|_{\ell,T}+|\mathbf{u}|_{\ell+1,T}\right\}.$$

Proof. Since $\Pi_{\mathcal{E}_h}(\mathbf{u})=\Pi_\Gamma(\mathbf{g})=\widehat{\mathbf{u}}_h$ on $\mathcal{E}_h^\partial$, we only need to compute the error for each $F\in\mathcal{E}_h^i$. In fact, we have

$$\begin{aligned}
\|\Pi_{\mathcal{E}_h}(\mathbf{u})-\widehat{\mathbf{u}}_h\|_h^2 \;&=\; \sum_{T\in\mathcal{T}_h}\sum_{F\in\partial T\setminus\Gamma} h_T\|\Pi_{\mathcal{E}_h}(\mathbf{u})-\boldsymbol{\lambda}_h\|_{0,F}^2\\
&\leq\; \widetilde{C}\sum_{T\in\mathcal{T}_h}\sum_{F\in\partial T\setminus\Gamma}\mathtt{h}\|\Pi_{\mathcal{E}_h}(\mathbf{u})-\boldsymbol{\lambda}_h\|_{0,F}^2 \;=\; 2\widetilde{C}\sum_{F\in\mathcal{E}_h^i}\mathtt{h}\|\Pi_{\mathcal{E}_h}(\mathbf{u})-\boldsymbol{\lambda}_h\|_{0,F}^2,
\end{aligned}$$

with $\widetilde{C}\geq 1$ depending only on the shape regularity of the mesh. Then, according to (3.9), (3.19) and the fact that $[\![\boldsymbol{\sigma}]\!]=\mathbf{0}$ on $\mathcal{E}_h^i$, we obtain that

$$\begin{aligned}
\|\Pi_{\mathcal{E}_h}(\mathbf{u})-\widehat{\mathbf{u}}_h\|_h^2 \;&\leq\; 2\widetilde{C}\sum_{F\in\mathcal{E}_h^i}\mathtt{h}\left\|\Pi_{\mathcal{E}_h}(\mathbf{u})-\{\!\{\mathbf{u}_h\}\!\}+\frac{1}{2}(\tau\mathtt{h})^{-1}[\![\boldsymbol{\sigma}_h]\!]\right\|_{0,F}^2\\
&\leq\; C\sum_{F\in\mathcal{E}_h^i}\left\{\|\mathtt{h}^{1/2}\left(\Pi_{\mathcal{E}_h}(\mathbf{u})-\{\!\{\mathbf{u}_h\}\!\}\right)\|_{0,F}^2+\frac{1}{4\tau}\|(\tau\mathtt{h})^{-1/2}[\![\boldsymbol{\sigma}-\boldsymbol{\sigma}_h]\!]\|_{0,F}^2\right\}\\
&\leq\; C\left\{\|\mathtt{h}^{1/2}\left(\Pi_{\mathcal{E}_h}(\mathbf{u})-\{\!\{\mathbf{u}_h\}\!\}\right)\|_{0,\mathcal{E}_h^i}^2 \;+\; \|\boldsymbol{\sigma}-\boldsymbol{\sigma}_h\|_{\Sigma_h}^2\right\}\\
&\leq\; C\left\{\|\mathtt{h}^{1/2}\Pi_{\mathcal{E}_h}(\mathbf{u}-\boldsymbol{\mathcal{P}}_{1,h}^k(\mathbf{u}))\|_{0,\mathcal{E}_h^i}^2 \;+\; \|\mathtt{h}^{1/2}\{\!\{\boldsymbol{\mathcal{P}}_{1,h}^k(\mathbf{u})-\mathbf{u}_h\}\!\}\|_{0,\mathcal{E}_h^i}^2 \;+\; \|\boldsymbol{\sigma}-\boldsymbol{\sigma}_h\|_{\Sigma_h}^2\right\},
\end{aligned}\tag{3.48}$$

where, denoting $\mathbf{X}_h^k:=\left\{\mathbf{v}_h\in\mathbf{C}(\bar\Omega)\;:\;\mathbf{v}_h|_T\in\mathbf{P}_k(T)\quad\forall\,T\in\mathcal{T}_h\right\}$, we let $\boldsymbol{\mathcal{P}}_{1,h}^k:\mathbf{H}^1(\Omega)\to\mathbf{X}_h^k$ be the orthogonal projector, which satisfies

$$\|\mathbf{v}-\boldsymbol{\mathcal{P}}_{1,h}^k(\mathbf{v})\|_{1,\Omega} \;\leq\; C_1\sum_{T\in\mathcal{T}_h} h_T^{\min\{\ell,k\}}|\mathbf{v}|_{\ell+1,T}\quad\forall\,\mathbf{v}\in\mathbf{H}^{\ell+1}(T),\quad\forall\,T\in\mathcal{T}_h \tag{3.49}$$

and

$$\|\mathbf{v}-\boldsymbol{\mathcal{P}}_{1,h}^k(\mathbf{v})\|_{0,\Omega} \;\leq\; C_0\sum_{T\in\mathcal{T}_h} h_T^{\min\{\ell+1,k+1\}}|\mathbf{v}|_{\ell+1,T}\quad\forall\,\mathbf{v}\in\mathbf{H}^{\ell+1}(T),\quad\forall\,T\in\mathcal{T}_h, \tag{3.50}$$

for $k\geq 1$ (see [71, Chapter 4] for details). Next, applying that $\|\Pi_{\mathcal{E}_h}\|\leq 1$ in the first term of (3.48), we find that

$$\|\Pi_{\mathcal{E}_h}(\mathbf{u})-\widehat{\mathbf{u}}_h\|_h \;\leq\; C\left\{\|\mathtt{h}^{1/2}(\mathbf{u}-\boldsymbol{\mathcal{P}}_{1,h}^k(\mathbf{u}))\|_{0,\mathcal{E}_h^i} \;+\; \|\mathtt{h}^{1/2}\{\!\{\boldsymbol{\mathcal{P}}_{1,h}^k(\mathbf{u})-\mathbf{u}_h\}\!\}\|_{0,\mathcal{E}_h^i} \;+\; \|\boldsymbol{\sigma}-\boldsymbol{\sigma}_h\|_{\Sigma_h}\right\}.$$

Consequently, using (3.16) and the analogue of the part $i)$ of Lemma 3.10 with $\mathbf{P}_k(\mathcal{T}_h)$ instead of V_h, we deduce that

$$\begin{aligned} \|\Pi_{\mathcal{E}_h}(\mathbf{u}) - \widehat{\mathbf{u}}_h\|_h &\leq C\Big\{\|\mathbf{u} - \boldsymbol{\mathcal{P}}_{1,h}^k(\mathbf{u})\|_{1,\Omega} \,+\, \|\boldsymbol{\mathcal{P}}_{1,h}^k(\mathbf{u}) - \mathbf{u}_h\|_{0,\Omega} \,+\, \|\boldsymbol{\sigma} - \boldsymbol{\sigma}_h\|_{\Sigma_h}\Big\} \\ &\leq C\Big\{\|\mathbf{u} - \boldsymbol{\mathcal{P}}_{1,h}^k(\mathbf{u})\|_{1,\Omega} \,+\, \|\mathbf{u} - \boldsymbol{\mathcal{P}}_{1,h}^k(\mathbf{u})\|_{0,\Omega} \,+\, \|\mathbf{u} - \mathbf{u}_h\|_{0,\Omega} \,+\, \|\boldsymbol{\sigma} - \boldsymbol{\sigma}_h\|_{\Sigma_h}\Big\}, \end{aligned}$$

which, together with (3.49), (3.50) and Theorem 3.3, complete the proof. □

3.5 Implementation considerations

In this section we describe some general aspects on the computational implementation of the discrete scheme proposed in Section 3.2. We remark that we refer to the original HDG system (3.8) since, as explained before, the equivalent reduced scheme given by (3.10) was introduced just for sake of the analysis. We begin by considering again problem (3.8) in a single element $T \in \mathcal{T}_h$ with Dirichlet's datum $\mathbf{g} = \mathbf{0}$ (as is usual, the boundary condition can be imposed later), that is

$$\begin{aligned} \int_T \boldsymbol{\psi}(\mathbf{t}_h) : \mathbf{s}_h - \int_T \mathbf{s}_h : \boldsymbol{\sigma}_h^{\mathrm{d}} &= 0, \\ \int_T \Big\{\mathbf{t}_h - \kappa_1\boldsymbol{\psi}(\mathbf{t}_h)\Big\} : \boldsymbol{\tau}_h^{\mathrm{d}} + \Big\{\kappa_1 \int_T \boldsymbol{\sigma}_h^{\mathrm{d}} : \boldsymbol{\tau}_h^{\mathrm{d}} + \kappa_2 \int_T \mathbf{div}(\boldsymbol{\sigma}_h)\cdot\mathbf{div}(\boldsymbol{\tau}_h)\Big\} & \\ + \int_T \mathbf{u}_h \cdot \mathbf{div}(\boldsymbol{\tau}_h) - \int_{\partial T} \boldsymbol{\tau}_h\boldsymbol{\nu}\cdot\boldsymbol{\lambda}_h &= -\kappa_2\int_T \mathbf{f}\cdot\mathbf{div}(\boldsymbol{\tau}_h), \\ -\int_T \mathbf{v}_h\cdot\mathbf{div}(\boldsymbol{\sigma}_h) + \int_{\partial T}\mathbf{S}\mathbf{u}_h\cdot\mathbf{v}_h - \int_{\partial T}\mathbf{S}\boldsymbol{\lambda}_h\cdot\mathbf{v}_h &= \int_T \mathbf{f}\cdot\mathbf{v}_h, \\ -\int_{\partial T}\boldsymbol{\sigma}_h\boldsymbol{\nu}\cdot\boldsymbol{\mu}_h + \int_{\partial T}\mathbf{S}\mathbf{u}_h\cdot\boldsymbol{\mu}_h - \int_{\partial T}\mathbf{S}\boldsymbol{\lambda}_h\cdot\boldsymbol{\mu}_h &= 0, \end{aligned}$$

for all $(\mathbf{s}_h, \boldsymbol{\tau}_h, \mathbf{v}_h, \boldsymbol{\mu}_h) \in \mathbb{P}_k(T)\times\mathbb{P}_k(T)\times\mathbf{P}_{k-1}(T)\times\mathbf{P}_k(\partial T)$.

Note that, because of the null mean value condition of the trace of $\boldsymbol{\sigma}_h$, that is $\int_\Omega \mathrm{tr}\,(\boldsymbol{\sigma}_h) = 0$, we can not establish the value of $\boldsymbol{\sigma}_h|_T$ only with the information from T (as it is natural in discontinuous Galerkin schemes). For that reason, and in order to rewrite the above local contribution in an equivalent form, we now define the local space

$$\Sigma_{h,0}(T) \;:=\; \Big\{\boldsymbol{\tau}\in\mathbb{P}_k(T) \;:\; \int_T \mathrm{tr}\,(\boldsymbol{\tau}) = 0\Big\},$$

for which there holds $\mathbb{P}_k(T) = \Sigma_{h,0}(T)\oplus \mathrm{P}_0(T)\mathbb{I}$, where $\mathbb{I}\in\mathrm{R}^{n\times n}$ is the identity matrix. Next, given $\boldsymbol{\sigma}_h, \boldsymbol{\tau}_h \in S_h$, we consider the local decomposition

$$\boldsymbol{\sigma}_h|_T \;=\; \widetilde{\boldsymbol{\sigma}}_h|_T \,+\, \rho_h|_T\,\mathbb{I} \quad\text{and}\quad \boldsymbol{\tau}_h|_T \;=\; \widetilde{\boldsymbol{\tau}}_h|_T \;+\; \zeta_h|_T\,\mathbb{I} \quad \forall\, T\in\mathcal{T}_h,$$

where $\widetilde{\boldsymbol{\sigma}}_h|_T,\ \widetilde{\boldsymbol{\tau}}_h|_T \in \Sigma_{h,0}(T),\ \ \rho_h|_T,\ \zeta_h|_T \in \mathrm{P}_0(T)$, and rewrite the above local contribution as

$$
\begin{aligned}
\int_T \boldsymbol{\psi}(\mathbf{t}_h) : \mathbf{s}_h - \int_T \mathbf{s}_h : \widetilde{\boldsymbol{\sigma}}_h^{\mathrm{d}} &= 0,\\
\int_T \Big\{\mathbf{t}_h - \kappa_1 \boldsymbol{\psi}(\mathbf{t}_h)\Big\} : \widetilde{\boldsymbol{\tau}}_h^{\mathrm{d}} + \Big\{\kappa_1 \int_T \widetilde{\boldsymbol{\sigma}}_h^{\mathrm{d}} : \widetilde{\boldsymbol{\tau}}_h^{\mathrm{d}} + \kappa_2 \int_T \mathbf{div}(\widetilde{\boldsymbol{\sigma}}_h)\cdot \mathbf{div}(\widetilde{\boldsymbol{\tau}}_h)\Big\} & \\
+ \int_T \mathbf{u}_h \cdot \mathbf{div}(\widetilde{\boldsymbol{\tau}}_h) - \int_{\partial T} \widetilde{\boldsymbol{\tau}}_h \boldsymbol{\nu}\cdot \boldsymbol{\lambda}_h &= -\kappa_2 \int_T \mathbf{f}\cdot \mathbf{div}(\widetilde{\boldsymbol{\tau}}_h),\\
-\int_T \mathbf{v}_h \cdot \mathbf{div}(\widetilde{\boldsymbol{\sigma}}_h) + \int_{\partial T} \mathbf{S}\mathbf{u}_h \cdot \mathbf{v}_h - \int_{\partial T} \mathbf{S}\boldsymbol{\lambda}_h \cdot \mathbf{v}_h &= \int_T \mathbf{f}\cdot \mathbf{v}_h,\\
-\int_{\partial T} \widetilde{\boldsymbol{\sigma}}_h \boldsymbol{\nu}\cdot \boldsymbol{\mu}_h + \int_{\partial T} \mathbf{S}\mathbf{u}_h \cdot \boldsymbol{\mu}_h - \int_{\partial T} \mathbf{S}\boldsymbol{\lambda}_h \cdot \boldsymbol{\mu}_h - \int_{\partial T} \rho_h \boldsymbol{\mu}_h \cdot \boldsymbol{\nu} &= 0,\\
-\int_{\partial T} \zeta_h \boldsymbol{\lambda}_h \cdot \boldsymbol{\nu} &= 0\,,
\end{aligned}
$$

for all $(\mathbf{s}_h, \widetilde{\boldsymbol{\tau}}_h, \mathbf{v}_h, \boldsymbol{\mu}_h, \zeta_h) \in \mathbb{P}_k(T) \times \Sigma_{h,0}(T) \times \mathbf{P}_{k-1}(T) \times \mathbf{P}_k(\partial T) \times \mathrm{P}_0(T)$. In addition, it is easy to see that the aforementioned condition on the trace of $\boldsymbol{\sigma}_h$ becomes

$$
\sum_{T\in\mathcal{T}_h} \rho_h|_T\,|T| \;=\; 0,
$$

which is imposed in the discrete system by means of a real Lagrange multiplier.

Then, applying the Newton-Raphson's method to the global nonlinear system, we translate the local contribution for the Newton's linear system in the mth iteration into the form

$$
\left(\begin{array}{ccc|cc}
\mathbf{DA}_1(\mathbf{t}_h^m) & \mathbf{B} & \mathbf{0} & \mathbf{0} & \mathbf{0}\\
-\mathbf{B}^T - \mathbf{DA}_2(\mathbf{t}_h^m) & \mathbf{H} & \mathbf{C} & -\mathbf{E} & \mathbf{0}\\
\mathbf{0} & -\mathbf{C}^T & \mathbf{K} & -\mathbf{F} & \mathbf{0}\\
\hline
\mathbf{0} & -\mathbf{E}^T & \mathbf{F}^T & -\mathbf{D} & \mathbf{G}\\
\mathbf{0} & \mathbf{0} & \mathbf{0} & \mathbf{G}^T & 0
\end{array}\right)
\left(\begin{array}{c}
\delta\mathbf{t}_h^m\\ \delta\widetilde{\boldsymbol{\sigma}}_h^m\\ \delta\mathbf{u}_h^m\\ \hline \delta\boldsymbol{\lambda}_h^m\\ \delta\rho_h^m
\end{array}\right)
=
\left(\begin{array}{c}
\mathbf{b}_1^m\\ \mathbf{b}_2^m\\ \mathbf{b}_3^m\\ \hline \mathbf{b}_4^m\\ \mathrm{b}_5^m
\end{array}\right),
$$

where $\delta\mathbf{t}_h^m$ corresponds to the mth update for the $\mathbf{t}_h$ variable, that is $\mathbf{t}_h^{m+1} = \mathbf{t}_h^m + \delta\mathbf{t}_h^m$, and similarly for the other variables. The discrete operators $\mathbf{DA}_i(\mathbf{r})$, $i \in \{1,2\}$, are the respective Gâteaux derivatives, given by

$$
[\mathbf{DA}_1(\mathbf{r})\mathbf{t},\mathbf{s}] \;:=\; \int_T \sum_{i,j,k,l=1}^{n} \frac{\partial}{\partial r_{kl}} \psi_{ij}(\mathbf{r}) t_{kl} s_{ij} \;=\; \int_T \frac{\mu'(|\mathbf{r}|)}{|\mathbf{r}|}(\mathbf{r}:\mathbf{t})(\mathbf{r}:\mathbf{s}) \;+\; \int_T \mu(|\mathbf{r}|)\mathbf{t}:\mathbf{s},
$$

and

$$
[\mathbf{DA}_2(\mathbf{r})\mathbf{t},\mathbf{s}] \;:=\; \kappa_1 [\mathbf{DA}_1(\mathbf{r})\mathbf{t},\mathbf{s}^{\mathrm{d}}],
$$

for all $\mathbf{r},\mathbf{t},\mathbf{s} \in \mathbb{L}^2(T)$, with $|\mathbf{r}| = \|\mathbf{r}\|_{\mathrm{R}^{n\times n}} \neq 0$. In turn, using the same notation given in [34], the operators $\mathbf{B}$, $\mathbf{C}$ and $\mathbf{H}$ are given as follows:

$$
\mathbf{B} \;:=\; \left[-\int_T \mathbf{s}:\boldsymbol{\tau}^{\mathrm{d}}\right] \;=\; -|\mathcal{J}_T| \begin{pmatrix} \frac{1}{2} & 0 & 0 & -\frac{1}{2}\\ 0 & 1 & 0 & 0\\ 0 & 0 & 1 & 0\\ -\frac{1}{2} & 0 & 0 & \frac{1}{2} \end{pmatrix} \otimes \mathbf{M},
$$

$$\mathbf{C} \;:=\; \left[\int_T \mathbf{v}\cdot\mathbf{div}(\boldsymbol{\tau})\right] \;=\; |\mathcal{J}_T|\,\mathbb{I}\otimes\left\{\begin{pmatrix}\partial_x\hat{x}\\ \partial_y\hat{x}\end{pmatrix}\otimes\mathbf{DX} \;+\; \begin{pmatrix}\partial_x\hat{y}\\ \partial_y\hat{y}\end{pmatrix}\otimes\mathbf{DY}\right\},$$

and

$$\begin{aligned}
\mathbf{H} \;&:=\; \left[\kappa_1\int_T \boldsymbol{\sigma}^{\mathrm{d}} : \boldsymbol{\tau}^{\mathrm{d}} + \kappa_2\int_T \mathbf{div}(\boldsymbol{\sigma})\cdot\mathbf{div}(\boldsymbol{\tau})\right]\\
&=\; -\kappa_1\mathbf{B} \;+\; |\mathcal{J}_T|\kappa_2\,\mathbb{I}\otimes\left\{\begin{pmatrix}(\partial_x\hat{x})^2 & \partial_x\hat{x}\partial_y\hat{x}\\ \partial_x\hat{x}\partial_y\hat{x} & (\partial_y\hat{x})^2\end{pmatrix}\otimes\mathbf{DXX} \;+\; \begin{pmatrix}\partial_x\hat{x}\partial_x\hat{y} & \partial_x\hat{x}\partial_y\hat{y}\\ \partial_y\hat{x}\partial_x\hat{y} & \partial_y\hat{x}\partial_y\hat{y}\end{pmatrix}\otimes\mathbf{DXY}\right.\\
&\qquad \left. +\; \begin{pmatrix}\partial_x\hat{x}\partial_x\hat{y} & \partial_x\hat{x}\partial_y\hat{y}\\ \partial_y\hat{x}\partial_x\hat{y} & \partial_y\hat{x}\partial_y\hat{y}\end{pmatrix}^T\otimes\mathbf{DXY}^T \;+\; \begin{pmatrix}(\partial_x\hat{y})^2 & \partial_x\hat{y}\partial_y\hat{y}\\ \partial_x\hat{y}\partial_y\hat{y} & (\partial_y\hat{y})^2\end{pmatrix}\otimes\mathbf{DYY}\right\},
\end{aligned}$$

where $\otimes$ is the Kronecker product, and given a basis $\{\hat{\varphi}_i\}$ of $\mathrm{P}_k(\hat{T})$, $\mathbf{M} := \left[\int_{\hat{T}}\hat{\varphi}_i\hat{\varphi}_j\right]$ is the mass matrix, $\mathbf{DX} := \left[\int_{\hat{T}}\hat{\varphi}_j\partial_{\hat{x}}\hat{\varphi}_i\right]$, $\mathbf{DY} := \left[\int_{\hat{T}}\hat{\varphi}_j\partial_{\hat{y}}\hat{\varphi}_i\right]$, $\mathbf{DXX} := \left[\int_{\hat{T}}\partial_{\hat{x}}\hat{\varphi}_i\partial_{\hat{x}}\hat{\varphi}_j\right]$, $\mathbf{DXY} := \left[\int_{\hat{T}}\partial_{\hat{x}}\hat{\varphi}_i\partial_{\hat{y}}\hat{\varphi}_j\right]$, and $\mathbf{DYY} := \left[\int_{\hat{T}}\partial_{\hat{y}}\hat{\varphi}_i\partial_{\hat{y}}\hat{\varphi}_j\right]$, all them precomputed on the reference cell $\hat{T}$. In particular, when $\{\hat{\varphi}_i\}$ is the Dubiner basis [57], we only need to delete the first column in the above definition of $\mathbf{B}$, the first row in $\mathbf{C}$ and the first row and the first column in $\mathbf{H}$, in order to hold the belonging to the space $\Sigma_{h,0}(T)$. All the other discrete operators can be calculated similarly as in [34].

It is important to note here that the local submatrix

$$\begin{pmatrix}\mathbf{DA}_1(\mathbf{t}_h^m) & \mathbf{B} & \mathbf{0}\\ -\mathbf{B}^T - \mathbf{DA}_2(\mathbf{t}_h^m) & \mathbf{H} & \mathbf{C}\\ \mathbf{0} & -\mathbf{C}^T & \mathbf{K}\end{pmatrix} \in \mathrm{R}^{(n^2d_q+(n^2d_q-1)+nd_u)\times(n^2d_q+(n^2d_q-1)+nd_u)},$$

with $d_q := \dim\mathrm{P}_k(T)$ and $d_u := \dim\mathrm{P}_{k-1}(T)$, is invertible when $\mu > 0$ and $|\mathbf{t}_h^m| \neq 0$. Then, as it is usual in the HDG methods, we can obtain the values of $\delta\mathbf{t}_h^m|_T$, $\delta\widetilde{\boldsymbol{\sigma}}_h^m|_T$ and $\delta\mathbf{u}_h^m|_T$ as functions of $\delta\boldsymbol{\lambda}_h^m|_T$ and $\delta\rho_h^m|_T$ (actually, they only depend on $\delta\boldsymbol{\lambda}_h^m|_T$). In other words, we can reduce the stencil of the global linear system on each iteration of the Newton's method.

Finally, we let

$$N_{\text{total}} \;:=\; (n^2d_q + n^2d_q + nd_u)\times(\#\text{ of element in }\mathcal{T}_h) \;+\; (nd_l)\times(\#\text{ of faces in }\mathcal{T}_h),$$

with $d_l := \dim\mathrm{P}_k(F)$, $F\in\partial T$, be the total number of degrees of freedom (without including those for the pressure). In other words, N_{total} is the total number of unknowns defining $\mathbf{t}_h$, $\boldsymbol{\sigma}_h$, $\mathbf{u}_h$ and $\boldsymbol{\lambda}_h$. On the other hand, we let

$$N_{\text{comp}} \;:=\; (nd_l)\times(\#\text{ of faces in }\mathcal{T}_h) \;+\; (\#\text{ of element in }\mathcal{T}_h) \;+\; 1$$

be the number of degrees of freedom effectively employed in the computations, i.e, the total number of unknowns defining $\boldsymbol{\lambda}_h$, ρ_h and the Lagrange multiplier.

3.6 Numerical results

In this section we present several numerical experiments illustrating the performance of the augmented HDG method introduced in Section 3.2. We set $\tau = 10^{-1}$ for each one of the 4 examples to be reported, which, as shown below, works fine in all the cases. An *a priori* verification of the hypotheses on τ in Lemma 3.13 would certainly require the explicit knowledge of all the constants involved, which, however, is rarely possible. On the other hand, we take the stabilization parameter $\kappa_1 = \frac{\alpha_0}{\gamma_0^2}$, which obviously satisfies the assumption $\kappa_1 \in \left(0, \frac{2\alpha_0}{\gamma_0^2}\right)$ in Lemma 3.6, and then, as suggested by the value of the strong monotonicity constant C_{SM} at the end of its proof, we simply choose $\kappa_2 = \frac{\kappa_1}{2}$. The corresponding nonlinear algebraic system arising from (3.8) is solved by the Newton method with a tolerance of 10^{-6} and taking as initial iteration the solution of the associated linear Stokes problem (four iterations were required to achieve the given tolerance in each example). Now, according to the definitions given in Section 3.5, we recall that N_{total} is the total number of degrees of freedom, and N_{comp} is the number of degrees of freedom involved in the implementation of the Newton's method. To this respect, and even though we understand that a meaningful comparison makes sense between the N_{comp} of two different methods, in Example 4 below we display the information concerning N_{comp} and N_{total} only to appreciate the reduction in the degrees of freedom provided by our method, which is one of the key aspects of the HDG approaches. We do not perform any comparison with other method since we are not aware of another HDG type procedure dealing with our nonlinear problem.

The numerical results presented below were obtained using a C++ code, which was developed following the same techniques from [34]. In turn, the linear systems are solved using the conjugate gradient method with a relative tolerance of 10^{-6}.

In Example 1 we follow [112, 43] and consider the linear Stokes problem given by the flow uncovered by Kovaszany [103]. This means that $\Omega := (-0.5, 1.5) \times (0, 2)$, $\mu = 0.1$, and the data $\mathbf{f}$ and $\mathbf{g}$ are chosen so that the exact solution is given by

$$\begin{aligned} \mathbf{u}(\mathbf{x}) &= \left(1 - \exp(\lambda x_1)\cos(2\pi x_2),\ \frac{\lambda}{2\pi}\exp(\lambda x_1)\sin(2\pi x_2)\right), \\ p(\mathbf{x}) &= \frac{1}{2}\exp(2\lambda x_1) - \frac{1}{8\lambda}\Big\{\exp(3\lambda) - \exp(-\lambda)\Big\}, \end{aligned}$$

for all $\mathbf{x} := (x_1, x_2)^{\mathrm{t}} \in \Omega$, where $\lambda := \frac{Re}{2} - \sqrt{\frac{Re^2}{4} + 4\pi^2}$ and $Re := \mu^{-1} = 10$ is the Reynolds number. It is easy to see in this linear case that $\alpha_0 = \gamma_0 = \mu$. Concerning the triangulations employed in our computations, we first consider seven meshes that are Cartesian refinements of a domain defined in terms of squares, and then we split each square into four congruent triangles.

In Example 2 we deal with the nonlinear version of Example 1. More precisely, we consider instead of $\mu = 0.1$ the kinematic viscosity function $\mu : \mathrm{R}^+ \to \mathrm{R}^+$ given by the Carreau law, that is $\mu(t) := \mu_0 + \mu_1(1 + t^2)^{(\beta-2)/2} \quad \forall\, t \in \mathrm{R}^+$, with $\mu_0 = \mu_1 = 0.5$ and $\beta = 1.5$. It is easy to check in this case that the assumptions (3.3) and (3.4) are satisfied with

$$\gamma_0 = \mu_0 + \mu_1\left\{\frac{|\beta - 2|}{2} + 1\right\} \quad \text{and} \quad \alpha_0 = \mu_0 .$$

Then, we let again $\Omega := (-0.5, 1.5) \times (0, 2)$, and choose the data $\mathbf{f}$ and $\mathbf{g}$ so that the exact solution is the same from Example 1. The set of triangulations utilized is also as in Example 1.

Next, in Example 3 we use the same nonlinearity μ from Example 2, consider the L-shaped domain $\Omega := (-1, 1)^2 \setminus [0, 1]^2$, and choose the data $\mathbf{f}$ and $\mathbf{g}$ so that the exact solution is given by

$$\begin{aligned} \mathbf{u}(\mathbf{x}) &= \Big(r^{2/3}\sin(\theta),\ -r^{2/3}\cos(\theta)\Big), \\ p(\mathbf{x}) &= \cos(x_1)\cos(x_2) - \sin^2(1), \end{aligned}$$

for all $\mathbf{x} := (x_1, x_2)^{\mathtt{t}} \in \Omega$, where $r := |\mathbf{x}| = \sqrt{x_1^2 + x_2^2}$ and $\theta := \arctan\left(\frac{x_2}{x_1}\right)$. We remark that $\nabla\mathbf{u}$ is singular at the origin, and hence lower rates of convergence are expected in our computations. The meshes are generated analogously to the previous examples.

Finally, in Example 4 we consider the three dimensional domain $\Omega := (0,1)^3$, and assume the same kinematic viscosity function μ from Examples 2 and 3. In addition, the data $\mathbf{f}$ and $\mathbf{g}$ are chosen so that the exact solution is given by

$$\mathbf{u}(\mathbf{x}) = \Big(x_1(\sin(2\pi x_3) - \sin(2\pi x_2)),\ x_2(\sin(2\pi x_1) - \sin(2\pi x_3)),\ x_3(\sin(2\pi x_2) - \sin(2\pi x_1))\Big),$$

$$p(\mathbf{x}) = x_1 x_2 x_3 \sin(2\pi x_1)\sin(2\pi x_2)\sin(2\pi x_3) + \frac{1}{8\pi^3},$$

for all $\mathbf{x} := (x_1, x_2, x_3)^{\mathtt{t}} \in \Omega$.

It is easy to check that $\mathbf{u}$ is divergence free and $\displaystyle\int_\Omega p = 0$ for each one of the aforedescribed examples.

It is important to remark here that we do not provide any postprocessing for the velocity $\mathbf{u}$ in the numerical results shown below. Nevertheless, we can report that we did perform some preliminary numerical experiments by using the postprocessing formulas given in [44], which yielded exactly the same order of $\mathbf{u}_h$, that is $\mathcal{O}(h^k)$, and hence no superconvergence was observed. The alternative formula given in [43] will be considered in a forthcoming related work.

In Tables 3.1 and 3.2 we summarize the convergence history of the augmented HDG method (3.8) as applied to Examples 1 and 2 for the polynomial degrees $k \in \{1, 2, 3\}$. We observe there, looking at the experimental rates of convergence, that the orders predicted for each k by Theorems 3.3 and 3.4, and estimates (3.46) and (3.47), are attained by all the unknowns for these smooth examples. Actually, the errors $\|\boldsymbol{\sigma} - \boldsymbol{\sigma}_h\|_{\Sigma_h}$ and $\|\mathbf{u} - \mathbf{u}_h\|_{0,\Omega}$ behave exactly as proved, whereas the remaining ones show higher orders of convergence. In particular, $\|\Pi_{\mathcal{E}_h}(\mathbf{u}) - \widehat{\mathbf{u}}_h\|_h$ presents a superconvergence phenomenon with two additional powers of h. In addition, it is interesting to notice that these numerical results provide the same rates of convergence obtained for the linear case in [43], and hence they might constitute numerical evidences supporting the conjecture that the *a priori* error estimates derived in the present chapter are not sharp. We plan to address this issue in a separate work. Nevertheless, as already mentioned at the beginning of Section 3.4, whether the projection-based error analysis developed in [43] will work or not in this nonlinear case is still an open problem.

Furthermore, preliminary numerical experiments for Example 2, using degree k instead of $k-1$ in the definition of the subspace V_h, showed that the convergence rates are the same of Table 3.2. Perhaps, the only advantages of this modification with respect to the approach of the present chapter are the possibility of using the polynomial degree $k = 0$ and the fact that the superconvergence behavior of the variable $\boldsymbol{\lambda}_h$ is recovered when $k = 1$. The above could very well mean that the restriction $k \geq 1$ and the degree $k-1$ for defining V_h are just technical assumptions of our analysis. On the other hand, even though the estimates given in Section 3.4 hold for τ small enough, the results provided in Table 3.3 for Example 2 insinuate the robustness of our method within a larger, but still limited, range of variability of this parameter. Indeed, we observe there that for fixed values of k and h, the errors of some variables behave pretty much of the same order when larger values of τ (up to $\tau = 10$) are employed. However, while for even larger values of the parameter such as $\tau \in \{100, 1000\}$ the method does not break down, we notice that in this case some errors begin to increase.

In Table 3.4 we summarize the convergence history of the augmented HDG method (3.8) as applied to Example 3 for the polynomial degrees $k \in \{1, 2, 3\}$. In this case, and because of the singularity at the origin of the exact solution, the theoretical orders of convergence are far to be attained. In fact, similarly as obtained in [34], $\|\mathbf{u}-\mathbf{u}_h\|_{0,\Omega}$ behaves as $\mathcal{O}(h^{\min\{k,4/3\}})$, whereas $\|\mathbf{t}-\mathbf{t}_h\|_{0,\Omega}=\mathcal{O}(h^{2/3})$. Also, $\|\boldsymbol{\sigma}-\boldsymbol{\sigma}_h\|_{0,\Omega}=\mathcal{O}(h^{2/3})$, $\|\Pi_{\mathcal{E}_h}(\mathbf{u})-\widehat{\mathbf{u}}_h\|_h=\mathcal{O}(h^{\min\{k,4/3\}})$, and thanks to (3.47), $\|p-p_h\|_{0,\Omega}=\mathcal{O}(h^{2/3})$ as well. Moreover, the behaviour of $\|\boldsymbol{\sigma}-\boldsymbol{\sigma}_h\|_{\Sigma_h}$ is explained by the fact that the *a priori* estimate for $\|\boldsymbol{\sigma}-\boldsymbol{\sigma}_h\|_{\Sigma_h}$ depends on the regularity of $\mathbf{div}(\boldsymbol{\sigma})$, which can be shown to belong precisely to $\mathbf{H}^{-1/3}(\Omega)$. A classical way of circumventing this drawback is the incorporation of an adaptive scheme based on *a posteriori* error estimates. This issue will also be addressed in a forthcoming paper.

On the other hand, in Table 3.5 we present the convergence history of the augmented HDG method (3.8) as applied to Example 4 for the polynomial degrees $k\in\{1,2,3\}$. The remarks in this case are exactly the same given above for Examples 1 and 2.

Finally, some components of the approximate and exact solutions for Examples 2, 3, and 4 are displayed in Figures 3.1–3.8. They all correspond to those obtained with the fourth mesh and for the polynomial degree k indicated in each case. Here we use the notations $\mathbf{t}_h=(t_{h,ij})_{i,j=1,n}$, $\boldsymbol{\sigma}_h=(\sigma_{h,ij})_{i,j=1,n}$, and $\mathbf{u}_h=(u_{h,i})_{i=1,n}$.

k	h	$\|\mathbf{t}-\mathbf{t}_h\|_{0,\Omega}$ error	order	$\|\boldsymbol{\sigma}-\boldsymbol{\sigma}_h\|_{0,\Omega}$ error	order	$\|\boldsymbol{\sigma}-\boldsymbol{\sigma}_h\|_{\Sigma_h}$ error	order	$\|\mathbf{u}-\mathbf{u}_h\|_{0,\Omega}$ error	order	$\|\Pi_{\mathcal{E}_h}(\mathbf{u})-\widehat{\mathbf{u}}_h\|_h$ error	order	$\|p-p_h\|_{0,\Omega}$ error	order
1	0.2000	1.14e-0	−−	3.03e-1	−−	5.11e-0	−−	4.77e-1	−−	9.21e-2	−−	1.98e-1	−−
	0.1333	5.27e-1	1.91	1.40e-1	1.90	3.51e-0	0.93	3.19e-1	1.00	3.49e-2	2.39	9.18e-2	1.90
	0.1000	3.01e-1	1.95	8.01e-2	1.95	2.66e-0	0.96	2.39e-1	1.00	1.81e-2	2.28	5.25e-2	1.95
	0.0800	1.94e-1	1.97	5.16e-2	1.97	2.14e-0	0.98	1.91e-1	1.00	1.11e-2	2.20	3.38e-2	1.97
	0.0667	1.35e-1	1.98	3.60e-2	1.98	1.79e-0	0.98	1.59e-1	1.00	7.49e-3	2.15	2.36e-2	1.98
	0.0571	9.97e-2	1.98	2.65e-2	1.98	1.53e-0	0.99	1.37e-1	1.00	5.41e-3	2.11	1.74e-2	1.98
	0.0500	7.65e-2	1.99	2.03e-2	1.99	1.34e-0	0.99	1.20e-1	1.00	4.10e-3	2.09	1.33e-2	1.99
2	0.2000	9.17e-2	−−	1.91e-2	−−	5.91e-1	−−	6.83e-2	−−	6.40e-3	−−	1.18e-2	−−
	0.1333	2.87e-2	2.86	5.97e-3	2.86	2.74e-1	1.90	3.02e-2	2.01	1.39e-3	3.77	3.70e-3	2.87
	0.1000	1.24e-2	2.91	2.58e-3	2.92	1.56e-1	1.95	1.70e-2	2.00	4.58e-4	3.85	1.60e-3	2.93
	0.0800	6.45e-3	2.94	1.33e-3	2.95	1.01e-1	1.97	1.09e-2	2.00	1.92e-4	3.89	8.26e-4	2.95
	0.0667	3.77e-3	2.95	7.77e-4	2.96	7.02e-2	1.98	7.54e-3	2.00	9.44e-5	3.91	4.81e-4	2.97
	0.0571	2.39e-3	2.96	4.92e-4	2.97	5.17e-2	1.98	5.54e-3	2.00	5.15e-5	3.92	3.04e-4	2.97
	0.0500	1.61e-3	2.96	3.31e-4	2.98	3.97e-2	1.99	4.24e-3	2.00	3.05e-5	3.93	2.04e-4	2.98
3	0.2000	5.81e-3	−−	1.20e-3	−−	5.04e-2	−−	7.31e-3	−−	2.57e-4	−−	7.45e-4	−−
	0.1333	1.20e-3	3.89	2.51e-4	3.87	1.56e-2	2.89	2.17e-3	3.00	3.64e-5	4.82	1.56e-4	3.86
	0.1000	3.87e-4	3.94	8.10e-5	3.93	6.71e-3	2.94	9.15e-4	3.00	8.91e-6	4.89	5.03e-5	3.93
	0.0800	1.60e-4	3.96	3.35e-5	3.95	3.46e-3	2.96	4.69e-4	3.00	2.97e-6	4.92	2.08e-5	3.95
	0.0667	7.76e-5	3.97	1.63e-5	3.97	2.01e-3	2.97	2.71e-4	3.00	1.21e-6	4.94	1.01e-5	3.97
	0.0571	4.20e-5	3.98	8.81e-6	3.98	1.27e-3	2.98	1.71e-4	3.00	5.62e-7	4.95	5.48e-6	3.98
	0.0500	2.47e-5	3.98	5.18e-6	3.98	8.53e-4	2.99	1.14e-4	3.00	2.90e-7	4.96	3.22e-6	3.98

Table 3.1: History of convergence for Example 1.

k	h	$\|\mathbf{t}-\mathbf{t}_h\|_{0,\Omega}$ error	order	$\|\boldsymbol{\sigma}-\boldsymbol{\sigma}_h\|_{0,\Omega}$ error	order	$\|\boldsymbol{\sigma}-\boldsymbol{\sigma}_h\|_{\Sigma_h}$ error	order	$\|\mathbf{u}-\mathbf{u}_h\|_{0,\Omega}$ error	order	$\|\Pi_{\mathcal{E}_h}(\mathbf{u})-\widehat{\mathbf{u}}_h\|_h$ error	order	$\|p-p_h\|_{0,\Omega}$ error	order
	0.2000	5.52e-1	−−	5.85e-1	−−	1.04e+1	−−	4.75e-1	−−	5.59e-2	−−	3.37e-1	−−
	0.1333	2.48e-1	1.97	2.64e-1	1.96	7.01e-0	0.98	3.17e-1	0.99	2.35e-2	2.14	1.53e-1	1.95
	0.1000	1.41e-1	1.98	1.50e-1	1.98	5.28e-0	0.99	2.38e-1	1.00	1.30e-2	2.07	8.64e-2	1.98
1	0.0800	9.02e-2	1.99	9.60e-2	1.99	4.23e-0	0.99	1.91e-1	1.00	8.19e-3	2.06	5.55e-2	1.99
	0.0667	6.28e-2	1.99	6.68e-2	1.99	3.53e-0	0.99	1.59e-1	1.00	5.65e-3	2.04	3.86e-2	1.99
	0.0571	4.62e-2	1.99	4.91e-2	1.99	3.03e-0	1.00	1.36e-1	1.00	4.13e-3	2.03	2.84e-2	1.99
	0.0500	3.54e-2	1.99	3.76e-2	1.99	2.65e-0	1.00	1.19e-1	1.00	3.15e-3	2.02	2.17e-2	1.99
	0.2000	4.77e-2	−−	4.06e-2	−−	1.31e-0	−−	5.95e-2	−−	2.62e-3	−−	1.92e-2	−−
	0.1333	1.44e-2	2.96	1.22e-2	2.96	5.90e-1	1.97	2.64e-2	2.00	5.68e-4	3.77	5.78e-3	2.96
	0.1000	6.10e-3	2.97	5.19e-3	2.98	3.30e-1	2.02	1.49e-2	2.00	1.86e-4	3.89	2.45e-3	2.98
2	0.0800	3.15e-3	2.96	2.69e-3	2.95	2.14e-1	1.93	9.50e-3	2.00	7.99e-5	3.78	1.27e-3	2.96
	0.0667	1.83e-3	2.98	1.56e-3	2.98	1.49e-1	1.99	6.60e-3	2.00	3.93e-5	3.89	7.37e-4	2.98
	0.0571	1.16e-3	2.98	9.85e-4	2.98	1.10e-1	1.99	4.85e-3	2.00	2.15e-5	3.91	4.65e-4	2.99
	0.0500	7.76e-4	2.98	6.61e-4	2.99	8.40e-2	2.00	3.71e-3	2.00	1.27e-5	3.93	3.12e-4	2.99
	0.2000	3.58e-3	−−	3.24e-3	−−	1.47e-1	−−	5.35e-3	−−	1.34e-4	−−	1.36e-3	−−
	0.1333	7.31e-4	3.92	6.95e-4	3.80	4.88e-2	2.72	1.58e-3	3.01	2.11e-5	4.56	2.95e-4	3.77
	0.1000	2.41e-4	3.87	2.30e-4	3.85	2.28e-2	2.64	6.64e-4	3.01	6.11e-6	4.30	9.64e-5	3.89
3	0.0800	9.83e-5	4.01	9.41e-5	4.00	1.10e-2	3.27	3.39e-4	3.00	1.82e-6	5.42	3.97e-5	3.98
	0.0667	4.79e-5	3.95	4.58e-5	3.96	6.42e-3	2.96	1.96e-4	3.00	7.53e-7	4.85	1.92e-5	3.98
	0.0571	2.60e-5	3.96	2.48e-5	3.97	4.06e-3	2.97	1.24e-4	3.00	3.55e-7	4.87	1.04e-5	4.00
	0.0500	1.53e-5	3.95	1.46e-5	3.97	2.74e-3	2.95	8.28e-5	3.00	1.86e-7	4.85	6.07e-6	4.01

Table 3.2: History of convergence for Example 2.

h	k	$\|\boldsymbol{\sigma}-\boldsymbol{\sigma}_h\|_{0,\Omega}$ $\tau=10^{-1}$	$\tau=10^{0}$	$\tau=10^{1}$	$\tau=10^{2}$	$\tau=10^{3}$
0.0571	1	4.9118e-2	6.5855e-2	2.8347e-1	2.3974e-0	1.7163e+1
0.0571	2	9.8544e-4	1.3358e-3	6.2561e-3	5.5194e-2	3.8630e-1
0.0667	3	4.5751e-5	5.5785e-5	2.3936e-4	2.1504e-3	1.5109e-2
0.0667	4	2.9174e-6	2.9876e-6	5.7542e-6	4.6312e-5	3.4693e-4
h	k	$\|\mathbf{u}-\mathbf{u}_h\|_{0,\Omega}$ $\tau=10^{-1}$	$\tau=10^{0}$	$\tau=10^{1}$	$\tau=10^{2}$	$\tau=10^{3}$
0.0571	1	1.3626e-1	1.3649e-1	1.3717e-1	1.5542e-1	2.7216e-1
0.0571	2	4.8468e-3	5.2903e-3	5.7489e-3	5.8752e-3	6.8390e-3
0.0667	3	1.9632e-4	2.3910e-4	3.0923e-4	3.3322e-4	3.7520e-4
0.0667	4	4.6136e-6	5.8874e-6	7.1539e-6	7.4307e-6	7.8061e-6
h	k	$\|\Pi_{\mathcal{E}_h}(\mathbf{u})-\widehat{\mathbf{u}}_h\|_h$ $\tau=10^{-1}$	$\tau=10^{0}$	$\tau=10^{1}$	$\tau=10^{2}$	$\tau=10^{3}$
0.0571	1	4.1323e-3	6.8604e-3	3.3457e-2	2.3303e-1	7.6095e-1
0.0571	2	2.1471e-5	3.8337e-5	2.0965e-4	1.8313e-3	1.2478e-2
0.0667	3	7.5312e-7	1.1598e-6	6.2942e-6	5.6190e-5	3.7855e-4
0.0667	4	3.8092e-8	4.0211e-8	1.0500e-7	9.0616e-7	6.6465e-6

Table 3.3: Example 2, some errors for different values of τ.

k	h	$\|\mathbf{t}-\mathbf{t}_h\|_{0,\Omega}$ error	order	$\|\boldsymbol{\sigma}-\boldsymbol{\sigma}_h\|_{0,\Omega}$ error	order	$\|\boldsymbol{\sigma}-\boldsymbol{\sigma}_h\|_{\Sigma_h}$ error	order	$\|\mathbf{u}-\mathbf{u}_h\|_{0,\Omega}$ error	order	$\|\Pi_{\mathcal{E}_h}(\mathbf{u})-\widehat{\mathbf{u}}_h\|_h$ error	order	$\|p-p_h\|_{0,\Omega}$ error	order
	0.1667	8.54e-2	−−	9.75e-2	−−	7.65e-0	−−	6.75e-2	−−	1.04e-2	−−	5.45e-2	−−
	0.1111	6.59e-2	0.64	6.95e-2	0.84	8.62e-0	-0.30	4.51e-2	0.99	7.16e-3	0.92	3.72e-2	0.94
	0.0833	5.47e-2	0.64	5.46e-2	0.84	9.39e-0	-0.30	3.39e-2	1.00	5.43e-3	0.96	2.83e-2	0.96
1	0.0667	4.74e-2	0.65	4.54e-2	0.83	1.00e+1	-0.30	2.71e-2	1.00	4.34e-3	1.00	2.29e-2	0.95
	0.0556	4.21e-2	0.65	3.91e-2	0.82	1.06e+1	-0.30	2.26e-2	1.00	3.60e-3	1.03	1.93e-2	0.95
	0.0455	3.69e-2	0.65	3.33e-2	0.81	1.13e+1	-0.30	1.85e-2	1.00	2.92e-3	1.05	1.60e-2	0.93
	0.0400	3.39e-2	0.65	3.01e-2	0.80	1.17e+1	-0.30	1.63e-2	1.00	2.54e-3	1.07	1.42e-2	0.92
	0.1667	6.09e-2	−−	5.32e-2	−−	6.84e-0	−−	2.45e-3	−−	5.47e-3	−−	2.23e-2	−−
	0.1111	4.67e-2	0.65	3.91e-2	0.76	7.72e-0	-0.30	1.33e-3	1.50	3.09e-3	1.41	1.56e-2	0.87
	0.0833	3.87e-2	0.66	3.16e-2	0.74	8.41e-0	-0.30	8.65e-4	1.50	2.07e-3	1.39	1.23e-2	0.82
2	0.0667	3.34e-2	0.66	2.69e-2	0.73	8.99e-0	-0.30	6.21e-4	1.48	1.52e-3	1.38	1.03e-2	0.80
	0.0556	2.96e-2	0.66	2.36e-2	0.72	9.50e-0	-0.30	4.75e-4	1.47	1.19e-3	1.37	8.96e-3	0.78
	0.0455	2.60e-2	0.66	2.04e-2	0.72	1.01e+1	-0.30	3.55e-4	1.46	9.03e-4	1.36	7.68e-3	0.77
	0.0400	2.39e-2	0.66	1.86e-2	0.72	1.05e+1	-0.30	2.95e-4	1.45	7.60e-4	1.35	6.97e-3	0.76
	0.1667	4.48e-2	−−	3.64e-2	−−	5.99e-0	−−	7.05e-4	−−	2.36e-3	−−	1.30e-2	−−
	0.1111	3.43e-2	0.66	2.73e-2	0.72	6.76e-0	-0.30	3.86e-4	1.48	1.29e-3	1.49	9.57e-3	0.76
	0.0833	2.84e-2	0.66	2.22e-2	0.71	7.37e-0	-0.30	2.55e-4	1.45	8.44e-4	1.47	7.73e-3	0.74
3	0.0667	2.45e-2	0.66	1.90e-2	0.71	7.89e-0	-0.30	1.85e-4	1.42	6.12e-4	1.45	6.57e-3	0.73
	0.0556	2.17e-2	0.66	1.67e-2	0.71	8.33e-0	-0.30	1.43e-4	1.41	4.71e-4	1.43	5.75e-3	0.73
	0.0455	1.91e-2	0.66	1.45e-2	0.70	8.85e-0	-0.30	1.09e-4	1.39	3.55e-4	1.41	4.98e-3	0.72
	0.0400	1.75e-2	0.66	1.32e-2	0.70	9.20e-0	-0.30	9.11e-5	1.37	2.97e-4	1.40	4.54e-3	0.72

Table 3.4: History of convergence for Example 3.

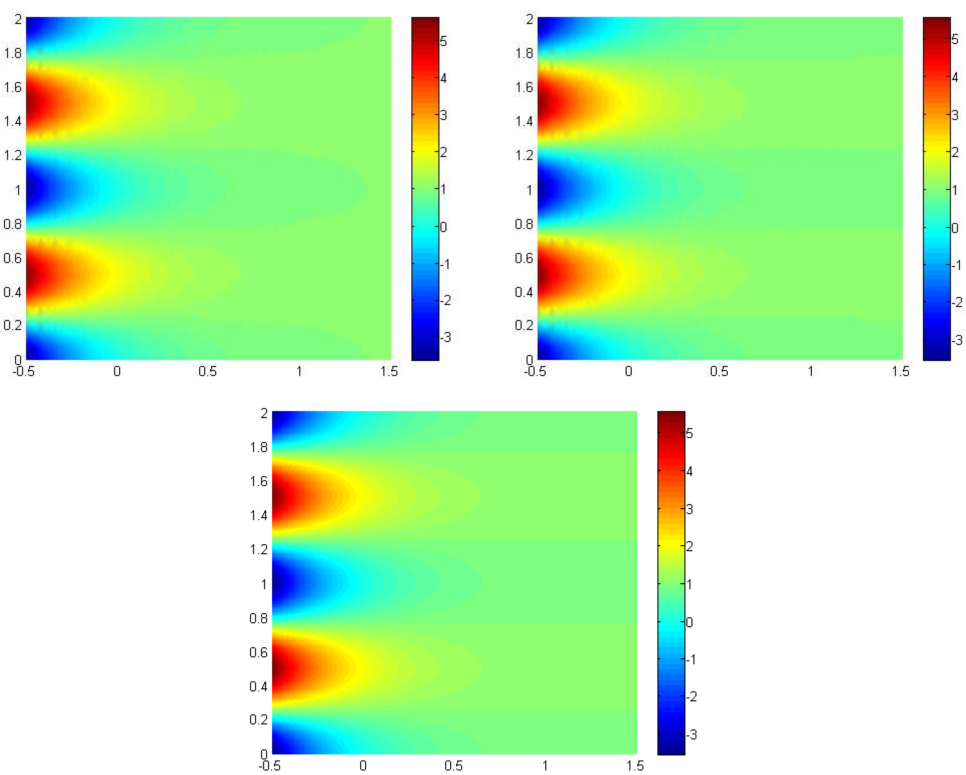

Figure 3.1: Example 2, $u_{h,1}$ for $k=2$ (top-left), for $k=3$ (top-right), and its exact value (bottom).

k	h	N_{total}	N_{comp}	$\lVert \mathbf{t} - \mathbf{t}_h \rVert_{0,\Omega}$ error	order	$\lVert \boldsymbol{\sigma} - \boldsymbol{\sigma}_h \rVert_{0,\Omega}$ error	order	$\lVert \boldsymbol{\sigma} - \boldsymbol{\sigma}_h \rVert_{\Sigma_h}$ error	order
1	0.3464	71100	15601	4.30e-1	−−	4.35e-1	−−	7.21e-0	−−
	0.2474	194040	41749	2.22e-1	1.96	2.30e-1	1.88	5.19e-0	0.98
	0.1925	411156	87481	1.35e-1	1.98	1.43e-1	1.91	4.06e-0	0.98
	0.1732	563400	119401	1.10e-1	2.00	1.16e-1	1.97	3.65e-0	1.01
	0.1332	1235052	259585	6.52e-2	1.98	6.94e-2	1.95	2.82e-0	0.98
	0.1083	2299392	480769	4.32e-2	1.99	4.60e-2	1.97	2.29e-0	0.99
	0.0962	3271752	682345	3.41e-2	2.00	3.64e-2	1.99	2.04e-0	1.00
2	0.3464	173700	30451	4.43e-2	−−	3.94e-2	−−	1.15e-0	−−
	0.2474	474516	81439	1.70e-2	2.85	1.49e-2	2.89	6.17e-1	1.86
	0.1925	1006020	170587	8.14e-3	2.92	7.13e-3	2.94	3.77e-1	1.96
	0.1732	1378800	232801	6.15e-3	2.66	5.51e-3	2.44	3.27e-1	1.34
	0.1332	3023748	505987	2.78e-3	3.03	2.44e-3	3.10	1.86e-1	2.15
	0.1083	5630976	936961	1.50e-3	2.97	1.31e-3	3.01	1.21e-1	2.07
	0.0962	8013168	1329697	1.06e-3	2.92	9.24e-4	2.95	9.61e-2	1.96
3	0.3464	342000	50251	5.96e-3	−−	6.29e-3	−−	2.55e-1	−−
	0.2474	934920	134359	1.92e-3	3.38	2.13e-3	3.22	1.16e-1	2.33
	0.1925	1982880	281395	8.53e-4	3.22	9.92e-4	3.04	6.79e-2	2.14
	0.1732	2718000	384001	5.33e-4	4.47	6.75e-4	3.65	4.75e-2	3.38
	0.1332	5962320	834523	1.88e-4	3.97	2.41e-4	3.94	2.16e-2	3.00
	0.1083	11105280	1545217	8.22e-5	3.98	1.05e-4	3.99	1.16e-2	2.99
	0.0962	15804720	2192833	5.15e-5	3.96	6.61e-5	3.93	8.18e-3	2.98

k	h	N_{total}	N_{comp}	$\lVert \mathbf{u} - \mathbf{u}_h \rVert_{0,\Omega}$ error	order	$\lVert \Pi_{\mathcal{E}_h}(\mathbf{u}) - \widehat{\mathbf{u}}_h \rVert_h$ error	order	$\lVert p - p_h \rVert_{0,\Omega}$ error	order
1	0.3464	71100	15601	2.64e-1	−−	1.66e-1	−−	1.86e-1	−−
	0.2474	194040	41749	1.89e-1	0.99	8.54e-2	1.98	1.01e-1	1.82
	0.1925	411156	87481	1.48e-1	0.99	5.18e-2	1.99	6.29e-2	1.87
	0.1732	563400	119401	1.33e-1	1.00	4.20e-2	2.00	5.12e-2	1.95
	0.1332	1235052	259585	1.02e-1	1.00	2.49e-2	1.99	3.08e-2	1.94
	0.1083	2299392	480769	8.31e-2	1.00	1.65e-2	2.00	2.05e-2	1.97
	0.0962	3271752	682345	7.39e-2	1.00	1.30e-2	2.00	1.62e-2	1.98
2	0.3464	173700	30451	4.03e-2	−−	6.07e-3	−−	1.33e-2	−−
	0.2474	474516	81439	2.07e-2	1.98	1.75e-3	3.70	4.61e-3	3.14
	0.1925	1006020	170587	1.26e-2	1.99	6.66e-4	3.84	2.13e-3	3.08
	0.1732	1378800	232801	1.02e-2	1.99	4.72e-4	3.26	1.60e-3	2.72
	0.1332	3023748	505987	6.04e-3	1.99	1.62e-4	4.07	6.95e-4	3.18
	0.1083	5630976	936961	3.99e-3	2.00	7.09e-5	3.99	3.65e-4	3.10
	0.0962	8013168	1329697	3.15e-3	2.00	4.48e-5	3.89	2.55e-4	3.04
3	0.3464	342000	50251	4.39e-3	−−	6.88e-4	−−	1.63e-3	−−
	0.2474	934920	134359	1.61e-3	2.98	1.62e-4	4.31	4.96e-4	3.54
	0.1925	1982880	281395	7.60e-4	2.99	5.67e-5	4.16	2.25e-4	3.14
	0.1732	2718000	384001	5.55e-4	2.99	3.20e-5	5.44	1.43e-4	4.31
	0.1332	5962320	834523	2.53e-4	2.99	8.67e-6	4.97	5.02e-5	3.99
	0.1083	11105280	1545217	1.36e-4	3.01	3.08e-6	4.98	2.20e-5	3.97
	0.0962	15804720	2192833	9.53e-5	3.00	1.72e-6	4.96	1.39e-5	3.93

Table 3.5: History of convergence for Example 4.

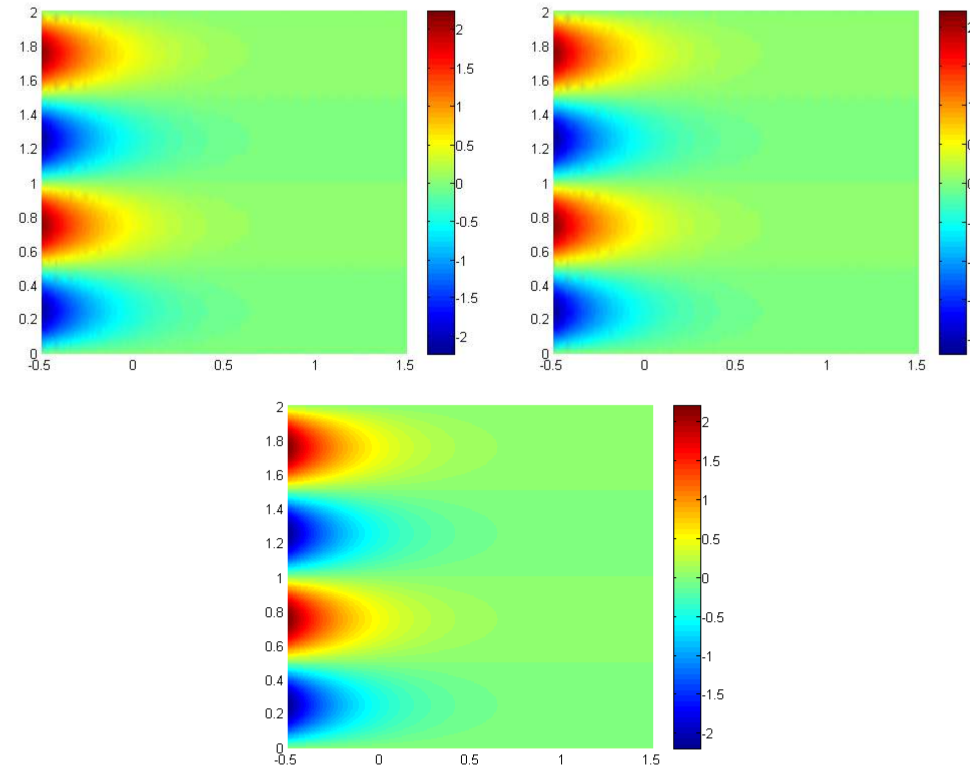

Figure 3.2: Example 2, $u_{h,2}$ for $k = 2$ (top-left), for $k = 3$ (top-right), and its exact value (bottom).

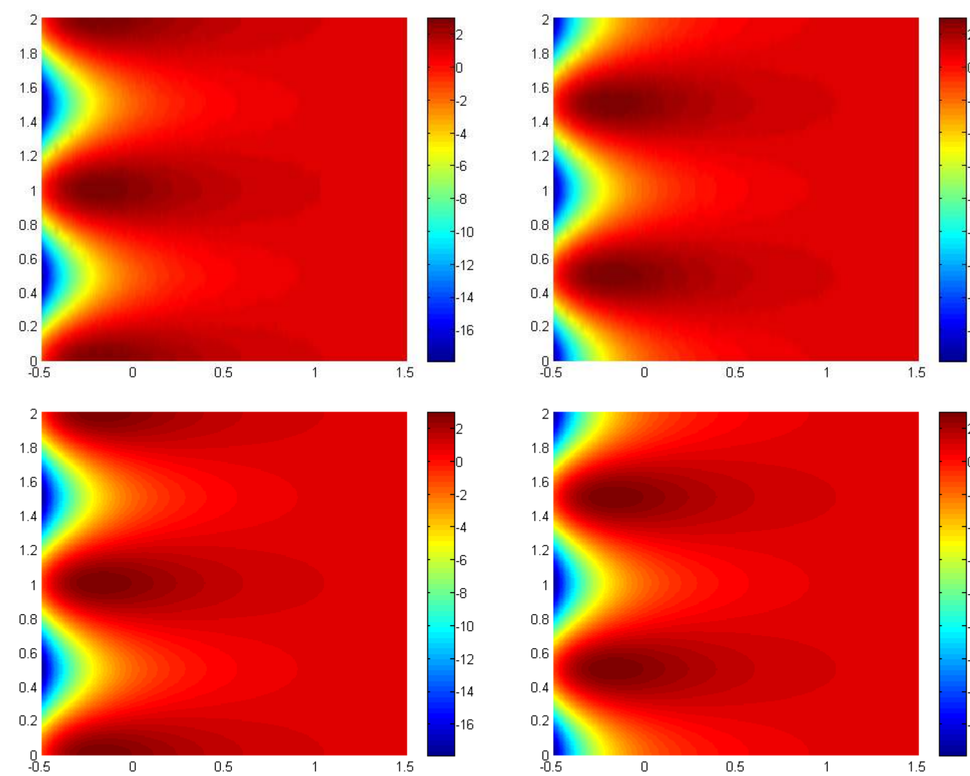

Figure 3.3: Example 2, $\sigma_{h,11}$ (top-left) $\sigma_{h,22}$ (top-right) for $k = 2$, and its exact values (bottom).

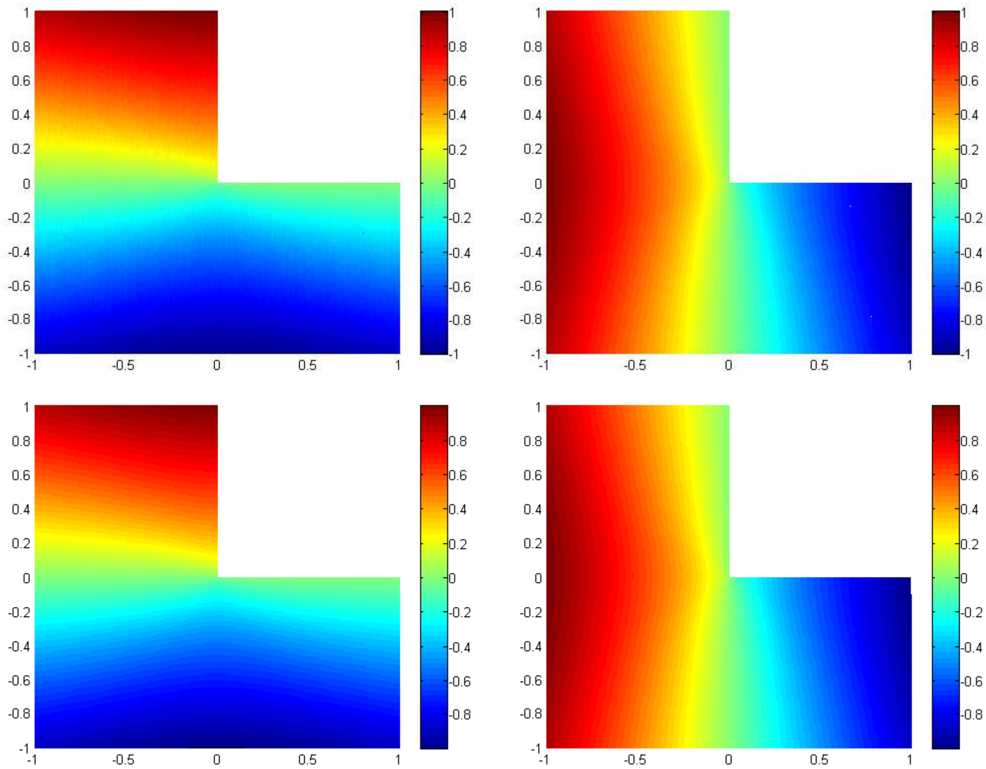

Figure 3.4: Example 3, $u_{h,1}$ (top-left) and $u_{h,2}$ (top-right) for $k = 2$, and its exact values (bottom).

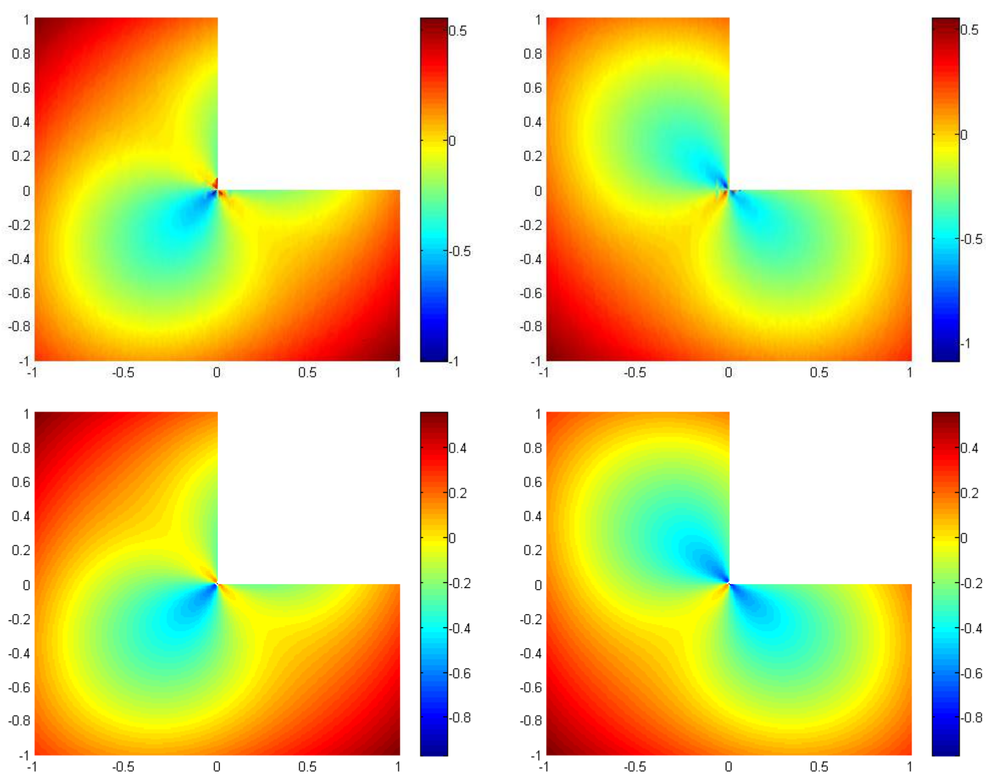

Figure 3.5: Example 3, $\sigma_{h,11}$ (top-left) and $\sigma_{h,22}$ (top-right) for $k = 2$, and its exact values (bottom).

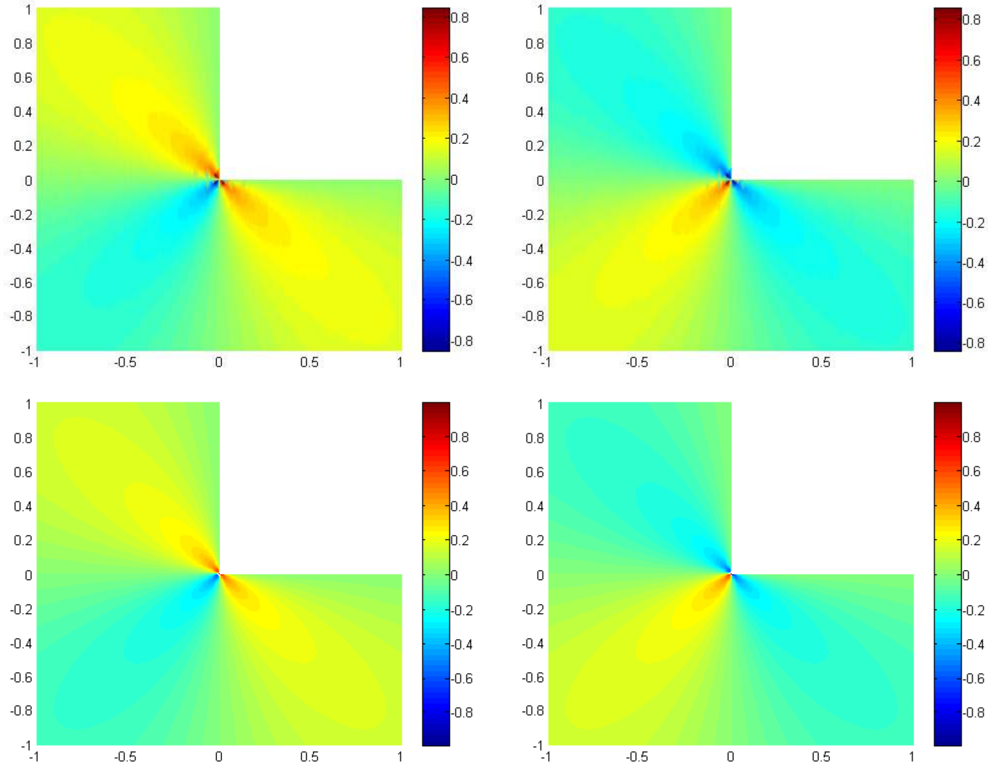

Figure 3.6: Example 3, $t_{h,11}$ (top-left) and $t_{h,22}$ (top-right) for $k=2$, and its exact values (bottom).

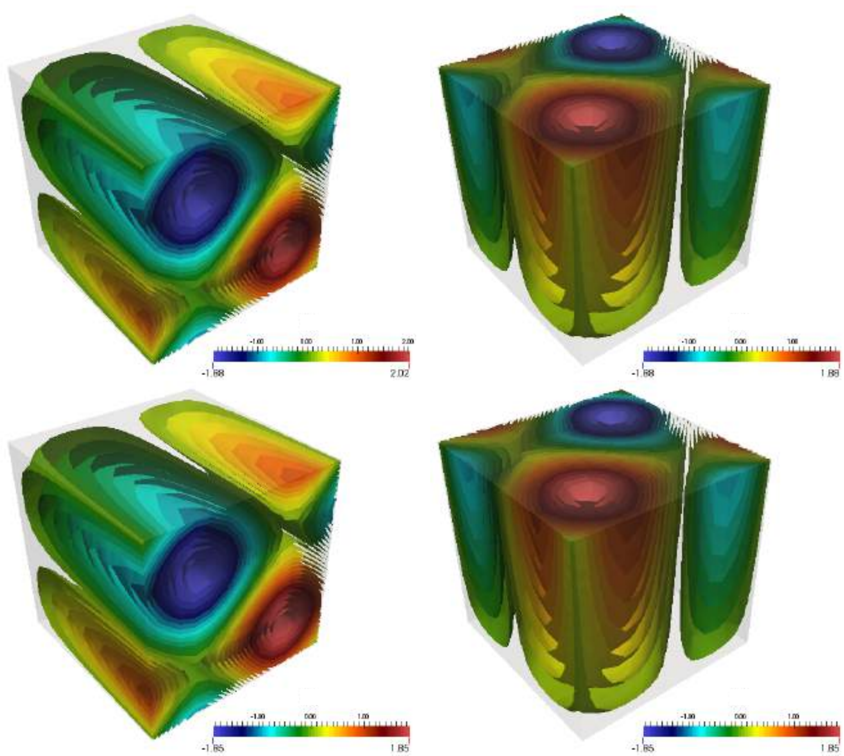

Figure 3.7: Example 4, iso-surfaces of $u_{h,1}$ (top-left) and $u_{h,3}$ (top-right) for $k=2$, and its exact values (bottom).

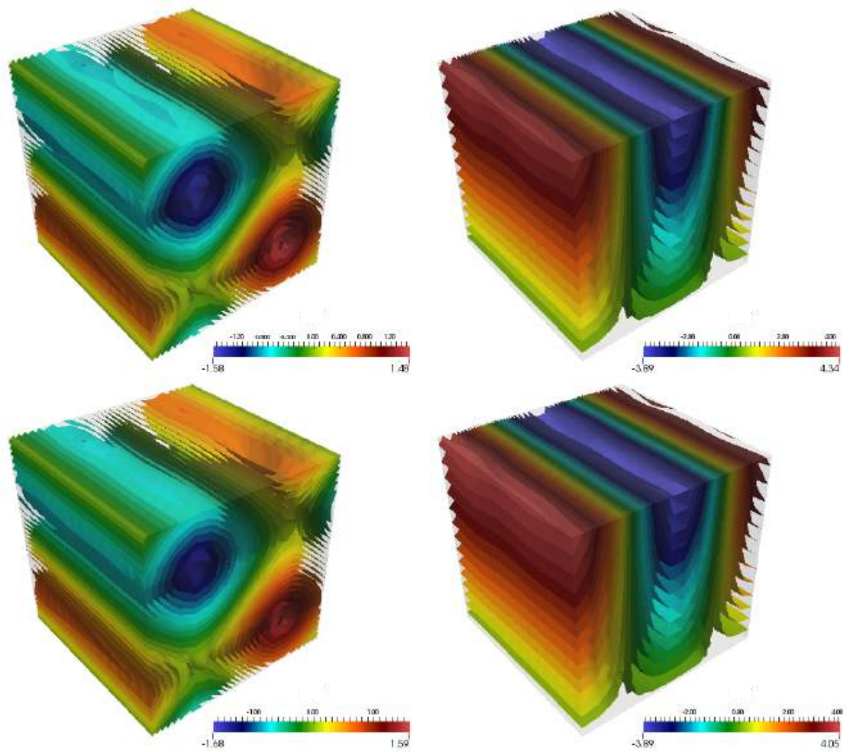

Figure 3.8: Example 4, iso-surfaces of $\sigma_{h,11}$ (top-left) and $\sigma_{h,32}$ (top-right) for $k = 2$, and its exact values (bottom).

CHAPTER 4

A priori and a posteriori error analyses of an augmented HDG method for a class of quasi-Newtonian Stokes flows

4.1 Introduction

The study of new and more efficient numerical methods for linear and nonlinear Stokes flows and related problems, has become a very active research area lately (see, e.g., [64, 83, 84, 112, 43], and the references therein). In particular, *a priori* and *a posteriori* error analyses of non-augmented and augmented mixed finite element methods for a quasi-Newtonian Stokes flow are developed in [84], whereas discontinuous Galerkin schemes are considered in [23] and more recently in [89] (i.e. Chapter 3). More precisely, the application of the local discontinuous Galerkin (LDG) method to the aforementioned nonlinear problem was studied in [23] by using a pseudostress-based formulation in which the velocity, its gradient, and the pressure complete the set of unknowns. On the other hand, a hybridizable discontinuous Galerkin (HDG) method for the same model and approach from [23] is introduced and analyzed in Chapter 3. This HDG formulation is enriched with two suitable redundant equations, thanks to which the well-posedness, that is the unique solvability, stability, and Céa's estimate of the proposed discrete scheme, can be easily established. Indeed, the resulting augmented HDG scheme is reformulated as a fixed point problem, which, under the assumption that certain stabilization parameter is small enough, allows to apply a nonlinear version of the Babuška-Brezzi theory and the classical Banach fixed-point theorem. However, according to the numerical experiments reported in Section 3.6, some of the unknowns show higher orders of convergence than predicted by the theoretical results, which suggests that the corresponding *a priori* error analysis is not sharp. In addition, those examples also showed that for large values of the stabilization parameter the method does not break down, thus insinuating that the restriction on the choice of this parameter could very well be just a technical assumption for the analysis. These drawbacks of the approach in Chapter 3 constitute the main motivation for the present contribution.

In the present chapter, we reconsider the nonlinear model and the associated augmented HDG formulation from Chapter 3, and provide a significant improvement of the corresponding analyses and results. In fact, after suitable redefinitions of the finite element subspaces approximating the pseudostress and velocity, and without resorting to any fixed-point strategy, but only applying a nonlinear version of the well known Babuška-Brezzi theory, we are able to prove in a cleaner way the well-posedness of the discrete scheme and to establish optimal orders of convergence for all the unknowns. Furthermore, a second contribution of this work consists of the derivation of a reliable and efficient residual-based *a posteriori* error estimator for our problem. Regarding this issue, it is important to remark here that the development of *a posteriori* error estimates for discontinuous Galerkin schemes is not as exhaustive as for conforming methods, which is confirmed by the scarce literature on the subject. One of the first results in this direction goes back to [24], where a new residual-based reliable *a posteriori* error estimator for the local discontinuous Galerkin approximations of linear and nonlinear diffusion problems in polygonal regions of R^2 is derived. The analysis in [24], which applies to convex and non-convex domains, is based on Helmholtz decompositions of the error and a suitable auxiliary polynomial function interpolating the Dirichlet datum. In turn, the first *a posteriori* error analysis of the HDG method for second-order elliptic problems was presented in [51]. A postprocessing variable was used there in order to prove reliability and efficiency of the proposed local *a posteriori* error indicator. More recently, an *a posteriori* error estimator for the HDG method applied to convection-diffusion equations with dominant convection was introduced in [35]. No postprocessed solution was employed in that approach. Other works dealing with the development of *a posteriori* error estimates for discontinuous Galerkin schemes include [23, 52] and the references therein. However, in spite of the aforementioned papers, there is still no contribution available in the literature on the *a posteriori* error analysis of HDG methods for nonlinear models in fluid mechanics. According to the above discussion, and as a first attempt in this regard, in this chapter we also develop a reliable and efficient residual-based *a posteriori* error estimator, and propose the associated adaptive algorithm, for the HDG approximation of the quasi-Newtonian Stokes flow from Chapter 3.

The rest of this work is organized as follows. In Section 4.2 we recall the augmented hybridizable discontinuous Galerkin formulation from Chapter 3, which involves the velocity, the pseudostress, the gradient of the velocity, and the trace of the velocity, as main unknowns. In Section 4.3 we show the unique solvability of this augmented HDG scheme by considering first an equivalent formulation, and then by applying a nonlinear version of the Babuška-Brezzi theory. The corresponding optimal *a priori* error estimates are then established in Section 4.4. Next, in Section 4.5 we derive a reliable and efficient residual-based *a posteriori* error estimator for arbitrary 2D polygonal domains and for polyhedral domains in 3D. Similarly as in [51], we use an element-by-element postprocessing formula for the pseudostress, which allows us to prove reliability and efficiency of the *a posteriori* estimator. Finally, several numerical results showing the good performance of the method, confirming the reliability and efficiency of the estimator, and illustrating the behaviour of the associated adaptive algorithm, even for a 3D example with a non-convex domain, are reported in Section 4.6.

We end this section with some notations to be used below. Given $n \in \{2,3\}$, the space of square matrices of order n with real entries is denoted by $\mathrm{R}^{n\times n}$. In addition, $\mathbb{I} := (\delta_{ij})$ is the identity matrix of $\mathrm{R}^{n\times n}$, and for any $\boldsymbol{\tau} := (\tau_{ij})$, $\boldsymbol{\zeta} := (\zeta_{ij}) \in \mathrm{R}^{n\times n}$, we write as usual

$$\boldsymbol{\tau}^{\mathtt{t}} \,:=\, (\tau_{ji})\,, \quad \mathrm{tr}\,(\boldsymbol{\tau}) \,:=\, \sum_{i=1}^{n} \tau_{ii}\,, \quad \boldsymbol{\tau}^{\mathtt{d}} \,:=\, \boldsymbol{\tau} - \frac{1}{n}\,\mathrm{tr}\,(\boldsymbol{\tau})\,\mathbb{I}\,, \quad \text{and} \quad \boldsymbol{\tau} : \boldsymbol{\zeta} \,:=\, \sum_{i,j=1}^{n} \tau_{ij}\zeta_{ij}\,.$$

Also, in what follows we utilize standard simplified terminology for Sobolev spaces and norms. In particular, if $\mathcal{O} \subset \mathrm{R}^n$ is a domain, $\mathcal{S} \subset \mathrm{R}^n$ is an open or closed Lipschitz curve if $n = 2$ (resp. surface if $n = 3$), and $r \in \mathrm{R}$, we define

$$\mathbf{H}^r(\mathcal{O}) \,:=\, [H^r(\mathcal{O})]^n\,, \quad \mathbb{H}^r(\mathcal{O}) \,:=\, [H^r(\mathcal{O})]^{n\times n}\,, \quad \text{and} \quad \mathbf{H}^r(\mathcal{S}) \,:=\, [H^r(\mathcal{S})]^n\,.$$

However, when $r = 0$ we usually write $\mathbf{L}^2(\mathcal{O})$, $\mathbb{L}^2(\mathcal{O})$, and $\mathbf{L}^2(\mathcal{S})$ instead of $\mathbf{H}^0(\mathcal{O})$, $\mathbb{H}^0(\mathcal{O})$, and $\mathbf{H}^0(\mathcal{S})$, respectively. The corresponding norms are denoted by $\|\cdot\|_{r,\mathcal{O}}$ and $\|\cdot\|_{r,\mathcal{S}}$. In general, given any Hilbert space H, we use $\mathbf{H}$ and $\mathbb{H}$ to denote H^n and $H^{n\times n}$, respectively. In addition, with div denoting the usual divergence operator, the Hilbert space

$$\mathbf{H}(\mathrm{div};\mathcal{O}) \;:=\; \left\{\mathbf{w}\in\mathbf{L}^2(\mathcal{O}) \;:\; \mathrm{div}(\mathbf{w})\in L^2(\mathcal{O})\right\}\,,$$

is standard in the realm of mixed problems (see, e.g. [19, 92, 71]). The space of matrix-valued functions whose rows belong to $\mathbf{H}(\mathrm{div};\mathcal{O})$ will be denoted $\mathbb{H}(\mathbf{div};\mathcal{O})$, where $\mathbf{div}$ stands for the action of div along each row of a tensor. The Hilbert norms of $\mathbf{H}(\mathrm{div};\mathcal{O})$ and $\mathbb{H}(\mathbf{div};\mathcal{O})$ are denoted by $\|\cdot\|_{\mathrm{div},\mathcal{O}}$ and $\|\cdot\|_{\mathbf{div},\mathcal{O}}$, respectively. Finally, we employ $\mathbf{0}$ to denote a generic null vector, null tensor or null operator, and use C or c, with or without subscripts, bars, tildes or hats, to denote generic constants independent of the discretization parameters, which may take different values at different places.

4.2 The augmented HDG method

4.2.1 The model problem

In order to define the boundary value problem of interest, we now let Ω be a bounded and simply connected polygonal domain in R^n with boundary Γ. As in [84], our goal is to determine the velocity $\mathbf{u}$, the pseudostress tensor $\boldsymbol{\sigma}$, and the pressure p of a steady flow occupying the region Ω, under the action of external forces. More precisely, given a volume force $\mathbf{f}\in\mathbf{L}^2(\Omega)$ and $\mathbf{g}\in\mathbf{H}^{1/2}(\Gamma)$, we seek a tensor field $\boldsymbol{\sigma}$, a vector field $\mathbf{u}$, and a scalar field p such that

$$\begin{aligned}
\boldsymbol{\sigma} \;&=\; \mu(|\nabla\mathbf{u}|)\,\nabla\mathbf{u}-p\,\mathbb{I} \quad \text{in} \quad \Omega\,, \qquad \mathbf{div}(\boldsymbol{\sigma}) \;=\; -\mathbf{f} \quad \text{in} \quad \Omega\,,\\
\mathrm{div}(\mathbf{u}) \;&=\; 0 \quad \text{in} \quad \Omega\,, \qquad \mathbf{u}=\mathbf{g} \quad \text{on} \quad \Gamma\,, \qquad \int_\Omega p \;=\; 0\,,
\end{aligned} \tag{4.1}$$

where $\mu:\mathrm{R}^+\to\mathrm{R}^+$ is the nonlinear kinematic viscosity function of the fluid, $\nabla\mathbf{u}$ is the tensor gradient of $\mathbf{u}$, and $|\cdot|$ is the Euclidean norm of $\mathrm{R}^{n\times n}$. As required by the incompressibility condition, we assume from now on that the datum $\mathbf{g}$ satisfies the compatibility condition $\int_\Gamma \mathbf{g}\cdot\boldsymbol{\nu}=0$, where $\boldsymbol{\nu}$ stands for the unit outward normal at Γ. The kind of nonlinear Stokes problem given by (4.1) appears in the modeling of a large class of non-Newtonian fluids (see, e.g. [12, 104, 108, 117]). In particular, the Ladyzhenskaya law is given by $\mu(t):=\mu_0+\mu_1 t^{\beta-2}\ \forall\, t\in\mathrm{R}^+$, with $\mu_0\geq 0$, $\mu_1>0$, and $\beta>1$, and the Carreau law for viscoplastic flows (see, e.g. [108, 117]) reads $\mu(t):=\mu_0+\mu_1(1+t^2)^{(\beta-2)/2}\ \forall\, t\in\mathrm{R}^+$, with $\mu_0\geq 0$, $\mu_1>0$, and $\beta\geq 1$.

We now let $\psi_{ij}:\mathrm{R}^{n\times n}\to\mathrm{R}$ be the mapping given by $\psi_{ij}(\mathbf{r}):=\mu(|\mathbf{r}|)r_{ij}$ for all $\mathbf{r}:=(r_{ij})\in\mathrm{R}^{n\times n}$, for all $i,j\in\{1,\dots,n\}$. Then, throughout this chapter we assume that μ is of class C^1 and that there exist $\gamma_0,\alpha_0>0$ such that for all $\mathbf{r}:=(r_{ij})$, $\mathbf{s}:=(s_{ij})\in\mathrm{R}^{n\times n}$, there holds

$$|\psi_{ij}(\mathbf{r})| \;\leq\; \gamma_0\,\|\mathbf{r}\|_{\mathrm{R}^{n\times n}}\,, \qquad \left|\frac{\partial}{\partial r_{kl}}\psi_{ij}(\mathbf{r})\right| \;\leq\; \gamma_0\,, \quad \forall\, i,j,k,l\in\{1,\dots,n\}\,, \tag{4.2}$$

and

$$\sum_{i,j,k,l=1}^{n}\frac{\partial}{\partial r_{kl}}\psi_{ij}(\mathbf{r})s_{ij}s_{kl} \;\;\geq\;\; \alpha_0\,\|\mathbf{s}\|^2_{\mathrm{R}^{n\times n}}\,. \tag{4.3}$$

It is easy to check that the Carreau law satisfies (4.2) and (4.3) for all $\mu_0>0$, and for all $\beta\in[1,2]$. In particular, with $\beta=2$ we recover the usual linear Stokes model.

On the other hand, we know from [84, Section 2.1] that the pair given by the first and third equations in (4.1) is equivalent to

$$\boldsymbol{\sigma} \;=\; \boldsymbol{\psi}(\nabla\mathbf{u}) - p\,\mathbb{I} \quad \text{in} \quad \Omega \qquad \text{and} \qquad p \;=\; -\frac{1}{n}\,\mathrm{tr}\,(\boldsymbol{\sigma}) \quad \text{in} \quad \Omega\,, \tag{4.4}$$

where $\boldsymbol{\psi} : \mathrm{R}^{n\times n} \to \mathrm{R}^{n\times n}$ is given by $\boldsymbol{\psi}(\mathbf{r}) := (\psi_{ij}(\mathbf{r}))$ for all $\mathbf{r} \in \mathrm{R}^{n\times n}$. Hence, replacing p by $-\frac{1}{n}\mathrm{tr}\,(\boldsymbol{\sigma})$ in the first equation of (4.1), and introducing the gradient $\mathbf{t} := \nabla\mathbf{u}$ in Ω as an auxiliary unknown, we arrive at the system

$$\begin{aligned}
\boldsymbol{\psi}(\mathbf{t}) - \boldsymbol{\sigma}^{\mathrm{d}} \;&=\; \mathbf{0} \quad \text{in} \quad \Omega\,, &\qquad \mathbf{t} - \nabla\mathbf{u} \;&=\; \mathbf{0} \quad \text{in} \quad \Omega\,,\\
-\mathbf{div}(\boldsymbol{\sigma}) \;&=\; \mathbf{f} \quad \text{in} \quad \Omega\,, &\qquad \mathrm{tr}\,(\mathbf{t}) \;&=\; 0 \quad \text{in} \quad \Omega\,,\\
\mathbf{u} \;&=\; \mathbf{g} \quad \text{on} \quad \Gamma\,, &\qquad \int_\Omega \mathrm{tr}\,(\boldsymbol{\sigma}) \;&=\; 0\,.
\end{aligned} \tag{4.5}$$

Next, we let $X_1 := \{\mathbf{s} \in \mathbb{L}^2(\Omega) \;:\; \mathrm{tr}\,(\mathbf{s}) = 0\}$ and $\mathbb{H}_0(\mathbf{div};\Omega) := \big\{\boldsymbol{\tau} \in \mathbb{H}(\mathbf{div};\Omega) \;:\; \int_\Omega \mathrm{tr}\,(\boldsymbol{\tau}) = 0\big\}$, and recall that the continuous formulation of (4.5), whose well-posedness has been established in [84, Section 2], reads: Find $(\mathbf{t},\boldsymbol{\sigma},\mathbf{u}) \in X_1 \times \mathbb{H}_0(\mathbf{div};\Omega) \times \mathbf{L}^2(\Omega)$ such that

$$\begin{aligned}
\int_\Omega \boldsymbol{\psi}(\mathbf{t}) : \mathbf{s} - \int_\Omega \boldsymbol{\sigma}^{\mathrm{d}} : \mathbf{s} \;&=\; 0 \quad \forall\, \mathbf{s} \in X_1\,,\\
-\int_\Omega \mathbf{t} : \boldsymbol{\tau}^{\mathrm{d}} - \int_\Omega \mathbf{u}\cdot\mathbf{div}(\boldsymbol{\tau}) \;&=\; -\,\langle \boldsymbol{\tau\nu},\mathbf{g}\rangle_\Gamma \quad \forall\, \boldsymbol{\tau} \in \mathbb{H}_0(\mathbf{div};\Omega)\,,\\
-\int_\Omega \mathbf{v}\cdot\mathbf{div}(\boldsymbol{\sigma}) \;&=\; \int_\Omega \mathbf{f}\cdot\mathbf{v} \quad \forall\, \mathbf{v} \in \mathbf{L}^2(\Omega)\,,
\end{aligned} \tag{4.6}$$

The *a priori* error analysis given below in Section 4.4 makes use of (4.6).

4.2.2 The hybridizable discontinuous Galerkin method

We begin by introducing some preliminary notations. Let $\mathcal{T}_h$ be a shape-regular triangulation of $\bar{\Omega}$ without the presence of hanging nodes, and let $\mathcal{E}_h$ be the set of faces F of $\mathcal{T}_h$. In addition, we let $\mathcal{E}_h^i$ and $\mathcal{E}_h^\partial$ be the set of interior and boundary faces, respectively, of $\mathcal{E}_h$, and set $\partial\mathcal{T}_h := \cup\{\partial T \;:\; T \in \mathcal{T}_h\}$. Next, given a domain $U \subseteq \mathrm{R}^n$ and a surface $G \subseteq \mathrm{R}^{n-1}$, we let $(\cdot,\cdot)_U$ (resp. $\langle\cdot,\cdot\rangle_G$) be the usual L^2, $\mathbf{L}^2$ and $\mathbb{L}^2$ (resp. L^2 and $\mathbf{L}^2$) inner products over U (resp. G). Then, we introduce the inner products:

$$(\cdot,\cdot)_{\mathcal{T}_h} \;:=\; \sum_{T\in\mathcal{T}_h} (\cdot,\cdot)_T\,, \quad \langle\cdot,\cdot\rangle_{\partial\mathcal{T}_h} \;:=\; \sum_{T\in\mathcal{T}_h} \langle\cdot,\cdot\rangle_{\partial T}\,, \quad \text{and} \quad \langle\cdot,\cdot\rangle_{\partial\mathcal{T}_h\setminus\Gamma} \;:=\; \sum_{T\in\mathcal{T}_h}\sum_{F\in\partial T\setminus\Gamma} \langle\cdot,\cdot\rangle_F\,.$$

On the other hand, given second-order tensorial and vectorial functions $\boldsymbol{\tau}$ and $\mathbf{v}$, respectively, and denoting by $\boldsymbol{\nu}^+$ and $\boldsymbol{\nu}^-$ the outward unit normal vectors on the boundaries of two neighboring elements T^+ and T^-, we let $(\boldsymbol{\tau}^\pm,\mathbf{v}^\pm)$ be the trace of $(\boldsymbol{\tau},\mathbf{v})$ on $F := \partial T^+ \cap \partial T^-$ from the interior of $T^\pm$. Then, we define the means $\{\!\{\cdot\}\!\}$ and jumps $[\![\cdot]\!]$ for $F \in \mathcal{E}_h^i$, as follows

$$\begin{aligned}
\{\!\{\boldsymbol{\tau}\}\!\} \;&:=\; \frac{1}{2}\left(\boldsymbol{\tau}^+ + \boldsymbol{\tau}^-\right)\,, &\qquad \{\!\{\mathbf{v}\}\!\} \;&:=\; \frac{1}{2}\left(\mathbf{v}^+ + \mathbf{v}^-\right)\,,\\
[\![\boldsymbol{\tau}]\!] \;&:=\; \boldsymbol{\tau}^+\boldsymbol{\nu}^+ + \boldsymbol{\tau}^-\boldsymbol{\nu}^-\,, &\qquad [\![\mathbf{v}]\!] \;&:=\; \mathbf{v}^+\otimes\boldsymbol{\nu}^+ + \mathbf{v}^-\otimes\boldsymbol{\nu}^-\,,
\end{aligned}$$

where $\otimes$ denotes the usual dyadic or tensor product.

Now we are ready to describe below the HDG method for the boundary value problem (4.5). To this end, given an integer $k \geq 0$ and a domain U, we let $\mathrm{P}_k(U)$ be the space of polynomials of total degree at most k defined on U. Then, the finite dimensional discontinuous subspaces are given by

$$
\begin{aligned}
S_h &:= \left\{ \mathbf{s} \in \mathbb{L}^2(\Omega) \ : \ \mathbf{s}|_T \in \mathbb{P}_k(T) \quad \forall\, T \in \mathcal{T}_h \right\}, \\
\Sigma_h &:= \left\{ \boldsymbol{\tau} \in \mathbb{L}^2(\Omega) \ : \ \boldsymbol{\tau}|_T \in \mathbb{RT}_k(T) \quad \forall\, T \in \mathcal{T}_h, \quad \text{and} \quad \int_\Omega \operatorname{tr}(\boldsymbol{\tau}) = 0 \right\}, \\
V_h &:= \left\{ \mathbf{v} \in \mathbf{L}^2(\Omega) \ : \ \mathbf{v}|_T \in \mathbf{P}_k(T) \quad \forall\, T \in \mathcal{T}_h \right\}, \\
M_h &:= \left\{ \boldsymbol{\mu} \in \mathbf{L}^2(\mathcal{E}_h^i) \ : \ \boldsymbol{\mu}|_F \in \mathbf{P}_k(F) \quad \forall\, F \in \mathcal{E}_h^i \right\},
\end{aligned}
$$

where $\mathbb{RT}_k(T) := \left\{ \boldsymbol{\tau} \in \mathbb{L}^2(T) \ : \ (\tau_{i1}, \ldots, \tau_{in})^{\mathrm{t}}|_T \in \mathbf{RT}_k(T) \quad \forall\, i \in \{1, \ldots, n\} \right\}$, $\mathbf{RT}_k(T)$ is the local Raviart-Thomas space of order k (see, e.g. [19, 116]), that is

$$
\mathbf{RT}_k(T) \ := \ \mathbf{P}_k(T) \ \oplus \ \mathrm{P}_k(T)\, \mathbf{x},
$$

$\mathbf{x} = \begin{pmatrix} x_1 \\ \vdots \\ x_n \end{pmatrix}$ is a generic vector of R^n, and, according to the notation introduced at the end of Section 4.1, $\mathbf{P}_k(T)$ denotes $[\mathrm{P}_k(T)]^n$. At this point we remark that, differently from Chapter 3 where the lowest polynomial degree that can be employed is $k = 1$, the present definitions of the subspaces S_h and M_h allow the utilization of $k = 0$. This fact and the foregoing definition of Σ_h will be useful in the new *a priori* error analysis to be developed below in Section 4.4.

Then, proceeding exactly as in [43, 89], the HDG formulation of the nonlinear model (4.5) reduces to: Find $(\mathbf{t}_h, \boldsymbol{\sigma}_h, \mathbf{u}_h, \boldsymbol{\lambda}_h) \in S_h \times \Sigma_h \times V_h \times M_h$, such that

$$
\begin{aligned}
(\boldsymbol{\psi}(\mathbf{t}_h), \mathbf{s}_h)_{\mathcal{T}_h} - (\mathbf{s}_h, \boldsymbol{\sigma}_h^{\mathtt{d}})_{\mathcal{T}_h} &= 0 \quad \forall\, \mathbf{s}_h \in S_h\,, \\
(\mathbf{t}_h, \boldsymbol{\tau}_h^{\mathtt{d}})_{\mathcal{T}_h} + (\mathbf{u}_h, \mathbf{div}_h(\boldsymbol{\tau}_h))_{\mathcal{T}_h} - \langle \boldsymbol{\tau}_h \boldsymbol{\nu}, \widehat{\mathbf{u}}_h \rangle_{\partial \mathcal{T}_h} &= 0 \quad \forall\, \boldsymbol{\tau}_h \in \Sigma_h\,, \\
(\boldsymbol{\sigma}_h, \nabla_h \mathbf{v}_h)_{\mathcal{T}_h} - \langle \widehat{\boldsymbol{\sigma}_h \boldsymbol{\nu}}, \mathbf{v}_h \rangle_{\partial \mathcal{T}_h} &= (\mathbf{f}, \mathbf{v}_h)_{\mathcal{T}_h} \quad \forall\, \mathbf{v}_h \in V_h\,, \\
\langle \widehat{\boldsymbol{\sigma}_h \boldsymbol{\nu}}, \boldsymbol{\mu}_h \rangle_{\partial \mathcal{T}_h \setminus \Gamma} &= 0 \quad \forall\, \boldsymbol{\mu}_h \in M_h\,,
\end{aligned}
\tag{4.7}
$$

where, letting Π_Γ be the $\mathbf{L}^2(\Gamma)$ projection onto the space of piecewise polynomials of degree $\leq k$ on $\mathcal{E}_h^\partial$, we define the numerical fluxes $\widehat{\mathbf{u}}_h$ and $\widehat{\boldsymbol{\sigma}_h \boldsymbol{\nu}}$ as

$$
\widehat{\mathbf{u}}_h \ := \ \begin{cases} \Pi_\Gamma(\mathbf{g}) & \text{on } \mathcal{E}_h^\partial\,, \\ \boldsymbol{\lambda}_h & \text{on } \mathcal{E}_h^i\,, \end{cases} \qquad \text{and} \qquad \widehat{\boldsymbol{\sigma}_h \boldsymbol{\nu}} \ := \ \boldsymbol{\sigma}_h \boldsymbol{\nu} - \mathbf{S}(\mathbf{u}_h - \widehat{\mathbf{u}}_h) \quad \text{on } \partial \mathcal{T}_h\,,
$$

where $\mathbf{S}$ is a stabilization operator to be defined below. Note that the condition $\widehat{\mathbf{u}}_h = \Pi_\Gamma(\mathbf{g})$ on $\mathcal{E}_h^\partial$ is usually imposed in the equivalent way $\langle \widehat{\mathbf{u}}_h, \boldsymbol{\mu}_h \rangle_\Gamma = \langle \mathbf{g}, \boldsymbol{\mu}_h \rangle_\Gamma \ \forall\, \boldsymbol{\mu}_h \in \mathbf{P}_k(\mathcal{E}_h)$, which is employed to perform the solvability analysis of (4.7). In addition, as in Chapter 3, we consider the special case in which $\mathbf{S}^+ = \mathbf{S}^-$ in each $F \in \mathcal{E}_h^i$, that is, $\mathbf{S}$ has only one value on each $F \in \mathcal{E}_h$. More precisely, given $F \in \mathcal{E}_h$, we assume that $\mathbf{S}|_F$ is a symmetric and positive definite constant tensor. Furthermore, observe that $\mathbf{S}^{-1}$ is well defined and symmetric and positive definite as well on each $F \in \mathcal{E}_h$. In (4.14) below, we select a particular choice for tensor $\mathbf{S}$ in order to establish the well-posedness of (4.8).

4.2.3 The augmented HDG formulation

In order to establish the unique solvability of the nonlinear problem (4.7), we now enrich the HDG formulation with two redundant equations arising from the constitutive and equilibrium equations, that is

$$\kappa_1(\boldsymbol{\sigma}_h^{\mathtt{d}} - \boldsymbol{\psi}(\mathbf{t}_h),\, \boldsymbol{\tau}_h^{\mathtt{d}})_{\mathcal{T}_h} \;=\; 0 \quad \forall\, \boldsymbol{\tau}_h \in \Sigma_h\,,$$

and

$$\kappa_2(\mathbf{div}_h(\boldsymbol{\sigma}_h),\, \mathbf{div}_h(\boldsymbol{\tau}_h))_{\mathcal{T}_h} \;=\; -\kappa_2(\mathbf{f},\, \mathbf{div}_h(\boldsymbol{\tau}_h))_{\mathcal{T}_h} \quad \forall\, \boldsymbol{\tau}_h \in \Sigma_h\,,$$

where $\kappa_1, \kappa_2 > 0$ are parameters to be determined later on. In this way, our augmented formulation becomes: Find $(\mathbf{t}_h, \boldsymbol{\sigma}_h, \mathbf{u}_h, \boldsymbol{\lambda}_h) \in S_h \times \Sigma_h \times V_h \times M_h$ such that

$$\begin{aligned}
(\boldsymbol{\psi}(\mathbf{t}_h), \mathbf{s}_h)_{\mathcal{T}_h} - (\mathbf{s}_h, \boldsymbol{\sigma}_h^{\mathtt{d}})_{\mathcal{T}_h} &= 0\,,\\
(\mathbf{t}_h, \boldsymbol{\tau}_h^{\mathtt{d}})_{\mathcal{T}_h} + (\mathbf{u}_h, \mathbf{div}_h(\boldsymbol{\tau}_h))_{\mathcal{T}_h} - \langle \boldsymbol{\tau}_h \boldsymbol{\nu}, \boldsymbol{\lambda}_h \rangle_{\partial\mathcal{T}_h \setminus \Gamma} &= \langle \boldsymbol{\tau}_h \boldsymbol{\nu}, \mathbf{g} \rangle_{\Gamma}\,,\\
-(\mathbf{v}_h, \mathbf{div}_h(\boldsymbol{\sigma}_h))_{\mathcal{T}_h} + \langle \mathbf{S}(\mathbf{u}_h - \boldsymbol{\lambda}_h), \mathbf{v}_h \rangle_{\partial\mathcal{T}_h \setminus \Gamma} + \langle \mathbf{S}\mathbf{u}_h, \mathbf{v}_h \rangle_{\Gamma} &= (\mathbf{f}, \mathbf{v}_h)_{\mathcal{T}_h} + \langle \mathbf{S}\mathbf{g}, \mathbf{v}_h \rangle_{\Gamma}\,,\\
\langle \boldsymbol{\sigma}_h \boldsymbol{\nu}, \boldsymbol{\mu}_h \rangle_{\partial\mathcal{T}_h \setminus \Gamma} - \langle \mathbf{S}(\mathbf{u}_h - \boldsymbol{\lambda}_h), \boldsymbol{\mu}_h \rangle_{\partial\mathcal{T}_h \setminus \Gamma} &= 0\,,\\
\kappa_1(\boldsymbol{\sigma}_h^{\mathtt{d}} - \boldsymbol{\psi}(\mathbf{t}_h), \boldsymbol{\tau}_h^{\mathtt{d}})_{\mathcal{T}_h} &= 0\,,\\
\kappa_2(\mathbf{div}_h(\boldsymbol{\sigma}_h), \mathbf{div}_h(\boldsymbol{\tau}_h))_{\mathcal{T}_h} &= -\kappa_2(\mathbf{f}, \mathbf{div}_h(\boldsymbol{\tau}_h))_{\mathcal{T}_h}\,,
\end{aligned} \tag{4.8}$$

for all $(\mathbf{s}_h, \boldsymbol{\tau}_h, \mathbf{v}_h, \boldsymbol{\mu}_h) \in S_h \times \Sigma_h \times V_h \times M_h$. Hence, in what follows we proceed as in Chapter 3 and derive an equivalent formulation to (4.8) (see (4.10) below), for which we prove its unique solvability. In addition, the *a priori* error estimates for (4.8) will also be based on the analysis of (4.10). We emphasize, however, that the introduction of this equivalent formulation is just for theoretical purposes and by no means for the explicit computation of the solution of (4.8), which is solved directly as we explain in Section 3.5.

It follows, proceeding as in [89, Section 2.2] (cf. (3.9)), that from the fourth equation in (4.8), we obtain

$$\boldsymbol{\lambda}_h \;=\; \{\!\!\{\mathbf{u}_h\}\!\!\} \;-\; \frac{1}{2}\,\mathbf{S}^{-1}\,[\![\boldsymbol{\sigma}_h]\!] \quad \text{on} \quad \mathcal{E}_h^i\,, \tag{4.9}$$

which, allows us to rewrite (4.8) as: Find $((\mathbf{t}_h, \boldsymbol{\sigma}_h), \mathbf{u}_h) \in H_h \times V_h$ such that

$$\begin{aligned}
[\mathcal{A}_h(\mathbf{t}_h, \boldsymbol{\sigma}_h), (\mathbf{s}_h, \boldsymbol{\tau}_h)] \;+\; [\mathcal{B}_h(\mathbf{s}_h, \boldsymbol{\tau}_h), \mathbf{u}_h] &= [\mathcal{F}_h, (\mathbf{s}_h, \boldsymbol{\tau}_h)] \quad \forall\, (\mathbf{s}_h, \boldsymbol{\tau}_h) \in H_h\,,\\
[\mathcal{B}_h(\mathbf{t}_h, \boldsymbol{\sigma}_h), \mathbf{v}_h] \;-\; [\mathcal{S}_h(\mathbf{u}_h), \mathbf{v}_h] &= [\mathcal{G}_h, \mathbf{v}_h] \quad \forall\, \mathbf{v}_h \in V_h\,,
\end{aligned} \tag{4.10}$$

where $H_h := S_h \times \Sigma_h$, and the operators $\mathcal{A}_h : H_h \to H_h'$, $\mathcal{B}_h : H_h \to V_h'$ and $\mathcal{S}_h : V_h \to V_h'$, and the functionals $\mathcal{F}_h : H_h \to \mathrm{R}$ and $\mathcal{G}_h : V_h \to \mathrm{R}$, are defined by

$$\begin{aligned}
[\mathcal{A}_h(\mathbf{t}_h, \boldsymbol{\sigma}_h), (\mathbf{s}_h, \boldsymbol{\tau}_h)] \;:=\;& (\boldsymbol{\psi}(\mathbf{t}_h), \mathbf{s}_h)_{\mathcal{T}_h} - (\mathbf{s}_h, \boldsymbol{\sigma}_h^{\mathtt{d}})_{\mathcal{T}_h} + (\mathbf{t}_h, \boldsymbol{\tau}_h^{\mathtt{d}})_{\mathcal{T}_h} + \frac{1}{2}\int_{\mathcal{E}_h^i} \mathbf{S}^{-1}[\![\boldsymbol{\sigma}_h]\!] \cdot [\![\boldsymbol{\tau}_h]\!]\\
&+ \kappa_1(\boldsymbol{\sigma}_h^{\mathtt{d}} - \boldsymbol{\psi}(\mathbf{t}_h), \boldsymbol{\tau}_h^{\mathtt{d}})_{\mathcal{T}_h} + \kappa_2(\mathbf{div}_h(\boldsymbol{\sigma}_h), \mathbf{div}_h(\boldsymbol{\tau}_h))_{\mathcal{T}_h}\,,
\end{aligned} \tag{4.11}$$

$$[\mathcal{B}_h(\mathbf{s}_h, \boldsymbol{\tau}_h), \mathbf{v}_h] \;:=\; (\mathbf{v}_h, \mathbf{div}_h(\boldsymbol{\tau}_h))_{\mathcal{T}_h} - \int_{\mathcal{E}_h^i} \{\!\!\{\mathbf{v}_h\}\!\!\} \cdot [\![\boldsymbol{\tau}_h]\!]\,, \tag{4.12}$$

$$[\mathcal{S}_h(\mathbf{u}_h), \mathbf{v}_h] \;:=\; \langle \mathbf{S}\mathbf{u}_h, \mathbf{v}_h \rangle_{\partial\mathcal{T}_h} - 2\int_{\mathcal{E}_h^i} \mathbf{S}\{\!\!\{\mathbf{u}_h\}\!\!\} \cdot \{\!\!\{\mathbf{v}_h\}\!\!\}\,, \tag{4.13}$$

$$[\mathcal{F}_h, (\mathbf{s}_h, \boldsymbol{\tau}_h)] \;:=\; \langle \boldsymbol{\tau}_h \boldsymbol{\nu}, \mathbf{g} \rangle_{\Gamma} - \kappa_2(\mathbf{f}, \mathbf{div}_h(\boldsymbol{\tau}_h))_{\mathcal{T}_h}\,,$$

$$[\mathcal{G}_h, \mathbf{v}_h] \;:=\; -(\mathbf{f}, \mathbf{v}_h)_{\mathcal{T}_h} - \langle \mathbf{S}\mathbf{g}, \mathbf{v}_h \rangle_{\Gamma}\,,$$

where $[\cdot,\cdot]$ stands in each case for the duality pairing induced by the corresponding operators and functionals. We remark in advance that we do not plan to use any fixed point strategy to derive the well-posedness of (4.10) (as we did in Chapter 3), which, as announced in Section 4.1, constitutes another advantage of the present approach. In addition, while the above operators and functionals are defined on discrete spaces, it is not difficult to see that they can act on continuous spaces as well. For example, $\mathcal{A}_h$ can actually be defined on $(S_h + \mathbb{L}^2(\Omega)) \times (\Sigma_h + \mathbb{H}(\mathbf{div};\Omega))$ and similarly for the other ones. In particular, this fact will be employed at the beginning of Section 4.4.

4.3 Solvability analysis

In this section, we establish the unique solvability of the nonlinear problem (4.10). To this end, and following [22, 23], we let $\mathtt{h} \in L^\infty(\mathcal{E}_h)$ be the function related to the local meshsizes, that is

$$\mathtt{h}(x) \quad := \quad \begin{cases} \min\{h_{T_1}, h_{T_2}\} & \text{if } x \in \operatorname{int}(\partial T_1 \cap \partial T_2)\,, \\ \qquad h_T & \text{if } x \in \operatorname{int}(\partial T \cap \Gamma)\,. \end{cases}$$

The main idea of our analysis consists of proving the conditions of the following abstract theorem.

Theorem 4.1. *Let X, M be Hilbert spaces and assume that:*

i) the operator $\mathcal{A} : X \to X'$ is Lipschitz continuous and strongly monotone, that is, there exist γ, $\alpha > 0$ such that

$$\|\mathcal{A}(\mathbf{s}_1) - \mathcal{A}(\mathbf{s}_2)\|_{X'} \;\leq\; \gamma\,\|\mathbf{s}_1 - \mathbf{s}_2\|_X \quad \forall\, \mathbf{s}_1, \mathbf{s}_2 \in X$$

and

$$[\mathcal{A}(\mathbf{s}_1) - \mathcal{A}(\mathbf{s}_2), \mathbf{s}_1 - \mathbf{s}_2] \;\geq\; \alpha\,\|\mathbf{s}_1 - \mathbf{s}_2\|_X^2 \quad \forall\, \mathbf{s}_1, \mathbf{s}_2 \in X;$$

ii) the linear operator $\mathcal{S}$ is positive semidefinite on M, that is

$$[\mathcal{S}(\boldsymbol{\tau}), \boldsymbol{\tau}] \;\geq\; 0 \quad \forall\, \boldsymbol{\tau} \in M;$$

iii) the linear operator $\mathcal{B}$ satisfies an inf-sup condition on $X \times M$, that is, there exists $\beta > 0$ such that

$$\sup_{\substack{\mathbf{s}\in X\\ \mathbf{s}\neq\mathbf{0}}} \frac{[\mathcal{B}(\mathbf{s}), \boldsymbol{\tau}]}{\|\mathbf{s}\|_X} \;\geq\; \beta\,\|\boldsymbol{\tau}\|_M \quad \forall\, \boldsymbol{\tau} \in M.$$

Then, given $\mathcal{F} \in X'$ and $\mathcal{G} \in M'$, there exists a unique solution $(\mathbf{t}, \boldsymbol{\sigma}) \in X \times M$ of the problem

$$\begin{aligned} [\mathcal{A}(\mathbf{t}), \mathbf{s}] \;+\; [\mathcal{B}^*(\boldsymbol{\sigma}), \mathbf{s}] \;&=\; [\mathcal{F}, \mathbf{s}] \quad \forall\, \mathbf{s} \in X, \\ [\mathcal{B}(\mathbf{t}), \boldsymbol{\tau}] \;-\; [\mathcal{S}(\boldsymbol{\sigma}), \boldsymbol{\tau}] \;&=\; [\mathcal{G}, \boldsymbol{\tau}] \quad \forall\, \boldsymbol{\tau} \in M. \end{aligned}$$

In addition, there exists $C > 0$, depending only on γ, α, β and $\|\mathcal{B}\|$, such that

$$\|(\mathbf{t}, \boldsymbol{\sigma})\|_{X\times M} \;\leq\; C\Big\{\|\mathcal{F}\|_{X'} \;+\; \|\mathcal{G}\|_{M'} \;+\; \|\mathcal{A}(\mathbf{0})\|_{X'}\Big\}.$$

Proof. See [77, Lemma 2.1]. □

In order to apply Theorem 4.1 to the augmented formulation (4.10), we now recall the following technical result from Chapter 3.

Lemma 4.1. *There exists a constant $c_1 > 0$, independent of h, such that*

$$\|\boldsymbol{\tau}_h\|_{0,\Omega}^2 \;\leq\; c_1\Big\{\|\boldsymbol{\tau}_h^{\mathtt{d}}\|_{0,\Omega}^2 \;+\; \|\mathbf{div}_h(\boldsymbol{\tau}_h)\|_{0,\Omega}^2 \;+\; \|\mathtt{h}^{-1/2}[\![\boldsymbol{\tau}_h]\!]\|_{0,\mathcal{E}_h^i}^2\Big\} \quad \forall\, \boldsymbol{\tau}_h \in \Sigma_h\,.$$

Proof. See Lemma 3.3. □

Now, similarly as in Chapter 3 (but with the stabilization parameter employed there given by $\tau = 1$), we set the tensor $\mathbf{S}$ as follows

$$\mathbf{S}|_F \;:=\; \mathtt{h}\,\mathbb{I} \qquad \forall\, F \in \mathcal{E}_h\,, \tag{4.14}$$

which certainly yields

$$\mathbf{S}^{-1}|_F \;:=\; \mathtt{h}^{-1}\,\mathbb{I} \qquad \forall\, F \in \mathcal{E}_h\,. \tag{4.15}$$

In addition, we consider the following definition of a norm onto Σ_h

$$\|\boldsymbol{\tau}_h\|_{\Sigma_h}^2 \;:=\; \|\boldsymbol{\tau}_h^{\mathtt{d}}\|_{0,\Omega}^2 \;+\; \|\mathbf{div}_h(\boldsymbol{\tau}_h)\|_{0,\Omega}^2 \;+\; \|\mathtt{h}^{-1/2}[\![\boldsymbol{\tau}_h]\!]\|_{0,\mathcal{E}_h^i}^2 \quad \forall\, \boldsymbol{\tau}_h \in \Sigma_h$$

which, according to Lemma 4.1, satisfies

$$\|\boldsymbol{\tau}_h\|_{0,\Omega} \;\;\leq\;\; c_2\|\boldsymbol{\tau}_h\|_{\Sigma_h} \quad \forall\, \boldsymbol{\tau}_h \in \Sigma_h\,, \tag{4.16}$$

with $c_2 := c_1^{1/2} > 0$. Note that the above suggests the following norm on $H_h := S_h \times \Sigma_h$

$$\|(\mathbf{s}_h, \boldsymbol{\tau}_h)\|_{H_h} \;:=\; \Big\{\|\mathbf{s}_h\|_{0,\Omega}^2 \;+\; \|\boldsymbol{\tau}_h\|_{\Sigma_h}^2\Big\}^{1/2} \quad \forall\, (\mathbf{s}_h, \boldsymbol{\tau}_h) \in H_h\,.$$

On the other hand, we define the nonlinear operator $\mathbb{A} : \mathbb{L}^2(\Omega) \to [\mathbb{L}^2(\Omega)]'$ by

$$[\mathbb{A}(\mathbf{r}),\, \mathbf{s}] \;:=\; \int_\Omega \boldsymbol{\psi}(\mathbf{r}) : \mathbf{s} \qquad \forall\, \mathbf{r},\, \mathbf{s} \in \mathbb{L}^2(\Omega)\,. \tag{4.17}$$

The following result shows that $\mathbb{A}$ is Lipschitz-continuous and strongly monotone.

Lemma 4.2. *Let γ_0 and α_0 be the constants from* (4.2) *and* (4.3)*, respectively. Then, for all $\mathbf{r}, \mathbf{s} \in \mathbb{L}^2(\Omega)$ there hold*

$$\|\mathbb{A}(\mathbf{r}) - \mathbb{A}(\mathbf{s})\|_{[\mathbb{L}^2(\Omega)]'} \;\leq\; \gamma_0\|\mathbf{r} - \mathbf{s}\|_{0,\Omega}, \quad \textit{and} \quad [\mathbb{A}(\mathbf{r}) - \mathbb{A}(\mathbf{s}), \mathbf{r} - \mathbf{s}] \;\geq\; \alpha_0\|\mathbf{r} - \mathbf{s}\|_{0,\Omega}^2\,.$$

Proof. It suffices to observe that for each $\widetilde{\mathbf{r}} \in \mathbb{L}^2(\Omega)$ the Gâteuax derivative $\mathcal{D}\mathbb{A}(\widetilde{\mathbf{r}})$ is a bilinear form on $\mathbb{L}^2(\Omega) \times \mathbb{L}^2(\Omega)$, which is uniformly bounded and uniformly $\mathbb{L}^2(\Omega)$-elliptic (see [84, Lemma 2.1] or [23, Section 3] for details). □

The following two lemmas, which establish that the nonlinear operator $\mathcal{A}_h$ defining the problem (4.10) shares the same properties of $\mathbb{A}$, were provided in Chapter 3.

Lemma 4.3. *Let $\mathcal{A}_h$ be the nonlinear operator defined by* (4.11)*. Then, there exists a constant $C_{\mathrm{LC}} > 0$, independent of h, such that*

$$\|\mathcal{A}_h(\mathbf{t}_h, \boldsymbol{\sigma}_h) - \mathcal{A}_h(\mathbf{s}_h, \boldsymbol{\tau}_h)\|_{H_h'} \;\leq\; C_{\mathrm{LC}}\, \|(\mathbf{t}_h, \boldsymbol{\sigma}_h) - (\mathbf{s}_h, \boldsymbol{\tau}_h)\|_{H_h} \quad \forall\, (\mathbf{t}_h, \boldsymbol{\sigma}_h), (\mathbf{s}_h, \boldsymbol{\tau}_h) \in H_h\,.$$

Proof. See Lemma 3.5. $\square$

Lemma 4.4. *Let $\mathcal{A}_h$ be the nonlinear operator defined by* (4.11)*, and assume that, given $\delta \in \left(0, \frac{2}{\gamma_0}\right)$, the parameter κ_1 lies in $\left(0, \frac{2\alpha_0\delta}{\gamma_0}\right)$, where α_0 and γ_0 are the positive constants from* (4.2) *and* (4.3)*. Then, there exists a constant $C_{\mathrm{SM}} > 0$, independent of h, such that*

$$[\mathcal{A}_h(\mathbf{t}_h, \boldsymbol{\sigma}_h) - \mathcal{A}_h(\mathbf{s}_h, \boldsymbol{\tau}_h), (\mathbf{t}_h, \boldsymbol{\sigma}_h) - (\mathbf{s}_h, \boldsymbol{\tau}_h)] \;\geq\; C_{\mathrm{SM}}\, \|(\mathbf{t}_h, \boldsymbol{\sigma}_h) - (\mathbf{s}_h, \boldsymbol{\tau}_h)\|^2_{H_h}\,,$$

for all $(\mathbf{t}_h, \boldsymbol{\sigma}_h), (\mathbf{s}_h, \boldsymbol{\tau}_h) \in H_h$.

Proof. See Lemma 3.6. $\square$

We remark here that the optimal choice of the stabilization parameter κ_1, that is the one yielding the largest value of the strong monotonicity constant C_{SM}, arises by taking $\delta = \frac{1}{\gamma_0}$ and $\kappa_1 = \frac{\alpha_0}{\gamma_0^2}$. This will be used in Section 4.6. Our next goal is to show the discrete inf-sup condition for the linear operator $\mathcal{B}_h$. More precisely, we have the following result.

Lemma 4.5. *There exists a constant $C_{\mathrm{inf}} > 0$, independent of h, such that*

$$\sup_{\substack{(\mathbf{s}_h, \boldsymbol{\tau}_h) \in H_h \\ (\mathbf{s}_h, \boldsymbol{\tau}_h) \neq \mathbf{0}}} \frac{[\mathcal{B}_h(\mathbf{s}_h, \boldsymbol{\tau}_h), \mathbf{v}_h]}{\|(\mathbf{s}_h, \boldsymbol{\tau}_h)\|_{H_h}} \;\geq\; C_{\mathrm{inf}}\, \|\mathbf{v}_h\|_{0,\Omega} \quad \forall\, \mathbf{v}_h \in V_h\,.$$

Proof. We adapt the proof of Lemma 3.7. Indeed, we begin by recalling from (4.12) that $\mathcal{B}_h$ does not depend on $\mathbf{s}_h$, and hence it suffices to show the existence of $C_{\mathrm{inf}} > 0$ such that

$$\sup_{\substack{\boldsymbol{\tau}_h \in \Sigma_h \\ \boldsymbol{\tau}_h \neq \mathbf{0}}} \frac{\displaystyle\int_\Omega \mathbf{v}_h \cdot \mathbf{div}_h(\boldsymbol{\tau}_h) - \int_{\mathcal{E}_h^i} \{\!\{\mathbf{v}_h\}\!\} \cdot [\![\boldsymbol{\tau}_h]\!]}{\|\boldsymbol{\tau}_h\|_{\Sigma_h}} \;\geq\; C_{\mathrm{inf}}\, \|\mathbf{v}_h\|_{0,\Omega} \quad \forall\, \mathbf{v}_h \in V_h\,.$$

To this end we let $\mathbb{RT}_k(\mathcal{T}_h)$ be the global Raviart-Thomas space of degree k, which is clearly contained in Σ_h, and note that

$$\sup_{\substack{\boldsymbol{\tau}_h \in \Sigma_h \\ \boldsymbol{\tau}_h \neq \mathbf{0}}} \frac{\displaystyle\int_\Omega \mathbf{v}_h \cdot \mathbf{div}_h(\boldsymbol{\tau}_h) - \int_{\mathcal{E}_h^i} \{\!\{\mathbf{v}_h\}\!\} \cdot [\![\boldsymbol{\tau}_h]\!]}{\|\boldsymbol{\tau}_h\|_{\Sigma_h}} \;\geq\; \sup_{\substack{\boldsymbol{\tau}_h \in \mathbb{RT}_k(\mathcal{T}_h) \backslash \{\mathbf{0}\} \\ \int_\Omega \mathrm{tr}(\boldsymbol{\tau}_h) = 0}} \frac{\displaystyle\int_\Omega \mathbf{v}_h \cdot \mathbf{div}(\boldsymbol{\tau}_h)}{\|\boldsymbol{\tau}_h\|_{\Sigma_h}}\,.$$

In this way, and observing that $\|\boldsymbol{\tau}_h\|_{\Sigma_h}$ is equivalent to $\|\boldsymbol{\tau}_h\|_{\mathbf{div},\Omega}$ $\forall\; \boldsymbol{\tau}_h \in \mathbb{RT}_k(\mathcal{T}_h)$ such that $\int_\Omega \mathrm{tr}\,(\boldsymbol{\tau}_h) = 0$, with constants independent of h, the rest of the proof follows from classical results from mixed finite element methods (see, e.g. [71, Section 4.2 and Lemma 2.6]). $\square$

The following lemma establishes the positive semidefiniteness of $\mathcal{S}_h$.

Lemma 4.6. *The operator $\mathcal{S}_h : V_h \to V_h'$ (cf. (4.13)) is positive semidefinite, that is,*

$$[\mathcal{S}_h(\mathbf{v}_h), \mathbf{v}_h] \;\geq\; 0 \quad \forall\, \mathbf{v}_h \in V_h\,.$$

Proof. It is clear from (4.13) and the symmetry of $\mathbf{S}$ that

$$
\begin{aligned}
[\mathcal{S}_h(\mathbf{v}_h),\mathbf{v}_h] &= \sum_{T\in\mathcal{T}_h}\sum_{F\in\partial T}\int_F \mathbf{S}\mathbf{v}_h\cdot\mathbf{v}_h - 2\int_{\mathcal{E}_h^i}\mathbf{S}\{\!\{\mathbf{v}_h\}\!\}\cdot\{\!\{\mathbf{v}_h\}\!\}\\
&= \int_{\mathcal{E}_h^i}\left(\mathbf{S}\mathbf{v}_h^+\cdot\mathbf{v}_h^+ + \mathbf{S}\mathbf{v}_h^-\cdot\mathbf{v}_h^-\right) - \frac{1}{2}\int_{\mathcal{E}_h^i}\left(\mathbf{S}\mathbf{v}_h^+\cdot\mathbf{v}_h^+ + 2\,\mathbf{S}\mathbf{v}_h^+\cdot\mathbf{v}_h^- + \mathbf{S}\mathbf{v}_h^-\cdot\mathbf{v}_h^-\right) + \int_{\mathcal{E}_h^\partial}\mathbf{S}\mathbf{v}_h\cdot\mathbf{v}_h\\
&= \frac{1}{2}\int_{\mathcal{E}_h^i}\left(\mathbf{S}\mathbf{v}_h^+\cdot\mathbf{v}_h^+ - 2\,\mathbf{S}\mathbf{v}_h^+\cdot\mathbf{v}_h^- + \mathbf{S}\mathbf{v}_h^-\cdot\mathbf{v}_h^-\right) + \int_{\mathcal{E}_h^\partial}\mathbf{S}\mathbf{v}_h\cdot\mathbf{v}_h\\
&= \frac{1}{2}\int_{\mathcal{E}_h^i}\mathbf{S}\left(\mathbf{v}_h^+ - \mathbf{v}_h^-\right)\cdot\left(\mathbf{v}_h^+ - \mathbf{v}_h^-\right) + \int_{\mathcal{E}_h^\partial}\mathbf{S}\mathbf{v}_h\cdot\mathbf{v}_h\,,
\end{aligned}
$$

which, thanks to the fact that $\mathbf{S}$ is a positive definite tensor on $\mathcal{E}_h$, completes the proof. □

Now we are ready to establish the main result of this section.

Theorem 4.2. *Assume that $\mathbf{f}\in\mathbf{L}^2(\Omega)$, $\mathbf{g}\in\mathbf{H}^{1/2}(\Gamma)$, and that, given $\delta\in\left(0,\frac{2}{\gamma_0}\right)$, the parameter κ_1 lies in $\left(0,\frac{2\alpha_0\delta}{\gamma_0}\right)$, where α_0 and γ_0 are the positive constants from* (4.2) *and* (4.3). *Then, there exists a unique $((\mathbf{t}_h,\boldsymbol{\sigma}_h),\mathbf{u}_h)\in H_h\times V_h$ solution of* (4.10). *Moreover, there holds*

$$
\|(\mathbf{t}_h,\boldsymbol{\sigma}_h)\|_{H_h} + \|\mathbf{u}_h\|_{0,\Omega} \le C\left\{\|\mathbf{f}\|_{0,\Omega} + \|\mathtt{h}^{-1/2}\mathbf{g}\|_{0,\mathcal{E}_h^\partial}\right\}.
$$

Proof. Thanks to Lemmas 4.3, 4.4, 4.5, and 4.6, the proof is a direct application of Theorem 4.1. □

4.4 A priori error analysis

We now aim to derive the *a priori* error estimates for the augmented HDG scheme (4.10). We begin by remarking that the proof from Section 3.4 is suitably adapted. Thus, since $\mathbf{u}\in\mathbf{L}^2(\Omega)$ and $\nabla\mathbf{u}=\mathbf{t}\in\mathbb{L}^2(\Omega)$ (cf. (4.5)), we observe that actually $\mathbf{u}\in\mathbf{H}^1(\Omega)$, which guarantees that the jump $[\![\mathbf{u}]\!]$ vanishes on any interior face of $\mathcal{T}_h$ and there holds $\{\!\{\mathbf{u}\}\!\}=\mathbf{u}$. In addition, since $\boldsymbol{\sigma}=\boldsymbol{\psi}(\nabla\mathbf{u})-p\,\mathbb{I}\in\mathbb{L}^2(\Omega)$ and $\mathbf{div}(\boldsymbol{\sigma})=-\mathbf{f}$ in Ω, with $\mathbf{f}\in\mathbf{L}^2(\Omega)$, we conclude that $\boldsymbol{\sigma}\in\mathbb{H}(\mathbf{div};\Omega)$, whence $[\![\boldsymbol{\sigma}]\!]=\mathbf{0}$ on each $F\in\mathcal{E}_h^i$. Then, it is easy to check that $(\mathbf{t},\boldsymbol{\sigma},\mathbf{u})$ satisfies the equations of (4.10), and then there holds

$$
\begin{aligned}
[\mathcal{A}_h(\mathbf{t},\boldsymbol{\sigma})-\mathcal{A}_h(\mathbf{t}_h,\boldsymbol{\sigma}_h),(\mathbf{s}_h,\boldsymbol{\tau}_h)] + [\mathcal{B}_h(\mathbf{s}_h,\boldsymbol{\tau}_h),\mathbf{u}-\mathbf{u}_h] &= 0 \quad \forall\,(\mathbf{s}_h,\boldsymbol{\tau}_h)\in H_h\,,\\
[\mathcal{B}_h((\mathbf{t},\boldsymbol{\sigma})-(\mathbf{t}_h,\boldsymbol{\sigma}_h)),\mathbf{v}_h] - [\mathcal{S}_h(\mathbf{u}-\mathbf{u}_h),\mathbf{v}_h] &= 0 \quad \forall\,\mathbf{v}_h\in V_h\,.
\end{aligned}
\tag{4.18}
$$

The following result establishes the Céa estimate for (4.6) and (4.10).

Lemma 4.7. *Let $(\mathbf{t},\boldsymbol{\sigma},\mathbf{u})\in\mathbb{L}^2(\Omega)\times\mathbb{H}(\mathbf{div};\Omega)\times\mathbf{L}^2(\Omega)$ and $((\mathbf{t}_h,\boldsymbol{\sigma}_h),\mathbf{u}_h)\in H_h\times V_h$ be the unique solutions of* (4.6) *and* (4.10), *respectively. Then, there exists $C>0$, independent of h, such that*

$$
\begin{aligned}
&\|(\mathbf{t},\boldsymbol{\sigma})-(\mathbf{t}_h,\boldsymbol{\sigma}_h)\|_{H_h} + \|\mathbf{u}-\mathbf{u}_h\|_{0,\Omega}\\
&\quad\le C\left\{\inf_{(\mathbf{s}_h,\boldsymbol{\tau}_h)\in H_h}\|(\mathbf{t},\boldsymbol{\sigma})-(\mathbf{s}_h,\boldsymbol{\tau}_h)\|_{H_h} + \inf_{\mathbf{v}_h\in V_h}\|\mathbf{u}-\mathbf{v}_h\|_{0,\Omega}\right\}.
\end{aligned}
$$

Proof. It is not difficult to see that $\mathcal{A}_h$ has a uniformly bounded and uniformly H_h-elliptic Gâteuax derivative, and hence the proof is a straightforward adaptation of the arguments from [77, Theorem 3.3], together with simple applications of the triangle inequality and (4.18). □

Next, in order to provide the rate of convergence of the discontinuous Galerkin scheme (4.10), we need the approximation properties of the finite element subspaces involved. For this purpose, given $T \in \mathcal{T}_h$, we let $\boldsymbol{\mathcal{P}}_T^k : \mathbb{L}^2(T) \to \mathbb{P}_k(T)$ and $\mathcal{P}_T^k : \mathbf{L}^2(T) \to \mathbf{P}_k(T)$ be the $\mathbb{L}^2(T)$ and $\mathbf{L}^2(T)$ − orthogonal projectors, respectively, which satisfy (see, e.g. [37, 71])

$$\|\mathbf{s} - \boldsymbol{\mathcal{P}}_T^k(\mathbf{s})\|_{0,T} \,\leq\, C\, h_T^{\min\{\ell,k+1\}} |\mathbf{s}|_{\ell,T} \quad \forall\, \mathbf{s} \in \mathbb{H}^\ell(T)\,, \quad \forall\, T \in \mathcal{T}_h\,, \tag{4.19}$$

and

$$\|\mathbf{v} - \mathcal{P}_T^k(\mathbf{v})\|_{0,T} \,\leq\, C\, h_T^{\min\{\ell,k+1\}} |\mathbf{v}|_{\ell,T} \quad \forall\, \mathbf{v} \in \mathbf{H}^\ell(T)\,, \quad \forall\, T \in \mathcal{T}_h\,. \tag{4.20}$$

Furthermore, let $\Pi_T^k : \mathbb{H}^1(T) \to \mathbb{RT}_k(T)$ be the Raviart-Thomas interpolation operator (see [19, 71, 116]), which, given $\boldsymbol{\tau} \in \mathbb{H}^1(\Omega)$, is characterized by the following identities:

$$\int_F \Pi_T^k(\boldsymbol{\tau})\boldsymbol{\nu} \cdot \boldsymbol{\mu} \;=\; \int_F \boldsymbol{\tau}\boldsymbol{\nu} \cdot \boldsymbol{\mu} \qquad \forall\, \boldsymbol{\mu} \in \mathbf{P}_k(F)\,, \quad \forall\, F \in \partial T\,, \quad \text{when } k \geq 0\,, \tag{4.21}$$

and

$$\int_T \Pi_T^k(\boldsymbol{\tau}) : \boldsymbol{\rho} \;=\; \int_T \boldsymbol{\tau} : \boldsymbol{\rho} \qquad \forall\, \boldsymbol{\rho} \in \mathbb{P}_{k-1}(T)\,, \quad \text{when } k \geq 1\,. \tag{4.22}$$

It is well-known that Π_T^k satisfies the approximation property

$$\|\boldsymbol{\tau} - \Pi_T^k(\boldsymbol{\tau})\|_{\mathbf{div},T} \;\leq\; C h_T^{\min\{\ell,k+1\}} \Big\{ |\boldsymbol{\tau}|_{\ell,T} \,+\, |\mathbf{div}(\boldsymbol{\tau})|_{\ell,T} \Big\} \quad \forall\, T \in \mathcal{T}_h\,, \tag{4.23}$$

for each $\boldsymbol{\tau} \in \mathbb{H}^\ell(T)$ such that $\mathbf{div}(\boldsymbol{\tau}) \in \mathbf{H}^\ell(T)$, with $\ell \geq 1$. Moreover, the interpolation operator Π_T^k can also be defined as a bounded linear operator from the larger space $\mathbb{H}^\ell(T) \cap \mathbb{H}(\mathbf{div}; T)$ into $\mathbb{RT}_k(T)$ for all $\ell \in (0, 1]$ (see, e.g. [96, Theorem 3.16]). In this case there holds (see [71, Lemma 3.19])

$$\|\boldsymbol{\tau} - \Pi_T^k(\boldsymbol{\tau})\|_{0,T} \;\leq\; C h_T^\ell \Big\{ |\boldsymbol{\tau}|_{\ell,T} \,+\, \|\mathbf{div}(\boldsymbol{\tau})\|_{0,T} \Big\} \quad \forall\, T \in \mathcal{T}_h\,,$$

which, thanks to (4.23) and interpolation estimates, implies for $\ell > 0$ that

$$\|\boldsymbol{\tau} - \Pi_T^k(\boldsymbol{\tau})\|_{\mathbf{div},T} \;\leq\; C h_T^{\min\{\ell,k+1\}} \Big\{ |\boldsymbol{\tau}|_{\ell,T} \,+\, \|\mathbf{div}(\boldsymbol{\tau})\|_{\ell,T} \Big\} \quad \forall\, T \in \mathcal{T}_h\,. \tag{4.24}$$

Next, observe that, given $Z := \{\boldsymbol{\tau} \in \mathbb{L}^2(\Omega) \;:\; \boldsymbol{\tau}|_T \in \mathbb{H}^\ell(T) \quad \forall\, T \in \mathcal{T}_h\}$, we can define $\Pi_{\Sigma_h} : \mathbb{H}(\mathbf{div}; \Omega) \cap Z \to \Sigma_h$ by

$$\Pi_{\Sigma_h}(\boldsymbol{\tau})|_T \;:=\; \Pi_T^k(\boldsymbol{\tau}|_T) \;+\; d\,\mathbb{I} \quad \forall\, T \in \mathcal{T}_h\,,$$

with $d := -\frac{1}{n|\Omega|} \sum\limits_{T \in \mathcal{T}_h} \int_T \operatorname{tr}\left(\Pi_T^k(\boldsymbol{\tau}|_T)\right) \in \mathrm{R}$. Then, it is easy to prove that

$$\|\boldsymbol{\tau} - \Pi_{\Sigma_h}(\boldsymbol{\tau})\|_{\Sigma_h}^2 \;\leq\; \sum_{T \in \mathcal{T}_h} \|\boldsymbol{\tau} - \Pi_T^k(\boldsymbol{\tau})\|_{\mathbf{div},T}^2 \quad \forall\, \boldsymbol{\tau} \in \mathbb{H}(\mathbf{div}; \Omega) \cap Z\,,$$

and hence, employing the estimate (4.24), we arrive at

$$\|\boldsymbol{\tau} - \Pi_{\Sigma_h}(\boldsymbol{\tau})\|_{\Sigma_h} \;\leq\; C \sum_{T \in \mathcal{T}_h} h_T^{\min\{\ell,k+1\}} \Big\{ |\boldsymbol{\tau}|_{\ell,T} \,+\, \|\mathbf{div}(\boldsymbol{\tau})\|_{\ell,T} \Big\}\,. \tag{4.25}$$

In this way, as a consequence of (4.19), (4.20), (4.25), and the usual interpolation estimates, we find that S_h, Σ_h and V_h satisfy the following approximation properties:

$(\mathbf{AP}_h^{\mathbf{t}})$ For each $\ell \geq 0$ and for each $\mathbf{s} \in \mathbb{H}^\ell(\Omega)$ there exists $\mathbf{s}_h \in S_h$ such that

$$\|\mathbf{s} - \mathbf{s}_h\|_{0,\Omega} \;\leq\; C \sum_{T\in\mathcal{T}_h} h_T^{\min\{\ell,k+1\}} |\mathbf{s}|_{\ell,T}\,.$$

$(\mathbf{AP}_h^{\boldsymbol{\sigma}})$ For each $\ell > 0$ and for each $\boldsymbol{\tau} \in \mathbb{H}^\ell(\Omega)$ with $\mathbf{div}(\boldsymbol{\tau}) \in \mathbf{H}^\ell(\Omega)$ there exists $\boldsymbol{\tau}_h \in \Sigma_h$ such that

$$\|\boldsymbol{\tau} - \boldsymbol{\tau}_h\|_{\Sigma_h} \;\leq\; C \sum_{T\in\mathcal{T}_h} h_T^{\min\{\ell,k+1\}} \Big\{ |\boldsymbol{\tau}|_{\ell,T} \;+\; \|\mathbf{div}(\boldsymbol{\tau})\|_{\ell,T} \Big\}\,.$$

$(\mathbf{AP}_h^{\mathbf{u}})$ For each $\ell \geq 0$ and for each $\mathbf{v} \in \mathbf{H}^\ell(\Omega)$ there exists $\mathbf{v}_h \in V_h$ such that

$$\|\mathbf{v} - \mathbf{v}_h\|_{0,\Omega} \;\leq\; C \sum_{T\in\mathcal{T}_h} h_T^{\min\{\ell,k+1\}} |\mathbf{v}|_{\ell,T}\,.$$

The following theorem establishes the theoretical rates of convergence of the discrete scheme (4.10), under suitable regularity assumptions on the exact solution.

Theorem 4.3. *Let $(\mathbf{t}, \boldsymbol{\sigma}, \mathbf{u}) \in \mathbb{L}^2(\Omega) \times \mathbb{H}(\mathbf{div};\Omega) \times \mathbf{L}^2(\Omega)$ and $((\mathbf{t}_h, \boldsymbol{\sigma}_h), \mathbf{u}_h) \in H_h \times V_h$ be the unique solutions of* (4.6) *and* (4.10)*, respectively. In addition, suppose that there exists an integer $\ell > 0$ such that $\mathbf{t}|_T \in \mathbb{H}^\ell(T)$, $\boldsymbol{\sigma}|_T \in \mathbb{H}^\ell(T)$, $\mathbf{div}(\boldsymbol{\sigma}|_T) \in \mathbf{H}^\ell(T)$ and $\mathbf{u}|_T \in \mathbf{H}^\ell(T)$, for all $T \in \mathcal{T}_h$. Then, there exists $C > 0$, independent of h and the polynomial approximation degree k, such that*

$$\begin{aligned} &\|\mathbf{t} - \mathbf{t}_h\|_{0,\Omega} \;+\; \|\boldsymbol{\sigma} - \boldsymbol{\sigma}_h\|_{\Sigma_h} \;+\; \|\mathbf{u} - \mathbf{u}_h\|_{0,\Omega} \\ &\quad\leq\; C \sum_{T\in\mathcal{T}_h} h_T^{\min\{\ell,k+1\}} \Big\{ |\mathbf{t}|_{\ell,T} \;+\; |\boldsymbol{\sigma}|_{\ell,T} \;+\; \|\mathbf{div}(\boldsymbol{\sigma})\|_{\ell,T} \;+\; |\mathbf{u}|_{\ell,T} \Big\}\,. \end{aligned}$$

Proof. It follows from the Céa estimate (cf. Lemma 4.7) and the approximation properties $(\mathbf{AP}_h^{\mathbf{t}})$, $(\mathbf{AP}_h^{\boldsymbol{\sigma}})$ and $(\mathbf{AP}_h^{\mathbf{u}})$. $\square$

Note from the previous theorem and (4.16) that we can also conclude that

$$\|\boldsymbol{\sigma} - \boldsymbol{\sigma}_h\|_{0,\Omega} \;\;\leq\;\; C \sum_{T\in\mathcal{T}_h} h_T^{\min\{\ell,k+1\}} \Big\{ |\mathbf{t}|_{\ell,T} + |\boldsymbol{\sigma}|_{\ell,T} + \|\mathbf{div}(\boldsymbol{\sigma})\|_{\ell,T} + |\mathbf{u}|_{\ell,T} \Big\}\,. \tag{4.26}$$

On the other hand, we know from (4.4) that $p = -\frac{1}{n}\mathrm{tr}\,(\boldsymbol{\sigma})$, which suggests to define the following postprocessed approximation of the pressure:

$$p_h \;:=\; -\frac{1}{n}\,\mathrm{tr}\,(\boldsymbol{\sigma}_h) \quad \text{in} \quad \Omega\,. \tag{4.27}$$

It follows that

$$\|p - p_h\|_{0,\Omega} \;=\; \frac{1}{n}\,\|\mathrm{tr}\,(\boldsymbol{\sigma} - \boldsymbol{\sigma}_h)\,\|_{0,\Omega} \;\leq\; \frac{1}{\sqrt{n}}\,\|\boldsymbol{\sigma} - \boldsymbol{\sigma}_h\|_{0,\Omega}\,, \tag{4.28}$$

which, thanks to (4.26), gives the *a priori* error estimate for the pressure.

Finally, in order to measure the error for the trace variable, namely $\widehat{\mathbf{u}}_h$ or $\boldsymbol{\lambda}_h$, we define the error:

$$\|\mathbf{u} - \widehat{\mathbf{u}}_h\|_h \;:=\; \left\{ \sum_{F\in\mathcal{E}_h^i} \left\| \mathrm{h}^{1/2}\big(\{\!\!\{\mathcal{P}_h^k(\mathbf{u})\}\!\!\} - \boldsymbol{\lambda}_h\big) \right\|_{0,F}^2 \right\}^{1/2}, \tag{4.29}$$

where $\mathcal{P}_h^k|_T := \mathcal{P}_T^k$, for each $T \in \mathcal{T}_h$. The corresponding *a priori* error estimate is established next.

Theorem 4.4. *Assume the same hypotheses of Theorem 4.3. Then, there exists $C > 0$, independent of h and the polynomial approximation degree k, such that*

$$\|\mathbf{u} - \widehat{\mathbf{u}}_h\|_h \;\le\; C \sum_{T\in\mathcal{T}_h} h_T^{\min\{\ell,k+1\}} \Big\{ |\mathbf{t}|_{\ell,T} + |\boldsymbol{\sigma}|_{\ell,T} + \|\mathbf{div}(\boldsymbol{\sigma})\|_{\ell,T} + |\mathbf{u}|_{\ell,T} \Big\}.$$

Proof. From (4.9), (4.15) and the fact that $[\![\boldsymbol{\sigma}]\!] = \mathbf{0}$ on $\mathcal{E}_h^i$, we obtain that

$$\begin{aligned}
\|\mathbf{u} - \widehat{\mathbf{u}}_h\|_h^2 \;&=\; \sum_{F\in\mathcal{E}_h^i} \left\| \mathtt{h}^{1/2} \left(\{\!\{\mathcal{P}_h^k(\mathbf{u})\}\!\} - \{\!\{\mathbf{u}_h\}\!\} + \frac{1}{2}\mathtt{h}^{-1}[\![\boldsymbol{\sigma}_h]\!] \right) \right\|_{0,F}^2 \\
&\le\; 2 \sum_{F\in\mathcal{E}_h^i} \left\{ \|\mathtt{h}^{1/2}\, \{\!\{\mathcal{P}_h^k(\mathbf{u}) - \mathbf{u}_h\}\!\}\|_{0,F}^2 + \frac{1}{4} \|\mathtt{h}^{-1/2}[\![\boldsymbol{\sigma} - \boldsymbol{\sigma}_h]\!]\|_{0,F}^2 \right\} \\
&\le\; C \Big\{ \|\mathtt{h}^{1/2} \{\!\{\mathcal{P}_h^k(\mathbf{u}) - \mathbf{u}_h\}\!\}\|_{0,\mathcal{E}_h^i}^2 \;+\; \|\boldsymbol{\sigma} - \boldsymbol{\sigma}_h\|_{\Sigma_h}^2 \Big\}.
\end{aligned} \tag{4.30}$$

Next, using the analogue of Lemma 3.10 part i), we deduce that

$$\|\mathtt{h}^{1/2} \{\!\{\mathcal{P}_h^k(\mathbf{u}) - \mathbf{u}_h\}\!\}\|_{0,\mathcal{E}_h^i} \;\le\; \widetilde{C}\, \|\mathcal{P}_h^k(\mathbf{u}) - \mathbf{u}_h\|_{0,\Omega}\,,$$

with $\widetilde{C}$ independent of h. Therefore, we conclude from (4.30) that

$$\begin{aligned}
\|\mathbf{u} - \widehat{\mathbf{u}}_h\|_h \;&\le\; C \Big\{ \|\mathcal{P}_h^k(\mathbf{u}) - \mathbf{u}_h\|_{0,\Omega} \;+\; \|\boldsymbol{\sigma} - \boldsymbol{\sigma}_h\|_{\Sigma_h} \Big\} \\
&\le\; C \Big\{ \|\mathbf{u} - \mathcal{P}_h^k(\mathbf{u})\|_{0,\Omega} \;+\; \|\mathbf{u} - \mathbf{u}_h\|_{0,\Omega} \;+\; \|\boldsymbol{\sigma} - \boldsymbol{\sigma}_h\|_{\Sigma_h} \Big\},
\end{aligned}$$

which, together with (4.20) and Theorem 4.3, complete the proof. □

4.5 A residual-based a posteriori error estimator

In this section we develop a residual-based *a posteriori* error analysis for the augmented HDG scheme (4.8). We begin by recalling that the equivalent formulation (4.10) was introduced in order to perform the solvability analysis and derive the *a priori* error estimates provided in Sections 4.3 and 4.4, respectively. In what follows we restrict ourselves to an arbitrary polygonal domain Ω in 2D, but keep in mind that the extension to polyhedral domains in 3D is quite straightforward (see, e.g. Section 1.4 for a related approach in this regard).

First we introduce some notations. Given $T \in \mathcal{T}_h$, we let

$$\|\boldsymbol{\tau}_h\|_{\Sigma_h(T)}^2 \;:=\; \|\boldsymbol{\tau}_h^{\mathtt{d}}\|_{0,T}^2 \;+\; \|\mathbf{div}(\boldsymbol{\tau}_h)\|_{0,T}^2 \;+\; \frac{1}{2} \sum_{F\in\partial T\cap\mathcal{E}_h^i} \|\mathtt{h}^{-1/2}[\![\boldsymbol{\tau}_h]\!]\|_{0,F}^2\,,$$

be the local contribution of the norm $\|\cdot\|_{\Sigma_h}$, that is,

$$\|\boldsymbol{\tau}_h\|_{\Sigma_h} \;=\; \left\{ \sum_{T\in\mathcal{T}_h} \|\boldsymbol{\tau}_h\|_{\Sigma_h(T)}^2 \right\}^{1/2}. \tag{4.31}$$

Also, for each edge $F \in \mathcal{E}_h$ we fix a unit normal vector $\boldsymbol{\nu}_F := (\nu_1, \nu_2)^{\mathtt{t}}$, and let $\boldsymbol{s}_F := (-\nu_2, \nu_1)^{\mathtt{t}}$ be the corresponding fixed unit tangential vector along F. Then, given $F \in \mathcal{E}_h^i$ such that $F = \partial T^+ \cap \partial T^-$, we let $[\![\boldsymbol{\tau}\boldsymbol{s}_F]\!]$ be the corresponding tangential jump across F, that is $[\![\boldsymbol{\tau}\boldsymbol{s}_F]\!] := (\boldsymbol{\tau}^+ - \boldsymbol{\tau}^-)\boldsymbol{s}_F$. From now on, when no confusion arises, we simply write $\boldsymbol{s}$ and $\boldsymbol{\nu}$ instead of $\boldsymbol{s}_F$ and $\boldsymbol{\nu}_F$, respectively. Finally, given scalar, vector and tensor valued fields v, $\boldsymbol{\varphi} := (\varphi_1, \varphi_2)$ and $\boldsymbol{\tau} := (\tau_{ij})$, respectively, we let

$$\mathbf{curl}(v) := \begin{pmatrix} \frac{\partial v}{\partial x_2} \\ -\frac{\partial v}{\partial x_1} \end{pmatrix}, \quad \underline{\mathbf{curl}}(\boldsymbol{\varphi}) := \begin{pmatrix} \mathbf{curl}(\varphi_1)^{\mathrm{t}} \\ \mathbf{curl}(\varphi_2)^{\mathrm{t}} \end{pmatrix}, \quad \text{and} \quad \mathrm{curl}(\boldsymbol{\tau}) := \begin{pmatrix} \frac{\partial \tau_{12}}{\partial x_1} - \frac{\partial \tau_{11}}{\partial x_2} \\ \frac{\partial \tau_{22}}{\partial x_1} - \frac{\partial \tau_{21}}{\partial x_2} \end{pmatrix}.$$

4.5.1 Flux postprocessing

We now follow [44, Section 5.1] (see also [45]) and introduce a postprocessed flux $\boldsymbol{\sigma}_h^\star$ for the variable $\boldsymbol{\sigma}_h$, that is, we let $\boldsymbol{\sigma}_h^\star$ be the unique element in $\mathbb{RT}_k(\mathcal{T}_h)$ such that

$$\int_T \boldsymbol{\sigma}_h^\star : \boldsymbol{\tau}_h = \int_T \boldsymbol{\sigma}_h : \boldsymbol{\tau}_h \quad \forall\, \boldsymbol{\tau}_h \in \mathbb{P}_{k-1}(T), \quad \forall\, T \in \mathcal{T}_h, \tag{4.32}$$

$$\int_F \boldsymbol{\sigma}_h^\star \boldsymbol{\nu} \cdot \boldsymbol{\mu}_h = \int_F \widehat{\boldsymbol{\sigma}_h \boldsymbol{\nu}} \cdot \boldsymbol{\mu}_h \quad \forall\, \boldsymbol{\mu}_h \in \mathbf{P}_k(F), \quad \forall\, F \in \partial T, \quad \forall\, T \in \mathcal{T}_h, \tag{4.33}$$

where $\mathbb{RT}_k(\mathcal{T}_h)$ is the global Raviart-Thomas subspace of degree k. It is important to observe here, thanks to the fourth equation of (4.7), that $\boldsymbol{\sigma}_h^\star \in \mathbb{H}(\mathbf{div};\Omega)$. In addition, from the third equation in (4.7) and the foregoing definition of $\boldsymbol{\sigma}_h^\star$, we have that

$$(\mathbf{f}, \mathbf{v}_h)_{\mathcal{T}_h} = (\boldsymbol{\sigma}_h, \nabla \mathbf{v}_h)_{\mathcal{T}_h} - \langle \widehat{\boldsymbol{\sigma}_h \boldsymbol{\nu}}, \mathbf{v}_h \rangle_{\partial \mathcal{T}_h} = (\boldsymbol{\sigma}_h^\star, \nabla \mathbf{v}_h)_{\mathcal{T}_h} - \langle \boldsymbol{\sigma}_h^\star \boldsymbol{\nu}, \mathbf{v}_h \rangle_{\partial \mathcal{T}_h} = -(\mathbf{div}(\boldsymbol{\sigma}_h^\star), \mathbf{v}_h)_{\mathcal{T}_h}$$

for all $\mathbf{v}_h \in V_h$. The above identity and the fact that $\mathbf{div}(\boldsymbol{\sigma}_h^\star)|_T \in \mathbf{P}_k(T)$ for each $T \in \mathcal{T}_h$ imply that

$$\mathbf{div}(\boldsymbol{\sigma}_h^\star) = -\mathcal{P}_h^k(\mathbf{f}) \quad \text{in} \quad \Omega,$$

where $\mathcal{P}_h^k : \mathbf{L}^2(\Omega) \to V_h$ is the $\mathbf{L}^2(\Omega)$-orthogonal projector. More precisely, $\mathcal{P}_h^k|_T := \mathcal{P}_T^k$ for each $T \in \mathcal{T}_h$.

Now, recalling that $\mathbb{H}(\mathbf{div};\Omega) = \mathbb{H}_0(\mathbf{div};\Omega) \oplus \mathrm{R}\,\mathbb{I}$, we denote by $\boldsymbol{\sigma}_{h,0}^\star$ the $\mathbb{H}_0(\mathbf{div};\Omega)$-component of $\boldsymbol{\sigma}_h^\star$. Equivalently, we write $\boldsymbol{\sigma}_h^\star = \boldsymbol{\sigma}_{h,0}^\star + d\,\mathbb{I}$, where $\boldsymbol{\sigma}_{h,0}^\star \in \mathbb{H}_0(\mathbf{div};\Omega)$ and $d := \frac{1}{n|\Omega|}\int_\Omega \mathrm{tr}\,(\boldsymbol{\sigma}_h^\star) \in \mathrm{R}$. Notice from (4.32) and the fact that $\int_\Omega \mathrm{tr}\,(\boldsymbol{\sigma}_h) = 0$, that $\boldsymbol{\sigma}_h^\star = \boldsymbol{\sigma}_{h,0}^\star$ when $k \geq 1$.

We end this section by remarking in advance that the *a posteriori* error estimator to be introduced below (cf. (4.36)) will depend on $\boldsymbol{\sigma}_{h,0}^\star$.

4.5.2 The a posteriori error estimator

We now recall from [84] that the augmented continuous formulation associated with (4.6) reads: Find $((\mathbf{t}, \boldsymbol{\sigma}), \mathbf{u}) \in H \times V$ such that

$$\begin{aligned} [\mathcal{A}(\mathbf{t}, \boldsymbol{\sigma}), (\mathbf{s}, \boldsymbol{\tau})] + [\mathcal{B}(\mathbf{s}, \boldsymbol{\tau}), \mathbf{u}] &= [\mathcal{F}, (\mathbf{s}, \boldsymbol{\tau})] \quad \forall\, (\mathbf{s}, \boldsymbol{\tau}) \in H, \\ [\mathcal{B}(\mathbf{t}, \boldsymbol{\sigma}), \mathbf{v}] &= [\mathcal{G}, \mathbf{v}] \qquad \forall\, \mathbf{v} \in V, \end{aligned} \tag{4.34}$$

where $H := \mathbb{L}^2(\Omega) \times \mathbb{H}_0(\mathbf{div};\Omega)$, $V := \mathbf{L}^2(\Omega)$ and the nonlinear operator $\mathcal{A} : H \to H'$, the linear operator $\mathcal{B} : H \to V'$, and the functionals $\mathcal{F} \in H'$ and $\mathcal{G} \in V'$, are defined by:

$$[\mathcal{A}(\mathbf{t}, \boldsymbol{\sigma}), (\mathbf{s}, \boldsymbol{\tau})] := \int_\Omega \boldsymbol{\psi}(\mathbf{t}) : \mathbf{s} - \int_\Omega \mathbf{s} : \boldsymbol{\sigma}^{\mathrm{d}} + \int_\Omega \mathbf{t} : \boldsymbol{\tau}^{\mathrm{d}} + \kappa_1 \int_\Omega (\boldsymbol{\sigma}^{\mathrm{d}} - \boldsymbol{\psi}(\mathbf{t})) : \boldsymbol{\tau}^{\mathrm{d}} + \kappa_2 \int_\Omega \mathbf{div}(\boldsymbol{\sigma}) \cdot \mathbf{div}(\boldsymbol{\tau}),$$

$$[\mathcal{B}(\mathbf{s},\boldsymbol{\tau}),\mathbf{v}] \;:=\; \int_\Omega \mathbf{v}\cdot\mathbf{div}(\boldsymbol{\tau}), \quad [\mathcal{F},(\mathbf{s},\boldsymbol{\tau})] \;:=\; \langle\boldsymbol{\tau\nu},\mathbf{g}\rangle_\Gamma - \kappa_2\int_\Omega \mathbf{f}\cdot\mathbf{div}(\boldsymbol{\tau}), \quad \text{and} \quad [\mathcal{G},\mathbf{v}] \;:=\; -\int_\Omega \mathbf{f}\cdot\mathbf{v}.$$

We know from the analysis developed in [84, Section 3.1] that the problem (4.34) is well-posed, for $\kappa_1 \in \left(0, \frac{2\alpha_0\delta}{\gamma_0}\right)$, with $\delta \in \left(0, \frac{2}{\gamma_0}\right)$, and $\kappa_2 > 0$. Certainly, the same is valid for the linear operator $\mathcal{M}$ obtained by adding the two equations on the left hand side of (4.34), after replacing $\mathbb{A}$ (cf. (4.17)) within $\mathcal{A}$ by the Gâteaux derivative $\mathcal{D}\mathbb{A}(\widetilde{\mathbf{r}})$ at any $\widetilde{\mathbf{r}}\in\mathbb{L}^2(\Omega)$, that is

$$\begin{aligned}[\,\mathcal{M}((\mathbf{s},\boldsymbol{\tau}),\mathbf{v}),\,((\mathbf{r},\boldsymbol{\rho}),\mathbf{w})\,] \;:=\; &\mathcal{D}\mathbb{A}(\widetilde{\mathbf{r}})(\mathbf{r},\mathbf{s}-\kappa_1\boldsymbol{\tau}^{\mathtt{d}}) - \int_\Omega \mathbf{s}:\boldsymbol{\rho}^{\mathtt{d}} + \int_\Omega \mathbf{r}:\boldsymbol{\tau}^{\mathtt{d}} + \kappa_1\int_\Omega \boldsymbol{\rho}^{\mathtt{d}}:\boldsymbol{\tau}^{\mathtt{d}}\\ &+ \kappa_2\int_\Omega \mathbf{div}(\boldsymbol{\rho})\cdot\mathbf{div}(\boldsymbol{\tau}) \;+\; [\mathcal{B}(\mathbf{s},\boldsymbol{\tau}),\mathbf{w}] \;+\; [\mathcal{B}(\mathbf{r},\boldsymbol{\rho}),\mathbf{v}]\,.\end{aligned}$$

Then, applying the respective continuous dependence result to $\mathcal{M}$, we obtain a global inf-sup condition, which means that there exists a constant $\widetilde{C} > 0$ such that

$$\widetilde{C}\,\|((\mathbf{r},\boldsymbol{\rho}),\mathbf{w})\|_{H\times V} \;\le\; \sup_{\substack{((\mathbf{s},\boldsymbol{\tau}),\mathbf{v})\in H\times V\\ ((\mathbf{s},\boldsymbol{\tau}),\mathbf{v})\neq\mathbf{0}}} \frac{[\,\mathcal{M}((\mathbf{s},\boldsymbol{\tau}),\mathbf{v}),\,((\mathbf{r},\boldsymbol{\rho}),\mathbf{w})\,]}{\|((\mathbf{s},\boldsymbol{\tau}),\mathbf{v})\|_{H\times V}} \tag{4.35}$$

for all $(\widetilde{\mathbf{r}},((\mathbf{r},\boldsymbol{\rho}),\mathbf{w}))\in\mathbb{L}^2(\Omega)\times(H\times V)$. This estimate will be employed below in Section 4.5.3 for the reliability of our *a posteriori* error estimator.

On the other hand, letting $((\mathbf{t},\boldsymbol{\sigma}),\mathbf{u})\in H\times V$ and $((\mathbf{t}_h,\boldsymbol{\sigma}_h),\mathbf{u}_h)\in H_h\times V_h$ be the unique solutions of the continuous and discrete formulations (4.34) and (4.8), respectively, we define for each $T\in\mathcal{T}_h$ a local error indicator θ_T as follows:

$$\begin{aligned}\theta_T^2 \;:=\; &\|(\boldsymbol{\sigma}^\star_{h,0}-\boldsymbol{\sigma}_h)^{\mathtt{d}}\|^2_{0,T} \;+\; \|\mathbf{div}(\boldsymbol{\sigma}^\star_{h,0}-\boldsymbol{\sigma}_h)\|^2_{0,T} \;+\; \|\mathbf{f}+\mathbf{div}(\boldsymbol{\sigma}_h)\|^2_{0,T} \;+\; \|\boldsymbol{\sigma}_h^{\mathtt{d}}-\boldsymbol{\psi}(\mathbf{t}_h)^{\mathtt{d}}\|^2_{0,T}\\ &+\; h_T^2\|\nabla\mathbf{u}_h-\mathbf{t}_h^{\mathtt{d}}\|^2_{0,T} \;+\; h_T^2\|\mathrm{curl}(\mathbf{t}_h^{\mathtt{d}})\|^2_{0,T} \;+\; h_T^2\|\mathrm{curl}(\boldsymbol{\sigma}_h^{\mathtt{d}}-\boldsymbol{\psi}(\mathbf{t}_h)^{\mathtt{d}})\|^2_{0,T}\\ &+\sum_{F\in\partial T\cap\mathcal{E}_h^i}\left\{h_F\|[\![\mathbf{t}_h^{\mathtt{d}}\boldsymbol{s}]\!]\|^2_{0,F} \;+\; \|\mathrm{h}^{-1/2}[\![\boldsymbol{\sigma}_h]\!]\|^2_{0,F} \;+\; h_F\left\|[\![\left(\boldsymbol{\sigma}_h^{\mathtt{d}}-\boldsymbol{\psi}(\mathbf{t}_h)^{\mathtt{d}}\right)\boldsymbol{s}]\!]\right\|^2_{0,F}\right\}\\ &+\sum_{F\in\partial T\cap\mathcal{E}_h^\partial} h_F\left\{\left\|\frac{d\mathbf{g}}{d\boldsymbol{s}}-\mathbf{t}_h^{\mathtt{d}}\boldsymbol{s}\right\|^2_{0,F} \;+\; \|\mathbf{g}-\mathbf{u}_h\|^2_{0,F} \;+\; \left\|\left(\boldsymbol{\sigma}_h^{\mathtt{d}}-\boldsymbol{\psi}(\mathbf{t}_h)^{\mathtt{d}}\right)\boldsymbol{s}\right\|^2_{0,F}\right\}.\end{aligned} \tag{4.36}$$

The residual character of each term on the right hand side of (4.36) is quite clear. As usual the expression $\boldsymbol{\theta} := \left\{\sum_{T\in\mathcal{T}_h}\theta_T^2\right\}^{1/2}$ is employed as the global residual error estimator.

The following theorem constitutes the main result of this section.

Theorem 4.5. *Assume that Ω is an arbitrary polygonal domain in* 2D *or an arbitrary polyhedral domain in* 3D. *Let $((\mathbf{t},\boldsymbol{\sigma}),\mathbf{u})\in H\times V$ and $((\mathbf{t}_h,\boldsymbol{\sigma}_h),\mathbf{u}_h)\in H_h\times V_h$ be the unique solutions of* (4.34) *and* (4.8)*, respectively, and suppose that $\mathbf{g}\in\mathbf{H}^1(\Gamma)$. Also, let $\boldsymbol{\sigma}_h^\star\in\mathbb{H}(\mathbf{div};\Omega)$ be the postprocessed flux given by* (4.32) *and* (4.33). *Then, there exist positive constants $C_{\mathtt{eff}}$ and $C_{\mathtt{rel}}$, independent of h, such that*

$$C_{\mathtt{eff}}\,\boldsymbol{\theta} \;+\; h.o.t. \;\le\; \|(\mathbf{t}-\mathbf{t}_h,\boldsymbol{\sigma}-\boldsymbol{\sigma}_h)\|_{H_h} \;+\; \|\mathbf{u}-\mathbf{u}_h\|_{0,\Omega} \;+\; \|\boldsymbol{\sigma}-\boldsymbol{\sigma}^\star_{h,0}\|_{\mathbf{div},\Omega} \;\le\; C_{\mathtt{rel}}\,\boldsymbol{\theta}\,, \tag{4.37}$$

where h.o.t. stands for one or several terms of higher order.

The proof of Theorem 4.5 is separated into the parts given by the next subsections. Firstly, we prove the reliability (upper bound in (4.37)) of the global error estimator, and then in Section 4.5.4 we derive the efficiency of the global error estimator (lower bound in (4.37)).

4.5.3 Reliability

We begin with the following preliminary estimate.

Lemma 4.8. *Let* $((\mathbf{t},\boldsymbol{\sigma}),\mathbf{u}) \in H \times V$ *and* $((\mathbf{t}_h,\boldsymbol{\sigma}_h),\mathbf{u}_h) \in H_h \times V_h$ *be the unique solutions of* (4.34) *and* (4.8)*, respectively. Also, let* $\boldsymbol{\sigma}_h^\star \in \mathbb{H}(\mathbf{div};\Omega)$ *be the postprocessed flux defined by* (4.32) *and* (4.33)*. Then, there exists* $C > 0$*, independent of* h*, such that*

$$\begin{aligned}
&\|(\mathbf{t}-\mathbf{t}_h,\boldsymbol{\sigma}-\boldsymbol{\sigma}_h)\|_{H_h} + \|\mathbf{u}-\mathbf{u}_h\|_{0,\Omega} + \|\boldsymbol{\sigma}-\boldsymbol{\sigma}_{h,0}^\star\|_{\mathbf{div},\Omega} \\
&\quad \le C\left\{\|\boldsymbol{\sigma}_h^{\mathtt{d}} - \boldsymbol{\psi}(\mathbf{t}_h)^{\mathtt{d}}\|_{0,\Omega} \,+\, \|\mathbf{f} + \mathbf{div}_h(\boldsymbol{\sigma}_h)\|_{0,\Omega} \,+\, \|\boldsymbol{\sigma}_{h,0}^\star - \boldsymbol{\sigma}_h\|_{\Sigma_h} \,+\, \|R\|_{\mathbb{H}_0(\mathbf{div};\Omega)'}\right\},
\end{aligned} \tag{4.38}$$

where $R \in \mathbb{H}_0(\mathbf{div};\Omega)'$ *is defined by*

$$\begin{aligned}
R(\boldsymbol{\tau}) \,:=\, &\int_\Omega \mathbf{t}_h^{\mathtt{d}} : \boldsymbol{\tau} \,+\, \int_\Omega \mathbf{u}_h \cdot \mathbf{div}(\boldsymbol{\tau}) - \langle \boldsymbol{\tau\nu}, \mathbf{g}\rangle_\Gamma \,+\, \kappa_1 \int_\Omega \left(\boldsymbol{\sigma}_h^{\mathtt{d}} - \boldsymbol{\psi}(\mathbf{t}_h)^{\mathtt{d}}\right) : \boldsymbol{\tau} \\
&+ \kappa_2 \int_\Omega (\mathbf{f} + \mathbf{div}_h(\boldsymbol{\sigma}_h)) \cdot \mathbf{div}(\boldsymbol{\tau}) \qquad \forall\, \boldsymbol{\tau} \in \mathbb{H}_0(\mathbf{div};\Omega)\,,
\end{aligned} \tag{4.39}$$

and $R(\boldsymbol{\tau}_h) \,=\, 0$ *for all* $\boldsymbol{\tau}_h \in \mathbb{RT}_k(\mathcal{T}_h) \cap \mathbb{H}_0(\mathbf{div};\Omega)$.

Proof. We begin by observing that

$$\|\boldsymbol{\sigma}-\boldsymbol{\sigma}_h\|_{\Sigma_h} \;\le\; \|\boldsymbol{\sigma}-\boldsymbol{\sigma}_{h,0}^\star\|_{\Sigma_h} \;+\; \|\boldsymbol{\sigma}_{h,0}^\star-\boldsymbol{\sigma}_h\|_{\Sigma_h} \;\le\; \|\boldsymbol{\sigma}-\boldsymbol{\sigma}_{h,0}^\star\|_{\mathbf{div},\Omega} \;+\; \|\boldsymbol{\sigma}_{h,0}^\star-\boldsymbol{\sigma}_h\|_{\Sigma_h}\,,$$

from which we readily deduce that

$$\begin{aligned}
&\|(\mathbf{t}-\mathbf{t}_h,\boldsymbol{\sigma}-\boldsymbol{\sigma}_h)\|_{H_h} + \|\mathbf{u}-\mathbf{u}_h\|_{0,\Omega} + \|\boldsymbol{\sigma}-\boldsymbol{\sigma}_{h,0}^\star\|_{\mathbf{div},\Omega} \\
&\qquad \le\; C\Big\{\|((\mathbf{t}-\mathbf{t}_h,\boldsymbol{\sigma}-\boldsymbol{\sigma}_{h,0}^\star),\mathbf{u}-\mathbf{u}_h)\|_{H\times V} \;+\; \|\boldsymbol{\sigma}_{h,0}^\star-\boldsymbol{\sigma}_h\|_{\Sigma_h}\Big\}\,.
\end{aligned} \tag{4.40}$$

Next, thanks to the mean value theorem, we know that there exists a convex combination of $\mathbf{t}$ and $\mathbf{t}_h$, say $\widetilde{\mathbf{r}}_h \in \mathbb{L}^2(\Omega)$, such that

$$\mathcal{D}\mathbb{A}(\widetilde{\mathbf{r}}_h)(\mathbf{t}-\mathbf{t}_h,\,\mathbf{s}) \;=\; [\mathbb{A}(\mathbf{t}),\,\mathbf{s}] \;-\; [\mathbb{A}(\mathbf{t}_h),\,\mathbf{s}] \quad \forall\, \mathbf{s} \in \mathbb{L}^2(\Omega)\,. \tag{4.41}$$

Hence, applying (4.35) to $\widetilde{\mathbf{r}} := \widetilde{\mathbf{r}}_h$ and the error $((\mathbf{r},\boldsymbol{\rho}),\mathbf{w}) := ((\mathbf{t}-\mathbf{t}_h,\boldsymbol{\sigma}-\boldsymbol{\sigma}_{h,0}^\star),\mathbf{u}-\mathbf{u}_h) \in H \times V$, and then using the identity (4.41) together with the definition of $\mathbb{A}$ (cf. (4.17)), we find that

$$\begin{aligned}
&\widetilde{C}\,\|((\mathbf{t}-\mathbf{t}_h,\boldsymbol{\sigma}-\boldsymbol{\sigma}_{h,0}^\star),\mathbf{u}-\mathbf{u}_h)\|_{H\times V} \\
&\le \sup_{\substack{((\mathbf{s},\boldsymbol{\tau}),\mathbf{v})\in H\times V\\ ((\mathbf{s},\boldsymbol{\tau}),\mathbf{v})\neq \mathbf{0}}} \left\{ \frac{[\mathcal{A}(\mathbf{t},\boldsymbol{\sigma}),(\mathbf{s},\boldsymbol{\tau})] + [\mathcal{B}(\mathbf{s},\boldsymbol{\tau}),\mathbf{u}] + [\mathcal{B}(\mathbf{t},\boldsymbol{\sigma}),\mathbf{v}] + \int_\Omega [(\boldsymbol{\sigma}_{h,0}^\star)^{\mathtt{d}} - \boldsymbol{\psi}(\mathbf{t}_h)^{\mathtt{d}}] : \mathbf{s} - \int_\Omega \mathbf{t}_h^{\mathtt{d}} : \boldsymbol{\tau}}{\|((\mathbf{s},\boldsymbol{\tau}),\mathbf{v})\|_{H\times V}} \right. \\
&\quad \left. -\; \frac{\kappa_1 \int_\Omega [(\boldsymbol{\sigma}_{h,0}^\star)^{\mathtt{d}} - \boldsymbol{\psi}(\mathbf{t}_h)^{\mathtt{d}}] : \boldsymbol{\tau} \,+\, \kappa_2 \int_\Omega \mathbf{div}(\boldsymbol{\sigma}_{h,0}^\star)\cdot\mathbf{div}(\boldsymbol{\tau}) + \int_\Omega \mathbf{u}_h \cdot \mathbf{div}(\boldsymbol{\tau}) + \int_\Omega \mathbf{v}\cdot\mathbf{div}(\boldsymbol{\sigma}_{h,0}^\star)}{\|((\mathbf{s},\boldsymbol{\tau}),\mathbf{v})\|_{H\times V}} \right\},
\end{aligned}$$

which, utilizing (4.34) and defining

$$\widetilde{R}(\boldsymbol{\tau}) \,:=\, R(\boldsymbol{\tau}) \,+\, \kappa_1 \int_\Omega (\boldsymbol{\sigma}_{h,0}^\star - \boldsymbol{\sigma}_h)^{\mathtt{d}} : \boldsymbol{\tau} \,+\, \kappa_2 \int_\Omega \mathbf{div}_h(\boldsymbol{\sigma}_{h,0}^\star - \boldsymbol{\sigma}_h)\cdot\mathbf{div}(\boldsymbol{\tau}) \qquad \forall\, \boldsymbol{\tau} \in \mathbb{H}_0(\mathbf{div};\Omega)\,,$$

gives

$$\widetilde{C}\|((\mathbf{t}-\mathbf{t}_h,\boldsymbol{\sigma}-\boldsymbol{\sigma}^\star_{h,0}),\mathbf{u}-\mathbf{u}_h)\|_{H\times V}$$
$$\leq \sup_{\substack{((\mathbf{s},\boldsymbol{\tau}),\mathbf{v})\in H\times V\\ ((\mathbf{s},\boldsymbol{\tau}),\mathbf{v})\neq\mathbf{0}}} \frac{\displaystyle\int_\Omega [(\boldsymbol{\sigma}^\star_{h,0})^{\mathtt{d}}-\boldsymbol{\psi}(\mathbf{t}_h)^{\mathtt{d}}]:\mathbf{s}-\int_\Omega[\mathbf{f}+\mathbf{div}(\boldsymbol{\sigma}^\star_{h,0})]\cdot\mathbf{v}-\widetilde{R}(\boldsymbol{\tau})}{\|((\mathbf{s},\boldsymbol{\tau}),\mathbf{v})\|_{H\times V}}\,.$$

Then, applying the Cauchy-Schwarz inequality it follows that

$$\widetilde{C}\|((\mathbf{t}-\mathbf{t}_h,\boldsymbol{\sigma}-\boldsymbol{\sigma}^\star_{h,0}),\mathbf{u}-\mathbf{u}_h)\|_{H\times V}\;\leq\;\|(\boldsymbol{\sigma}^\star_{h,0})^{\mathtt{d}}-\boldsymbol{\psi}(\mathbf{t}_h)^{\mathtt{d}}\|_{0,\Omega}\;+\;\|\mathbf{f}+\mathbf{div}(\boldsymbol{\sigma}^\star_{h,0})\|_{0,\Omega}$$
$$+\;\|\boldsymbol{\sigma}^\star_{h,0}-\boldsymbol{\sigma}_h\|_{0,\Omega}\;+\;\|\mathbf{div}_h(\boldsymbol{\sigma}^\star_{h,0}-\boldsymbol{\sigma}_h)\|_{0,\Omega}\;+\|R\|_{\mathbb{H}_0(\mathbf{div};\Omega)'}\,,$$

which, together with (4.40) and the straightforward estimates

$$\|(\boldsymbol{\sigma}^\star_{h,0})^{\mathtt{d}}-\boldsymbol{\psi}(\mathbf{t}_h)^{\mathtt{d}}\|_{0,\Omega}\;\leq\;\|\boldsymbol{\sigma}_h^{\mathtt{d}}-\boldsymbol{\psi}(\mathbf{t}_h)^{\mathtt{d}}\|_{0,\Omega}+\|(\boldsymbol{\sigma}^\star_{h,0}-\boldsymbol{\sigma}_h)^{\mathtt{d}}\|_{0,\Omega}\,,$$

$$\|(\boldsymbol{\sigma}^\star_{h,0}-\boldsymbol{\sigma}_h)^{\mathtt{d}}\|_{0,\Omega}\;+\;\|\mathbf{div}_h(\boldsymbol{\sigma}^\star_{h,0}-\boldsymbol{\sigma}_h)\|_{0,\Omega}\;\leq\;\|\boldsymbol{\sigma}^\star_{h,0}-\boldsymbol{\sigma}_h\|_{\Sigma_h}\,,$$

and

$$\|\mathbf{f}+\mathbf{div}(\boldsymbol{\sigma}^\star_{h,0})\|_{0,\Omega}\leq\|\mathbf{f}+\mathbf{div}_h(\boldsymbol{\sigma}_h)\|_{0,\Omega}\;+\;\|\mathbf{div}_h(\boldsymbol{\sigma}^\star_{h,0}-\boldsymbol{\sigma}_h)\|_{0,\Omega}\,,$$

imply (4.38). Finally, from the second, fifth and sixth equations in (4.8), we know that

$$\int_\Omega \mathbf{t}_h^{\mathtt{d}}:\boldsymbol{\tau}_h\;+\;\int_\Omega\mathbf{u}_h\cdot\mathbf{div}_h(\boldsymbol{\tau}_h)\;-\;\int_{\mathcal{E}_h^i}[\![\boldsymbol{\tau}_h]\!]\cdot\boldsymbol{\lambda}_h\;+\;\kappa_1\int_\Omega[\boldsymbol{\sigma}_h^{\mathtt{d}}-\boldsymbol{\psi}(\mathbf{t}_h)^{\mathtt{d}}]:\boldsymbol{\tau}_h$$
$$+\;\kappa_2\int_\Omega\mathbf{div}_h(\boldsymbol{\sigma}_h)\cdot\mathbf{div}_h(\boldsymbol{\tau}_h)\;=\;\langle\boldsymbol{\tau}_h\boldsymbol{\nu},\mathbf{g}\rangle_\Gamma\;-\;\kappa_2\int_\Omega\mathbf{f}\cdot\mathbf{div}_h(\boldsymbol{\tau}_h)$$

for all $\boldsymbol{\tau}_h\in\Sigma_h$, which yields, in particular, $R(\boldsymbol{\tau}_h)=0$ for all $\boldsymbol{\tau}_h\in\mathbb{RT}(\mathcal{T}_h)\cap\mathbb{H}_0(\mathbf{div};\Omega)$, thus completing the proof. □

We now aim to bound $\|R\|_{\mathbb{H}_0(\mathbf{div};\Omega)'} := \sup\limits_{\substack{\boldsymbol{\tau}\in\mathbb{H}_0(\mathbf{div};\Omega)\\ \boldsymbol{\tau}\neq\mathbf{0}}}\dfrac{R(\boldsymbol{\tau})}{\|\boldsymbol{\tau}\|_{\mathbf{div},\Omega}}$ on the right-hand side of (4.38). For this purpose, and because of the vanishing property of R established by Lemma 4.8, we replace $R(\boldsymbol{\tau})$ in the above supremum by $R(\boldsymbol{\tau}-\boldsymbol{\tau}_h)$ with a suitable choice of $\boldsymbol{\tau}_h\in\mathbb{RT}_k(\mathcal{T}_h)\cap\mathbb{H}_0(\mathbf{div};\Omega)$. More precisely, proceeding exactly as in [72, Section 4.2], we now set $X_h := \big\{v\in C(\bar\Omega)\,:\,v|_T\in P_1(T)\quad\forall\,T\in\mathcal{T}_h\big\}$ and introduce the Clément interpolation operator $\mathcal{I}_h : H^1(\Omega)\to X_h$ (cf. [40]). A vectorial version of $\mathcal{I}_h$, say $\boldsymbol{\mathcal{I}}_h:\mathbf{H}^1(\Omega)\to\mathbf{X}_h$, which is defined componentwise by $\mathcal{I}_h$, is also required. The following lemma establishes the local approximation properties of $\mathcal{I}_h$.

Lemma 4.9. *There exist constants $c_1,c_2>0$, independent of h, such that for all $v\in H^1(\Omega)$ there holds*

$$\|v-\mathcal{I}_h(v)\|_{0,T}\;\leq\;c_1h_T\|v\|_{1,\Delta(T)}\quad\forall\,T\in\mathcal{T}_h\,,$$

and

$$\|v-\mathcal{I}_h(v)\|_{0,F}\;\leq\;c_2h_F^{1/2}\|v\|_{1,\Delta(F)}\quad\forall\,F\in\mathcal{E}_h\,,$$

where $\Delta(T)$ and $\Delta(F)$ are the union of all elements intersecting with T and F, respectively.

Proof. See [40]. □

Next, for each $\boldsymbol{\tau} \in \mathbb{H}_0(\mathbf{div};\Omega)$ we consider its Helmholtz decomposition (see, e.g. [72, Section 4.2] or Chapter 1, Lemma 1.7 for details)

$$\boldsymbol{\tau} \;=\; \nabla\mathbf{z} \;+\; \underline{\mathbf{curl}}(\boldsymbol{\chi})\,, \tag{4.42}$$

where $\mathbf{z} \in \mathbf{H}^2(\Omega)$ and $\boldsymbol{\chi} \in \mathbf{H}^1(\Omega)$ satisfy $\Delta\mathbf{z} = \mathbf{div}(\boldsymbol{\tau})$ in Ω, $\int_\Omega \boldsymbol{\chi} = \mathbf{0}$, and the stability estimate

$$\|\mathbf{z}\|_{2,\Omega} \;+\; \|\boldsymbol{\chi}\|_{1,\Omega} \;\leq\; C\,\|\boldsymbol{\tau}\|_{\mathbf{div},\Omega}\,. \tag{4.43}$$

Next, we let $\boldsymbol{\zeta} := \nabla\mathbf{z} \in \mathbb{H}^1(\Omega)$, $\boldsymbol{\chi}_h := \boldsymbol{\mathcal{I}}_h(\boldsymbol{\chi})$, and define

$$\boldsymbol{\tau}_h \;:=\; \Pi_h^k(\boldsymbol{\zeta}) \;+\; \underline{\mathbf{curl}}(\boldsymbol{\chi_h}) \;+\; c\,\mathbb{I} \;\in\; \mathbb{RT}_k(\mathcal{T}_h)\cap\mathbb{H}_0(\mathbf{div};\Omega)\,, \tag{4.44}$$

where Π_h^k is the global Raviart-Thomas interpolation operator introduced before (cf. (4.21) and (4.22)). Here, the constant c is chosen so that $\boldsymbol{\tau}_h$, which is already in $\mathbb{RT}_k(\mathcal{T}_h)$, belongs to $\mathbb{H}_0(\mathbf{div};\Omega)$. Equivalently, $\boldsymbol{\tau}_h$ is the $\mathbb{H}_0(\mathbf{div};\Omega)$-component of $\Pi_h^k(\boldsymbol{\zeta})+\underline{\mathbf{curl}}(\boldsymbol{\chi_h})$. We refer to (4.44) as a discrete Helmholtz decomposition of $\boldsymbol{\tau}_h$. Therefore, we can write

$$\boldsymbol{\tau}-\boldsymbol{\tau}_h \;=\; \boldsymbol{\tau}-\Pi_h^k(\boldsymbol{\zeta})-\underline{\mathbf{curl}}(\boldsymbol{\chi_h})-c\,\mathbb{I} \;=\; \boldsymbol{\zeta}-\Pi_h^k(\boldsymbol{\zeta}) \;+\; \underline{\mathbf{curl}}(\boldsymbol{\chi}-\boldsymbol{\chi_h}) \;-\; c\,\mathbb{I}\,, \tag{4.45}$$

which, using that $\mathbf{div}(\Pi_h^k(\boldsymbol{\tau})) = \mathcal{P}_h^k(\mathbf{div}(\boldsymbol{\tau}))$ and that $\mathbf{div}(\boldsymbol{\zeta}) = \Delta\mathbf{z} = \mathbf{div}(\boldsymbol{\tau})$ in Ω, and denoting by $\mathbf{I}$ a generic identity operator, yields

$$\mathbf{div}(\boldsymbol{\tau}-\boldsymbol{\tau}_h) \;=\; \mathbf{div}(\boldsymbol{\zeta}-\Pi_h^k(\boldsymbol{\zeta})) \;=\; (\mathbf{I}-\mathcal{P}_h^k)(\mathbf{div}(\boldsymbol{\zeta})) \;=\; (\mathbf{I}-\mathcal{P}_h^k)(\mathbf{div}(\boldsymbol{\tau}))\,.$$

Then, replacing each $\boldsymbol{\tau} \in \mathbb{H}_0(\mathbf{div};\Omega)$ by its Helmholtz decomposition (4.42), employing the associated discrete element $\boldsymbol{\tau}_h$ given by (4.44), recalling from Lemma 4.8 that $R(\boldsymbol{\tau}_h) = 0$, and observing that R vanishes $c\,\mathbb{I}$ as well, we deduce from (4.39) and (4.45) that $R(\boldsymbol{\tau}) = R(\boldsymbol{\tau}-\boldsymbol{\tau}_h)$ is decomposed as

$$R(\boldsymbol{\tau}) \;=\; R_1(\boldsymbol{\zeta}-\Pi_h^k(\boldsymbol{\zeta})) \;+\; R_2(\boldsymbol{\chi}-\boldsymbol{\chi}_h)\,, \tag{4.46}$$

where

$$\begin{aligned} R_1(\boldsymbol{\zeta}-\Pi_h^k(\boldsymbol{\zeta})) \;:=\; & \int_\Omega \mathbf{t}_h^{\mathtt{d}} : (\boldsymbol{\zeta}-\Pi_h^k(\boldsymbol{\zeta})) \;+\; \int_\Omega \mathbf{u}_h\cdot\mathbf{div}(\boldsymbol{\zeta}-\Pi_h^k(\boldsymbol{\zeta})) \;-\; \Big\langle(\boldsymbol{\zeta}-\Pi_h^k(\boldsymbol{\zeta}))\boldsymbol{\nu},\mathbf{g}\Big\rangle_\Gamma \\ & +\;\kappa_1\int_\Omega \big(\boldsymbol{\sigma}_h^{\mathtt{d}}-(\boldsymbol{\psi}(\mathbf{t}_h))^{\mathtt{d}}\big) : (\boldsymbol{\zeta}-\Pi_h^k(\boldsymbol{\zeta})) \;+\; \kappa_2\int_\Omega (\mathbf{f}+\mathbf{div}_h(\boldsymbol{\sigma}_h))\cdot\mathbf{div}(\boldsymbol{\zeta}-\Pi_h^k(\boldsymbol{\zeta})) \end{aligned}$$

and

$$\begin{aligned} R_2(\boldsymbol{\chi}-\boldsymbol{\chi}_h) \;:=\; & \int_\Omega \mathbf{t}_h^{\mathtt{d}} : \underline{\mathbf{curl}}(\boldsymbol{\chi}-\boldsymbol{\chi}_h) \;-\; \langle\underline{\mathbf{curl}}(\boldsymbol{\chi}-\boldsymbol{\chi}_h)\boldsymbol{\nu},\mathbf{g}\rangle_\Gamma \\ & +\;\kappa_1\int_\Omega \big(\boldsymbol{\sigma}_h^{\mathtt{d}}-(\boldsymbol{\psi}(\mathbf{t}_h))^{\mathtt{d}}\big) : \underline{\mathbf{curl}}(\boldsymbol{\chi}-\boldsymbol{\chi}_h)\,. \end{aligned}$$

The following two lemmas provide suitable upper bounds for $|R_1(\boldsymbol{\zeta}-\Pi_h^k(\boldsymbol{\zeta}))|$ and $|R_2(\boldsymbol{\chi}-\boldsymbol{\chi}_h)|$, which will yield the required estimate for $\|R\|_{\mathbb{H}_0(\mathbf{div};\Omega)'}$.

Lemma 4.10. *There exists $C_1 > 0$, independent of h, such that*

$$|R_1(\boldsymbol{\zeta}-\Pi_h^k(\boldsymbol{\zeta}))| \;\leq\; C_1\left\{\sum_{T\in\mathcal{T}_h}\theta_{1,T}^2\right\}^{1/2}\|\boldsymbol{\tau}\|_{\mathbf{div},\Omega}\,,$$

where

$$\begin{aligned} \theta_{1,T}^2 \;:=\; & h_T^2\,\|\nabla\mathbf{u}_h-\mathbf{t}_h^{\mathtt{d}}\|_{0,T}^2 \;+\; h_T^2\,\|\boldsymbol{\sigma}_h^{\mathtt{d}}-\boldsymbol{\psi}(\mathbf{t}_h)^{\mathtt{d}}\|_{0,T}^2 \\ & +\;\|\mathbf{f}+\mathbf{div}(\boldsymbol{\sigma}_h)\|_{0,T}^2 \;+\; \sum_{F\in\partial T\cap\mathcal{E}_h^\partial} h_F\,\|\mathbf{g}-\mathbf{u}_h\|_{0,F}^2\,. \end{aligned}$$

Lemma 4.11. *Assume that* $\mathbf{g} \in \mathbf{H}^1(\Gamma)$*. Then there exists* $C_2 > 0$*, independent of* h*, such that*

$$|R_2(\boldsymbol{\chi} - \boldsymbol{\chi}_h)| \;\leq\; C_2 \left\{ \sum_{T \in \mathcal{T}_h} \theta_{2,T}^2 \right\}^{1/2} \|\boldsymbol{\tau}\|_{\mathbf{div},\Omega} \,,$$

where

$$\begin{aligned}
\theta_{2,T}^2 \;:=\;& h_T^2 \, \|\mathrm{curl}(\mathbf{t}_h^{\mathtt{d}})\|_{0,T}^2 \;+\; h_T^2 \, \|\mathrm{curl}\left(\boldsymbol{\sigma}_h^{\mathtt{d}} - \boldsymbol{\psi}(\mathbf{t}_h)^{\mathtt{d}}\right)\|_{0,T}^2 \\
&+ \sum_{F \in \partial T \cap \mathcal{E}_h^i} h_F \left\{ \|[\![\mathbf{t}_h^{\mathtt{d}} \boldsymbol{s}]\!]\|_{0,F}^2 \;+\; \|[\![(\boldsymbol{\sigma}_h^{\mathtt{d}} - \boldsymbol{\psi}(\mathbf{t}_h)^{\mathtt{d}}) \boldsymbol{s}]\!]\|_{0,F}^2 \right\} \\
&+ \sum_{F \in \partial T \cap \mathcal{E}_h^\partial} h_F \left\{ \left\| \frac{d\mathbf{g}}{d\boldsymbol{s}} - \mathbf{t}_h^{\mathtt{d}} \boldsymbol{s} \right\|_{0,F}^2 \;+\; \|(\boldsymbol{\sigma}_h^{\mathtt{d}} - \boldsymbol{\psi}(\mathbf{t}_h)^{\mathtt{d}}) \boldsymbol{s}\|_{0,F}^2 \right\}.
\end{aligned}$$

The proofs of Lemmas 4.10 and 4.11 follow by using exactly the same arguments from [83, Lemmas 4.3 and 4.4] (see, also [84, Lemmas 4.3 and 4.4]). Indeed, the main tools employed are integration by parts, the Cauchy-Schwarz inequality, the approximation properties provided by Lemma 4.9, the identities (4.21) and (4.22) characterizing Π_h^k, the approximation properties of Π_h^k, the fact that the number of triangles in $\Delta(T)$ and $\Delta(F)$ are bounded, and the stability estimate (4.43). We omit further details here and refer to the aforementioned works.

Finally, it readily follows from (4.46) and Lemmas 4.10 and 4.11 that

$$\|R\|_{\mathbb{H}_0(\mathbf{div};\Omega)'} \;\leq\; C \left\{ \sum_{T \in \mathcal{T}_h} \left(\theta_{1,T}^2 + \theta_{2,T}^2 \right) \right\}^{1/2} . \tag{4.47}$$

In this way, and having in mind that the term $h_T^2 \|\boldsymbol{\sigma}_h^{\mathtt{d}} - \boldsymbol{\psi}(\mathbf{t}_h)^{\mathtt{d}}\|_{0,T}^2$ is dominated by $\|\boldsymbol{\sigma}_h^{\mathtt{d}} - \boldsymbol{\psi}(\mathbf{t}_h)^{\mathtt{d}}\|_{0,T}^2$, we conclude from (4.31), Lemma 4.8, and (4.47), the reliability of the *a posteriori* error estimator $\boldsymbol{\theta}$ (upper bound in (4.37)).

4.5.4 Efficiency

In this section we establish the efficiency of our *a posteriori* error estimator $\boldsymbol{\theta}$ (lower bound in (4.37)). In other words, we provide suitable upper bounds for the thirteen terms defining the local error indicator θ_T^2 (cf. (4.36)). We first notice that the converse of the derivation of (4.34) from (4.5) holds true. Indeed, it is easy to show, applying integration by parts backwardly and using appropriate test functions, that the unique solution $((\mathbf{t}, \boldsymbol{\sigma}), \mathbf{u}) \in H \times V$ of (4.34) solves the original problem (4.5). Then, using that $\mathbf{f} = -\mathbf{div}(\boldsymbol{\sigma})$ in Ω, it follows that

$$\|\mathbf{f} + \mathbf{div}(\boldsymbol{\sigma}_h)\|_{0,T}^2 \;\;=\;\; \|\mathbf{div}(\boldsymbol{\sigma} - \boldsymbol{\sigma}_h)\|_{0,T}^2 \,. \tag{4.48}$$

Also, after adding and subtracting $\boldsymbol{\sigma}$, we have

$$\begin{aligned}
&\|(\boldsymbol{\sigma}_{h,0}^\star - \boldsymbol{\sigma}_h)^{\mathtt{d}}\|_{0,T}^2 \;+\; \|\mathbf{div}(\boldsymbol{\sigma}_{h,0}^\star - \boldsymbol{\sigma}_h)\|_{0,T}^2 \;+\; \sum_{F \in \partial T \cap \mathcal{E}_h^i} \|\mathtt{h}^{-1/2} [\![\boldsymbol{\sigma}_h]\!]\|_{0,F}^2 \\
&\qquad \leq\; 2 \left\{ \|\boldsymbol{\sigma} - \boldsymbol{\sigma}_h\|_{\Sigma_h(T)}^2 \;+\; \|\boldsymbol{\sigma} - \boldsymbol{\sigma}_{h,0}^\star\|_{\mathbf{div},T}^2 \right\} .
\end{aligned} \tag{4.49}$$

Next, using that $\boldsymbol{\sigma}^{\mathtt{d}} = \boldsymbol{\psi}(\mathbf{t}) = \boldsymbol{\psi}(\mathbf{t})^{\mathtt{d}}$ in Ω and applying the Lipschitz-continuity of $\mathbb{A}$ (cf. Lemma 4.2), but restricted to the triangle $T \in \mathcal{T}_h$ instead of Ω, we deduce that

$$\begin{aligned} \|\boldsymbol{\sigma}_h^{\mathtt{d}} - \boldsymbol{\psi}(\mathbf{t}_h)^{\mathtt{d}}\|_{0,T}^2 \,&\leq\, 2\,\|(\boldsymbol{\sigma} - \boldsymbol{\sigma}_h)^{\mathtt{d}}\|_{0,T}^2 \;+\; 2\,\|\boldsymbol{\psi}(\mathbf{t}) - \boldsymbol{\psi}(\mathbf{t}_h)\|_{0,T}^2 \\ &\leq\, 2\left\{\|(\boldsymbol{\sigma} - \boldsymbol{\sigma}_h)^{\mathtt{d}}\|_{0,T}^2 \;+\; \gamma_0^2\,\|\mathbf{t} - \mathbf{t}_h\|_{0,T}^2\right\}. \end{aligned} \tag{4.50}$$

On the other hand, in order to bound the terms involving the mesh parameters h_T and h_F, we proceed as in [83] and [84] (see also [72]). The techniques applied there are based on triangle-bubble and edge-bubble functions, extension operators, and discrete trace and inverse inequalities. Hence, the estimates of the remaining eight terms defining θ_T^2 (cf. (4.36)) are given as follows.

Lemma 4.12. *There exist $C_1, C_2 > 0$, independent of h, such that*

$$h_T^2\|\mathrm{curl}(\mathbf{t}_h^{\mathtt{d}})\|_{0,T}^2 \;\leq\; C_1\,\|\mathbf{t} - \mathbf{t}_h\|_{0,T}^2 \quad \forall\, T \in \mathcal{T}_h\,,$$

and

$$h_F\|[\![\mathbf{t}_h^{\mathtt{d}}\boldsymbol{s}]\!]\|_{0,F}^2 \;\leq\; C_2\,\|\mathbf{t} - \mathbf{t}_h\|_{0,\omega_F}^2 \quad \forall\, F \in \mathcal{E}_h^i\,,$$

where $\omega_F := \cup\{\, T \in \mathcal{T}_h \;:\; F \in \partial T\}$.

Proof. It suffices to apply the general results stated in [83, Lemmas 4.9 and 4.10] to $\boldsymbol{\rho}_h = \mathbf{t}_h^{\mathtt{d}}$ and $\boldsymbol{\rho} = \mathbf{t} = \mathbf{t}^{\mathtt{d}}$, noting that $\mathrm{curl}(\boldsymbol{\rho}) = \mathrm{curl}(\nabla\mathbf{u}) = \mathbf{0}$ in Ω. □

Lemma 4.13. *There exist $C_3, C_4 > 0$, independent of h, such that*

$$h_T^2\|\mathrm{curl}(\boldsymbol{\sigma}_h^{\mathtt{d}} - \boldsymbol{\psi}(\mathbf{t}_h)^{\mathtt{d}})\|_{0,T}^2 \;\leq\; C_3\left\{\|\mathbf{t} - \mathbf{t}_h\|_{0,T}^2 \;+\; \|(\boldsymbol{\sigma} - \boldsymbol{\sigma}_h)^{\mathtt{d}}\|_{0,T}^2\right\} \quad \forall\, T \in \mathcal{T}_h\,,$$

and

$$h_F\|[\![(\boldsymbol{\sigma}_h^{\mathtt{d}} - \boldsymbol{\psi}(\mathbf{t}_h)^{\mathtt{d}})\boldsymbol{s}]\!]\|_{0,F}^2 \;\leq\; C_4\left\{\|\mathbf{t} - \mathbf{t}_h\|_{0,\omega_F}^2 \;+\; \|(\boldsymbol{\sigma} - \boldsymbol{\sigma}_h)^{\mathtt{d}}\|_{0,\omega_F}^2\right\} \quad \forall\, F \in \mathcal{E}_h\,,$$

where, we define $[\![(\boldsymbol{\sigma}_h^{\mathtt{d}} - \boldsymbol{\psi}(\mathbf{t}_h)^{\mathtt{d}})\boldsymbol{s}]\!] := (\boldsymbol{\sigma}_h^{\mathtt{d}} - \boldsymbol{\psi}(\mathbf{t}_h)^{\mathtt{d}})\boldsymbol{s}$ on $\mathcal{E}_h^{\partial}$.

Proof. As in the proof of Lemma 4.12, it suffices now to apply the general results stated in [83, Lemmas 4.9 and 4.10] to $\boldsymbol{\rho}_h = \boldsymbol{\sigma}_h^{\mathtt{d}} - \boldsymbol{\psi}(\mathbf{t}_h)^{\mathtt{d}}$ and $\boldsymbol{\rho} = \boldsymbol{\sigma}^{\mathtt{d}} - \boldsymbol{\psi}(\mathbf{t})^{\mathtt{d}} = \mathbf{0}$ in Ω, and then use the Lipschitz-continuity of $\mathbb{A}$ (cf. Lemma 4.2) restricted to T and ω_F. □

Lemma 4.14. *There exists $C_5 > 0$, independent of h, such that*

$$h_T^2\|\nabla\mathbf{u}_h - \mathbf{t}_h^{\mathtt{d}}\|_{0,T}^2 \;\leq\; C_5\left\{\|\mathbf{u} - \mathbf{u}_h\|_{0,T}^2 \;+\; h_T^2\|\mathbf{t} - \mathbf{t}_h\|_{0,T}^2\right\} \quad \forall\, T \in \mathcal{T}_h\,.$$

Proof. As in [84, Lemma 4.8], it follows from the proof of [83, Lemma 4.13]. □

Lemma 4.15. *Assume that $\mathbf{g}$ is piecewise polynomial. Then there exists $C_6 > 0$, independent of h, such that*

$$h_F\left\|\frac{d\mathbf{g}}{d\boldsymbol{s}} - \mathbf{t}_h^{\mathtt{d}}\boldsymbol{s}\right\|_{0,F}^2 \;\leq\; C_6\,\|\mathbf{t} - \mathbf{t}_h\|_{0,T}^2 \quad \forall\, F \in \mathcal{E}_h^{\partial}\,, \tag{4.51}$$

where T is the triangle of $\mathcal{T}_h$ having F as an edge.

Proof. It is a slight modification of the proof of [83, Lemma 4.15]. In fact, it suffices to replace $\frac{1}{2\mu}\boldsymbol{\sigma}_h$ by our $\mathbf{t}_h$ and use now that $\frac{d\mathbf{g}}{d\boldsymbol{\mathcal{S}}} = (\nabla\mathbf{u})\boldsymbol{\mathcal{S}} = \mathbf{t}\boldsymbol{\mathcal{S}} = \mathbf{t}^{\mathtt{d}}\boldsymbol{\mathcal{S}}$ on Γ. □

Lemma 4.16. *There exists $C_7 > 0$, independent of h, such that*

$$h_F\|\mathbf{g} - \mathbf{u}_h\|_{0,F}^2 \;\leq\; C_7\left\{\|\mathbf{u} - \mathbf{u}_h\|_{0,T}^2 \;+\; h_T^2\|\mathbf{t} - \mathbf{t}_h\|_{0,T}^2\right\} \quad \forall\, F \in \mathcal{E}_h^{\partial}\,,$$

where T is the triangle of $\mathcal{T}_h$ having F as an edge.

Proof. Similarly to the previous lemmas, it follows by replacing $\frac{1}{2\mu}\boldsymbol{\sigma}_h$ by our $\mathbf{t}_h$ in the proof of [83, Lemma 4.14], and then using that $\nabla\mathbf{u} = \mathbf{t} = \mathbf{t}^{\mathtt{d}}$ in Ω and $\mathbf{u} = \mathbf{g}$ on Γ. The estimate given by Lemma 4.14 is also employed here. □

We remark here that if $\mathbf{g}$ were not a piecewise polynomial, but a sufficiently smooth function, then higher order terms given by the errors arising from suitable polynomial approximations would appear in (4.51). This explains the eventual expression *h.o.t.* in (4.37). Consequently, the efficiency of $\boldsymbol{\theta}$ follows directly from estimates (4.48), (4.49) and (4.50), together with Lemmas 4.12 throughout 4.16, after summing up over $T \in \mathcal{T}_h$.

4.6 Numerical results

In this section we present four numerical examples illustrating the good performance of our augmented HDG method, confirming the reliability and efficiency of the *a posteriori* error estimator $\boldsymbol{\theta}$, and showing the behaviour of the associated adaptive algorithm. We remark that we refer to the original HDG system (4.8) since, as explained before, the equivalent reduced scheme given by (4.10) was introduced just for the sake of the analysis. In addition, in all the computations, we consider polynomial degrees $k \in \{0, 1, 2\}$. We begin by setting additional notations. In what follows, N denotes the total number of unknowns of (4.8), whereas $N_{\rm comp}$ stands for the number of unknowns effectively employed in the computations (involved in the resolution of the corresponding linear systems). In other words, N is the total number of degrees of freedom defining $\mathbf{t}_h$, $\boldsymbol{\sigma}_h$, $\mathbf{u}_h$, and $\boldsymbol{\lambda}_h$. On the other hand, as is natural in the HDG implementations, we can reduce N to $N_{\rm comp}$, where in the case of (4.8), $N_{\rm comp}$ is the total number of degrees of freedom defining $\boldsymbol{\lambda}_h$, plus one constant for each $T \in \mathcal{T}_h$, which has the task of imposing the condition $\int_\Omega \operatorname{tr}(\boldsymbol{\sigma}) = 0$ (see Section 3.5 for details). In turn, the individual and total errors are defined by

$$\begin{array}{llllll} \mathsf{e}(\mathbf{t}) & := & \|\mathbf{t} - \mathbf{t}_h\|_{0,\Omega}\,, \quad & \mathsf{e}(\boldsymbol{\sigma}) & := & \|\boldsymbol{\sigma} - \boldsymbol{\sigma}_h\|_{\Sigma_h}\,, \quad & \mathsf{e}(\mathbf{u}) & := & \|\mathbf{u} - \mathbf{u}_h\|_{0,\Omega}\,, \\ \mathsf{e}_0(\boldsymbol{\sigma}) & := & \|\boldsymbol{\sigma} - \boldsymbol{\sigma}_h\|_{0,\Omega}\,, \quad & \mathsf{e}(\boldsymbol{\lambda}) & := & \|\mathbf{u} - \widehat{\mathbf{u}}_h\|_h\,, \quad & \mathsf{e}(p) & := & \|p - p_h\|_{0,\Omega}\,, \end{array}$$

$$\mathsf{e}^\star(\boldsymbol{\sigma}) \;:=\; \|\boldsymbol{\sigma} - \boldsymbol{\sigma}_{h,0}^\star\|_{\mathbf{div},\Omega}\,, \quad \mathsf{e}(\mathbf{t},\boldsymbol{\sigma},\mathbf{u}) \;:=\; \left\{[\mathsf{e}(\mathbf{t})]^2 \;+\; [\mathsf{e}(\boldsymbol{\sigma})]^2 \;+\; [\mathsf{e}(\mathbf{u})]^2\right\}^{1/2},$$

where p_h is computed by the postprocessing formulae (4.27), whereas $\|\mathbf{u} - \widehat{\mathbf{u}}_h\|_h$ is defined in (4.29). The effectivity index with respect to $\boldsymbol{\theta}$ is given by

$$\mathtt{eff}(\boldsymbol{\theta}) \;:=\; \left\{[\mathsf{e}(\mathbf{t},\boldsymbol{\sigma},\mathbf{u})]^2 \;+\; [\mathsf{e}^\star(\boldsymbol{\sigma})]^2\right\}^{1/2} / \;\boldsymbol{\theta}\,,$$

and the experimental rates of convergence are defined as

$$\begin{aligned} \mathtt{r}(\mathbf{t}) &:= \frac{\log(\mathtt{e}(\mathbf{t})/\mathtt{e}'(\mathbf{t}))}{\log(h/h')}, & \mathtt{r}(\boldsymbol{\sigma}) &:= \frac{\log(\mathtt{e}(\boldsymbol{\sigma})/\mathtt{e}'(\boldsymbol{\sigma}))}{\log(h/h')}, \\ \mathtt{r}(\mathbf{u}) &:= \frac{\log(\mathtt{e}(\mathbf{u})/\mathtt{e}'(\mathbf{u}))}{\log(h/h')}, & \mathtt{r}(\mathbf{t},\boldsymbol{\sigma},\mathbf{u}) &:= \frac{\log(\mathtt{e}(\mathbf{t},\boldsymbol{\sigma},\mathbf{u})/\mathtt{e}'(\mathbf{t},\boldsymbol{\sigma},\mathbf{u}))}{\log(h/h')}, \end{aligned}$$

and similarly for $\mathtt{r}_0(\boldsymbol{\sigma})$, $\mathtt{r}(\boldsymbol{\lambda})$, $\mathtt{r}(p)$ and $\mathtt{r}^\star(\boldsymbol{\sigma})$, where $\mathtt{e}$ and $\mathtt{e}'$ denote the corresponding errors for two consecutive triangulations with mesh sizes h and h', respectively. Nevertheless, when the adaptive algorithm is applied (see details below), the expression $\log(h/h')$ appearing in the computation of the above rates is replaced by $-\frac{1}{2}\log(N/N')$, where N and N' denote the corresponding total degrees of freedom of each triangulation.

The numerical results presented below were obtained using a C++ code. The corresponding nonlinear algebraic systems arising from (4.8) are solved by the Newton-Raphson method with a tolerance of 10^{-6} and taking as initial iteration the solution of the associated linear Stokes problem. In all the examples less than four iterations were required to achieve the given tolerance. In turn, the linear systems were solved using the Conjugate Gradient method as the main solver. In addition, for the adaptive 3D mesh generation (cf. Example 4), we use the software TetGen developed in [120]. The examples to be considered in this section are described next. Example 1 and 2 (linear and nonlinear, respectively) are employed to illustrate the performance of the augmented HDG scheme (4.8) and to confirm the reliability and efficiency of the *a posteriori* error estimator $\boldsymbol{\theta}$. Examples 3 and 4 are utilized to show the behaviour of the associated adaptive algorithm, which applies the following procedure:

(1) Start with a coarse mesh $\mathcal{T}_h$.

(2) Solve the linear version of the discrete problem (4.8), in order to obtain an initial guess $\mathbf{x}_0$, for the Newton iterations.

(3) Solve the discrete problem (4.8) for the actual mesh $\mathcal{T}_h$, with the actual initial guess $\mathbf{x}_0$.

(4) Compute θ_T (cf. (4.36)) for each triangle $T \in \mathcal{T}_h$,

(5) Evaluate stopping criterion and decide to finish or go to next step.

(6) Use *red-green-blue* procedure (cf. [126]) to refine each $T' \in \mathcal{T}_h$ whose indicator $\theta_{T'}$ satisfies

$$\theta_{T'} \;\geq\; \frac{1}{2}\max\{\theta_T \;:\; T\in\mathcal{T}_h\}\,.$$

(7) Use the solution given by step 3 and the new mesh to interpolate a new initial guess $\widetilde{\mathbf{x}}_0$ and then replace $\mathbf{x}_0$ by $\widetilde{\mathbf{x}}_0$.

(8) Define the new mesh as actual mesh $\mathcal{T}_h$ and go to step 3.

For Example 1 we take $\mu = 1$ and for the remaining three examples we consider the nonlinear function $\mu : \mathrm{R}^+ \to \mathrm{R}^+$ given by the Carreau law

$$\mu(t) \;:=\; \mu_0 \;+\; \mu_1(1+t^2)^{(\beta-2)/2} \quad \forall\, t\in\mathrm{R}^+,$$

with $\mu_0 = \mu_1 = 0.5$ and $\beta = 1.5$. It is easy to check that the assumptions (4.2) and (4.3) are satisfied with

$$\gamma_0 \;=\; \mu_0 \;+\; \mu_1 \left\{ \frac{|\beta - 2|}{2} + 1 \right\} \qquad \text{and} \qquad \alpha_0 \;=\; \mu_0 \,.$$

Hence, for the implementation of the augmented HDG scheme (4.8) we use the stabilization parameter $\kappa_1 = \frac{\alpha_0}{\gamma_0^2}$, which obviously satisfies the assumption in Lemma 4.4, and then, as in Chapter 3, we simply choose $\kappa_2 = \frac{\kappa_1}{2}$.

In Example 1 we consider $\Omega =]-1,1[^2$, and choose the data $\mathbf{f}$ and $\mathbf{g}$ so that the exact solution is given for each $\mathbf{x} := (x_1, x_2)^{\mathtt{t}} \in \Omega$ by

$$\mathbf{u}(\mathbf{x}) \;=\; \begin{pmatrix} \sin(\pi\, x_1)\, \cos(\pi\, x_2) \\ -\cos(\pi\, x_1)\, \sin(\pi\, x_2) \end{pmatrix}$$

and

$$p(\mathbf{x}) \;=\; 4\, x_2^2 \cos(6\, x_1) \;-\; \frac{2}{9} \sin(6)\,.$$

It is easy to check that $\mathbf{u}$ is divergence free, and $(\mathbf{u}, p)$ is regular in the whole domain Ω.

In Example 2 we consider $\Omega = (0,1)^2$, and choose the data $\mathbf{f}$ and $\mathbf{g}$ so that the exact solution is given for each $\mathbf{x} := (x_1, x_2)^{\mathtt{t}} \in \Omega$ by

$$\mathbf{u}(\mathbf{x}) \;=\; \begin{pmatrix} (1 + x_1 - \exp(x_1))\, (1 - \cos(x_2)) \\ (\exp(x_1) - 1)\, (x_2 - \sin(x_2)) \end{pmatrix}$$

and

$$p(\mathbf{x}) \;=\; \frac{1}{2} \exp(2\pi x_1) \;+\; \frac{1}{4\pi} (1 - \exp(2\pi))\,.$$

Note that $\mathbf{u}$ is divergence free and $(\mathbf{u}, p)$ is regular in the whole domain Ω.

Next, in Example 3 we consider the L-shaped domain $\Omega = \,]-1,1[^2 \setminus [0,1]^2$, and choose $\mathbf{f}$ and $\mathbf{g}$ so that the exact solution is given for each $\mathbf{x} := (x_1, x_2)^{\mathtt{t}} \in \Omega$ by

$$\mathbf{u}(\mathbf{x}) \;=\; \mathbf{curl}\left(\sqrt{(x_1 - 0.01)^2 \;+\; (x_2 - 0.01)^2} \right)$$

and

$$p(\mathbf{x}) \;=\; \frac{1}{x_2 \;+\; 1.1} \;-\; \frac{1}{3} \ln(231)\,.$$

Note that $\mathbf{u}$ and p are singular at $(0.01, 0.01)$ and along the line $x_2 = -1.1$, respectively. Hence, we should expect regions of high gradients around the origin, which is the middle corner of the L, and along the line $x_2 = -1$.

Finally, in Example 4 we consider the non-convex three dimensional domain

$$\Omega \;:=\;]-\tfrac{3}{4}, \tfrac{3}{4}[\times]-\tfrac{3}{4}, \tfrac{3}{4}[\times]-\tfrac{1}{4}, \tfrac{1}{4}[\;\setminus\; \left\{ [-\tfrac{3}{4}, -\tfrac{1}{4}] \times [-\tfrac{3}{4}, \tfrac{1}{4}] \times [-\tfrac{1}{4}, \tfrac{1}{4}] \;\cup\; [\tfrac{1}{4}, \tfrac{3}{4}] \times [-\tfrac{3}{4}, \tfrac{1}{4}] \times [-\tfrac{1}{4}, \tfrac{1}{4}] \right\},$$

and choose the data $\mathbf{f}$ and $\mathbf{g}$ so that the exact solution is given for each $\mathbf{x} := (x_1, x_2, x_3)^{\mathtt{t}} \in \Omega$ by

$$\begin{aligned} \mathbf{u}(\mathbf{x}) \;=\; \mathbf{curl}\Big(& \sqrt{(x_1 + 0.3)^2 \;+\; (x_2 - 0.2)^2 \;+\; (x_3 - 0.3)^2} \\ & \;+\; \sqrt{(x_1 - 0.3)^2 \;+\; (x_2 - 0.2)^2 \;+\; (x_3 - 0.3)^2} \Big) \end{aligned}$$

and

$$p(\mathbf{x}) \;=\; \frac{1}{x_2 \;+\; 0.85} \;+\; \frac{4}{5}\ln\left(\frac{11}{64}\right).$$

Note that Ω is a T-shaped domain and that $\mathbf{u}$ and p are singular at $(-0.3, 0.2, 0.3)$ and $(0.3, 0.2, 0.3)$, and along the plane $x_2 = -0.85$, respectively. Hence, similarly to Example 3, we should expect regions of high gradients around $(-0.25, 0.25, 0.25)$ and $(0.25, 0.25, 0.25)$, which are the middle corners of the T, and along the plane $x_2 = -0.75$.

In Tables 4.1, 4.2, 4.3, and 4.4, we summarize the convergence history of the augmented HDG scheme (4.8) as applied to Example 1 and 2, for a sequence of quasi-uniform triangulations of each domain. We notice there that the rate of convergence $O(h^{k+1})$ predicted by (4.26), (4.28) and Theorems 4.3 and 4.4 is attained by all the unknowns. In particular, as observed in the tenth column of Table 4.3, the convergence of $\mathbf{u}_h$ is a bit faster than expected, which could correspond to either a superconvergence phenomenon or a special feature of Example 2. A similar phenomenon holds for the variable $\boldsymbol{\lambda}_h$ in Table 4.4. We also remark the good behaviour of the *a posteriori* error estimator $\boldsymbol{\theta}$ in this case. In particular, in Table 4.1, we see that the effectivity index $\texttt{eff}(\boldsymbol{\theta})$ remains always in the neighborhood of 0.95, 0.70, and 0.55 for $k \in \{0, 1, 2\}$, respectively, which illustrates the reliability and efficiency result provided by Theorem 4.5.

Next, in Tables 4.5 to 4.12, we provide the convergence history of the quasi-uniform and adaptive schemes as applied to Examples 3 and 4. Now, the stopping criterion in Example 3 corresponds to a maximum of 20 iterations, whereas in Example 4 it corresponds to a maximum of 9 iterations. We observe here, as expected, that the errors of the adaptive methods decrease faster than those obtained by the quasi-uniform ones. This fact is better illustrated in Figures 4.1 and 4.4, where we display the errors $\texttt{e}(\mathbf{t}, \boldsymbol{\sigma}, \mathbf{u})$ vs. the degrees of freedom N for both refinements. In addition, the effectivity indices remain again bounded from above and below, which confirms the reliability and efficiency of $\boldsymbol{\theta}$ for the associated adaptive algorithm as well. Some intermediate meshes obtained with this procedure are displayed in Figures 4.2 and 4.5. Notice here that the adapted meshes concentrate the refinements around the origin and the line $x_2 = -1$ in Example 3, and around the points $(-0.25, 0.25, 0.25)$ and $(0.25, 0.25, 0.25)$ and the plane $x_2 = -0.75$ in Example 4, which means that the method is in fact able to recognize the regions with high gradients of the solutions. Finally, in Figures 4.3 and 4.6, we display some components of the discrete solutions for both examples.

k	h	N	N_{comp}	$\mathtt{e}(\mathbf{t})$	$\mathtt{r}(\mathbf{t})$	$\mathtt{e}(\boldsymbol{\sigma})$	$\mathtt{r}(\boldsymbol{\sigma})$	$\mathtt{e}(\mathbf{u})$	$\mathtt{r}(\mathbf{u})$	$\mathtt{e}(\mathbf{t},\boldsymbol{\sigma},\mathbf{u})$	$\mathtt{r}(\mathbf{t},\boldsymbol{\sigma},\mathbf{u})$	$\mathtt{eff}(\boldsymbol{\theta})$
	0.1250	15424	4161	8.30e-1	−−	3.53e-0	−−	1.32e-1	−−	3.63e-0	−−	0.9624
	0.1000	24080	6481	6.67e-1	0.98	2.83e-0	1.00	1.05e-1	1.01	2.91e-0	0.99	0.9580
	0.0833	34656	9313	5.57e-1	0.99	2.36e-0	1.00	8.77e-2	1.00	2.42e-0	1.00	0.9554
	0.0714	47152	12657	4.78e-1	0.99	2.02e-0	1.00	7.51e-2	1.00	2.08e-0	1.00	0.9536
0	0.0625	61568	16513	4.19e-1	0.99	1.77e-0	1.00	6.57e-2	1.00	1.82e-0	1.00	0.9523
	0.0556	77904	20881	3.72e-1	0.99	1.57e-0	1.00	5.84e-2	1.00	1.62e-0	1.00	0.9514
	0.0417	138432	37057	2.80e-1	1.00	1.18e-0	1.00	4.38e-2	1.00	1.21e-0	1.00	0.9496
	0.0313	246016	65793	2.10e-1	1.00	8.85e-1	1.00	3.28e-2	1.00	9.10e-1	1.00	0.9484
	0.0208	553344	147841	1.40e-1	1.00	5.90e-1	1.00	2.19e-2	1.00	6.07e-1	1.00	0.9474
	0.0156	983552	262657	1.05e-1	1.00	4.43e-1	1.00	1.64e-2	1.00	4.55e-1	1.00	0.9469
	0.1250	41088	7297	4.07e-2	−−	2.12e-1	−−	7.96e-3	−−	2.16e-1	−−	0.7057
	0.1000	64160	11361	2.62e-2	1.98	1.36e-1	2.00	5.09e-3	2.00	1.39e-1	2.00	0.7033
	0.0833	92352	16321	1.82e-2	1.99	9.45e-2	2.00	3.54e-3	2.00	9.63e-2	2.00	0.7017
	0.0714	125664	22177	1.34e-2	1.99	6.94e-2	2.00	2.60e-3	2.00	7.07e-2	2.00	0.7005
1	0.0625	164096	28929	1.03e-2	1.99	5.31e-2	2.00	1.99e-3	2.00	5.42e-2	2.00	0.6997
	0.0556	207648	36577	8.13e-3	1.99	4.20e-2	2.00	1.57e-3	2.00	4.28e-2	2.00	0.6991
	0.0417	369024	64897	4.58e-3	1.99	2.36e-2	2.00	8.84e-4	2.00	2.41e-2	2.00	0.6978
	0.0313	655872	115201	2.58e-3	2.00	1.33e-2	2.00	4.97e-4	2.00	1.35e-2	2.00	0.6968
	0.0208	1475328	258817	1.15e-3	2.00	5.91e-3	2.00	2.21e-4	2.00	6.02e-3	2.00	0.6959
	0.0156	2622464	459777	6.46e-4	2.00	3.32e-3	2.00	1.24e-4	2.00	3.39e-3	2.00	0.6954
	0.1250	76992	10433	1.58e-3	−−	9.64e-3	−−	3.19e-4	−−	9.78e-3	−−	0.5638
	0.1000	120240	16241	8.08e-4	3.00	4.94e-3	3.00	1.63e-4	3.00	5.01e-3	3.00	0.5604
	0.0833	173088	23329	4.68e-4	3.00	2.86e-3	3.00	9.46e-5	3.00	2.90e-3	3.00	0.5583
	0.0714	235536	31697	2.95e-4	3.00	1.80e-3	3.00	5.96e-5	3.00	1.83e-3	3.00	0.5568
2	0.0625	307584	41345	1.98e-4	3.00	1.21e-3	3.00	3.99e-5	3.00	1.22e-3	3.00	0.5557
	0.0556	389232	52273	1.39e-4	3.00	8.47e-4	3.00	2.80e-5	3.00	8.59e-4	3.00	0.5548
	0.0417	691776	92737	5.86e-5	3.00	3.57e-4	3.00	1.18e-5	3.00	3.62e-4	3.00	0.5532
	0.0313	1229568	164609	2.47e-5	3.00	1.51e-4	3.00	4.99e-6	3.00	1.53e-4	3.00	0.5519
	0.0208	2765952	369793	7.33e-6	3.00	4.47e-5	3.00	1.48e-6	3.00	4.53e-5	3.00	0.5508
	0.0156	4916736	656897	3.10e-6	2.99	1.91e-5	2.96	6.24e-7	3.00	1.93e-5	2.96	0.5514

Table 4.1: Example 1, quasi-uniform scheme (Part 1).

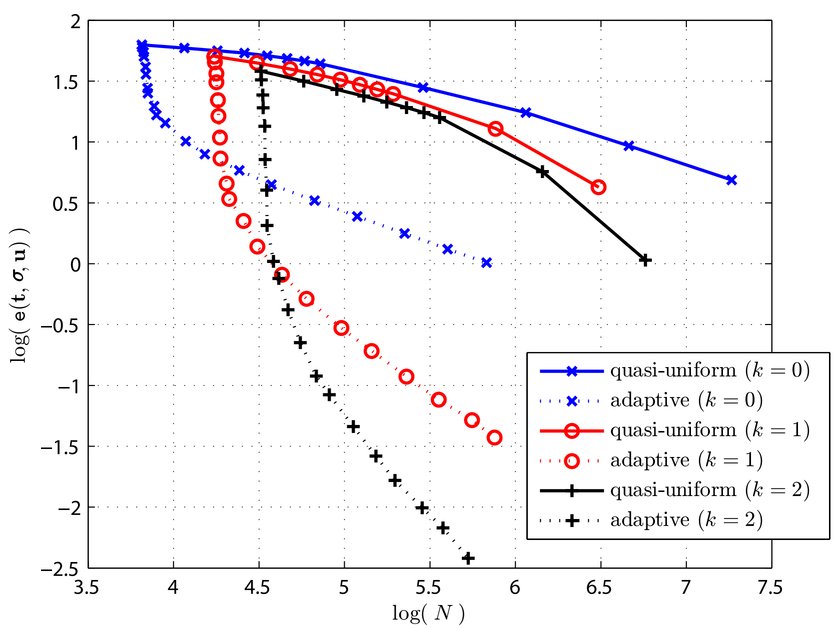

Figure 4.1: Example 3, $\mathtt{e}(\mathbf{t},\boldsymbol{\sigma},\mathbf{u})$ vs. N.

k	h	N	N_{comp}	$\mathtt{e}_0(\boldsymbol{\sigma})$	$\mathtt{r}_0(\boldsymbol{\sigma})$	$\mathtt{e}(\boldsymbol{\lambda})$	$\mathtt{r}(\boldsymbol{\lambda})$	$\mathtt{e}(p)$	$\mathtt{r}(p)$	$\mathtt{e}^\star(\boldsymbol{\sigma})$	$\mathtt{r}^\star(\boldsymbol{\sigma})$
	0.1250	15424	4161	9.57e-1	−−	1.14e-1	−−	4.43e-1	−−	3.58e-0	−−
	0.1000	24080	6481	7.63e-1	1.02	9.00e-2	1.04	3.49e-1	1.07	2.87e-0	1.00
	0.0833	34656	9313	6.34e-1	1.02	7.45e-2	1.03	2.87e-1	1.06	2.39e-0	1.00
	0.0714	47152	12657	5.42e-1	1.01	6.36e-2	1.02	2.44e-1	1.05	2.05e-0	1.00
0	0.0625	61568	16513	4.74e-1	1.01	5.55e-2	1.02	2.13e-1	1.04	1.79e-0	1.00
	0.0556	77904	20881	4.21e-1	1.01	4.93e-2	1.02	1.88e-1	1.04	1.59e-0	1.00
	0.0417	138432	37057	3.15e-1	1.01	3.68e-2	1.01	1.40e-1	1.03	1.19e-0	1.00
	0.0313	246016	65793	2.36e-1	1.01	2.76e-2	1.01	1.04e-1	1.02	8.96e-1	1.00
	0.0208	553344	147841	1.57e-1	1.00	1.84e-2	1.00	6.94e-2	1.01	5.97e-1	1.00
	0.0156	983552	262657	1.18e-1	1.00	1.38e-2	1.00	5.19e-2	1.01	4.48e-1	1.00
	0.1250	41088	7297	4.77e-2	−−	1.63e-2	−−	2.18e-2	−−	2.13e-1	−−
	0.1000	64160	11361	3.06e-2	1.99	1.04e-2	1.99	1.40e-2	2.01	1.36e-1	2.00
	0.0833	92352	16321	2.13e-2	1.99	7.26e-3	1.99	9.69e-3	2.01	9.48e-2	2.00
	0.0714	125664	22177	1.57e-2	1.99	5.34e-3	1.99	7.11e-3	2.00	6.97e-2	2.00
1	0.0625	164096	28929	1.20e-2	2.00	4.09e-3	2.00	5.44e-3	2.00	5.33e-2	2.00
	0.0556	207648	36577	9.48e-3	2.00	3.23e-3	2.00	4.30e-3	2.00	4.21e-2	2.00
	0.0417	369024	64897	5.34e-3	2.00	1.82e-3	2.00	2.42e-3	2.00	2.37e-2	2.00
	0.0313	655872	115201	3.00e-3	2.00	1.02e-3	2.00	1.36e-3	2.00	1.33e-2	2.00
	0.0208	1475328	258817	1.34e-3	2.00	4.56e-4	2.00	6.03e-4	2.00	5.93e-3	2.00
	0.0156	2622464	459777	7.52e-4	2.00	2.56e-4	2.00	3.39e-4	2.00	3.33e-3	2.00
	0.1250	76992	10433	2.15e-3	−−	4.43e-4	−−	1.01e-3	−−	9.73e-3	−−
	0.1000	120240	16241	1.10e-3	3.01	2.26e-4	3.01	5.12e-4	3.03	4.98e-3	3.00
	0.0833	173088	23329	6.34e-4	3.01	1.31e-4	3.01	2.95e-4	3.02	2.88e-3	3.00
	0.0714	235536	31697	3.99e-4	3.01	8.22e-5	3.00	1.86e-4	3.02	1.82e-3	3.00
2	0.0625	307584	41345	2.67e-4	3.00	5.51e-5	3.00	1.24e-4	3.01	1.22e-3	3.00
	0.0556	389232	52273	1.87e-4	3.00	3.87e-5	3.00	8.70e-5	3.01	8.54e-4	3.00
	0.0417	691776	92737	7.90e-5	3.00	1.63e-5	3.00	3.66e-5	3.01	3.60e-4	3.00
	0.0313	1229568	164609	3.33e-5	3.00	6.88e-6	3.00	1.54e-5	3.00	1.52e-4	3.00
	0.0208	2765952	369793	9.87e-6	3.00	2.04e-6	3.00	4.57e-6	3.00	4.51e-5	3.00
	0.0156	4916736	656897	4.18e-6	2.99	8.62e-7	3.00	1.94e-6	2.98	1.90e-5	3.00

Table 4.2: Example 1, quasi-uniform scheme (Part 2).

k	h	N	N_{comp}	$\mathtt{e}(\mathbf{t})$	$\mathtt{r}(\mathbf{t})$	$\mathtt{e}(\boldsymbol{\sigma})$	$\mathtt{r}(\boldsymbol{\sigma})$	$\mathtt{e}(\mathbf{u})$	$\mathtt{r}(\mathbf{u})$	$\mathtt{e}(\mathbf{t}, \boldsymbol{\sigma}, \mathbf{u})$	$\mathtt{r}(\mathbf{t}, \boldsymbol{\sigma}, \mathbf{u})$	$\mathtt{eff}(\boldsymbol{\theta})$
	0.0625	15424	4161	8.48e-0	−−	3.15e+1	−−	1.06e-1	−−	3.26e+1	−−	1.0010
	0.0500	24080	6481	6.66e-0	1.08	2.52e+1	0.99	6.68e-2	2.07	2.61e+1	1.00	1.0019
	0.0417	34656	9313	5.46e-0	1.10	2.10e+1	0.99	4.57e-2	2.09	2.17e+1	1.00	1.0042
	0.0357	47152	12657	4.60e-0	1.11	1.81e+1	1.00	3.31e-2	2.10	1.86e+1	1.00	1.0071
0	0.0313	61568	16513	3.96e-0	1.12	1.58e+1	1.00	2.50e-2	2.10	1.63e+1	1.00	1.0103
	0.0278	77904	20881	3.47e-0	1.13	1.41e+1	1.00	1.95e-2	2.11	1.45e+1	1.00	1.0136
	0.0208	138432	37057	2.50e-0	1.14	1.05e+1	1.00	1.06e-2	2.11	1.08e+1	1.01	1.0231
	0.0156	246016	65793	1.79e-0	1.16	7.91e-0	1.00	5.81e-3	2.09	8.11e-0	1.01	1.0343
	0.0104	553344	147841	1.12e-0	1.17	5.28e-0	1.00	2.54e-3	2.04	5.39e-0	1.01	1.0513
	0.0078	983552	262657	7.98e-1	1.16	3.96e-0	1.00	1.44e-3	1.96	4.04e-0	1.01	1.0627
	0.0625	41088	7297	2.07e-1	−−	1.19e-0	−−	9.63e-4	−−	1.21e-0	−−	0.7779
	0.0500	64160	11361	1.32e-1	2.04	7.65e-1	1.99	4.96e-4	2.97	7.76e-1	1.99	0.7845
	0.0417	92352	16321	9.12e-2	2.01	5.32e-1	1.99	2.90e-4	2.95	5.40e-1	1.99	0.7877
	0.0357	125664	22177	6.70e-2	2.00	3.91e-1	1.99	1.84e-4	2.94	3.97e-1	1.99	0.7895
1	0.0313	164096	28929	5.13e-2	1.99	3.00e-1	1.99	1.24e-4	2.94	3.04e-1	1.99	0.7906
	0.0278	207648	36577	4.06e-2	1.99	2.37e-1	2.00	8.80e-5	2.93	2.41e-1	2.00	0.7913
	0.0208	369024	64897	2.29e-2	1.99	1.33e-1	2.00	3.79e-5	2.93	1.35e-1	2.00	0.7925
	0.0156	655872	115201	1.29e-2	1.99	7.51e-2	2.00	1.63e-5	2.92	7.62e-2	2.00	0.7933
	0.0104	1475328	258817	5.76e-3	1.99	3.34e-2	2.00	5.07e-6	2.89	3.39e-2	2.00	0.7940
	0.0078	2622464	459777	3.24e-3	1.99	1.88e-2	2.00	2.25e-6	2.83	1.91e-2	2.00	0.7943
	0.0625	76992	10433	4.68e-3	−−	3.29e-2	−−	1.28e-5	−−	3.32e-2	−−	0.6260
	0.0500	120240	16241	2.41e-3	2.97	1.69e-2	2.98	5.28e-6	3.96	1.71e-2	2.98	0.6244
	0.0417	173088	23329	1.40e-3	2.98	9.80e-3	2.99	2.56e-6	3.96	9.90e-3	2.99	0.6233
	0.0357	235536	31697	8.83e-4	2.98	6.18e-3	2.99	1.39e-6	3.97	6.24e-3	2.99	0.6224
2	0.0313	307584	41345	5.93e-4	2.99	4.14e-3	2.99	8.18e-7	3.97	4.18e-3	2.99	0.6218
	0.0278	389232	52273	4.17e-4	2.99	2.91e-3	3.00	5.13e-7	3.97	2.94e-3	3.00	0.6213
	0.0208	691776	92737	1.76e-4	2.99	1.23e-3	3.00	1.64e-7	3.96	1.24e-3	3.00	0.6202
	0.0156	1229568	164609	7.45e-5	2.99	5.19e-4	3.00	5.25e-8	3.95	5.24e-4	3.00	0.6194
	0.0104	2765952	369793	2.21e-5	3.00	1.54e-4	3.00	1.07e-8	3.93	1.55e-4	3.00	0.6190
	0.0078	4916736	656897	9.34e-6	3.00	6.49e-5	3.00	3.40e-9	3.98	6.55e-5	3.00	0.6196

Table 4.3: Example 2, quasi-uniform scheme (Part 1).

k	h	N	N_{comp}	$\mathtt{e}_0(\boldsymbol{\sigma})$	$\mathtt{r}_0(\boldsymbol{\sigma})$	$\mathtt{e}(\boldsymbol{\lambda})$	$\mathtt{r}(\boldsymbol{\lambda})$	$\mathtt{e}(p)$	$\mathtt{r}(p)$	$\mathtt{e}^\star(\boldsymbol{\sigma})$	$\mathtt{r}^\star(\boldsymbol{\sigma})$
	0.0625	15424	4161	8.22e-0	−−	3.00e-1	−−	3.93e-0	−−	3.19e+1	−−
	0.0500	24080	6481	6.59e-0	0.99	1.89e-1	2.07	3.14e-0	1.01	2.56e+1	0.99
	0.0417	34656	9313	5.49e-0	1.00	1.29e-1	2.09	2.61e-0	1.01	2.14e+1	0.99
	0.0357	47152	12657	4.71e-0	1.00	9.33e-2	2.10	2.24e-0	1.01	1.83e+1	1.00
0	0.0313	61568	16513	4.12e-0	1.00	7.03e-2	2.11	1.96e-0	1.01	1.60e+1	1.00
	0.0278	77904	20881	3.66e-0	1.00	5.48e-2	2.12	1.74e-0	1.01	1.43e+1	1.00
	0.0208	138432	37057	2.75e-0	1.00	2.97e-2	2.13	1.30e-0	1.01	1.07e+1	1.00
	0.0156	246016	65793	2.06e-0	1.00	1.61e-2	2.13	9.73e-1	1.01	8.03e-0	1.00
	0.0104	553344	147841	1.37e-0	1.00	6.84e-3	2.11	6.48e-1	1.00	5.36e-0	1.00
	0.0078	983552	262657	1.03e-0	1.00	3.77e-3	2.07	4.85e-1	1.00	4.02e-0	1.00
	0.0625	41088	7297	2.95e-1	−−	3.69e-3	−−	1.38e-1	−−	1.21e-0	−−
	0.0500	64160	11361	1.90e-1	1.98	1.89e-3	2.99	8.86e-2	1.99	7.75e-1	1.99
	0.0417	92352	16321	1.32e-1	1.98	1.10e-3	2.97	6.16e-2	1.99	5.39e-1	1.99
	0.0357	125664	22177	9.73e-2	1.99	6.97e-4	2.96	4.53e-2	1.99	3.97e-1	1.99
1	0.0313	164096	28929	7.46e-2	1.99	4.70e-4	2.96	3.47e-2	1.99	3.04e-1	1.99
	0.0278	207648	36577	5.90e-2	1.99	3.32e-4	2.96	2.75e-2	2.00	2.40e-1	2.00
	0.0208	369024	64897	3.33e-2	1.99	1.42e-4	2.96	1.55e-2	2.00	1.35e-1	2.00
	0.0156	655872	115201	1.87e-2	1.99	6.05e-5	2.96	8.70e-3	2.00	7.61e-2	2.00
	0.0104	1475328	258817	8.35e-3	2.00	1.83e-5	2.95	3.87e-3	2.00	3.38e-2	2.00
	0.0078	2622464	459777	4.70e-3	2.00	7.86e-6	2.93	2.18e-3	2.00	1.90e-2	2.00
	0.0625	76992	10433	7.44e-3	−−	5.44e-5	−−	3.60e-3	−−	3.33e-2	−−
	0.0500	120240	16241	3.81e-3	2.99	2.24e-5	3.98	1.84e-3	3.01	1.71e-2	2.98
	0.0417	173088	23329	2.21e-3	3.00	1.08e-5	3.99	1.06e-3	3.01	9.91e-3	2.99
	0.0357	235536	31697	1.39e-3	3.00	5.85e-6	3.99	6.68e-4	3.01	6.25e-3	2.99
2	0.0313	307584	41345	9.32e-4	3.00	3.43e-6	3.99	4.47e-4	3.01	4.19e-3	2.99
	0.0278	389232	52273	6.55e-4	3.00	2.14e-6	3.99	3.13e-4	3.01	2.94e-3	3.00
	0.0208	691776	92737	2.76e-4	3.00	6.80e-7	3.99	1.32e-4	3.01	1.24e-3	3.00
	0.0156	1229568	164609	1.17e-4	2.99	2.16e-7	3.99	5.58e-5	2.99	5.25e-4	3.00
	0.0104	2765952	369793	3.56e-5	2.93	4.28e-8	3.99	1.75e-5	2.85	1.56e-4	3.00
	0.0078	4916736	656897	1.50e-5	3.00	1.36e-8	3.98	7.42e-6	2.99	6.62e-5	2.97

Table 4.4: Example 2, quasi-uniform scheme (Part 2).

k	h	N	N_{comp}	$\mathtt{e}(\mathbf{t})$	$\mathtt{r}(\mathbf{t})$	$\mathtt{e}(\boldsymbol{\sigma})$	$\mathtt{r}(\boldsymbol{\sigma})$	$\mathtt{e}(\mathbf{u})$	$\mathtt{r}(\mathbf{u})$	$\mathtt{e}(\mathbf{t},\boldsymbol{\sigma},\mathbf{u})$	$\mathtt{r}(\mathbf{t},\boldsymbol{\sigma},\mathbf{u})$	$\mathtt{eff}(\boldsymbol{\theta})$
	0.1667	6528	1777	2.32e-0	−−	6.27e+1	−−	1.12e-1	−−	6.27e+1	−−	1.4002
	0.1250	11584	3137	2.08e-0	0.38	5.91e+1	0.20	8.63e-2	0.91	5.92e+1	0.20	1.4031
	0.1000	18080	4881	1.90e-0	0.39	5.62e+1	0.23	7.01e-2	0.93	5.62e+1	0.23	1.4046
	0.0833	26016	7009	1.77e-0	0.40	5.37e+1	0.25	5.92e-2	0.93	5.37e+1	0.25	1.4054
	0.0714	35392	9521	1.66e-0	0.40	5.11e+1	0.31	5.13e-2	0.93	5.11e+1	0.31	1.4060
0	0.0625	46208	12417	1.58e-0	0.41	4.86e+1	0.38	4.53e-2	0.92	4.86e+1	0.38	1.4064
	0.0556	58464	15697	1.50e-0	0.42	4.62e+1	0.43	4.07e-2	0.92	4.62e+1	0.43	1.4067
	0.0500	72160	19361	1.43e-0	0.43	4.39e+1	0.48	3.70e-2	0.92	4.40e+1	0.48	1.4069
	0.0250	288320	77121	9.90e-1	0.53	2.80e+1	0.65	1.90e-2	0.96	2.80e+1	0.65	1.4068
	0.0125	1152640	307841	5.08e-1	0.96	1.74e+1	0.69	9.32e-3	1.03	1.74e+1	0.69	1.4068
	0.0063	4609280	1230081	2.63e-1	0.95	9.28e-0	0.91	4.66e-3	1.00	9.29e-0	0.91	1.4064
	0.0031	18434560	4917761	1.35e-1	0.97	4.87e-0	0.93	2.33e-3	1.00	4.87e-0	0.93	1.4065
	0.1667	17376	3121	1.51e-0	−−	5.05e+1	−−	2.57e-2	−−	5.05e+1	−−	1.3935
	0.1250	30848	5505	1.33e-0	0.44	4.45e+1	0.44	1.92e-2	1.02	4.45e+1	0.44	1.3972
	0.1000	48160	8561	1.20e-0	0.46	3.97e+1	0.51	1.56e-2	0.94	3.97e+1	0.51	1.3990
	0.0833	69312	12289	1.10e-0	0.49	3.58e+1	0.56	1.30e-2	0.98	3.58e+1	0.56	1.3998
1	0.0714	94304	16689	1.01e-0	0.54	3.25e+1	0.64	1.10e-2	1.07	3.25e+1	0.64	1.4003
	0.0625	123136	21761	9.34e-1	0.61	2.95e+1	0.71	9.43e-3	1.19	2.95e+1	0.71	1.4005
	0.0556	155808	27505	8.62e-1	0.68	2.70e+1	0.76	8.08e-3	1.31	2.70e+1	0.76	1.4004
	0.0500	192320	33921	7.95e-1	0.76	2.49e+1	0.78	6.94e-3	1.44	2.49e+1	0.78	1.4001
	0.0250	768640	135041	3.46e-1	1.20	1.29e+1	0.95	1.96e-3	1.82	1.29e+1	0.95	1.3964
	0.0125	3073280	538881	1.08e-1	1.69	4.24e-0	1.60	5.09e-4	1.95	4.25e-0	1.60	1.3916
	0.1667	32544	4465	1.14e-0	−−	3.81e+1	−−	1.36e-2	−−	3.82e+1	−−	1.3820
	0.1250	57792	7873	9.77e-1	0.53	3.16e+1	0.66	1.02e-2	0.99	3.16e+1	0.66	1.3843
	0.1000	90240	12241	8.51e-1	0.62	2.70e+1	0.71	7.78e-3	1.24	2.70e+1	0.71	1.3837
	0.0833	129888	17569	7.44e-1	0.74	2.38e+1	0.69	5.89e-3	1.52	2.38e+1	0.69	1.3826
2	0.0714	176736	23857	6.50e-1	0.88	2.13e+1	0.73	4.52e-3	1.71	2.13e+1	0.73	1.3817
	0.0625	230784	31105	5.68e-1	1.00	1.92e+1	0.78	3.54e-3	1.83	1.92e+1	0.78	1.3811
	0.0556	292032	39313	4.98e-1	1.12	1.74e+1	0.82	2.83e-3	1.90	1.74e+1	0.82	1.3809
	0.0500	360480	48481	4.38e-1	1.22	1.59e+1	0.88	2.32e-3	1.91	1.59e+1	0.88	1.3810
	0.0250	1440960	192961	1.64e-1	1.42	5.71e-0	1.47	6.65e-4	1.80	5.71e-0	1.47	1.3776
	0.0125	5761920	769921	2.48e-2	2.72	1.07e-0	2.42	8.10e-5	3.04	1.07e-0	2.42	1.3646

Table 4.5: Example 3, quasi-uniform scheme (Part 1).

k	h	N	N_{comp}	$\mathtt{e}_0(\boldsymbol{\sigma})$	$\mathtt{r}_0(\boldsymbol{\sigma})$	$\mathtt{e}(\boldsymbol{\lambda})$	$\mathtt{r}(\boldsymbol{\lambda})$	$\mathtt{e}(p)$	$\mathtt{r}(p)$	$\mathtt{e}^\star(\boldsymbol{\sigma})$	$\mathtt{r}^\star(\boldsymbol{\sigma})$
	0.1667	6528	1777	1.95e-0	−−	1.51e-1	−−	8.88e-1	−−	6.27e+1	−−
	0.1250	11584	3137	1.60e-0	0.69	1.06e-1	1.23	6.78e-1	0.94	5.91e+1	0.20
	0.1000	18080	4881	1.38e-0	0.65	7.88e-2	1.32	5.60e-1	0.86	5.62e+1	0.23
	0.0833	26016	7009	1.24e-0	0.60	6.17e-2	1.35	4.90e-1	0.73	5.37e+1	0.25
	0.0714	35392	9521	1.14e-0	0.57	5.02e-2	1.33	4.45e-1	0.62	5.11e+1	0.31
0	0.0625	46208	12417	1.06e-0	0.54	4.23e-2	1.28	4.14e-1	0.54	4.86e+1	0.38
	0.0556	58464	15697	9.94e-1	0.53	3.68e-2	1.20	3.91e-1	0.49	4.62e+1	0.43
	0.0500	72160	19361	9.41e-1	0.52	3.27e-2	1.12	3.72e-1	0.47	4.40e+1	0.48
	0.0250	288320	77121	6.22e-1	0.60	1.63e-2	1.00	2.46e-1	0.60	2.80e+1	0.65
	0.0125	1152640	307841	3.40e-1	0.87	7.92e-3	1.04	1.48e-1	0.73	1.74e+1	0.69
	0.0063	4609280	1230081	1.78e-1	0.93	3.94e-3	1.01	7.90e-2	0.91	9.29e-0	0.91
	0.0031	18434560	4917761	9.12e-2	0.96	1.97e-3	1.00	4.18e-2	0.92	4.85e-0	0.94
	0.1667	17376	3121	1.03e-0	−−	3.73e-2	−−	3.88e-1	−−	5.05e+1	−−
	0.1250	30848	5505	8.87e-1	0.53	2.50e-2	1.39	3.47e-1	0.39	4.45e+1	0.44
	0.1000	48160	8561	7.87e-1	0.54	2.03e-2	0.92	3.14e-1	0.44	3.97e+1	0.51
	0.0833	69312	12289	7.07e-1	0.59	1.75e-2	0.82	2.82e-1	0.59	3.58e+1	0.56
1	0.0714	94304	16689	6.37e-1	0.67	1.53e-2	0.89	2.51e-1	0.77	3.25e+1	0.64
	0.0625	123136	21761	5.76e-1	0.75	1.33e-2	1.02	2.22e-1	0.93	2.95e+1	0.71
	0.0556	155808	27505	5.22e-1	0.84	1.16e-2	1.18	1.95e-1	1.07	2.70e+1	0.76
	0.0500	192320	33921	4.74e-1	0.92	1.00e-2	1.35	1.72e-1	1.20	2.49e+1	0.78
	0.0250	768640	135041	2.03e-1	1.22	2.90e-3	1.79	7.65e-2	1.17	1.29e+1	0.95
	0.0125	3073280	538881	6.80e-2	1.58	7.74e-4	1.90	2.83e-2	1.43	4.25e-0	1.60
	0.1667	32544	4465	7.79e-1	−−	2.14e-2	−−	3.21e-1	−−	3.82e+1	−−
	0.1250	57792	7873	6.34e-1	0.72	1.72e-2	0.75	2.49e-1	0.88	3.16e+1	0.66
	0.1000	90240	12241	5.29e-1	0.81	1.35e-2	1.09	1.94e-1	1.12	2.70e+1	0.71
	0.0833	129888	17569	4.46e-1	0.94	1.03e-2	1.49	1.51e-1	1.38	2.38e+1	0.69
2	0.0714	176736	23857	3.79e-1	1.05	7.86e-3	1.76	1.19e-1	1.54	2.13e+1	0.73
	0.0625	230784	31105	3.26e-1	1.12	6.05e-3	1.95	9.80e-2	1.45	1.92e+1	0.78
	0.0556	292032	39313	2.85e-1	1.17	4.71e-3	2.12	8.57e-2	1.14	1.74e+1	0.82
	0.0500	360480	48481	2.51e-1	1.19	3.73e-3	2.23	7.89e-2	0.79	1.59e+1	0.88
	0.0250	1440960	192961	9.61e-2	1.39	9.78e-4	1.93	3.51e-2	1.17	5.71e-0	1.47
	0.0125	5761920	769921	1.60e-2	2.58	1.32e-4	2.89	7.01e-3	2.32	1.07e-0	2.42

Table 4.6: Example 3, quasi-uniform scheme (Part 2).

k	h	N	N_{comp}	$\mathtt{e}(\mathbf{t})$	$\mathtt{r}(\mathbf{t})$	$\mathtt{e}(\boldsymbol{\sigma})$	$\mathtt{r}(\boldsymbol{\sigma})$	$\mathtt{e}(\mathbf{u})$	$\mathtt{r}(\mathbf{u})$	$\mathtt{e}(\mathbf{t},\boldsymbol{\sigma},\mathbf{u})$	$\mathtt{r}(\mathbf{t},\boldsymbol{\sigma},\mathbf{u})$	$\mathtt{eff}(\boldsymbol{\theta})$
	0.1667	6528	1777	2.32e-0	−−	6.27e+1	−−	1.12e-1	−−	6.27e+1	−−	1.4002
	0.1667	6560	1787	2.25e-0	12.24	5.98e+1	19.43	1.11e-1	2.77	5.98e+1	19.42	1.4032
	0.1667	6680	1819	2.01e-0	12.35	5.46e+1	9.96	1.03e-1	8.55	5.46e+1	9.96	1.4029
	0.1667	6712	1829	1.96e-0	10.19	5.03e+1	34.82	1.03e-1	-0.11	5.03e+1	34.79	1.4030
	0.1667	6862	1869	1.73e-0	11.43	4.14e+1	17.54	1.00e-1	2.82	4.14e+1	17.53	1.4004
	0.1667	6894	1879	1.62e-0	28.69	3.59e+1	61.79	9.99e-2	0.22	3.59e+1	61.72	1.3964
	0.1667	7044	1919	1.50e-0	7.05	2.76e+1	24.23	9.92e-2	0.65	2.77e+1	24.19	1.3876
	0.1667	7076	1929	1.40e-0	31.43	2.51e+1	42.26	9.92e-2	-0.01	2.51e+1	42.22	1.3817
	0.1667	7706	2097	1.22e-0	3.11	1.96e+1	5.77	9.39e-2	1.29	1.97e+1	5.76	1.3732
0	0.1667	7952	2167	1.20e-0	1.48	1.66e+1	10.69	9.38e-2	0.03	1.66e+1	10.64	1.3589
	0.1667	8956	2445	1.12e-0	1.12	1.42e+1	2.59	8.84e-2	1.01	1.43e+1	2.58	1.3509
	0.1667	11788	3209	8.35e-1	2.14	1.01e+1	2.50	8.05e-2	0.68	1.01e+1	2.50	1.3355
	0.1667	15242	4155	7.45e-1	0.88	7.91e-0	1.90	7.99e-2	0.05	7.94e-0	1.89	1.3082
	0.1667	24258	6571	5.66e-1	1.18	5.81e-0	1.33	7.34e-2	0.37	5.83e-0	1.33	1.3042
	0.1667	37464	10141	4.75e-1	0.81	4.44e-0	1.24	6.78e-2	0.37	4.46e-0	1.24	1.2817
	0.1667	66906	18023	3.58e-1	0.98	3.28e-0	1.04	5.51e-2	0.71	3.30e-0	1.04	1.2765
	0.1667	118938	31995	2.73e-1	0.94	2.43e-0	1.04	4.51e-2	0.69	2.45e-0	1.04	1.2697
	0.1667	224564	60225	1.98e-1	1.00	1.76e-0	1.02	3.32e-2	0.96	1.77e-0	1.02	1.2672
	0.1179	400954	107321	1.47e-1	1.02	1.31e-0	1.03	2.46e-2	1.04	1.31e-0	1.03	1.2676
	0.0833	678522	181565	1.14e-1	0.96	1.01e-0	0.96	1.92e-2	0.94	1.02e-0	0.96	1.2694
	0.1667	17376	3121	1.51e-0	−−	5.05e+1	−−	2.57e-2	−−	5.05e+1	−−	1.3935
	0.1667	17460	3139	1.38e-0	36.69	4.52e+1	46.17	2.11e-2	82.12	4.52e+1	46.17	1.3942
	0.1667	17780	3195	1.17e-0	18.64	3.65e+1	23.28	1.58e-2	32.16	3.66e+1	23.27	1.3957
	0.1667	17864	3213	9.39e-1	93.28	3.10e+1	69.70	1.31e-2	77.25	3.10e+1	69.73	1.3910
	0.1667	18264	3283	7.45e-1	20.86	2.21e+1	30.67	1.10e-2	15.87	2.21e+1	30.66	1.3910
	0.1667	18348	3301	5.13e-1	162.37	1.63e+1	131.38	1.04e-2	25.24	1.63e+1	131.41	1.3733
	0.1667	18748	3371	3.97e-1	23.78	1.08e+1	37.96	1.01e-2	2.73	1.09e+1	37.94	1.3603
	0.1667	18832	3389	3.44e-1	64.33	7.35e-0	174.39	1.01e-2	2.34	7.35e-0	174.20	1.3173
	0.1667	20512	3683	2.50e-1	7.45	4.53e-0	11.30	8.34e-3	4.36	4.54e-0	11.29	1.2751
1	0.1667	21164	3807	2.40e-1	2.80	3.39e-0	18.58	8.33e-3	0.08	3.40e-0	18.52	1.1999
	0.1667	25756	4637	1.28e-1	6.37	2.24e-0	4.20	5.42e-3	4.38	2.25e-0	4.21	1.2490
	0.1667	30972	5563	1.02e-1	2.43	1.38e-0	5.26	5.33e-3	0.19	1.38e-0	5.25	1.1836
	0.1667	43124	7749	6.13e-2	3.10	8.08e-1	3.24	3.63e-3	2.32	8.11e-1	3.24	1.1605
	0.1667	60180	10747	4.58e-2	1.75	5.11e-1	2.75	3.39e-3	0.41	5.13e-1	2.74	1.1110
	0.1667	96308	17109	2.55e-2	2.48	2.93e-1	2.37	2.13e-3	1.98	2.94e-1	2.37	1.1020
	0.1667	144196	25595	1.79e-2	1.76	1.91e-1	2.11	1.68e-3	1.18	1.92e-1	2.11	1.0779
	0.1667	230180	40695	1.10e-2	2.09	1.18e-1	2.07	1.06e-3	1.97	1.18e-1	2.07	1.0757
	0.1667	355122	62644	7.01e-3	2.07	7.60e-2	2.02	6.95e-4	1.93	7.63e-2	2.02	1.0785
	0.1667	556068	98029	4.56e-3	1.92	5.18e-2	1.70	4.37e-4	2.07	5.20e-2	1.71	1.1008
	0.1179	756780	133213	3.48e-3	1.75	3.69e-2	2.20	3.36e-4	1.70	3.71e-2	2.20	1.0715
	0.1667	32544	4465	1.14e-0	−−	3.81e+1	−−	1.36e-2	−−	3.82e+1	−−	1.3820
	0.1667	32700	4491	9.31e-1	83.69	3.23e+1	69.58	9.27e-3	160.96	3.23e+1	69.59	1.3736
	0.1667	33300	4571	7.69e-1	21.12	2.43e+1	31.23	6.12e-3	45.68	2.43e+1	31.22	1.3785
	0.1667	33456	4597	5.02e-1	181.93	1.91e+1	103.60	3.84e-3	199.63	1.91e+1	103.67	1.3664
	0.1667	34206	4697	3.55e-1	31.27	1.34e+1	31.75	2.52e-3	37.96	1.34e+1	31.75	1.3775
	0.1667	34362	4723	1.96e-1	260.23	7.17e-0	275.69	2.08e-3	84.06	7.17e-0	275.68	1.3466
	0.1667	35112	4823	1.36e-1	34.28	4.02e-0	53.71	1.93e-3	7.05	4.02e-0	53.70	1.3306
	0.1667	35268	4849	8.51e-2	210.62	2.06e-0	301.40	1.89e-3	8.17	2.06e-0	301.28	1.2150
	0.1667	38418	5269	5.12e-2	11.89	1.04e-0	15.92	1.42e-3	6.79	1.04e-0	15.91	1.1440
2	0.1667	41286	5667	3.37e-2	11.60	7.56e-1	8.92	7.14e-4	19.02	7.57e-1	8.93	1.1769
	0.1667	46734	6435	1.97e-2	8.70	4.17e-1	9.59	6.18e-4	2.32	4.18e-1	9.59	1.1348
	0.1667	55146	7567	1.41e-2	3.99	2.24e-1	7.51	5.82e-4	0.73	2.24e-1	7.50	1.0367
	0.1667	68520	9371	7.84e-3	5.42	1.19e-1	5.82	3.55e-4	4.56	1.19e-1	5.81	0.9950
	0.1667	81510	11181	5.18e-3	4.77	8.38e-2	4.06	2.56e-4	3.75	8.39e-2	4.06	1.0125
	0.1667	112740	15371	3.23e-3	2.92	4.57e-2	3.73	1.96e-4	1.66	4.58e-2	3.73	0.9695
	0.1667	152826	20747	1.90e-3	3.49	2.62e-2	3.67	1.30e-4	2.70	2.62e-2	3.67	0.9415
	0.1667	197430	26741	1.26e-3	3.19	1.65e-2	3.59	9.45e-5	2.47	1.66e-2	3.58	0.9201
	0.1667	284766	38547	7.45e-4	2.88	9.83e-3	2.84	5.76e-5	2.70	9.86e-3	2.84	0.9165
	0.1667	377358	50929	4.71e-4	3.25	6.73e-3	2.69	3.73e-5	3.10	6.75e-3	2.69	0.9631
	0.1667	530172	71403	2.75e-4	3.18	3.79e-3	3.38	2.21e-5	3.07	3.80e-3	3.38	0.9386

Table 4.7: Example 3, adaptive scheme (Part 1).

k	h	N	N_{comp}	$\mathtt{e}_0(\boldsymbol{\sigma})$	$\mathtt{r}_0(\boldsymbol{\sigma})$	$\mathtt{e}(\boldsymbol{\lambda})$	$\mathtt{r}(\boldsymbol{\lambda})$	$\mathtt{e}(p)$	$\mathtt{r}(p)$	$\mathtt{e}^{\star}(\boldsymbol{\sigma})$	$\mathtt{r}^{\star}(\boldsymbol{\sigma})$
	0.1667	6528	1777	1.95e-0	−−	1.51e-1	−−	8.88e-1	−−	6.27e+1	−−
	0.1667	6560	1787	1.96e-0	-1.11	1.49e-1	3.61	9.33e-1	-20.12	5.98e+1	19.41
	0.1667	6680	1819	1.63e-0	19.89	1.13e-1	30.42	7.05e-1	30.85	5.46e+1	9.96
	0.1667	6712	1829	1.63e-0	1.35	1.17e-1	-12.66	7.21e-1	-9.38	5.03e+1	34.81
	0.1667	6862	1869	1.47e-0	9.43	1.03e-1	11.70	6.53e-1	9.00	4.14e+1	17.54
	0.1667	6894	1879	1.41e-0	16.11	1.05e-1	-7.57	6.26e-1	18.19	3.59e+1	61.76
	0.1667	7044	1919	1.36e-0	3.45	1.02e-1	2.51	6.15e-1	1.69	2.76e+1	24.21
	0.1667	7076	1929	1.33e-0	11.24	1.02e-1	-1.83	6.07e-1	5.64	2.51e+1	42.22
	0.1667	7706	2097	1.26e-0	1.23	1.01e-1	0.33	5.83e-1	0.94	1.96e+1	5.76
0	0.1667	7952	2167	1.25e-0	0.74	1.01e-1	0.09	5.75e-1	0.85	1.66e+1	10.67
	0.1667	8956	2445	1.18e-0	0.92	9.32e-2	1.28	5.56e-1	0.58	1.42e+1	2.58
	0.1667	11788	3209	8.42e-1	2.46	7.04e-2	2.04	3.85e-1	2.67	1.01e+1	2.50
	0.1667	15242	4155	7.39e-1	1.01	6.83e-2	0.24	3.37e-1	1.04	7.92e-0	1.89
	0.1667	24258	6571	5.82e-1	1.03	6.18e-2	0.43	2.69e-1	0.97	5.82e-0	1.33
	0.1667	37464	10141	4.77e-1	0.91	5.54e-2	0.50	2.18e-1	0.97	4.44e-0	1.24
	0.1667	66906	18023	3.65e-1	0.93	4.49e-2	0.72	1.66e-1	0.93	3.29e-0	1.04
	0.1667	118938	31995	2.77e-1	0.96	3.65e-2	0.72	1.26e-1	0.96	2.44e-0	1.04
	0.1667	224564	60225	2.02e-1	1.00	2.64e-2	1.02	9.17e-2	1.01	1.76e-0	1.02
	0.1179	400954	107321	1.51e-1	1.01	1.98e-2	0.98	6.86e-2	1.00	1.31e-0	1.03
	0.0833	678522	181565	1.17e-1	0.95	1.57e-2	0.88	5.36e-2	0.94	1.02e-0	0.96
	0.1667	17376	3121	1.03e-0	−−	3.73e-2	−−	3.88e-1	−−	5.05e+1	−−
	0.1667	17460	3139	9.23e-1	46.63	3.29e-2	52.18	3.36e-1	60.65	4.52e+1	46.18
	0.1667	17780	3195	7.68e-1	20.33	2.44e-2	32.88	3.02e-1	11.57	3.66e+1	23.28
	0.1667	17864	3213	6.18e-1	92.18	2.28e-2	28.35	2.34e-1	108.31	3.10e+1	69.71
	0.1667	18264	3283	4.76e-1	23.64	1.90e-2	16.39	1.77e-1	25.37	2.21e+1	30.67
	0.1667	18348	3301	3.71e-1	107.87	1.87e-2	8.30	1.55e-1	57.42	1.63e+1	131.37
	0.1667	18748	3371	3.08e-1	17.45	1.81e-2	2.83	1.33e-1	13.91	1.09e+1	37.95
	0.1667	18832	3389	2.82e-1	38.94	1.80e-2	2.32	1.21e-1	41.75	7.35e-0	174.34
	0.1667	20512	3683	2.32e-1	4.57	1.52e-2	4.03	1.01e-1	4.40	4.54e-0	11.30
1	0.1667	21164	3807	2.27e-1	1.30	1.51e-2	0.09	9.89e-2	1.12	3.39e-0	18.56
	0.1667	25756	4637	1.34e-1	5.38	9.56e-3	4.68	6.27e-2	4.64	2.25e-0	4.20
	0.1667	30972	5563	9.71e-2	3.49	9.15e-3	0.47	4.39e-2	3.88	1.38e-0	5.26
	0.1667	43124	7749	5.97e-2	2.94	6.00e-3	2.55	2.69e-2	2.96	8.09e-1	3.24
	0.1667	60180	10747	4.42e-2	1.80	5.56e-3	0.46	1.98e-2	1.84	5.12e-1	2.75
	0.1667	96308	17109	2.43e-2	2.54	3.50e-3	1.96	1.07e-2	2.60	2.94e-1	2.37
	0.1667	144196	25595	1.76e-2	1.61	2.71e-3	1.27	7.86e-3	1.54	1.92e-1	2.11
	0.1667	230180	40695	1.07e-2	2.12	1.71e-3	1.96	4.77e-3	2.14	1.18e-1	2.07
	0.1667	355122	62644	6.81e-3	2.09	1.11e-3	1.99	3.03e-3	2.10	7.61e-2	2.02
	0.1667	556068	98029	4.50e-3	1.84	7.09e-4	2.01	2.01e-3	1.82	5.19e-2	1.70
	0.1179	756780	133213	3.37e-3	1.87	5.61e-4	1.53	1.50e-3	1.89	3.70e-2	2.20
	0.1667	32544	4465	7.79e-1	−−	2.14e-2	−−	3.21e-1	−−	3.82e+1	−−
	0.1667	32700	4491	5.95e-1	112.89	1.31e-2	205.94	2.08e-1	181.79	3.23e+1	69.59
	0.1667	33300	4571	4.68e-1	26.36	1.06e-2	22.95	1.61e-1	28.10	2.43e+1	31.23
	0.1667	33456	4597	3.22e-1	160.02	5.91e-3	250.50	1.24e-1	110.42	1.91e+1	103.60
	0.1667	34206	4697	2.17e-1	35.82	3.92e-3	36.92	8.14e-2	38.16	1.34e+1	31.75
	0.1667	34362	4723	1.30e-1	224.05	3.28e-3	79.35	5.26e-2	191.77	7.17e-0	275.68
	0.1667	35112	4823	9.03e-2	33.84	3.07e-3	5.89	3.64e-2	34.17	4.02e-0	53.71
	0.1667	35268	4849	6.83e-2	125.52	3.04e-3	5.06	3.14e-2	66.56	2.06e-0	301.34
	0.1667	38418	5269	4.79e-2	8.31	2.38e-3	5.69	2.23e-2	8.05	1.04e-0	15.91
2	0.1667	41286	5667	3.83e-2	6.24	1.38e-3	15.15	1.82e-2	5.61	7.56e-1	8.92
	0.1667	46734	6435	1.96e-2	10.79	1.10e-3	3.69	8.97e-3	11.40	4.17e-1	9.59
	0.1667	55146	7567	1.28e-2	5.18	1.04e-3	0.69	5.84e-3	5.19	2.24e-1	7.51
	0.1667	68520	9371	6.80e-3	5.80	6.31e-4	4.58	3.00e-3	6.12	1.19e-1	5.82
	0.1667	81510	11181	5.09e-3	3.34	4.54e-4	3.79	2.28e-3	3.19	8.38e-2	4.06
	0.1667	112740	15371	2.94e-3	3.39	3.56e-4	1.49	1.31e-3	3.42	4.58e-2	3.73
	0.1667	152826	20747	1.76e-3	3.35	2.33e-4	2.79	7.79e-4	3.41	2.62e-2	3.67
	0.1667	197430	26741	1.18e-3	3.15	1.70e-4	2.47	5.19e-4	3.17	1.65e-2	3.59
	0.1667	284766	38547	7.26e-4	2.65	1.04e-4	2.70	3.21e-4	2.61	9.84e-3	2.84
	0.1667	377358	50929	4.55e-4	3.32	6.77e-5	3.02	2.02e-4	3.31	6.74e-3	2.69
	0.1667	530172	71403	2.62e-4	3.24	4.03e-5	3.05	1.16e-4	3.26	3.79e-3	3.38

Table 4.8: Example 3, adaptive scheme (Part 2).

k	h	N	N_{comp}	$\mathtt{e}(\mathbf{t})$	$\mathtt{r}(\mathbf{t})$	$\mathtt{e}(\boldsymbol{\sigma})$	$\mathtt{r}(\boldsymbol{\sigma})$	$\mathtt{e}(\mathbf{u})$	$\mathtt{r}(\mathbf{u})$	$\mathtt{e}(\mathbf{t}, \boldsymbol{\sigma}, \mathbf{u})$	$\mathtt{r}(\mathbf{t}, \boldsymbol{\sigma}, \mathbf{u})$	$\mathtt{eff}(\boldsymbol{\theta})$
	0.4330	7464	1945	1.27e-0	−−	8.00e-0	−−	2.97e-1	−−	8.10e-0	−−	1.0827
	0.2165	58656	14497	7.62e-1	0.73	4.98e-0	0.68	1.50e-1	0.98	5.04e-0	0.68	1.0795
	0.1443	196776	47737	5.37e-1	0.86	3.63e-0	0.78	9.97e-2	1.01	3.68e-0	0.78	1.0847
	0.1083	465024	111745	4.14e-1	0.91	2.84e-0	0.86	7.51e-2	0.98	2.87e-0	0.86	1.0833
	0.0866	906600	216601	3.37e-1	0.92	2.33e-0	0.89	6.00e-2	1.01	2.35e-0	0.90	1.0835
0	0.0722	1564704	372385	2.83e-1	0.96	1.97e-0	0.92	4.99e-2	1.01	1.99e-0	0.92	1.0825
	0.0619	2482536	589177	2.44e-1	0.96	1.69e-0	0.97	4.28e-2	0.99	1.71e-0	0.97	1.0788
	0.0541	3703296	877057	2.14e-1	0.97	1.49e-0	0.97	3.76e-2	0.99	1.50e-0	0.97	1.0764
	0.0481	5270184	1246105	1.91e-1	0.97	1.33e-0	0.96	3.33e-2	1.01	1.34e-0	0.96	1.0759
	0.0433	7226400	1706401	1.73e-1	0.97	1.20e-0	0.98	3.00e-2	1.00	1.21e-0	0.98	1.0746
	0.0394	9615144	2268025	1.57e-1	0.99	1.09e-0	0.96	2.73e-2	1.00	1.10e-0	0.96	1.0751
	0.0361	12479616	2941057	1.44e-1	0.99	1.00e-0	0.98	2.50e-2	1.01	1.01e-0	0.98	1.0744
	0.4330	27432	5353	4.64e-1	−−	3.85e-0	−−	3.41e-2	−−	3.88e-0	−−	0.8809
	0.2165	216288	39649	1.82e-1	1.35	1.63e-0	1.24	9.96e-3	1.78	1.64e-0	1.24	0.8804
	0.1443	726408	130249	9.26e-2	1.67	8.85e-1	1.50	4.56e-3	1.93	8.89e-1	1.51	0.8962
	0.1083	1717632	304513	5.63e-2	1.73	5.51e-1	1.64	2.62e-3	1.92	5.54e-1	1.64	0.8968
1	0.0866	3349800	589801	3.75e-2	1.82	3.72e-1	1.76	1.69e-3	1.97	3.74e-1	1.76	0.9016
	0.0722	5782752	1013473	2.66e-2	1.88	2.70e-1	1.76	1.17e-3	2.00	2.72e-1	1.76	0.9089
	0.0619	9176328	1602889	2.00e-2	1.86	2.01e-1	1.93	8.68e-4	1.95	2.02e-1	1.93	0.8985
	0.0541	13690368	2385409	1.55e-2	1.90	1.55e-1	1.91	6.68e-4	1.97	1.56e-1	1.91	0.8956
	0.0481	19484712	3388393	1.23e-2	1.93	1.24e-1	1.91	5.28e-4	2.00	1.25e-1	1.91	0.8955
	0.4330	64944	10465	2.04e-1	−−	1.86e-0	−−	9.39e-3	−−	1.87e-0	−−	0.6302
	0.2165	513216	77377	5.56e-2	1.88	5.44e-1	1.77	1.82e-3	2.37	5.46e-1	1.77	0.6435
2	0.1443	1724976	254017	2.12e-2	2.37	2.26e-1	2.16	6.18e-4	2.67	2.27e-1	2.17	0.6779
	0.1083	4080384	593665	1.04e-2	2.49	1.15e-1	2.34	2.84e-4	2.70	1.16e-1	2.35	0.6728
	0.0866	7959600	1149601	5.75e-3	2.65	6.49e-2	2.57	1.52e-4	2.80	6.52e-2	2.57	0.6759
	0.0722	13742784	1975105	3.46e-3	2.78	4.05e-2	2.59	8.81e-5	2.99	4.06e-2	2.59	0.6764

Table 4.9: Example 4, quasi-uniform scheme (Part 1).

k	h	N	N_{comp}	$\mathtt{e}_0(\boldsymbol{\sigma})$	$\mathtt{r}_0(\boldsymbol{\sigma})$	$\mathtt{e}(\boldsymbol{\lambda})$	$\mathtt{r}(\boldsymbol{\lambda})$	$\mathtt{e}(p)$	$\mathtt{r}(p)$	$\mathtt{e}^\star(\boldsymbol{\sigma})$	$\mathtt{r}^\star(\boldsymbol{\sigma})$
0	0.4330	7464	1945	1.07e-0	−−	2.35e-1	−−	4.28e-1	−−	8.02e-0	−−
	0.2165	58656	14497	6.34e-1	0.75	1.23e-1	0.93	2.50e-1	0.78	5.00e-0	0.68
	0.1443	196776	47737	4.43e-1	0.89	8.19e-2	1.01	1.71e-1	0.93	3.64e-0	0.78
	0.1083	465024	111745	3.38e-1	0.93	6.08e-2	1.03	1.29e-1	0.98	2.85e-0	0.86
	0.0866	906600	216601	2.73e-1	0.96	4.87e-2	0.99	1.03e-1	1.02	2.33e-0	0.90
	0.0722	1564704	372385	2.28e-1	0.99	4.03e-2	1.04	8.54e-2	1.03	1.97e-0	0.92
	0.0619	2482536	589177	1.96e-1	0.99	3.45e-2	1.01	7.29e-2	1.03	1.70e-0	0.97
	0.0541	3703296	877057	1.72e-1	0.99	3.01e-2	1.01	6.35e-2	1.03	1.49e-0	0.97
	0.0481	5270184	1246105	1.53e-1	0.99	2.68e-2	0.99	5.62e-2	1.04	1.33e-0	0.96
	0.0433	7226400	1706401	1.38e-1	1.00	2.41e-2	1.00	5.04e-2	1.04	1.20e-0	0.98
	0.0394	9615144	2268025	1.25e-1	1.00	2.19e-2	1.01	4.57e-2	1.03	1.09e-0	0.96
	0.0361	12479616	2941057	1.15e-1	1.01	2.01e-2	1.02	4.17e-2	1.04	1.00e-0	0.98
1	0.4330	27432	5353	3.63e-1	−−	5.98e-2	−−	1.33e-1	−−	3.85e-0	−−
	0.2165	216288	39649	1.32e-1	1.45	1.85e-2	1.69	4.43e-2	1.58	1.63e-0	1.24
	0.1443	726408	130249	6.75e-2	1.66	8.83e-3	1.83	2.27e-2	1.65	8.85e-1	1.50
	0.1083	1717632	304513	4.08e-2	1.75	5.14e-3	1.88	1.37e-2	1.76	5.52e-1	1.64
	0.0866	3349800	589801	2.71e-2	1.83	3.37e-3	1.89	9.11e-3	1.82	3.73e-1	1.76
	0.0722	5782752	1013473	1.93e-2	1.87	2.36e-3	1.96	6.44e-3	1.90	2.70e-1	1.76
	0.0619	9176328	1602889	1.44e-2	1.89	1.75e-3	1.93	4.78e-3	1.93	2.01e-1	1.93
	0.0541	13690368	2385409	1.11e-2	1.92	1.35e-3	1.93	3.69e-3	1.94	1.56e-1	1.91
	0.0481	19484712	3388393	8.87e-3	1.94	1.08e-3	1.95	2.94e-3	1.94	1.24e-1	1.91
2	0.4330	64944	10465	1.39e-1	−−	1.74e-2	−−	4.08e-2	−−	1.86e-0	−−
	0.2165	513216	77377	3.63e-2	1.94	3.56e-3	2.29	1.06e-2	1.95	5.44e-1	1.77
	0.1443	1724976	254017	1.41e-2	2.33	1.28e-3	2.52	4.25e-3	2.25	2.26e-1	2.16
	0.1083	4080384	593665	6.91e-3	2.48	5.95e-4	2.67	2.10e-3	2.45	1.15e-1	2.34
	0.0866	7959600	1149601	3.84e-3	2.64	3.26e-4	2.70	1.19e-3	2.54	6.49e-2	2.57
	0.0722	13742784	1975105	2.31e-3	2.79	1.92e-4	2.91	7.10e-4	2.84	4.05e-2	2.59

Table 4.10: Example 4, quasi-uniform scheme (Part 2).

k	h	N	N_{comp}	$\mathtt{e}(\mathbf{t})$	$\mathtt{r}(\mathbf{t})$	$\mathtt{e}(\boldsymbol{\sigma})$	$\mathtt{r}(\boldsymbol{\sigma})$	$\mathtt{e}(\mathbf{u})$	$\mathtt{r}(\mathbf{u})$	$\mathtt{e}(\mathbf{t},\boldsymbol{\sigma},\mathbf{u})$	$\mathtt{r}(\mathbf{t},\boldsymbol{\sigma},\mathbf{u})$	$\mathtt{eff}(\boldsymbol{\theta})$
	0.4330	7464	1945	1.27e-0	−−	8.00e-0	−−	2.97e-1	−−	8.10e-0	−−	1.0827
	0.4330	12174	3113	1.01e-0	0.94	6.10e-0	1.11	2.37e-1	0.93	6.19e-0	1.10	1.0485
	0.4330	25077	6310	8.65e-1	0.42	4.30e-0	0.97	2.16e-1	0.25	4.40e-0	0.95	0.9371
	0.4330	74127	18307	6.10e-1	0.64	2.92e-0	0.71	1.46e-1	0.72	2.99e-0	0.71	0.9193
0	0.2795	153618	37469	4.73e-1	0.70	2.44e-0	0.49	1.10e-1	0.79	2.49e-0	0.50	0.9611
	0.2275	422067	101816	3.50e-1	0.59	1.64e-0	0.79	8.45e-2	0.52	1.68e-0	0.78	0.9044
	0.2165	699573	167837	2.86e-1	0.80	1.45e-0	0.50	6.58e-2	0.99	1.48e-0	0.51	0.9476
	0.1768	1956981	466720	2.11e-1	0.59	9.76e-1	0.76	5.12e-2	0.49	1.00e-0	0.76	0.8957
	0.1250	3822273	906633	1.64e-1	0.76	8.06e-1	0.57	3.85e-2	0.86	8.23e-1	0.58	0.9301
	0.4330	27432	5353	4.64e-1	−−	3.85e-0	−−	3.41e-2	−−	3.88e-0	−−	0.8809
	0.4330	44796	8549	2.56e-1	2.42	2.27e-0	2.15	2.04e-2	2.10	2.29e-0	2.15	0.8580
	0.4330	87576	16461	1.70e-1	1.23	1.10e-0	2.18	1.81e-2	0.35	1.11e-0	2.16	0.6720
	0.4330	186330	34163	1.05e-1	1.26	8.81e-1	0.58	1.10e-2	1.32	8.87e-1	0.59	0.8235
1	0.4330	353526	64371	6.93e-2	1.31	4.20e-1	2.31	8.59e-3	0.78	4.26e-1	2.29	0.6572
	0.2795	705015	126520	4.41e-2	1.31	3.35e-1	0.65	4.21e-3	2.07	3.38e-1	0.67	0.7822
	0.2500	1384584	247005	2.89e-2	1.25	1.70e-1	2.01	3.27e-3	0.75	1.72e-1	1.99	0.6428
	0.2296	2227491	394576	2.02e-2	1.51	1.36e-1	0.95	2.31e-3	1.45	1.37e-1	0.96	0.7173
	0.1768	4218372	742429	1.15e-2	1.76	8.02e-2	1.65	1.30e-3	1.80	8.10e-2	1.65	0.6923
	0.4330	64944	10465	2.04e-1	−−	1.86e-0	−−	9.39e-3	−−	1.87e-0	−−	0.6302
	0.4330	106140	16703	7.31e-2	4.18	8.31e-1	3.27	3.15e-3	4.44	8.34e-1	3.28	0.7124
	0.4330	195594	30339	3.91e-2	2.05	2.77e-1	3.60	2.62e-3	0.60	2.79e-1	3.58	0.4474
	0.4330	268422	41196	2.67e-2	2.42	2.47e-1	0.71	1.81e-3	2.35	2.49e-1	0.73	0.5931
2	0.4330	449226	67867	1.79e-2	1.56	1.82e-1	1.20	1.24e-3	1.47	1.82e-1	1.20	0.6436
	0.3783	900066	134396	9.40e-3	1.85	6.68e-2	2.88	6.81e-4	1.72	6.75e-2	2.86	0.4727
	0.3536	1345116	198767	5.82e-3	2.38	5.62e-2	0.86	3.84e-4	2.85	5.65e-2	0.88	0.6289
	0.3125	1638588	241631	4.68e-3	2.20	4.40e-2	2.49	3.13e-4	2.08	4.42e-2	2.48	0.6046
	0.2795	2625642	385834	2.44e-3	2.77	2.35e-2	2.65	1.60e-4	2.84	2.37e-2	2.65	0.6021

Table 4.11: Example 4, adaptive scheme (Part 1).

k	h	N	N_{comp}	$\mathtt{e}_0(\boldsymbol{\sigma})$	$\mathtt{r}_0(\boldsymbol{\sigma})$	$\mathtt{e}(\boldsymbol{\lambda})$	$\mathtt{r}(\boldsymbol{\lambda})$	$\mathtt{e}(p)$	$\mathtt{r}(p)$	$\mathtt{e}^\star(\boldsymbol{\sigma})$	$\mathtt{r}^\star(\boldsymbol{\sigma})$
	0.4330	7464	1945	1.07e-0	−−	2.35e-1	−−	4.28e-1	−−	8.02e-0	−−
	0.4330	12174	3113	9.60e-1	0.44	2.45e-1	-0.18	4.12e-1	0.16	6.13e-0	1.10
	0.4330	25077	6310	7.23e-1	0.79	2.29e-1	0.19	2.83e-1	1.04	4.31e-0	0.97
	0.4330	74127	18307	5.08e-1	0.65	1.66e-1	0.59	2.02e-1	0.63	2.92e-0	0.72
0	0.2795	153618	37469	4.16e-1	0.55	1.37e-1	0.53	1.70e-1	0.47	2.44e-0	0.49
	0.2275	422067	101816	2.93e-1	0.69	1.00e-1	0.62	1.15e-1	0.77	1.64e-0	0.79
	0.2165	699573	167837	2.38e-1	0.83	7.63e-2	1.08	9.15e-2	0.92	1.45e-0	0.50
	0.1768	1956981	466720	1.68e-1	0.68	5.98e-2	0.47	6.18e-2	0.76	9.74e-1	0.77
	0.1250	3822273	906633	1.31e-1	0.73	4.46e-2	0.88	4.82e-2	0.74	8.05e-1	0.57
	0.4330	27432	5353	3.63e-1	−−	5.98e-2	−−	1.33e-1	−−	3.85e-0	−−
	0.4330	44796	8549	2.69e-1	1.22	4.41e-2	1.24	1.17e-1	0.51	2.28e-0	2.14
	0.4330	87576	16461	1.38e-1	2.00	3.83e-2	0.43	5.04e-2	2.52	1.10e-0	2.19
	0.4330	186330	34163	9.61e-2	0.96	2.43e-2	1.21	3.84e-2	0.72	8.82e-1	0.58
1	0.4330	353526	64371	5.63e-2	1.67	1.88e-2	0.79	2.06e-2	1.95	4.20e-1	2.32
	0.2795	705015	126520	3.81e-2	1.13	9.25e-3	2.06	1.45e-2	1.02	3.36e-1	0.65
	0.2500	1384584	247005	2.30e-2	1.50	7.20e-3	0.74	8.09e-3	1.73	1.70e-1	2.01
	0.2296	2227491	394576	1.66e-2	1.36	5.11e-3	1.44	6.07e-3	1.21	1.36e-1	0.95
	0.1768	4218372	742429	1.03e-2	1.51	2.90e-3	1.77	3.70e-3	1.55	9.91e-2	0.99
	0.4330	64944	10465	1.39e-1	−−	1.74e-2	−−	4.08e-2	−−	1.86e-0	−−
	0.4330	106140	16703	7.28e-2	2.63	7.72e-3	3.32	2.97e-2	1.29	8.32e-1	3.27
	0.4330	195594	30339	3.04e-2	2.85	6.05e-3	0.80	1.03e-2	3.46	2.77e-1	3.60
	0.4330	268422	41196	2.33e-2	1.68	4.23e-3	2.26	8.88e-3	0.96	2.48e-1	0.70
2	0.4330	449226	67867	1.63e-2	1.38	2.90e-3	1.46	6.35e-3	1.30	1.82e-1	1.20
	0.3783	900066	134396	7.29e-3	2.32	1.67e-3	1.59	2.48e-3	2.70	6.69e-2	2.88
	0.3536	1345116	198767	5.10e-3	1.78	9.28e-4	2.92	1.95e-3	1.20	5.63e-2	0.86
	0.3125	1638588	241631	4.01e-3	2.43	7.54e-4	2.11	1.50e-3	2.68	4.40e-2	2.49
	0.2795	2625642	385834	2.15e-3	2.65	3.78e-4	2.93	8.08e-4	2.61	2.25e-2	2.84

Table 4.12: Example 4, adaptive scheme (Part 2).

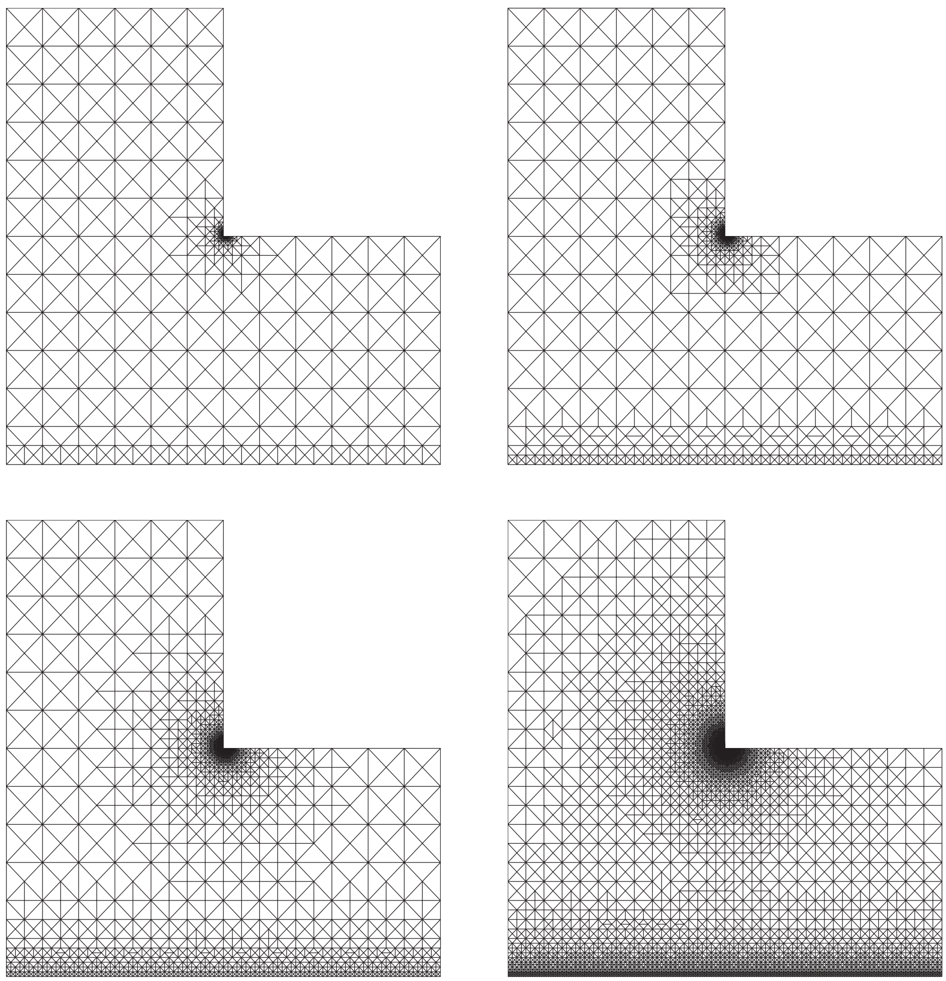

Figure 4.2: Example 3, adapted meshes for $k = 0$ with 11788, 24258, 66906, and 224564 degrees of freedom.

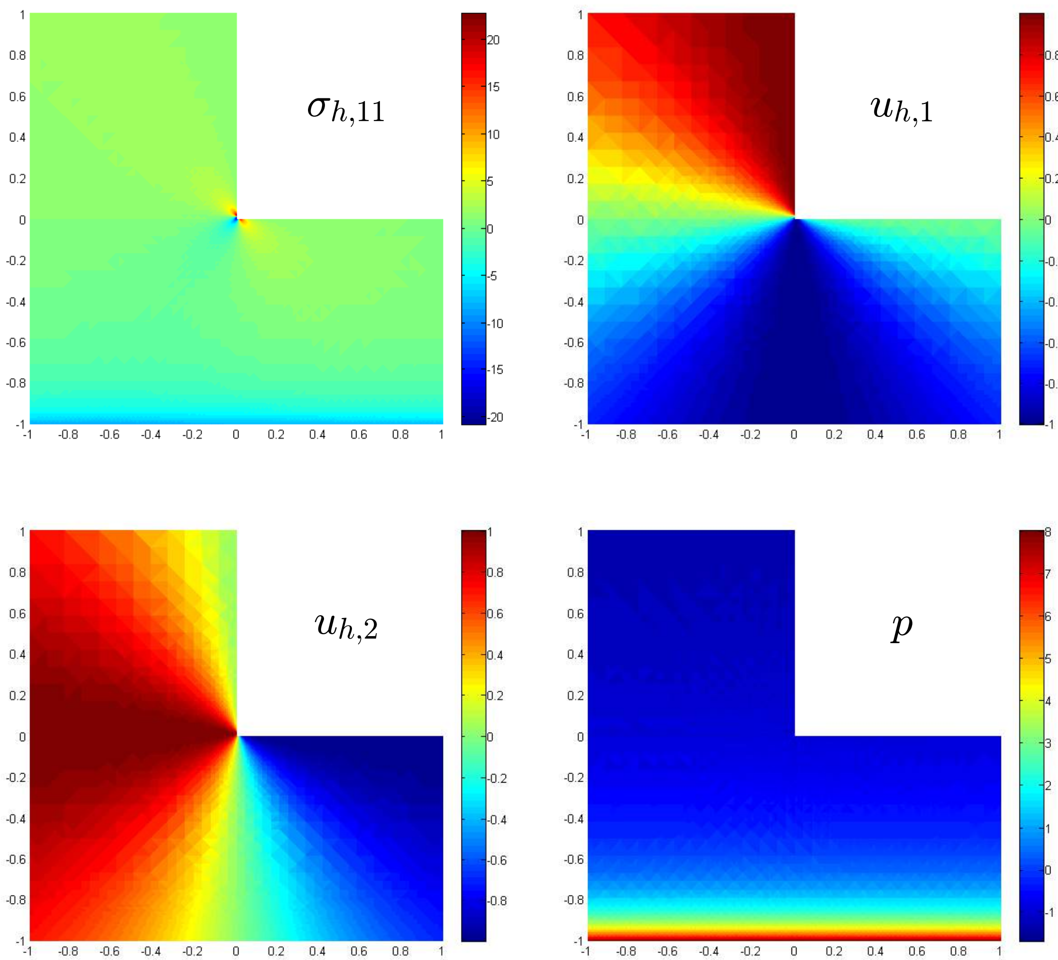

Figure 4.3: Example 3, some components of the approximate solutions ($k = 0$ and $N = 118938$) for the adaptive scheme.

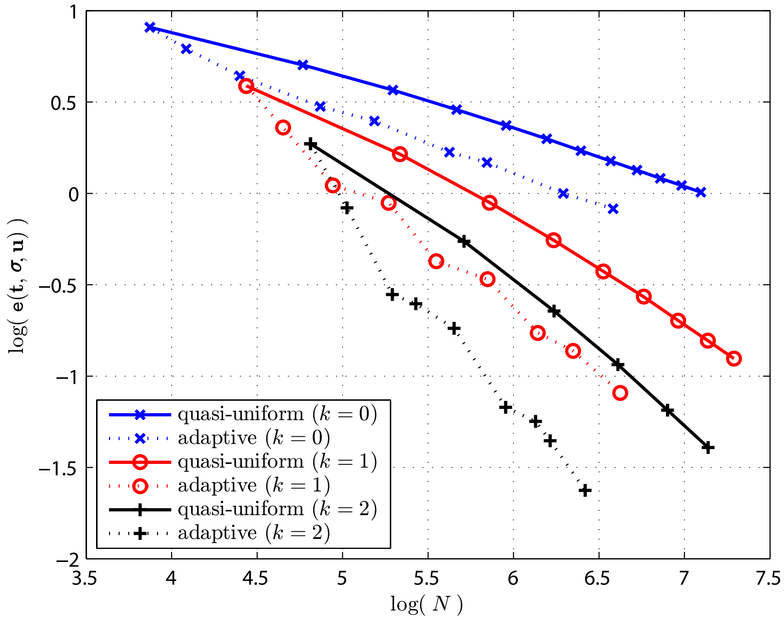

Figure 4.4: Example 4, $\mathsf{e}(\mathbf{t}, \boldsymbol{\sigma}, \mathbf{u})$ vs. N.

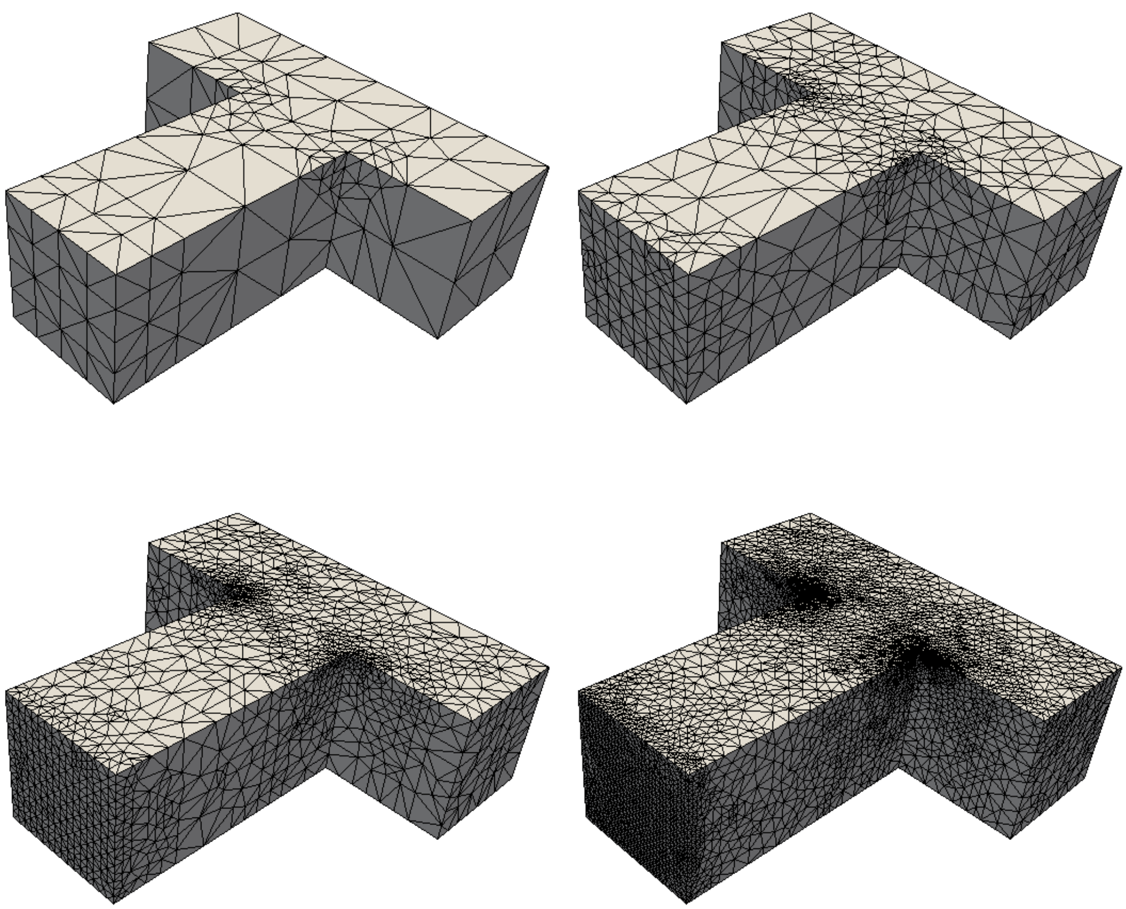

Figure 4.5: Example 4, adapted meshes for $k = 0$ with 25077, 153618, 699573, and 3822273 degrees of freedom.

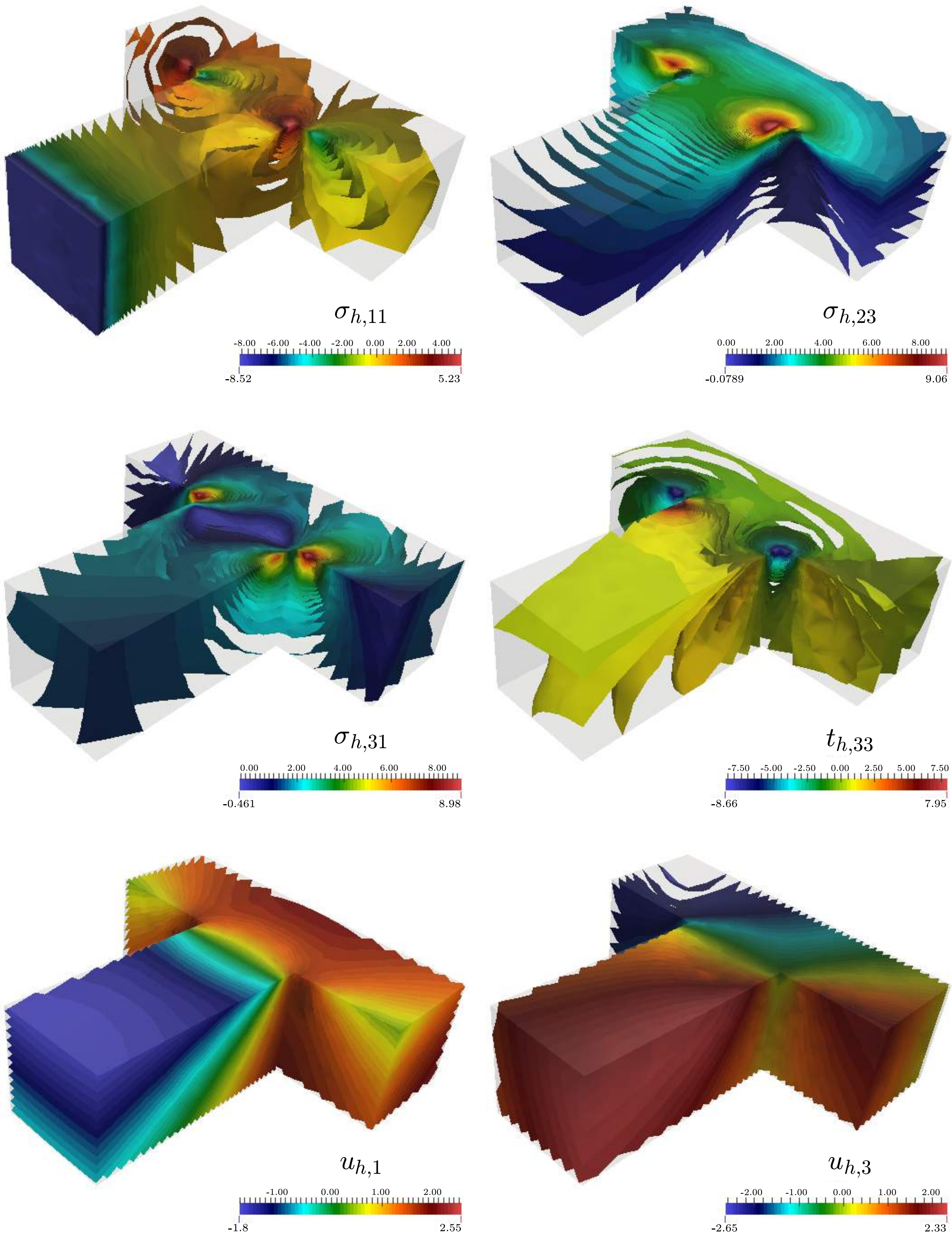

Figure 4.6: Example 4, iso-surfaces of some components of the approximate solutions ($k = 2$ and $N = 1638588$) for the adaptive scheme.

CHAPTER 5

Analysis of the HDG method for the Stokes-Darcy coupling

5.1 Introduction

The derivation of suitable numerical methods for the coupling of fluid flow with porous media flow, modelled by the Stokes and Darcy equations, has been increasing during recent years (see e.g., [15, 28, 38, 55, 56, 59, 60, 65, 81, 85, 88, 101, 105, 114, 115, 124, 128], and the references therein). The above list includes different kind of problems. In particular, porous media with cracks, and the incorporation of other linear and nonlinear equations in the coupled problem, such as Brinkman and Forchheimer. This model has applications in different areas of interest, such as chemical and petroleum engineering, hydrology, and environmental sciences, to name a few. That is the reason why it has gained relevance through the last decades, and the cause of the numerical analysis community has been putting so much effort in developing more accurate and efficient methods for solving this problem. Now, with respect to the historical perspective, we recall here that the first fully-mixed finite element method for the 2D Stokes-Darcy coupled problem has been introduced and analyzed recently in [86]. This approach allows the introduction of further unknowns of physical interest as well as the utilization of the same family of finite element subspaces in both media, without requiring any stabilization term. Moreover, the fact that dual-mixed formulations are considered in both domains yields as the main unknowns the pseudostress and the velocity in the fluid, together with the velocity and the pressure in the porous medium. The pressure and the gradient of the velocity in the fluid can then be computed through a very simple post-process of the above unknowns, in which no numerical differentiation is applied, and hence no further sources of error arise. In addition, due to the fully-mixed approach utilized, the transmission conditions become essential, and hence they have to be imposed weakly, which leads to the incorporation of two additional unknowns to the system, namely the traces of the Darcy pressure and the Stokes velocity on the coupling interface Σ. These new unknowns are also variables of importance from a physical point of view. Then, in order to prove the unique solvability of the resulting continuous formulation, that the well known Fredholm and Babuška-Brezzi theories are applied, which also contribute to derive sufficient conditions on the finite element subspaces ensuring that the associated Galerkin scheme becomes well-posed. Among the several different ways in which the equations and unknowns can be ordered, the one yielding a doubly mixed structure is chosen, for which the inf-sup conditions of the off-diagonal bilinear forms follow straightforwardly. Moreover, the arguments of the continuous analysis can be easily adapted to the discrete case. In particular, a feasible choice of subspaces is given by Raviart-Thomas elements of lowest order and piecewise constants for the velocities and pressures, respectively, in both domains, together with continuous piecewise linear elements for the additional unknowns on the interface.

On the other hand, the hybridizable discontinuous Galerkin (HDG) method, introduced in [42] for diffusion problems, is one of the several high-order discretization schemes that benefit from the hybridization technique originally applied in [50] to the local discontinuous Galerkin (LDG) method for time dependent convection-diffusion problems. The main advantages of HDG methods include a substantial reduction of the globally coupled degrees of freedom (which was a criticism for the discontinuous Galerkin (DG) methods for elliptic problems during the last decade), and the fact that convergence is obtained even for the polynomial degree $k = 0$. Additionally, the approximate flux converges with order $k+1$ for $k \geq 0$, and an element-by-element computation of a new approximation of the scalar variable is possible, which converges with order $k+2$ for $k \geq 1$ (see e.g. [41, 45, 43]). Nevertheless, and up to our knowledge, there is still no contribution in the literature concerning HDG for fully-mixed Stokes-Darcy systems.

According to the above discussion, we are interested in this chapter in applying the HDG approach to the coupled Stokes and Darcy flows problem studied in [86]. To this end, we plan to employ the same techniques given in the context of HDG schemes for the Stokes and Darcy uncoupled equations. More precisely, for Stokes problem, the hybridization for DG methods was initially introduced in [31] and then analyzed in [112, 43]. Lately, an overview of the recent work by Cockburn and co-workers on the devising of HDG methods for the Stokes equations of incompressible flow was provided in [49]. For the Darcy law, we are particularly interested in [44], where it was introduced the new projection-based technique for the study of the *a priori* error analysis of hybridizable discontinuous Galerkin methods. In addition, we follow [48], to derive a way to deal with the weak stress symmetry, and then show the optimal rate of convergence for all unknowns. The rest of this chapter is organized as follows. In Section 5.2 we present the main aspects of the continuous problem, which includes the geometry and the coupled model. Then, in Section 5.3 we introduce the hybridizable discontinuous Galerkin formulation for the coupled problem. More precisely, we present the finite dimensional discontinuous subspaces and we show the unique solvability of HDG scheme. The corresponding *a priori* error estimates are derived in Section 5.4. In particular, we use projections whose design are inspired by the form of the numerical traces of the method, which is an innovative technique applied for the error analysis of HDG approximations. Finally, several numerical experiments validating the good performance of the method and confirming the rates of convergence derived are reported in Section 5.5.

We end the present section with further notations to be used below. Given a non-null space H, we set $\mathbf{H} := H^n$ and $\mathbb{H} := H^{n\times n}$. Also, given $\boldsymbol{\tau} := (\tau_{ij})$, $\boldsymbol{\zeta} := (\zeta_{ij}) \in \mathrm{R}^{n\times n}$, we write as usual

$$\boldsymbol{\tau}^{\mathtt{t}} \;:=\; (\tau_{ji})\,, \quad \operatorname{tr}(\boldsymbol{\tau}) \;:=\; \sum_{i=1}^{n}\tau_{ii}\,, \quad \boldsymbol{\tau}^{\mathtt{d}} \;:=\; \boldsymbol{\tau} - \frac{1}{n}\operatorname{tr}(\boldsymbol{\tau})\,\mathbb{I}\,, \quad \text{and} \quad \boldsymbol{\tau}:\boldsymbol{\zeta} \;:=\; \sum_{i,j=1}^{n}\tau_{ij}\zeta_{ij}\,.$$

Also, in what follows we utilize the standard terminology for Sobolev spaces and norms, employ $\mathbf{0}$ to denote a generic null vector, null tensor or null operator, and use C, with or without subscripts, bars, tildes or hats, to denote generic constants independent of the discretization parameters, which may take different values at different places.

5.2 The coupled problem

In order to describe the geometry of the problem, we let Ω_S and Ω_D be bounded and simply connected polyhedral domains in R^n, $n \in \{2,3\}$, such that $\partial\Omega_S \cap \partial\Omega_D = \Sigma \neq \emptyset$. Then, we let

$\Gamma_S := \partial\Omega_S \setminus \bar{\Sigma}$, $\Gamma_D := \partial\Omega_D \setminus \bar{\Sigma}$, and denote by $\mathbf{n}$ the unit normal vector on the boundaries, which is chosen pointing outward from $\Omega_S \cup \Sigma \cup \Omega_D$ (and hence inward to Ω_D when seen on Σ). On Σ we also consider unit tangent vectors, which are given by $\mathbf{t} = \mathbf{t}_1$ when $n = 2$ (see Figure 5.1 below) and by $\{\mathbf{t}_1, \mathbf{t}_2\}$, when $n = 3$.

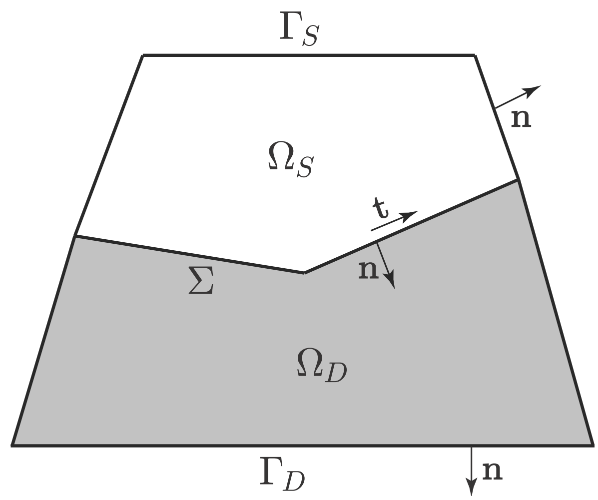

Figure 5.1: Sketch of the 2D geometry for the Stokes-Darcy coupling.

The model consists of two separate groups of equations and a set of coupling terms. In Ω_S, the governing equations are those of the Stokes problem, which are written in the following stress-velocity-pressure formulation:

$$\begin{gathered}\boldsymbol{\sigma}_S = \nu\,\mathbf{e}(\mathbf{u}_S) - p_S\,\mathbb{I} \quad \text{in} \quad \Omega_S\,, \qquad \mathbf{div}(\boldsymbol{\sigma}_S) + \mathbf{f}_S = \mathbf{0} \quad \text{in} \quad \Omega_S\,, \\ \operatorname{div}(\mathbf{u}_S) = 0 \quad \text{in} \quad \Omega_S\,, \qquad \mathbf{u}_S = \mathbf{0} \quad \text{on} \quad \Gamma_S\,, \qquad \int_{\Omega_S} p_S = 0\,, \end{gathered} \tag{5.1}$$

where $\nu > 0$ is the viscosity of the fluid, $\boldsymbol{\sigma}_S$ is the stress tensor, $\mathbf{u}_S$ is the fluid velocity, p_S is the pressure, $\mathbb{I}$ is the $n \times n$ identity matrix, $\mathbf{f}_S \in \mathbf{L}^2(\Omega_S)$ is a known source term, $\mathbf{div}$ is the usual divergence operator div acting row-wise on each tensor, and

$$\mathbf{e}(\mathbf{u}_S) := \frac{1}{2}\left(\nabla\mathbf{u}_S + (\nabla\mathbf{u}_S)^{\mathtt{t}}\right)$$

is the strain tensor (or symmetric part of the velocity gradient). Now, introducing the vorticity (or skew-symmetric part of the velocity gradient) $\boldsymbol{\rho}_S := \frac{1}{2}\left(\nabla\mathbf{u}_S - (\nabla\mathbf{u}_S)^{\mathtt{t}}\right)$ as a further unknown, and using that $\operatorname{tr}(\nabla\mathbf{u}_S) = \operatorname{div}(\mathbf{u}_S) = 0$ in Ω_S, and the relation $\nabla\mathbf{u}_S - \boldsymbol{\rho}_S = \mathbf{e}(\mathbf{u}_S)$ in Ω_S, we observe that the equations in (5.1) can be rewritten equivalently as

$$\begin{gathered}\frac{1}{\nu}\boldsymbol{\sigma}_S^{\mathtt{d}} = \nabla\mathbf{u}_S - \boldsymbol{\rho}_S \quad \text{in} \quad \Omega_S\,, \qquad \mathbf{div}(\boldsymbol{\sigma}_S) + \mathbf{f}_S = \mathbf{0} \quad \text{in} \quad \Omega_S\,, \\ \boldsymbol{\sigma}_S = \boldsymbol{\sigma}_S^{\mathtt{t}} \quad \text{in} \quad \Omega_S\,, \qquad p_S = -\frac{1}{n}\operatorname{tr}(\boldsymbol{\sigma}_S) \quad \text{in} \quad \Omega_S\,, \\ \mathbf{u}_S = \mathbf{0} \quad \text{on} \quad \Gamma_S\,, \qquad \int_{\Omega_S} \operatorname{tr}(\boldsymbol{\sigma}_S) = 0\,. \end{gathered} \tag{5.2}$$

In turn, in Ω_D we consider the following Darcy model:

$$\begin{gathered}\mathbf{u}_D = -\mathbf{K}\nabla p_D \quad \text{in} \quad \Omega_D\,, \qquad \operatorname{div}(\mathbf{u}_D) = f_D \quad \text{in} \quad \Omega_D\,, \\ \mathbf{u}_D \cdot \mathbf{n} = 0 \quad \text{on} \quad \Gamma_D\,, \end{gathered} \tag{5.3}$$

where $\mathbf{u}_D$ and p_D denote the velocity and pressure, respectively, and the source term $f_D \in L^2(\Omega_D)$ is such that $\int_{\Omega_D} f_D = 0$. The tensor valued function $\mathbf{K}$, which describes the permeability of Ω_D divided by the viscosity ν, satisfies $\mathbf{K}^{\mathtt{t}} = \mathbf{K}$, and has $L^\infty(\Omega_D)$ components. Also, we assume that there exists $\alpha_{\mathbf{K}} > 0$ such that

$$\mathbf{w} \cdot \mathbf{K}(\mathbf{x})\mathbf{w} \quad \geq \quad \alpha_{\mathbf{K}} \|\mathbf{w}\|^2_{\mathrm{R}^n} \,,$$

for almost all $\mathbf{x} \in \Omega_D$, and for all $\mathbf{w} \in \mathrm{R}^n$. Finally, the transmission conditions on Σ are given by

$$\begin{aligned} \mathbf{u}_S \cdot \mathbf{n} \quad &= \quad \mathbf{u}_D \cdot \mathbf{n} \quad \text{on} \quad \Sigma\,, \\ \boldsymbol{\sigma}_S \mathbf{n} \;+\; \sum_{\ell=1}^{n-1} \kappa_\ell^{-1} (\mathbf{u}_S \cdot \mathbf{t}_\ell) \mathbf{t}_\ell \quad &= \quad -p_D \mathbf{n} \quad \text{on} \quad \Sigma\,, \end{aligned} \tag{5.4}$$

where $\{\kappa_1, \ldots, \kappa_{n-1}\}$ is a set of positive frictional constants that can be determined experimentally. The first equation in (5.4) is the conservation of mass, and the second one establishes the balance of normal forces and the Beavers-Joseph-Saffman law.

5.3 The HDG method

5.3.1 Notation

We begin by introducing some preliminary notations. Let $\mathcal{T}_h^S$ and $\mathcal{T}_h^D$ be respective triangulations of the domains Ω_S and Ω_D without the presence of hanging nodes, which are formed by shape-regular n-simplex of diameter h_T and assume that they match in Σ so that $\mathcal{T}_h^S \cup \mathcal{T}_h^D$ is a triangulation of $\Omega_S \cup \Sigma \cup \Omega_D$. In addition, let $\mathcal{E}_h^*$ be the set of faces F of $\mathcal{T}_h^*$, and $\partial \mathcal{T}_h^* := \cup \{\partial T \;:\; T \in \mathcal{T}_h^*\} \quad \forall\, * \in \{S, D\}$. Next, let $(\cdot,\cdot)_U$ denote the usual L^2, $\mathbf{L}^2$ and $\mathbb{L}^2$ inner product over the domain $U \subseteq \mathrm{R}^n$, and similarly let $\langle \cdot,\cdot \rangle_G$ be the L^2 and $\mathbf{L}^2$ inner product over the surface $G \subseteq \mathrm{R}^{n-1}$. Then, for each $* \in \{S, D\}$ we introduce the inner products:

$$(\cdot,\cdot)_{\mathcal{T}_h^*} \;:=\; \sum_{T \in \mathcal{T}_h^*} (\cdot,\cdot)_T\,, \quad \langle \cdot,\cdot \rangle_{\partial \mathcal{T}_h^*} \;:=\; \sum_{T \in \mathcal{T}_h^*} \langle \cdot,\cdot \rangle_{\partial T}\,, \quad \text{and} \quad \langle \cdot,\cdot \rangle_{\partial \mathcal{T}_h^* \setminus \Sigma} \;:=\; \sum_{T \in \mathcal{T}_h^*} \sum_{F \in \partial T \setminus \Sigma} \langle \cdot,\cdot \rangle_F\,.$$

Furthermore, given $r \geq 0$ and $* \in \{S, D\}$, we define

$$H^r(\mathcal{T}_h^*) \;:=\; \left\{ v \in L^2(\Omega_*) \;:\; v|_T \in H^r(T) \quad \forall\, T \in \mathcal{T}_h^* \right\}\,,$$

whence $\mathbf{H}^r(\mathcal{T}_h^*)$ and $\mathbb{H}^r(\mathcal{T}_h^*)$ denote the vectorial and tensorial versions of $H^r(\mathcal{T}_h^*)$, respectively.

On the other hand, let $\mathbf{n}^+$ and $\mathbf{n}^-$ be the outward unit normal vectors on the boundaries of two neighboring elements T^+ and T^-, respectively. We use $\boldsymbol{\tau}^\pm$ to denote the traces of $\boldsymbol{\tau}$ on $F := \partial T^+ \cap \partial T^-$ from the interior of $T^\pm$, where $\boldsymbol{\tau}$ is a second-order tensorial function. Then, we define the jumps $[\![\cdot]\!]$ of tensor variables on each interior face as follows

$$[\![\boldsymbol{\tau}]\!] \;:=\; \boldsymbol{\tau}^+ \mathbf{n}^+ \;+\; \boldsymbol{\tau}^- \mathbf{n}^-\,.$$

5.3.2 Subspaces

Next, given $k \geq 1$, and U a domain or either a closed or open Lipschitz curve if $n = 2$ (resp. surface if $n = 3$), we let $\mathrm{P}_k(U)$ be the space of polynomials of total degree at most k defined on U. In addition, given $T \in \mathcal{T}_h^S \cup \mathcal{T}_h^D$, we let

$$\mathbb{A}(T) \ := \ \mathbb{P}_k(T) \cap \mathbb{L}^2_{\text{skew}}(T)\,,$$

and (see [93, 48])

$$\mathbb{B}(T) \ := \ \text{curl}\left(\text{curl}\left(\mathbb{A}(T)\right) b_T\right)\,,$$

where $\mathbb{L}^2_{\text{skew}}(T) := \{\boldsymbol{\eta} \in \mathbb{L}^2(T) \,:\, \boldsymbol{\eta} + \boldsymbol{\eta}^{\mathtt{t}} = \mathbf{0}\}$ is the subspace of skew-symmetric tensors of $\mathbb{L}^2(T)$, and b_T is the scalar bubble function in $\mathrm{P}_{n+1}(T)$. Furthermore, in three space dimensions the ith row of $\text{curl}(\boldsymbol{\tau})$ is nothing but $\text{curl}(\cdot)$ applied to the ith row of $\boldsymbol{\tau}$. In the two-dimensional case, given vector and tensor valued fields $\mathbf{v} := (v_1, v_2)$ and $\boldsymbol{\tau} := (\tau_{ij})$, respectively, we let

$$\text{curl}(\mathbf{v}) \ := \ \begin{pmatrix} \frac{\partial v_1}{\partial x_2} & -\frac{\partial v_1}{\partial x_1} \\ \frac{\partial v_2}{\partial x_2} & -\frac{\partial v_2}{\partial x_1} \end{pmatrix} \quad \text{and} \quad \text{curl}(\boldsymbol{\tau}) \ := \ \begin{pmatrix} \frac{\partial \tau_{12}}{\partial x_1} - \frac{\partial \tau_{11}}{\partial x_2} \\ \frac{\partial \tau_{22}}{\partial x_1} - \frac{\partial \tau_{21}}{\partial x_2} \end{pmatrix}.$$

Then, the finite dimensional discontinuous subspaces are given by

$$\begin{aligned}
\mathbb{S}_h \ &:= \ \left\{\boldsymbol{\tau} \in \mathbb{L}^2(\Omega_S) \ : \ \boldsymbol{\tau}|_T \in \mathbb{P}_k(T) + \mathbb{B}(T) \quad \forall\, T \in \mathcal{T}_h^S\right\}\,,\\
\mathbb{A}_h \ &:= \ \left\{\boldsymbol{\eta} \in \mathbb{L}^2(\Omega_S) \ : \ \boldsymbol{\eta}|_T \in \mathbb{A}(T) \quad \forall\, T \in \mathcal{T}_h^S\right\}\,,\\
\mathbf{V}_h^* \ &:= \ \left\{\mathbf{v} \in \mathbf{L}^2(\Omega_*) \ : \ \mathbf{v}|_T \in \mathbf{P}_k(T) \quad \forall\, T \in \mathcal{T}_h^*\right\} \qquad \forall\, * \in \{S, D\}\,,\\
\mathbf{M}_h \ &:= \ \left\{\boldsymbol{\mu} \in \mathbf{L}^2(\mathcal{E}_h^S) \ : \ \boldsymbol{\mu}|_F \in \mathbf{P}_k(F) \quad \forall\, F \in \mathcal{E}_h^S \quad \text{and} \quad \boldsymbol{\mu}|_{\Gamma_S} \ = \ \mathbf{0}\right\}\,,\\
P_h \ &:= \ \left\{q \in L^2(\Omega_D) \ : \ q|_T \in \mathrm{P}_k(T) \quad \forall\, T \in \mathcal{T}_h^D\right\}\,,\\
N_h \ &:= \ \left\{\psi \in L^2(\mathcal{E}_h^D) \ : \ \psi|_F \in \mathrm{P}_k(F) \quad \forall\, F \in \mathcal{E}_h^D\right\}\,.
\end{aligned}$$

The purpose of enriching here the space $\mathbb{S}_h$ with $\mathbb{B}(T)$ will become clear in the *a priori* error analysis given below in Section 5.4. Note that if $\boldsymbol{\tau}_{S,h} \in \mathbb{B}_h := \{\boldsymbol{\tau} \in \mathbb{L}^2(\Omega_S) \ : \ \boldsymbol{\tau}|_T \in \mathbb{B}(T) \quad \forall\, T \in \mathcal{T}_h^S\}$, we have that

$$\mathbf{div}(\boldsymbol{\tau}_{S,h}) \ = \ \mathbf{0} \quad \text{in} \quad \Omega_S \quad \text{and} \quad \boldsymbol{\tau}_{S,h}\mathbf{n} \ = \ \mathbf{0} \quad \text{in} \quad \mathcal{E}_h^S\,. \tag{5.5}$$

Finally, for convenience of further analysis, we define the subspace

$$\widetilde{\mathbb{S}}_h \ := \ \{\boldsymbol{\tau} \in \mathbb{L}^2(\Omega_S) \ : \ \boldsymbol{\tau}|_T \in \mathbb{P}_k(T) \quad \forall\, T \in \mathcal{T}_h^S\}$$

and notice that

$$\mathbb{S}_h \ = \ \widetilde{\mathbb{S}}_h \ + \ \mathbb{B}_h\,.$$

5.3.3 Formulation

Proceeding as in [44, 43, 48], we deduce that the HDG formulation of the coupled system (5.2)-(5.3)-(5.4) reduces to: Find $(\boldsymbol{\sigma}_{S,h}, \mathbf{u}_{S,h}, \boldsymbol{\rho}_{S,h}, \boldsymbol{\lambda}_{S,h}, \mathbf{u}_{D,h}, p_{D,h}, \varphi_{D,h}) \in \mathbb{S}_h \times \mathbf{V}_h^S \times \mathbb{A}_h \times \mathbf{M}_h \times \mathbf{V}_h^D \times P_h \times N_h$, such that

$$\begin{aligned}
\frac{1}{\nu}(\boldsymbol{\sigma}^{\mathtt{d}}_{S,h},\boldsymbol{\tau}^{\mathtt{d}}_{S,h})_{\mathcal{T}_h^S} + (\mathbf{u}_{S,h},\mathbf{div}(\boldsymbol{\tau}_{S,h}))_{\mathcal{T}_h^S} - \langle\boldsymbol{\tau}_{S,h}\mathbf{n},\widehat{\mathbf{u}}_{S,h}\rangle_{\partial\mathcal{T}_h^S}&\\
+ (\boldsymbol{\rho}_{S,h},\boldsymbol{\tau}_{S,h})_{\mathcal{T}_h^S} &= 0\,, &(5.6a)\\
(\boldsymbol{\sigma}_{S,h},\nabla\mathbf{v}_{S,h})_{\mathcal{T}_h^S} - \left\langle\widehat{\boldsymbol{\sigma}_{S,h}\mathbf{n}},\mathbf{v}_{S,h}\right\rangle_{\partial\mathcal{T}_h^S} &= (\mathbf{f}_S,\mathbf{v}_{S,h})_{\mathcal{T}_h^S}\,, &(5.6b)\\
(\boldsymbol{\eta}_{S,h},\boldsymbol{\sigma}_{S,h})_{\mathcal{T}_h^S} &= 0\,, &(5.6c)\\
\left\langle\widehat{\boldsymbol{\sigma}_{S,h}\mathbf{n}},\boldsymbol{\mu}_{S,h}\right\rangle_{\partial\mathcal{T}_h^S\setminus\Sigma} &= 0\,, &(5.6d)\\
(\mathbf{K}^{-1}\mathbf{u}_{D,h},\mathbf{v}_{D,h})_{\mathcal{T}_h^D} - (p_{D,h},\operatorname{div}(\mathbf{v}_{D,h}))_{\mathcal{T}_h^D} + \langle\mathbf{v}_{D,h}\cdot\mathbf{n},\widehat{p}_{D,h}\rangle_{\partial\mathcal{T}_h^D\setminus\Sigma}&\\
- \langle\mathbf{v}_{D,h}\cdot\mathbf{n},\widehat{p}_{D,h}\rangle_{\Sigma} &= 0\,, &(5.6e)\\
-(\mathbf{u}_{D,h},\nabla q_{D,h})_{\mathcal{T}_h^D} + \left\langle\widehat{\mathbf{u}_{D,h}\cdot\mathbf{n}},q_{D,h}\right\rangle_{\partial\mathcal{T}_h^D\setminus\Sigma} - \left\langle\widehat{\mathbf{u}_{D,h}\cdot\mathbf{n}},q_{D,h}\right\rangle_{\Sigma} &= (f_D,q_{D,h})_{\mathcal{T}_h^D}\,, &(5.6f)\\
\left\langle\widehat{\mathbf{u}_{D,h}\cdot\mathbf{n}},\psi_{D,h}\right\rangle_{\partial\mathcal{T}_h^D\setminus\Sigma} &= 0\,, &(5.6g)\\
\left\langle\widehat{\mathbf{u}}_{S,h}\cdot\mathbf{n} - \widehat{\mathbf{u}_{D,h}\cdot\mathbf{n}},\psi_{D,h}\right\rangle_{\Sigma} &= 0\,, &(5.6h)\\
\left\langle\widehat{\boldsymbol{\sigma}_{S,h}\mathbf{n}} \;+\; \sum_{\ell=1}^{n-1}\kappa_\ell^{-1}(\widehat{\mathbf{u}}_{S,h}\cdot\mathbf{t}_\ell)\mathbf{t}_\ell \;+\; \widehat{p}_{D,h}\mathbf{n},\; \boldsymbol{\mu}_{S,h}\right\rangle_{\Sigma} &= 0\,, &(5.6i)\\
(\operatorname{tr}(\boldsymbol{\sigma}_{S,h}),1)_{\Omega_S} &= 0\,, &(5.6j)
\end{aligned}$$

for all $(\boldsymbol{\tau}_{S,h},\mathbf{v}_{S,h},\boldsymbol{\eta}_{S,h},\boldsymbol{\mu}_{S,h},\mathbf{v}_{D,h},q_{D,h},\psi_{D,h}) \in \mathbb{S}_h\times\mathbf{V}_h^S\times\mathbb{A}_h\times\mathbf{M}_h\times\mathbf{V}_h^D\times P_h\times N_h$, with the numerical fluxes $\widehat{\mathbf{u}}_{S,h}$, $\widehat{\boldsymbol{\sigma}_{S,h}\mathbf{n}}$, $\widehat{p}_{D,h}$ and $\widehat{\mathbf{u}_{D,h}\cdot\mathbf{n}}$ given by

$$\widehat{\mathbf{u}}_{S,h} = \boldsymbol{\lambda}_{S,h} \quad\text{in}\quad \mathcal{E}_h^S\,, \qquad \widehat{\boldsymbol{\sigma}_{S,h}\mathbf{n}} = \boldsymbol{\sigma}_{S,h}\mathbf{n} - \mathbf{S}(\mathbf{u}_{S,h} - \widehat{\mathbf{u}}_{S,h}) \quad\text{in}\quad \partial\mathcal{T}_h^S\,,$$

$$\widehat{p}_{D,h} = \varphi_{D,h} \quad\text{in}\quad \mathcal{E}_h^D\,, \qquad\text{and}\qquad \widehat{\mathbf{u}_{D,h}\cdot\mathbf{n}} = \begin{cases} \mathbf{u}_{D,h}\cdot\mathbf{n} + \tau(p_{D,h} - \widehat{p}_{D,h}) & \text{on}\quad \partial\mathcal{T}_h^D\setminus\Sigma\,,\\ \mathbf{u}_{D,h}\cdot\mathbf{n} - \tau(p_{D,h} - \widehat{p}_{D,h}) & \text{on}\quad \Sigma\,,\end{cases}$$

where $\mathbf{S}$ is an stabilization tensor to be defined below, and $\tau > 0$ is a constant function in $\mathcal{E}_h^D$.

From (5.6) we observe that equations (5.6a)-(5.6b)-(5.6c) and (5.6j) arise from the application of the HDG approximation to the Stokes system (5.2), and similarly (5.6e) and (5.6f) arise from the Darcy system (5.3). In addition, expressions (5.6d) and (5.6g) are the weak imposition of the continuity of the normal component of the fluxes, as it is natural in HDG schemes. In particular, note that the Neumann condition $\mathbf{u}_D\cdot\mathbf{n} = 0$ on Γ_D is considered in (5.6g). Finally, equations (5.6h) and (5.6i) constitute the HDG setting of the transmission conditions (5.4) on Σ.

On the other hand, the definition of $\widehat{\mathbf{u}_{D,h}\cdot\mathbf{n}}$ is consistent with that given in [44], that is $\widehat{\mathbf{u}}_{D,h} := \mathbf{u}_{D,h} + \tau(p_{D,h} - \widehat{p}_{D,h})\mathbf{n}$ on $\partial\mathcal{T}_h^D$, for some non-negative penalty function τ defined on $\partial\mathcal{T}_h^D$, which we assume to be constant on each face of the triangulation. To this respect, note first that problem (5.6) can be reformulated as: Find $(\boldsymbol{\sigma}_{S,h},\mathbf{u}_{S,h},\boldsymbol{\rho}_{S,h},\boldsymbol{\lambda}_{S,h},\mathbf{u}_{D,h},p_{D,h},\varphi_{D,h}) \in \mathbb{S}_h\times\mathbf{V}_h^S\times\mathbb{A}_h\times\mathbf{M}_h\times\mathbf{V}_h^D\times$

$P_h \times N_h$, such that

$$
\begin{aligned}
\frac{1}{\nu}(\boldsymbol{\sigma}^{\mathtt{d}}_{S,h}, \boldsymbol{\tau}^{\mathtt{d}}_{S,h})_{\mathcal{T}_h^S} + (\mathbf{u}_{S,h}, \mathbf{div}(\boldsymbol{\tau}_{S,h}))_{\mathcal{T}_h^S} - \langle \boldsymbol{\tau}_{S,h}\mathbf{n}, \boldsymbol{\lambda}_{S,h}\rangle_{\partial\mathcal{T}_h^S}& \\
+ (\boldsymbol{\rho}_{S,h}, \boldsymbol{\tau}_{S,h})_{\mathcal{T}_h^S} &= 0\,, && (5.7a)\\
-(\mathbf{v}_{S,h}, \mathbf{div}(\boldsymbol{\sigma}_{S,h}))_{\mathcal{T}_h^S} + \langle \mathbf{S}(\mathbf{u}_{S,h} - \boldsymbol{\lambda}_{S,h}), \mathbf{v}_{S,h}\rangle_{\partial\mathcal{T}_h^S} &= (\mathbf{f}_S, \mathbf{v}_{S,h})_{\mathcal{T}_h^S}\,, && (5.7b)\\
(\boldsymbol{\eta}_{S,h}, \boldsymbol{\sigma}_{S,h})_{\mathcal{T}_h^S} &= 0\,, && (5.7c)\\
\left\langle \boldsymbol{\sigma}_{S,h}\mathbf{n}, \boldsymbol{\mu}_{S,h}\right\rangle_{\partial\mathcal{T}_h^S\setminus\Sigma} - \left\langle \mathbf{S}(\mathbf{u}_{S,h} - \boldsymbol{\lambda}_{S,h}), \boldsymbol{\mu}_{S,h}\right\rangle_{\partial\mathcal{T}_h^S\setminus\Sigma} &= 0\,, && (5.7d)\\
(\mathbf{K}^{-1}\mathbf{u}_{D,h}, \mathbf{v}_{D,h})_{\mathcal{T}_h^D} - (p_{D,h}, \operatorname{div}(\mathbf{v}_{D,h}))_{\mathcal{T}_h^D} + \langle \mathbf{v}_{D,h}\cdot\mathbf{n}, \varphi_{D,h}\rangle_{\partial\mathcal{T}_h^D\setminus\Sigma}& \\
- \langle \mathbf{v}_{D,h}\cdot\mathbf{n}, \varphi_{D,h}\rangle_{\Sigma} &= 0\,, && (5.7e)\\
(q_{D,h}, \operatorname{div}(\mathbf{u}_{D,h}))_{\mathcal{T}_h^D} + \langle \tau(p_{D,h} - \varphi_{D,h}), q_{D,h}\rangle_{\partial\mathcal{T}_h^D} &= (f_D, q_{D,h})_{\mathcal{T}_h^D}\,, && (5.7f)\\
\langle \mathbf{u}_{D,h}\cdot\mathbf{n}, \psi_{D,h}\rangle_{\partial\mathcal{T}_h^D\setminus\Sigma} + \langle \tau(p_{D,h} - \varphi_{D,h}), \psi_{D,h}\rangle_{\partial\mathcal{T}_h^D\setminus\Sigma} &= 0\,, && (5.7g)\\
\langle \boldsymbol{\lambda}_{S,h}\cdot\mathbf{n}, \psi_{D,h}\rangle_{\Sigma} - \langle \mathbf{u}_{D,h}\cdot\mathbf{n}, \psi_{D,h}\rangle_{\Sigma} + \langle \tau(p_{D,h} - \varphi_{D,h}), \psi_{D,h}\rangle_{\Sigma} &= 0\,, && (5.7h)\\
\left\langle \boldsymbol{\sigma}_{S,h}\mathbf{n}, \boldsymbol{\mu}_{S,h}\right\rangle_{\Sigma} - \left\langle \mathbf{S}(\mathbf{u}_{S,h} - \boldsymbol{\lambda}_{S,h}), \boldsymbol{\mu}_{S,h}\right\rangle_{\Sigma} + \sum_{\ell=1}^{n-1} \kappa_\ell^{-1}\left\langle \boldsymbol{\lambda}_{S,h}\cdot\mathbf{t}_\ell, \boldsymbol{\mu}_{S,h}\cdot\mathbf{t}_\ell\right\rangle_{\Sigma}& \\
+ \left\langle \boldsymbol{\mu}_{S,h}\cdot\mathbf{n}, \varphi_{D,h}\right\rangle_{\Sigma} &= 0\,, && (5.7i)\\
(\operatorname{tr}(\boldsymbol{\sigma}_{S,h}), 1)_{\Omega_S} &= 0\,, && (5.7j)
\end{aligned}
$$

for all $(\boldsymbol{\tau}_{S,h}, \mathbf{v}_{S,h}, \boldsymbol{\eta}_{S,h}, \boldsymbol{\mu}_{S,h}, \mathbf{v}_{D,h}, q_{D,h}, \psi_{D,h}) \in \mathbb{S}_h \times \mathbf{V}_h^S \times \mathbb{A}_h \times \mathbf{M}_h \times \mathbf{V}_h^D \times P_h \times N_h$, where (5.6b) and (5.6f) has been rewritten, respectively, using that

$$
(\boldsymbol{\sigma}_{S,h}, \nabla\mathbf{v}_{S,h})_{\mathcal{T}_h^S} \;=\; -(\mathbf{v}_{S,h}, \mathbf{div}(\boldsymbol{\sigma}_{S,h}))_{\mathcal{T}_h^S} \;+\; \langle \boldsymbol{\sigma}_{S,h}\mathbf{n}, \mathbf{v}_{S,h}\rangle_{\partial\mathcal{T}_h^S}
$$

and

$$
-(\mathbf{u}_{D,h}, \nabla q_{D,h})_{\mathcal{T}_h^D} \;=\; (q_{D,h}, \operatorname{div}(\mathbf{u}_{D,h}))_{\mathcal{T}_h^D} \;-\; \langle \mathbf{u}_{D,h}\cdot\mathbf{n}, q_{D,h}\rangle_{\partial\mathcal{T}_h^D\setminus\Sigma} \;+\; \langle \mathbf{u}_{D,h}\cdot\mathbf{n}, q_{D,h}\rangle_{\Sigma}\,.
$$

We complete the definition of the HDG method by describing the stabilization tensor $\mathbf{S}$. We first recall that general conditions for $\mathbf{S}$ were proposed in [43]. In particular, given $F \in \mathcal{E}_h^S$, we assume that $\mathbf{S}|_F$ is a symmetric and positive definite constant tensor.

5.3.4 Solvability analysis

The following theorem establishes the unique solvability of the HDG scheme (5.7).

Theorem 5.1. *There exists a unique solution for the linear problem* (5.7).

Proof. We first note that the existence of the solution follows from its uniqueness. Thus, it suffices to show that when the right-hand sides of (5.7) vanish, then $\boldsymbol{\sigma}_{S,h}$, $\mathbf{u}_{S,h}$, $\boldsymbol{\rho}_{S,h}$, $\boldsymbol{\lambda}_{S,h}$, $\mathbf{u}_{D,h}$, $p_{D,h}$, and

$\varphi_{D,h}$ also vanish. Indeed, assuming that $\mathbf{f}_S = \mathbf{0}$ and $f_D = 0$, and taking $\boldsymbol{\tau}_{S,h} = \boldsymbol{\sigma}_{S,h}$, $\mathbf{v}_{S,h} = \mathbf{u}_{S,h}$, $\boldsymbol{\eta}_{S,h} = \boldsymbol{\rho}_{S,h}$ and $\boldsymbol{\mu}_{S,h} = \boldsymbol{\lambda}_{S,h}$ in (5.7a), (5.7b), (5.7c), (5.7d) and (5.7i), we easily obtain

$$\begin{aligned} \frac{1}{\nu}\|\boldsymbol{\sigma}^{\mathtt{d}}_{S,h}\|^2_{0,\Omega_S} \,+\, \langle \mathbf{S}(\mathbf{u}_{S,h} - \boldsymbol{\lambda}_{S,h}), \mathbf{u}_{S,h} - \boldsymbol{\lambda}_{S,h}\rangle_{\partial\mathcal{T}_h^S} & \\ +\, \sum_{\ell=1}^{n-1} \kappa_\ell^{-1}\|\boldsymbol{\lambda}_{S,h}\cdot\mathbf{t}_\ell\|^2_{0,\Sigma} \,+\, \langle \boldsymbol{\lambda}_{S,h}\cdot\mathbf{n}, \varphi_{D,h}\rangle_\Sigma \;&=\; 0\,. \end{aligned} \tag{5.8}$$

Similarly, taking $\mathbf{v}_{D,h} = \mathbf{u}_{D,h}$, $q_{D,h} = p_{D,h}$ and $\psi_{D,h} = \varphi_{D,h}$ in (5.7e), (5.7f), (5.7g), and (5.7h), we find that

$$(\mathbf{K}^{-1}\mathbf{u}_{D,h}, \mathbf{u}_{D,h})_{\mathcal{T}_h^D} + \langle \tau(p_{D,h} - \varphi_{D,h}), p_{D,h} - \varphi_{D,h}\rangle_{\partial\mathcal{T}_h^D} - \langle \boldsymbol{\lambda}_{S,h}\cdot\mathbf{n}, \varphi_{D,h}\rangle_\Sigma \;=\; 0\,. \tag{5.9}$$

Next, adding (5.8) and (5.9), and using the properties of $\mathbf{S}$, $\mathbf{K}$ and the fact that $\nu, \kappa_1, \ldots, \kappa_{n-1}, \tau > 0$, it follows that

$$\boldsymbol{\sigma}^{\mathtt{d}}_{S,h} = \mathbf{0} \quad\text{in}\quad \Omega_S\,, \quad \mathbf{u}_{S,h} = \boldsymbol{\lambda}_{S,h} \quad\text{on}\quad \mathcal{E}_h^S\,, \quad \boldsymbol{\lambda}_{S,h}\cdot\mathbf{t}_\ell = 0 \quad\text{in}\quad \Sigma \quad \forall\, \ell\in\{1,\ldots,n-1\}\,,$$

$$\mathbf{u}_{D,h} = \mathbf{0} \quad\text{in}\quad \Omega_D\,, \quad\text{and}\quad p_{D,h} = \varphi_{D,h} \quad\text{on}\quad \mathcal{E}_h^D\,.$$

Now, using that $\mathbf{u}_{S,h} = \boldsymbol{\lambda}_{S,h}$ on $\mathcal{E}_h^S$ and (5.5), we deduce from (5.7b) and (5.7d) that $\mathbf{div}(\boldsymbol{\sigma}_{S,h}) = \mathbf{0}$ in $\mathcal{T}_h^S$ and $[\![\boldsymbol{\sigma}_{S,h}]\!] = \mathbf{0}$ on $\mathcal{E}_h^S\setminus(\Sigma\cup\Gamma_S)$, which together with $\boldsymbol{\sigma}^{\mathtt{d}}_{S,h} = \mathbf{0}$ in Ω_S implies that $\boldsymbol{\sigma}_{S,h} = c\,\mathbb{I}$ in Ω_S, where $c\in\mathrm{R}$. Thus, applying (5.7j) we arrive to $\boldsymbol{\sigma}_{S,h} = \mathbf{0}$ in Ω_S. In turn, according to the foregoing analysis, and integrating by parts the second terms in (5.7a) and (5.7e), we see that (5.7) reduces to the system:

$$-(\nabla\mathbf{u}_{S,h}, \boldsymbol{\tau}_{S,h})_{\mathcal{T}_h^S} + (\boldsymbol{\rho}_{S,h}, \boldsymbol{\tau}_{S,h})_{\mathcal{T}_h^S} \;=\; 0 \quad \forall\, \boldsymbol{\tau}_{S,h}\in\mathbb{S}_h\,, \tag{5.10}$$

$$(\nabla p_{D,h}, \mathbf{v}_{D,h})_{\mathcal{T}_h^D} \;=\; 0 \quad \forall\, \mathbf{v}_{D,h}\in\mathbf{V}_h^D\,, \tag{5.11}$$

$$\langle \boldsymbol{\lambda}_{S,h}\cdot\mathbf{n}, \psi_{D,h}\rangle_\Sigma \;=\; 0 \quad \forall\, \psi_{D,h}\in N_h\,, \tag{5.12}$$

$$\langle \boldsymbol{\mu}_{S,h}\cdot\mathbf{n}, \varphi_{D,h}\rangle_\Sigma \;=\; 0 \quad \forall\, \boldsymbol{\mu}_{S,h}\in\mathbf{M}_h\,. \tag{5.13}$$

It is clear from (5.12) that $\boldsymbol{\lambda}_{S,h}\cdot\mathbf{n} = 0$ on Σ, which together with the fact that $\boldsymbol{\lambda}_{S,h}\cdot\mathbf{t}_\ell = 0$ on Σ $\forall\,\ell\in\{1,\ldots,n-1\}$ implies that $\boldsymbol{\lambda}_{S,h} = \mathbf{u}_{S,h} = \mathbf{0}$ on $\partial\Omega_S$. In addition, it follows from (5.10) that $\boldsymbol{\rho}_{S,h} = \nabla\mathbf{u}_{S,h}$ in Ω_S, which establishes that $\mathbf{e}(\mathbf{u}_{S,h}) = \mathbf{0}$ in Ω_S, and hence $\mathbf{u}_{S,h}$ belongs to the space of infinitesimal rigid motions (see [17, Exercise 11.x.2]). In this way, using that $\mathbf{u}_{S,h} = \mathbf{0}$ on $\partial\Omega_S$, it is easy to prove that $\mathbf{u}_{S,h} = \mathbf{0}$ in Ω_S, and then we conclude that $\boldsymbol{\rho}_{S,h} = \mathbf{0}$ in Ω_S and $\boldsymbol{\lambda}_{S,h} = \mathbf{0}$ on $\mathcal{E}_h^S$. Finally, from (5.11) we have that $\nabla p_{D,h} = \mathbf{0}$ in $\mathcal{T}_h^D$, which using that $p_{D,h}$ is continuous in Ω_D ($p_{D,h} = \varphi_{D,h}$ in $\mathcal{E}_h^D$), yields $p_{D,h}$ constant in Ω_D. But, recalling that $\varphi_{D,h} = 0$ on Σ (cf. (5.13)), we deduce that $p_{D,h} = 0$ in Ω_S, which gives $\varphi_{D,h} = p_{D,h} = 0$ in $\mathcal{E}_h^D$ and completes the proof. □

5.4 A priori error analysis

We now aim to derive the *a priori* error estimates for the HDG scheme (5.7). To this end, we use the projection-based error analysis developed in [44, 43, 48].

5.4.1 The projections

The projected functions are denoted by

$$\begin{array}{rcl}\Pi_S \ : \ \mathbb{H}^1(\mathcal{T}_h^S)\times\mathbf{H}^1(\mathcal{T}_h^S) & \longrightarrow & \widetilde{\mathbb{S}}_h\times\mathbf{V}_h^S \\ (\boldsymbol{\Phi}_S,\boldsymbol{\varphi}_S) & \longmapsto & \Pi_S(\boldsymbol{\Phi}_S,\boldsymbol{\varphi}_S) \ := \ (\Pi\boldsymbol{\Phi}_S,\Pi\boldsymbol{\varphi}_S)\,,\end{array}$$

and

$$\begin{array}{rcl}\Pi_D \ : \ \mathbf{H}^1(\mathcal{T}_h^D)\times H^1(\mathcal{T}_h^D) & \longrightarrow & \mathbf{V}_h^D\times P_h \\ (\boldsymbol{\varphi}_D,\phi_D) & \longmapsto & \Pi_D(\boldsymbol{\varphi}_D,\phi_D) \ := \ (\Pi\boldsymbol{\varphi}_D,\Pi\phi_D)\,,\end{array}$$

where, as usual, we denote $\Pi\boldsymbol{\Phi}_S$ and $\Pi\boldsymbol{\varphi}_S$ only for convenience, since it is clear that $\Pi\boldsymbol{\Phi}_S$ and $\Pi\boldsymbol{\varphi}_S$ depend both on $\boldsymbol{\Phi}_S$ and $\boldsymbol{\varphi}_S$. The same convention is applied to $\Pi\boldsymbol{\varphi}_D$ and $\Pi\phi_D$.

Next, given $(\boldsymbol{\Phi}_S,\boldsymbol{\varphi}_S)\in\mathbb{H}^1(\mathcal{T}_h^S)\times\mathbf{H}^1(\mathcal{T}_h^S)$, the values of the projection $\Pi_S(\boldsymbol{\Phi}_S,\boldsymbol{\varphi}_S)$ on any $T\in\mathcal{T}_h^S$ are fixed by requiring that the components satisfy the equations

$$(\Pi\boldsymbol{\Phi}_S,\boldsymbol{\tau}_S)_T \;=\; (\boldsymbol{\Phi}_S,\boldsymbol{\tau}_S)_T \quad \forall\,\boldsymbol{\tau}_S\in\mathbb{P}_{k-1}(T)\,, \tag{5.14a}$$

$$(\Pi\boldsymbol{\varphi}_S,\mathbf{v}_S)_T \;=\; (\boldsymbol{\varphi}_S,\mathbf{v}_S)_T \quad \forall\,\mathbf{v}_S\in\mathbf{P}_{k-1}(T)\,, \tag{5.14b}$$

$$\langle\Pi\boldsymbol{\Phi}_S\mathbf{n}-\mathbf{S}\Pi\boldsymbol{\varphi}_S,\boldsymbol{\mu}_S\rangle_F \;=\; \langle\boldsymbol{\Phi}_S\mathbf{n}-\mathbf{S}\boldsymbol{\varphi}_S,\boldsymbol{\mu}_S\rangle_F \quad \forall\,\boldsymbol{\mu}_S\in\mathbf{P}_k(F)\,,\quad \forall\,F\in\partial T\,. \tag{5.14c}$$

Similarly, given $(\boldsymbol{\varphi}_D,\phi_D)\in\mathbf{H}^1(\mathcal{T}_h^D)\times H^1(\mathcal{T}_h^D)$, the values of the projection $\Pi_D(\boldsymbol{\varphi}_D,\phi_D)$ on any $T\in\mathcal{T}_h^D$ are determined by requiring that

$$(\Pi\boldsymbol{\varphi}_D,\mathbf{v}_D)_T \;=\; (\boldsymbol{\varphi}_D,\mathbf{v}_D)_T \quad \forall\,\mathbf{v}_D\in\mathbf{P}_{k-1}(T)\,, \tag{5.15a}$$

$$(\Pi\phi_D,q_D)_T \;=\; (\phi_D,q_D)_T \quad \forall\,q_D\in\mathrm{P}_{k-1}(T)\,, \tag{5.15b}$$

$$\langle\Pi\boldsymbol{\varphi}_D\cdot\mathbf{n}+\tau\Pi\phi_D,\psi_D\rangle_F \;=\; \langle\boldsymbol{\varphi}_D\cdot\mathbf{n}+\tau\phi_D,\psi_D\rangle_F \quad \forall\,\psi_D\in\mathrm{P}_k(F)\,,\quad \forall\,F\in\partial T\setminus\Sigma\,, \tag{5.15c}$$

$$\langle\Pi\boldsymbol{\varphi}_D\cdot\mathbf{n}-\tau\Pi\phi_D,\psi_D\rangle_F \;=\; \langle\boldsymbol{\varphi}_D\cdot\mathbf{n}-\tau\phi_D,\psi_D\rangle_F \quad \forall\,\psi_D\in\mathrm{P}_k(F)\,,\quad \forall\,F\in\partial T\cap\Sigma\,. \tag{5.15d}$$

As in [44, 43], both projections are defined in order to preserve the numerical traces (cf. equations (5.7d), (5.7g), (5.7h) and (5.7i)). Also, as it is normal in this approach, the fact that Π_S and Π_D are well-defined arises from the fact that (5.14) and (5.15) are square linear systems, so that the existence of each projection follows from its uniqueness. In view of this, we develop next estimates for any $(\Pi\boldsymbol{\Phi}_S,\Pi\boldsymbol{\varphi}_S)\in\widetilde{\mathbb{S}}_h\times\mathbf{V}_h^S$ satisfying (5.14) without assuming uniqueness *a priori*. Then, we will use the approximation estimates below to prove unisolvency (see Theorem 5.3). The same format is applied to $(\Pi\boldsymbol{\varphi}_D,\Pi\phi_D)\in\mathbf{V}_h^D\times P_h$. Since the main ideas are given in [44, 43] for general choices of $\mathbf{S}$ and τ, in what follows we only give a summary of the proofs for the well-posedness and the approximation properties of the projections. In particular, for the special choice $\mathbf{S}:=\alpha\,\mathbb{I}$, $\alpha\in\mathrm{R}$, the ith row of $\Pi\boldsymbol{\Phi}_S$ and the ith component of $\Pi\boldsymbol{\varphi}_S$ are nothing but the two components of the projection for the diffusion case given in [44].

Now, we set $\mathrm{P}_k(T)^\perp$ be the orthogonal of $\mathrm{P}_{k-1}(T)$ within $\mathrm{P}_k(T)$, that is

$$\mathrm{P}_k(T)^\perp \;:=\; \{p\in\mathrm{P}_k(T)\ :\ (p,q)_T \;=\; 0 \quad \forall\,q\in\mathrm{P}_{k-1}(T)\}\,,$$

and, according to our notation from the Introduction, we set $\mathbf{P}_k(T)^\perp:=[\mathrm{P}_k(T)^\perp]^n$. Thus, the following lemma establishes a characterization of $\Pi\boldsymbol{\varphi}_S$.

Lemma 5.1. *Let* $(\Pi\boldsymbol{\Phi}_S, \Pi\boldsymbol{\varphi}_S) \in \widetilde{\mathbb{S}}_h \times \mathbf{V}_h^S$ *satisfying* (5.14)*. Then, for each* $T \in \mathcal{T}_h^S$, $\Pi\boldsymbol{\varphi}_S|_T$ *is the only element of* $\mathbf{P}_k(T)$ *such that*

$$\begin{aligned}
(\Pi\boldsymbol{\varphi}_S, \mathbf{v}_S)_T &= (\boldsymbol{\varphi}_S, \mathbf{v}_S)_T \quad \forall\, \mathbf{v}_S \in \mathbf{P}_{k-1}(T)\,,\\
\langle \mathbf{S}\Pi\boldsymbol{\varphi}_S, \mathbf{v}_S\rangle_{\partial T} &= -(\mathbf{div}(\boldsymbol{\Phi}_S), \mathbf{v}_S)_T \,+\, \langle \mathbf{S}\boldsymbol{\varphi}_S, \mathbf{v}_S\rangle_{\partial T} \quad \forall\, \mathbf{v}_S \in \mathbf{P}_k(T)^{\perp}.
\end{aligned}$$

Proof. It follows by applying the same techniques from [43, Proposition 4.2]. □

We now collect estimates for $\Pi\boldsymbol{\varphi}_S - \boldsymbol{\varphi}_S$ and $\Pi\boldsymbol{\Phi}_S - \boldsymbol{\Phi}_S$. Note that the assumed local regularity of the pair $(\boldsymbol{\Phi}_S, \boldsymbol{\varphi}_S)$ is clear from the right-hand side of each estimate.

Theorem 5.2. *Given* $(\Pi\boldsymbol{\Phi}_S, \Pi\boldsymbol{\varphi}_S) \in \widetilde{\mathbb{S}}_h \times \mathbf{V}_h^S$ *satisfying* (5.14)*, there exists* $C > 0$*, depending only on* $\mathbf{S}$*, such that for each* $T \in \mathcal{T}_h^S$ *there hold*

$$\|\Pi\boldsymbol{\varphi}_S - \boldsymbol{\varphi}_S\|_{0,T} \;\leq\; C\Big\{ h_T^{\ell_{\boldsymbol{\varphi}_S}+1} |\boldsymbol{\varphi}_S|_{\ell_{\boldsymbol{\varphi}_S}+1,T} \,+\, h_T^{\ell_{\boldsymbol{\Phi}_S}+1} |\mathbf{div}(\boldsymbol{\Phi}_S)|_{\ell_{\boldsymbol{\Phi}_S},T} \Big\}\,,$$

and

$$\|\Pi\boldsymbol{\Phi}_S - \boldsymbol{\Phi}_S\|_{0,T} \;\leq\; C\Big\{ h_T^{\ell_{\boldsymbol{\Phi}_S}+1} |\boldsymbol{\Phi}_S|_{\ell_{\boldsymbol{\Phi}_S}+1,T} \,+\, h_T^{\ell_{\boldsymbol{\varphi}_S}+1} |\boldsymbol{\varphi}_S|_{\ell_{\boldsymbol{\varphi}_S}+1,T} \,+\, h_T^{\ell_{\boldsymbol{\Phi}_S}+1} |\mathbf{div}(\boldsymbol{\Phi}_S)|_{\ell_{\boldsymbol{\Phi}_S},T} \Big\}\,,$$

for $\ell_{\boldsymbol{\Phi}_S}, \ell_{\boldsymbol{\varphi}_S} \in [0, k]$.

Proof. Using Lemma 5.1, it follows from a slight modification of the proofs of [43, Lemma 4.5] and [43, Propositions 4.6 and 4.7]. □

Now, we are ready to establish that the projection $\Pi_S\big(\boldsymbol{\Phi}_S, \boldsymbol{\varphi}_S\big) := \big(\Pi\boldsymbol{\Phi}_S, \Pi\boldsymbol{\varphi}_S\big)$ is well defined, whereas the respective approximation estimates are already given in the foregoing theorem.

Theorem 5.3. *The projection* Π_S *is well defined.*

Proof. Let us first observe that the number of independent equations arising from (5.14) is given by

$$\begin{aligned}
n^2 \dim \mathrm{P}_{k-1}(T &\qquad \text{for (5.14a)}\,,\\
n \dim \mathrm{P}_{k-1}(T) &\qquad \text{for (5.14b)}\,,\\
n\,(n+1) \dim \mathrm{P}_k(F) &\qquad \text{for (5.14c)}\,,
\end{aligned}$$

which yields a total of $n\,(n+1) \dim \mathrm{P}_k(T)$. In turn, the corresponding number of unknowns is

$$\begin{aligned}
n^2 \dim \mathrm{P}_k(T) &\qquad \text{for } \Pi\boldsymbol{\Phi}_S\,,\\
n \dim \mathrm{P}_k(T) &\qquad \text{for } \Pi\boldsymbol{\varphi}_S\,,
\end{aligned}$$

which gives $n\,(n+1) \dim \mathrm{P}_k(T)$. It follows that (5.14) is a square linear system, and hence, setting $\boldsymbol{\Phi}_S = \mathbf{0}$ and $\boldsymbol{\varphi}_S = \mathbf{0}$ in the approximation estimates (cf. Theorem 5.2), we find that the projection must vanish, which establishes the unisolvency of (5.14). □

As previously announced, a similar approach is used to establish that the projection $\Pi_D\big(\boldsymbol{\varphi}_D, \boldsymbol{\phi}_D\big) := \big(\Pi\boldsymbol{\varphi}_D, \Pi\boldsymbol{\phi}_D\big)$ (cf. (5.15)) is well defined, and that corresponding approximation properties hold.

Theorem 5.4. *The projection Π_D is well defined. In addition, there exist $C > 0$, independent of $T \in \mathcal{T}_h^D$ and τ, such that*

$$\|\Pi\phi_D - \phi_D\|_{0,T} \;\leq\; C\Big\{ h_T^{\ell_{\phi_D}+1} |\phi_D|_{\ell_{\phi_D}+1,T} \;+\; \tau^{-1} h_T^{\ell_{\boldsymbol{\varphi}_D}+1} |\mathrm{div}(\boldsymbol{\varphi}_D)|_{\ell_{\boldsymbol{\varphi}_D},T} \Big\},$$

and

$$\|\Pi\boldsymbol{\varphi}_D - \boldsymbol{\varphi}_D\|_{0,T} \;\leq\; C\Big\{ h_T^{\ell_{\boldsymbol{\varphi}_D}+1} |\boldsymbol{\varphi}_D|_{\ell_{\boldsymbol{\varphi}_D}+1,T} \;+\; \tau\, h_T^{\ell_{\phi_D}+1} |\phi_D|_{\ell_{\phi_D}+1,T} \Big\},$$

where $\ell_{\boldsymbol{\varphi}_D}, \ell_{\phi_D} \in [0,k]$.

Proof. The proof can be carried out similarly as for Theorem 5.3. More precisely, it follows by applying the same techniques employed in the proof of [44, Propositions A.1, A.2 and A.3]. $\square$

We end this section by introducing other projections. First, consider $\boldsymbol{\mathcal{P}}_A : \mathbb{L}^2(\Omega_S) \to \mathbb{A}_h$ the $\mathbb{L}^2$ orthogonal projector, for which it is well known (see, e.g. [37, 71]) that there holds

$$\|\boldsymbol{\mathcal{P}}_A(\mathbf{s}) - \mathbf{s}\|_{0,T} \;\leq\; C\, h_T^{\ell_{\mathbf{s}}}\, |\mathbf{s}|_{\ell_{\mathbf{s}},T} \quad \forall\, \mathbf{s} \in \mathbb{H}^{\ell_{\mathbf{s}}}(T)\,, \quad \forall\, T \in \mathcal{T}_h^S\,, \tag{5.16}$$

where $\ell_{\mathbf{s}} \in [0, k+1]$. Also, we consider

$$\boldsymbol{P}_M \,:\, \mathbf{L}^2(\mathcal{E}_h^S) \longrightarrow \mathbf{M}_h \quad \text{and} \quad P_N \,:\, L^2(\mathcal{E}_h^D) \longrightarrow N_h\,, \tag{5.17}$$

the corresponding $\mathbf{L}^2$ and L^2 orthogonal projections, respectively.

5.4.2 The a priori error estimates

Similary as in [44, 43, 48], our first goal in this section is to provide upper estimates for the approximation errors, namely, $\mathrm{E}^{\boldsymbol{\sigma}_S} := \Pi\boldsymbol{\sigma}_S - \boldsymbol{\sigma}_{S,h}$, $\mathrm{E}^{\mathbf{u}_S} := \Pi\mathbf{u}_S - \mathbf{u}_{S,h}$, $\mathrm{E}^{\boldsymbol{\rho}_S} := \boldsymbol{\mathcal{P}}_A(\boldsymbol{\rho}_S) - \boldsymbol{\rho}_{S,h}$, $\mathrm{E}^{\mathbf{u}_D} := \Pi\mathbf{u}_D - \mathbf{u}_{D,h}$, $\mathrm{E}^{p_D} := \Pi p_D - p_{D,h}$, $\mathrm{E}^{\widehat{\mathbf{u}}_S} := \boldsymbol{P}_M(\mathbf{u}_S) - \boldsymbol{\lambda}_{S,h}$ and $\mathrm{E}^{\widehat{p}_D} := P_N(p_D) - \varphi_{D,h}$. In what follows we assume that the exact solution $(\boldsymbol{\sigma}_S, \mathbf{u}_S, \mathbf{u}_D, p_D)$ of our problem (5.2)-(5.3)-(5.4) is regular enough to apply Π_S and Π_D. That is, $(\boldsymbol{\sigma}_S, \mathbf{u}_S, \mathbf{u}_D, p_D)$ belongs to $\mathbb{H}^1(\mathcal{T}_h^S) \times \mathbf{H}^2(\mathcal{T}_h^S) \times \mathbf{H}^1(\mathcal{T}_h^D) \times H^2(\mathcal{T}_h^D)$ and admits the regularity estimate

$$\sum_{T\in\mathcal{T}_h^S} \Big\{ \|\boldsymbol{\sigma}_S\|_{1,T} \,+\, \|\mathbf{u}_S\|_{2,T} \Big\} + \sum_{T\in\mathcal{T}_h^D} \Big\{ \|\mathbf{u}_D\|_{1,T} \,+\, \|p_D\|_{2,T} \Big\} \;\leq\; C_{\mathrm{reg}} \Big\{ \|\mathbf{f}_S\|_{0,\Omega_S} \,+\, \|f_D\|_{0,\Omega_D} \Big\}. \tag{5.18}$$

The purpose of assuming that $\nabla\mathbf{u}_S \in \mathbb{H}^1(\mathcal{T}_h^S)$ and $\nabla p_D \in \mathbf{H}^1(\mathcal{T}_h^D)$ will become clear in the proof of Lemma 5.6 below.

Next, for the consistency of the HDG approximation, we note that the exact solution $\big(\boldsymbol{\sigma}_S,\, \mathbf{u}_S,\, \boldsymbol{\rho}_S := \frac{1}{2}(\nabla\mathbf{u}_S - (\nabla\mathbf{u}_S)^{\mathtt{t}}),\, \boldsymbol{\lambda}_S := \mathbf{u}_S|_{\mathcal{E}_h^S},\, \mathbf{u}_D,\, p_D,\, \varphi_D := p_D|_{\mathcal{E}_h^D}\big)$, satisfies also (5.7). Hence, after applying the definition of the projections (see (5.14) and (5.15)) Π_S, Π_D, $\boldsymbol{\mathcal{P}}_A$, $\boldsymbol{P}_M$ and P_N, together with the identities (5.5), and integrating by parts, we find from (5.7) that

$$
\begin{aligned}
\frac{1}{\nu}(\boldsymbol{\sigma}_S^{\mathtt{d}}, \boldsymbol{\tau}_{S,h}^{\mathtt{d}})_{\mathcal{T}_h^S} + (\Pi \mathbf{u}_S, \mathbf{div}(\boldsymbol{\tau}_{S,h}))_{\mathcal{T}_h^S} - \langle \boldsymbol{\tau}_{S,h}\mathbf{n}, \boldsymbol{P}_M(\mathbf{u}_S)\rangle_{\partial\mathcal{T}_h^S} & \\
+ (\boldsymbol{\rho}_S, \boldsymbol{\tau}_{S,h})_{\mathcal{T}_h^S} &= 0\,, \\
-(\mathbf{v}_{S,h}, \mathbf{div}(\Pi\boldsymbol{\sigma}_S))_{\mathcal{T}_h^S} + \langle \mathbf{S}(\Pi\mathbf{u}_S - \boldsymbol{P}_M(\mathbf{u}_S)), \mathbf{v}_{S,h}\rangle_{\partial\mathcal{T}_h^S} &= (\mathbf{f}_S, \mathbf{v}_{S,h})_{\mathcal{T}_h^S}\,, \\
(\boldsymbol{\eta}_{S,h}, \boldsymbol{\sigma}_S)_{\mathcal{T}_h^S} &= 0\,, \\
\left\langle \Pi\boldsymbol{\sigma}_S\mathbf{n}, \boldsymbol{\mu}_{S,h}\right\rangle_{\partial\mathcal{T}_h^S\setminus\Sigma} - \left\langle \mathbf{S}(\Pi\mathbf{u}_S - \boldsymbol{P}_M(\mathbf{u}_S)), \boldsymbol{\mu}_{S,h}\right\rangle_{\partial\mathcal{T}_h^S\setminus\Sigma} &= 0\,, \\
(\mathbf{K}^{-1}\mathbf{u}_{D,h}, \mathbf{v}_{D,h})_{\mathcal{T}_h^D} - (\Pi p_D, \mathrm{div}(\mathbf{v}_{D,h}))_{\mathcal{T}_h^D} + \langle \mathbf{v}_{D,h}\cdot\mathbf{n}, P_N(p_D)\rangle_{\partial\mathcal{T}_h^D\setminus\Sigma} & \\
- \ \langle \mathbf{v}_{D,h}\cdot\mathbf{n}, P_N(p_D)\rangle_{\Sigma} &= 0\,, \\
(q_{D,h}, \mathrm{div}(\Pi\mathbf{u}_D))_{\mathcal{T}_h^D} + \langle \tau(\Pi p_D - P_N(p_D)), q_{D,h}\rangle_{\partial\mathcal{T}_h^D} &= (f_D, q_{D,h})_{\mathcal{T}_h^D}\,, \\
\langle \Pi\mathbf{u}_D\cdot\mathbf{n}, \psi_{D,h}\rangle_{\partial\mathcal{T}_h^D\setminus\Sigma} + \langle \tau(\Pi p_D - P_N(p_D)), \psi_{D,h}\rangle_{\partial\mathcal{T}_h^D\setminus\Sigma} &= 0\,, \\
\langle \boldsymbol{P}_M(\mathbf{u}_S)\cdot\mathbf{n}, \psi_{D,h}\rangle_{\Sigma} - \langle \Pi\mathbf{u}_D\cdot\mathbf{n}, \psi_{D,h}\rangle_{\Sigma} + \langle \tau(\Pi p_D - P_N(p_D)), \psi_{D,h}\rangle_{\Sigma} &= 0\,, \\
\left\langle \Pi\boldsymbol{\sigma}_S\mathbf{n}, \boldsymbol{\mu}_{S,h}\right\rangle_{\Sigma} - \left\langle \mathbf{S}(\Pi\mathbf{u}_S - \boldsymbol{P}_M(\mathbf{u}_S)), \boldsymbol{\mu}_{S,h}\right\rangle_{\Sigma} + \sum_{\ell=1}^{n-1}\kappa_\ell^{-1}\left\langle \boldsymbol{P}_M(\mathbf{u}_S)\cdot\mathbf{t}_\ell, \boldsymbol{\mu}_{S,h}\cdot\mathbf{t}_\ell\right\rangle_{\Sigma} & \\
+ \ \left\langle \boldsymbol{\mu}_{S,h}\cdot\mathbf{n}, P_N(p_D)\right\rangle_{\Sigma} &= 0\,, \\
(\mathrm{tr}\,(\Pi\boldsymbol{\sigma}_S)\,, 1)_{\Omega_S} &= 0\,,
\end{aligned}
$$

for all $(\boldsymbol{\tau}_{S,h}, \mathbf{v}_{S,h}, \boldsymbol{\eta}_{S,h}, \boldsymbol{\mu}_{S,h}, \mathbf{v}_{D,h}, q_{D,h}, \psi_{D,h}) \in \mathbb{S}_h \times \mathbf{V}_h^S \times \mathbb{A}_h \times \mathbf{M}_h \times \mathbf{V}_h^D \times P_h \times N_h$. Now, subtracting (5.7) from the above set of equations, and performing simple algebraic manipulations (see [44, 43, 48] for details), we obtain the error equations:

$$
\begin{aligned}
\frac{1}{\nu}((\mathrm{E}^{\boldsymbol{\sigma}_S})^{\mathtt{d}}, \boldsymbol{\tau}_{S,h}^{\mathtt{d}})_{\mathcal{T}_h^S} + (\mathrm{E}^{\mathbf{u}_S}, \mathbf{div}(\boldsymbol{\tau}_{S,h}))_{\mathcal{T}_h^S} - \left\langle \boldsymbol{\tau}_{S,h}\mathbf{n}, \mathrm{E}^{\widehat{\mathbf{u}}_S}\right\rangle_{\partial\mathcal{T}_h^S} + (\mathrm{E}^{\boldsymbol{\rho}_S}, \boldsymbol{\tau}_{S,h})_{\mathcal{T}_h^S} & \\
= \ \frac{1}{\nu}(\Pi\boldsymbol{\sigma}_S - \boldsymbol{\sigma}_S, \boldsymbol{\tau}_{S,h}^{\mathtt{d}})_{\mathcal{T}_h^S} + (\boldsymbol{\mathcal{P}}_A(\boldsymbol{\rho}_S) - \boldsymbol{\rho}_S, \boldsymbol{\tau}_{S,h})_{\mathcal{T}_h^S}\,, & \qquad (5.19a) \\
-(\mathbf{v}_{S,h}, \mathbf{div}(\mathrm{E}^{\boldsymbol{\sigma}_S}))_{\mathcal{T}_h^S} + \left\langle \mathbf{S}(\mathrm{E}^{\mathbf{u}_S} - \mathrm{E}^{\widehat{\mathbf{u}}_S}), \mathbf{v}_{S,h}\right\rangle_{\partial\mathcal{T}_h^S} \ = \ 0\,, & \qquad (5.19b) \\
(\boldsymbol{\eta}_{S,h}, \mathrm{E}^{\boldsymbol{\sigma}_S})_{\mathcal{T}_h^S} \ = \ (\boldsymbol{\eta}_{S,h}, \Pi\boldsymbol{\sigma}_S - \boldsymbol{\sigma}_S)_{\mathcal{T}_h^S}\,, & \qquad (5.19c) \\
\left\langle \mathrm{E}^{\boldsymbol{\sigma}_S}\mathbf{n}, \boldsymbol{\mu}_{S,h}\right\rangle_{\partial\mathcal{T}_h^S} - \left\langle \mathbf{S}(\mathrm{E}^{\mathbf{u}_S} - \mathrm{E}^{\widehat{\mathbf{u}}_S}), \boldsymbol{\mu}_{S,h}\right\rangle_{\partial\mathcal{T}_h^S} + \sum_{\ell=1}^{n-1}\kappa_\ell^{-1}\left\langle \mathrm{E}^{\widehat{\mathbf{u}}_S}\cdot\mathbf{t}_\ell, \boldsymbol{\mu}_{S,h}\cdot\mathbf{t}_\ell\right\rangle_{\Sigma} & \\
+ \ \left\langle \boldsymbol{\mu}_{S,h}\cdot\mathbf{n}, \mathrm{E}^{\widehat{p}_D}\right\rangle_{\Sigma} \ = \ 0\,, & \qquad (5.19d) \\
(\mathbf{K}^{-1}\mathrm{E}^{\mathbf{u}_D}, \mathbf{v}_{D,h})_{\mathcal{T}_h^D} - (\mathrm{E}^{p_D}, \mathrm{div}(\mathbf{v}_{D,h}))_{\mathcal{T}_h^D} + \left\langle \mathbf{v}_{D,h}\cdot\mathbf{n}, \mathrm{E}^{\widehat{p}_D}\right\rangle_{\partial\mathcal{T}_h^D\setminus\Sigma} - \left\langle \mathbf{v}_{D,h}\cdot\mathbf{n}, \mathrm{E}^{\widehat{p}_D}\right\rangle_{\Sigma} & \\
= \ (\mathbf{K}^{-1}(\Pi\mathbf{u}_D - \mathbf{u}_D), \mathbf{v}_{D,h})_{\mathcal{T}_h^D}\,, & \qquad (5.19e) \\
(q_{D,h}, \mathrm{div}(\mathrm{E}^{\mathbf{u}_D}))_{\mathcal{T}_h^D} + \left\langle \tau(\mathrm{E}^{p_D} - \mathrm{E}^{\widehat{p}_D}), q_{D,h}\right\rangle_{\partial\mathcal{T}_h^D} \ = \ 0\,, & \qquad (5.19f) \\
\left\langle \mathrm{E}^{\widehat{\mathbf{u}}_S}\cdot\mathbf{n}, \psi_{D,h}\right\rangle_{\Sigma} + \langle \mathrm{E}^{\mathbf{u}_D}\cdot\mathbf{n}, \psi_{D,h}\rangle_{\partial\mathcal{T}_h^D\setminus\Sigma} - \langle \mathrm{E}^{\mathbf{u}_D}\cdot\mathbf{n}, \psi_{D,h}\rangle_{\Sigma} & \\
+ \ \left\langle \tau(\mathrm{E}^{p_D} - \mathrm{E}^{\widehat{p}_D}), \psi_{D,h}\right\rangle_{\partial\mathcal{T}_h^D} \ = \ 0\,, & \qquad (5.19g) \\
(\mathrm{tr}\,(\mathrm{E}^{\boldsymbol{\sigma}_S})\,, 1)_{\Omega_S} \ = \ 0\,, & \qquad (5.19h)
\end{aligned}
$$

for all $(\boldsymbol{\tau}_{S,h}, \mathbf{v}_{S,h}, \boldsymbol{\eta}_{S,h}, \boldsymbol{\mu}_{S,h}, \mathbf{v}_{D,h}, q_{D,h}, \psi_{D,h}) \in \mathbb{S}_h \times \mathbf{V}_h^S \times \mathbb{A}_h \times \mathbf{M}_h \times \mathbf{V}_h^D \times P_h \times N_h$.

Estimating $\mathrm{E}^{\boldsymbol{\rho}_S}$

We begin by determining an estimate for $\mathrm{E}^{\boldsymbol{\rho}_S}$. To do this, we follow [48] and consider the orthogonal decomposition

$$\mathrm{E}^{\boldsymbol{\rho}_S} \;=\; \mathrm{E}_0^{\boldsymbol{\rho}_S} \;+\; \mathrm{E}_c^{\boldsymbol{\rho}_S}\,,$$

where $\int_T \mathrm{E}_0^{\boldsymbol{\rho}_S}|_T = \mathbf{0}$ and $\mathrm{E}_c^{\boldsymbol{\rho}_S}|_T \in \mathbb{P}_0(T)$ for each $T \in \mathcal{T}_h^S$. This means that for each $T \in \mathcal{T}_h^S$ and for all $i,j \in \{1,\dots,n\}$ there exist unique $(\mathrm{E}_0^{\boldsymbol{\rho}_S}|_T)_{ij} \in L_0^2(T)$ and $(\mathrm{E}_c^{\boldsymbol{\rho}_S}|_T)_{ij} := \frac{1}{|T|}\int_T (\mathrm{E}^{\boldsymbol{\rho}_S}|_T)_{ij} \in \mathrm{R}$ such that $(\mathrm{E}^{\boldsymbol{\rho}_S}|_T)_{ij} = (\mathrm{E}_0^{\boldsymbol{\rho}_S}|_T)_{ij} + (\mathrm{E}_c^{\boldsymbol{\rho}_S}|_T)_{ij}$.

Next, in order to bound these two terms separately, we denote by $\mathbb{A}_h^0$ the subspace to which $\mathrm{E}_0^{\boldsymbol{\rho}_S}$ belongs, that is

$$\mathbb{A}_h^0 \;:=\; \left\{ \boldsymbol{\eta}_{S,h} \in \mathbb{A}_h \;:\; (\boldsymbol{\eta}_{S,h}, \boldsymbol{\tau})_T \;= 0 \quad \forall\, \boldsymbol{\tau} \in \mathbb{P}_0(T)\,, \quad \forall\, T \in \mathcal{T}_h^S \right\}\,.$$

The following two lemmas provide the upper bounds for $\|\mathrm{E}_0^{\boldsymbol{\rho}_S}\|_{0,\Omega_S}$ and $\|\mathrm{E}_c^{\boldsymbol{\rho}_S}\|_{0,\Omega_S}$.

Lemma 5.2. *There exists $C > 0$, independent of the meshsize, such that*

$$\|\mathrm{E}_0^{\boldsymbol{\rho}_S}\|_{0,\Omega_S} \;\leq\; C\Big\{ \|(\mathrm{E}^{\boldsymbol{\sigma}_S})^{\mathtt{d}}\|_{0,\Omega_S} \;+\; \|\Pi\boldsymbol{\sigma}_S - \boldsymbol{\sigma}_S\|_{0,\Omega_S} \;+\; \|\boldsymbol{\mathcal{P}}_A(\boldsymbol{\rho}_S) - \boldsymbol{\rho}_S\|_{0,\Omega_S} \Big\}\,.$$

Proof. We follow similarly as in the proof of [48, Theorem 3.6] for the three-dimensional case, keeping in mind that the proof for two dimensions should be even simpler. Indeed, we know from the discrete surjectivity result provided by [93, Lemma 2.9] (see also [48, Lemma 3.7]) that, given $\underline{\boldsymbol{\eta}} := \mathrm{E}_0^{\boldsymbol{\rho}_S} \in \mathbb{A}_h^0$, there exists $\widetilde{\boldsymbol{\tau}}_{S,h} \in \mathbb{B}_h$ such that

$$(\widetilde{\boldsymbol{\tau}}_{S,h}, \boldsymbol{\eta}_{S,h})_{\mathcal{T}_h^S} \quad=\quad (\mathrm{E}_0^{\boldsymbol{\rho}_S}, \boldsymbol{\eta}_{S,h})_{\mathcal{T}_h^S} \quad \forall\, \boldsymbol{\eta}_{S,h} \in \mathbb{A}_h \tag{5.20}$$

and

$$\|\widetilde{\boldsymbol{\tau}}_{S,h}\|_{0,\Omega_S} \quad\leq\quad C\,\|\mathrm{E}_0^{\boldsymbol{\rho}_S}\|_{0,\Omega_S}\,, \tag{5.21}$$

where $C > 0$ is independent of $\underline{\boldsymbol{\eta}}$ and the meshsize. Next, we take $\boldsymbol{\tau}_{S,h} = \widetilde{\boldsymbol{\tau}}_{S,h}$ in the error equation (5.19a), and then apply the identities (5.5) to obtain

$$\begin{aligned}\frac{1}{\nu}((\mathrm{E}^{\boldsymbol{\sigma}_S})^{\mathtt{d}}, (\widetilde{\boldsymbol{\tau}}_{S,h})^{\mathtt{d}})_{\mathcal{T}_h^S} + (\mathrm{E}_0^{\boldsymbol{\rho}_S}, \widetilde{\boldsymbol{\tau}}_{S,h})_{\mathcal{T}_h^S} + (\mathrm{E}_c^{\boldsymbol{\rho}_S}, \widetilde{\boldsymbol{\tau}}_{S,h})_{\mathcal{T}_h^S} \quad&=\quad \frac{1}{\nu}(\Pi\boldsymbol{\sigma}_S - \boldsymbol{\sigma}_S, (\widetilde{\boldsymbol{\tau}}_{S,h})^{\mathtt{d}})_{\mathcal{T}_h^S} \\ &\quad+ (\boldsymbol{\mathcal{P}}_A(\boldsymbol{\rho}_S) - \boldsymbol{\rho}_S, \widetilde{\boldsymbol{\tau}}_{S,h})_{\mathcal{T}_h^S}\,.\end{aligned} \tag{5.22}$$

In turn, it follows from (5.20) that

$$(\widetilde{\boldsymbol{\tau}}_{S,h}, \mathrm{E}_0^{\boldsymbol{\rho}_S})_{\mathcal{T}_h^S} \;=\; (\mathrm{E}_0^{\boldsymbol{\rho}_S}, \mathrm{E}_0^{\boldsymbol{\rho}_S})_{\mathcal{T}_h^S} \;=\; \|\mathrm{E}_0^{\boldsymbol{\rho}_S}\|^2_{0,\Omega_S}$$

and

$$(\widetilde{\boldsymbol{\tau}}_{S,h}, \mathrm{E}_c^{\boldsymbol{\rho}_S})_{\mathcal{T}_h^S} \;=\; (\mathrm{E}_0^{\boldsymbol{\rho}_S}, \mathrm{E}_c^{\boldsymbol{\rho}_S})_{\mathcal{T}_h^S} \;=\; 0\,,$$

which implies together with (5.22), that

$$\|\mathrm{E}_0^{\boldsymbol{\rho}_S}\|^2_{0,\Omega_S} \;=\; -\frac{1}{\nu}((\mathrm{E}^{\boldsymbol{\sigma}_S})^{\mathtt{d}}, (\widetilde{\boldsymbol{\tau}}_{S,h})^{\mathtt{d}})_{\mathcal{T}_h^S} + \frac{1}{\nu}(\Pi\boldsymbol{\sigma}_S - \boldsymbol{\sigma}_S, (\widetilde{\boldsymbol{\tau}}_{S,h})^{\mathtt{d}})_{\mathcal{T}_h^S} + (\boldsymbol{\mathcal{P}}_A(\boldsymbol{\rho}_S) - \boldsymbol{\rho}_S, \widetilde{\boldsymbol{\tau}}_{S,h})_{\mathcal{T}_h^S}\,.$$

In this way, applying the Cauchy-Schwarz inequality and estimate (5.21) we conclude the proof. □

Lemma 5.3. *There exists $C > 0$, independent of the meshsize, such that*

$$\|\mathrm{E}_c^{\boldsymbol{\rho}_S}\|_{0,\Omega_S} \;\leq\; C\Big\{\|(\mathrm{E}^{\boldsymbol{\sigma}_S})^{\mathtt{d}}\|_{0,\Omega_S} \;+\; \|\Pi\boldsymbol{\sigma}_S - \boldsymbol{\sigma}_S\|_{0,\Omega_S} \;+\; \|\boldsymbol{\mathcal{P}}_A(\boldsymbol{\rho}_S) - \boldsymbol{\rho}_S\|_{0,\Omega_S}\Big\}.$$

Proof. Given $\mathrm{E}_c^{\boldsymbol{\rho}_S} \in \mathbb{A}_h^c := \{\boldsymbol{\eta} \in \mathbb{A}_h : \boldsymbol{\eta}|_T \in \mathbb{P}_0(T) \;\; \forall\, T \in \mathcal{T}_h^S\}$, we know from [9, Section 11.7, Theorem 11.9] (see also [80, Lemma 5.2]) that there exists $\widetilde{\boldsymbol{\tau}}_{S,h} \in \{\boldsymbol{\tau} \in \mathbb{H}(\mathbf{div};\Omega_S) \;:\; \boldsymbol{\tau}|_T \in \mathbb{P}_1(T) \;\; \forall\, T \in \mathcal{T}_h^S\}$ such that $\mathbf{div}(\widetilde{\boldsymbol{\tau}}_{S,h}) = \mathbf{0}$ in Ω_S, $\widetilde{\boldsymbol{\tau}}_{S,h}\mathbf{n} = \mathbf{0}$ on $\partial\Omega_S$,

$$(\widetilde{\boldsymbol{\tau}}_{S,h}, \boldsymbol{\eta}_{S,h})_{\mathcal{T}_h^S} \;=\; (\mathrm{E}_c^{\boldsymbol{\rho}_S}, \boldsymbol{\eta}_{S,h})_{\mathcal{T}_h^S} \quad \forall\, \boldsymbol{\eta}_{S,h} \in \mathbb{A}_h^c\,, \tag{5.23}$$

and

$$\|\widetilde{\boldsymbol{\tau}}_{S,h}\|_{\mathbf{div},\Omega_S} \;\leq\; C\,\|\mathrm{E}_c^{\boldsymbol{\rho}_S}\|_{0,\Omega_S}\,, \tag{5.24}$$

where $C > 0$ is independent of the meshsize. Then, replacing $\boldsymbol{\tau}_{S,h} = \widetilde{\boldsymbol{\tau}}_{S,h}$ in the error equation (5.19a), we obtain that

$$\begin{aligned}
&\frac{1}{\nu}((\mathrm{E}^{\boldsymbol{\sigma}_S})^{\mathtt{d}}, (\widetilde{\boldsymbol{\tau}}_{S,h})^{\mathtt{d}})_{\mathcal{T}_h^S} - \Big\langle \widetilde{\boldsymbol{\tau}}_{S,h}\mathbf{n}, \mathrm{E}^{\widehat{\mathbf{u}}_S}\Big\rangle_{\partial\mathcal{T}_h^S} + (\mathrm{E}_0^{\boldsymbol{\rho}_S}, \widetilde{\boldsymbol{\tau}}_{S,h})_{\mathcal{T}_h^S} + (\mathrm{E}_c^{\boldsymbol{\rho}_S}, \widetilde{\boldsymbol{\tau}}_{S,h})_{\mathcal{T}_h^S} \\
&\quad = \frac{1}{\nu}(\Pi\boldsymbol{\sigma}_S - \boldsymbol{\sigma}_S, \widetilde{\boldsymbol{\tau}}_{S,h}^{\mathtt{d}})_{\mathcal{T}_h^S} + (\boldsymbol{\mathcal{P}}_A(\boldsymbol{\rho}_S) - \boldsymbol{\rho}_S, \widetilde{\boldsymbol{\tau}}_{S,h})_{\mathcal{T}_h^S}\,.
\end{aligned}$$

Now, from (5.23) we have $(\mathrm{E}_c^{\boldsymbol{\rho}_S}, \widetilde{\boldsymbol{\tau}}_{S,h})_{\mathcal{T}_h^S} = (\mathrm{E}_c^{\boldsymbol{\rho}_S}, \mathrm{E}_c^{\boldsymbol{\rho}_S})_{\mathcal{T}_h^S} = \|\mathrm{E}_c^{\boldsymbol{\rho}_S}\|_{0,\Omega_S}^2$, and using that $\widetilde{\boldsymbol{\tau}}_{S,h}\mathbf{n} = \mathbf{0}$ on $\partial\Omega_S$, we see that

$$\Big\langle \widetilde{\boldsymbol{\tau}}_{S,h}\mathbf{n}, \mathrm{E}^{\widehat{\mathbf{u}}_S}\Big\rangle_{\partial\mathcal{T}_h^S} \;=\; \Big\langle \widetilde{\boldsymbol{\tau}}_{S,h}\mathbf{n}, \mathrm{E}^{\widehat{\mathbf{u}}_S}\Big\rangle_{\partial\Omega_S} \;=\; 0\,.$$

Thus, from the foregoing identities we deduce that

$$\begin{aligned}
\|\mathrm{E}_c^{\boldsymbol{\rho}_S}\|_{0,\Omega_S}^2 \;=\;& -\frac{1}{\nu}((\mathrm{E}^{\boldsymbol{\sigma}_S})^{\mathtt{d}}, (\widetilde{\boldsymbol{\tau}}_{S,h})^{\mathtt{d}})_{\mathcal{T}_h^S} - (\mathrm{E}_0^{\boldsymbol{\rho}_S}, \widetilde{\boldsymbol{\tau}}_{S,h})_{\mathcal{T}_h^S} + \frac{1}{\nu}(\Pi\boldsymbol{\sigma}_S - \boldsymbol{\sigma}_S, (\widetilde{\boldsymbol{\tau}}_{S,h})^{\mathtt{d}})_{\mathcal{T}_h^S} \\
&+ (\boldsymbol{\mathcal{P}}_A(\boldsymbol{\rho}_S) - \boldsymbol{\rho}_S, \widetilde{\boldsymbol{\tau}}_{S,h})_{\mathcal{T}_h^S}\,,
\end{aligned}$$

from which, applying the Cauchy-Schwarz inequality, estimate (5.24) and Lemma 5.2, the proof is completed. □

As a consequence of Lemmas 5.2 and 5.3 we conclude the estimate for $\mathrm{E}^{\boldsymbol{\rho}_S}$ given by

$$\|\mathrm{E}^{\boldsymbol{\rho}_S}\|_{0,\Omega_S} \;\leq\; C\Big\{\|(\mathrm{E}^{\boldsymbol{\sigma}_S})^{\mathtt{d}}\|_{0,\Omega_S} \;+\; \|\Pi\boldsymbol{\sigma}_S - \boldsymbol{\sigma}_S\|_{0,\Omega_S} \;+\; \|\boldsymbol{\mathcal{P}}_A(\boldsymbol{\rho}_S) - \boldsymbol{\rho}_S\|_{0,\Omega_S}\Big\}. \tag{5.25}$$

Estimating $\mathrm{E}^{\boldsymbol{\sigma}_S}$ and $\mathrm{E}^{\mathbf{u}_D}$

The following two lemmas show how to use the previous results to obtain estimates for $\|\mathrm{E}^{\boldsymbol{\sigma}_S}\|_{0,\Omega_S}$ and $\|\mathrm{E}^{\mathbf{u}_D}\|_{0,\Omega_D}$. To do that, in what follows we denote

$$\|\boldsymbol{\mu}\|_{\mathbf{S}} \;:=\; \langle \mathbf{S}\boldsymbol{\mu}, \boldsymbol{\mu}\rangle_{\partial\mathcal{T}_h^S}^{1/2} \qquad \forall\, \boldsymbol{\mu} \in \mathbf{L}^2(\mathcal{E}_h^S)\,.$$

Lemma 5.4. *There exists $C > 0$, independent of the meshsize, such that*

$$\begin{aligned}
\|(\mathrm{E}^{\boldsymbol{\sigma}_S})^{\mathtt{d}}\|_{0,\Omega_S} \;+\; \|\mathrm{E}^{\mathbf{u}_S} - \mathrm{E}^{\widehat{\mathbf{u}}_S}\|_{\mathbf{S}} \;+\; \|\mathrm{E}^{\mathbf{u}_D}\|_{0,\Omega_D} \;\leq\;& C\Big\{\|\Pi\boldsymbol{\sigma}_S - \boldsymbol{\sigma}_S\|_{0,\Omega_S} + \|\boldsymbol{\mathcal{P}}_A(\boldsymbol{\rho}_S) - \boldsymbol{\rho}_S\|_{0,\Omega_S} \\
&+ \|\Pi\mathbf{u}_D - \mathbf{u}_D\|_{0,\Omega_D}\Big\}.
\end{aligned}$$

Proof. Taking $\boldsymbol{\tau}_{S,h} := \mathrm{E}^{\boldsymbol{\sigma}_S}$, $\mathbf{v}_{S,h} := \mathrm{E}^{\mathbf{u}_S}$, $\boldsymbol{\eta}_{S,h} := -\mathrm{E}^{\boldsymbol{\rho}_S}$, $\boldsymbol{\mu}_{S,h} := \mathrm{E}^{\widehat{\mathbf{u}}_S}$, $\mathbf{v}_{D,h} := \mathrm{E}^{\mathbf{u}_D}$, $q_{D,h} := \mathrm{E}^{p_D}$, and $\psi_{D,h} := -\mathrm{E}^{p_D}$ in the error equations (5.19), and summing all them, we arrive at

$$
\begin{aligned}
&\frac{1}{\nu}\|(\mathrm{E}^{\boldsymbol{\sigma}_S})^{\mathtt{d}}\|^2_{0,\Omega_S} \;+\; \|\mathrm{E}^{\mathbf{u}_S} - \mathrm{E}^{\widehat{\mathbf{u}}_S}\|^2_{\mathbf{S}} \;+\; \sum_{\ell=1}^{n-1} \kappa_\ell^{-1}\|\mathrm{E}^{\widehat{\mathbf{u}}_S}\cdot \mathbf{t}_\ell\|^2_{0,\Sigma} \\
&\quad + (\mathbf{K}^{-1}\mathrm{E}^{\mathbf{u}_D}, \mathrm{E}^{\mathbf{u}_D})_{\mathcal{T}_h^D} \;+\; \Big\langle \tau(\mathrm{E}^{p_D} - \mathrm{E}^{\widehat{p}_D}), \mathrm{E}^{p_D} - \mathrm{E}^{\widehat{p}_D}\Big\rangle_{\partial\mathcal{T}_h^D} \\
=\;& \frac{1}{\nu}(\Pi\boldsymbol{\sigma}_S - \boldsymbol{\sigma}_S, (\mathrm{E}^{\boldsymbol{\sigma}_S})^{\mathtt{d}})_{\mathcal{T}_h^S} \;+\; (\boldsymbol{\mathcal{P}}_A(\boldsymbol{\rho}_S) - \boldsymbol{\rho}_S, (\mathrm{E}^{\boldsymbol{\sigma}_S})^{\mathtt{d}})_{\mathcal{T}_h^S} \\
&\quad - (\mathrm{E}^{\boldsymbol{\rho}_S}, \Pi\boldsymbol{\sigma}_S - \boldsymbol{\sigma}_S)_{\mathcal{T}_h^S} \;+\; (\mathbf{K}^{-1}(\Pi\mathbf{u}_D - \mathbf{u}_D), \mathrm{E}^{\mathbf{u}_D})_{\mathcal{T}_h^D}\,.
\end{aligned} \tag{5.26}
$$

In particular, according to the properties of $\mathbf{K}^{-1}$, $\mathbf{S}$ and τ, and applying the Cauchy-Schwarz and Young inequality, we deduce from (5.26) that

$$
\begin{aligned}
&\|(\mathrm{E}^{\boldsymbol{\sigma}_S})^{\mathtt{d}}\|^2_{0,\Omega_S} \;+\; \|\mathrm{E}^{\mathbf{u}_S} - \mathrm{E}^{\widehat{\mathbf{u}}_S}\|^2_{\mathbf{S}} \;+\; \|\mathrm{E}^{\mathbf{u}_D}\|^2_{0,\Omega_D} \\
&\quad \le\; \widetilde{C}\Big\{\|\Pi\boldsymbol{\sigma}_S - \boldsymbol{\sigma}_S\|_{0,\Omega_S}\|(\mathrm{E}^{\boldsymbol{\sigma}_S})^{\mathtt{d}}\|_{0,\Omega_S} + \|\boldsymbol{\mathcal{P}}_A(\boldsymbol{\rho}_S) - \boldsymbol{\rho}_S\|_{0,\Omega_S}\|(\mathrm{E}^{\boldsymbol{\sigma}_S})^{\mathtt{d}}\|_{0,\Omega_S} \\
&\qquad +\; \|\Pi\boldsymbol{\sigma}_S - \boldsymbol{\sigma}_S\|_{0,\Omega_S}\|\mathrm{E}^{\boldsymbol{\rho}_S}\|_{0,\Omega_S} + \|\Pi\mathbf{u}_D - \mathbf{u}_D\|_{0,\Omega_D}\|\mathrm{E}^{\mathbf{u}_D}\|_{0,\Omega_D}\Big\} \\
&\quad \le\; \frac{1}{2}\widetilde{C}\bigg\{\frac{1}{\delta_1}\|\Pi\boldsymbol{\sigma}_S - \boldsymbol{\sigma}_S\|^2_{0,\Omega_S} + \delta_1\|(\mathrm{E}^{\boldsymbol{\sigma}_S})^{\mathtt{d}}\|^2_{0,\Omega_S} + \frac{1}{\delta_2}\|\boldsymbol{\mathcal{P}}_A(\boldsymbol{\rho}_S) - \boldsymbol{\rho}_S\|^2_{0,\Omega_S} + \delta_2\|(\mathrm{E}^{\boldsymbol{\sigma}_S})^{\mathtt{d}}\|^2_{0,\Omega_S} \\
&\qquad +\; \frac{1}{\delta_3}\|\Pi\boldsymbol{\sigma}_S - \boldsymbol{\sigma}_S\|^2_{0,\Omega_S} + \delta_3\|\mathrm{E}^{\boldsymbol{\rho}_S}\|^2_{0,\Omega_S} + \frac{1}{\delta_4}\|\Pi\mathbf{u}_D - \mathbf{u}_D\|^2_{0,\Omega_D} + \delta_4\|\mathrm{E}^{\mathbf{u}_D}\|^2_{0,\Omega_D}\bigg\}\,,
\end{aligned}
$$

for all $\delta_i > 0$, $i \in \{1,2,3,4\}$. Next, utilizing (5.25) we find that the previous inequality becomes

$$
\begin{aligned}
&\|(\mathrm{E}^{\boldsymbol{\sigma}_S})^{\mathtt{d}}\|^2_{0,\Omega_S} \;+\; \|\mathrm{E}^{\mathbf{u}_S} - \mathrm{E}^{\widehat{\mathbf{u}}_S}\|^2_{\mathbf{S}} \;+\; \|\mathrm{E}^{\mathbf{u}_D}\|^2_{0,\Omega_D} \\
&\quad \le\; \widehat{C}\left\{\left(\frac{1}{\delta_1} + \frac{1}{\delta_3} + \delta_3\right)\|\Pi\boldsymbol{\sigma}_S - \boldsymbol{\sigma}_S\|^2_{0,\Omega_S} + \left(\frac{1}{\delta_2} + \delta_3\right)\|\boldsymbol{\mathcal{P}}_A(\boldsymbol{\rho}_S) - \boldsymbol{\rho}_S\|^2_{0,\Omega_S}\right. \\
&\qquad \left. +\; \frac{1}{\delta_4}\|\Pi\mathbf{u}_D - \mathbf{u}_D\|^2_{0,\Omega_D} + (\delta_1 + \delta_2 + \delta_3)\,\|(\mathrm{E}^{\boldsymbol{\sigma}_S})^{\mathtt{d}}\|^2_{0,\Omega_S} + \delta_4\|\mathrm{E}^{\mathbf{u}_D}\|^2_{0,\Omega_D}\right\}\,,
\end{aligned}
$$

which yields

$$
\begin{aligned}
&\Big\{1 - \widehat{C}(\delta_1 + \delta_2 + \delta_3)\Big\}\,\|(\mathrm{E}^{\boldsymbol{\sigma}_S})^{\mathtt{d}}\|^2_{0,\Omega_S} \;+\; \|\mathrm{E}^{\mathbf{u}_S} - \mathrm{E}^{\widehat{\mathbf{u}}_S}\|^2_{\mathbf{S}} \;+\; (1 - \widehat{C}\delta_4)\|\mathrm{E}^{\mathbf{u}_D}\|^2_{0,\Omega_D} \\
&\quad \le\; \widehat{C}\left\{\left(\frac{1}{\delta_1} + \frac{1}{\delta_3} + \delta_3\right)\|\Pi\boldsymbol{\sigma}_S - \boldsymbol{\sigma}_S\|^2_{0,\Omega_S} + \left(\frac{1}{\delta_2} + \delta_3\right)\|\boldsymbol{\mathcal{P}}_A(\boldsymbol{\rho}_S) - \boldsymbol{\rho}_S\|^2_{0,\Omega_S}\right. \\
&\qquad \left. +\; \frac{1}{\delta_4}\|\Pi\mathbf{u}_D - \mathbf{u}_D\|^2_{0,\Omega_D}\right\} \qquad \forall\ \delta_i > 0, \quad i \in \{1,2,3,4\}.
\end{aligned}
$$

Finally, suitable choices of $\delta_i > 0$, $i \in \{1,2,3,4\}$, complete the proof. □

Lemma 5.5. *There exists $C > 0$, independent of the meshsize, such that*

$$
\|\mathrm{E}^{\boldsymbol{\sigma}_S}\|_{0,\Omega_S} \;\le\; C\Big\{\|\Pi\boldsymbol{\sigma}_S - \boldsymbol{\sigma}_S\|_{0,\Omega_S} + \|\boldsymbol{\mathcal{P}}_A(\boldsymbol{\rho}_S) - \boldsymbol{\rho}_S\|_{0,\Omega_S} + \|\Pi\mathbf{u}_D - \mathbf{u}_D\|_{0,\Omega_D}\Big\}.
$$

Proof. From the identity $\|\mathrm{E}^{\boldsymbol{\sigma}_S}\|^2_{0,\Omega_S} = \|(\mathrm{E}^{\boldsymbol{\sigma}_S})^{\mathtt{d}}\|^2_{0,\Omega_S} + \frac{1}{n}\|\mathrm{tr}\,(\mathrm{E}^{\boldsymbol{\sigma}_S})\,\|^2_{0,\Omega_S}$ and Lemma 5.4, it is clear that we only need to bound $\|\mathrm{tr}\,(\mathrm{E}^{\boldsymbol{\sigma}_S})\,\|_{0,\Omega_S}$, for which we proceed in what follows as in [43, Proposition

3.4]. In fact, we first recall here a well-known result (see, e.g. [92, Corollary 2.4 in Chapter I]), which establishes that there exists $\beta > 0$ such that

$$\beta\,\|q\|_{0,\Omega_S} \;\le\; \sup_{\substack{\mathbf{w}\in\mathbf{H}_0^1(\Omega_S)\\ \mathbf{w}\neq\mathbf{0}}} \frac{(q,\mathrm{div}(\mathbf{w}))_{\mathcal{T}_h^S}}{\|\mathbf{w}\|_{1,\Omega_S}} \qquad \forall\, q\in L_0^2(\Omega_S)\,.$$

Then, applying this inequality to $q := \mathrm{tr}\,(\mathrm{E}^{\boldsymbol{\sigma}_S}) \in L_0^2(\Omega_S)$ (cf. (5.19h)), we readily have

$$\|\mathrm{tr}\,(\mathrm{E}^{\boldsymbol{\sigma}_S})\,\|_{0,\Omega_S} \;\le\; \frac{1}{\beta}\sup_{\substack{\mathbf{w}\in\mathbf{H}_0^1(\Omega_S)\\ \mathbf{w}\neq\mathbf{0}}} \frac{(\mathrm{tr}\,(\mathrm{E}^{\boldsymbol{\sigma}_S})\,,\mathrm{div}(\mathbf{w}))_{\mathcal{T}_h^S}}{\|\mathbf{w}\|_{1,\Omega_S}}\,. \tag{5.27}$$

Next, let $\mathbf{P}:\mathbf{H}^1(\mathcal{T}_h^S)\to\mathbf{V}_h^S$ be any projection such that, given $\mathbf{w}\in\mathbf{H}^1(\mathcal{T}_h^S)$, there holds $(\mathbf{P}(\mathbf{w})-\mathbf{w},\mathbf{v})_T = 0 \quad \forall\,\mathbf{v}\in\mathbf{P}_{k-1}(T), \quad \forall\, T\in\mathcal{T}_h^S$. In particular, it suffices to take $\mathbf{P}:\mathbf{H}^1(\mathcal{T}_h^S)\to\mathbf{V}_h^S$ as the orthogonal projector with respect to the $\mathbf{L}^2(\Omega_S)$ inner product, which verifies $(\mathbf{P}(\mathbf{w})-\mathbf{w},\mathbf{v})_T = 0$ $\forall\,\mathbf{v}\in\mathbf{P}_k(T), \forall\, T\in\mathcal{T}_h^S$. It follows, integrating by parts on each $T\in\mathcal{T}_h^S$, and at the end incorporating the projectors $\boldsymbol{P}_M$ (cf. (5.17)) and $\mathbf{P}$, that for each $\mathbf{w}\in\mathbf{H}_0^1(\Omega_S)$ there holds

$$\begin{aligned}
\frac{1}{n}(\mathrm{tr}\,(\mathrm{E}^{\boldsymbol{\sigma}_S})\,,\mathrm{div}(\mathbf{w}))_{\mathcal{T}_h^S} \;&=\; -\frac{1}{n}(\nabla\mathrm{tr}\,(\mathrm{E}^{\boldsymbol{\sigma}_S})\,,\mathbf{w})_{\mathcal{T}_h^S} + \frac{1}{n}\,\langle \mathbf{w}\cdot\mathbf{n},\mathrm{tr}\,(\mathrm{E}^{\boldsymbol{\sigma}_S})\rangle_{\partial\mathcal{T}_h^S}\\
&=\; \left(\mathbf{div}\left(-\frac{1}{n}\mathrm{tr}\,(\mathrm{E}^{\boldsymbol{\sigma}_S})\,\mathbb{I}\right),\mathbf{w}\right)_{\mathcal{T}_h^S} + \frac{1}{n}\,\langle \mathbf{w}\cdot\mathbf{n},\mathrm{tr}\,(\mathrm{E}^{\boldsymbol{\sigma}_S})\rangle_{\partial\mathcal{T}_h^S}\\
&=\; \left(\mathbf{div}\left((\mathrm{E}^{\boldsymbol{\sigma}_S})^{\mathrm{d}}\right),\mathbf{w}\right)_{\mathcal{T}_h^S} - (\mathbf{div}(\mathrm{E}^{\boldsymbol{\sigma}_S}),\mathbf{w})_{\mathcal{T}_h^S} + \frac{1}{n}\,\langle \mathbf{w}\cdot\mathbf{n},\mathrm{tr}\,(\mathrm{E}^{\boldsymbol{\sigma}_S})\rangle_{\partial\mathcal{T}_h^S}\\
&=\; -((\mathrm{E}^{\boldsymbol{\sigma}_S})^{\mathrm{d}},\nabla\mathbf{w})_{\mathcal{T}_h^S} + \left\langle(\mathrm{E}^{\boldsymbol{\sigma}_S})^{\mathrm{d}}\mathbf{n},\mathbf{w}\right\rangle_{\partial\mathcal{T}_h^S} - (\mathbf{div}(\mathrm{E}^{\boldsymbol{\sigma}_S}),\mathbf{w})_{\mathcal{T}_h^S} + \left\langle\left(\frac{1}{n}\mathrm{tr}\,(\mathrm{E}^{\boldsymbol{\sigma}_S})\,\mathbb{I}\right)\mathbf{n},\mathbf{w}\right\rangle_{\partial\mathcal{T}_h^S}\\
&=\; -((\mathrm{E}^{\boldsymbol{\sigma}_S})^{\mathrm{d}},\nabla\mathbf{w})_{\mathcal{T}_h^S} - (\mathbf{div}(\mathrm{E}^{\boldsymbol{\sigma}_S}),\mathbf{w})_{\mathcal{T}_h^S} + \langle\mathrm{E}^{\boldsymbol{\sigma}_S}\mathbf{n},\mathbf{w}\rangle_{\partial\mathcal{T}_h^S}\\
&=\; -((\mathrm{E}^{\boldsymbol{\sigma}_S})^{\mathrm{d}},\nabla\mathbf{w})_{\mathcal{T}_h^S} - (\mathbf{div}(\mathrm{E}^{\boldsymbol{\sigma}_S}),\mathbf{P}(\mathbf{w}))_{\mathcal{T}_h^S} + \langle\mathrm{E}^{\boldsymbol{\sigma}_S}\mathbf{n},\boldsymbol{P}_M(\mathbf{w})\rangle_{\partial\mathcal{T}_h^S} \qquad \forall\,\mathbf{w}\in\mathbf{H}_0^1(\Omega_S)\,.
\end{aligned}$$

Now, employing the error equation (5.19b) and (5.19d) with $\mathbf{v}_{S,h} := \mathbf{P}(\mathbf{w})$ and $\boldsymbol{\mu}_{S,h} := \boldsymbol{P}_M(\mathbf{w})$, respectively, we deduce together with the foregoing equation that

$$\begin{aligned}
\frac{1}{n}(\mathrm{tr}\,(\mathrm{E}^{\boldsymbol{\sigma}_S})\,,\mathrm{div}(\mathbf{w}))_{\mathcal{T}_h^S} \;&=\; -((\mathrm{E}^{\boldsymbol{\sigma}_S})^{\mathrm{d}},\nabla\mathbf{w})_{\mathcal{T}_h^S} - \left\langle\mathbf{S}(\mathrm{E}^{\mathbf{u}_S}-\mathrm{E}^{\widehat{\mathbf{u}}_S}),\mathbf{P}(\mathbf{w})\right\rangle_{\partial\mathcal{T}_h^S}\\
&\quad+\;\left\langle\mathbf{S}(\mathrm{E}^{\mathbf{u}_S}-\mathrm{E}^{\widehat{\mathbf{u}}_S}),\boldsymbol{P}_M(\mathbf{w})\right\rangle_{\partial\mathcal{T}_h^S} - \sum_{\ell=1}^{n-1}\kappa_\ell^{-1}\left\langle\mathrm{E}^{\widehat{\mathbf{u}}_S}\cdot\mathbf{t}_\ell,\boldsymbol{P}_M(\mathbf{w})\cdot\mathbf{t}_\ell\right\rangle_\Sigma - \left\langle\boldsymbol{P}_M(\mathbf{w})\cdot\mathbf{n},\mathrm{E}^{\widehat{p}_D}\right\rangle_\Sigma\\
&=\; -((\mathrm{E}^{\boldsymbol{\sigma}_S})^{\mathrm{d}},\nabla\mathbf{w})_{\mathcal{T}_h^S} - \left\langle\mathbf{S}(\mathrm{E}^{\mathbf{u}_S}-\mathrm{E}^{\widehat{\mathbf{u}}_S}),\mathbf{P}(\mathbf{w})-\boldsymbol{P}_M(\mathbf{w})\right\rangle_{\partial\mathcal{T}_h^S}\\
&\quad-\;\sum_{\ell=1}^{n-1}\kappa_\ell^{-1}\left\langle\mathrm{E}^{\widehat{\mathbf{u}}_S}\cdot\mathbf{t}_\ell,\mathbf{w}\cdot\mathbf{t}_\ell\right\rangle_\Sigma - \left\langle\mathbf{w}\cdot\mathbf{n},\mathrm{E}^{\widehat{p}_D}\right\rangle_\Sigma\\
&=\; -((\mathrm{E}^{\boldsymbol{\sigma}_S})^{\mathrm{d}},\nabla\mathbf{w})_{\mathcal{T}_h^S} - \left\langle\mathbf{S}(\mathrm{E}^{\mathbf{u}_S}-\mathrm{E}^{\widehat{\mathbf{u}}_S}),\mathbf{P}(\mathbf{w})-\boldsymbol{P}_M(\mathbf{w})\right\rangle_{\partial\mathcal{T}_h^S}\,,
\end{aligned}$$

where the terms on Σ vanish because $\mathbf{w}=\mathbf{0}$ on $\partial\Omega_S$. In this way, we find that

$$\begin{aligned}
(\mathrm{tr}\,(\mathrm{E}^{\boldsymbol{\sigma}_S})\,,\mathrm{div}(\mathbf{w}))_{\mathcal{T}_h^S} \;&\le\; n\left\{\|(\mathrm{E}^{\boldsymbol{\sigma}_S})^{\mathrm{d}}\|_{0,\Omega_S}|\mathbf{w}|_{1,\Omega_S} \;+\; \|\mathrm{E}^{\mathbf{u}_S}-\mathrm{E}^{\widehat{\mathbf{u}}_S}\|_{\mathbf{S}}\|\mathbf{P}(\mathbf{w})-\boldsymbol{P}_M(\mathbf{w})\|_{\mathbf{S}}\right\}\\
&\le\; n\left\{\|(\mathrm{E}^{\boldsymbol{\sigma}_S})^{\mathrm{d}}\|_{0,\Omega_S} \;+\; \|\mathrm{E}^{\mathbf{u}_S}-\mathrm{E}^{\widehat{\mathbf{u}}_S}\|_{\mathbf{S}}\frac{\|\mathbf{P}(\mathbf{w})-\boldsymbol{P}_M(\mathbf{w})\|_{\mathbf{S}}}{\|\mathbf{w}\|_{1,\Omega_S}}\right\}\|\mathbf{w}\|_{1,\Omega_S} \quad \forall\,\mathbf{w}\in\mathbf{H}_0^1(\Omega_S)\,,
\end{aligned}$$

which, replaced back into (5.27), yields

$$\|\mathrm{tr}\,(\mathrm{E}^{\boldsymbol{\sigma}_S})\|_{0,\Omega_S} \;\leq\; \frac{n}{\beta}\,\Psi(\mathbf{S})\left\{\|(\mathrm{E}^{\boldsymbol{\sigma}_S})^{\mathtt{d}}\|_{0,\Omega_S} \;+\; \|\mathrm{E}^{\mathbf{u}_S} - \mathrm{E}^{\widehat{\mathbf{u}}_S}\|_{\mathbf{S}}\right\}, \tag{5.28}$$

where

$$\Psi(\mathbf{S}) \;:=\; \max\left\{1,\; \sup_{\substack{\mathbf{w}\in\mathbf{H}^1_0(\Omega_S)\\ \mathbf{w}\neq\mathbf{0}}} \frac{\|\mathbf{P}(\mathbf{w}) - \boldsymbol{P}_M(\mathbf{w})\|_{\mathbf{S}}}{\|\mathbf{w}\|_{1,\Omega_S}}\right\}.$$

The above expression is bounded by a constant depending on $\mathbf{S}$ (see [43, Proposition 3.9] for details), and hence Lemma 5.4 and (5.28) complete the proof. $\square$

Estimating $\mathrm{E}^{\mathbf{u}_S}$ and E^{p_D}

In order to estimate $\|\mathrm{E}^{\mathbf{u}_S}\|_{0,\Omega_S}$ and $\|\mathrm{E}^{p_D}\|_{0,\Omega_D}$, we now proceed as in [44, 43, 48] and incorporate a suitable auxiliary problem. More precisely, in what follows we consider the continuous problem (5.2)-(5.3)-(5.4) with sources given by $\mathbf{f}_S := -\mathrm{E}^{\mathbf{u}_S} \in \mathbf{L}^2(\Omega_S)$ and $f_D := \mathrm{E}^{p_D} \in L^2(\Omega_D)$, that is:

$$\begin{aligned}
\frac{1}{\nu}\boldsymbol{\Phi}_S^{\mathtt{d}} \;-\; \nabla\boldsymbol{\varphi}_S \;+\; \boldsymbol{\gamma}_S &= \mathbf{0} && \text{in } \Omega_S, && (5.29a)\\
\mathbf{div}(\boldsymbol{\Phi}_S) &= \mathrm{E}^{\mathbf{u}_S} && \text{in } \Omega_S\,, && (5.29b)\\
\boldsymbol{\Phi}_S \;-\; \boldsymbol{\Phi}_S^{\mathtt{t}} &= \mathbf{0} && \text{in } \Omega_S\,, && (5.29c)\\
\boldsymbol{\varphi}_S &= \mathbf{0} && \text{on } \Gamma_S\,, && (5.29d)\\
\mathbf{K}^{-1}\boldsymbol{\psi}_D \;+\; \nabla\phi_D &= \mathbf{0} && \text{in } \Omega_D\,, && (5.29e)\\
\mathrm{div}(\boldsymbol{\psi}_D) &= \mathrm{E}^{p_D} && \text{in } \Omega_D\,, && (5.29f)\\
\boldsymbol{\psi}_D\cdot\mathbf{n} &= 0 && \text{on } \Gamma_D\,, && (5.29g)\\
\boldsymbol{\varphi}_S\cdot\mathbf{n} \;-\; \boldsymbol{\psi}_D\cdot\mathbf{n} &= 0 && \text{on } \Sigma\,, && (5.29h)\\
\boldsymbol{\Phi}_S\mathbf{n} \;+\; \sum_{\ell=1}^{n-1}\kappa_\ell^{-1}(\boldsymbol{\varphi}_S\cdot\mathbf{t}_\ell)\mathbf{t}_\ell \;+\; \phi_D\mathbf{n} &= \mathbf{0} && \text{on } \Sigma\,, && (5.29i)
\end{aligned}$$

where $\boldsymbol{\gamma}_S := \frac{1}{2}\left(\nabla\boldsymbol{\varphi}_S - (\nabla\boldsymbol{\varphi}_S)^{\mathtt{t}}\right)$. According to (5.18), we know that there holds

$$\sum_{T\in\mathcal{T}_h^S}\left\{\|\boldsymbol{\Phi}_S\|_{1,T} + \|\boldsymbol{\varphi}_S\|_{2,T}\right\} + \sum_{T\in\mathcal{T}_h^D}\left\{\|\boldsymbol{\psi}_D\|_{1,T} + \|\phi_D\|_{2,T}\right\} \;\leq\; C_{\mathrm{reg}}\left\{\|\mathrm{E}^{\mathbf{u}_S}\|_{0,\Omega_S} + \|\mathrm{E}^{p_D}\|_{0,\Omega_D}\right\}, \tag{5.30}$$

and certainly $\mathbf{div}(\boldsymbol{\Phi}_S) \in \mathbf{L}^2(\Omega_S)$ and $\mathrm{div}(\boldsymbol{\psi}_D) \in L^2(\Omega_D)$.

Lemma 5.6. *There holds*

$$\begin{aligned}
\|\mathrm{E}^{\mathbf{u}_S}\|_{0,\Omega_S} + \;\|\mathrm{E}^{p_D}\|_{0,\Omega_D} \;\leq\; C\,h\Big\{&\|(\mathrm{E}^{\boldsymbol{\sigma}_S})^{\mathtt{d}}\|_{0,\Omega_S} + \|\mathrm{E}^{\boldsymbol{\rho}_S}\|_{0,\Omega_S} + \|\mathrm{E}^{\mathbf{u}_D}\|_{0,\Omega_D}\\
&+ \|\Pi\boldsymbol{\sigma}_S - \boldsymbol{\sigma}_S\|_{0,\Omega_S} + \|\boldsymbol{\mathcal{P}}_A(\boldsymbol{\rho}_S) - \boldsymbol{\rho}_S\|_{0,\Omega_S} + \|\Pi\mathbf{u}_D - \mathbf{u}_D\|_{0,\Omega_D}\Big\}.
\end{aligned}$$

Proof. First, note from (5.30) that we can apply Π_S and Π_D to the solution of (5.29), and hence we can set $\Pi_S(\boldsymbol{\Phi}_S,\boldsymbol{\varphi}_S) := (\Pi\boldsymbol{\Phi}_S, \Pi\boldsymbol{\varphi}_S)$ and $\Pi_D(\boldsymbol{\psi}_D,\phi_D) := (\Pi\boldsymbol{\psi}_D, \Pi\phi_D)$. Then, from (5.29a), (5.29b), (5.29e) and (5.29f) we have

$$
\begin{aligned}
\|\mathrm{E}^{\mathbf{u}_S}\|^2_{0,\Omega_S} \,+\, \|\mathrm{E}^{p_D}\|^2_{0,\Omega_D} \;&=\; (\mathrm{E}^{\mathbf{u}_S},\mathrm{E}^{\mathbf{u}_S})_{\mathcal{T}_h^S} \,+\, (\mathrm{E}^{p_D},\mathrm{E}^{p_D})_{\mathcal{T}_h^D} \;=\; (\mathrm{E}^{\mathbf{u}_S},\mathbf{div}(\mathbf{\Phi}_S))_{\mathcal{T}_h^S}\\
&+\, (\mathrm{E}^{\boldsymbol{\sigma}_S},\frac{1}{\nu}\mathbf{\Phi}_S^{\mathtt{d}} - \nabla\boldsymbol{\varphi}_S + \boldsymbol{\gamma}_S)_{\mathcal{T}_h^S} + (\mathrm{E}^{p_D},\mathrm{div}(\boldsymbol{\psi}_D))_{\mathcal{T}_h^D} - (\mathrm{E}^{\mathbf{u}_D},\mathbf{K}^{-1}\boldsymbol{\psi}_D + \nabla\phi_D)_{\mathcal{T}_h^D}\\
=\;& (\mathrm{E}^{\mathbf{u}_S},\mathbf{div}(\Pi\mathbf{\Phi}_S))_{\mathcal{T}_h^S} + (\Pi\boldsymbol{\varphi}_S,\mathrm{div}(\mathrm{E}^{\boldsymbol{\sigma}_S}))_{\mathcal{T}_h^S} + (\boldsymbol{\mathcal{P}}_A(\boldsymbol{\gamma}_S),\mathrm{E}^{\boldsymbol{\sigma}_S})_{\mathcal{T}_h^S} + (\mathrm{E}^{p_D},\mathrm{div}(\Pi\boldsymbol{\psi}_D))_{\mathcal{T}_h^D}\\
&+\, (\Pi\phi_D,\mathrm{div}(\mathrm{E}^{\mathbf{u}_D})_{\mathcal{T}_h^D} + \frac{1}{\nu}((\mathrm{E}^{\boldsymbol{\sigma}_S})^{\mathtt{d}},\mathbf{\Phi}_S)_{\mathcal{T}_h^S} - ((\mathrm{E}^{\boldsymbol{\sigma}_S})^{\mathtt{d}},\boldsymbol{\mathcal{P}}_A(\boldsymbol{\gamma}_S) - \boldsymbol{\gamma}_S)_{\mathcal{T}_h^S} - (\mathbf{K}^{-1}\mathrm{E}^{\mathbf{u}_D},\boldsymbol{\psi}_D)_{\mathcal{T}_h^D}\\
&-\, \langle(\Pi\mathbf{\Phi}_S - \mathbf{\Phi}_S)\mathbf{n},\mathrm{E}^{\mathbf{u}_S}\rangle_{\partial\mathcal{T}_h^S} - \langle\mathrm{E}^{\boldsymbol{\sigma}_S}\mathbf{n},\boldsymbol{\varphi}_S\rangle_{\partial\mathcal{T}_h^S} - \langle(\Pi\boldsymbol{\psi}_D - \boldsymbol{\psi}_D)\cdot\mathbf{n},\mathrm{E}^{p_D}\rangle_{\partial\mathcal{T}_h^D\setminus\Sigma}\\
&+\, \langle(\Pi\boldsymbol{\psi}_D - \boldsymbol{\psi}_D)\cdot\mathbf{n},\mathrm{E}^{p_D}\rangle_\Sigma - \langle\mathrm{E}^{\mathbf{u}_D}\cdot\mathbf{n},\phi_D\rangle_{\partial\mathcal{T}_h^D\setminus\Sigma} + \langle\mathrm{E}^{\mathbf{u}_D}\cdot\mathbf{n},\phi_D\rangle_\Sigma\,.
\end{aligned}
$$

Now, using the error equations (5.19a), (5.19b), (5.19c), (5.19e) and (5.19f) in the first five terms of the above identity, and employing that $\mathbf{\Phi}_S$ is a symmetric tensor (cf. (5.29c)), we deduce that

$$
\|\mathrm{E}^{\mathbf{u}_S}\|^2_{0,\Omega_S} \,+\, \|\mathrm{E}^{p_D}\|^2_{0,\Omega_D} \;=\; S_1 \,+\, S_2 \,+\, S_3 \,-\, \langle\mathrm{E}^{\mathbf{u}_D}\cdot\mathbf{n},\phi_D\rangle_{\partial\mathcal{T}_h^D\setminus\Sigma} \,+\, \langle\mathrm{E}^{\mathbf{u}_D}\cdot\mathbf{n},\phi_D\rangle_\Sigma\,, \tag{5.31}
$$

where the intermediate terms S_i, $i\in\{1,2,3\}$, are given by

$$
\begin{aligned}
S_1 \;:=\;& -\frac{1}{\nu}((\mathrm{E}^{\boldsymbol{\sigma}_S})^{\mathtt{d}},\Pi\mathbf{\Phi}_S - \mathbf{\Phi}_S)_{\mathcal{T}_h^S} - ((\mathrm{E}^{\boldsymbol{\sigma}_S})^{\mathtt{d}},\boldsymbol{\mathcal{P}}_A(\boldsymbol{\gamma}_S) - \boldsymbol{\gamma}_S)_{\mathcal{T}_h^S} - (\mathrm{E}^{\boldsymbol{\rho}_S},\Pi\mathbf{\Phi}_S - \mathbf{\Phi}_S)_{\mathcal{T}_h^S}\\
&+\, (\boldsymbol{\mathcal{P}}_A(\boldsymbol{\rho}_S) - \boldsymbol{\rho}_S,\Pi\mathbf{\Phi}_S - \mathbf{\Phi}_S)_{\mathcal{T}_h^S} + \frac{1}{\nu}(\Pi\boldsymbol{\sigma}_S - \boldsymbol{\sigma}_S,(\Pi\mathbf{\Phi}_S)^{\mathtt{d}})_{\mathcal{T}_h^S} + (\boldsymbol{\mathcal{P}}_A(\boldsymbol{\gamma}_S),\Pi\boldsymbol{\sigma}_S - \boldsymbol{\sigma}_S)_{\mathcal{T}_h^S}\\
&+\, (\mathbf{K}^{-1}\mathrm{E}^{\mathbf{u}_D},\Pi\boldsymbol{\psi}_D - \boldsymbol{\psi}_D)_{\mathcal{T}_h^D} - (\mathbf{K}^{-1}(\Pi\mathbf{u}_D - \mathbf{u}_D),\Pi\boldsymbol{\psi}_D)_{\mathcal{T}_h^D}\,,
\end{aligned}
$$

$$
S_2 \;:=\; \left\langle\Pi\mathbf{\Phi}_S\mathbf{n},\mathrm{E}^{\widehat{\mathbf{u}}_S}\right\rangle_{\partial\mathcal{T}_h^S} - \langle(\Pi\mathbf{\Phi}_S - \mathbf{\Phi}_S)\mathbf{n},\mathrm{E}^{\mathbf{u}_S}\rangle_{\partial\mathcal{T}_h^S} + \left\langle\mathbf{S}(\mathrm{E}^{\mathbf{u}_S} - \mathrm{E}^{\widehat{\mathbf{u}}_S}),\Pi\boldsymbol{\varphi}_S\right\rangle_{\partial\mathcal{T}_h^S} - \langle\mathrm{E}^{\boldsymbol{\sigma}_S}\mathbf{n},\boldsymbol{\varphi}_S\rangle_{\partial\mathcal{T}_h^S}\,,
$$

and

$$
\begin{aligned}
S_3 \;:=\;& \left\langle\Pi\boldsymbol{\psi}_D\cdot\mathbf{n},\mathrm{E}^{\widehat{p}_D}\right\rangle_{\partial\mathcal{T}_h^D\setminus\Sigma} - \left\langle\Pi\boldsymbol{\psi}_D\cdot\mathbf{n},\mathrm{E}^{\widehat{p}_D}\right\rangle_\Sigma - \langle(\Pi\boldsymbol{\psi}_D - \boldsymbol{\psi}_D)\cdot\mathbf{n},\mathrm{E}^{p_D}\rangle_{\partial\mathcal{T}_h^D\setminus\Sigma}\\
&+\, \langle(\Pi\boldsymbol{\psi}_D - \boldsymbol{\psi}_D)\cdot\mathbf{n},\mathrm{E}^{p_D}\rangle_\Sigma - \left\langle\tau(\mathrm{E}^{p_D} - \mathrm{E}^{\widehat{p}_D}),\Pi\phi_D\right\rangle_{\partial\mathcal{T}_h^D}\,.
\end{aligned}
$$

Next, performing some simple algebraic manipulations, we find that

$$
\begin{aligned}
S_2 \;=\;& -\left\langle\mathrm{E}^{\mathbf{u}_S} - \mathrm{E}^{\widehat{\mathbf{u}}_S},(\Pi\mathbf{\Phi}_S - \mathbf{\Phi}_S)\mathbf{n} - \mathbf{S}(\Pi\boldsymbol{\varphi}_S - \boldsymbol{\varphi}_S)\right\rangle_{\partial\mathcal{T}_h^S} + \left\langle\mathbf{\Phi}_S\mathbf{n},\mathrm{E}^{\widehat{\mathbf{u}}_S}\right\rangle_{\partial\mathcal{T}_h^S}\\
&-\, \left\langle\mathrm{E}^{\boldsymbol{\sigma}_S}\mathbf{n} - \mathbf{S}(\mathrm{E}^{\mathbf{u}_S} - \mathrm{E}^{\widehat{\mathbf{u}}_S}),\boldsymbol{\varphi}_S\right\rangle_{\partial\mathcal{T}_h^S}
\end{aligned} \tag{5.32}
$$

and

$$
\begin{aligned}
S_3 \;=\;& -\left\langle\mathrm{E}^{p_D} - \mathrm{E}^{\widehat{p}_D},(\Pi\boldsymbol{\psi}_D - \boldsymbol{\psi}_D)\cdot\mathbf{n} + \tau(\Pi\phi_D - \phi_D)\right\rangle_{\partial\mathcal{T}_h^D\setminus\Sigma}\\
&+\, \left\langle\mathrm{E}^{p_D} - \mathrm{E}^{\widehat{p}_D},(\Pi\boldsymbol{\psi}_D - \boldsymbol{\psi}_D)\cdot\mathbf{n} - \tau(\Pi\phi_D - \phi_D)\right\rangle_\Sigma\\
&+\, \left\langle\boldsymbol{\psi}_D\cdot\mathbf{n},\mathrm{E}^{\widehat{p}_D}\right\rangle_{\partial\mathcal{T}_h^D\setminus\Sigma} - \left\langle\boldsymbol{\psi}_D\cdot\mathbf{n},\mathrm{E}^{\widehat{p}_D}\right\rangle_\Sigma - \left\langle\tau(\mathrm{E}^{p_D} - \mathrm{E}^{\widehat{p}_D}),\phi_D\right\rangle_{\partial\mathcal{T}_h^D}\,.
\end{aligned}
$$

Then, from (5.14c) with $\boldsymbol{\mu}_S := \mathrm{E}^{\mathbf{u}_S} - \mathrm{E}^{\widehat{\mathbf{u}}_S}$, we note that (5.32) reduces to

$$
S_2 \;=\; \left\langle\mathbf{\Phi}_S\mathbf{n},\mathrm{E}^{\widehat{\mathbf{u}}_S}\right\rangle_{\partial\mathcal{T}_h^S} - \left\langle\mathrm{E}^{\boldsymbol{\sigma}_S}\mathbf{n} - \mathbf{S}(\mathrm{E}^{\mathbf{u}_S} - \mathrm{E}^{\widehat{\mathbf{u}}_S}),\boldsymbol{P}_M(\boldsymbol{\varphi}_S)\right\rangle_{\partial\mathcal{T}_h^S}\,,
$$

from which, applying (5.19d) with $\boldsymbol{\mu}_{S,h} := \boldsymbol{P}_M(\boldsymbol{\varphi}_S)$, the continuity of $\boldsymbol{\Phi}_S\mathbf{n}$, the fact that $\mathrm{E}^{\widehat{\mathbf{u}}_S} = \mathbf{0}$ on Γ_S, and (5.29i), we deduce that

$$
\begin{aligned}
S_2 &= \left\langle \boldsymbol{\Phi}_S\mathbf{n}, \mathrm{E}^{\widehat{\mathbf{u}}_S} \right\rangle_\Sigma + \sum_{\ell=1}^{n-1} \kappa_\ell^{-1} \left\langle \mathrm{E}^{\widehat{\mathbf{u}}_S} \cdot \mathbf{t}_\ell, \boldsymbol{P}_M(\boldsymbol{\varphi}_S) \cdot \mathbf{t}_\ell \right\rangle_\Sigma + \left\langle \boldsymbol{P}_M(\boldsymbol{\varphi}_S) \cdot \mathbf{n}, \mathrm{E}^{\widehat{p}_D} \right\rangle_\Sigma \\
&= \left\langle \boldsymbol{\Phi}_S\mathbf{n} \;+\; \sum_{\ell=1}^{n-1} \kappa_\ell^{-1} (\boldsymbol{\varphi}_S \cdot \mathbf{t}_\ell)\mathbf{t}_\ell,\; \mathrm{E}^{\widehat{\mathbf{u}}_S} \right\rangle_\Sigma \;+\; \left\langle \boldsymbol{\varphi}_S \cdot \mathbf{n}, \mathrm{E}^{\widehat{p}_D} \right\rangle_\Sigma \\
&= -\left\langle \phi_D\mathbf{n}, \mathrm{E}^{\widehat{\mathbf{u}}_S} \right\rangle_\Sigma \;+\; \left\langle \boldsymbol{\varphi}_S \cdot \mathbf{n}, \mathrm{E}^{\widehat{p}_D} \right\rangle_\Sigma \\
&= -\left\langle \mathrm{E}^{\widehat{\mathbf{u}}_S} \cdot \mathbf{n}, \phi_D \right\rangle_\Sigma \;+\; \left\langle \boldsymbol{\varphi}_S \cdot \mathbf{n}, \mathrm{E}^{\widehat{p}_D} \right\rangle_\Sigma .
\end{aligned}
\tag{5.33}
$$

On the other hand, from (5.15c), (5.15d), and (5.19g) with $\psi_{D,h} := P_N(\phi_D)$, we have

$$
S_3 \;=\; \left\langle \boldsymbol{\psi}_D \cdot \mathbf{n}, \mathrm{E}^{\widehat{p}_D} \right\rangle_{\partial\mathcal{T}_h^D\setminus\Sigma} - \left\langle \boldsymbol{\psi}_D \cdot \mathbf{n}, \mathrm{E}^{\widehat{p}_D} \right\rangle_\Sigma + \left\langle \mathrm{E}^{\widehat{\mathbf{u}}_S} \cdot \mathbf{n}, \phi_D \right\rangle_\Sigma + \langle \mathrm{E}^{\mathbf{u}_D} \cdot \mathbf{n}, \phi_D \rangle_{\partial\mathcal{T}_h^D\setminus\Sigma} - \langle \mathrm{E}^{\mathbf{u}_D} \cdot \mathbf{n}, \phi_D \rangle_\Sigma \,,
$$

which, using the continuity of $\boldsymbol{\psi}_D \cdot \mathbf{n}$ and (5.29g), becomes

$$
S_3 \;=\; -\left\langle \boldsymbol{\psi}_D \cdot \mathbf{n}, \mathrm{E}^{\widehat{p}_D} \right\rangle_\Sigma + \left\langle \mathrm{E}^{\widehat{\mathbf{u}}_S} \cdot \mathbf{n}, \phi_D \right\rangle_\Sigma + \langle \mathrm{E}^{\mathbf{u}_D} \cdot \mathbf{n}, \phi_D \rangle_{\partial\mathcal{T}_h^D\setminus\Sigma} - \langle \mathrm{E}^{\mathbf{u}_D} \cdot \mathbf{n}, \phi_D \rangle_\Sigma \,.
$$

In this way, from (5.33) and (5.29h), we find that

$$
\begin{aligned}
S_2 \;+\; S_3 &= \left\langle \boldsymbol{\varphi}_S \cdot \mathbf{n} - \boldsymbol{\psi}_D \cdot \mathbf{n}, \mathrm{E}^{\widehat{p}_D} \right\rangle_\Sigma + \langle \mathrm{E}^{\mathbf{u}_D} \cdot \mathbf{n}, \phi_D \rangle_{\partial\mathcal{T}_h^D\setminus\Sigma} - \langle \mathrm{E}^{\mathbf{u}_D} \cdot \mathbf{n}, \phi_D \rangle_\Sigma \\
&= \langle \mathrm{E}^{\mathbf{u}_D} \cdot \mathbf{n}, \phi_D \rangle_{\partial\mathcal{T}_h^D\setminus\Sigma} \;-\; \langle \mathrm{E}^{\mathbf{u}_D} \cdot \mathbf{n}, \phi_D \rangle_\Sigma \,,
\end{aligned}
$$

and replacing the above expression back into (5.31), we obtain

$$
\begin{aligned}
&\|\mathrm{E}^{\mathbf{u}_S}\|_{0,\Omega_S}^2 \;+\; \|\mathrm{E}^{p_D}\|_{0,\Omega_D}^2 \;=\; S_1 \\
&\quad= -\frac{1}{\nu}((\mathrm{E}^{\boldsymbol{\sigma}_S})^{\mathtt{d}}, \Pi\boldsymbol{\Phi}_S - \boldsymbol{\Phi}_S)_{\mathcal{T}_h^S} - ((\mathrm{E}^{\boldsymbol{\sigma}_S})^{\mathtt{d}}, \boldsymbol{\mathcal{P}}_A(\boldsymbol{\gamma}_S) - \boldsymbol{\gamma}_S)_{\mathcal{T}_h^S} \\
&\qquad - (\mathrm{E}^{\boldsymbol{\rho}_S}, \Pi\boldsymbol{\Phi}_S - \boldsymbol{\Phi}_S)_{\mathcal{T}_h^S} - (\boldsymbol{\mathcal{P}}_A(\boldsymbol{\rho}_S) - \boldsymbol{\rho}_S, \Pi\boldsymbol{\Phi}_S - \boldsymbol{\Phi}_S)_{\mathcal{T}_h^S} + \frac{1}{\nu}(\Pi\boldsymbol{\sigma}_S - \boldsymbol{\sigma}_S, (\Pi\boldsymbol{\Phi}_S - \boldsymbol{\Phi}_S)^{\mathtt{d}})_{\mathcal{T}_h^S} \\
&\qquad + (\Pi\boldsymbol{\sigma}_S - \boldsymbol{\sigma}_S, \boldsymbol{\mathcal{P}}_A(\boldsymbol{\gamma}_S) - \boldsymbol{\gamma}_S)_{\mathcal{T}_h^S} + (\mathbf{K}^{-1}\mathrm{E}^{\mathbf{u}_D}, \Pi\boldsymbol{\psi}_D - \boldsymbol{\psi}_D)_{\mathcal{T}_h^D} \\
&\qquad - (\mathbf{K}^{-1}(\Pi\mathbf{u}_D - \mathbf{u}_D), \Pi\boldsymbol{\psi}_D - \boldsymbol{\psi}_D)_{\mathcal{T}_h^D} + (\Pi\boldsymbol{\sigma}_S - \boldsymbol{\sigma}_S, \frac{1}{\nu}\boldsymbol{\Phi}_S^{\mathtt{d}} + \boldsymbol{\gamma}_S)_{\mathcal{T}_h^S} - (\Pi\mathbf{u}_D - \mathbf{u}_D, \mathbf{K}^{-1}\boldsymbol{\psi}_D)_{\mathcal{T}_h^D} \\
&\quad= -\frac{1}{\nu}((\mathrm{E}^{\boldsymbol{\sigma}_S})^{\mathtt{d}}, \Pi\boldsymbol{\Phi}_S - \boldsymbol{\Phi}_S)_{\mathcal{T}_h^S} - ((\mathrm{E}^{\boldsymbol{\sigma}_S})^{\mathtt{d}}, \boldsymbol{\mathcal{P}}_A(\boldsymbol{\gamma}_S) - \boldsymbol{\gamma}_S)_{\mathcal{T}_h^S} \\
&\qquad - (\mathrm{E}^{\boldsymbol{\rho}_S}, \Pi\boldsymbol{\Phi}_S - \boldsymbol{\Phi}_S)_{\mathcal{T}_h^S} - (\boldsymbol{\mathcal{P}}_A(\boldsymbol{\rho}_S) - \boldsymbol{\rho}_S, \Pi\boldsymbol{\Phi}_S - \boldsymbol{\Phi}_S)_{\mathcal{T}_h^S} + \frac{1}{\nu}(\Pi\boldsymbol{\sigma}_S - \boldsymbol{\sigma}_S, (\Pi\boldsymbol{\Phi}_S - \boldsymbol{\Phi}_S)^{\mathtt{d}})_{\mathcal{T}_h^S} \\
&\qquad + (\Pi\boldsymbol{\sigma}_S - \boldsymbol{\sigma}_S, \boldsymbol{\mathcal{P}}_A(\boldsymbol{\gamma}_S) - \boldsymbol{\gamma}_S)_{\mathcal{T}_h^S} + (\mathbf{K}^{-1}\mathrm{E}^{\mathbf{u}_D}, \Pi\boldsymbol{\psi}_D - \boldsymbol{\psi}_D)_{\mathcal{T}_h^D} \\
&\qquad - (\mathbf{K}^{-1}(\Pi\mathbf{u}_D - \mathbf{u}_D), \Pi\boldsymbol{\psi}_D - \boldsymbol{\psi}_D)_{\mathcal{T}_h^D} + (\Pi\boldsymbol{\sigma}_S - \boldsymbol{\sigma}_S, \nabla\boldsymbol{\varphi}_S)_{\mathcal{T}_h^S} + (\Pi\mathbf{u}_D - \mathbf{u}_D, \nabla\phi_D)_{\mathcal{T}_h^D} \,,
\end{aligned}
$$

where in the last identity we have applied (5.29a) and (5.29e). Now, from (5.14a) and (5.15a) we note that

$$
(\Pi\boldsymbol{\sigma}_S - \boldsymbol{\sigma}_S, \nabla\boldsymbol{\varphi}_S)_{\mathcal{T}_h^S} \;=\; (\Pi\boldsymbol{\sigma}_S - \boldsymbol{\sigma}_S, \nabla\boldsymbol{\varphi}_S - \boldsymbol{P}_0(\nabla\boldsymbol{\varphi}_S))_{\mathcal{T}_h^S}
$$

and

$$
(\Pi\mathbf{u}_D - \mathbf{u}_D, \nabla\phi_D)_{\mathcal{T}_h^D} \;=\; (\Pi\mathbf{u}_D - \mathbf{u}_D, \nabla\phi_D - P_0(\nabla\phi_D))_{\mathcal{T}_h^D}
$$

where $\boldsymbol{P}_0|_T$ and $P_0|_K$ are the $\mathbf{L}^2(T)$ and $L^2(K)$ projections onto $\mathbf{P}_0(T)$ and $\mathrm{P}_0(K)$, respectively, for each $T \in \mathcal{T}_h^S$ and $K \in \mathcal{T}_h^D$. Hence, applying the Cauchy-Schwarz inequality, we obtain

$$\begin{aligned}\|\mathrm{E}^{\mathbf{u}_S}\|_{0,\Omega_S}^2 + \|\mathrm{E}^{p_D}\|_{0,\Omega_D}^2 \;\leq\; & C\Big\{\|(\mathrm{E}^{\boldsymbol{\sigma}_S})^{\mathtt{d}}\|_{0,\Omega_S} + \|\mathrm{E}^{\boldsymbol{\rho}_S}\|_{0,\Omega_S} + \|\mathrm{E}^{\mathbf{u}_D}\|_{0,\Omega_D} + \|\Pi\boldsymbol{\sigma}_S - \boldsymbol{\sigma}_S\|_{0,\Omega_S} \\ & + \|\boldsymbol{\mathcal{P}}_A(\boldsymbol{\rho}_S) - \boldsymbol{\rho}_S\|_{0,\Omega_S} + \|\Pi\mathbf{u}_D - \mathbf{u}_D\|_{0,\Omega_D}\Big\}\Big\{\|\Pi\boldsymbol{\Phi}_S - \boldsymbol{\Phi}_S\|_{0,\Omega_S} + \|\boldsymbol{\mathcal{P}}_A(\boldsymbol{\gamma}_S) - \boldsymbol{\gamma}_S\|_{0,\Omega_S} \\ & + \|\Pi\boldsymbol{\psi}_D - \boldsymbol{\psi}_D\|_{0,\Omega_D} + \|\boldsymbol{P}_0(\nabla\boldsymbol{\varphi}_S) - \nabla\boldsymbol{\varphi}_S\|_{0,\Omega_S} + \|P_0(\nabla\phi_D) - \nabla\phi_D\|_{0,\Omega_D}\Big\},\end{aligned}$$

from which, using the approximation properties of Π_S and Π_D (cf. Theorems 5.2 and 5.4), and those of $\boldsymbol{\mathcal{P}}_A$ (cf. (5.16)), $\boldsymbol{P}_0$ and P_0 (see, e.g. [37]), we deduce that

$$\begin{aligned}\|\mathrm{E}^{\mathbf{u}_S}\|_{0,\Omega_S}^2 + \|\mathrm{E}^{p_D}\|_{0,\Omega_D}^2 \;\leq\; & C\,h\Big\{\|(\mathrm{E}^{\boldsymbol{\sigma}_S})^{\mathtt{d}}\|_{0,\Omega_S} + \|\mathrm{E}^{\boldsymbol{\rho}_S}\|_{0,\Omega_S} + \|\mathrm{E}^{\mathbf{u}_D}\|_{0,\Omega_D} + \|\Pi\boldsymbol{\sigma}_S - \boldsymbol{\sigma}_S\|_{0,\Omega_S} \\ & + \|\boldsymbol{\mathcal{P}}_A(\boldsymbol{\rho}_S) - \boldsymbol{\rho}_S\|_{0,\Omega_S} + \|\Pi\mathbf{u}_D - \mathbf{u}_D\|_{0,\Omega_D}\Big\}\Big\{\sum_{T\in\mathcal{T}_h^S}\Big(|\boldsymbol{\Phi}_S|_{1,T} + |\boldsymbol{\varphi}_S|_{1,\Omega_S} + \|\mathbf{div}(\boldsymbol{\Phi}_S)\|_{0,T} \\ & + |\boldsymbol{\gamma}_S|_{1,T} + |\nabla\boldsymbol{\varphi}_S|_{1,T}\Big) + \sum_{T\in\mathcal{T}_h^D}\Big(|\boldsymbol{\psi}_D|_{1,T} + |\phi_D|_{1,T} + |\nabla\phi_D|_{1,T}\Big)\Big\}.\end{aligned}$$

Finally, the regularity estimate (5.30) and (5.29b) finish the proof. $\square$

Estimating $\mathrm{E}^{\widehat{\mathbf{u}}_S}$ and $\mathrm{E}^{\widehat{p}_D}$

Our next goal is to derive estimates for the trace variables. To this end, as in [43, 44], we measure the errors of quantities defined on $\partial\mathcal{T}_h^S$ and $\partial\mathcal{T}_h^D$ with the seminorms:

$$\|\boldsymbol{\mu}_{S,h}\|_h \;:=\; \left\{\sum_{T\in\mathcal{T}_h^S} h_T\|\boldsymbol{\mu}_{S,h}\|_{0,\partial T}^2\right\}^{1/2} \quad\text{and}\quad \|\psi_{D,h}\|_h \;:=\; \left\{\sum_{T\in\mathcal{T}_h^D} h_T\|\psi_{D,h}\|_{0,\partial T}^2\right\}^{1/2},$$

respectively. In this way, the following lemma uses ideas from [43, Lemma 3.7] and [44, Theorem 4.1] to obtain estimates for $\|\mathrm{E}^{\widehat{\mathbf{u}}_S}\|_h$ and $\|\mathrm{E}^{\widehat{p}_D}\|_h$.

Lemma 5.7. *There hold*

$$\|\mathrm{E}^{\widehat{\mathbf{u}}_S}\|_h \leq C\left\{h\Big(\|(\mathrm{E}^{\boldsymbol{\sigma}_S})^{\mathtt{d}}\|_{0,\Omega_S} + \|\mathrm{E}^{\boldsymbol{\rho}_S}\|_{0,\Omega_S} + \|\Pi\boldsymbol{\sigma}_S - \boldsymbol{\sigma}_S\|_{0,\Omega_S} + \|\boldsymbol{\mathcal{P}}_A(\boldsymbol{\rho}_S) - \boldsymbol{\rho}_S\|_{0,\Omega_S}\Big) + \|\mathrm{E}^{\mathbf{u}_S}\|_{0,\Omega_S}\right\}$$

and

$$\|\mathrm{E}^{\widehat{p}_D}\|_h \;\leq\; C\left\{h\Big(\|\mathrm{E}^{\mathbf{u}_D}\|_{0,\Omega_D} + \|\Pi\mathbf{u}_D - \mathbf{u}_D\|_{0,\Omega_D}\Big) \;+\; \|\mathrm{E}^{p_D}\|_{0,\Omega_D}\right\}.$$

Proof. The proof follows from a straightforward adaptation of the proofs in [43, Lemma 3.7] and [44, Theorem 4.1]. The main tools employed are the error equations (5.19a) and (5.19e), a standard scaling argument (see [18]), the Cauchy-Schwarz inequality, and an inverse inequality. $\square$

The main result

As a consequence of the lemmas provided in the previous sections, now we are able to establish the *a priori* error estimates for the HDG scheme (5.7).

Theorem 5.5. *There exists $C > 0$, independent of h, such that*

$$\begin{aligned}
&\|\boldsymbol{\sigma}_S - \boldsymbol{\sigma}_{S,h}\|_{0,\Omega_S} \ + \ \|\boldsymbol{\rho}_S - \boldsymbol{\rho}_{S,h}\|_{0,\Omega_S} \ + \ \|\mathbf{u}_D - \mathbf{u}_{D,h}\|_{0,\Omega_D} \\
&\quad \leq \ C\Big\{ \|\Pi\boldsymbol{\sigma}_S - \boldsymbol{\sigma}_S\|_{0,\Omega_S} + \|\boldsymbol{\mathcal{P}}_A(\boldsymbol{\rho}_S) - \boldsymbol{\rho}_S\|_{0,\Omega_S} + \|\Pi\mathbf{u}_D - \mathbf{u}_D\|_{0,\Omega_D} \Big\},
\end{aligned}$$

$$\begin{aligned}
&\|\mathbf{u}_S - \mathbf{u}_{S,h}\|_{0,\Omega_S} \\
&\quad \leq \ C\Big\{ \|\Pi\boldsymbol{\sigma}_S - \boldsymbol{\sigma}_S\|_{0,\Omega_S} + \|\Pi\mathbf{u}_S - \mathbf{u}_S\|_{0,\Omega_S} + \|\boldsymbol{\mathcal{P}}_A(\boldsymbol{\rho}_S) - \boldsymbol{\rho}_S\|_{0,\Omega_S} + \|\Pi\mathbf{u}_D - \mathbf{u}_D\|_{0,\Omega_D} \Big\},
\end{aligned}$$

$$\begin{aligned}
&\|p_D - p_{D,h}\|_{0,\Omega_D} \\
&\quad \leq \ C\Big\{ \|\Pi\boldsymbol{\sigma}_S - \boldsymbol{\sigma}_S\|_{0,\Omega_S} + \|\boldsymbol{\mathcal{P}}_A(\boldsymbol{\rho}_S) - \boldsymbol{\rho}_S\|_{0,\Omega_S} + \|\Pi\mathbf{u}_D - \mathbf{u}_D\|_{0,\Omega_D} + \|\Pi p_D - p_D\|_{0,\Omega_D} \Big\},
\end{aligned}$$

and

$$\begin{aligned}
&\|\mathrm{E}^{\widehat{\mathbf{u}}_S}\|_h \ + \ \|\mathrm{E}^{\widehat{p}_D}\|_h \\
&\quad \leq \ C\,h\Big\{ \|\Pi\boldsymbol{\sigma}_S - \boldsymbol{\sigma}_S\|_{0,\Omega_S} + \|\boldsymbol{\mathcal{P}}_A(\boldsymbol{\rho}_S) - \boldsymbol{\rho}_S\|_{0,\Omega_S} + \|\Pi\mathbf{u}_D - \mathbf{u}_D\|_{0,\Omega_D} \Big\}.
\end{aligned}$$

Moreover, the following theorem provides the corresponding theoretical rates of convergence.

Theorem 5.6. *There exists $C > 0$, independent of h, such that*

$$\begin{aligned}
&\|\boldsymbol{\sigma}_S - \boldsymbol{\sigma}_{S,h}\|_{0,\Omega_S} \ + \ \|\mathbf{u}_S - \mathbf{u}_{S,h}\|_{0,\Omega_S} \ + \ \|\boldsymbol{\rho}_S - \boldsymbol{\rho}_{S,h}\|_{0,\Omega_S} \ + \ \|\mathbf{u}_D - \mathbf{u}_{D,h}\|_{0,\Omega_D} \\
&\quad \leq \ C\,h^{\min\{\ell_{\boldsymbol{\sigma}_S}+1,\ell_{\mathbf{u}_S}+1,\ell_{\boldsymbol{\rho}_S}\}} \sum_{T\in\mathcal{T}_h^S} \Big\{ |\boldsymbol{\sigma}_S|_{\ell_{\boldsymbol{\sigma}_S}+1,T} + |\mathbf{u}_S|_{\ell_{\mathbf{u}_S}+1,T} + |\boldsymbol{\rho}_S|_{\ell_{\boldsymbol{\rho}_S},T} + |\mathbf{div}(\boldsymbol{\sigma}_S)|_{\ell_{\boldsymbol{\sigma}_S},T} \Big\} \\
&\qquad + \ C\,h^{\min\{\ell_{\mathbf{u}_D}+1,\ell_{p_D}+1\}} \sum_{T\in\mathcal{T}_h^D} \Big\{ |\mathbf{u}_D|_{\ell_{\mathbf{u}_D}+1,T} + |p_D|_{\ell_{p_D}+1,T} \Big\},
\end{aligned}$$

$$\begin{aligned}
&\|p_D - p_{D,h}\|_{0,\Omega_D} \\
&\quad \leq \ C\,h^{\min\{\ell_{\boldsymbol{\sigma}_S}+1,\ell_{\mathbf{u}_S}+1,\ell_{\boldsymbol{\rho}_S}\}} \sum_{T\in\mathcal{T}_h^S} \Big\{ |\boldsymbol{\sigma}_S|_{\ell_{\boldsymbol{\sigma}_S}+1,T} + |\mathbf{u}_S|_{\ell_{\mathbf{u}_S}+1,T} + |\boldsymbol{\rho}_S|_{\ell_{\boldsymbol{\rho}_S},T} + |\mathbf{div}(\boldsymbol{\sigma}_S)|_{\ell_{\boldsymbol{\sigma}_S},T} \Big\} \\
&\qquad + \ C\,h^{\min\{\ell_{\mathbf{u}_D}+1,\ell_{p_D}+1\}} \sum_{T\in\mathcal{T}_h^D} \Big\{ |\mathbf{u}_D|_{\ell_{\mathbf{u}_D}+1,T} + |p_D|_{\ell_{p_D}+1,T} + |\mathrm{div}(\mathbf{u}_D)|_{\ell_{\mathbf{u}_D},T} \Big\},
\end{aligned}$$

and

$$\begin{aligned}
&\|\boldsymbol{P}_M(\mathbf{u}_S) - \boldsymbol{\lambda}_{S,h}\|_h \ + \ \|P_N(p_D) - \varphi_{D,h}\|_h \\
&\quad \leq \ C\,h^{1+\min\{\ell_{\boldsymbol{\sigma}_S}+1,\ell_{\mathbf{u}_S}+1,\ell_{\boldsymbol{\rho}_S}\}} \sum_{T\in\mathcal{T}_h^S} \Big\{ |\boldsymbol{\sigma}_S|_{\ell_{\boldsymbol{\sigma}_S}+1,T} + |\mathbf{u}_S|_{\ell_{\mathbf{u}_S}+1,T} + |\boldsymbol{\rho}_S|_{\ell_{\boldsymbol{\rho}_S},T} + |\mathbf{div}(\boldsymbol{\sigma}_S)|_{\ell_{\boldsymbol{\sigma}_S},T} \Big\} \\
&\qquad + \ C\,h^{1+\min\{\ell_{\mathbf{u}_D}+1,\ell_{p_D}+1\}} \sum_{T\in\mathcal{T}_h^D} \Big\{ |\mathbf{u}_D|_{\ell_{\mathbf{u}_D}+1,T} + |p_D|_{\ell_{p_D}+1,T} \Big\},
\end{aligned}$$

for $\ell_{\boldsymbol{\sigma}_S}, \ell_{\mathbf{u}_S}, \ell_{\mathbf{u}_D}, \ell_{p_D} \in [0,k]$ and $\ell_{\boldsymbol{\rho}_S} \in [0,k+1]$.

Proof. It follows from Theorem 5.5 and the approximation properties of Π_S and Π_D (cf. Theorems 5.2 and 5.4), and those of $\boldsymbol{\mathcal{P}}_A$ (cf. (5.16)). $\square$

In addition, we know from (5.2) that $p_S = -\frac{1}{n}\,\mathrm{tr}\,(\boldsymbol{\sigma}_S)$, which suggests to define the following postprocessed approximation of the pressure:

$$p_{S,h} \;:=\; -\frac{1}{n}\,\mathrm{tr}\,(\boldsymbol{\sigma}_{S,h}) \quad \text{in} \quad \Omega_S\,, \tag{5.34}$$

and therefore

$$\|p_S - p_{S,h}\|_{0,\Omega_S} \;=\; \frac{1}{n}\,\|\mathrm{tr}\,(\boldsymbol{\sigma}_S - \boldsymbol{\sigma}_{S,h})\,\|_{0,\Omega_S} \;\leq\; \|\boldsymbol{\sigma}_S - \boldsymbol{\sigma}_{S,h}\|_{0,\Omega_S}\,, \tag{5.35}$$

which, thanks to Theorem 5.6, gives the *a priori* error estimate for the pressure in the fluid as well.

5.5 Numerical results

In this section we present three numerical experiments illustrating the performance of the HDG method (5.7) introduced and analyzed in Section 5.3. We let N_{total} be the total number of degrees of freedom, and N_{comp} be the number of degrees of freedom effectively employed in the computations (involved in the resolution of the corresponding linear system). In other words, N_{total} is the total number of unknowns defining $\boldsymbol{\sigma}_{S,h}$, $\mathbf{u}_{S,h}$, $\boldsymbol{\rho}_{S,h}$, $\boldsymbol{\lambda}_{S,h}$, $\mathbf{u}_{D,h}$, $p_{D,h}$ and $\varphi_{D,h}$, whereas N_{comp} is the total number of unknowns defining $\boldsymbol{\lambda}_{S,h}$ and $\varphi_{D,h}$ plus one constant for each $T \in \mathcal{T}_h^S$, which take care of the condition $\int_{\Omega_S} \mathrm{tr}\,(\boldsymbol{\sigma}_S) = 0$ (see Chapter 3, Section 3.5 for details). Also, the individual errors are defined by

$$\begin{gathered}
\mathtt{e}(\boldsymbol{\sigma}_S) \;:=\; \|\boldsymbol{\sigma}_S - \boldsymbol{\sigma}_{S,h}\|_{0,\Omega_S}\,, \quad \mathtt{e}(\mathbf{u}_S) \;:=\; \|\mathbf{u}_S - \mathbf{u}_{S,h}\|_{0,\Omega_S}\,, \quad \mathtt{e}(\boldsymbol{\rho}_S) \;:=\; \|\boldsymbol{\rho}_S - \boldsymbol{\rho}_{S,h}\|_{0,\Omega_S}\,,\\
\mathtt{e}(\boldsymbol{\lambda}_S) \;:=\; \|\boldsymbol{P}_M(\mathbf{u}_S) - \boldsymbol{\lambda}_{S,h}\|_h\,, \quad \mathtt{e}(p_S) \;:=\; \|p_S - p_{S,h}\|_{0,\Omega_S}\,, \quad \mathtt{e}(\mathbf{u}_D) \;:=\; \|\mathbf{u}_D - \mathbf{u}_{D,h}\|_{0,\Omega_D}\,,\\
\mathtt{e}(p_D) \;:=\; \|p_D - p_{D,h}\|_{0,\Omega_D}\,, \quad \text{and} \quad \mathtt{e}(\varphi_D) \;:=\; \|P_N(p_D) - \varphi_{D,h}\|_h\,,
\end{gathered}$$

where $p_{S,h}$ is computed by the postprocessing formulae (5.34). Then, we define the experimental rates of convergence as

$$\mathtt{r}(\cdot) \;:=\; \frac{\log\big(\mathtt{e}(\cdot)\,/\,\mathtt{e}'(\cdot)\big)}{\log(h\,/\,h')}\,,$$

where $\mathtt{e}$ and $\mathtt{e}'$ denote the corresponding errors for two consecutive triangulations with mesh sizes h and h', respectively.

The examples to be considered in this section are described next. In all of them we choose $\nu = 1$, $\kappa_1 = \ldots = \kappa_{n-1} = 1$, $\mathbf{S}|_F = \mathbb{I}$ for all $F \in \mathcal{E}_h^S$, and $\tau|_F = 1$ in each $F \in \mathcal{E}_h^D$. Example 1 ($n = 2$) and 2 ($n = 3$) are used to illustrate the performance of the HDG scheme (5.7) and to corroborate the rates of convergence given in Theorem 5.6, when the solution is regular enough and the domains are convex. Example 3 ($n = 2$) is utilized to illustrate the behaviour of the same estimate for non convex domains and solutions with low regularity. We use $k \in \{1, 2, 3\}$ and $k \in \{1, 2\}$ for the 2D and 3D numerical experiments, respectively. The numerical results presented below were obtained using a C++ code, which was developed following the same techniques from [34] (see also Chapter 3).

In Example 1 we consider the regions $\Omega_S := (0,1) \times (0,1)$ and $\Omega_D := (0,1) \times (-1,0)$, $\mathbf{K} = \mathbb{I}$, and the data $\mathbf{f}_S$ and f_D are chosen so that the exact solution is given by

$$\begin{aligned}
\mathbf{u}_S(\mathbf{x}) \;&=\; \mathbf{curl}\Big(x_1 x_2^2 (x_1 - 1)(x_2 - 1)\sin(\pi x_1)\sin(\pi x_2)\Big)\,,\\
p_S(\mathbf{x}) \;&=\; \cos(\pi x_1)\cos(\pi x_2)\,,
\end{aligned}$$

for all $\mathbf{x} := (x_1, x_2) \in \Omega_S$, and

$$p_D(\mathbf{x}) \quad = \quad \cos(\pi x_1)\cos(\pi x_2) \quad \forall\, \mathbf{x} := (x_1, x_2) \in \Omega_D\,,$$

where $\mathbf{curl}(v) := \left(\frac{\partial v}{\partial x_2},\ -\frac{\partial v}{\partial x_1}\right)^{\mathtt{t}}$. Concerning the triangulations employed in our computations, we first consider seven meshes that are Cartesian refinements of a domain defined in terms of squares, and then we split each square into four congruent triangles.

In Example 2 we consider $\Omega_S := (0,1)^2 \times \left(\frac{1}{2}, 1\right)$ and $\Omega_D := (0,1)^2 \times \left(0, \frac{1}{2}\right)$, $\mathbf{K} = \left(\begin{smallmatrix} 2 & -1 & 0 \\ -1 & 2 & -1 \\ 0 & -1 & 2 \end{smallmatrix}\right)$, and choose the data $\mathbf{f}_S$ and f_D so that the exact solution is given by

$$\begin{aligned}
\mathbf{u}_S(\mathbf{x}) \quad &= \quad \mathrm{curl}\begin{pmatrix} x_1^2(1-x_1)^2 x_2^2(1-x_2)^2(1-x_3)^2(1-2x_3)^3\sin(\pi x_1) \\ x_1^2(1-x_1)^2 x_2^2(1-x_2)^2(1-x_3)^2(1-2x_3)^3\sin(\pi x_2) \\ x_1^2(1-x_1)^2 x_2^2(1-x_2)^2(1-x_3)^2(1-2x_3)^3\sin(\pi x_3) \end{pmatrix}, \\
p_S(\mathbf{x}) \quad &= \quad \cos(\pi x_2)\cos(\pi x_3)\exp(x_1)\,,
\end{aligned}$$

for all $\mathbf{x} := (x_1, x_2, x_3) \in \Omega_S$, and

$$p_D(\mathbf{x}) \quad = \quad x_1 x_2 x_3 (1-x_1)(1-x_2)(1-2x_3)^2 \sin(2\pi x_1)\sin(2\pi x_2)\sin(\pi x_3)\,,$$

for all $\mathbf{x} := (x_1, x_2, x_3) \in \Omega_D$.

Finally, in Example 3 we consider $\mathbf{K} = 5\,\mathbb{I}$, $\Omega_D := (-1,1)\times(-2,-1)$, and let Ω_S be the L-shaped domain given by $(-1,1)^2 \setminus [0,1]^2$. Then we choose $\mathbf{f}_S$ and f_D so that the exact solution is given by

$$\begin{aligned}
\mathbf{u}_S(\mathbf{x}) \quad &= \quad \mathbf{curl}\left(3(x_1^2 + x_2^2)^{5/6}(x_2+1)^3\right)\,, \\
p_S(\mathbf{x}) \quad &= \quad \frac{1}{5}(x_1^3 - 3x_1)\cos(\pi x_2)\,,
\end{aligned}$$

for all $\mathbf{x} := (x_1, x_2) \in \Omega_S$, and

$$p_D(\mathbf{x}) \quad = \quad \frac{1}{5}(x_1^3 - 3x_1)\cos(\pi x_2) \quad \forall\, \mathbf{x} := (x_1, x_2) \in \Omega_D\,.$$

Note that $\mathbf{u}_S$ is divergence free, $\int_{\Omega_S} p_S = 0$, and $\nabla \mathbf{u}_S$ has a singularity at the origin. In addition, it is easy to check that this solution satisfies $\mathbf{u}_S \cdot \mathbf{n} = \mathbf{u}_D \cdot \mathbf{n}$ on Σ, and the boundary condition $\mathbf{u}_D \cdot \mathbf{n} = 0$ on Γ_D. However, the Dirichlet condition for the Stokes velocity on Γ_S is non-homogeneous ($\mathbf{u}_S = \mathbf{g} \neq \mathbf{0}$ on Γ_S). For that reason, we have modified our implementation to allow non-zero Dirichlet conditions. It is important to remark here that all the analysis in the previous sections can be extended straightforwardly to this case by eliminating the condition $\boldsymbol{\mu}|_{\Gamma_S} = \mathbf{0}$ in the definition of the subspace $\mathbf{M}_h$, and then considering in (5.7) the new equation $\left\langle \widehat{\mathbf{u}}_{S,h}, \boldsymbol{\mu}_{S,h} \right\rangle_{\Gamma_S} = \left\langle \mathbf{g}, \boldsymbol{\mu}_{S,h} \right\rangle_{\Gamma_S}\ \forall\, \boldsymbol{\mu}_{S,h} \in \mathbf{M}_h$.

In Tables 5.1−5.4 we summarize the convergence history of the HDG method (5.7) as applied to Examples 1 and 2. We observe there, looking at the experimental rates of convergence, that the orders predicted for each k by Theorem 5.6, are attained in all the unknowns for these smooth examples. In particular, $\|\boldsymbol{P}_M(\mathbf{u}_S) - \boldsymbol{\lambda}_{S,h}\|_h$ and $\|P_N(p_D) - \varphi_{D,h}\|_h$ present a superconvergence with an additional powers of h, also as predicted in Theorem 5.6.

On the other hand, in Tables 5.5−5.6 we summarize the convergence history of the HDG method (5.7) as applied to Example 3 for the polynomial degrees $k \in \{1, 2, 3\}$. In this case, and because of the singularity at the origin of the exact solution, the theoretical orders of convergence are far to be attained. In fact, it is easy to show that $\mathbf{u}_S$ belong to $\mathbf{H}^{4/3}(\Omega_S)$, whence $\boldsymbol{\sigma}_S \in \mathbb{H}^{2/3}(\Omega_S)$, which implies that we can expect $\|\Pi\boldsymbol{\sigma}_S - \boldsymbol{\sigma}_S\|_{0,\Omega_S} = \mathcal{O}(h^{2/3})$. We use here that Π_S can also be defined for $\boldsymbol{\sigma}_S \in \mathbb{H}^\delta(\mathcal{T}_h^S)$ with $\delta > 1/2$. Thus, thanks to Theorem 5.6 and (5.35), we can explain the *a priori* estimates in Tables 5.5−5.6 for $\boldsymbol{\sigma}_S$, $\mathbf{u}_S$, $\boldsymbol{\rho}_S$, p_S, and also for $\|\boldsymbol{P}_M(\mathbf{u}_S) - \boldsymbol{\lambda}_{S,h}\|_h$ and $\|P_N(p_D) - \varphi_{D,h}\|_h$, which must converge with $\mathcal{O}(h^{1+2/3})$. In addition, the convergence of $\mathbf{u}_D$ and p_D is a bit faster than expected, which could correspond to a special feature of this example.

Finally, some components of the approximate solutions for the three examples are displayed in Figures 5.2, 5.3 and 5.4. They all correspond to those obtained with the fourth mesh and for the polynomial degree $k = 2$. Here we use the notations $\boldsymbol{\sigma}_{S,h} = (\,[\boldsymbol{\sigma}_{S,h}]_{ij}\,)_{i,j=1,\dots,n}$, $\boldsymbol{\rho}_{S,h} = (\,[\boldsymbol{\rho}_{S,h}]_{ij}\,)_{i,j=1,\dots,n}$, and $\mathbf{u}_{*,h} = (\,[\mathbf{u}_{*,h}]_i\,)_{i=1,\dots,n}$ for $* \in \{S, D\}$.

k	h	N_{total}	N_{comp}	$\mathtt{e}(\boldsymbol{\sigma}_S)$	$\mathtt{r}(\boldsymbol{\sigma}_S)$	$\mathtt{e}(\mathbf{u}_S)$	$\mathtt{r}(\mathbf{u}_S)$	$\mathtt{e}(\boldsymbol{\rho}_S)$	$\mathtt{r}(\boldsymbol{\rho}_S)$	$\mathtt{e}(\boldsymbol{\lambda}_S)$	$\mathtt{r}(\boldsymbol{\lambda}_S)$	$\mathtt{e}(p_S)$	$\mathtt{r}(p_S)$
	0.2000	8290	2091	2.00e-2	−−	4.15e-3	−−	1.70e-2	−−	1.42e-3	−−	8.56e-3	−−
	0.1000	32980	8181	5.42e-3	1.89	1.06e-3	1.97	4.83e-3	1.82	2.01e-4	2.81	2.39e-3	1.84
	0.0667	74070	18271	2.47e-3	1.94	4.74e-4	1.99	2.23e-3	1.90	6.23e-5	2.90	1.10e-3	1.91
1	0.0500	131560	32361	1.41e-3	1.96	2.67e-4	1.99	1.28e-3	1.93	2.68e-5	2.93	6.30e-4	1.94
	0.0400	205450	50451	9.06e-4	1.97	1.71e-4	2.00	8.28e-4	1.95	1.39e-5	2.94	4.07e-4	1.95
	0.0333	295740	72541	6.32e-4	1.97	1.19e-4	2.00	5.79e-4	1.96	8.11e-6	2.96	2.85e-4	1.96
	0.0286	402430	98631	4.66e-4	1.98	8.74e-5	2.00	4.28e-4	1.97	5.14e-6	2.96	2.10e-4	1.97
	0.2000	15435	3036	1.65e-3	−−	3.11e-4	−−	1.55e-3	−−	8.22e-5	−−	6.99e-4	−−
	0.1000	61470	11871	2.05e-4	3.01	3.99e-5	2.96	1.92e-4	3.01	5.00e-6	4.04	8.58e-5	3.03
	0.0667	138105	26506	6.04e-5	3.01	1.19e-5	2.98	5.66e-5	3.01	9.80e-7	4.02	2.53e-5	3.01
2	0.0500	245340	46941	2.55e-5	3.00	5.04e-6	2.99	2.39e-5	3.00	3.09e-7	4.01	1.06e-5	3.01
	0.0400	383175	73176	1.30e-5	3.00	2.58e-6	2.99	1.22e-5	3.00	1.27e-7	4.00	5.43e-6	3.01
	0.0333	551610	105211	7.54e-6	3.00	1.50e-6	2.99	7.07e-6	3.00	6.10e-8	4.00	3.14e-6	3.00
	0.0286	750645	143046	4.75e-6	3.00	9.43e-7	3.00	4.45e-6	3.00	3.29e-8	4.00	1.98e-6	3.00
	0.2000	24580	3981	1.08e-4	−−	2.10e-5	−−	9.98e-5	−−	4.05e-6	−−	4.27e-5	−−
	0.1000	97960	15561	7.14e-6	3.93	1.34e-6	3.97	6.63e-6	3.91	1.31e-7	4.95	2.79e-6	3.93
	0.0667	220140	34741	1.43e-6	3.96	2.66e-7	3.99	1.33e-6	3.95	1.75e-8	4.97	5.59e-7	3.97
3	0.0500	391120	61521	4.58e-7	3.96	8.45e-8	3.99	4.27e-7	3.96	4.20e-9	4.97	1.78e-7	3.97
	0.0400	610900	95901	1.89e-7	3.96	3.47e-8	3.98	1.76e-7	3.96	1.39e-9	4.97	7.37e-8	3.96
	0.0333	879480	137881	9.18e-8	3.97	1.68e-8	3.98	8.56e-8	3.96	5.61e-10	4.96	3.58e-8	3.96
	0.0286	1196860	187461	4.99e-8	3.96	9.10e-9	3.98	4.65e-8	3.96	2.69e-10	4.77	1.94e-8	3.96

Table 5.1: History of convergence for Example 1 (Stokes variables).

k	h	N_{total}	N_{comp}	$\mathtt{e}(\mathbf{u}_D)$	$\mathtt{r}(\mathbf{u}_D)$	$\mathtt{e}(p_D)$	$\mathtt{r}(p_D)$	$\mathtt{e}(\varphi_D)$	$\mathtt{r}(\varphi_D)$
	0.2000	8290	2091	2.50e-2	−−	8.45e-3	−−	1.40e-3	−−
	0.1000	32980	8181	6.33e-3	1.98	2.12e-3	1.99	1.82e-4	2.94
	0.0667	74070	18271	2.82e-3	1.99	9.45e-4	2.00	5.46e-5	2.97
1	0.0500	131560	32361	1.59e-3	1.99	5.32e-4	2.00	2.32e-5	2.98
	0.0400	205450	50451	1.02e-3	2.00	3.40e-4	2.00	1.19e-5	2.99
	0.0333	295740	72541	7.08e-4	2.00	2.36e-4	2.00	6.90e-6	2.99
	0.0286	402430	98631	5.21e-4	2.00	1.74e-4	2.00	4.34e-6	3.00
	0.2000	15435	3036	1.08e-3	−−	3.51e-4	−−	4.18e-5	−−
	0.1000	61470	11871	1.36e-4	2.99	4.42e-5	2.99	2.62e-6	4.00
	0.0667	138105	26506	4.04e-5	3.00	1.31e-5	3.00	5.19e-7	4.00
2	0.0500	245340	46941	1.70e-5	3.00	5.53e-6	3.00	1.65e-7	3.98
	0.0400	383175	73176	8.73e-6	3.00	2.83e-6	3.00	6.79e-8	3.98
	0.0333	551610	105211	5.05e-6	3.00	1.64e-6	3.00	3.29e-8	3.98
	0.0286	750645	143046	3.19e-6	2.99	1.03e-6	3.00	1.78e-8	3.98
	0.2000	24580	3981	3.83e-5	−−	1.17e-5	−−	1.24e-6	−−
	0.1000	97960	15561	2.39e-6	4.00	7.34e-7	3.99	3.98e-8	4.96
	0.0667	220140	34741	4.75e-7	3.99	1.46e-7	3.99	5.43e-9	4.91
3	0.0500	391120	61521	1.50e-7	3.99	4.64e-8	3.98	1.32e-9	4.92
	0.0400	610900	95901	6.22e-8	3.96	1.91e-8	3.98	4.53e-10	4.79
	0.0333	879480	137881	3.02e-8	3.97	9.23e-9	3.98	1.93e-10	4.68
	0.0286	1196860	187461	1.65e-8	3.92	5.01e-9	3.96	9.53e-11	4.58

Table 5.2: History of convergence for Example 1 (Darcy variables).

k	h	N_{total}	N_{comp}	$\mathtt{e}(\boldsymbol{\sigma}_S)$	$\mathtt{r}(\boldsymbol{\sigma}_S)$	$\mathtt{e}(\mathbf{u}_S)$	$\mathtt{r}(\mathbf{u}_S)$	$\mathtt{e}(\boldsymbol{\rho}_S)$	$\mathtt{r}(\boldsymbol{\rho}_S)$	$\mathtt{e}(\boldsymbol{\lambda}_S)$	$\mathtt{r}(\boldsymbol{\lambda}_S)$	$\mathtt{e}(p_S)$	$\mathtt{r}(p_S)$
	0.4330	21696	5569	5.69e-2	−−	6.43e-3	−−	3.30e-2	−−	6.79e-3	−−	2.32e-2	−−
	0.2887	72360	17929	3.16e-2	1.45	2.88e-3	1.98	1.81e-2	1.49	2.41e-3	2.56	1.01e-2	2.05
	0.2165	170496	41473	1.82e-2	1.92	1.62e-3	1.99	1.13e-2	1.63	1.12e-3	2.67	5.66e-3	2.02
1	0.1732	331800	79801	1.18e-2	1.94	1.04e-3	1.99	7.70e-3	1.71	6.06e-4	2.74	3.60e-3	2.02
	0.1443	571968	136513	8.30e-3	1.94	7.25e-4	1.99	5.58e-3	1.76	3.65e-4	2.78	2.47e-3	2.08
	0.1237	906696	215209	6.13e-3	1.96	5.33e-4	1.99	4.23e-3	1.80	2.37e-4	2.81	1.81e-3	2.00
	0.1083	1351680	319489	4.71e-3	1.98	4.09e-4	1.99	3.32e-3	1.83	1.62e-4	2.83	1.40e-3	1.94
	0.4330	50688	10945	5.19e-3	−−	6.20e-4	−−	3.45e-3	−−	5.04e-4	−−	2.16e-3	−−
	0.2887	169344	35209	1.89e-3	2.49	1.86e-4	2.97	1.17e-3	2.67	1.27e-4	3.40	6.49e-4	2.97
	0.2165	399360	81409	8.81e-4	2.66	7.99e-5	2.93	5.31e-4	2.74	4.33e-5	3.75	2.86e-4	2.85
2	0.1732	777600	156601	4.71e-4	2.81	4.12e-5	2.97	2.86e-4	2.78	1.87e-5	3.76	1.48e-4	2.94
	0.1443	1340928	267841	2.77e-4	2.91	2.40e-5	2.97	1.72e-4	2.80	9.35e-6	3.80	8.65e-5	2.96
	0.1237	2126208	422185	1.76e-4	2.94	1.52e-5	2.97	1.12e-4	2.78	5.14e-6	3.89	5.46e-5	2.99
	0.1083	3170304	626689	1.18e-4	2.98	1.02e-5	2.99	7.79e-5	2.72	3.06e-6	3.89	3.68e-5	2.95

Table 5.3: History of convergence for Example 2 (Stokes variables).

k	h	N_{total}	N_{comp}	$\texttt{e}(\mathbf{u}_D)$	$\texttt{r}(\mathbf{u}_D)$	$\texttt{e}(p_D)$	$\texttt{r}(p_D)$	$\texttt{e}(\varphi_D)$	$\texttt{r}(\varphi_D)$
	0.4330	21696	5569	3.47e-3	−−	8.44e-4	−−	3.80e-4	−−
	0.2887	72360	17929	1.72e-3	1.73	4.27e-4	1.68	1.46e-4	2.36
	0.2165	170496	41473	1.01e-3	1.84	2.53e-4	1.82	7.35e-5	2.39
1	0.1732	331800	79801	6.62e-4	1.90	1.65e-4	1.89	4.13e-5	2.58
	0.1443	571968	136513	4.66e-4	1.93	1.16e-4	1.93	2.53e-5	2.70
	0.1237	906696	215209	3.45e-4	1.95	8.61e-5	1.95	1.60e-5	2.97
	0.1083	1351680	319489	2.66e-4	1.96	6.63e-5	1.96	1.07e-5	2.99
	0.4330	50688	10945	1.21e-3	−−	2.86e-4	−−	6.78e-5	−−
	0.2887	169344	35209	4.09e-4	2.68	9.57e-5	2.70	1.45e-5	3.81
	0.2165	399360	81409	1.82e-4	2.81	4.25e-5	2.82	4.78e-6	3.85
2	0.1732	777600	156601	9.57e-5	2.88	2.23e-5	2.89	2.01e-6	3.89
	0.1443	1340928	267841	5.62e-5	2.92	1.31e-5	2.92	9.76e-7	3.95
	0.1237	2126208	422185	3.56e-5	2.95	8.30e-6	2.95	5.31e-7	3.95
	0.1083	3170304	626689	2.40e-5	2.96	5.59e-6	2.96	3.14e-7	3.94

Table 5.4: History of convergence for Example 2 (Darcy variables).

k	h	N_{total}	N_{comp}	$\texttt{e}(\boldsymbol{\sigma}_S)$	$\texttt{r}(\boldsymbol{\sigma}_S)$	$\texttt{e}(\mathbf{u}_S)$	$\texttt{r}(\mathbf{u}_S)$	$\texttt{e}(\boldsymbol{\rho}_S)$	$\texttt{r}(\boldsymbol{\rho}_S)$	$\texttt{e}(\boldsymbol{\lambda}_S)$	$\texttt{r}(\boldsymbol{\lambda}_S)$	$\texttt{e}(p_S)$	$\texttt{r}(p_S)$
	0.0500	178040	43641	1.19e-1	−−	5.00e-2	−−	1.48e-1	−−	3.80e-3	−−	4.01e-2	−−
	0.0400	278050	68051	1.02e-1	0.68	4.27e-2	0.71	1.27e-1	0.69	2.79e-3	1.39	3.44e-2	0.69
	0.0333	400260	97861	9.01e-2	0.67	3.76e-2	0.69	1.12e-1	0.68	2.18e-3	1.36	3.04e-2	0.68
1	0.0286	544670	133071	8.13e-2	0.67	3.39e-2	0.68	1.01e-1	0.67	1.77e-3	1.34	2.74e-2	0.67
	0.0250	711280	173681	7.44e-2	0.67	3.09e-2	0.68	9.22e-2	0.67	1.48e-3	1.33	2.51e-2	0.67
	0.0222	900090	219691	6.88e-2	0.67	2.86e-2	0.68	8.52e-2	0.67	1.27e-3	1.32	2.32e-2	0.67
	0.0200	1111100	271101	6.41e-2	0.66	2.66e-2	0.67	7.94e-2	0.67	1.10e-3	1.31	2.16e-2	0.67
	0.0500	331860	63061	6.94e-2	−−	3.22e-2	−−	8.82e-2	−−	9.79e-4	−−	1.83e-2	−−
	0.0400	518325	98326	5.99e-2	0.66	2.78e-2	0.67	7.60e-2	0.67	7.00e-4	1.50	1.58e-2	0.66
	0.0333	746190	141391	5.31e-2	0.66	2.46e-2	0.67	6.73e-2	0.67	5.33e-4	1.49	1.40e-2	0.66
2	0.0286	1015455	192256	4.80e-2	0.66	2.22e-2	0.67	6.07e-2	0.67	4.25e-4	1.47	1.27e-2	0.66
	0.0250	1326120	250921	4.39e-2	0.66	2.03e-2	0.67	5.56e-2	0.67	3.50e-4	1.46	1.16e-2	0.66
	0.0222	1678185	317386	4.06e-2	0.66	1.88e-2	0.67	5.14e-2	0.67	2.95e-4	1.45	1.07e-2	0.66
	0.0200	2071650	391651	3.79e-2	0.66	1.75e-2	0.67	4.79e-2	0.67	2.53e-4	1.44	9.99e-3	0.66
	0.0500	528880	82481	5.01e-2	−−	2.31e-2	−−	5.99e-2	−−	4.27e-4	−−	1.26e-2	−−
	0.0400	826100	128601	4.32e-2	0.66	1.99e-2	0.66	5.16e-2	0.67	2.95e-4	1.65	1.08e-2	0.66
	0.0333	1189320	184921	3.83e-2	0.66	1.77e-2	0.66	4.57e-2	0.67	2.18e-4	1.65	9.59e-3	0.67
3	0.0286	1618540	251441	3.46e-2	0.66	1.59e-2	0.67	4.13e-2	0.67	1.69e-4	1.65	8.66e-3	0.67
	0.0250	2113760	328161	3.16e-2	0.66	1.46e-2	0.67	3.78e-2	0.67	1.36e-4	1.65	7.92e-3	0.67
	0.0222	2674980	415081	2.93e-2	0.66	1.35e-2	0.67	3.49e-2	0.67	1.12e-4	1.65	7.33e-3	0.67
	0.0200	3302200	512201	2.73e-2	0.66	1.26e-2	0.67	3.25e-2	0.67	9.40e-5	1.65	6.83e-3	0.67

Table 5.5: History of convergence for Example 3 (Stokes variables).

k	h	N_{total}	N_{comp}	$\mathtt{e}(\mathbf{u}_D)$	$\mathtt{r}(\mathbf{u}_D)$	$\mathtt{e}(p_D)$	$\mathtt{r}(p_D)$	$\mathtt{e}(\varphi_D)$	$\mathtt{r}(\varphi_D)$
1	0.0500	178040	43641	2.84e-3	−−	2.98e-3	−−	8.30e-3	−−
	0.0400	278050	68051	1.82e-3	1.99	2.21e-3	1.32	6.37e-3	1.19
	0.0333	400260	97861	1.27e-3	1.98	1.75e-3	1.29	5.13e-3	1.19
	0.0286	544670	133071	9.36e-4	1.98	1.44e-3	1.27	4.27e-3	1.19
	0.0250	711280	173681	7.19e-4	1.97	1.22e-3	1.26	3.64e-3	1.19
	0.0222	900090	219691	5.70e-4	1.97	1.05e-3	1.25	3.16e-3	1.19
	0.0200	1111100	271101	4.64e-4	1.96	9.22e-4	1.24	2.79e-3	1.19
2	0.0500	331860	63061	6.38e-5	−−	4.82e-4	−−	1.50e-3	−−
	0.0400	518325	98326	4.65e-5	1.42	3.72e-4	1.16	1.16e-3	1.15
	0.0333	746190	141391	3.68e-5	1.28	3.01e-4	1.17	9.36e-4	1.16
	0.0286	1015455	192256	3.05e-5	1.22	2.51e-4	1.17	7.81e-4	1.17
	0.0250	1326120	250921	2.60e-5	1.18	2.15e-4	1.18	6.67e-4	1.18
	0.0222	1678185	317386	2.27e-5	1.16	1.87e-4	1.18	5.81e-4	1.18
	0.0200	2071650	391651	2.01e-5	1.15	1.65e-4	1.18	5.13e-4	1.18
3	0.0500	528880	82481	5.12e-6	−−	3.83e-5	−−	1.19e-4	−−
	0.0400	826100	128601	4.32e-6	0.76	3.08e-5	0.98	9.56e-5	0.98
	0.0333	1189320	184921	3.76e-6	0.77	2.55e-5	1.03	7.92e-5	1.03
	0.0286	1618540	251441	3.34e-6	0.76	2.16e-5	1.06	6.73e-5	1.06
	0.0250	2113760	328161	3.03e-6	0.74	1.87e-5	1.08	5.82e-5	1.08
	0.0222	2674980	415081	2.78e-6	0.72	1.65e-5	1.10	5.11e-5	1.10
	0.0200	3302200	512201	2.58e-6	0.69	1.46e-5	1.11	4.55e-5	1.11

Table 5.6: History of convergence for Example 3 (Darcy variables).

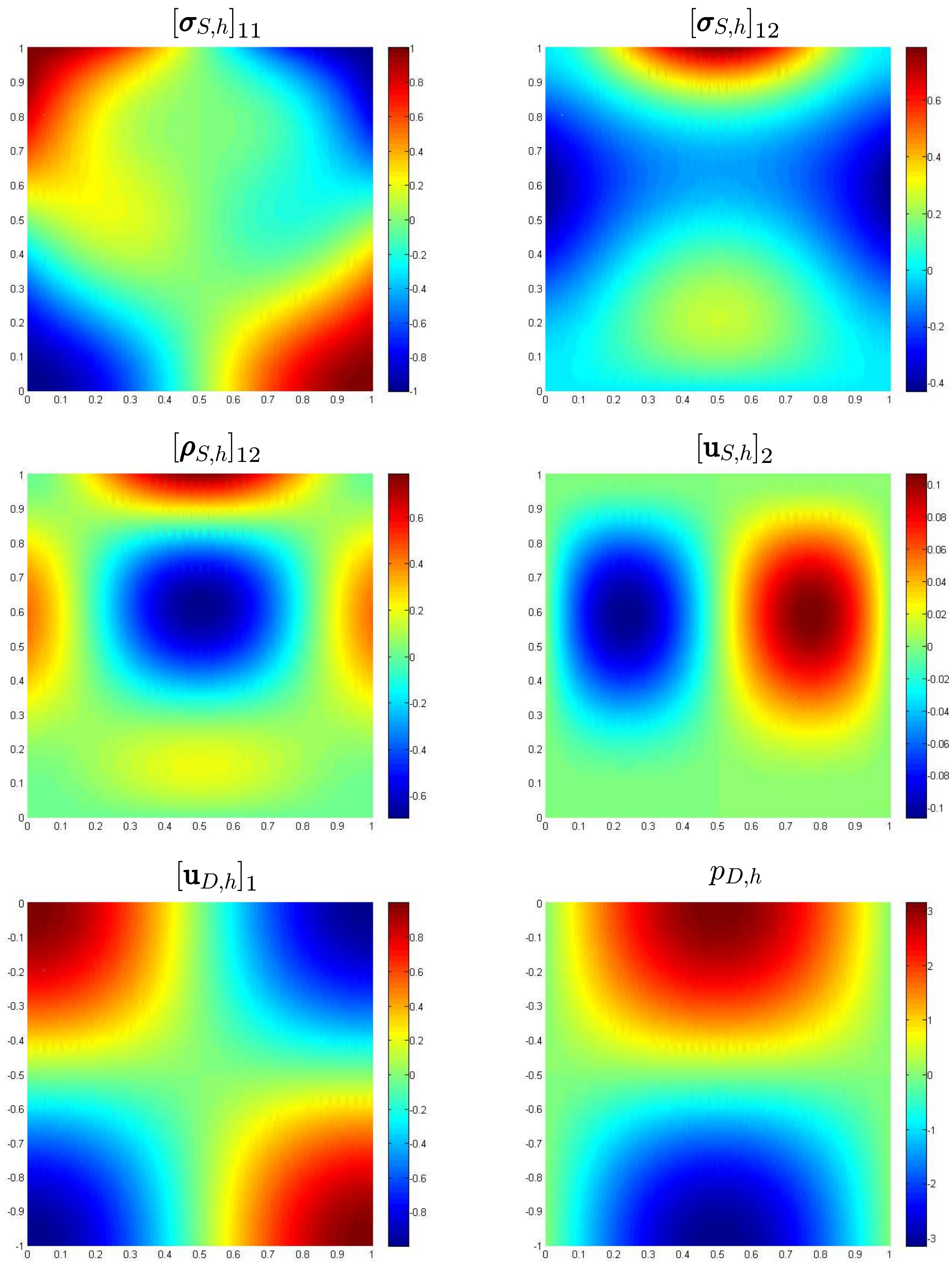

Figure 5.2: Example 1, some components of the approximate solutions.

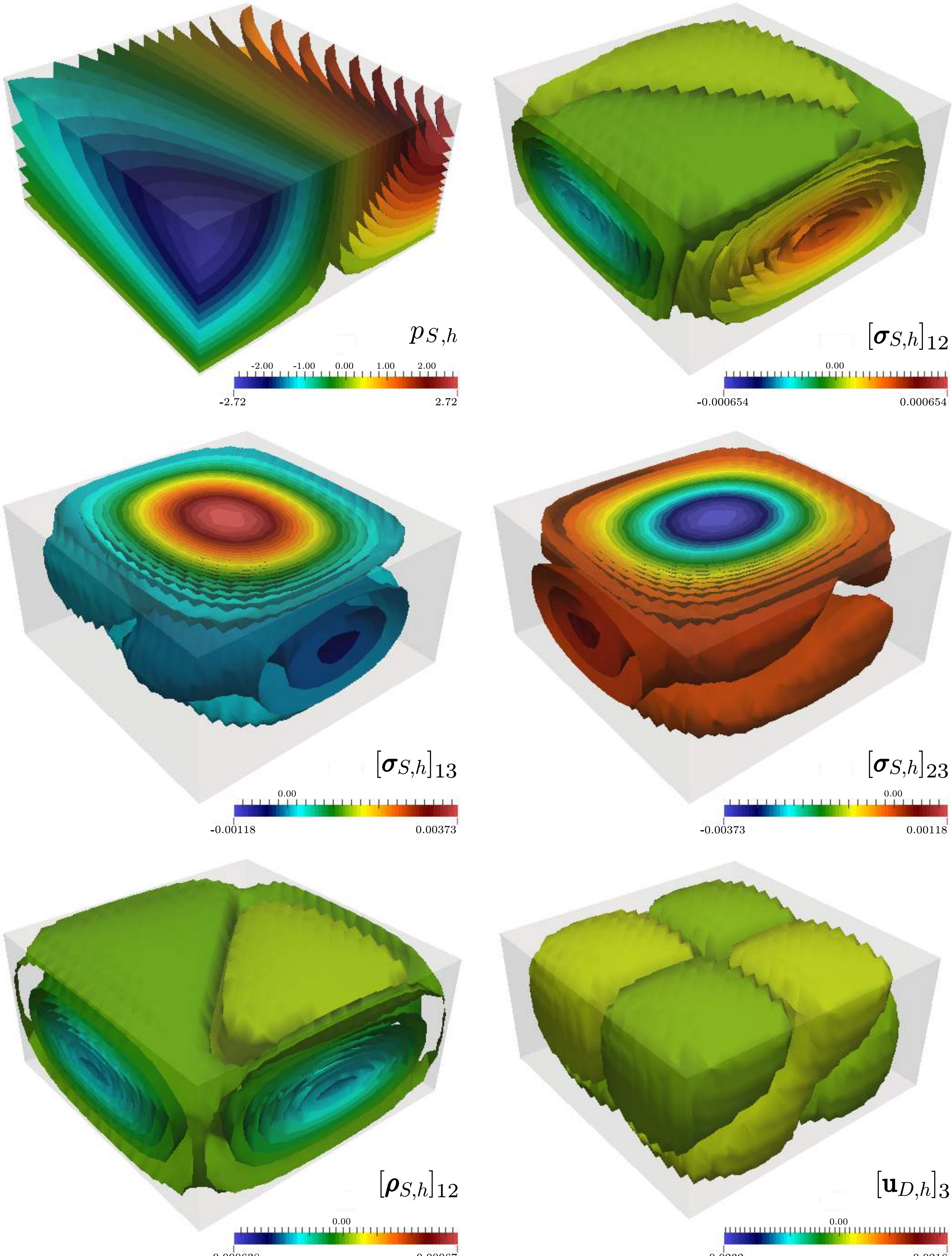

Figure 5.3: Example 2, iso-surfaces of some components of the approximate solutions.

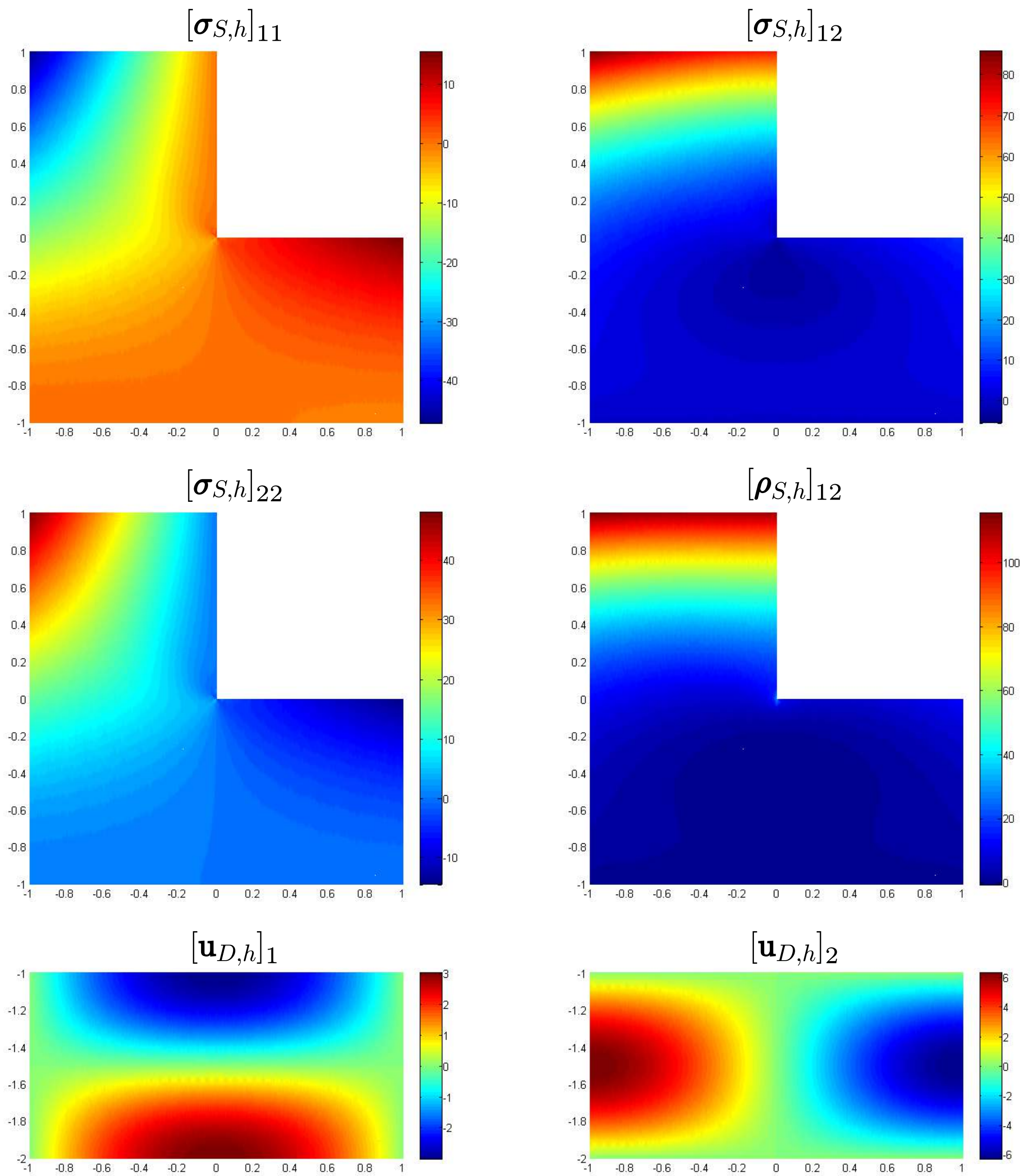

Figure 5.4: Example 3, some components of the approximate solutions.

CHAPTER 6

Design of H(div) conforming and DG methods for incompressible Euler's equations

6.1 Introduction

In this chapter we study H(div) conforming and DG finite element methods for the incompressible Euler equations in both two and three dimensions. Our methods are based on the velocity-pressure formulation. Let Ω be a bounded and simply connected polygonal domain in R^d, $d \in \{2,3\}$, with boundary Γ. The velocity $\mathbf{u} \in \mathbf{H}_0^1(\Omega) := [H_0^1(\Omega)]^d$, and the pressure $p \in L_0^2(\Omega)$ satisfy

$$\begin{aligned} \mathbf{u}_t + \mathbf{u}\cdot\nabla\mathbf{u} + \nabla p &= \mathbf{0} && \text{in} \quad (0,T)\times\Omega, \\ \operatorname{div}(\mathbf{u}) &= 0 && \text{in} \quad (0,T)\times\Omega, \\ \mathbf{u}\cdot\mathbf{n} &= \mathbf{0} && \text{on} \quad (0,T)\times\Gamma, \\ \mathbf{u}(0,\mathbf{x}) &= \mathbf{u}_0(\mathbf{x}) && \text{in} \quad \Omega, \end{aligned} \tag{6.1}$$

where $\mathbf{u}_t = \partial_t \mathbf{u}$ is the time derivative, $\nabla\mathbf{u}$ is the tensor gradient of $\mathbf{u}$, and $T > 0$.

The goal of this chapter is to define methods that are L^2 stable, and, for DG methods, are also locally conservative. The methods are inspired by the work [46] where they developed locally conservative DG methods for the steady state Navier-Stokes equations. There they take Newton iterations to solve numerically the equations and in each step they postprocess the DG approximation to get a new approximation that belongs to H(div) and is divergence free. Here we apply this idea to DG methods in each time step for Euler's equations. However, we first consider H(div) conforming elements as they seem natural for incompressible Euler's equations and are easier to analyze. In order to make the H(div) elements L^2 stable, one has to add numerical fluxes of the nonlinear term on the interfaces of the triangulation. We start with the semi-discrete method, using both central and upwind fluxes, and then analyze a backward Euler time stepping method. Once we have developed H(div) conforming methods, it guides us in developing DG methods using the post-processing idea used in [46]. In [46] upwind fluxes are used, but it is important to note that central numerical fluxes can also guarantee L^2 stability for Euler's equations.

The development and study of finite element methods for incompressible flows have a long history; see for example the books of Temam [123] and Girault and Raviart [92]. More recently there has been an interest in using H(div) conforming methods for these problems [47] since they produce divergence free approximations. However, to the best of our knowledge, an analysis of these methods for the inviscid problem (i.e. Euler's equation) has not been considered. On the other hand, there has been recent work on proving convergence rates for other finite element methods for problems with arbitrarily low viscosity [20].

We give an error analysis for both the semi-discrete methods and the backward Euler time stepping methods. The error estimate for the velocity in the L^2 norm converges with rate $O(h^k)$ if the velocity space contains the polynomials of degree k. Notice that this is sub-optimal by one order. However, numerical experiments suggest that these results are not sharp for some polynomial orders and using a central numerical flux. In particular, the error estimate will not give an error estimate for the lowest-order Raviart-Thomas element. However, on structured grids our numerical experiments show that the lowest-order Raviart-Thomas elements seem to be converging. Moreover, when using the upwind numerical flux numerical experiments suggest that the method is optimal. However, at the present time we are not able to prove this result. Our estimates assume that the velocity belongs to $W^{1,\infty}$. Of course, these *a priori* estimates are not known (and might not hold) in three dimensions for general smooth initial data. However, in two dimensions the *a priori* estimates were proved by Kato [102] for smooth initial data.

In addition to providing numerical experiments to check the order of convergence of our methods, we give numerical experiments to show how the methods behave in high gradient flows. We see that using upwind flux the method seems to do very well and comparable to DG methods that use the vorticity-potential formulation [106].

The chapter is organized as follows. In the next section we present the semi-discrete methods and prove error estimates. In section 6.3 we present the backward Euler methods. Finally, in section 6.4 we provide some numerical examples.

6.2 Semi-discrete methods

We begin by introducing some preliminary notations. Let $\mathcal{T}_h$ be a shape-regular and quasi-uniform triangulation of $\overline{\Omega}$ without the presence of hanging nodes, and let $\mathcal{E}_h$ be the set of edges/faces F of $\mathcal{T}_h$. In addition, we denote by $\mathcal{E}_h^i$ and $\mathcal{E}_h^\partial$ the set of interior and boundary faces, respectively, of $\mathcal{E}_h$, and we set $\partial\mathcal{T}_h := \cup\{\partial T \;:\; T \in \mathcal{T}_h\}$.

Next, let $(\cdot,\cdot)_U$ denote the usual L^2 and $\mathbf{L}^2 := [L^2]^d$ inner product over the domain $U \subset \mathrm{R}^d$, and similarly let $\langle \cdot,\cdot\rangle_G$ be the L^2 and $\mathbf{L}^2$ inner product over the surface $G \subset \mathrm{R}^{d-1}$. Then, we introduce the inner products:

$$(\cdot,\cdot)_{\mathcal{T}_h} \;:=\; \sum_{T\in\mathcal{T}_h} (\cdot,\cdot)_T \quad \text{and} \quad \langle\cdot,\cdot\rangle_{\partial\mathcal{T}_h} \;:=\; \sum_{T\in\mathcal{T}_h} \langle\cdot,\cdot\rangle_{\partial T}\,.$$

On the other hand, let $\mathbf{n}^+$ and $\mathbf{n}^-$ be the outward unit normal vectors on the boundaries of two neighboring elements T^+ and T^-, respectively. We use $(\boldsymbol{\tau}^\pm, \mathbf{v}^\pm, q^\pm)$ to denote the traces of $(\boldsymbol{\tau}, \mathbf{v}, q)$ on $F := \overline{T}^+ \cap \overline{T}^-$ from the interior of $T^\pm$, where $\boldsymbol{\tau}$, $\mathbf{v}$ and q are second-order tensorial, vectorial and scalar functions, respectively. Then, we define the means $\{\!\{\cdot\}\!\}$ and jumps $[\![\cdot]\!]$ for $F \in \mathcal{E}_h^i$, as follows

$$\begin{aligned}
\{\!\{\boldsymbol{\tau}\}\!\} &:= \frac{1}{2}\left(\boldsymbol{\tau}^+ + \boldsymbol{\tau}^-\right), & \{\!\{\mathbf{v}\}\!\} &:= \frac{1}{2}\left(\mathbf{v}^+ + \mathbf{v}^-\right), & \{\!\{q\}\!\} &:= \frac{1}{2}\left(q^+ + q^-\right),\\
[\![\boldsymbol{\tau}\mathbf{n}]\!] &:= \boldsymbol{\tau}^+\mathbf{n}^+ + \boldsymbol{\tau}^-\mathbf{n}^-, & [\![\mathbf{v}\cdot\mathbf{n}]\!] &:= \mathbf{v}^+\cdot\mathbf{n}^+ + \mathbf{v}^-\cdot\mathbf{n}^-, & [\![q\mathbf{n}]\!] &:= q^+\mathbf{n}^+ + q^-\mathbf{n}^-.
\end{aligned}$$

The method is derived using the conservative or divergence form of the equation. To this end, denoting $\otimes$ as the usual dyadic or tensor product, that is, $(\mathbf{u}\otimes\mathbf{v})_{ij} = (\mathbf{u}^{\mathrm{t}}\mathbf{v})_{ij} = u_i v_j$, we consider the formula

$$\mathbf{div}(\mathbf{u}\otimes\mathbf{v}) \;=\; \mathbf{v}\cdot\nabla\mathbf{u} \;+\; \mathrm{div}(\mathbf{v})\,\mathbf{u}, \tag{6.2}$$

together with the divergence-free condition, to write the problem (6.1) in the form

$$\begin{aligned} \mathbf{u}_t + \mathbf{div}(\mathbf{u}\otimes\mathbf{u}) + \nabla p \;=\; \mathbf{0} \quad \text{in} \quad (0,T)\times\Omega, \qquad \mathrm{div}(\mathbf{u}) \;=\; 0 \quad \text{in} \quad (0,T)\times\Omega\,, \\ \mathbf{u}\cdot\mathbf{n} \;=\; \mathbf{0} \quad \text{on} \quad (0,T)\times\Gamma\,, \qquad \mathbf{u}(0,\mathbf{x}) \;=\; \mathbf{u}_0(\mathbf{x}) \quad \text{in} \quad \Omega\,, \end{aligned} \tag{6.3}$$

where $\mathbf{div}$ denotes the usual divergence operator div acting along each row of the corresponding tensor.

Finally, given an integer $\ell \geq 0$ and a subset U of R^d, we denote by $\mathrm{P}_\ell(U)$ the space of polynomials defined in U of total degree at most ℓ, with $\mathbf{P}_\ell(U) := [\mathrm{P}_\ell(U)]^d$. Furthermore, for each $T \in \mathcal{T}_h$, we define the local Raviart-Thomas space of order ℓ (see, e.g. [19, 116])

$$\mathbf{RT}_\ell(T) \;:=\; \mathbf{P}_\ell(T) \;+\; \mathrm{P}_\ell(T)\,\mathbf{x}$$

where $\mathbf{x} = \begin{pmatrix} x_1 \\ \vdots \\ x_d \end{pmatrix}$ is a generic vector of R^d. In addition, we set

$$\mathbf{ND}_\ell(T) \;:=\; \mathbf{P}_\ell(T) \;+\; \mathbf{P}_\ell(T)\times\mathbf{x}$$

be the local Nédélec space of order ℓ on $T \in \mathcal{T}_h$.

6.2.1 H(div) conforming methods

In this section, we define H(div) conforming finite element schemes associated with the model problem (6.3). We start by introducing the method using the central flux, but in a later section we present the method using the upwind flux. For simplicity we only consider the Raviart-Thomas finite element spaces, but we note that one can use instead the BDM finite elements (see, e.g. [19, 116]). The globally defined Raviart-Thomas spaces are given by $\mathbf{V}_h$ for the velocity and Q_h for the pressure, given by

$$\begin{aligned} \mathbf{V}_h \;&:=\; \{\mathbf{v}\in\mathbf{H}(\mathrm{div};\Omega) \;:\; \mathbf{v}|_T \in \mathbf{RT}_k(T) \quad \forall\, T\in\mathcal{T}_h \quad \text{and} \quad \mathbf{v}\cdot\mathbf{n} = \mathbf{0} \;\; \text{on} \;\; \Gamma\}\,, \\ Q_h \;&:=\; \left\{q\in L^2_0(\Omega) \;:\; q|_T \in P_k(T) \quad \forall\, T\in\mathcal{T}_h\right\}. \end{aligned}$$

Now, the finite element method is defined by: Find $(\mathbf{u}_h, p_h) \in \mathbf{V}_h \times Q_h$, such that

$$\begin{aligned} (\partial_t\mathbf{u}_h,\mathbf{v}_h)_{\mathcal{T}_h} - (\mathbf{u}_h\otimes\mathbf{u}_h, \nabla_h\mathbf{v}_h)_{\mathcal{T}_h} - (p_h, \mathrm{div}(\mathbf{v}_h))_{\mathcal{T}_h} + \langle\widehat{\boldsymbol{\sigma}}(\mathbf{u}_h,p_h)\mathbf{n},\mathbf{v}_h\rangle_{\partial\mathcal{T}_h} \;&=\; 0, \\ (q_h, \mathrm{div}(\mathbf{u}_h))_{\mathcal{T}_h} \;&=\; 0, \\ \mathbf{u}_h(0,\mathbf{x}) \;=\; \mathbf{u}_{h,0}(\mathbf{x}) \quad \text{in } \Omega&, \end{aligned} \tag{6.4}$$

for all $(\mathbf{v}_h, q_h) \in \mathbf{V}_h \times Q_h$, where ∇_h is the broken gradient, $\mathbf{u}_{h,0}$ is some projection of $\mathbf{u}_0$ on $\mathbf{V}_h$, and $\widehat{\boldsymbol{\sigma}}(\mathbf{u}_h, p_h)$ represents the numerical flux of $\mathbf{u}\otimes\mathbf{u} + p\,\mathbb{I}$ on $\mathcal{E}_h$. In particular, we take $\widehat{\boldsymbol{\sigma}}(\mathbf{u}_h, p_h) := \mathbf{u}_h\otimes\mathbf{u}_h + p_h\mathbb{I}$ on $\mathcal{E}_h^\partial$ and for $\mathcal{E}_h^i$ we define

$$\widehat{\boldsymbol{\sigma}}(\mathbf{u}_h,p_h) \;:=\; \{\!\{\mathbf{u}_h\}\!\}\otimes\{\!\{\mathbf{u}_h\}\!\} \;+\; \{\!\{p_h\}\!\}\mathbb{I}\,. \tag{6.5}$$

This is the method using the central flux. In a later section we introduce the method using the upwind flux which seems to do better numerically.

Next, using the above definition for $\widehat{\boldsymbol{\sigma}}$, together with the formula (6.2), the fact that $\mathbf{u}_h$ is divergence free (from the second equation in (6.4)), and integration by parts, we can rewrite (6.4) as: Find $(\mathbf{u}_h, p_h) \in \mathbf{V}_h \times Q_h$, such that

$$\begin{aligned} (\partial_t \mathbf{u}_h, \mathbf{v}_h)_{\mathcal{T}_h} + (\mathbf{u}_h \cdot \nabla_h \mathbf{u}_h, \mathbf{v}_h)_{\mathcal{T}_h} - \sum_{F \in \mathcal{E}_h^i} \langle [\![(\mathbf{u}_h \otimes \mathbf{u}_h)\mathbf{n}]\!], \{\!\{ \mathbf{v}_h \}\!\} \rangle_F - (p_h, \operatorname{div}(\mathbf{v}_h))_{\mathcal{T}_h} &= 0, \\ (q_h, \operatorname{div}(\mathbf{u}_h))_{\mathcal{T}_h} &= 0, \\ \mathbf{u}_h(0, \mathbf{x}) = \mathbf{u}_{h,0}(\mathbf{x}) \quad &\text{in } \Omega, \end{aligned} \tag{6.6}$$

for all $(\mathbf{v}_h, q_h) \in \mathbf{V}_h \times Q_h$.

It will be useful to rewrite the $[\![(\mathbf{u}_h \otimes \mathbf{u}_h)\mathbf{n}]\!]|_F$. Let $F = \overline{T}^+ \cap \overline{T}^-$. Then,

$$[\![(\mathbf{u}_h \otimes \mathbf{u}_h)\mathbf{n}]\!] = [\![(\mathbf{u}_h \cdot \mathbf{n})\mathbf{u}_h]\!] = (\mathbf{u}_h^+ \cdot \mathbf{n}^+)\mathbf{u}_h^+ + (\mathbf{u}_h^- \cdot \mathbf{n}^-)\mathbf{u}_h^-.$$

In addition, from the fact that $\mathbf{u}_h^+ \cdot \mathbf{n}^+ = \mathbf{u}_h^- \cdot \mathbf{n}^+$, since $\mathbf{u}_h \in \mathbf{H}(\operatorname{div}; \Omega)$, it follows that

$$[\![(\mathbf{u}_h \otimes \mathbf{u}_h)\mathbf{n}]\!] = (\mathbf{u}_h^+ \cdot \mathbf{n}^+)\mathbf{u}_h^+ - (\mathbf{u}_h^- \cdot \mathbf{n}^+)\mathbf{u}_h^- = (\mathbf{u}_h^+ \cdot \mathbf{n}^+)(\mathbf{u}_h^+ - \mathbf{u}_h^-).$$

From now on we will use the notation (without loss of generality) $[\![\mathbf{v}]\!] := \mathbf{v}^+ - \mathbf{v}^-$. Also, we use the notation $(\mathbf{u}_h \cdot \mathbf{n})|_F = (\mathbf{u}_h^+ \cdot \mathbf{n}^+)|_F$. Hence, we write

$$[\![(\mathbf{u}_h \otimes \mathbf{u}_h)\mathbf{n}]\!] = (\mathbf{u}_h \cdot \mathbf{n})[\![\mathbf{u}_h]\!].$$

Now from this we see that the third term in the right-hand side of first equation in (6.6) is consistent, since $[\![\mathbf{u}]\!] = \mathbf{0}$ on $\mathcal{E}_h^i$ when $\mathbf{u}$ is smooth.

Lemma 6.1 (Conservation of energy). *Given $\mathbf{u}_h \in \mathbf{V}_h$ the solution of* (6.6)*, we have*

$$\frac{d}{dt} \|\mathbf{u}_h\|_{L^2(\Omega)}^2 = 0.$$

Proof. Taking $\mathbf{v}_h := \mathbf{u}_h$ in the first equation of (6.6) and using that $\mathbf{u}_h$ is divergence free, it follows

$$\frac{1}{2}\frac{d}{dt} \|\mathbf{u}_h\|_{L^2(\Omega)}^2 + (\mathbf{u}_h \cdot \nabla_h \mathbf{u}_h, \mathbf{u}_h)_{\mathcal{T}_h} - \sum_{F \in \mathcal{E}_h^i} \langle (\mathbf{u}_h \cdot \mathbf{n})[\![\mathbf{u}_h]\!], \{\!\{ \mathbf{u}_h \}\!\} \rangle_F = 0. \tag{6.7}$$

Thus, note that

$$\begin{aligned} (\mathbf{u}_h \cdot \nabla_h \mathbf{u}_h, \mathbf{u}_h)_{\mathcal{T}_h} &= \frac{1}{2} \sum_{T \in \mathcal{T}_h} \int_T \mathbf{u}_h \cdot \nabla(|\mathbf{u}_h|^2) = \frac{1}{2} \sum_{T \in \mathcal{T}_h} \left\{ - \int_T \operatorname{div}(\mathbf{u}_h)|\mathbf{u}_h|^2 + \int_{\partial T} (\mathbf{u}_h \cdot \mathbf{n})|\mathbf{u}_h|^2 \right\} \\ &= \frac{1}{2} \sum_{T \in \mathcal{T}_h} \int_{\partial T} (\mathbf{u}_h \cdot \mathbf{n})|\mathbf{u}_h|^2 = \frac{1}{2} \sum_{F \in \mathcal{E}_h^i} \int_F \{\!\{ \mathbf{u}_h \}\!\} \cdot [\![|\mathbf{u}_h|^2 \mathbf{n}]\!] \\ &= \sum_{F \in \mathcal{E}_h^i} \int_F (\mathbf{u}_h \cdot \mathbf{n})[\![\mathbf{u}_h]\!] \cdot \{\!\{ \mathbf{u}_h \}\!\}, \end{aligned} \tag{6.8}$$

which, together with (6.7) complete the proof. $\square$

We remark here that, from the previous lemma, integrating in time over $(0, t)$, we can deduce that $\|\mathbf{u}_h(t, \cdot)\|_{L^2(\Omega)} = \|\mathbf{u}_{h,0}\|_{L^2(\Omega)}$ for each $t \in (0, T)$. That is, we proved that the scheme (6.6) is stable.

Error estimates

Our next goal is to obtain error estimates for the scheme (6.6). In order to do that, we now introduce the Raviart-Thomas interpolation operator (see [19, 116]) $\mathbf{\Pi}_h^k : \mathbf{H}^1(\Omega) \to \mathbf{V}_h$, which satisfies the following approximation properties: for each $\mathbf{v} \in \mathbf{H}^m(\Omega)$, with $1 \leq m \leq k+1$, there holds

$$\|\mathbf{v} - \mathbf{\Pi}_h^k(\mathbf{v})\|_{L^2(T)} + h_T \|\nabla(\mathbf{v} - \mathbf{\Pi}_h^k(\mathbf{v}))\|_{L^2(T)} \;\leq\; C\, h_T^m |\mathbf{v}|_{m,T} \quad \forall\, T \in \mathcal{T}_h. \tag{6.9}$$

Moreover, we also have the following bounds

$$\|\mathbf{v} - \mathbf{\Pi}_h^k(\mathbf{v})\|_{L^\infty(T)} + h_T \|\nabla(\mathbf{v} - \mathbf{\Pi}_h^k(\mathbf{v}))\|_{L^\infty(T)} \;\leq\; C\, h_T \|\nabla \mathbf{v}\|_{L^\infty(T)} \quad \forall\, T \in \mathcal{T}_h. \tag{6.10}$$

In addition, let $\mathcal{P}_h^k : L^2(\Omega) \to Q_h$ be the L^2-orthogonal projector. Hence, for each $q \in H^m(\Omega)$, with $0 \leq m \leq k+1$, there holds (see, e.g. [37])

$$\|q - \mathcal{P}_h^k(q)\|_{L^2(T)} \;\leq\; C\, h_T^m |q|_{H^m(T)} \quad \forall\, T \in \mathcal{T}_h. \tag{6.11}$$

We now aim to derive the *a priori* error estimates for the scheme (6.6). To this end, thanks to the triangle inequality, we only need to provide estimates for the approximation errors, namely, $\mathrm{E}^{\mathbf{u}} := \mathbf{\Pi}_h^k(\mathbf{u}) - \mathbf{u}_h$ and $\mathrm{E}^p := \mathcal{P}_h^k(p) - p_h$. To do this, we use the fact that the exact solution satisfies the approximation method (6.6), in order to obtain the error equations:

$$\begin{aligned}
(\partial_t(\mathbf{u} - \mathbf{u}_h), \mathbf{v}_h)_{\mathcal{T}_h} \;+\; (\mathbf{u} \cdot \nabla_h \mathbf{u} - \mathbf{u}_h \cdot \nabla_h \mathbf{u}_h, \mathbf{v}_h)_{\mathcal{T}_h} & \\
- \sum_{F \in \mathcal{E}_h^i} \langle (\mathbf{u}_h \cdot \mathbf{n}) [\![\mathbf{u} - \mathbf{u}_h]\!], \{\!\{ \mathbf{v}_h \}\!\} \rangle_F \;-\; (p - p_h, \operatorname{div}(\mathbf{v}_h))_{\mathcal{T}_h} &= 0, \\
(q_h, \operatorname{div}(\mathbf{u} - \mathbf{u}_h))_{\mathcal{T}_h} &= 0,
\end{aligned}$$

for all $(\mathbf{v}_h, q_h) \in \mathbf{V}_h \times Q_h$. In addition, from the property $\operatorname{div}(\mathbf{\Pi}_h^k(\mathbf{u})) = \mathcal{P}_h^k(\operatorname{div}(\mathbf{u})) = 0$, we can rewrite the error equations in the form

$$\begin{aligned}
&(\partial_t \mathrm{E}^{\mathbf{u}}, \mathbf{v}_h)_{\mathcal{T}_h} \;+\; (\mathbf{u} \cdot \nabla_h \mathbf{u} - \mathbf{u}_h \cdot \nabla_h \mathbf{u}_h, \mathbf{v}_h)_{\mathcal{T}_h} \;-\; \sum_{F \in \mathcal{E}_h^i} \langle (\mathbf{u}_h \cdot \mathbf{n}) [\![\mathrm{E}^{\mathbf{u}}]\!], \{\!\{ \mathbf{v}_h \}\!\} \rangle_F \;-\; (\mathrm{E}^p, \operatorname{div}(\mathbf{v}_h))_{\mathcal{T}_h} \\
&= (\partial_t(\mathbf{\Pi}_h^k(\mathbf{u}) - \mathbf{u}), \mathbf{v}_h)_{\mathcal{T}_h} \;-\; \sum_{F \in \mathcal{E}_h^i} \Big\langle (\mathbf{u}_h \cdot \mathbf{n}) [\![\mathbf{\Pi}_h^k(\mathbf{u}) - \mathbf{u}]\!], \{\!\{ \mathbf{v}_h \}\!\} \Big\rangle_F \;-\; (\mathcal{P}_h^k(p) - p, \operatorname{div}(\mathbf{v}_h))_{\mathcal{T}_h}, \qquad (6.12) \\
&\qquad\qquad (q_h, \operatorname{div}(\mathrm{E}^{\mathbf{u}}))_{\mathcal{T}_h} \;=\; 0,
\end{aligned}$$

for all $(\mathbf{v}_h, q_h) \in \mathbf{V}_h \times Q_h$, where it is important to remark here that $\mathrm{E}^{\mathbf{u}}$ is divergence free.

Theorem 6.1. *Assume that $\mathbf{u} \in W^{1,\infty}([0,T] \times \Omega)^d$ is uniformly bounded. Also, suppose that $\mathcal{T}_h$ is quasi-uniform. Then, there exists $C > 0$, independent of h, such that*

$$\|(\mathbf{u} - \mathbf{u}_h)(T, \cdot)\|_{L^2(\Omega)} \;\leq\; C(u)\, h^k\, B(u),$$

where

$$C(u) \;:=\; (1 + C(1 + C_u)) \exp(C(1 + C_u)T),$$

with $C_u := \|\mathbf{u}\|_{W^{1,\infty}([0,T] \times \Omega)}$. Also,

$$B(u) \;:=\; h\|\mathbf{u}_0\|_{H^{k+1}(\Omega)} + \|\mathbf{u}\|_{L^2(0,T;H^{k+1}(\Omega))} + h\|\mathbf{u}_t\|_{L^2(0,T;H^{k+1}(\Omega))}\,.$$

Proof. We begin by choosing $\mathbf{v}_h := \mathrm{E}^{\mathbf{u}}$ in (6.12). Thus, we have

$$\begin{aligned}\frac{1}{2}\frac{d}{dt}\|\mathrm{E}^{\mathbf{u}}\|^2_{L^2(\Omega)} &= \underbrace{-(\mathbf{u}\cdot\nabla_h\mathbf{u}-\mathbf{u}_h\cdot\nabla_h\mathbf{u}_h,\mathrm{E}^{\mathbf{u}})_{\mathcal{T}_h}}_{I_1} + \underbrace{\sum_{F\in\mathcal{E}_h^i}\langle(\mathbf{u}_h\cdot\mathbf{n})[\![\mathrm{E}^{\mathbf{u}}]\!],\{\!\{\mathrm{E}_h^{\mathbf{u}}\}\!\}\rangle_F}_{I_2}\\ &\quad + (\mathbf{\Pi}_h^k(\mathbf{u}_t)-\mathbf{u}_t,\mathrm{E}^{\mathbf{u}})_{\mathcal{T}_h} \underbrace{- \sum_{F\in\mathcal{E}_h^i}\left\langle(\mathbf{u}_h\cdot\mathbf{n})[\![\mathbf{\Pi}_h^k(\mathbf{u})-\mathbf{u}]\!],\{\!\{\mathrm{E}^{\mathbf{u}}\}\!\}\right\rangle_F}_{I_3},\end{aligned} \tag{6.13}$$

where we have used the fact that $\partial_t\mathbf{\Pi}_h^k(\mathbf{u}) = \mathbf{\Pi}_h^k(\mathbf{u}_t)$. Next, note that

$$\begin{aligned} I_1 &= -(\mathbf{u}\cdot\nabla_h\{\mathbf{u}-\mathbf{\Pi}_h^k(\mathbf{u})\},\mathrm{E}^{\mathbf{u}})_{\mathcal{T}_h} - ((\mathbf{u}-\mathbf{u}_h)\cdot\nabla_h\mathbf{\Pi}_h^k(\mathbf{u}),\mathrm{E}^{\mathbf{u}})_{\mathcal{T}_h} - (\mathbf{u}_h\cdot\nabla_h\mathrm{E}^{\mathbf{u}},\mathrm{E}^{\mathbf{u}})_{\mathcal{T}_h},\\ &= -(\mathbf{u}\cdot\nabla_h\{\mathbf{u}-\mathbf{\Pi}_h^k(\mathbf{u})\},\mathrm{E}^{\mathbf{u}})_{\mathcal{T}_h} - ((\mathbf{u}-\mathbf{u}_h)\cdot\nabla_h\mathbf{\Pi}_h^k(\mathbf{u}),\mathrm{E}^{\mathbf{u}})_{\mathcal{T}_h} - I_2,\end{aligned}$$

where in the last term, we apply the same arguments of (6.8) by using $\mathrm{E}^{\mathbf{u}}$ instead of $\mathbf{u}_h$ in the last two functions. Furthermore, using (6.10) we deduce that

$$\begin{aligned} I_1 + I_2 &\le C_u\|\nabla_h\{\mathbf{\Pi}_h^k(\mathbf{u})-\mathbf{u}\}\|_{L^2(\Omega)}\|\mathrm{E}^{\mathbf{u}}\|_{L^2(\Omega)} + CC_u\|\mathbf{u}-\mathbf{u}_h\|_{L^2(\Omega)}\|\mathrm{E}^{\mathbf{u}}\|_{L^2(\Omega)}\\ &\le C_u\|\nabla_h\{\mathbf{\Pi}_h^k(\mathbf{u})-\mathbf{u}\}\|_{L^2(\Omega)}\|\mathrm{E}^{\mathbf{u}}\|_{L^2(\Omega)} + CC_u\Big\{\|\mathbf{\Pi}_h^k(\mathbf{u})-\mathbf{u}\|_{L^2(\Omega)}+\|\mathrm{E}^{\mathbf{u}}\|_{L^2(\Omega)}\Big\}\|\mathrm{E}^{\mathbf{u}}\|_{L^2(\Omega)}\\ &\le C\,C_u\|\mathrm{E}^{\mathbf{u}}\|^2_{L^2(\Omega)} + C\,C_u\left\{\|\mathbf{\Pi}_h^k(\mathbf{u})-\mathbf{u}\|^2_{L^2(\Omega)} + \|\nabla_h\{\mathbf{\Pi}_h^k(\mathbf{u})-\mathbf{u}\}\|^2_{L^2(\Omega)}\right\}.\end{aligned} \tag{6.14}$$

On the other hand, for I_3 it follows

$$\begin{aligned} I_3 &= -\sum_{F\in\mathcal{E}_h^i}\left\langle(\mathrm{E}^{\mathbf{u}}\cdot\mathbf{n})[\![\mathbf{\Pi}_h^k(\mathbf{u})-\mathbf{u}]\!],\{\!\{\mathrm{E}^{\mathbf{u}}\}\!\}\right\rangle_F + \sum_{F\in\mathcal{E}_h^i}\left\langle(\mathbf{\Pi}_h^k(\mathbf{u})\cdot\mathbf{n})[\![\mathbf{\Pi}_h^k(\mathbf{u})-\mathbf{u}]\!],\{\!\{\mathrm{E}^{\mathbf{u}}\}\!\}\right\rangle_F\\ &\le Ch^{-1}\|\mathbf{\Pi}_h^k(\mathbf{u})-\mathbf{u}\|_{L^\infty(\Omega)}\sum_{F\in\mathcal{E}_h^i}h_F\|\{\!\{\mathrm{E}^{\mathbf{u}}\}\!\}\|^2_{L^2(F)}\\ &\quad + C\|\mathbf{\Pi}_h^k(\mathbf{u})\|_{L^\infty(\Omega)}\left(\sum_{F\in\mathcal{E}_h^i}h_F^{-1}\|[\![\mathbf{\Pi}_h^k(\mathbf{u})-\mathbf{u}]\!]\|^2_{L^2(F)}\right)^{1/2}\left(\sum_{F\in\mathcal{E}_h^i}h_F\|\{\!\{\mathrm{E}^{\mathbf{u}}\}\!\}\|^2_{L^2(F)}\right)^{1/2}.\end{aligned} \tag{6.15}$$

In addition, given $\mathbf{v}\in\mathbf{H}^1(\mathcal{T}_h)$ and applying a discrete trace inequality, we observe that

$$\begin{aligned}\sum_{F\in\mathcal{E}_h^i}h_F^{-1}\|[\![\mathbf{v}]\!]\|^2_{L^2(F)} &\le 2\sum_{F\in\mathcal{E}_h^i}h_F^{-1}\Big(\|\mathbf{v}^+\|^2_{L^2(F)}+\|\mathbf{v}^-\|^2_{L^2(F)}\Big) \le 2\sum_{T\in\mathcal{T}_h}\sum_{F\in\partial T}h_F^{-1}\|\mathbf{v}\|^2_{L^2(F)}\\ &\le 2\,C_{\mathrm{tr}}\sum_{T\in\mathcal{T}_h}\sum_{F\in\partial T}h_F^{-1}\Big\{h_T^{-1}\|\mathbf{v}\|^2_{L^2(T)}+h_T\|\nabla\mathbf{v}\|^2_{L^2(T)}\Big\}\\ &\le \widehat{C}\Big\{h^{-2}\|\mathbf{v}\|^2_{L^2(\Omega)} + \|\nabla_h\mathbf{v}\|^2_{L^2(\Omega)}\Big\},\end{aligned} \tag{6.16}$$

and, in the same way together with an inverse inequality we obtain

$$\sum_{F\in\mathcal{E}_h^i}h_F\|\{\!\{\mathrm{E}^{\mathbf{u}}\}\!\}\|^2_{L^2(F)} \le \widehat{C}\,\|\mathrm{E}^{\mathbf{u}}\|^2_{L^2(\Omega)}. \tag{6.17}$$

Hence, replacing (6.16) and (6.17) in (6.15) and using (6.10) we deduce that

$$I_3 \le C\,C_u\|\mathrm{E}^{\mathbf{u}}\|^2_{L^2(\Omega)} + C\,C_u\left\{h^{-2}\|\mathbf{\Pi}_h^k(\mathbf{u})-\mathbf{u}\|^2_{L^2(\Omega)} + \|\nabla_h\{\mathbf{\Pi}_h^k(\mathbf{u})-\mathbf{u}\}\|^2_{L^2(\Omega)}\right\}. \tag{6.18}$$

Now, we return to (6.13), which satisfies that

$$\frac{1}{2}\frac{d}{dt}\|\mathrm{E}^{\mathbf{u}}\|^2_{L^2(\Omega)} \;\leq\; \frac{1}{2}\|\mathrm{E}^{\mathbf{u}}\|^2_{L^2(\Omega)} + \frac{1}{2}\|\mathbf{\Pi}^k_h(\mathbf{u}_t)-\mathbf{u}_t\|^2_{L^2(\Omega)} + (I_1+I_2) + I_3,$$

where, replacing (6.14) and (6.18), we obtain that

$$\begin{aligned}\frac{d}{dt}\|\mathrm{E}^{\mathbf{u}}\|^2_{L^2(\Omega)} \;&\leq\; C(1+C_u)\|\mathrm{E}^{\mathbf{u}}\|^2_{L^2(\Omega)} + C\|\mathbf{\Pi}^k_h(\mathbf{u}_t)-\mathbf{u}_t\|^2_{L^2(\Omega)}\\ &\quad + CC_u\left\{h^{-2}\|\mathbf{\Pi}^k_h(\mathbf{u})-\mathbf{u}\|^2_{L^2(\Omega)} + \|\nabla_h\{\mathbf{\Pi}^k_h(\mathbf{u})-\mathbf{u}\}\|^2_{L^2(\Omega)}\right\}.\end{aligned}$$

Hence, applying (6.9) we get

$$\frac{d}{dt}\|\mathrm{E}^{\mathbf{u}}\|^2_{L^2(\Omega)} \;\leq\; C(1+C_u)\|\mathrm{E}^{\mathbf{u}}\|^2_{L^2(\Omega)} + C(1+C_u)\,h^{2k}\left(h^2\|\mathbf{u}_t\|^2_{H^{k+1}(\Omega)} + \|\mathbf{u}\|^2_{H^{k+1}(\Omega)}\right).$$

which, applying the Gronwall's inequality (see, e.g. [61]), yields

$$\begin{aligned}\|\mathrm{E}^{\mathbf{u}}(T,\cdot)\|^2_{L^2(\Omega)} \;&\leq\; \exp(C(1+C_u)T)\Big\{\|\mathrm{E}^{\mathbf{u}}(0,\cdot)\|^2_{L^2(\Omega)}\\ &\quad + C(1+C_u)\left(h^2\|\mathbf{u}_t\|^2_{L^2(0,T;H^{k+1}(\Omega))} + \|\mathbf{u}\|^2_{L^2(0,T;H^{k+1}(\Omega))}\right)\Big\}.\end{aligned}$$

Finally, we use that $\|\mathrm{E}^{\mathbf{u}}(0,\cdot)\|^2_{L^2(\Omega)} \leq C\,h^{2(k+1)}\|\mathbf{u}_0\|^2_{H^{k+1}(\Omega)}$ to complete the proof. □

The next goal is to establish error estimates for the pressure variable. To do this, we first obtain an estimate for $\partial_t(\mathbf{u}-\mathbf{u}_h)$, which is the subject of the next result.

Lemma 6.2. *Assume the same hypotheses of Theorem* 6.1*. Then, there exists $C>0$, independent of h, such that*

$$\begin{aligned}\|\partial_t\mathrm{E}^{\mathbf{u}}(T,\cdot)\|_{L^2(\Omega)} \;&\leq\; (C(u)h^{k-d/2}B(u)+C_u)h^{k-1}\Big\{C(u)\,B(u) + \|\mathbf{u}(T,\cdot)\|_{H^{k+1}(\Omega)}\Big\}\\ &\quad + Ch^{k+1}\|\mathbf{u}_t(T,\cdot)\|_{H^{k+1}(\Omega)}.\end{aligned}$$

Proof. First, we take $\mathbf{v}_h := \partial_t\mathrm{E}^{\mathbf{u}}$ in (6.12) and using that $\mathrm{div}(\partial_t\mathrm{E}^{\mathbf{u}}) = \partial_t\mathrm{div}(\mathrm{E}^{\mathbf{u}}) = 0$, we obtain

$$\begin{aligned}\|\partial_t\mathrm{E}^{\mathbf{u}}\|^2_{L^2(\Omega)} \;&=\; -(\mathbf{u}\cdot\nabla_h\mathbf{u}-\mathbf{u}_h\cdot\nabla_h\mathbf{u}_h,\partial_t\mathrm{E}^{\mathbf{u}})_{\mathcal{T}_h} + \sum_{F\in\mathcal{E}^i_h}\langle(\mathbf{u}_h\cdot\mathbf{n})[\![\mathrm{E}^{\mathbf{u}}]\!],\{\!\{\partial_t\mathrm{E}^{\mathbf{u}}\}\!\}\rangle_F\\ &\quad + (\mathbf{\Pi}^k_h(\mathbf{u}_t)-\mathbf{u}_t,\partial_t\mathrm{E}^{\mathbf{u}})_{\mathcal{T}_h} - \sum_{F\in\mathcal{E}^i_h}\Big\langle(\mathbf{u}_h\cdot\mathbf{n})[\![\mathbf{\Pi}^k_h(\mathbf{u})-\mathbf{u}]\!],\{\!\{\partial_t\mathrm{E}^{\mathbf{u}}\}\!\}\Big\rangle_F\\ &\leq\; \|\mathbf{u}\cdot\nabla_h\mathbf{u}-\mathbf{u}_h\cdot\nabla_h\mathbf{u}_h\|_{L^2(\Omega)}\|\partial_t\mathrm{E}^{\mathbf{u}}\|_{L^2(\Omega)} + \|\mathbf{\Pi}^k_h(\mathbf{u}_t)-\mathbf{u}_t\|_{L^2(\Omega)}\|\partial_t\mathrm{E}^{\mathbf{u}}\|_{L^2(\Omega)}\\ &\quad + C\|\mathbf{u}_h\|_{L^\infty(\Omega)}\left(\sum_{F\in\mathcal{E}^i_h}h_F^{-1}\|[\![\mathrm{E}^{\mathbf{u}}]\!]\|^2_{L^2(F)}\right)^{1/2}\left(\sum_{F\in\mathcal{E}^i_h}h_F\|\{\!\{\partial_t\mathrm{E}^{\mathbf{u}}\}\!\}\|^2_{L^2(F)}\right)^{1/2}\\ &\quad + C\|\mathbf{u}_h\|_{L^\infty(\Omega)}\left(\sum_{F\in\mathcal{E}^i_h}h_F^{-1}\|[\![\mathbf{\Pi}^k_h(\mathbf{u})-\mathbf{u}]\!]\|^2_{L^2(F)}\right)^{1/2}\left(\sum_{F\in\mathcal{E}^i_h}h_F\|\{\!\{\partial_t\mathrm{E}^{\mathbf{u}}\}\!\}\|^2_{L^2(F)}\right)^{1/2}.\end{aligned}$$

Next, using (6.16) and (6.17), we deduce after some algebraic manipulation that

$$\begin{aligned}\|\partial_t\mathrm{E}^{\mathbf{u}}\|_{L^2(\Omega)} \;\leq\; C\Big\{&h^{-1}\|\mathbf{u}_h\|_{L^\infty(\Omega)}\|\mathrm{E}^{\mathbf{u}}\|_{L^2(\Omega)} + \|\mathbf{u}\cdot\nabla_h\mathbf{u}-\mathbf{u}_h\cdot\nabla_h\mathbf{u}_h\|_{L^2(\Omega)}\\ &+ \|\mathbf{\Pi}^k_h(\mathbf{u}_t)-\mathbf{u}_t\|_{L^2(\Omega)} + \|\mathbf{u}_h\|_{L^\infty(\Omega)}(h^{-1}\|\mathbf{\Pi}^k_h(\mathbf{u})-\mathbf{u}\|_{L^2(\Omega)} + \|\nabla_h(\mathbf{\Pi}^k_h(\mathbf{u})-\mathbf{u})\|_{L^2(\Omega)})\Big\}.\end{aligned}$$

To bound the nonlinear term we add and subtract terms to get

$$
\begin{aligned}
\|\mathbf{u}\cdot\nabla_h\mathbf{u}-\mathbf{u}_h\cdot\nabla_h\mathbf{u}_h\|_{L^2(\Omega)} &= \|(\mathbf{u}-\mathbf{u}_h)\cdot\nabla_h\mathbf{u}+\mathbf{u}_h\cdot\nabla_h(\mathbf{u}-\mathbf{u}_h)\|_{L^2(\Omega)}\\
&\le C_u\|\mathbf{u}-\mathbf{u}_h\|_{L^2(\Omega)}+\|\mathbf{u}_h\|_{L^\infty(\Omega)}\|\nabla_h(\mathbf{u}-\mathbf{u}_h)\|_{L^2(\Omega)}\\
&\le C_u\|\mathbf{u}-\mathbf{u}_h\|_{L^2(\Omega)}+\|\mathbf{u}_h\|_{L^\infty(\Omega)}(\|\nabla_h(\mathbf{u}-\mathbf{\Pi}_h^k\mathbf{u})\|_{L^2(\Omega)}+Ch^{-1}\|\mathrm{E}^{\mathbf{u}}\|_{L^2(\Omega)})\\
&\le C_u\|\mathrm{E}^{\mathbf{u}}\|_{L^2(\Omega)}+C_u\|\mathbf{\Pi}_h^k(\mathbf{u})-\mathbf{u}\|_{L^2(\Omega)}\\
&\quad+\|\mathbf{u}_h\|_{L^\infty(\Omega)}(\|\nabla_h(\mathbf{u}-\mathbf{\Pi}_h^k\mathbf{u})\|_{L^2(\Omega)}+Ch^{-1}\|\mathrm{E}^{\mathbf{u}}\|_{L^2(\Omega)}),
\end{aligned}
$$

where we have used an inverse estimate. Therefore,

$$
\begin{aligned}
\|\partial_t\mathrm{E}^{\mathbf{u}}\|_{L^2(\Omega)} \le C\Big\{&(h^{-1}\|\mathbf{u}_h\|_{L^\infty(\Omega)}+C_u)\|\mathrm{E}^{\mathbf{u}}\|_{L^2(\Omega)}+\|\mathbf{\Pi}_h^k(\mathbf{u}_t)-\mathbf{u}_t\|_{L^2(\Omega)}\\
&+\|\mathbf{u}_h\|_{L^\infty(\Omega)}\|\nabla_h(\mathbf{\Pi}_h^k(\mathbf{u})-\mathbf{u})\|_{L^2(\Omega)}+(h^{-1}\|\mathbf{u}_h\|_{L^\infty(\Omega)}+C_u)\|\mathbf{\Pi}_h^k(\mathbf{u})-\mathbf{u}\|_{L^2(\Omega)}\Big\}.
\end{aligned}
$$

We can bound $\|\mathbf{u}_h\|_{L^\infty(\Omega)}$ using an inverse estimate

$$
\|\mathbf{u}_h\|_{L^\infty(\Omega)} \le \|\mathrm{E}^{\mathbf{u}}\|_{L^\infty(\Omega)}+\|\mathbf{\Pi}_h^k(\mathbf{u})\|_{L^\infty(\Omega)} \le C\,h^{-d/2}\|\mathrm{E}^{\mathbf{u}}\|_{L^2(\Omega)}+C\,C_u. \tag{6.19}
$$

Hence,

$$
\begin{aligned}
\|\partial_t\mathrm{E}^{\mathbf{u}}(t)\|_{L^2(\Omega)} \le C\Big\{&h^{-1}(h^{-d/2}\|\mathrm{E}^{\mathbf{u}}\|_{L^2(\Omega)}+C_u)\|\mathrm{E}^{\mathbf{u}}\|_{L^2(\Omega)}+\|\mathbf{\Pi}_h^k(\mathbf{u}_t)-\mathbf{u}_t\|_{L^2(\Omega)}\\
&+(h^{-d/2}\|\mathrm{E}^{\mathbf{u}}\|_{L^2(\Omega)}+C_u)\Big(\|\nabla_h(\mathbf{\Pi}_h^k(\mathbf{u})-\mathbf{u})\|_{L^2(\Omega)}+h^{-1}\|\mathbf{\Pi}_h^k(\mathbf{u})-\mathbf{u}\|_{L^2(\Omega)}\Big)\Big\}.
\end{aligned}
$$

Finally, using Theorem 6.1 and (6.9) establishes the result. □

Note that in the above proof we have also proved

$$
\begin{aligned}
\|(\mathbf{u}\cdot\nabla_h\mathbf{u}-\mathbf{u}_h\cdot\nabla_h\mathbf{u}_h)(T,\cdot)\|_{L^2(\Omega)} \le\;& (C(u)h^{k-d/2}B(u)+C_u)h^{k-1}\Big\{C(u)\,B(u)+\|\mathbf{u}(T,\cdot)\|_{H^{k+1}(\Omega)}\Big\}\\
&+Ch^{k+1}\|\partial_t\mathbf{u}(T,\cdot)\|_{H^{k+1}(\Omega)}\,.
\end{aligned} \tag{6.20}
$$

We end this section with the *a priori* error estimate for the pressure, which is established next.

Theorem 6.2. *Assume the hypothesis of Theorem* 6.1*. Then, there exists* $C>0$*, independent of* h*, such that*

$$
\begin{aligned}
\|(p-p_h)(T,\cdot)\|_{L^2(\Omega)} \le\;& (C(u)h^{k-d/2}B(u)+C_u+C\,h)h^{k-1}\Big\{C(u)\,B(u)+\|\mathbf{u}(T,\cdot)\|_{H^{k+1}(\Omega)}\Big\}\\
&+Ch^{k+1}\Big\{\|\mathbf{u}_t(T,\cdot)\|_{H^{k+1}(\Omega)}+\|p(T,\cdot)\|_{H^{k+1}(\Omega)}\Big\}\,.
\end{aligned}
$$

Proof. We begin by recalling here the discrete inf-sup given by

$$
\beta\,\|q_h\|_{L^2(\Omega)} \le \sup_{\substack{\mathbf{v}_h\in\mathbf{V}_h\\ \mathbf{v}_h\neq\mathbf{0}}}\frac{(q_h,\mathrm{div}(\mathbf{v}_h))_{\mathcal{T}_h}}{\|\mathbf{v}_h\|_{H(\mathrm{div};\Omega)}} \qquad \forall\, q_h\in Q_h, \tag{6.21}
$$

which, in particular for $q_h := \mathrm{E}^p$, it follows

$$
\|\mathrm{E}^p\|_{L^2(\Omega)} \le \frac{1}{\beta}\sup_{\substack{\mathbf{v}_h\in\mathbf{V}_h\\ \mathbf{v}_h\neq\mathbf{0}}}\frac{(\mathrm{E}^p,\mathrm{div}(\mathbf{v}_h))_{\mathcal{T}_h}}{\|\mathbf{v}_h\|_{H(\mathrm{div};\Omega)}}. \tag{6.22}
$$

Now, from the error equation (6.12) and proceeding as in the proof of Lemma 6.2, we have

$$
\begin{aligned}
(\mathrm{E}^p, \mathrm{div}(\mathbf{v}_h))_{\mathcal{T}_h} \;&=\; (\partial_t \mathrm{E}^{\mathbf{u}}, \mathbf{v}_h)_{\mathcal{T}_h} \,+\, (\mathbf{u}\cdot\nabla_h \mathbf{u} - \mathbf{u}_h\cdot\nabla_h \mathbf{u}_h, \mathbf{v}_h)_{\mathcal{T}_h} \,-\, \sum_{F\in\mathcal{E}_h^i} \langle (\mathbf{u}_h\cdot\mathbf{n})[\![\mathrm{E}^{\mathbf{u}}]\!], \{\!\{\mathbf{v}_h\}\!\}\rangle_F \\
&\quad -\, (\mathbf{\Pi}_h^k(\mathbf{u}_t) - \mathbf{u}_t, \mathbf{v}_h)_{\mathcal{T}_h} \,+\, \sum_{F\in\mathcal{E}_h^i} \Big\langle (\mathbf{u}_h\cdot\mathbf{n})[\![\mathbf{\Pi}_h^k(\mathbf{u}) - \mathbf{u}]\!], \{\!\{\mathbf{v}_h\}\!\}\Big\rangle_F \,+\, (\mathcal{P}_h^k(p) - p, \mathrm{div}(\mathbf{v}_h))_{\mathcal{T}_h} \\
&\le\; \|\partial_t \mathrm{E}^{\mathbf{u}}\|_{L^2(\Omega)}\|\mathbf{v}_h\|_{L^2(\Omega)} \,+\, \|\mathbf{u}\cdot\nabla_h\mathbf{u} - \mathbf{u}_h\cdot\nabla_h\mathbf{u}_h\|_{L^2(\Omega)}\|\mathbf{v}_h\|_{L^2(\Omega)} \,+\, Ch^{-1}\|\mathrm{E}^{\mathbf{u}}\|_{L^2(\Omega)}\|\mathbf{v}_h\|_{L^2(\Omega)} \\
&\quad +\, C\Big\{h^{-1}\|\mathbf{\Pi}_h^k(\mathbf{u}) - \mathbf{u}\|_{L^2(\Omega)} \,+\, \|\nabla_h(\mathbf{\Pi}_h^k(\mathbf{u}) - \mathbf{u})|_{L^2(\Omega)}\Big\}\|\mathbf{v}_h\|_{L^2(\Omega)} \\
&\quad +\, \|\mathbf{\Pi}_h^k(\mathbf{u}_t) - \mathbf{u}_t\|_{L^2(\Omega)}\|\mathbf{v}_h\|_{L^2(\Omega)} \,+\, \|\mathcal{P}_h^k(p) - p\|_{L^2(\Omega)}\|\mathrm{div}(\mathbf{v}_h)\|_{L^2(\Omega)}.
\end{aligned}
$$

The above result together with (6.22) establishes

$$
\begin{aligned}
\|\mathrm{E}^p\|_{L^2(\Omega)} \;\le\; C\Big\{&\|\partial_t\mathrm{E}^{\mathbf{u}}\|_{L^2(\Omega)} \,+\, \|\mathbf{u}\cdot\nabla_h\mathbf{u} - \mathbf{u}_h\cdot\nabla_h\mathbf{u}_h\|_{L^2(\Omega)} \,+\, h^{-1}\|\mathrm{E}^{\mathbf{u}}\|_{L^2(\Omega)} \\
&+\, h^{-1}\|\mathbf{\Pi}_h^k(\mathbf{u}) - \mathbf{u}\|_{L^2(\Omega)} \,+\, \|\nabla_h(\mathbf{\Pi}_h^k(\mathbf{u}) - \mathbf{u})\|_{L^2(\Omega)} \,+\, \|\mathbf{\Pi}_h^k(\mathbf{u}_t) - \mathbf{u}_t\|_{L^2(\Omega)} \,+\, \|\mathcal{P}_h^k(p) - p\|_{L^2(\Omega)}\Big\}.
\end{aligned}
$$

Therefore, thanks to $\|p - p_h\|_{L^2(\Omega)} \le \|\mathrm{E}^p\|_{L^2(\Omega)} + \|\mathcal{P}_h^k(p) - p\|_{L^2(\Omega)}$, (6.20), Lemma 6.2 and the approximation properties (6.9) and (6.11), we can easily complete the proof. □

Notice the the error estimate for the pressure predicts $O(h^{k-1})$ (for $k \ge 2$) in two and three dimensions.

Using an upwind flux

Here, we introduce an alternative version of the conforming method (6.6), analyzed in previous sections. In order to do that, we begin by redefining the numerical flux $\widehat{\boldsymbol{\sigma}}$ (cf. (6.5)) in a new general form, given by:

$$
\widehat{\boldsymbol{\sigma}}(\mathbf{u}_h, p_h) \;:=\; \widehat{\mathbf{u}}_h^{\mathbf{w}} \otimes \{\!\{\mathbf{u}_h\}\!\} \;+\; \{\!\{p_h\}\!\}\,\mathbb{I}\,,
$$

where $\widehat{\mathbf{u}}_h^{\mathbf{w}}$ is a new numerical trace for $\mathbf{u}_h$ related with the convective term. In particular, taking $\widehat{\mathbf{u}}_h^{\mathbf{w}} := \{\!\{\mathbf{u}_h\}\!\} = \frac{1}{2}\left(\mathbf{u}_h^{\mathrm{int}} + \mathbf{u}_h^{\mathrm{ext}}\right)$ we arrive exactly to the scheme (6.6). That is, the method (6.6) correspond to a *central scheme*.

On the other hand, for some problems with high gradients, it is more natural to use an *upwind scheme*, in order to get better accuracy and order of convergence. In Section 6.4 we will present some examples of this. In fact, we see numerically that using upwind flux gives optimal convergence rates for both the velocity and pressure variables.

According to above, we consider the following upwind flux

$$
\widehat{\mathbf{u}}_h^{\mathbf{w}} \;:=\; \begin{cases} \mathbf{u}_h^{\mathrm{int}} & \text{if} \quad \mathbf{u}_h\cdot\mathbf{n} \ge 0, \\ \mathbf{u}_h^{\mathrm{ext}} & \text{if} \quad \mathbf{u}_h\cdot\mathbf{n} < 0. \end{cases}
$$

This definition is given in the same way of that presented in [106] for the vorticity, and it is not difficult to check that we can obtain again the method (6.6), with an extra term given by a weighted full jumps onto $\mathcal{E}_h^i$. That is, we seek $\mathbf{u}_h \in \mathbf{V}_h$ and $p_h \in Q_h$, such that

$$\begin{aligned}(\partial_t \mathbf{u}_h, \mathbf{v}_h)_{\mathcal{T}_h} + (\mathbf{u}_h \cdot \nabla_h \mathbf{u}_h, \mathbf{v}_h)_{\mathcal{T}_h} - \sum_{F\in\mathcal{E}_h^i} \langle (\mathbf{u}_h \cdot \mathbf{n}) [\![\mathbf{u}_h]\!], \{\!\{\mathbf{v}_h\}\!\}\rangle_F \\ + \sum_{F\in\mathcal{E}_h^i} \langle |\mathbf{u}_h \cdot \mathbf{n}| [\![\mathbf{u}_h]\!], [\![\mathbf{v}_h]\!]\rangle_F - (p_h, \mathrm{div}(\mathbf{v}_h))_{\mathcal{T}_h} &= 0 \quad \forall\, \mathbf{v}_h \in \mathbf{V}_h, \qquad (6.23)\\ (q_h, \mathrm{div}(\mathbf{u}_h))_{\mathcal{T}_h} &= 0 \quad \forall\, q_h \in Q_h,\\ \mathbf{u}_h(0,\mathbf{x}) = \mathbf{u}_{h,0}(\mathbf{x}) \quad \text{in } \Omega.\end{aligned}$$

It is important to remark here, that the introduction of this new term does not pose any difficulty in order to prove stability and convergence. In fact, both follow the same arguments, using that when $\mathbf{v}_h = \mathbf{u}_h$ this term is positive. In particular, the error estimates are basically the same and the stability, see remark after the proof of Lemma 6.1, now is given by $\|\mathbf{u}_h(t,\cdot)\|_{L^2(\Omega)} \le \|\mathbf{u}_{h,0}\|_{L^2(\Omega)}$ for each $t \in (0,T)$.

6.2.2 DG schemes

In this section, we introduce a discontinuous Galerkin method for the model problem (6.3). The velocity space will consist of polynomials of degree $k+1$ for the fully discontinuous subspace

$$\mathbf{V}_h^{\mathrm{dg}} \;:=\; \left\{\mathbf{v} \in \mathbf{L}^2(\Omega) \,:\, \mathbf{v}|_T \in \mathbf{P}_{k+1}(T) \quad \forall\, T \in \mathcal{T}_h \quad \text{and} \quad \mathbf{v}\cdot\mathbf{n} = \mathbf{0} \;\text{ on }\; \Gamma\right\},$$

whereas, the pressure space remains unchanged. That is,

$$Q_h \;:=\; \left\{q \in L_0^2(\Omega) \,:\, q|_T \in P_k(T) \quad \forall\, T \in \mathcal{T}_h\right\}.$$

In the previous section we only defined the jumps and averages on the interior faces/edges. Here we also define them on boundary faces. That is, for $F \in \mathcal{E}_h^\partial$, as is usual, we set

$$\{\!\{\mathbf{v}\}\!\} := \mathbf{v}, \qquad [\![\mathbf{v}\cdot\mathbf{n}]\!] := \mathbf{v}\cdot\mathbf{n} \qquad \text{and} \qquad \{\!\{q\}\!\} := q.$$

Thus, in order to define the approximation scheme, we first introduce a postprocessed flux. For each $\mathbf{v} \in \mathbf{H}^1(\mathcal{T}_h)$, we find $\mathbf{v}^\star \in \mathbf{P}_{k+1}(\mathcal{T}_h)$ such that

$$\int_F (\mathbf{v}^\star \cdot \mathbf{n}) q \;=\; \int_F (\{\!\{\mathbf{v}\}\!\} \cdot \mathbf{n}) q \quad \forall\, q \in \mathrm{P}_{k+1}(F), \quad \forall\, F \in \partial T, \qquad (6.24)$$

$$\int_T \mathbf{v}^\star \cdot \mathbf{p} \;=\; \int_T \mathbf{v}\cdot\mathbf{p} \quad \forall\, \mathbf{p} \in \mathbf{ND}_{k-1}(T), \qquad (6.25)$$

for each $T \in \mathcal{T}_h$. Note that if $\mathbf{v}_h \in \mathbf{V}_h^{\mathrm{dg}}$ then $\mathbf{v}^\star \in \mathbf{BDM}_{k+1}^0(\Omega)$ where,

$$\begin{aligned}\mathbf{BDM}_{k+1}(\Omega) &:= \{\mathbf{v} \in \mathbf{H}(\mathrm{div};\Omega) \,:\, \mathbf{v}|_T \in \mathbf{P}_{k+1}(T) \quad \forall\, T \in \mathcal{T}_h\}\\ \mathbf{BDM}_{k+1}^0(\Omega) &:= \{\mathbf{v} \in \mathbf{BDM}_{k+1}(\Omega) \,:\, \mathbf{v}\cdot\mathbf{n} = 0 \;\text{ on }\; \Gamma\}.\end{aligned}$$

For this postprocessed flux, we have the following result.

Lemma 6.3. *Given $T \in \mathcal{T}_h$ and $\mathbf{v}_h \in \mathbf{P}_{k+1}(T)$, there is exists a constants $C^\star > 0$, independent of T, such that*

$$\|\mathbf{v}_h^\star - \mathbf{v}_h\|_{L^2(T)} \;\le\; C^\star\, h_T^{1/2} \sum_{F\in\partial T} \|[\![\mathbf{v}_h\cdot\mathbf{n}]\!]\|_{L^2(F)}\,.$$

Proof. We proceed as in [45, Lemma 4.2]. Indeed, if we set $\boldsymbol{\delta} := \mathbf{v}_h^\star - \mathbf{v}_h \in \mathbf{P}_{k+1}(T)$ we have that $\boldsymbol{\delta}$ satisfying the equations

$$\begin{aligned}\int_F (\boldsymbol{\delta}\cdot\mathbf{n})q &= \int_F (\{\!\{\mathbf{v}_h\}\!\} - \mathbf{v}_h)\cdot\mathbf{n}q \quad \forall\, q \in \mathrm{P}_{k+1}(F), \quad \forall\, F \in \partial T,\\ \int_T \boldsymbol{\delta}\cdot\mathbf{p} &= 0 \quad \forall\, \mathbf{p} \in \mathbf{ND}_{k-1}(T).\end{aligned}$$

The result together with a scaling argument (see [19]), imply that

$$\|\boldsymbol{\delta}\|_{L^2(T)} \leq C\, h_T^{1/2} \|(\{\!\{\mathbf{v}_h\}\!\} - \mathbf{v}_h)\cdot\mathbf{n}\|_{0,\partial T}\,,$$

which, using the fact that $(\{\!\{\mathbf{v}_h\}\!\} - \mathbf{v}_h)\cdot\mathbf{n} = \pm[\![\mathbf{v}_h\cdot\mathbf{n}]\!]$, we complete the proof. □

Now, similar as in (6.4), we consider the Galerkin scheme: Find $(\mathbf{u}_h, p_h) \in \mathbf{V}_h^{\mathrm{dg}} \times Q_h$, such that

$$\begin{aligned}(\partial_t\mathbf{u}_h, \mathbf{v}_h)_{\mathcal{T}_h} - (\mathbf{u}_h\otimes\mathbf{u}_h^\star, \nabla_h\mathbf{v}_h)_{\mathcal{T}_h} - (p_h, \mathrm{div}_h(\mathbf{v}_h))_{\mathcal{T}_h} + \langle\widehat{\boldsymbol{\sigma}}(\mathbf{u}_h,p_h)\mathbf{n}, \mathbf{v}_h\rangle_{\partial\mathcal{T}_h} &= 0,\\ -(\nabla_h q_h, \mathbf{u}_h)_{\mathcal{T}_h} + \langle\widehat{\mathbf{u}}_h\cdot\mathbf{n}, q_h\rangle_{\partial\mathcal{T}_h} &= 0,\\ \mathbf{u}_h(0,\mathbf{x}) &= \mathbf{u}_{h,0}(\mathbf{x}) \quad \text{in } \Omega,\end{aligned} \tag{6.26}$$

for all $(\mathbf{v}_h, q_h) \in \mathbf{V}_h^{\mathrm{dg}} \times Q_h$, where

$$\widehat{\boldsymbol{\sigma}}(\mathbf{u}_h,p_h) := \{\!\{\mathbf{u}_h\}\!\}\otimes\{\!\{\mathbf{u}_h^\star\}\!\} + \{\!\{p_h\}\!\}\,\mathbb{I} + \alpha\, h_F^{-1}[\![\mathbf{u}_h\cdot\mathbf{n}]\!]\,\mathbb{I}, \tag{6.27}$$

and $\alpha > 0$ is stabilization parameter. In addition, we define the numerical flux $\widehat{\mathbf{u}}_h$ as

$$\widehat{\mathbf{u}}_h := \{\!\{\mathbf{u}_h\}\!\} \text{ on } \mathcal{E}_h.$$

Thus, from the second equation of (6.26) and the definition of $\mathbf{u}_h^\star$ (cf. (6.24) and (6.25)), we note that

$$0 = -(\nabla_h q_h, \mathbf{u}_h)_{\mathcal{T}_h} + \langle\widehat{\mathbf{u}}_h\cdot\mathbf{n}, q_h\rangle_{\partial\mathcal{T}_h} = -(\nabla_h q_h, \mathbf{u}_h^\star)_{\mathcal{T}_h} + \langle\mathbf{u}_h^\star\cdot\mathbf{n}, q_h\rangle_{\partial\mathcal{T}_h} = (q_h, \mathrm{div}(\mathbf{u}_h^\star))_{\mathcal{T}_h}$$

for all $q_h \in Q_h$. The above identity and the fact that $\mathrm{div}(\mathbf{u}_h^\star)|_T \in \mathrm{P}_k(T)$ for each $T \in \mathcal{T}_h$, imply that $\mathbf{u}_h^\star$ is divergence-free. This conclusion and the fact that $\mathbf{u}_h^\star$ has a continuous normal component are the main reasons that while we consider $\mathbf{u}_h^\star$ instead of $\mathbf{u}_h$ in the method (6.26).

Then, using integration by parts, the fact that $\mathbf{div}(\mathbf{u}_h\otimes\mathbf{u}_h^\star) = \mathbf{u}_h^\star\cdot\nabla\mathbf{u}_h$ (cf. (6.2)), and the definition of the numerical fluxes, it is not difficult to check that the above DG scheme is as follows: Find $\mathbf{u}_h \in \mathbf{V}_h^{\mathrm{dg}}$ and $p_h \in Q_h$ such that

$$\begin{aligned}(\partial_t\mathbf{u}_h, \mathbf{v}_h)_{\mathcal{T}_h} + (\mathbf{u}_h^\star\cdot\nabla_h\mathbf{u}_h, \mathbf{v}_h)_{\mathcal{T}_h} + \alpha\sum_{F\in\mathcal{E}_h^i} h_F^{-1}\langle[\![\mathbf{u}_h\cdot\mathbf{n}]\!], [\![\mathbf{v}_h\cdot\mathbf{n}]\!]\rangle_F &\\ - \sum_{F\in\mathcal{E}_h^i}\langle(\mathbf{u}_h^\star\cdot\mathbf{n})[\![\mathbf{u}_h]\!], \{\!\{\mathbf{v}_h\}\!\}\rangle_F - (p_h, \mathrm{div}_h(\mathbf{v}_h))_{\mathcal{T}_h} + \sum_{F\in\mathcal{E}_h^i}\langle[\![\mathbf{v}_h\cdot\mathbf{n}]\!], \{\!\{p_h\}\!\}\rangle_F &= 0,\\ (q_h, \mathrm{div}_h(\mathbf{u}_h))_{\mathcal{T}_h} - \sum_{F\in\mathcal{E}_h^i}\langle[\![\mathbf{u}_h\cdot\mathbf{n}]\!], \{\!\{q_h\}\!\}\rangle_F &= 0,\\ \mathbf{u}_h(0,\mathbf{x}) &= \mathbf{u}_{h,0}(\mathbf{x}) \quad \text{in } \Omega,\end{aligned} \tag{6.28}$$

for all $(\mathbf{v}_h, q_h) \in \mathbf{V}_h^{\mathrm{dg}} \times Q_h$. It is important to note here, that $\mathbf{u}_h$ is not necessarily divergence-free as in the method of Section 6.2.1. In addition, unlike the methods in the previous section, the DG method (6.28) is locally conservative.

Lemma 6.4 (Stability). *Given $\mathbf{u}_h \in \mathbf{V}_h^{\mathrm{dg}}$ the solution of* (6.28). *Then, we have*

$$\frac{d}{dt}\,\|\mathbf{u}_h\|^2_{L^2(\Omega)} \;\leq\; 0.$$

Proof. We take $\mathbf{v}_h := \mathbf{u}_h$ and $q_h := p_h$ in (6.28), and then we deduce

$$\frac{1}{2}\frac{d}{dt}\,\|\mathbf{u}_h\|^2_{L^2(\Omega)} \,+\, (\mathbf{u}_h^\star\cdot\nabla_h\mathbf{u}_h,\mathbf{u}_h)_{\mathcal{T}_h} \,+\, \alpha\sum_{F\in\mathcal{E}_h^i} h_F^{-1}\|[\![\mathbf{u}_h\cdot\mathbf{n}]\!]\|^2_{L^2(F)} \\ -\,\sum_{F\in\mathcal{E}_h^i}\langle(\mathbf{u}_h^\star\cdot\mathbf{n})[\![\mathbf{u}_h]\!],\{\!\{\mathbf{u}_h\}\!\}\rangle_F \;=\; 0\,.$$

Next, with that same arguments of (6.8), we have

$$(\mathbf{u}_h^\star\cdot\nabla_h\mathbf{u}_h,\mathbf{u}_h)_{\mathcal{T}_h} \,-\, \sum_{F\in\mathcal{E}_h^i}\langle(\mathbf{u}_h^\star\cdot\mathbf{n})[\![\mathbf{u}_h]\!],\{\!\{\mathbf{u}_h\}\!\}\rangle_F \;=\; 0,$$

which establish that

$$\frac{1}{2}\frac{d}{dt}\,\|\mathbf{u}_h\|^2_{L^2(\Omega)} \,+\, \alpha\sum_{F\in\mathcal{E}_h^i} h_F^{-1}\|[\![\mathbf{u}_h\cdot\mathbf{n}]\!]\|^2_{L^2(F)} \;=\; 0.$$

Finally, from the fact that $\alpha > 0$, we complete the proof. □

Error estimates for DG method

Now we are ready to provide error estimates for the DG scheme (6.28). We will need to define the BDM/Nédélec projection.

$$\int_F ((\mathbf{\Pi}_h^{\mathrm{BDM}}\mathbf{v}-\mathbf{v})\cdot\mathbf{n})q \;=\; 0 \quad \forall\, q\in \mathrm{P}_{k+1}(F), \quad \forall\, F\in\partial T, \tag{6.29}$$

$$\int_T (\mathbf{\Pi}_h^{\mathrm{BDM}}(\mathbf{v})-\mathbf{v})\cdot\mathbf{p} \;=\; 0 \quad \forall\, \mathbf{p}\in \mathbf{ND}_{k-1}(T)\,. \tag{6.30}$$

We have the following approximation results for $1\leq m\leq k+2$.

$$\|\mathbf{v}-\mathbf{\Pi}_h^{\mathrm{BDM}}(\mathbf{v})\|_{L^2(T)} + h_T\|\nabla(\mathbf{v}-\mathbf{\Pi}_h^{\mathrm{BDM}}(\mathbf{v}))\|_{L^2(T)} \;\leq\; C\,h_T^m|\mathbf{v}|_{m,T} \quad \forall\, T\in\mathcal{T}_h. \tag{6.31}$$

Moreover, we also have the following bounds

$$\|\mathbf{v}-\mathbf{\Pi}_h^{\mathrm{BDM}}(\mathbf{v})\|_{L^\infty(T)} + h_T\|\nabla(\mathbf{v}-\mathbf{\Pi}_h^{\mathrm{BDM}}(\mathbf{v}))\|_{L^\infty(T)} \;\leq\; C\,h_T\|\nabla\mathbf{v}\|_{L^\infty(T)} \quad \forall\, T\in\mathcal{T}_h. \tag{6.32}$$

Let now $\mathrm{E}^{\mathbf{u}} = \mathbf{\Pi}_h^{\mathrm{BDM}}(\mathbf{u})-\mathbf{u}_h$ and $\mathrm{E}^p = \mathcal{P}_h^k(p)-p_h$. Then, we follow (6.12) and consider the error equations:

$$
\begin{aligned}
&(\partial_t \mathrm{E}^{\mathbf{u}}, \mathbf{v}_h)_{\mathcal{T}_h} \;+\; (\mathbf{u}\cdot\nabla_h\mathbf{u} - \mathbf{u}_h^\star\cdot\nabla_h\mathbf{u}_h, \mathbf{v}_h)_{\mathcal{T}_h} \;+\; \alpha \sum_{F\in\mathcal{E}_h^i} h_F^{-1}\,\langle [\![\mathrm{E}^{\mathbf{u}}\cdot\mathbf{n}]\!], [\![\mathbf{v}_h\cdot\mathbf{n}]\!]\rangle_F \\
&\quad - \sum_{F\in\mathcal{E}_h^i} \langle(\mathbf{u}_h^\star\cdot\mathbf{n})[\![\mathrm{E}^{\mathbf{u}}]\!], \{\!\{\mathbf{v}_h\}\!\}\rangle_F \;-\; (\mathrm{E}^p, \mathrm{div}_h(\mathbf{v}_h))_{\mathcal{T}_h} \;+\; \sum_{F\in\mathcal{E}_h^i} \langle [\![\mathbf{v}_h\cdot\mathbf{n}]\!], \{\!\{\mathrm{E}^p\}\!\}\rangle_F \\
&\; = \; (\partial_t(\mathbf{\Pi}_h^{\mathrm{BDM}}(\mathbf{u}) - \mathbf{u}), \mathbf{v}_h)_{\mathcal{T}_h} \;+\; \alpha \sum_{F\in\mathcal{E}_h^i} h_F^{-1}\left\langle [\![(\mathbf{\Pi}_h^{\mathrm{BDM}}(\mathbf{u}) - \mathbf{u})\cdot\mathbf{n}]\!], [\![\mathbf{v}_h\cdot\mathbf{n}]\!]\right\rangle_F \\
&\quad - \sum_{F\in\mathcal{E}_h^i} \left\langle(\mathbf{u}_h^\star\cdot\mathbf{n})[\![\mathbf{\Pi}_h^{\mathrm{BDM}}(\mathbf{u}) - \mathbf{u}]\!], \{\!\{\mathbf{v}_h\}\!\}\right\rangle_F \;-\; (\mathcal{P}_h^k(p) - p, \mathrm{div}_h(\mathbf{v}_h))_{\mathcal{T}_h} \\
&\quad + \sum_{F\in\mathcal{E}_h^i} \left\langle [\![\mathbf{v}_h\cdot\mathbf{n}]\!], \{\!\{\mathcal{P}_h^k(p) - p\}\!\}\right\rangle_F, \qquad (6.33)\\
&(q_h, \mathrm{div}_h(\mathrm{E}^{\mathbf{u}}))_{\mathcal{T}_h} \;-\; \sum_{F\in\mathcal{E}_h^i} \langle [\![\mathrm{E}^{\mathbf{u}}\cdot\mathbf{n}]\!], \{\!\{q_h\}\!\}\rangle_F \;=\; 0,
\end{aligned}
$$

for all $(\mathbf{v}_h, q_h) \in \mathbf{V}_h^{\mathrm{dg}} \times Q_h$.

Theorem 6.3. *Assume that $\mathbf{u} \in W^{1,\infty}([0,T]\times\Omega)^d$. Also, suppose that $\mathcal{T}_h$ is quasi-uniform. Then, there exists $C > 0$, independent of h, such that*

$$\|(\mathbf{u} - \mathbf{u}_h)(T,\cdot)\|_{L^2(\Omega)} \;\leq\; C(u)h^{k+1}B(u)$$

where

$$C(u) \;:=\; (1 + C(1+C_u))\exp(C(1+C_u)T),$$

with $C_u := \|\mathbf{u}\|_{W^{1,\infty}([0,T]\times\Omega)}$. Also,

$$B(u) \;\;:=\;\; h\|\mathbf{u}_0\|_{H^{k+2}(\Omega)} + \|\mathbf{u}\|_{L^2(0,T;H^{k+2}(\Omega))} + h\|\mathbf{u}_t\|_{L^2(0,T;H^{k+2}(\Omega))} + \|p\|_{L^2(0,T;H^{k+1}(\Omega))}\,.$$

Proof. We begin by choosing $\mathbf{v}_h := \mathrm{E}^{\mathbf{u}}$ and $q_h := \mathrm{E}^p$ in the error equations (6.33). Then, we have that

$$
\begin{aligned}
&\frac{1}{2}\frac{d}{dt}\|\mathrm{E}^{\mathbf{u}}\|_{L^2(\Omega)}^2 + \alpha\sum_{F\in\mathcal{E}_h^i} h_F^{-1}\|[\![\mathrm{E}^{\mathbf{u}}\cdot\mathbf{n}]\!]\|_{L^2(F)}^2 \;=\; \underbrace{-(\mathbf{u}\cdot\nabla_h\mathbf{u} - \mathbf{u}_h^\star\cdot\nabla_h\mathbf{u}_h, \mathrm{E}^{\mathbf{u}})_{\mathcal{T}_h}}_{I_1} \\
&\quad + \underbrace{\sum_{F\in\mathcal{E}_h^i} \langle(\mathbf{u}_h^\star\cdot\mathbf{n})[\![\mathrm{E}^{\mathbf{u}}]\!], \{\!\{\mathrm{E}^{\mathbf{u}}\}\!\}\rangle_F}_{I_2} + (\mathbf{\Pi}_h^{\mathrm{BDM}}(\mathbf{u}_t) - \mathbf{u}_t, \mathrm{E}^{\mathbf{u}})_{\mathcal{T}_h} \\
&\quad + \underbrace{\alpha\sum_{F\in\mathcal{E}_h^i} h_F^{-1}\left\langle[\![(\mathbf{\Pi}_h^{\mathrm{BDM}}(\mathbf{u}) - \mathbf{u})\cdot\mathbf{n}]\!], [\![\mathrm{E}^{\mathbf{u}}\cdot\mathbf{n}]\!]\right\rangle_F}_{I_3} \underbrace{-\sum_{F\in\mathcal{E}_h^i}\left\langle(\mathbf{u}_h^\star\cdot\mathbf{n})[\![\mathbf{\Pi}_h^{\mathrm{BDM}}(\mathbf{u}) - \mathbf{u}]\!], \{\!\{\mathrm{E}^{\mathbf{u}}\}\!\}\right\rangle_F}_{I_4} \\
&\quad - \underbrace{(\mathcal{P}_h^k(p) - p, \mathrm{div}_h(\mathrm{E}^{\mathbf{u}}))_{\mathcal{T}_h}}_{I_5} + \underbrace{\sum_{F\in\mathcal{E}_h^i}\left\langle[\![\mathrm{E}^{\mathbf{u}}\cdot\mathbf{n}]\!], \{\!\{\mathcal{P}_h^k(p) - p\}\!\}\right\rangle_F}_{I_6}. \qquad (6.34)
\end{aligned}
$$

Next, we want to find bounds for I_i, $i = 1,\ldots,6$. First since $\mathrm{div}_h(\mathrm{E}^{\mathbf{u}})$ is a piecewise polynomial of degree k we have $I_5 = 0$. Also, note that by (6.29) $I_3 = 0$. Before we bound the rest of the terms. We note that by Lemma 6.3 and $[\![\mathbf{\Pi}_h^{\mathrm{BDM}}(\mathbf{u})\cdot\mathbf{n}]\!]=0$, we know

$$\|\mathbf{u}_h-\mathbf{u}_h^\star\|_{L^2(\Omega)}^2 \;\le\; C\sum_{F\in\mathcal{E}_h} h_F\|[\![\mathbf{u}_h\cdot\mathbf{n}]\!]\|_{L^2(F)}^2 \;=\; C\sum_{F\in\mathcal{E}_h} h_F\|[\![\mathrm{E}^{\mathbf{u}}\cdot\mathbf{n}]\!]\|_{L^2(F)}^2 \;\le\; C\|\mathrm{E}^{\mathbf{u}}\|_{L^2(\Omega)}^2. \quad (6.35)$$

Now we bound I_1, using that

$$\begin{aligned} I_1 &= -(\mathbf{u}\cdot\nabla_h\left\{\mathbf{u}-\mathbf{\Pi}_h^{\mathrm{BDM}}(\mathbf{u})\right\},\mathrm{E}^{\mathbf{u}})_{\mathcal{T}_h} - ((\mathbf{u}-\mathbf{u}_h^\star)\cdot\nabla_h\mathbf{\Pi}_h^{\mathrm{BDM}}(\mathbf{u}),\mathrm{E}^{\mathbf{u}})_{\mathcal{T}_h} - (\mathbf{u}_h^\star\cdot\nabla_h\mathrm{E}^{\mathbf{u}},\mathrm{E}^{\mathbf{u}})_{\mathcal{T}_h},\\ &= -(\mathbf{u}\cdot\nabla_h\left\{\mathbf{u}-\mathbf{\Pi}_h^{\mathrm{BDM}}(\mathbf{u})\right\},\mathrm{E}^{\mathbf{u}})_{\mathcal{T}_h} - ((\mathbf{u}-\mathbf{u}_h^\star)\cdot\nabla_h\mathbf{\Pi}_h^{\mathrm{BDM}}(\mathbf{u}),\mathrm{E}^{\mathbf{u}})_{\mathcal{T}_h} - I_2, \end{aligned}$$

where in last term, we apply the same argument of (6.8) as in the proof of Theorem 6.1. Furthermore, using that $\|\mathbf{u}\|_{L^\infty(\Omega)}\le C_u$ and $\|\nabla_h\mathbf{\Pi}_h^{\mathrm{BDM}}(\mathbf{u})\|_{L^\infty(\Omega)}\le C\,C_u$ (see (6.32)), we deduce that

$$\begin{aligned} I_1+I_2 &\le C_u\|\nabla_h\{\mathbf{\Pi}_h^{\mathrm{BDM}}(\mathbf{u})-\mathbf{u}\}\|_{L^2(\Omega)}\|\mathrm{E}^{\mathbf{u}}\|_{L^2(\Omega)} + C\,C_u\|\mathbf{u}-\mathbf{u}_h^\star\|_{L^2(\Omega)}\|\mathrm{E}^{\mathbf{u}}\|_{L^2(\Omega)}\\ &\le CC_u\Big\{\|\nabla_h\{\mathbf{\Pi}_h^{\mathrm{BDM}}(\mathbf{u})-\mathbf{u}\}\|_{L^2(\Omega)}+\|\mathbf{\Pi}_h^{\mathrm{BDM}}(\mathbf{u})-\mathbf{u}\|_{L^2(\Omega)}+\|\mathrm{E}^{\mathbf{u}}\|_{L^2(\Omega)}\Big\}\|\mathrm{E}^{\mathbf{u}}\|_{L^2(\Omega)}\\ &\quad + C\,C_u\|\mathbf{u}_h-\mathbf{u}_h^\star\|_{L^2(\Omega)}\|\mathrm{E}^{\mathbf{u}}\|_{L^2(\Omega)}\\ &\le C\,C_u\,\|\mathrm{E}^{\mathbf{u}}\|_{L^2(\Omega)}^2 + C\,C_u\|\mathbf{\Pi}_h^{\mathrm{BDM}}(\mathbf{u})-\mathbf{u}\|_{L^2(\Omega)}^2 + C\,C_u\|\nabla_h\{\mathbf{\Pi}_h^{\mathrm{BDM}}(\mathbf{u})-\mathbf{u}\}\|_{L^2(\Omega)}^2, \end{aligned} \quad (6.36)$$

where we also used (6.35).

In the case of I_4, from $\|\mathbf{\Pi}_h^{\mathrm{BDM}}(\mathbf{u})\|_{L^\infty(\Omega)}\le C_u$, note that

$$\begin{aligned} I_4 &= \sum_{F\in\mathcal{E}_h^i}\big\langle(\{\!\{\mathbf{u}_h^\star\}\!\}\cdot\mathbf{n})[\![\mathbf{\Pi}_h^{\mathrm{BDM}}(\mathbf{u})-\mathbf{u}]\!],\{\!\{\mathrm{E}^{\mathbf{u}}\}\!\}\big\rangle_F\\ &= \sum_{F\in\mathcal{E}_h^i}\big\langle(\{\!\{\mathbf{u}_h^\star-\mathbf{u}_h\}\!\}\cdot\mathbf{n})[\![\mathbf{\Pi}_h^{\mathrm{BDM}}(\mathbf{u})-\mathbf{u}]\!],\{\!\{\mathrm{E}^{\mathbf{u}}\}\!\}\big\rangle_F\\ &\quad - \sum_{F\in\mathcal{E}_h^i}\big\langle(\{\!\{\mathrm{E}^{\mathbf{u}}\}\!\}\cdot\mathbf{n})[\![\mathbf{\Pi}_h^{\mathrm{BDM}}(\mathbf{u})-\mathbf{u}]\!],\{\!\{\mathrm{E}^{\mathbf{u}}\}\!\}\big\rangle_F\\ &\quad + \sum_{F\in\mathcal{E}_h^i}\big\langle(\{\!\{\mathbf{\Pi}_h^{\mathrm{BDM}}(\mathbf{u})\}\!\}\cdot\mathbf{n})[\![\mathbf{\Pi}_h^{\mathrm{BDM}}(\mathbf{u})-\mathbf{u}]\!],\{\!\{\mathrm{E}^{\mathbf{u}}\}\!\}\big\rangle_F\\ &\le \|\mathbf{\Pi}_h^{\mathrm{BDM}}(\mathbf{u})-\mathbf{u}\|_{L^\infty(\Omega)}\left(\sum_{F\in\mathcal{E}_h^i}h_F^{-1}\|\{\!\{\mathbf{u}_h^\star-\mathbf{u}_h\}\!\}\|_{L^2(F)}^2\right)^{1/2}\left(\sum_{F\in\mathcal{E}_h^i}h_F\|\{\!\{\mathrm{E}^{\mathbf{u}}\}\!\}\|_{L^2(F)}^2\right)^{1/2}\\ &\quad + \|\mathbf{\Pi}_h^{\mathrm{BDM}}(\mathbf{u})-\mathbf{u}\|_{L^\infty(\Omega)}\sum_{F\in\mathcal{E}_h^i}\|\{\!\{\mathrm{E}^{\mathbf{u}}\}\!\}\|_{L^2(F)}^2\\ &\quad + C_u\left(\sum_{F\in\mathcal{E}_h^i}h_F^{-1}\|[\![\mathbf{\Pi}_h^{\mathrm{BDM}}(\mathbf{u})-\mathbf{u}]\!]\|_{L^2(F)}^2\right)^{1/2}\left(\sum_{F\in\mathcal{E}_h^i}h_F\|\{\!\{\mathrm{E}^{\mathbf{u}}\}\!\}\|_{L^2(F)}^2\right)^{1/2}, \end{aligned}$$

and from (6.16), (6.17), and (6.35) with an inverse inequality, we deduce that

$$\begin{aligned} I_4 &\le \|\mathbf{u}_h-\mathbf{u}_h^\star\|_{L^2(\Omega)}\left(Ch^{-1}\|\mathbf{\Pi}_h^{\mathrm{BDM}}(\mathbf{u})-\mathbf{u}\|_{L^\infty(\Omega)}\right)\|\mathrm{E}^{\mathbf{u}}\|_{L^2(\Omega)}\\ &\quad + \left(Ch^{-1}\|\mathbf{\Pi}_h^{\mathrm{BDM}}(\mathbf{u})-\mathbf{u}\|_{L^\infty(\Omega)}\right)\|\mathrm{E}^{\mathbf{u}}\|_{L^2(\Omega)}^2 + C\,C_u\Big\{h^{-2}\|\mathbf{\Pi}_h^{\mathrm{BDM}}(\mathbf{u})-\mathbf{u}\|_{L^2(\Omega)}^2\\ &\quad + \|\nabla_h\{\mathbf{\Pi}_h^{\mathrm{BDM}}(\mathbf{u})-\mathbf{u}\}\|_{L^2(\Omega)}^2\Big\} + C\,C_u\|\mathrm{E}^{\mathbf{u}}\|_{L^2(\Omega)}^2\\ &\le C\left(1+h^{-1}\|\mathbf{\Pi}_h^{\mathrm{BDM}}(\mathbf{u})-\mathbf{u}\|_{L^\infty(\Omega)}\right)\|\mathrm{E}^{\mathbf{u}}\|_{L^2(\Omega)}^2\\ &\quad + Ch^{-2}\|\mathbf{\Pi}_h^{\mathrm{BDM}}(\mathbf{u})-\mathbf{u}\|_{L^2(\Omega)}^2 + C\|\nabla_h\{\mathbf{\Pi}_h^{\mathrm{BDM}}(\mathbf{u})-\mathbf{u}\}\|_{L^2(\Omega)}^2. \end{aligned}$$

In addition, applying (6.32), we conclude that

$$I_4 \;\leq\; C\,C_u\,\|\mathrm{E}^{\mathbf{u}}\|^2_{L^2(\Omega)} \,+\, C\,C_u\Big\{h^{-2}\|\mathbf{\Pi}_h^{\mathrm{BDM}}(\mathbf{u})-\mathbf{u}\|^2_{L^2(\Omega)} \,+\, \|\nabla_h\{\mathbf{\Pi}_h^{\mathrm{BDM}}(\mathbf{u})-\mathbf{u}\}\|^2_{L^2(\Omega)}\Big\}. \quad (6.37)$$

Now, in similar way to (6.16), given $q \in H^1(\mathcal{T}_h)$ we have that

$$\sum_{F\in\mathcal{E}_h^i} h_F\|\{\!\{q\}\!\}\|^2_{L^2(F)} \;\leq\; \widehat{C}\Big\{\|q\|^2_{L^2(\Omega)} \,+\, h^2\|\nabla_h q\|^2_{L^2(\Omega)}\Big\},$$

which allows us to deduce

$$\begin{aligned} I_6 \;&=\; \sum_{F\in\mathcal{E}_h}\Big\langle h_F^{-1/2}[\![\mathrm{E}^{\mathbf{u}}\cdot\mathbf{n}]\!], h_F^{1/2}\{\!\{\mathcal{P}_h^k(p)-p\}\!\}\Big\rangle_F \;\leq\; \frac{\alpha}{2}\sum_{F\in\mathcal{E}_h} h_F^{-1}\|[\![\mathrm{E}^{\mathbf{u}}\cdot\mathbf{n}]\!]\|^2_{L^2(F)} \\ &\quad+\; C\sum_{F\in\mathcal{E}_h^i} h_F\|\{\!\{\mathcal{P}_h^k(p)-p\}\!\}\|^2_{L^2(F)} \\ &\leq\; \frac{\alpha}{2}\sum_{F\in\mathcal{E}_h} h_F^{-1}\|[\![\mathrm{E}^{\mathbf{u}}\cdot\mathbf{n}]\!]\|^2_{L^2(F)} \,+\, C\,\|\mathcal{P}_h^k(p)-p\|^2_{L^2(\Omega)} \,+\, C\,h^2\|\nabla_h\{\mathcal{P}_h^k(p)-p\}\|^2_{L^2(\Omega)}. \quad (6.38)\end{aligned}$$

On the other hand, replacing (6.36)–(6.38) in (6.34), we obtain that

$$\begin{aligned}&\frac{1}{2}\frac{d}{dt}\|\mathrm{E}^{\mathbf{u}}\|^2_{L^2(\Omega)} \,+\, \frac{\alpha}{2}\sum_{F\in\mathcal{E}_h^i} h_F^{-1}\|[\![\mathrm{E}^{\mathbf{u}}\cdot\mathbf{n}]\!]\|^2_{L^2(F)} \;\leq\; C\,C_u\|\mathrm{E}^{\mathbf{u}}\|^2_{L^2(\Omega)} \,+\, \frac{1}{2}\|\mathbf{\Pi}_h^{\mathrm{BDM}}(\mathbf{u}_t)-\mathbf{u}_t\|^2_{L^2(\Omega)} \\ &+ C\,C_u\Big\{h^{-2}\|\mathbf{\Pi}_h^{\mathrm{BDM}}(\mathbf{u})-\mathbf{u}\|^2_{L^2(\Omega)} \,+\, \|\nabla_h\{\mathbf{\Pi}_h^{\mathrm{BDM}}\mathbf{u}-\mathbf{u}\}\|^2_{L^2(\Omega)}\Big\} \,+\, C\,\|\mathcal{P}_h^k(p)-p\|^2_{L^2(\Omega)} \\ &+ Ch^2\|\nabla_h\{\mathcal{P}_h^k(p)-p\}\|^2_{L^2(\Omega)}.\end{aligned}$$

Hence, using (6.31) we have

$$\begin{aligned}\frac{d}{dt}\|\mathrm{E}^{\mathbf{u}}\|^2_{L^2(\Omega)} \;&\leq\; C(1+C_u)\|\mathrm{E}^{\mathbf{u}}\|^2_{L^2(\Omega)} \\ &\quad+\, C(1+C_u)\,h^{2(k+1)}\Big\{h^2\|\mathbf{u}_t\|^2_{H^{k+2}(\Omega)} + \|\mathbf{u}\|^2_{H^{k+2}(\Omega)} + \|p\|_{H^{k+1}(\Omega)}\Big\}.\end{aligned}$$

Finally, applying Gronwall's inequality gives the result. □

Theorem 6.4. *Assuming the hypothesis of the previous theorem we have the existence of a $C > 0$, independent of h, such that*

$$\begin{aligned}\|(p-p_h)(T,\cdot)\|_{L^2(\Omega)} \;&\leq\; (C(u)h^{k+1-d/2}B(u) + C_u + C\,)h^k\Big\{C(u)\,B(u) + \|\mathbf{u}(T,\cdot)\|_{H^{k+2}(\Omega)}\Big\} \\ &\quad+\, Ch^{k+1}\Big\{h\|\mathbf{u}_t(T,\cdot)\|_{H^{k+2}(\Omega)} + \|p(T,\cdot)\|_{H^{k+1}(\Omega)}\Big\}.\end{aligned}$$

Proof. Similar to the proof of Theorem 6.2. □

Upwind flux for DG method

Similarly as Section 6.2.1, we now introduce a DG method using an upwind flux. Indeed, as before, we redefine the numerical flux $\widehat{\boldsymbol{\sigma}}$ (see (6.27)) in the form

$$\widehat{\boldsymbol{\sigma}}(\mathbf{u}_h, p_h) \;:=\; \widehat{\mathbf{u}}_h^{\mathbf{w}}\otimes\{\!\{\mathbf{u}_h^{\star}\}\!\} \;+\; \{\!\{p_h\}\!\}\,\mathbb{I} \;+\; \alpha\,h_F^{-1}[\![\mathbf{u}_h\cdot\mathbf{n}]\!]\,\mathbb{I},$$

where we take $\widehat{\mathbf{u}}_h^{\mathbf{w}}$ as

$$\widehat{\mathbf{u}}_h^{\mathbf{w}} \;:=\; \begin{cases} \mathbf{u}_h^{\text{int}} & \text{if} \quad \mathbf{u}_h^\star \cdot \mathbf{n} \geq 0, \\ \mathbf{u}_h^{\text{ext}} & \text{if} \quad \mathbf{u}_h^\star \cdot \mathbf{n} < 0. \end{cases}$$

Once again, with this definition we can obtain again the method (6.28), with an extra consistent term given by

$$\sum_{F \in \mathcal{E}_h^i} \langle\, |\mathbf{u}_h^\star \cdot \mathbf{n}|\, [\![\mathbf{u}_h]\!],\; [\![\mathbf{v}_h]\!] \rangle_F\,,$$

which, allow us to prove stability and convergence in the same way of before, using the fact that when $\mathbf{v}_h = \mathbf{u}_h$ the above term is positive. Summarizing, we find $\mathbf{u}_h \in \mathbf{V}_h^{\text{dg}}$ and $p_h \in Q_h$ such that

$$\begin{aligned} (\partial_t \mathbf{u}_h, \mathbf{v}_h)_{\mathcal{T}_h} \,+\, (\mathbf{u}_h^\star \cdot \nabla_h \mathbf{u}_h, \mathbf{v}_h)_{\mathcal{T}_h} \,+\, \alpha \sum_{F \in \mathcal{E}_h^i} h_F^{-1} \langle [\![\mathbf{u}_h \cdot \mathbf{n}]\!], [\![\mathbf{v}_h \cdot \mathbf{n}]\!] \rangle_F & \\ -\, \sum_{F \in \mathcal{E}_h^i} \langle\, (\mathbf{u}_h^\star \cdot \mathbf{n})\, [\![\mathbf{u}_h]\!], \{\!\{ \mathbf{v}_h \}\!\} \rangle_F \,+\, \sum_{F \in \mathcal{E}_h^i} \langle\, |\mathbf{u}_h^\star \cdot \mathbf{n}|\, [\![\mathbf{u}_h]\!],\; [\![\mathbf{v}_h]\!] \rangle_F & \\ -\, (p_h, \operatorname{div}_h(\mathbf{v}_h))_{\mathcal{T}_h} \,+\, \sum_{F \in \mathcal{E}_h^i} \langle [\![\mathbf{v}_h \cdot \mathbf{n}]\!], \{\!\{ p_h \}\!\} \rangle_F &\;=\; 0, \\ (q_h, \operatorname{div}_h(\mathbf{u}_h))_{\mathcal{T}_h} \,-\, \sum_{F \in \mathcal{E}_h^i} \langle [\![\mathbf{u}_h \cdot \mathbf{n}]\!], \{\!\{ q_h \}\!\} \rangle_F &\;=\; 0, \\ \mathbf{u}_h(0, \mathbf{x}) \;=\; \mathbf{u}_{h,0}(\mathbf{x}) \quad \text{in } \Omega, & \end{aligned} \tag{6.39}$$

for all $(\mathbf{v}_h, q_h) \in \mathbf{V}_h^{\text{dg}} \times Q_h$.

6.3 Fully-discrete methods

In this section we define fully-discrete versions of both approaches introduced in Section 6.2. In order to do that, for the time discretization we consider the backward Euler method, that is, we write

$$\mathbf{u}_t(t_{n+1}, \,\cdot\,) \;=\; \frac{1}{\Delta t} \big\{ \mathbf{u}(t_{n+1}, \,\cdot\,) \,-\, \mathbf{u}(t_n, \,\cdot\,) \big\} \,+\, \mathbf{E}_0(t_{n+1}), \tag{6.40}$$

where $\Delta t > 0$ is the time step, $t_n := n\Delta t$, $0 \leq n \leq N$, and $\mathbf{E}_0(t_{n+1})$ is the truncation error. We know that

$$\|\mathbf{E}_0(t_{n+1})\|_{L^2(\Omega)} \;\leq\; C \int_{t_n}^{t_{n+1}} \|\mathbf{u}_{tt}(s, \cdot)\|_{L^2(\Omega)}\, ds. \tag{6.41}$$

For simplicity of the following analysis we denote $\mathbf{u}^n := \mathbf{u}(t_n, \,\cdot\,)$ for the exact value and $\mathbf{u}_h^n := \mathbf{u}_h(t_n, \,\cdot\,)$ for the approximation. Also, given $\mathbf{\Pi}_h^k$ the corresponding projection used before in each case, respectively, we define $\mathbf{e}_{\mathbf{u}}^n := \mathbf{\Pi}_h^k(\mathbf{u}^n) - \mathbf{u}_h^n$ as the discrete error. Similar convention is used for the pressure variable.

On the other hand, using (6.40) we have that the exact solution of (6.1) satisfies that

$$\begin{aligned} (\mathbf{u}^{n+1}, \mathbf{v}_h)_{\mathcal{T}_h} \,+\, \Delta t (\mathbf{u}^{n+1} \cdot \nabla \mathbf{u}^{n+1}, \mathbf{v}_h)_{\mathcal{T}_h} \,-\, \Delta t (p^{n+1}, \operatorname{div}(\mathbf{v}_h))_{\mathcal{T}_h} &\;=\; (\mathbf{u}^n, \mathbf{v}_h)_{\mathcal{T}_h} \\ &\qquad -\, \Delta t (\mathbf{E}_0(t_{n+1}), \mathbf{v}_h)_{\mathcal{T}_h}, \\ (q_h, \operatorname{div}(\mathbf{u}^{n+1}))_{\mathcal{T}_h} &\;=\; 0, \end{aligned}$$

or equivalently,

$$
\begin{aligned}
(\mathbf{u}^{n+1}, \mathbf{v}_h)_{\mathcal{T}_h} \,+\, \Delta t(\mathbf{u}^n \cdot \nabla \mathbf{u}^{n+1}, \mathbf{v}_h)_{\mathcal{T}_h} \,-\, \Delta t(p^{n+1}, \mathrm{div}(\mathbf{v}_h))_{\mathcal{T}_h} \;&=\; (\mathbf{u}^n, \mathbf{v}_h)_{\mathcal{T}_h} \\
+\, \Delta t((\mathbf{u}^n - \mathbf{u}^{n+1}) \cdot \nabla \mathbf{u}^{n+1}, \mathbf{v}_h)_{\mathcal{T}_h} \,&-\, \Delta t(\mathbf{E}_0(t_{n+1}), \mathbf{v}_h)_{\mathcal{T}_h}, \\
(q_h, \mathrm{div}(\mathbf{u}^{n+1}))_{\mathcal{T}_h} \;&=\; 0,
\end{aligned}
\tag{6.42}
$$

for all $(\mathbf{v}_h, q_h) \in \mathbf{V}_h^{\mathrm{dg}} \times Q_h$. We recall here that $\mathbf{V}_h \subset \mathbf{V}_h^{\mathrm{dg}}$.

6.3.1 H(div) conforming methods

Next, using (6.40) in the semi-discrete method (6.6), we introduce the fully-discrete approximation as: Find $(\mathbf{u}_h^{n+1}, p_h^{n+1}) \in \mathbf{V}_h \times Q_h$ such that

$$
\begin{aligned}
(\mathbf{u}_h^{n+1}, \mathbf{v}_h)_{\mathcal{T}_h} \,+\, \Delta t(\mathbf{u}_h^n \cdot \nabla_h \mathbf{u}_h^{n+1}, \mathbf{v}_h)_{\mathcal{T}_h} \,-\, \Delta t \sum_{F \in \mathcal{E}_h^i} \big\langle (\mathbf{u}_h^n \cdot \mathbf{n}) [\![\mathbf{u}_h^{n+1}]\!], \{\!\{ \mathbf{v}_h \}\!\} \big\rangle_F & \\
-\, \Delta t(p_h^{n+1}, \mathrm{div}(\mathbf{v}_h))_{\mathcal{T}_h} \;&=\; (\mathbf{u}_h^n, \mathbf{v}_h)_{\mathcal{T}_h}, \\
(q_h, \mathrm{div}(\mathbf{u}_h^{n+1}))_{\mathcal{T}_h} \;&=\; 0,
\end{aligned}
\tag{6.43}
$$

for all $(\mathbf{v}_h, q_h) \in \mathbf{V}_h \times Q_h$. Note that we eliminated the nonlinearity of the problem using the previous approximation. Also, it follows from the proof of Lemma 6.1 that when we take $\mathbf{v}_h := \mathbf{u}_h^{n+1}$ in (6.43), we have

$$
\|\mathbf{u}_h^{n+1}\|_{L^2(\Omega)}^2 \;=\; (\mathbf{u}_h^n, \mathbf{u}_h^{n+1})_{\mathcal{T}_h},
$$

which establish that $\|\mathbf{u}_h^{n+1}\|_{L^2(\Omega)} \le \|\mathbf{u}_h^n\|_{L^2(\Omega)}$, that is, the method (6.43) is stable.

Our next goal is establish an error estimate for the velocity.

Theorem 6.5. *Assume that $\mathbf{u} \in W^{1,\infty}([0,T] \times \Omega)^d$ is uniformly bounded. Also, suppose that $\mathcal{T}_h$ is quasi-uniform. Then, there exists $C > 0$, independent of h, such that*

$$
\|\mathbf{u}^n - \mathbf{u}_h^n\|_{L^2(\Omega)} \;\le\; C\, \exp(C\, C_u\, T)\, (h^k + \Delta t)\, A(u), \qquad \textit{for all } \; 0 \le n \le N\,,
$$

with $C_u := \|\mathbf{u}\|_{W^{1,\infty}([0,T]\times\Omega)}$. Also, where

$$
\begin{aligned}
A(u) \;:=\; & (h\sqrt{T} + C_u T^{3/2}) \|\mathbf{u}_t\|_{L^2(0,T;H^{k+1}(\Omega))} \,+\, C_u \sqrt{T} \|\mathbf{u}_t\|_{L^2(0,T;L^2(\Omega))} \,+\, \sqrt{T} \|\mathbf{u}_{tt}\|_{L^2(0,T;L^2(\Omega))} \\
& +\, (C_u T + h) \|\mathbf{u}_0\|_{H^{k+1}(\Omega)}\,.
\end{aligned}
$$

Proof. We begin by subtracting equation (6.42) from equation (6.43) together with the fact that $[\![\mathbf{u}^{n+1}]\!] = \mathbf{0}$ on $\mathcal{E}_h^i$, in order to obtain the error equation

$$
\begin{aligned}
& (\mathbf{e}_{\mathbf{u}}^{n+1}, \mathbf{v}_h)_{\mathcal{T}_h} \,+\, \Delta t(\mathbf{u}^n \cdot \nabla_h \mathbf{u}^{n+1} - \mathbf{u}_h^n \cdot \nabla_h \mathbf{u}_h^{n+1}, \mathbf{v}_h)_{\mathcal{T}_h} \,-\, \Delta t \sum_{F \in \mathcal{E}_h^i} \big\langle (\mathbf{u}_h^n \cdot \mathbf{n}) [\![\mathbf{e}_{\mathbf{u}}^{n+1}]\!], \{\!\{ \mathbf{v}_h \}\!\} \big\rangle_F \\
& \quad -\, \Delta t(p^{n+1} - p_h^{n+1}, \mathrm{div}(\mathbf{v}_h))_{\mathcal{T}_h} \;=\; (\mathbf{u}^n - \mathbf{u}_h^n, \mathbf{v}_h)_{\mathcal{T}_h} \,+\, (\mathbf{\Pi}_h^k(\mathbf{u}^{n+1}) - \mathbf{u}^{n+1}, \mathbf{v}_h)_{\mathcal{T}_h} \\
& \quad +\, \Delta t((\mathbf{u}^n - \mathbf{u}^{n+1}) \cdot \nabla \mathbf{u}^{n+1}, \mathbf{v}_h)_{\mathcal{T}_h} \,-\, \Delta t \sum_{F \in \mathcal{E}_h^i} \Big\langle (\mathbf{u}_h^n \cdot \mathbf{n}) [\![\mathbf{\Pi}_h^k(\mathbf{u}^{n+1}) - \mathbf{u}^{n+1}]\!], \{\!\{ \mathbf{v}_h \}\!\} \Big\rangle_F \\
& \quad -\, \Delta t(\mathbf{E}_0(t_{n+1}), \mathbf{v}_h)_{\mathcal{T}_h}.
\end{aligned}
\tag{6.44}
$$

Now, we take $\mathbf{v}_h := \mathbf{e}_{\mathbf{u}}^{n+1}$ and using that $\operatorname{div}(\mathbf{e}_{\mathbf{u}}^{n+1}) = 0$ in Ω, it follows that

$$\begin{aligned}
\|\mathbf{e}_{\mathbf{u}}^{n+1}\|^2_{L^2(\Omega)} \;&=\; \underbrace{-\Delta t(\mathbf{u}^n\cdot\nabla_h\mathbf{u}^{n+1} - \mathbf{u}_h^n\cdot\nabla_h\mathbf{u}_h^{n+1}, \mathbf{e}_{\mathbf{u}}^{n+1})_{\mathcal{T}_h}}_{I_1} \;+\; \underbrace{\Delta t\sum_{F\in\mathcal{E}_h^i}\big\langle(\mathbf{u}_h^n\cdot\mathbf{n})[\![\mathbf{e}_{\mathbf{u}}^{n+1}]\!], \{\!\{\mathbf{e}_{\mathbf{u}}^{n+1}\}\!\}\big\rangle_F}_{I_2} \\
&+ (\mathbf{u}^n - \mathbf{u}_h^n, \mathbf{e}_{\mathbf{u}}^{n+1})_{\mathcal{T}_h} \;+\; (\mathbf{\Pi}_h^k(\mathbf{u}^{n+1}) - \mathbf{u}^{n+1}, \mathbf{e}_{\mathbf{u}}^{n+1})_{\mathcal{T}_h} \;+\; \Delta t((\mathbf{u}^n - \mathbf{u}^{n+1})\cdot\nabla\mathbf{u}^{n+1}, \mathbf{e}_{\mathbf{u}}^{n+1})_{\mathcal{T}_h} \\
&- \underbrace{\Delta t\sum_{F\in\mathcal{E}_h^i}\Big\langle(\mathbf{u}_h^n\cdot\mathbf{n})[\![\mathbf{\Pi}_h^k(\mathbf{u}^{n+1}) - \mathbf{u}^{n+1}]\!], \{\!\{\mathbf{e}_{\mathbf{u}}^{n+1}\}\!\}\Big\rangle_F}_{I_3} \;-\; \Delta t(\mathbf{E}_0(t_{n+1}), \mathbf{e}_{\mathbf{u}}^{n+1})_{\mathcal{T}_h},
\end{aligned}\tag{6.45}$$

which, in similar way to (6.14), we note that

$$\begin{aligned}
I_1 \,+\, I_2 \;&=\; -\Delta t(\mathbf{u}^n\cdot\nabla_h\{\mathbf{u}^{n+1} - \mathbf{\Pi}_h^k(\mathbf{u}^{n+1})\}, \mathbf{e}_{\mathbf{u}}^{n+1})_{\mathcal{T}_h} \;-\; \Delta t((\mathbf{u}^n - \mathbf{u}_h^n)\cdot\nabla_h\mathbf{\Pi}_h^k(\mathbf{u}^{n+1}), \mathbf{e}_{\mathbf{u}}^{n+1})_{\mathcal{T}_h} \\
&\le\; \Delta t\Big\{C_u\|\nabla_h\{\mathbf{\Pi}_h^k(\mathbf{u}^{n+1}) - \mathbf{u}^{n+1}\}\|_{L^2(\Omega)} + C\,C_u\|\mathbf{\Pi}_h^k(\mathbf{u}^n) - \mathbf{u}^n\|_{L^2(\Omega)} \\
&\quad +\; C\,C_u\|\mathbf{e}_{\mathbf{u}}^n\|_{L^2(\Omega)}\Big\}\|\mathbf{e}_{\mathbf{u}}^{n+1}\|_{L^2(\Omega)},
\end{aligned}\tag{6.46}$$

where, we used that $\|\mathbf{u}^n\|_{L^\infty(\Omega)} \le C_u$ and $\|\nabla_h\mathbf{\Pi}_h^k(\mathbf{u}^{n+1})\|_{L^\infty(\Omega)} \le C\,C_u$. Also, follows (6.15) and using (6.16), (6.17) and (6.10), we have

$$\begin{aligned}
I_3 \;&\le\; C\,\Delta t\left\{h^{-1}\|\mathbf{\Pi}_h^k(\mathbf{u}^{n+1}) - \mathbf{u}^{n+1}\|_{L^\infty(\Omega)}\left(\sum_{F\in\mathcal{E}_h^i} h_F\|\{\!\{\mathbf{e}_{\mathbf{u}}^n\}\!\}\|^2_{L^2(F)}\right)^{\frac12}\right. \\
&\quad \left. +\; \|\mathbf{\Pi}_h^k(\mathbf{u}^n)\|_{L^\infty(\Omega)}\left(\sum_{F\in\mathcal{E}_h^i} h_F^{-1}\|[\![\mathbf{\Pi}_h^k(\mathbf{u}^{n+1}) - \mathbf{u}^{n+1}]\!]\|^2_{L^2(F)}\right)^{\frac12}\right\}\left(\sum_{F\in\mathcal{E}_h^i} h_F\|\{\!\{\mathbf{e}_{\mathbf{u}}^{n+1}\}\!\}\|^2_{L^2(F)}\right)^{\frac12} \\
&\le\; C\,C_u\Delta t\Big\{\|\mathbf{e}_{\mathbf{u}}^n\|_{L^2(\Omega)} + h^{-1}\|\mathbf{\Pi}_h^k(\mathbf{u}^{n+1}) - \mathbf{u}^{n+1}\|_{L^2(\Omega)} \\
&\quad +\; \|\nabla_h\{\mathbf{\Pi}_h^k(\mathbf{u}^{n+1}) - \mathbf{u}^{n+1}\}\|_{L^2(\Omega)}\Big\}\|\mathbf{e}_{\mathbf{u}}^{n+1}\|_{L^2(\Omega)}.
\end{aligned}\tag{6.47}$$

On the other hand, we return to (6.45), and observe

$$\begin{aligned}
\|\mathbf{e}_{\mathbf{u}}^{n+1}\|^2_{L^2(\Omega)} \;\;&\le\;\; \Big\{\|\mathbf{e}_{\mathbf{u}}^n\|_{L^2(\Omega)} \,+\, \|\mathbf{\Pi}_h^k(\mathbf{u}^{n+1} - \mathbf{u}^n) - (\mathbf{u}^{n+1} - \mathbf{u}^n)\|_{L^2(\Omega)} \,+\, C_u\Delta t\|\mathbf{u}^{n+1} - \mathbf{u}^n\|_{L^2(\Omega)} \\
&\quad +\; \Delta t\|\mathbf{E}_0(t_{n+1})\|_{L^2(\Omega)}\Big\}\|\mathbf{e}_{\mathbf{u}}^{n+1}\|_{L^2(\Omega)} \,+\, (I_1 + I_2) \,+\, I_3,
\end{aligned}$$

which, replacing (6.46) and (6.47), we deduce that

$$\begin{aligned}
\|\mathbf{e}_{\mathbf{u}}^{n+1}\|_{L^2(\Omega)} \;\;&\le\;\; (1 + CC_u\Delta t)\,\|\mathbf{e}_{\mathbf{u}}^n\|_{L^2(\Omega)} \,+\, \|\mathbf{\Pi}_h^k(\mathbf{u}^{n+1} - \mathbf{u}^n) - (\mathbf{u}^{n+1} - \mathbf{u}^n)\|_{L^2(\Omega)} \\
&\quad +\; C\,C_u\,\Delta t\Big\{\|\mathbf{\Pi}_h^k(\mathbf{u}^n) - \mathbf{u}^n\|_{L^2(\Omega)} \,+\, h^{-1}\|\mathbf{\Pi}_h^k(\mathbf{u}^{n+1}) - \mathbf{u}^{n+1}\|_{L^2(\Omega)}. \\
&\quad +\; \|\nabla_h\{\mathbf{\Pi}_h^k(\mathbf{u}^{n+1}) - \mathbf{u}^{n+1}\}\|_{L^2(\Omega)}\Big\} \\
&\quad +\; \Delta t\Big\{C_u\,\|\mathbf{u}^{n+1} - \mathbf{u}^n\|_{L^2(\Omega)} \,+\, \|\mathbf{E}_0(t_{n+1})\|_{L^2(\Omega)}\Big\}.
\end{aligned}$$

Next, using that

$$(\mathbf{u}^{n+1} - \mathbf{u}^n)(\mathbf{x}) \;\;=\;\; \int_{t_n}^{t_{n+1}} \mathbf{u}_t(s,\mathbf{x})\,ds\,, \tag{6.48}$$

together with (6.9), it follows that

$$\|\mathbf{\Pi}_h^k(\mathbf{u}^{n+1}-\mathbf{u}^n)-(\mathbf{u}^{n+1}-\mathbf{u}^n)\|_{L^2(\Omega)} \;\leq\; C h^{k+1}\int_{t_n}^{t_{n+1}}\|\mathbf{u}_t(s,\cdot)\|_{H^{k+1}(\Omega)}\,ds\,.$$

Similarly, we can show

$$\Delta t\, C_u\,\|\mathbf{u}^{n+1}-\mathbf{u}^n\|_{L^2(\Omega)} \;\leq\; \Delta t\, C\, C_u\int_{t_n}^{t_{n+1}}\|\mathbf{u}_t(s,\cdot)\|_{L^2(\Omega)}\,ds$$

and, from (6.41),

$$\Delta t\,\|\mathbf{E}_0(t_{n+1})\|_{L^2(\Omega)} \;\leq\; C\,\Delta t\int_{t_n}^{t_{n+1}}\|\mathbf{u}_{tt}(s,\cdot)\|_{L^2(\Omega)}\,ds\,.$$

In addition, using that

$$\mathbf{u}^{n+1}(\mathbf{x}) \;=\; \mathbf{u}_0(\mathbf{x}) \;+\; \int_0^{t_{n+1}}\mathbf{u}_t(s,\mathbf{x})\,ds\,,$$

and (6.9), we have

$$h^{-1}\|\mathbf{\Pi}_h^k(\mathbf{u}^{n+1})-\mathbf{u}^{n+1}\|_{L^2(\Omega)} \;\leq\; C h^k\left\{\|\mathbf{u}_0\|_{H^{k+1}(\Omega)} \;+\; \int_0^{t_{n+1}}\|\mathbf{u}_t(s,\cdot)\|_{H^{k+1}(\Omega)}\,ds\right\}.$$

Analogously, we can show

$$\begin{aligned}
&C\,C_u\,\Delta t\left\{\|\mathbf{\Pi}_h^k(\mathbf{u}^n)-\mathbf{u}^n\|_{L^2(\Omega)} \;+\; h^{-1}\|\mathbf{\Pi}_h^k(\mathbf{u}^{n+1})-\mathbf{u}^{n+1}\|_{L^2(\Omega)} + \;\|\nabla_h\{\mathbf{\Pi}_h^k(\mathbf{u}^{n+1})-\mathbf{u}^{n+1}\}\|_{L^2(\Omega)}\right\}\\
&\quad\leq\; C\,C_u\,\Delta t\, h^k\left\{\|\mathbf{u}_0\|_{H^{k+1}(\Omega)} \;+\; \int_0^{t_{n+1}}\|\mathbf{u}_t(s,\cdot)\|_{H^{k+1}(\Omega)}\,ds\right\}.
\end{aligned}$$

Therefore, gathering together all the above equations, we deduce that

$$\|\mathbf{e}_{\mathbf{u}}^{n+1}\|_{L^2(\Omega)} \;\leq\; (1+CC_u\Delta t)\,\|\mathbf{e}_{\mathbf{u}}^n\|_{L^2(\Omega)} \;+\; C(\Delta t+h^k)B(u,n)\,, \tag{6.49}$$

where

$$\begin{aligned}
B(u,n) \;:=\; & h\int_{t_n}^{t_{n+1}}\|\mathbf{u}_t(s,\cdot)\|_{H^{k+1}(\Omega)}\,ds \;+\; C_u\int_{t_n}^{t_{n+1}}\|\mathbf{u}_t(s,\cdot)\|_{L^2(\Omega)}\,ds \;+\; \int_{t_n}^{t_{n+1}}\|\mathbf{u}_{tt}(s,\cdot)\|_{L^2(\Omega)}\,ds\\
& +\;\Delta t\,C_u\left\{\|\mathbf{u}_0\|_{H^{k+1}(\Omega)} + \int_0^{t_{n+1}}\|\mathbf{u}_t(s,\cdot)\|_{H^{k+1}(\Omega)}\,ds\right\}.
\end{aligned}$$

Now, from the recurrence relation (6.49), we obtain that

$$\begin{aligned}
\|\mathbf{e}_{\mathbf{u}}^n\|_{L^2(\Omega)} \;&\leq\; (1+C\,C_u\Delta t)^n\,\|\mathbf{e}_{\mathbf{u}}^0\|_{L^2(\Omega)} \;+\; C\left\{\sum_{i=0}^{n-1}(1+C_u\Delta t)^i B(u,n-1-i)\right\}(h^k+\Delta t)\\
&\leq\; C\,(1+C\,C_u\Delta t)^n\,(h^k+\Delta t)\left\{h\|\mathbf{u}_0\|_{H^{k+1}(\Omega)} \;+\; \sum_{i=0}^{n-1}B(u,n-1-i)\right\}\\
&=\; C\left(1+C\,\frac{C_u\,T}{n}\right)^n(h^k+\Delta t)\left\{h\|\mathbf{u}_0\|_{H^{k+1}(\Omega)} \;+\; \sum_{i=0}^{n-1}B(u,n-1-i)\right\}.
\end{aligned}$$

Finally, noting that

$$
\begin{aligned}
\sum_{i=0}^{n-1} B(u, n-1-i) \;&\le\; h \int_0^{t_n} \|\mathbf{u}_t(s,\cdot)\|_{H^{k+1}(\Omega)}\, ds \;+\; C_u \int_0^{t_n} \|\mathbf{u}_t(s,\cdot)\|_{L^2(\Omega)}\, ds \\
&+\; \int_0^{t_n} \|\mathbf{u}_{tt}(s,\cdot)\|_{L^2(\Omega)}\, ds \;+\; C_u t_n \left\{ \|\mathbf{u}_0\|_{H^{k+1}(\Omega)} \;+\; \int_0^{t_n} \|\mathbf{u}_t(s,\cdot)\|_{H^{k+1}(\Omega)}\, ds \right\},
\end{aligned}
$$

the result now follows by using Cauchy-Schwarz inequality. □

Now, we establish the *a priori* error estimate for the pressure, and for that we first consider the next result.

Lemma 6.5. *Assuming the hypothesis of the previous theorem we have the existence of a $C > 0$, independent of h, such that for all $0 \le n \le N$*

$$
\begin{aligned}
\left\| \frac{\mathbf{u}^{n+1} - \mathbf{u}_h^{n+1}}{\Delta t} - \frac{\mathbf{u}^n - \mathbf{u}_h^n}{\Delta t} \right\|_{L^2(\Omega)} \;&\le\; C\, C_{h,\Delta t}(u) \exp(C\, C_u\, T) \left(h^{k-1} + \frac{\Delta t}{h} \right) A(u) \\
&+\; C \left\{ 1 + C_{h,\Delta t}(u) \right\} (h^k + \Delta t)\, D_n(u)\,,
\end{aligned}
$$

where

$$
C_{h,\Delta t}(u) \;:=\; \exp(C\, C_u\, T)\, h^{-d/2}\, (h^k + \Delta t)\, A(u) \;+\; C_u
$$

and

$$
\begin{aligned}
D_n(u) \;:=\;& h\, \|\mathbf{u}_t\|_{L^\infty(t_n, t_{n+1}; H^{k+1}(\Omega))} \;+\; \|\mathbf{u}_t\|_{L^\infty(t_n, t_{n+1}; L^2(\Omega))} \;+\; \|\mathbf{u}_{tt}\|_{L^\infty(t_n, t_{n+1}; L^2(\Omega))} \\
&+\; \|\mathbf{u}\|_{L^\infty(t_n, t_{n+1}; H^{k+1}(\Omega))}\,.
\end{aligned}
$$

Proof. From the error equation (6.44) we have

$$
\begin{aligned}
(\boldsymbol{\delta}_h, \mathbf{v}_h)_{\mathcal{T}_h} \;=\;& -(\mathbf{u}^n \cdot \nabla_h \mathbf{u}^{n+1} - \mathbf{u}_h^n \cdot \nabla_h \mathbf{u}_h^{n+1}, \mathbf{v}_h)_{\mathcal{T}_h} \;+\; \sum_{F \in \mathcal{E}_h^i} \left\langle (\mathbf{u}_h^n \cdot \mathbf{n}) [\![\mathbf{u}^{n+1} - \mathbf{u}_h^{n+1}]\!], \{\!\{ \mathbf{v}_h \}\!\} \right\rangle_F \\
&+\; (p^{n+1} - p_h^{n+1}, \mathrm{div}(\mathbf{v}_h))_{\mathcal{T}_h} \;+\; \frac{1}{\Delta t} (\boldsymbol{\Pi}_h^k (\mathbf{u}^{n+1} - \mathbf{u}^n) - (\mathbf{u}^{n+1} - \mathbf{u}^n), \mathbf{v}_h)_{\mathcal{T}_h} \\
&+\; ((\mathbf{u}^n - \mathbf{u}^{n+1}) \cdot \nabla \mathbf{u}^{n+1}, \mathbf{v}_h)_{\mathcal{T}_h} \;-\; (\mathbf{E}_0(t_{n+1}), \mathbf{v}_h)_{\mathcal{T}_h} \qquad \forall\ \mathbf{v}_h \in \mathbf{V}_h\,,
\end{aligned}
$$

where $\boldsymbol{\delta}_h := \frac{1}{\Delta t}(\mathbf{e}_{\mathbf{u}}^{n+1} - \mathbf{e}_{\mathbf{u}}^n)$. Then, taking $\mathbf{v}_h := \boldsymbol{\delta}_h$ and using that $\mathrm{div}(\boldsymbol{\delta}_h) = 0$, we deduce that

$$
\begin{aligned}
\|\boldsymbol{\delta}_h\|_{L^2(\Omega)}^2 \;\le\;& \|\mathbf{u}^n \cdot \nabla_h \mathbf{u}^{n+1} - \mathbf{u}_h^n \cdot \nabla_h \mathbf{u}_h^{n+1}\|_{L^2(\Omega)} \|\boldsymbol{\delta}_h\|_{L^2(\Omega)} \\
&+\; C \|\mathbf{u}_h^n\|_{L^\infty(\Omega)} \left(\sum_{F \in \mathcal{E}_h^i} h_F^{-1} \| [\![\mathbf{u}^{n+1} - \mathbf{u}_h^{n+1}]\!] \|_{L^2(F)}^2 \right)^{1/2} \left(\sum_{F \in \mathcal{E}_h^i} h_F \| \{\!\{ \boldsymbol{\delta}_h \}\!\} \|_{L^2(F)}^2 \right)^{1/2} \\
&+\; \left\| \boldsymbol{\Pi}_h^k \left(\frac{\mathbf{u}^{n+1} - \mathbf{u}^n}{\Delta t} \right) - \left(\frac{\mathbf{u}^{n+1} - \mathbf{u}^n}{\Delta t} \right) \right\|_{L^2(\Omega)} \|\boldsymbol{\delta}_h\|_{L^2(\Omega)} \\
&+\; C_u \|\mathbf{u}^{n+1} - \mathbf{u}^n\|_{L^2(\Omega)} \|\boldsymbol{\delta}_h\|_{L^2(\Omega)} \;+\; \|\mathbf{E}_0(t_{n+1})\|_{L^2(\Omega)} \|\boldsymbol{\delta}_h\|_{L^2(\Omega)}\,.
\end{aligned}
$$

Now, we follow the proof of Lemma 6.2, to obtain that

$$
\begin{aligned}
\|\mathbf{u}^n \cdot \nabla_h \mathbf{u}^{n+1} - \mathbf{u}_h^n \cdot \nabla_h \mathbf{u}_h^{n+1}\|_{L^2(\Omega)} \;&\le\; C_u \|\mathbf{u}^n - \mathbf{u}_h^n\|_{L^2(\Omega)} \\
+\; C\, (h^{-d/2} \|\mathbf{e}_{\mathbf{u}}^n\|_{L^2(\Omega)} + C_u) &\Big\{ h^{-1} \|\mathbf{e}_{\mathbf{u}}^{n+1}\|_{L^2(\Omega)} \;+\; \|\nabla_h \{ \boldsymbol{\Pi}_h^k (\mathbf{u}^{n+1}) - \mathbf{u}^{n+1} \}\|_{L^2(\Omega)} \Big\}\,,
\end{aligned} \tag{6.50}
$$

and from (6.16) and (6.19) we have

$$\|\mathbf{u}_h^n\|_{L^\infty(\Omega)} \left(\sum_{F\in\mathcal{E}_h^i} h_F^{-1} \|[\![\mathbf{u}^{n+1} - \mathbf{u}_h^{n+1}]\!]\|_{L^2(F)}^2 \right)^{\frac{1}{2}} \le C\,(h^{-d/2}\|\mathbf{e}_{\mathbf{u}}^n\|_{L^2(\Omega)} + C_u)\Big\{ h^{-1}\|\mathbf{u}^{n+1} - \mathbf{u}_h^{n+1}\|_{L^2(\Omega)}$$
$$+ h^{-1}\|\mathbf{\Pi}_h^k(\mathbf{u}^{n+1}) - \mathbf{u}^{n+1}\|_{L^2(\Omega)} + \|\nabla_h\{\mathbf{\Pi}_h^k(\mathbf{u}^{n+1}) - \mathbf{u}^{n+1}\}\|_{L^2(\Omega)}\Big\}. \tag{6.51}$$

Next, applying (6.50) and (6.51), together with (6.17), it follows that

$$\begin{aligned}
\|\boldsymbol{\delta}_h\|_{L^2(\Omega)} \;\le\;& C_u\|\mathbf{u}^n - \mathbf{u}_h^n\|_{L^2(\Omega)} \;+\; Ch^{-1}(h^{-d/2}\|\mathbf{e}_{\mathbf{u}}^n\|_{L^2(\Omega)} + C_u)\|\mathbf{u}^{n+1} - \mathbf{u}_h^{n+1}\|_{L^2(\Omega)} \\
&+ C(h^{-d/2}\|\mathbf{e}_{\mathbf{u}}^n\|_{L^2(\Omega)} + C_u)\Big\{ h^{-1}\|\mathbf{\Pi}_h^k(\mathbf{u}^{n+1}) - \mathbf{u}^{n+1}\|_{L^2(\Omega)} \\
&+ \|\nabla_h\{\mathbf{\Pi}_h^k(\mathbf{u}^{n+1}) - \mathbf{u}^{n+1}\}\|_{L^2(\Omega)}\Big\} \;+\; \left\|\mathbf{\Pi}_h^k\left(\frac{\mathbf{u}^{n+1} - \mathbf{u}^n}{\Delta t}\right) - \left(\frac{\mathbf{u}^{n+1} - \mathbf{u}^n}{\Delta t}\right)\right\|_{L^2(\Omega)} \\
&+ C_u\|\mathbf{u}^{n+1} - \mathbf{u}^n\|_{L^2(\Omega)} \;+\; \|\mathbf{E}_0(t_{n+1})\|_{L^2(\Omega)}\,.
\end{aligned}$$

On the other hand, using the fact that

$$\left\|\frac{\mathbf{u}^{n+1} - \mathbf{u}_h^{n+1}}{\Delta t} - \frac{\mathbf{u}^n - \mathbf{u}_h^n}{\Delta t}\right\|_{L^2(\Omega)} \;\le\; \left\|\mathbf{\Pi}_h^k\left(\frac{\mathbf{u}^{n+1} - \mathbf{u}^n}{\Delta t}\right) - \left(\frac{\mathbf{u}^{n+1} - \mathbf{u}^n}{\Delta t}\right)\right\|_{L^2(\Omega)} \;+\; \|\boldsymbol{\delta}_h\|_{L^2(\Omega)}\,,$$

we have

$$\begin{aligned}
\left\|\frac{\mathbf{u}^{n+1} - \mathbf{u}_h^{n+1}}{\Delta t} - \frac{\mathbf{u}^n - \mathbf{u}_h^n}{\Delta t}\right\|_{L^2(\Omega)} \;\le\;& C_u\|\mathbf{u}^n - \mathbf{u}_h^n\|_{L^2(\Omega)} \\
&+ Ch^{-1}(h^{-d/2}\|\mathbf{e}_{\mathbf{u}}^n\|_{L^2(\Omega)} + C_u)\|\mathbf{u}^{n+1} - \mathbf{u}_h^{n+1}\|_{L^2(\Omega)} \\
&+ C(h^{-d/2}\|\mathbf{e}_{\mathbf{u}}^n\|_{L^2(\Omega)} + C_u)\Big\{ h^{-1}\|\mathbf{\Pi}_h^k(\mathbf{u}^{n+1}) - \mathbf{u}^{n+1}\|_{L^2(\Omega)} \\
&+ \|\nabla_h\{\mathbf{\Pi}_h^k(\mathbf{u}^{n+1}) - \mathbf{u}^{n+1}\}\|_{L^2(\Omega)}\Big\} \;+\; 2\left\|\mathbf{\Pi}_h^k\left(\frac{\mathbf{u}^{n+1} - \mathbf{u}^n}{\Delta t}\right) - \left(\frac{\mathbf{u}^{n+1} - \mathbf{u}^n}{\Delta t}\right)\right\|_{L^2(\Omega)} \\
&+ C_u\|\mathbf{u}^{n+1} - \mathbf{u}^n\|_{L^2(\Omega)} \;+\; \|\mathbf{E}_0(t_{n+1})\|_{L^2(\Omega)}\,.
\end{aligned} \tag{6.52}$$

Next, we proceed as in the last part of the proof of Theorem 6.5. Indeed, from (6.9), we obtain that

$$\begin{aligned}
& h^{-1}\|\mathbf{\Pi}_h^k(\mathbf{u}^{n+1}) - \mathbf{u}^{n+1}\|_{L^2(\Omega)} + \|\nabla_h\{\mathbf{\Pi}_h^k(\mathbf{u}^{n+1}) - \mathbf{u}^{n+1}\}\|_{L^2(\Omega)} \\
&\le\; Ch^k\,\|\mathbf{u}^{n+1}\|_{H^{k+1}(\Omega)} \;\le\; Ch^k\,\|\mathbf{u}\|_{L^\infty(t_n,t_{n+1};H^{k+1}(\Omega))}
\end{aligned}$$

Similarly, from (6.48) and (6.9), we have

$$\begin{aligned}
\left\|\mathbf{\Pi}_h^k\left(\frac{\mathbf{u}^{n+1} - \mathbf{u}^n}{\Delta t}\right) - \left(\frac{\mathbf{u}^{n+1} - \mathbf{u}^n}{\Delta t}\right)\right\|_{L^2(\Omega)} \;\le\;& Ch^{k+1}\left\{\frac{1}{\Delta t}\int_{t_n}^{t_{n+1}} \|\mathbf{u}_t(s,\cdot)\|_{H^{k+1}(\Omega)}\,ds\right\} \\
\le\;& Ch^{k+1}\|\mathbf{u}_t\|_{L^\infty(t_n,t_{n+1};H^{k+1}(\Omega))}\,.
\end{aligned}$$

In addition, using again (6.48) and (6.41), we deduce, respectively, that

$$\|\mathbf{u}^{n+1} - \mathbf{u}^n\|_{L^2(\Omega)} \;\le\; \int_{t_n}^{t_{n+1}} \|\mathbf{u}_t(s,\cdot)\|_{L^2(\Omega)}\,ds \;\le\; \Delta t\,\|\mathbf{u}_t\|_{L^\infty(t_n,t_{n+1};L^2(\Omega))}\,,$$

and

$$\|\mathbf{E}_0(t_{n+1})\|_{L^2(\Omega)} \;\le\; C\int_{t_n}^{t_{n+1}} \|\mathbf{u}_{tt}(s,\cdot)\|_{L^2(\Omega)}\,ds \;\le\; C\,\Delta t\,\|\mathbf{u}_{tt}\|_{L^\infty(t_n,t_{n+1};L^2(\Omega))}\,.$$

The result now follows after applying the previous theorem and the last four estimates into (6.52). $\square$

Theorem 6.6. *Assume the hypothesis of Theorem 6.5. Then, there exists $C>0$, independent of h, such that for all $0\le n\le N$ the following estimate holds*

$$\begin{aligned}\|p^n - p_h^n\|_{L^2(\Omega)} &\le C\,C_{h,\Delta t}(u)\exp(C\,C_u\,T)\left(h^{k-1}+\frac{\Delta t}{h}\right)A(u)\\ &\quad + C\left\{1+C_{h,\Delta t}(u)\right\}(h^k+\Delta t)\,D_n(u)\,,\\ &\quad + Ch^{k+1}\|p(t_n,\cdot)\|_{H^{k+1}(\Omega)}.\end{aligned}$$

Proof. We proceed as in the proof of Theorem 6.2. Indeed, from error equation (6.44), we deduce that

$$\begin{aligned}(\mathbf{e}_p^{n+1},\mathrm{div}(\mathbf{v}_h))_{\mathcal{T}_h} &= \Delta t^{-1}((\mathbf{u}^{n+1}-\mathbf{u}_h^{n+1})-(\mathbf{u}^n-\mathbf{u}_h^n),\mathbf{v}_h)_{\mathcal{T}_h} + (\mathbf{u}^n\cdot\nabla_h\mathbf{u}^{n+1}-\mathbf{u}_h^n\cdot\nabla_h\mathbf{u}_h^{n+1},\mathbf{v}_h)_{\mathcal{T}_h}\\ &\quad - ((\mathbf{u}^n-\mathbf{u}^{n+1})\cdot\nabla\mathbf{u}^{n+1},\mathbf{v}_h)_{\mathcal{T}_h} - \sum_{F\in\mathcal{E}_h^i}\left\langle(\mathbf{u}_h^n\cdot\mathbf{n})[\![\mathbf{u}^{n+1}-\mathbf{u}_h^{n+1}]\!],\{\!\{\mathbf{v}_h\}\!\}\right\rangle_F\\ &\quad + (\mathcal{P}_h^k(p^{n+1})-p^{n+1},\mathrm{div}(\mathbf{v}_h))_{\mathcal{T}_h} + (\mathbf{E}_0(t_{n+1}),\mathbf{v}_h)_{\mathcal{T}_h}\\ &\le \left\|\frac{\mathbf{u}^{n+1}-\mathbf{u}_h^{n+1}}{\Delta t}-\frac{\mathbf{u}^n-\mathbf{u}_h^n}{\Delta t}\right\|_{L^2(\Omega)}\|\mathbf{v}_h\|_{L^2(\Omega)} + \|\mathbf{u}^n\cdot\nabla_h\mathbf{u}^{n+1}-\mathbf{u}_h^n\cdot\nabla_h\mathbf{u}_h^{n+1}\|_{L^2(\Omega)}\|\mathbf{v}_h\|_{L^2(\Omega)}\\ &\quad + C\|\mathbf{u}_h^n\|_{L^\infty(\Omega)}\left(\sum_{F\in\mathcal{E}_h^i}h_F^{-1}\|[\![\mathbf{u}^{n+1}-\mathbf{u}_h^{n+1}]\!]\|_{L^2(F)}^2\right)^{1/2}\left(\sum_{F\in\mathcal{E}_h^i}h_F\|\{\!\{\mathbf{v}_h\}\!\}\|_{L^2(F)}^2\right)^{1/2}\\ &\quad + C_u\|\mathbf{u}^{n+1}-\mathbf{u}^n\|_{L^2(\Omega)}\|\mathbf{v}_h\|_{L^2(\Omega)} + \|\mathcal{P}_h^k(p^{n+1})-p^{n+1}\|_{L^2(\Omega)}\|\mathrm{div}(\mathbf{v}_h)\|_{L^2(\Omega)}\\ &\quad + \|\mathbf{E}_0(t_{n+1})\|_{L^2(\Omega)}\|\mathbf{v}_h\|_{L^2(\Omega)}\,.\end{aligned}$$

Thus, using (6.50), (6.51) and (6.17), we obtain that

$$\begin{aligned}(\mathbf{e}_p^{n+1},\mathrm{div}(\mathbf{v}_h))_{\mathcal{T}_h} &\le C\Bigg\{\left\|\frac{\mathbf{u}^{n+1}-\mathbf{u}_h^{n+1}}{\Delta t}-\frac{\mathbf{u}^n-\mathbf{u}_h^n}{\Delta t}\right\|_{L^2(\Omega)} + C_u\|\mathbf{u}^n-\mathbf{u}_h^n\|_{L^2(\Omega)}\\ &\quad + Ch^{-1}(h^{-d/2}\|\mathbf{e}_{\mathbf{u}}^n\|_{L^2(\Omega)}+C_u)\|\mathbf{u}^{n+1}-\mathbf{u}_h^{n+1}\|_{L^2(\Omega)}\\ &\quad + C(h^{-d/2}\|\mathbf{e}_{\mathbf{u}}^n\|_{L^2(\Omega)}+C_u)\Big\{h^{-1}\|\mathbf{\Pi}_h^k(\mathbf{u}^{n+1})-\mathbf{u}^{n+1}\|_{L^2(\Omega)}\\ &\quad + \|\nabla_h\{\mathbf{\Pi}_h^k(\mathbf{u}^{n+1})-\mathbf{u}^{n+1}\}\|_{L^2(\Omega)}\Big\}\\ &\quad + C_u\|\nabla_h\{\mathbf{\Pi}_h^k(\mathbf{u}^{n+1})-\mathbf{u}^{n+1}\}\|_{L^2(\Omega)} + C_u\|\mathbf{u}^{n+1}-\mathbf{u}^n\|_{L^2(\Omega)}\\ &\quad + \|\mathcal{P}_h^k(p^{n+1})-p^{n+1}\|_{L^2(\Omega)} + \|\mathbf{E}_0(t_{n+1})\|_{L^2(\Omega)}\Bigg\}\|\mathbf{v}_h\|_{H(\mathrm{div};\Omega)}\,,\end{aligned}$$

which, together with the inf-sup condition (6.21), Lemma 6.5, Theorem 6.5, (6.11), and the last estimates obtained in the proof of Lemma 6.5, we can complete the proof. □

We end this section by remarking that we can extend the previous analysis for the upwind version of the method (cf. (6.23)) given by: Find $(\mathbf{u}_h^{n+1}, p_h^{n+1}) \in \mathbf{V}_h \times Q_h$ such that

$$\begin{aligned}
(\mathbf{u}_h^{n+1}, \mathbf{v}_h)_{\mathcal{T}_h} \,+\, \Delta t(\mathbf{u}_h^{n} \cdot \nabla_h \mathbf{u}_h^{n+1}, \mathbf{v}_h)_{\mathcal{T}_h} \,-\, \Delta t \sum_{F\in\mathcal{E}_h^i} \big\langle\, (\mathbf{u}_h^n \cdot \mathbf{n})\, [\![\mathbf{u}_h^{n+1}]\!], \{\!\{ \mathbf{v}_h \}\!\} \big\rangle_F & \\
+\, \Delta t \sum_{F\in\mathcal{E}_h^i} \big\langle\, |\mathbf{u}_h^n \cdot \mathbf{n}|\, [\![\mathbf{u}_h^{n+1}]\!], [\![\mathbf{v}_h]\!] \big\rangle_F \,-\, \Delta t(p_h^{n+1}, \mathrm{div}(\mathbf{v}_h))_{\mathcal{T}_h} &\;=\; (\mathbf{u}_h^n, \mathbf{v}_h)_{\mathcal{T}_h}, \quad (6.53)\\
(q_h, \mathrm{div}(\mathbf{u}_h^{n+1}))_{\mathcal{T}_h} &\;=\; 0,
\end{aligned}$$

for all $(\mathbf{v}_h, q_h) \in \mathbf{V}_h \times Q_h$.

6.3.2 DG schemes

Here we only mention that when we combine the techniques used in sections 6.2.2 and 6.3.1 we can also obtain the same error estimates for DG schemes (6.28) and (6.39). The fully-discrete versions of both methods, using (6.40), are given by: Find $\mathbf{u}_h \in \mathbf{V}_h^{\mathrm{dg}}$ and $p_h \in Q_h$ such that

$$\begin{aligned}
(\mathbf{u}_h^{n+1}, \mathbf{v}_h)_{\mathcal{T}_h} \,+\, \Delta t((\mathbf{u}_h^\star)^n \cdot \nabla_h \mathbf{u}_h^{n+1}, \mathbf{v}_h)_{\mathcal{T}_h} \,+\, \alpha \Delta t \sum_{F\in\mathcal{E}_h^i} h_F^{-1} \big\langle [\![\mathbf{u}_h^{n+1} \cdot \mathbf{n}]\!], [\![\mathbf{v}_h \cdot \mathbf{n}]\!] \big\rangle_F & \\
-\Delta t \sum_{F\in\mathcal{E}_h^i} \big\langle\, ((\mathbf{u}_h^\star)^n \cdot \mathbf{n})\, [\![\mathbf{u}_h^{n+1}]\!], \{\!\{ \mathbf{v}_h \}\!\} \big\rangle_F \,-\, \Delta t(p_h^{n+1}, \mathrm{div}_h(\mathbf{v}_h))_{\mathcal{T}_h} & \\
+\, \Delta t \sum_{F\in\mathcal{E}_h^i} \big\langle [\![\mathbf{v}_h \cdot \mathbf{n}]\!], \{\!\{ p_h^{n+1} \}\!\} \big\rangle_F &\;=\; (\mathbf{u}_h^n, \mathbf{v}_h)_{\mathcal{T}_h},\\
(q_h, \mathrm{div}_h(\mathbf{u}_h^{n+1}))_{\mathcal{T}_h} \,-\, \sum_{F\in\mathcal{E}_h^i} \big\langle [\![\mathbf{u}_h^{n+1} \cdot \mathbf{n}]\!], \{\!\{ q_h \}\!\} \big\rangle_F &\;=\; 0,\\
\mathbf{u}_h(0, \mathbf{x}) &\;=\; \mathbf{u}_{h,0}(\mathbf{x}) \quad \text{in } \Omega, \qquad (6.54)
\end{aligned}$$

for all $(\mathbf{v}_h, q_h) \in \mathbf{V}_h^{\mathrm{dg}} \times Q_h$ for the central flux, and: Find $\mathbf{u}_h \in \mathbf{V}_h^{\mathrm{dg}}$ and $p_h \in Q_h$ such that

$$\begin{aligned}
(\mathbf{u}_h^{n+1}, \mathbf{v}_h)_{\mathcal{T}_h} \,+\, \Delta t((\mathbf{u}_h^\star)^n \cdot \nabla_h \mathbf{u}_h^{n+1}, \mathbf{v}_h)_{\mathcal{T}_h} \,+\, \alpha \Delta t \sum_{F\in\mathcal{E}_h^i} h_F^{-1} \big\langle [\![\mathbf{u}_h^{n+1} \cdot \mathbf{n}]\!], [\![\mathbf{v}_h \cdot \mathbf{n}]\!] \big\rangle_F & \\
-\, \Delta t \sum_{F\in\mathcal{E}_h^i} \big\langle\, ((\mathbf{u}_h^\star)^n \cdot \mathbf{n})\, [\![\mathbf{u}_h^{n+1}]\!], \{\!\{ \mathbf{v}_h \}\!\} \big\rangle_F \,+\, \Delta t \sum_{F\in\mathcal{E}_h^i} \big\langle\, |(\mathbf{u}_h^\star)^n \cdot \mathbf{n}|\, [\![\mathbf{u}_h^{n+1}]\!], [\![\mathbf{v}_h]\!] \big\rangle_F & \\
-\, \Delta t(p_h^{n+1}, \mathrm{div}_h(\mathbf{v}_h))_{\mathcal{T}_h} \,+\, \Delta t \sum_{F\in\mathcal{E}_h^i} \big\langle [\![\mathbf{v}_h \cdot \mathbf{n}]\!], \{\!\{ p_h^{n+1} \}\!\} \big\rangle_F &\;=\; (\mathbf{u}_h^n, \mathbf{v}_h)_{\mathcal{T}_h},\\
(q_h, \mathrm{div}_h(\mathbf{u}_h^{n+1}))_{\mathcal{T}_h} \,-\, \sum_{F\in\mathcal{E}_h^i} \big\langle [\![\mathbf{u}_h^{n+1} \cdot \mathbf{n}]\!], \{\!\{ q_h \}\!\} \big\rangle_F &\;=\; 0,\\
\mathbf{u}_h(0, \mathbf{x}) &\;=\; \mathbf{u}_{h,0}(\mathbf{x}) \quad \text{in } \Omega, \qquad (6.55)
\end{aligned}$$

for all $(\mathbf{v}_h, q_h) \in \mathbf{V}_h^{\mathrm{dg}} \times Q_h$ for the upwind flux.

Theorem 6.7. *Assume that $\mathbf{u} \in W^{1,\infty}([0,T] \times \Omega)^d$ and $p \in L^\infty([0,T] \times \Omega)$ are uniformly bounded. Also, suppose that $\mathcal{T}_h$ is quasi-uniform. Then, there exists $C > 0$, independent of h, such that*

$$\|\mathbf{u}^n - \mathbf{u}_h^n\|_{L^2(\Omega)} \;\le\; C\, \exp(C\, C_u\, T)\, (h^{k+1} + \Delta t)\, A(u,p), \qquad \textit{for all } \; 0 \,\le\, n \,\le\, N\,,$$

where $C_u := \|\mathbf{u}\|_{W^{1,\infty}([0,T]\times\Omega)}$ and

$$\begin{aligned}
A(u,p) \;\;:=\;\; & (h\sqrt{T} + C_u T^{3/2}) \|\mathbf{u}_t\|_{L^2(0,T;H^{k+2}(\Omega))} \,+\, C_u \sqrt{T} \|\mathbf{u}_t\|_{L^2(0,T;L^2(\Omega))} \,+\, \sqrt{T} \|\mathbf{u}_{tt}\|_{L^2(0,T;L^2(\Omega))}\\
& +\, (C_u T + h) \|\mathbf{u}_0\|_{H^{k+2}(\Omega)} \,+\, \sqrt{T} \|p\|_{L^\infty(0,T;H^{k+1}(\Omega))}\,.
\end{aligned}$$

Proof. It follows straightforwardly from the proof of Theorems 6.3 and 6.5. □

Theorem 6.8. *Assume the hypothesis of Theorem* 6.7. *In addition, assume that the parameter* α *lies in* $(0, \alpha_0 \Delta t)$, *for some* $\alpha_0 > 0$ *independent of* h. *Then, there exists* $C > 0$, *independent of* h, *such that for all* $0 \leq n \leq N$ *the following estimate holds*

$$\begin{aligned}\|p^n - p_h^n\|_{L^2(\Omega)} \;\leq\; & C\, C_{h,\Delta t}(u,p) \exp(C\, C_u\, T) \left(h^k + \frac{\Delta t}{h} \right) A(u,p) \\ & + C \left\{ 1 + C_{h,\Delta t}(u,p) \right\} (h^k + \Delta t)\, D_n(u,p)\,, \\ & + C h^{k+1} \|p(t_n,\cdot)\|_{H^{k+1}(\Omega)}\end{aligned}$$

where

$$C_{h,\Delta t}(u,p) \;:=\; \exp(C\, C_u\, T)\, h^{-d/2}\, (h^{k+1} + \Delta t)\, A(u,p) \;+\; C_u$$

and

$$\begin{aligned} D_n(u,p) \;:=\; & h^2\, \|\mathbf{u}_t\|_{L^\infty(t_n,t_{n+1};H^{k+2}(\Omega))} \;+\; \|\mathbf{u}_t\|_{L^\infty(t_n,t_{n+1};L^2(\Omega))} \;+\; \|\mathbf{u}_{tt}\|_{L^\infty(t_n,t_{n+1};L^2(\Omega))} \\ & + \|\mathbf{u}\|_{L^\infty(t_n,t_{n+1};H^{k+2}(\Omega))} \;+\; \|p\|_{L^\infty(t_n,t_{n+1};H^{k+1}(\Omega))}\,. \end{aligned}$$

Proof. Similar as the proof of Theorem 6.6. □

6.4 Numerical results

In this section, we present some numerical results for two dimensional problem (i.e. $d = 2$), illustrating the performance of the fully discrete schemes analyzed in Sections 6.3.1 and 6.3.2. In all the computations we consider four uniform meshes that are Cartesian refinements of a domain defined in terms of squares, and then we split each square into two congruent triangles. Also, we consider polynomial degree $k \in \{0, 1, 2\}$ and for the DG schemes, we use only $\alpha = 1$. In addition, the numerical results presented below were obtained using a MATLAB code, where the zero integral mean condition for the pressure is imposed via a real Lagrange multiplier.

In Example 1 we follow [106] and consider the Taylor-Green vortex (see [36]). That is, we set $\Omega := [0, 2\pi]^2$, and the exact solution is given by

$$\begin{aligned}\mathbf{u}(t,\mathbf{x}) \;&=\; \Big(\sin(x_1)\cos(x_2) e^{-2t/Re},\; -\cos(x_1)\sin(x_2) e^{-2t/Re} \Big)^{\mathtt{t}}\,, \\ p(t,\mathbf{x}) \;&=\; \frac{1}{4} \big(\cos(2x_1) \,+\, \cos(2x_2) \big) e^{-4t/Re}\,,\end{aligned}$$

for all $\mathbf{x} := (x_1, x_2)^{\mathtt{t}} \in \Omega$ and $t \in (0,1)$, where $Re = 100$ is the Reynolds number. It is easy to check that $\mathbf{u}$ is divergence free and $\int_\Omega p = 0$. Here, we compute the approximation of $\mathbf{u}$ at $t = 1$, where we consider $\Delta t = 1/160 = 0.00625$. In Table 6.1 we present the results obtained for Raviart-Thomas schemes (6.43) and (6.53), whereas in Table 6.2 we use DG schemes (6.54) and (6.55).

We see that the estimates we obtained using the Raviart-Thomas spaces and the central flux are sharp for the velocity when $k = 1$. However, for $k = 0$, $k = 2$ the convergence rates are higher than predicted theoretically. In particular, we could not prove convergence for $k = 0$, however numerically the method seems to be converging with order 1. Similarly, for DG method using the central flux the estimate we gave seem to be sharp for the velocity for $k = 0$ and $k = 2$ (notice that the velocity space contains polynomials of degree $k+1$ for the DG space), but numerically the case $k=1$ does better than the theory predicts. Finally, using the upwind flux for both the Raviart-Thomas method or the DG method one observes numerically optimal convergence rates for both the velocity and pressure variables. Unfortunately, we cannot prove these optimal error estimates.

k	h	d.o.f	Central flux $\|\mathbf{u}-\mathbf{u}_h\|_{L^2(\Omega)}$ error	order	Central flux $\|p-p_h\|_{L^2(\Omega)}$ error	order	Upwind flux $\|\mathbf{u}-\mathbf{u}_h\|_{L^2(\Omega)}$ error	order	Upwind flux $\|p-p_h\|_{L^2(\Omega)}$ error	order
0	0.7405	745	1.14e-0	−−	4.69e-1	−−	1.50e-0	−−	8.69e-1	−−
	0.3702	2929	5.70e-1	1.00	2.08e-1	1.17	8.82e-1	0.76	5.17e-1	0.75
	0.2468	6553	3.80e-1	1.00	1.35e-1	1.07	6.29e-1	0.83	3.68e-1	0.84
	0.1851	11617	2.85e-1	1.00	1.00e-1	1.04	4.90e-1	0.87	2.86e-1	0.88
1	0.7405	2353	5.84e-1	−−	1.48e-1	−−	1.75e-1	−−	9.86e-2	−−
	0.3702	9313	2.97e-1	0.98	6.65e-2	1.15	4.40e-2	2.00	2.68e-2	1.88
	0.2468	20881	1.98e-1	1.00	4.32e-2	1.07	1.94e-2	2.01	1.22e-2	1.94
	0.1851	37057	1.49e-1	1.00	3.22e-2	1.02	1.09e-2	2.01	6.91e-3	1.96
2	0.7405	4825	2.15e-2	−−	6.53e-3	−−	1.28e-2	−−	5.19e-3	−−
	0.3702	19153	3.31e-3	2.70	9.53e-4	2.78	1.53e-3	3.06	6.80e-4	2.93
	0.2468	42985	8.61e-4	3.32	3.09e-4	2.78	4.36e-4	3.09	2.13e-4	2.87
	0.1851	76321	3.52e-4	3.11	1.39e-4	2.78	1.79e-4	3.08	9.49e-5	2.81

Table 6.1: History of convergence for Example 1, Raviart-Thomas scheme with $t=1$.

k	h	d.o.f	Central flux $\|\mathbf{u}-\mathbf{u}_h\|_{L^2(\Omega)}$ error	order	Central flux $\|p-p_h\|_{L^2(\Omega)}$ error	order	Upwind flux $\|\mathbf{u}-\mathbf{u}_h\|_{L^2(\Omega)}$ error	order	Upwind flux $\|p-p_h\|_{L^2(\Omega)}$ error	order
0	0.7405	2017	5.13e-1	−−	3.83e-1	−−	2.85e-1	−−	3.81e-1	−−
	0.3702	8065	2.39e-1	1.10	1.89e-1	1.02	8.17e-2	1.80	1.88e-1	1.02
	0.2468	18145	1.57e-1	1.03	1.25e-1	1.01	3.85e-2	1.85	1.25e-1	1.01
	0.1851	32257	1.18e-1	1.01	9.39e-2	1.01	2.24e-2	1.89	9.34e-2	1.01
1	0.7405	4321	4.48e-2	−−	4.83e-2	−−	3.41e-2	−−	4.80e-2	−−
	0.3702	17281	6.48e-3	2.79	1.20e-2	2.01	4.60e-3	2.89	1.20e-2	2.00
	0.2468	38881	2.01e-3	2.89	5.32e-3	2.00	1.37e-3	2.99	5.32e-3	2.00
	0.1851	69121	8.72e-4	2.90	3.00e-3	2.00	5.75e-4	3.01	2.99e-3	2.00
2	0.7405	7489	4.83e-3	−−	4.14e-3	−−	2.23e-3	−−	4.12e-3	−−
	0.3702	29953	5.89e-4	3.03	5.52e-4	2.91	1.49e-4	3.90	5.50e-4	2.91
	0.2468	67393	1.74e-4	3.00	1.76e-4	2.82	3.10e-5	3.88	1.71e-4	2.89
	0.1851	119809	7.36e-5	3.00	8.31e-5	2.61	1.03e-5	3.83	7.82e-5	2.71

Table 6.2: History of convergence for Example 1, DG scheme with $t=1$.

For Example 2 we consider the double shear layer problem taken from [14] (see also [106]). We solve the Euler equation (6.1) in the domain $\Omega := [0,2\pi]^2$ with a periodic boundary condition and an initial data given by $\mathbf{u}_0(\mathbf{x}) = (u_1^0(\mathbf{x}), u_2^0(\mathbf{x}))^{\mathtt{t}}$, with

$$u_1^0(\mathbf{x}) = \begin{cases} \tanh((x_2-\pi/2)/\rho) & x_2 \le \pi \\ \tanh((3\pi/2-x_2)/\rho) & x_2 > \pi \end{cases}, \quad \text{and} \quad u_2^0(\mathbf{x}) = \delta\sin(x_1),$$

for all $\mathbf{x} := (x_1, x_2)^{\mathtt{t}} \in \Omega$, where we take $\rho = \pi/15$ and $\delta = 0.05$.

In Figures 6.1−6.6, we present some contours of the vorticity $\omega_h := \mathrm{curl}(\mathbf{u}_h) = \partial_{x_1} u_2 - \partial_{x_2} u_1$ at $t = 6$ and $t = 8$ to show the resolution. We use 99 contours between -4.9 and 4.9, using the previous four meshes, where $h \in \{0.7405, 0.3702, 0.2468, 0.1851\}$. For this Figures, we use the DG scheme with the central flux (cf. (6.54)). Analogously, in Figures 6.7−6.12 we use the DG scheme with the upwind flux (cf. (6.55)). In all this figures, we take $\Delta t = 8/200 = 0.04$.

We see that the method using the upwind flux seems to do much better than the method using the central flux. In particular, when using $k = 2$ and using the upwind flux the method seems to do quite well. In fact, the method seems to be comparable to DG methods using the vorticity-potential formulation and high-order time integrators developed by Liu and Shu in [106].

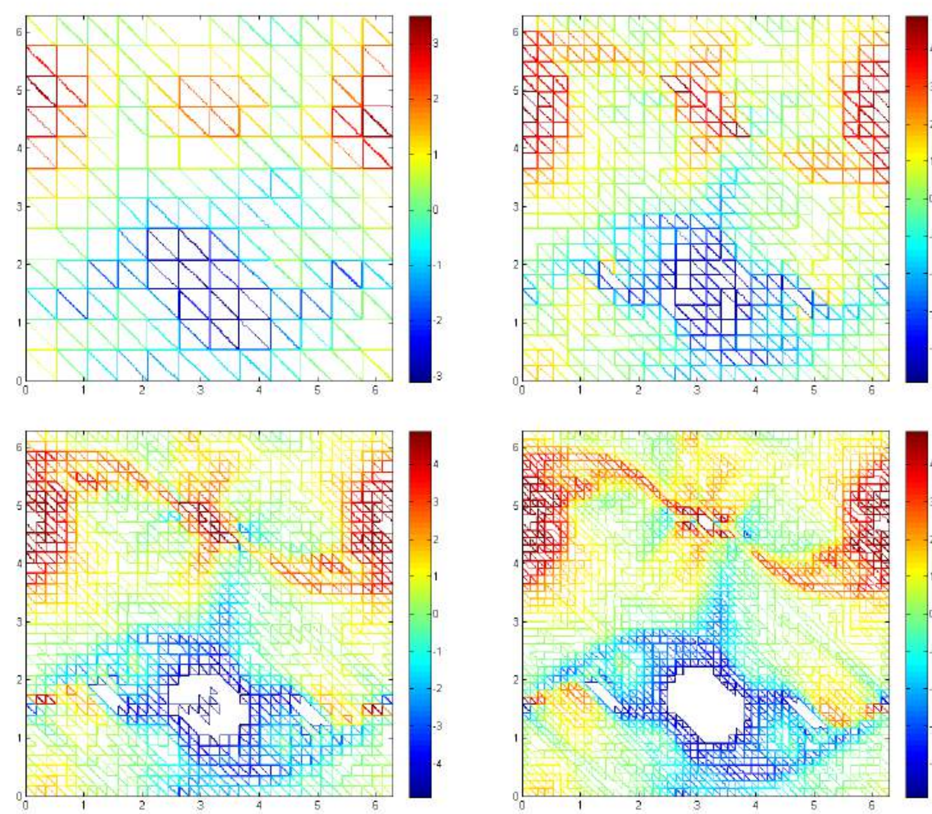

Figure 6.1: Example 2 (DG + central flux), contours for the vorticity with $k = 0$ and $t = 6$.

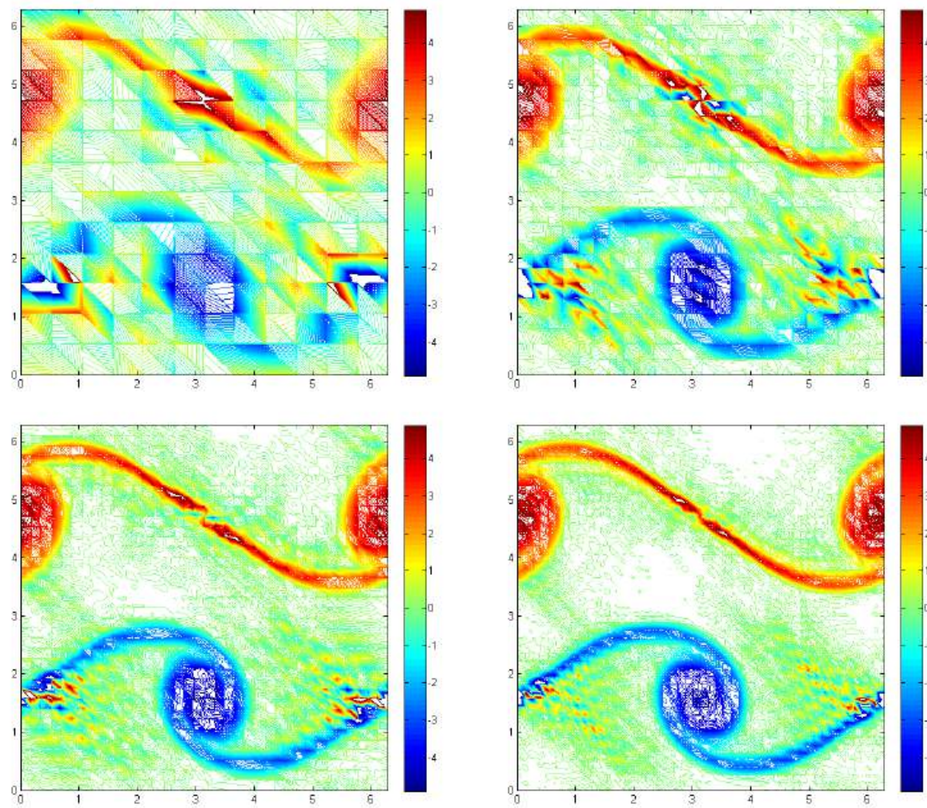

Figure 6.2: Example 2 (DG + central flux), contours for the vorticity with $k = 1$ and $t = 6$.

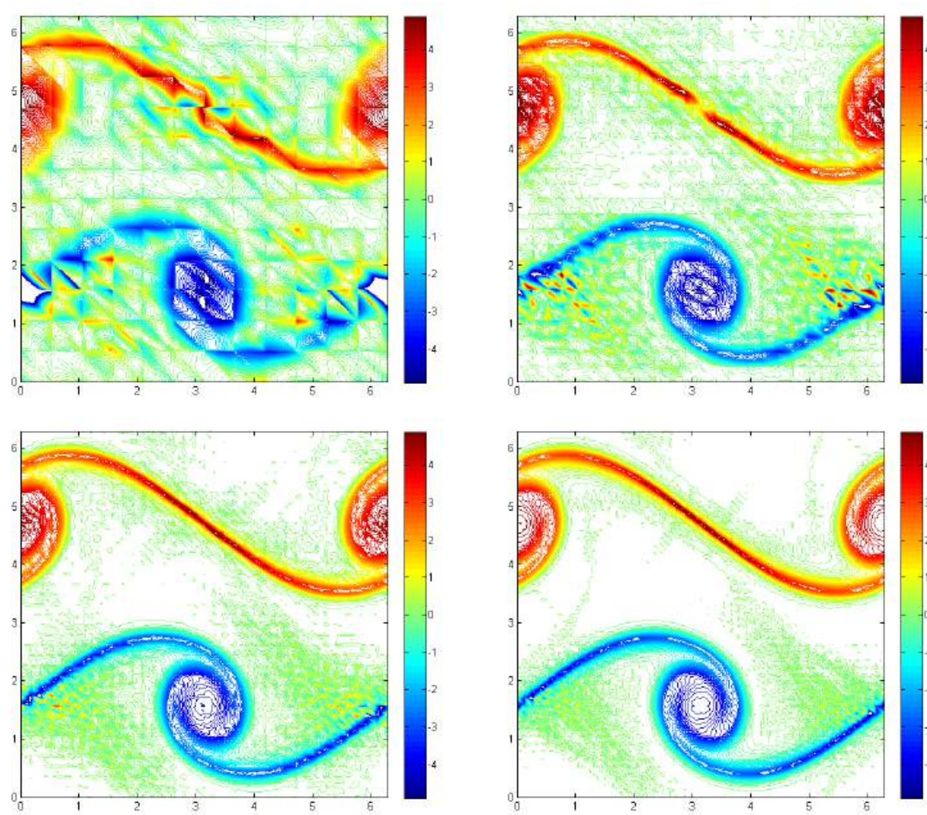

Figure 6.3: Example 2 (DG + central flux), contours for the vorticity with $k = 2$ and $t = 6$.

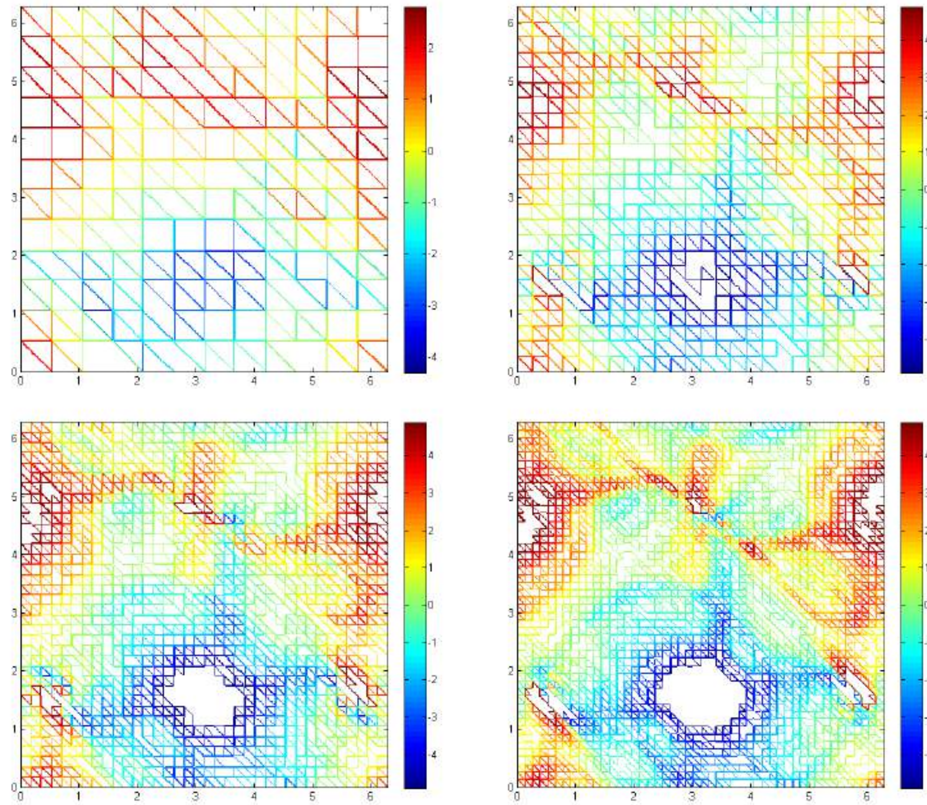

Figure 6.4: Example 2 (DG + central flux), contours for the vorticity with $k = 0$ and $t = 8$.

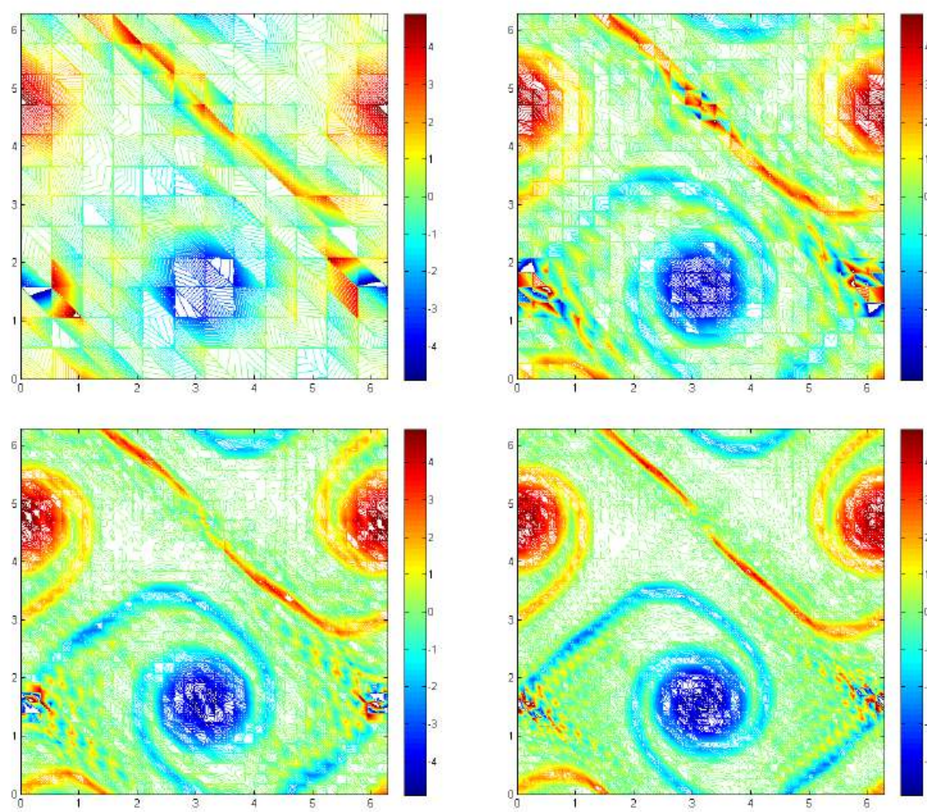

Figure 6.5: Example 2 (DG + central flux), contours for the vorticity with $k = 1$ and $t = 8$.

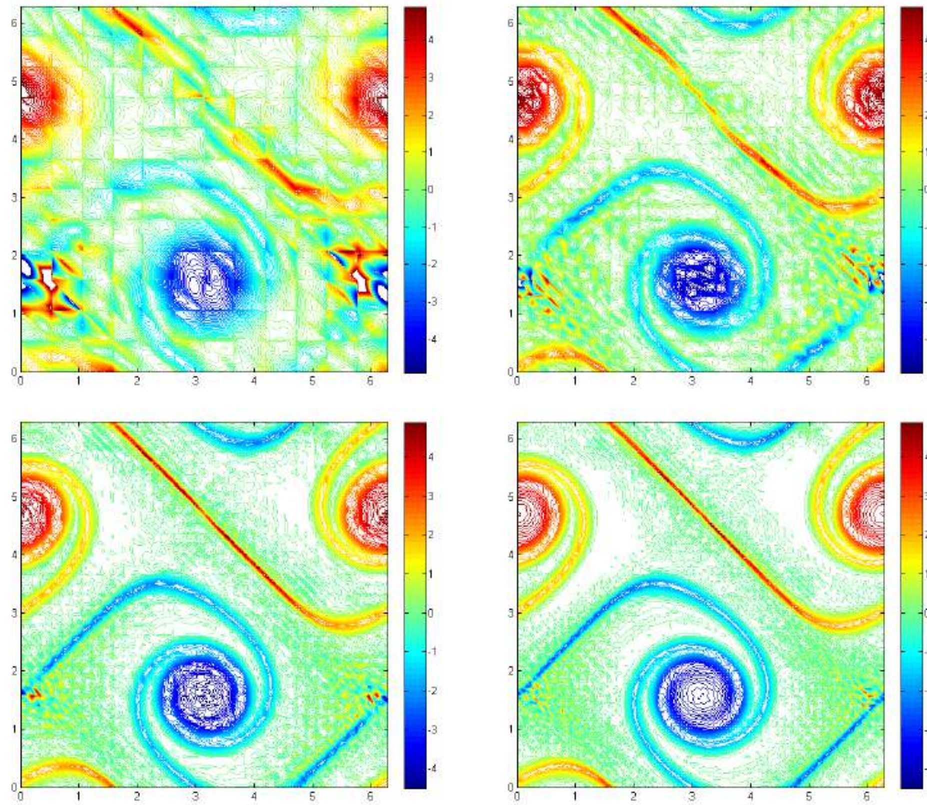

Figure 6.6: Example 2 (DG + central flux), contours for the vorticity with $k = 2$ and $t = 8$.

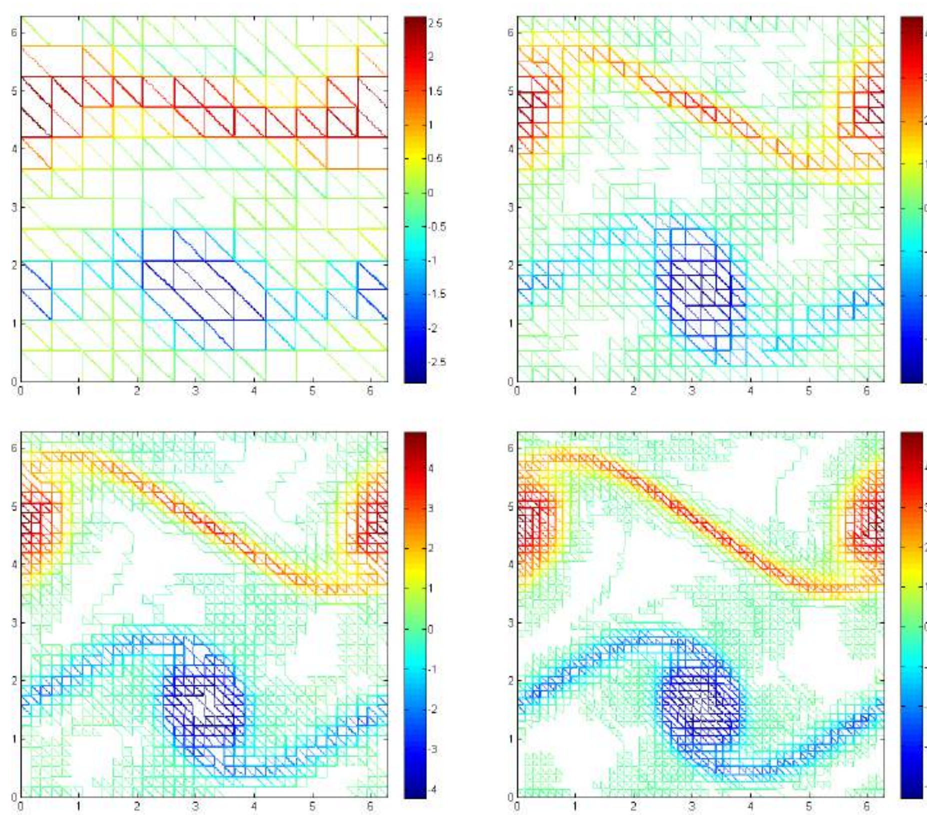

Figure 6.7: Example 2 (DG + upwind flux), contours for the vorticity with $k = 0$ and $t = 6$.

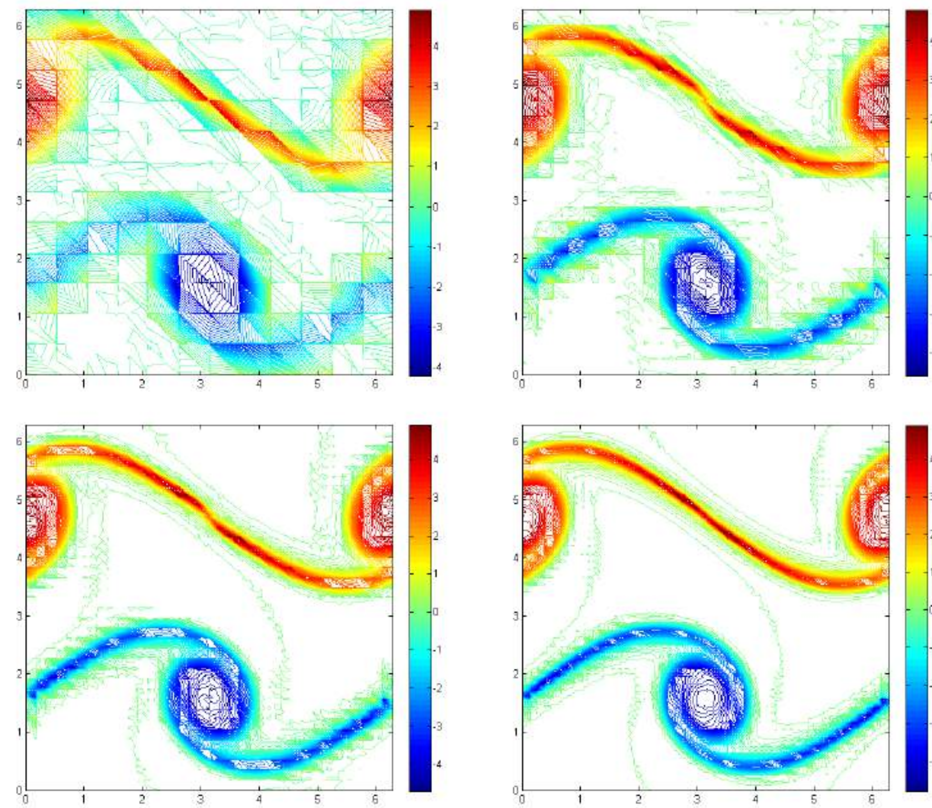

Figure 6.8: Example 2 (DG + upwind flux), contours for the vorticity with $k = 1$ and $t = 6$.

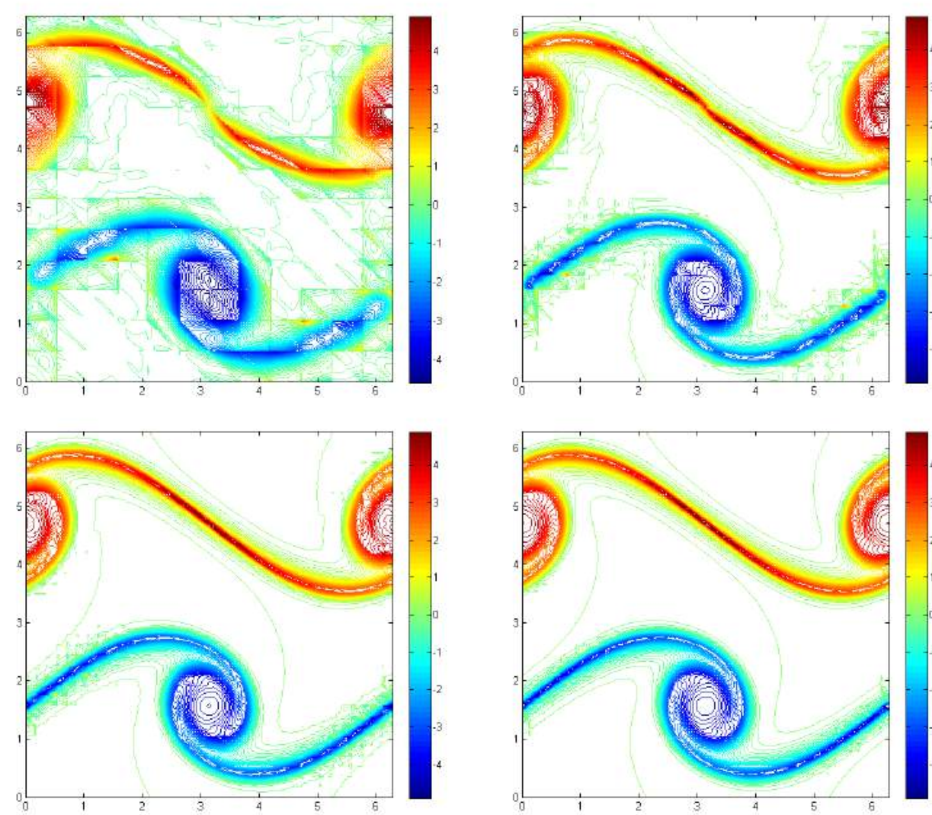

Figure 6.9: Example 2 (DG + upwind flux), contours for the vorticity with $k = 2$ and $t = 6$.

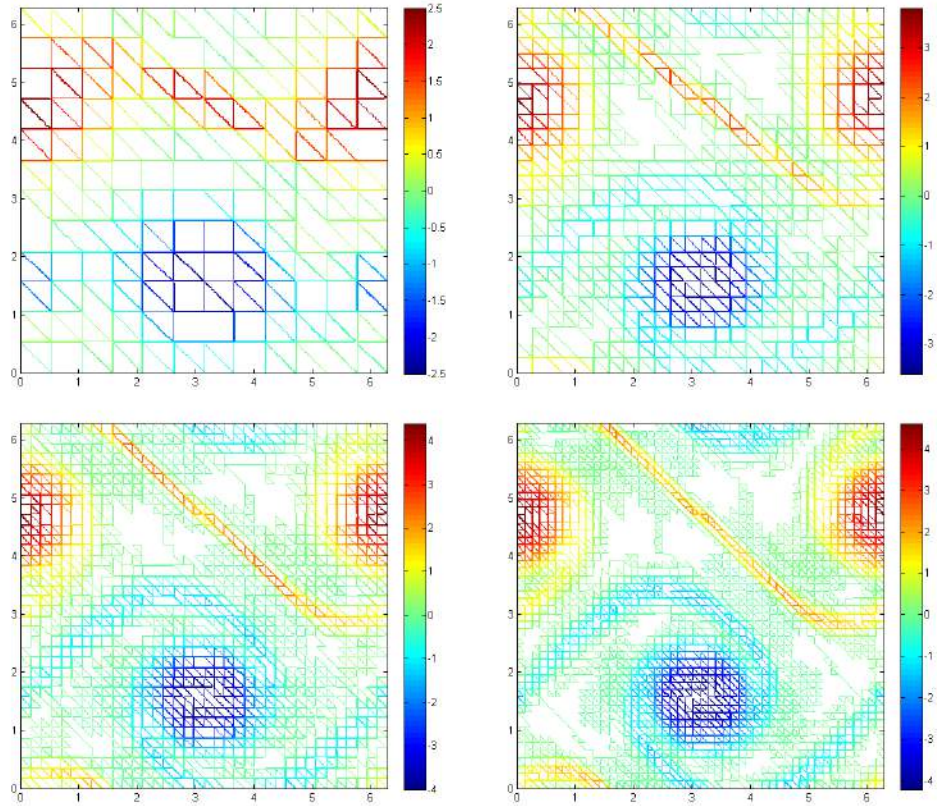

Figure 6.10: Example 2 (DG + upwind flux), contours for the vorticity with $k = 0$ and $t = 8$.

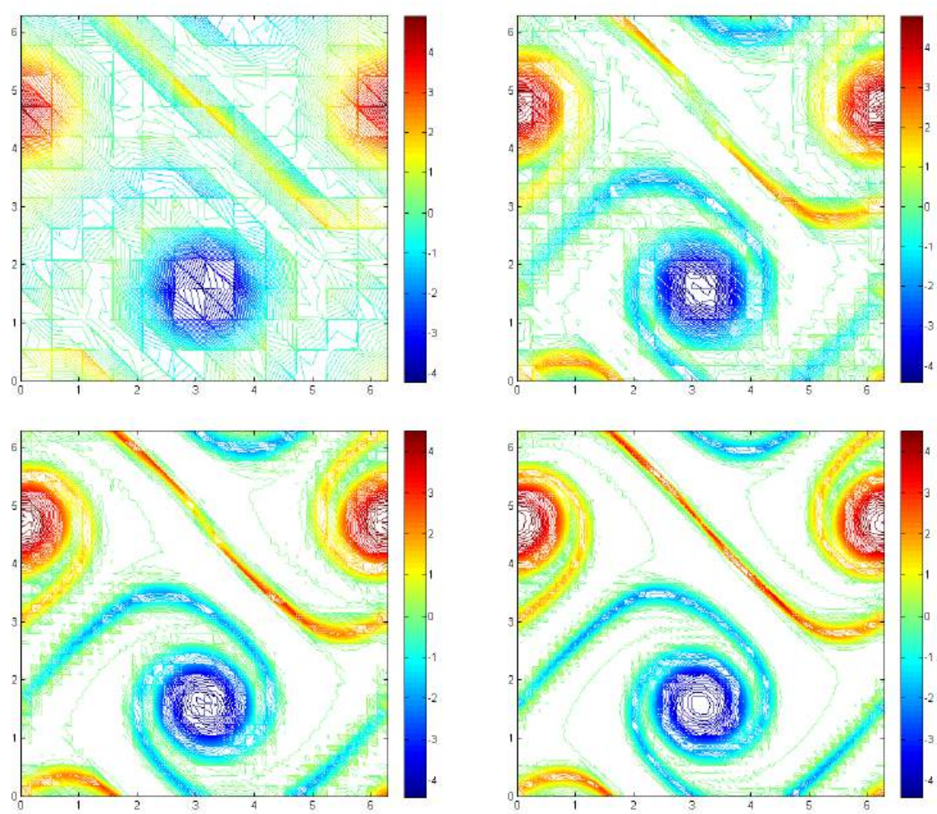

Figure 6.11: Example 2 (DG + upwind flux), contours for the vorticity with $k = 1$ and $t = 8$.

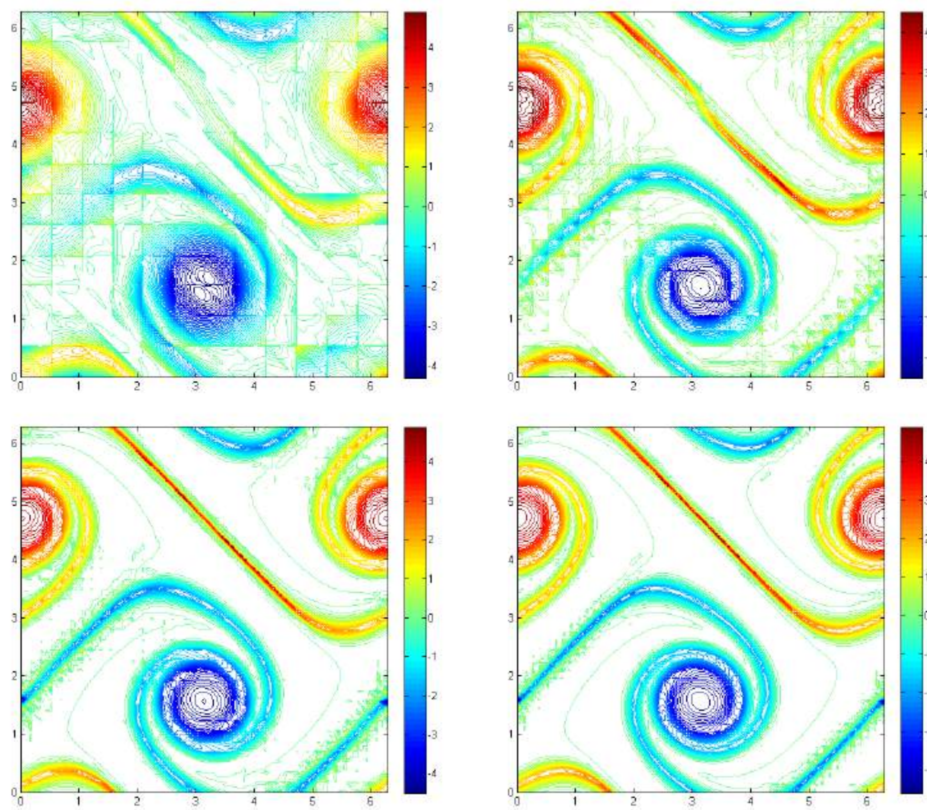

Figure 6.12: Example 2 (DG + upwind flux), contours for the vorticity with $k = 2$ and $t = 8$.

Conclusions and future works

Conclusions

In this thesis we developed mixed finite element methods for a set of partial differential equations of physical interest in continuum mechanics. We considered H(div) conforming and discontinuous Galerkin schemes in order to obtain original contributions and then to improve the existing literature on the subject. Here, not only the theoretical analysis is presented, but we also designed computational tools and strategies for the efficient implementations of the proposed methods.

The main conclusions of this work are:

1. We derived a pseudostress-based dual-mixed formulation for the linear elasticity problem with non-homogeneous Dirichlet boundary conditions, and then we showed its well-posedness. Furthermore, we introduced and analyzed the associated mixed finite element method. In particular, we established that Raviart-Thomas spaces of order $k \geq 0$ for the pseudostress and piecewise polynomials of degree $\leq k$ for the displacement can be employed, which, in the 3D case, yields a global number of unknowns behaving approximately as only 9 times the number of tetrahedra of the triangulation when $k = 0$. In classical approaches, this factor increases to 12.5 when one uses the PEERS elements with $k = 0$. In addition, we introduced an element-by-element postprocessing formula for the symmetric stress, which yields an optimally convergent approximation of this unknown with respect to the broken $\mathbb{H}(\mathbf{div})$-norm. Finally, a reliable and efficient residual-based *a posteriori* error estimator was developed for polyhedral domains in 3D.

2. We introduced an augmented continuous formulation for nonlinear Brinkman model and analyzed its solvability. In this way, the original unknowns given by the velocity and pressure, were easily recovered through a simple postprocessing. In addition, since the Neumann boundary condition becomes essential, we imposed it in a weak sense, which yields the introduction of the trace of the fluid velocity over the Neumann boundary as the associated Lagrange multiplier. In particular, a feasible choice of finite element subspaces for the associated mixed finite element method, was given by Raviart-Thomas elements of order $k \geq 0$ for the pseudostress, piecewise polynomials of degree $\leq k$ for the gradient of the velocity, and continuous piecewise polynomials of degree $\leq k + 1$ for the Lagrange multiplier. On the other hand, we extended a previous approach for the respective linear model to the present nonlinear case, and developed a reliable and efficient residual-based *a posteriori* error estimator for our Galerkin scheme. Numerical results confirmed the good performance and robustness of the scheme, together with the reliability and efficiency of the *a posteriori* estimator.

3. We proposed an augmented hybridizable discontinuous Galerkin formulation for nonlinear Stokes models arising in quasi-Newtonian fluids. This method approximates with good precision physical quantities such as the velocity, the pseudostress and the velocity gradient. In addition, we studied the unique solvability of the augmented HDG scheme by considering an equivalent formulation and then applying a nonlinear version of the Babuška-Brezzi theory and the classical Banach fixed-point theorem. The corresponding *a priori* error estimates were derived without the usual projection-based approach. We also derived a reliable and efficient residual-based *a posteriori* error estimator for this problem, and proposed the associated adaptive algorithm for the nonlinear HDG approximation. Finally, we provided several numerical results illustrating the performance of the method, confirming the theoretical properties of the estimator, and showing the expected behaviour of the associated adaptive algorithm. Some general aspects concerning the computational implementation of the HDG method were also discussed.

4. In the area of transmission problems, we contributed with the analysis of the HDG method for the Stokes and Darcy coupling problem. More precisely, we presented the finite dimensional discontinuous subspaces for a fully-mixed formulation in which the main unknowns were given by the stress, the vorticity, the velocity, and the trace of the velocity, all them in the fluid, together with the velocity, the pressure, and the trace of the pressure in the porous medium. Furthermore, we showed the unique solvability of the HDG scheme for this problem. The corresponding *a priori* error estimates were derived using the projection-based error analysis in order to simplify the corresponding study. In other words, we used projections whose design were inspired by the form of the numerical traces of the method, which is an innovative technique applied for the error analysis of HDG approximations. Finally, several numerical experiments validating the good performance of the method and confirming the rates of convergence were reported.

5. In relation to unsteady state problems, we developed H(div) conforming and discontinuous Galerkin finite element methods for incompressible Euler equations in two and three dimensions. Here, we used velocity-pressure formulations instead of the classical vorticity−stream-function approaches. We established the corresponding *a priori* error estimates, however, the reported numerical experiments, showing higher orders than predicted, support the conjecture that our analysis was not sharp, at least for the upwind methods. It would be interesting to see if a new analysis can lead to the optimal estimates for the upwind schemes. Despite this, the numerical behavior of the methods classified them as good alternative approximation schemes for this kind of partial differential systems.

Future works

1. We are interested in extending the results and techniques of Chapters 3 and 4 to the nonlinear Brinkman model considered in Chapter 2. At first glance, the extension looks immediate, but there is one issue with the augmented equation defined by the divergence. In fact, for our Brinkman model, the equation is given now by:

$$\kappa_2\,(\mathbf{div}_h(\boldsymbol{\sigma}_h), \mathbf{div}_h(\boldsymbol{\tau}_h))_{\mathcal{T}_h} \;-\; \alpha\,\kappa_2\,(\mathbf{u}_h, \mathbf{div}_h(\boldsymbol{\tau}_h))_{\mathcal{T}_h} \;=\; -\kappa_2\,(\mathbf{f}, \mathbf{div}_h(\boldsymbol{\tau}_h))_{\mathcal{T}_h} \quad \forall\, \boldsymbol{\tau}_h \in \Sigma_h.$$

The second term on the left-hand side of the above identity, implies that the nonlinear saddle-point problem obtained for the equivalent formulation is now non-symmetric. It is because of this that we will expect to obtain some restrictions for the parameter $\alpha > 0$ in order to establish the solvability analysis.

2. We plan to derive a reliable and efficient residual-based *a posteriori* error estimator for the HDG method applied to the Stokes-Darcy coupling system, introduced in Chapter 5. Possibly, we will extend the same approach given in Chapter 4 for this problem, which means that we will introduce postprocessing variables, in order to apply a global continuous inf-sup condition.

3. We plan to study the application of the HDG method to a nonlinear version of the Stokes-Darcy coupled problem described in Chapter 5. More precisely, we aim to the extension of the respective linear model presented in Chapter 5 to the nonlinear case analyzed in [81].

4. We plan to develop and analyze a fully-mixed HDG approximation for certain fluid-solid interaction problems (see, e.g. [78, 80]). As in previous works, the media are governed by the elastodynamic and acoustic equations in time-harmonic regime, respectively. In addition, the transmission conditions are given by the equilibrium of forces and the equality of the corresponding normal displacements, and the fluid is supposed to occupy an annular region surrounding the solid, so that a Robin boundary condition imitating the behavior of the Sommerfeld condition is imposed on its exterior boundary.

Conclusiones y trabajos futuros

Conclusiones

En esta tesis se desarrollaron métodos de elementos finitos mixtos para un conjunto de ecuaciones diferenciales parciales de interés físico en mecánica de medios continuos. Se consideraron esquemas conformes en H(div) y de Galerkin discontinuo, con el fin de obtener contribuciones originales y así enriquecer la literatura existente en el área. Aquí no sólo se presentó el análisis teórico, si no que además se diseñaron herramientas computaciones y estrategias para la implementación eficiente de los métodos propuestos.

Las conclusiones principales de este trabajo corresponden a:

1. Se derivó una formulación dual-mixta basada en pseudo-esfuerzo, para el problema de elasticidad lineal con condiciones de contorno de Dirichlet no homogéneas. Se probó que la misma era bien puesta. Más aún, se introdujo y se analizó el método de elementos finitos mixto asociado. En particular, se estableció que es posible emplear los espacios de Raviart-Thomas de orden $k \geq 0$ para el pseudo-esfuerzo, así como polinomios a trozos de grado $\leq k$ para el desplazamiento, donde para el caso 3D, se tiene que el número global de incógnitas se comporta aproximadamente como 9 veces el número de tetraedros en la triangulación, cuando $k = 0$. En enfoques clásicos, este factor se incrementa a 12.5, cuando se utilizan los elementos PEERS con $k = 0$. Adicionalmente, se introdujo un post-procesamiento para el esfuerzo simétrico, con el cual se obtiene una aproximación con convergencia óptima para esta incógnita, con respecto a la norma $\mathbb{H}(\mathbf{div})$ por tramos. Finalmente, se desarrolló un estimador de error *a posteriori* residual, el cual es confiable y eficiente para dominios poliédricos en 3D.

2. Se introdujo una formulación aumentada para el modelo de Brinkman no lineal y se analizó su solubilidad. En este sentido, la velocidad y presión original fueron fácilmente recuperadas a través de simples post-procesamientos. Además, dado que la condición de contorno de Neumann se vuelve esencial, la misma se impuso de manera débil, lo que lleva a la introducción de la traza de la velocidad del fluido sobre la frontera Neumann como el multiplicador de Lagrange asociado. En particular para el método discreto, recomandamos elegir los subespacios de elementos finitos mixtos dados por los elementos de Raviart-Thomas de orden $k \geq 0$ para el pseudo-esfuerzo, polinomios a trozos de grado $\leq k$ para el gradiente de la velocidad, así como polinomios continuos a trozos de grado $\leq k+1$ para el multiplicador de Lagrange. Por otro lado, se extendió un enfoque previo para el respectivo modelo lineal, al caso no lineal presente, y con ello se derivó un estimador de error *a posteriori* residual, confiable y eficiente, para el esquema de Galerkin. Resultados numéricos confirmaron el buen rendimiento del esquema, junto con la confiabilidad y la eficiencia del estimador *a posteriori*.

3. Se propuso una formulación aumentada de Galerkin discontinuo hibridizado, para modelos no lineales de Stokes provenientes de fluidos cuasi-Newtonianos. Este método aproximó con buena precisión cantidades físicas como: la velocidad, el pseudo-esfuerzo y el gradiente de la velocidad. Además, se estudió la solubilidad única del esquema HDG aumentado, a través de una formulación equivalente y de la aplicación de una versión no lineal de la teoría de Babuška-Brezzi y del teorema clásico de punto fijo de Banach. Las estimaciones de error *a priori* correspondientes fueron derivadas sin el enfoque usual por proyecciones. Más aún, se derivó un estimador de error *a posteriori* residual, confiable y eficiente, para este problema. Además, se propuso el algoritmo adaptativo asociado para la aproximación HDG no lineal. Finalmente, se presentaron varios resultados numéricos que ilustraron el rendimiento del método y confirmaron las propiedades teóricas del estimador. Algunos aspectos generales, referentes a la implementación computacional del método HDG, también fueron discutidos.

4. En el área de problemas de transmisión, se contribuyó con el análisis del método HDG aplicado a las ecuaciones acopladas de Stokes y Darcy. Más precisamente, se presentaron los subespacios discontinuos de dimensión finita para una formulación completamente mixta, en la cual las incógnitas principales fueron: el esfuerzo, la vorticidad, la velocidad y la traza de la velocidad, todas ellas en el fluido; junto con la velocidad, la presión y la traza de la presión en el medio poroso. Para este esquema HDG se probó la solubilidad única y las correspondientes estimaciones de error *a priori* fueron derivadas utilizando el análisis de error basado en proyecciones, lo que simplificó dicho estudio. Es decir, se usaron proyecciones cuyo diseño fue inspirado por la forma que tienen las trazas numéricas del método. Finalmente, se reportaron varios experimentos numéricos, los cuales validaron el buen rendimiento del esquema propuesto, así como los órdenes de convergencia predichos.

5. Con respecto a problemas evolutivos, se desarrollaron métodos de elementos finitos conformes en H(div) y de Galerkin discontinuo, para las ecuaciones incompresibles de Euler en dos y tres dimensiones. Los mismos estan basados en formulaciones variacionales cuyas incógnitas principales vienen dadas por la velocidad y la presión. Se probaron estimaciones de error, sin embargo, los experimentos numéricos sugirieron que el análisis propuesto no fue acertado, al menos para los métodos con flujo *upwind*. Sería interesante ver si un nuevo análisis puede probar las estimaciones óptimas para los esquemas *upwind*. A pesar de esto, el comportamiento numérico de los métodos, los clasifica como buenos esquemas de aproximación alternativos para esta clase de sistemas diferenciales parciales.

Trabajos futuros

1. Se extenderán los resultados y técnicas de los Capítulos 3 y 4 al modelo de Brinkman no lineal considerado en el Capítulo 2. A primera vista esta extensión parece inmediata, sin embargo, existe una dificultad con la ecuación aumentada definida por la divergencia. Más precisamente, en el caso del modelo de Brinkman, dicha ecuación viene dada ahora por:

$$\kappa_2\,(\mathbf{div}_h(\boldsymbol{\sigma}_h),\mathbf{div}_h(\boldsymbol{\tau}_h))_{\mathcal{T}_h} \;-\; \alpha\,\kappa_2\,(\mathbf{u}_h,\mathbf{div}_h(\boldsymbol{\tau}_h))_{\mathcal{T}_h} \;=\; -\kappa_2\,(\mathbf{f},\mathbf{div}_h(\boldsymbol{\tau}_h))_{\mathcal{T}_h} \quad \forall\ \boldsymbol{\tau}_h\in\Sigma_h.$$

El segundo término en el lado izquierdo de la identidad anterior, implica que el problema de punto-silla no lineal obtenido por la formulación equivalente es ahora no simétrico. Es debido a esto que se espera obtener algunas restricciones para el parámetro $\alpha > 0$, con las cuales se garantice el análisis de solubilidad.

2. Se derivará un estimador de error *a posteriori* residual, confiable y eficiente, para el método HDG aplicado al sistema acoplado de Stokes-Darcy, introducido en el Capítulo 5. Posiblemente, se extenderá el mismo enfoque dado en el Capítulo 4 para este problema. Es decir, se considerará la introducción de variables post-procesadas, para así poder recurrir a una condición inf-sup global y continua.

3. Se estudiará la aplicación del método HDG para una versión no lineal del problema acoplado de Stokes-Darcy, descrito en el Capítulo 5. Más precisamente, el objetivo es una extensión para el respectivo modelo lineal presentado en el Capítulo 5 al caso no lineal analizado en [81].

4. Se desarrollará y analizará una aproximación HDG completamente mixta, para ciertos problemas de interacción solido-fluido (ver por ejemplo [78, 80]). Similar a a trabajos previos, los medios están determinados por las ecuaciones de elastodinámica y acústica en un régimen de tiempo armónico, respectivamente. Adicionalmente, las condiciones de transmisión están dadas por el equilibrio de fuerzas y la igualdad de los correspondientes desplazamientos normales. Más aún, se supone que el líquido ocupa una región anular que rodea el sólido, de modo que se impone en el exterior de su frontera, una condición de contorno Robin, la cual imita el comportamiento de la condición de Sommerfeld.

References

[1] S. Adams and B. Cockburn, *A mixed finite element method for elasticity in three dimensions*, Journal of Scientific Computing, 25 (2005), pp. 515–521.

[2] C. Amrouche, C. Bernardi, M. Dauge, and V. Girault, *Vector potentials in three-dimensional nonsmooth domains*, Mathematical Methods in the Applied Sciences, 21 (1998), pp. 823–864.

[3] D. N. Arnold, *An interior penalty finite element method with discontinuous elements*, SIAM Journal on Numerical Analysis, 19 (1982), pp. 742–760.

[4] D. N. Arnold, F. Brezzi, and J. Douglas, *PEERS: A new mixed finite element method for plane elasticity*, Japan Journal of Applied Mathematics, 1 (1984), pp. 347–367.

[5] D. N. Arnold, J. Douglas, and C. P. Gupta, *A family of higher order mixed finite element methods for plane elasticity*, Numerische Mathematik, 45 (1984), pp. 1–22.

[6] D. N. Arnold and R. S. Falk, *A new mixed formulation for elasticity*, Numerische Mathematik, 53 (1988), pp. 13–30.

[7] ——, *Mixed finite element methods for linear elasticity with weakly imposed symmetry*, Mathematics of Computation, 76 (2007), pp. 1699–1723.

[8] D. N. Arnold, R. S. Falk, and R. Winther, *Differential complexes and stability of finite element methods. II: The elasticity complex. In: Compatible Spatial Discretizations, D.N. Arnold, P. Bochev, R. Lehoucq, R. Nicolaides, and M. Shashkov, eds*, IMA Volumes in Mathematics and its Applications, Springer Verlag, 142 (2005), pp. 47–67.

[9] ——, *Finite element exterior calculus, homological techniques, and applications*, Acta Numerica, 15 (2006), pp. 1–155.

[10] D. N. Arnold and R. Winther, *Mixed finite elements for elasticity*, Numerische Mathematik, 92 (2002), pp. 401–419.

[11] I. Babuška and G. N. Gatica, *On the mixed finite element method with Lagrange multipliers*, Numerical Methods for Partial Differential Equations, 19 (2003), pp. 192–210.

[12] J. Baranger, K. Najib, and D. Sandri, *Numerical analysis of a three-fields model for a quasi-Newtonian flow*, Computer Methods in Applied Mechanics and Engineering, 109 (1993), pp. 281–292.

[13] T. P. Barrios, G. N. Gatica, M. González, and N. Heuer, *A residual based a posteriori error estimator for an augmented mixed finite element method in linear elasticity*, ESAIM: Mathematical Modelling and Numerical Analysis, 40 (2007), pp. 843–869.

[14] J. Bell, P. Colella, and H. Glaz, *A second order projection method for the incompressible Navier-Stokes equations*, Journal of Computational Physics, 85 (1989), pp. 257–283.

[15] C. Bernardi, F. Hecht, and O. Pironneau, *Coupling Darcy and Stokes equations for porous media with cracks*, ESAIM: Mathematical Modelling and Numerical Analysis, 39 (2005), pp. 7–35.

[16] D. Boffi, F. Brezzi, and M. Fortin, *Reduced symmetry elements in linear elasticity*, Communications on Pure and Applied Analysis, 8 (2009), pp. 95–121.

[17] S. C. Brenner and L. R. Scott, *The Mathematical Theory of Finite Element Methods*, Springer, third ed., 2008.

[18] F. Brezzi, J. Douglas, and L. D. Marini, *Two families of mixed finite elements for second order elliptic problems*, Numerische Mathematik, 47 (1985), pp. 217–235.

[19] F. Brezzi and M. Fortin, *Mixed and Hybrid Finite Element Methods*, Springer Verlag, 1991.

[20] E. Burman and M. A. Fernández, *Continuous interior penalty finite element method for the time-dependent Navier-Stokes equations: space discretization and convergence*, Numerische Mathematik, 107 (2007), pp. 39–77.

[21] E. Burman and P. Hansbo, *A unified stabilized method for Stokes' and Darcy's equations*, Journal of Computational and Applied Mathematics, 198 (2007), pp. 35–51.

[22] R. Bustinza and G. N. Gatica, *A local discontinuous Galerkin method for nonlinear diffusion problems with mixed boundary conditions*, Journal of Scientific Computing, 26 (2004), pp. 152–177.

[23] ——, *A mixed local discontinuous Galerkin for a class of nonlinear problems in fluid mechanics*, Journal of Computational Physics, 207 (2005), pp. 427–456.

[24] R. Bustinza, G. N. Gatica, and B. Cockburn, *An a posteriori error estimate for the local discontinuous Galerkin method applied to linear and nonlinear diffusion problems*, Journal of Scientific Computing, 22-23 (2005), pp. 147–185.

[25] Z. Cai, C. Tong, P. S. Vassilevski, and C. Wang, *Mixed finite element methods for incompressible flow: stationary Stokes equations*, Numerical Methods for Partial Differential Equations, 26 (2010), pp. 957–978.

[26] Z. Cai, C. Wang, and S. Zhang, *Mixed finite element methods for incompressible flow: stationary Navier-Stokes equations*, SIAM Journal on Numerical Analysis, 48 (2010), pp. 79–94.

[27] Z. Cai and S. Zhang, *Mixed methods for stationary Navier-Stokes equations based on pseudostress-pressure-velocity formulation*, Mathematics of Computation, 81 (2012), pp. 1903–1927.

[28] J. Camaño, G. N. Gatica, R. Oyarzúa, R. Ruiz-Baier, and P. Venegas, *New fully-mixed finite element methods for the Stokes-Darcy coupling*, Computer Methods in Applied Mechanics and Engineering, 295 (2015), pp. 362–395.

[29] J. Camaño, G. N. Gatica, R. Oyarzúa, and G. Tierra, *An augmented mixed finite element method for the Navier-Stokes equations with variable viscosity*, Preprint 2015-09, Centro de Investigación en Ingeniería Matemática (CI^{2}MA), Universidad de Concepción, Chile, (2015).

[30] J. Camaño, R. Oyarzúa, and G. Tierra, *Analysis of an augmented mixed-FEM for the Navier-Stokes problem*, Preprint 2014-33, Centro de Investigación en Ingeniería Matemática (CI^{2}MA), Universidad de Concepción, Chile, (2014).

[31] J. Carrero, B. Cockburn, and D. Schötzau, *Hybridized, globally divergence-free LDG methods. Part I: The Stokes problem*, Mathematics of Computation, 75 (2006), pp. 533–563.

[32] C. Carstensen, *A posteriori error estimate for the mixed finite element method*, Mathematics of Computation, 66 (1997), pp. 465–476.

[33] C. Carstensen and G. Dolzmann, *A posteriori error estimates for mixed FEM in elasticity*, Numerische Mathematik, 81 (1998), pp. 187–209.

[34] P. E. Castillo and F. A. Sequeira, *Computational aspects of the local discontinuous Galerkin method on unstructured grids in three dimensions*, Mathematical and Computer Modelling, 57 (2013), pp. 2279–2288.

[35] H. Chen, J. Li, and W. Qiu, *Robust a posteriori error estimates for hdg method for convection-diffusion equations*, IMA Journal of Numerical Analysis, (2015).

[36] A. J. Chorin, *Numerical solution of the navier-stokes equations*, Mathematics of Computation, 22 (1968), pp. 745–762.

[37] P. G. Ciarlet, *The Finite Element Method for Elliptic Problems*, Nort-Holland, 1978.

[38] F. Cimolin and M. Discacciati, *Navier-Stokes/Forchheimer models for filtration through porous media*, Applied Numerical Mathematics, 72 (2013), pp. 205–224.

[39] P. Clément, *Un problème d'approximation par éléments finis*, PhD thesis, Ecole Polytechnique Fédérale de Lausane, 1973.

[40] ——, *Approximation by finite element functions using local regularisation*, ESAIM: Mathematical Modelling and Numerical Analysis, 9 (1975), pp. 77–84.

[41] B. Cockburn, B. Dong, and J. Guzmán, *A superconvergent LDG-hybridizable Galerkin method for second-order elliptic problems*, Mathematics of Computation, 77 (2008), pp. 1887–1916.

[42] B. Cockburn, J. Gopalakrishnan, and R. Lazarov, *Unified hybridization of discontinuous Galerkin, mixed and continuous Galerkin methods for second order elliptic problems*, SIAM Journal on Numerical Analysis, 47 (2009), pp. 1319–1365.

[43] B. Cockburn, J. Gopalakrishnan, N. C. Nguyen, J. Peraire, and F. J. Sayas, *Analysis of HDG methods for Stokes flow*, Mathematics of Computation, 80 (2011), pp. 723–760.

[44] B. Cockburn, J. Gopalakrishnan, and F. J. Sayas, *A projection-based error analysis of HDG methods*, Mathematics of Computation, 79 (2010), pp. 1351–1367.

[45] B. Cockburn, J. Guzmán, and H. Wang, *Superconvergent discontinuous Galerkin methods for second-order elliptic problems*, Mathematics of Computation, 78 (2009), pp. 1–24.

[46] B. Cockburn, G. Kanschat, and D. Schötzau, *A locally conservative LDG method for the incompressible Navier-Stokes equations*, Mathematics of Computation, 74 (2005), pp. 1067–1095.

[47] ——, *A note on discontinuous Galerkin divergence-free solutions of the Navier-Stokes equations*, Journal of Scientific Computing, 31 (2007), pp. 61–73.

[48] B. Cockburn and K. Shi, *Superconvergent HDG methods for linear elasticity with weakly symmetric stress*, IMA Journal of Numerical Analysis, 33 (2013), pp. 747–770.

[49] ——, *Devising HDG methods for Stokes flow: An overview*, Computers & Fluids, 98 (2014), pp. 221–229.

[50] B. Cockburn and C. Shu, *The local discontinuous Galerkin method for time-dependent convection-diffusion systems*, SIAM Journal on Numerical Analysis, 35 (1998), pp. 2440–2463.

[51] B. Cockburn and W. Zhang, *A posteriori error estimates for HDG methods*, Journal of Scientific Computing, 51 (2012), pp. 582–607.

[52] ——, *A posteriori error analysis for hybridizable discontinuous Galerkin methods for second order elliptic problems*, SIAM Journal on Numerical Analysis, 51 (2013), pp. 676–693.

[53] E. Colmenares, G. N. Gatica, and R. Oyarzúa, *Analysis of an augmented mixed-primal formulation for the stationary Boussinesq problem*, Numerical Methods for Partial Differential Equations, DOI:http://dx.doi.org/10.1002/num.22001, (2015).

[54] S. Congreve, P. Houston, E. Süli, and T. P. Whiler, *Discontinuous Galerkin finite element approximation of quasilinear elliptic boundary value problems II: Strongly monotone quasi-Newtonian flows*, IMA Journal of Numerical Analysis, 33 (2013), pp. 1386–1415.

[55] M. Discacciati, *Domain Decomposition Methods for the Coupling of Surface and Groundwater Flows*, PhD thesis, Ecole Polytechnique Fédérale de Lausanne, 2004.

[56] M. Discacciati, E. Miglio, and A. Quarteroni, *Mathematical and numerical models for coupling surface and groundwater flows*, Applied Numerical Mathematics, 43 (2002), pp. 57–74.

[57] M. Dubiner, *Spectral methods on triangles and other domains*, Journal of Scientific Computing, 6 (1991), pp. 345–390.

[58] V. J. Ervin, J. S. Howell, and I. Stanculescu, *A dual-mixed approximation method for a three-field model of a nonlinear generalized Stokes problem*, Computer Methods in Applied Mechanics and Engineering, 197 (2008), pp. 2886–2900.

[59] V. J. Ervin, E. W. Jenkins, and S. Sun, *Coupled generalized nonlinear Stokes flow with flow through a porous medium*, SIAM Journal on Numerical Analysis, 47 (2009), pp. 929–952.

[60] ——, *Coupling nonlinear Stokes and Darcy flow using mortar finite elements*, Applied Numerical Mathematics, 61 (2011), pp. 1198–1222.

[61] L. C. Evans, *Partial Differential Equations*, American Mathematical Society, 2 ed., 2010.

[62] M. Farhloul, *Dual hybrid methods for the elasticity and the Stokes problems: a unified approach*, Canadian Applied Mathematics Quarterly, 3 (1995), pp. 399–418.

[63] M. Farhloul and M. Fortin, *Dual hybrid methods for the elasticity and the Stokes problems: a unified approach*, Numerische Mathematik, 76 (1997), pp. 419–440.

[64] L. Figueroa, G. N. Gatica, and A. Márquez, *Augmented mixed finite element methods for the stationary Stokes equations*, Journal of Scientific Computing, 31 (2008/09), pp. 1082–1119.

[65] J. Galvis and M. Sarkis, *Non-matching mortar discretization analysis for the coupling Stokes-Darcy equations*, Electronic Transactions on Numerical Analysis, 26 (2007), pp. 350–384.

[66] A. I. Garralda-Guillem, G. N. Gatica, A. Márquez, and M. Ruiz-Galán, *A posteriori error analysis of twofold saddle point variational formulations for nonlinear boundary value problems*, IMA Journal of Numerical Analysis, 34 (2014), pp. 326–361.

[67] G. N. Gatica, *Solvability and Galerkin approximations of a class of nonlinear operator equations*, Zeitschrift für Analysis und ihre Anwendungen, 21 (2002), pp. 761–781.

[68] ——, *A note on the efficiency of residual-based a-posteriori error estimators for some mixed finite element methods*, Electronic Transactions on Numerical Analysis, 17 (2004), pp. 218–233.

[69] ——, *Analysis of a new augmented mixed finite element method for linear elasticity allowing* $\mathbb{RT}_0 - \mathbb{P}_1 - \mathbb{P}_0$ *approximations*, ESAIM: Mathematical Modelling and Numerical Analysis, 40 (2006), pp. 1–28.

[70] ——, *An augmented mixed finite element method for linear elasticity with non-homogeneous Dirichlet conditions*, Electronic Transactions on Numerical Analysis, 26 (2007), pp. 421–438.

[71] ——, *A Simple Introduction to the Mixed Finite Element Method: Theory and Applications*, SpringerBriefs in Mathematics, Springer Cham Heidelberg New York Dordrecht London, 2014.

[72] G. N. Gatica, L. F. Gatica, and A. Márquez, *Analysis of a pseudostress-based mixed finite element method for the Brinkman model of porous media flow*, Numerische Mathematik, 126 (2014), pp. 635–677.

[73] G. N. Gatica, L. F. Gatica, and F. A. Sequeira, *Analysis of an augmented pseudostress-based mixed formulation for a nonlinear Brinkman model of porous media flow*, Computer Methods in Applied Mechanics and Engineering, 289 (2015), pp. 104–130.

[74] ——, *A* $\mathbb{RT}_k - \mathbf{P}_k$ *approximation for linear elasticity yielding a broken* $\mathbb{H}(\mathbf{div})$ *convergent post-processed stress*, Applied Mathematics Letters, 49 (2015), pp. 133–140.

[75] ——, *A priori and a posteriori error analyses of a pseudostress-based mixed formulation for linear elasticity*, Preprint 2015-14, Centro de Investigación en Ingeniería Matemática (CI^2MA), Universidad de Concepción, Chile, (2015).

[76] G. N. Gatica, M. González, and S. Meddahi, *A low-order mixed finite element method for a class of quasi-Newtonian Stokes flows. I: a priori error analysis*, Computer Methods in Applied Mechanics and Engineering, 193 (2004), pp. 881–892.

[77] G. N. Gatica, N. Heuer, and S. Meddahi, *On the numerical analysis of nonlinear twofold saddle point problems*, IMA Journal of Numerical Analysis, 23 (2003), pp. 301–330.

[78] G. N. Gatica, A. Márquez, and S. Meddahi, *Analysis of the coupling of primal and dual-mixed finite element methods for a two-dimensional fluid-solid interaction problem*, SIAM Journal on Numerical Analysis, 45 (2007), pp. 2072–2097.

[79] G. N. Gatica, A. Márquez, and S. Meddahi, *An augmented mixed finite element method for 3D linear elasticity problems*, Journal of Computational and Applied Mathematics, 231 (2009), pp. 526–540.

[80] G. N. Gatica, A. Márquez, and S. Meddahi, *Analysis of the coupling of Lagrange and Arnold-Falk-Winther finite elements for a fluid-solid interaction problem in three dimensions*, SIAM Journal on Numerical Analysis, 50 (2012), pp. 1648–1674.

[81] G. N. Gatica, A. Márquez, R. Oyarzúa, and R. Rebolledo, *Analysis of an augmented fully-mixed approach for the coupling of quasi-Newtonian fluids and porous media*, Computer Methods in Applied Mechanics and Engineering, 270 (2014), pp. 76–112.

[82] G. N. Gatica, A. Márquez, and W. Rudolph, *A priori and a posteriori error analyses of augmented twofold saddle point formulations for nonlinear elasticity problems*, Computer Methods in Applied Mechanics and Engineering, 264 (2013), pp. 23–48.

[83] G. N. Gatica, A. Márquez, and M. A. Sánchez, *Analysis of a velocity-pressure-pseudostress formulation for the stationary Stokes equations*, Computer Methods in Applied Mechanics and Engineering, 199 (2010), pp. 1064–1079.

[84] ——, *A priori and a posteriori error analyses of a velocity-pseudostress formulation for a class of quasi-Newtonian Stokes flows*, Computer Methods in Applied Mechanics and Engineering, 200 (2011), pp. 1619–1636.

[85] G. N. Gatica, S. Meddahi, and R. Oyarzúa, *A conforming mixed finite-element method for the coupling of fluid flow with porous media flow*, IMA Journal of Numerical Analysis, 29 (2009), pp. 86–108.

[86] G. N. Gatica, R. Oyarzúa, and F.-J. Sayas, *Analysis of fully-mixed finite element methods for the Stokes-Darcy coupled problem*, Mathematics of Computation, 80 (2011), pp. 1911–1948.

[87] ——, *A residual-based a posteriori error estimator for a fully-mixed formulation of the Stokes-Darcy coupled problem*, Computer Methods in Applied Mechanics and Engineering, 200 (2011), pp. 1877–1891.

[88] ——, *A twofold saddle point approach for the coupling of fluid flow with nonlinear porous media flow*, IMA Journal of Numerical Analysis, 32 (2012), pp. 845–887.

[89] G. N. Gatica and F. A. Sequeira, *Analysis of an augmented HDG method for a class of quasi-Newtonian Stokes flows*, Journal of Scientific Computing, 65 (2015), pp. 1270–1308.

[90] ——, *Analysis of the HDG method for the Stokes-Darcy coupling*, Preprint 2015-23, Centro de Investigación en Ingeniería Matemática (CI^2MA), Universidad de Concepción, Chile, (2015).

[91] ——, *A priori and a posteriori error analyses of an augmented HDG method for a class of quasi-Newtonian Stokes flows*, Preprint 2015-32, Centro de Investigación en Ingeniería Matemática (CI^{2}MA), Universidad de Concepción, Chile, (2015).

[92] V. Girault and P. A. Raviart, *Finite Element Methods for Navier-Stokes Equations. Theory and Algorithms*, Springer Series in Computational Mathematics, Vol. 5. Berlin: Springer, 1986.

[93] J. Guzmán, *A unified analysis of several mixed methods for elasticity with weak stress symmetry*, Journal of Scientific Computing, 44 (2010), pp. 156–169.

[94] J. Guzmán, F. A. Sequeira, and C.-W. Shu, *H(div) conforming and DG methods for incompressible Euler's equations*, Preprint 2015-19, Centro de Investigación en Ingeniería Matemática (CI^{2}MA), Universidad de Concepción, Chile, (2015).

[95] P. Hansbo and M. Juntunen, *Weakly imposed dirichlet boundary conditions for the Brinkman model of porous media flow*, Applied Numerical Mathematics, 59 (2009), pp. 1274–1289.

[96] R. Hiptmair, *Finite elements in computational electromagnetism*, Acta Numerica, 11 (2002), pp. 237–339.

[97] P. Houston, J. Robson, and E. Süli, *Discontinuous Galerkin finite element approximation of quasilinear elliptic boundary value problems. I. The scalar case*, IMA Journal of Numerical Analysis, 25 (2005), pp. 726–749.

[98] J. S. Howell, *Dual-mixed finite element approximation of Stokes and nonlinear Stokes problems using trace-free velocity gradients*, Journal of Computational and Applied Mathematics, 231 (2009), pp. 780–792.

[99] J. S. Howell and N. J. Walkington, *Dual-mixed finite element methods for the Navier-Stokes equations*, ESAIM: Mathematical Modelling and Numerical Analysis, 47 (2013), pp. 789–805.

[100] M. Juntunen and R. Stenberg, *Analysis of finite element methods for the Brinkman problem*, Calcolo, 47 (2010), pp. 129–147.

[101] T. Karper, K.-A. Mardal, and R. Winther, *Unified finite element discretizations of coupled Darcy-Stokes flow*, Numerical Methods for Partial Differential Equations, 25 (2009), pp. 311–326.

[102] T. Kato, *On classical solutions of the two-dimensional non-stationary Euler equation*, Archive for Rational Mechanics and Analysis, 14 (1967), pp. 188–200.

[103] L. I. G. Kovasznay, *Laminar flow behind a two-dimensional grid*, Proceedings of the Cambridge Philosophical Society, 44 (1948), pp. 58–62.

[104] O. Ladyzhenskaya, *New equations for the description of the viscous incompressible fluids and solvability in the large for the boundary value problems of them, in: Boundary Value Problems of Mathematical Physics V*, Providence, RI: AMS, 1970.

[105] W. J. Layton, F. Schieweck, and I. Yotov, *Coupling fluid flow with porous media flow*, SIAM Journal on Numerical Analysis, 40 (2003), pp. 2195–2218.

[106] J.-G. Liu and C.-W. Shu, *A High-Order Discontinuous Galerkin Method for 2D Incompressible Flows*, Journal of Computational Physics, 160 (2000), pp. 577–596.

[107] M. Lonsing and R. Verfürth, *On the stability of BDMS and PEERS elements*, Numerische Mathematik, 99 (2004), pp. 131–140.

[108] A. F. D. Loula and J. N. C. Guerreiro, *Finite element analysis of nonlinear creeping flows*, Computer Methods in Applied Mechanics and Engineering, 99 (1990), pp. 87–109.

[109] A. Márquez, S. Meddahi, and F.-J. Sayas, *Strong coupling of finite element methods for the Stokes-Darcy problem*, IMA Journal of Numerical Analysis, DOI:http://dx.doi.org/10.1093/imanum/dru023 (2014).

[110] W. McLean, *Strongly Elliptic Systems and Boundary Integral Equations*, Cambridge University Press, London, 2000.

[111] N. C. Nguyen, J. Peraire, and B. Cockburn, *An implicit high-order hybridizable discontinuous Galerkin method for nonlinear convection-diffusion equations*, Journal of Computational Physics, 228 (2009), pp. 8841–8855.

[112] ——, *A hybridizable discontinuous Galerkin method for Stokes flow*, Computer Methods in Applied Mechanics and Engineering, 199 (2010), pp. 582–597.

[113] A. Quarteroni and A. Valli, *Numerical Approximation of Partial Differential Equations*, Springer, Heidelberg, 1996.

[114] B. Rivière, *Analysis of a discontinuous finite element method for coupled Stokes and Darcy problems*, Journal of Scientific Computing, 22-23 (2005), pp. 479–500.

[115] B. Rivière and I. Yotov, *Locally conservative coupling of Stokes and Darcy flows*, SIAM Journal on Numerical Analysis, 42 (2005), pp. 1959–1977.

[116] J. E. Roberts and J. M. Thomas, *Mixed and Hybrid Methods. In Handbook of Numerical Analysis, edited by P.G. Ciarlet and J.L. Lions, vol. II, Finite Element Methods (Part 1)*, Nort-Holland, Amsterdam, 1991.

[117] D. Sandri, *Sur l'approximation numérique des écoulements quasi-Newtoniens dont la viscosité suit la loi puissance ou la loi de Carreau*, ESAIM: Mathematical Modelling and Numerical Analysis, 27 (1993), pp. 131–155.

[118] B. Scheurer, *Existence et approximation de point selles pour certain problemes non linéaires*, ESAIM: Mathematical Modelling and Numerical Analysis, 11 (1977), pp. 369–400.

[119] D. Schötzau, C. Schwab, and A. Toselli, *Mixed hp-DGFEM for incompressible flows*, SIAM Journal on Numerical Analysis, 40 (2003), pp. 2171–2194.

[120] H. Si, *TetGen: A Quality Tetrahedral Mesh Generator and 3D Delaunay Triangulator v.1.5 User's manual*, Tech. Report 13, Weierstrass Institute for Applied Analysis and Stochastics, Berlin, 2013.

[121] R. Stenberg, *A family of mixed finite elements for the elasticity problem*, Numerische Mathematik, 53 (1988), pp. 513–538.

[122] ———, *Two low-order mixed methods for the elasticity problem*, The mathematics of finite elements and applications, VI (Uxbridge, 1987), Academic Press, London, (1988), pp. 271–280.

[123] R. Temam, *Navier-Stokes equations. Theory and numerical analysis*, Studies in Mathematics and its Applications, North-Holland Publishing Co., Amsterdam, 1984.

[124] J. M. Urquiza, D. N'Dri, A. Garon, and M. C. Delfour, *Coupling Stokes and Darcy equations*, Applied Numerical Mathematics, 58 (2008), pp. 525–538.

[125] R. Verfürth, *A posteriori error estimation and adaptive-mesh-refinement techniques*, Journal of Computational and Applied Mathematics, 50 (1994), pp. 67–83.

[126] ———, *A Review of A Posteriori Error Estimation and Adaptive-Mesh-Refinement Techniques*, Wiley-Teubner, Chichester, 1996.

[127] ———, *A Posteriori Error Estimation Techniques for Finite Element Methods*, Oxford University Press, 2013.

[128] X. Xie, J. Xu, and G. Xue, *Uniformly stable finite element methods for Darcy-Stokes-Brinkman models*, Journal of Computational Mathematics, 26 (2008), pp. 437–455.